



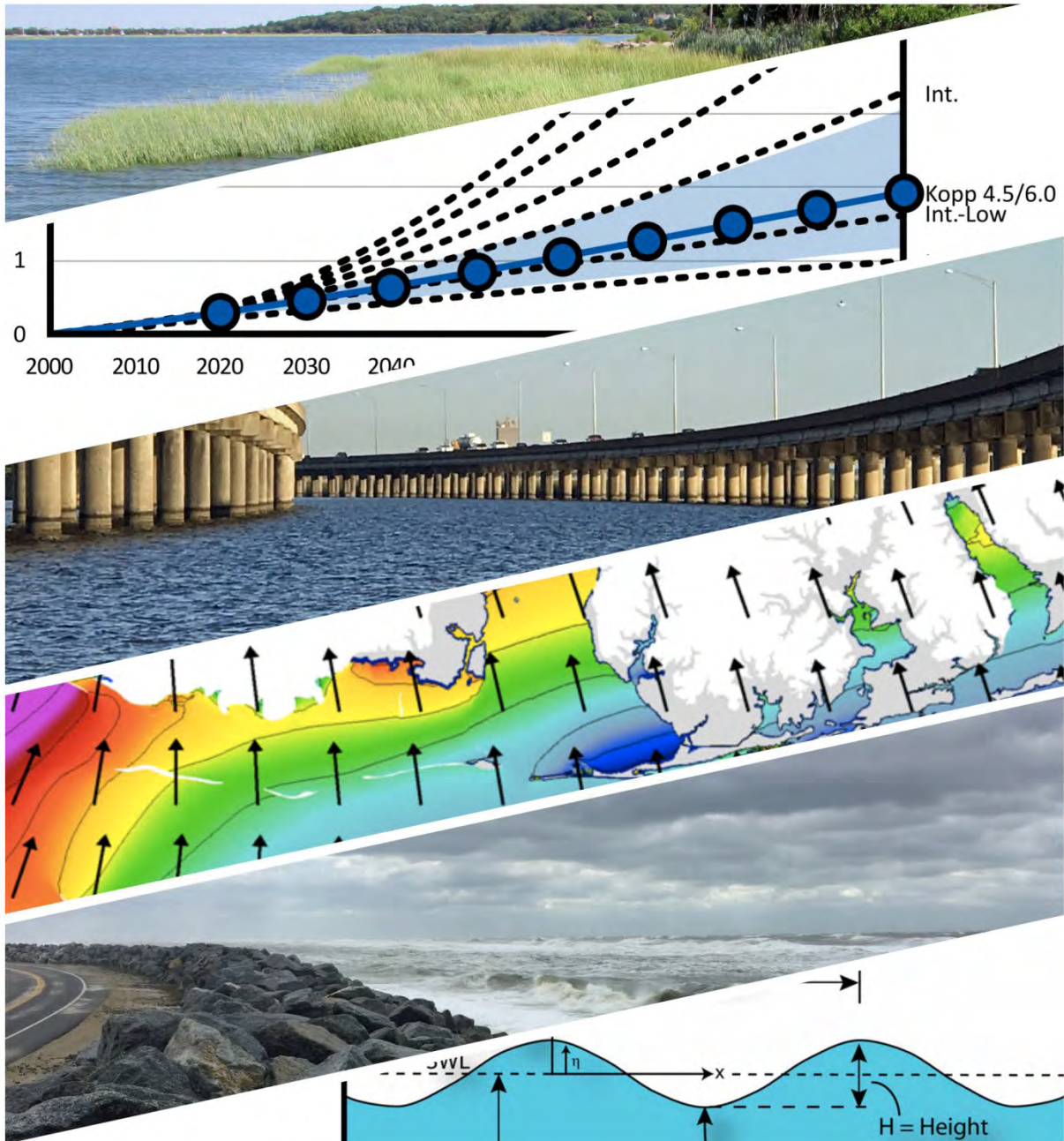
U.S. Department  
of Transportation

**Federal Highway  
Administration**

Publication No. FHWA-HIF-19-059

January 2020

Hydraulic Engineering Circular No. 25



# Highways in the Coastal Environment

Third Edition

*Page Intentionally Left Blank*



*Page Intentionally Left Blank*

# Table of Contents

Table of Contents..... i

List of Figures ..... ix

List of Tables..... xx

List of Symbols..... xxi

Acknowledgements.....xxiv

Notice.....xxiv

Non-Binding Contents.....xxiv

Quality Assurance Statement ..... xxv

Supporting Purpose ..... xxv

Glossary.....xxvi

List of Acronyms .....xliv

Part 1 – Background & Context ..... 1

Chapter 1 - Introduction .....3

    1.1 Purpose and Scope.....3

    1.2 Organization .....4

    1.3 Target Audience.....6

    1.4 Units in this Manual.....6

Chapter 2 - Federal Policy for Coastal Highways .....7

    2.1 Federal Highway and the Coast: National Overview.....7

    2.2 FHWA Statutes & Regulations .....7

        2.2.1 FHWA Statute.....7

        2.2.2 Appropriation Language .....9

        2.2.3 FHWA Regulations .....9

    2.3 Other Federal Agency Coastal Statutes & Regulations ..... 11

        2.3.1 Rivers and Harbors Act of 1899 [33 U.S.C. § 401 and § 403]..... 11

        2.3.2 General Bridge Act of 1946 [33 U.S.C. § 525 through 533] ..... 11

        2.3.3 Transportation Act of 1966 [Public Law 89-670]..... 11

        2.3.4 Coastal Zone Management Act [16 U.S.C. § 1451-1466] ..... 12

        2.3.5 National Environmental Policy Act [42 U.S.C. § 4321, et seq.] ..... 12

        2.3.6 Clean Water Act [33 U.S.C. § 1251-1387]..... 12

        2.3.7 Endangered Species Act [16 U.S.C. § 1531-1544] ..... 13

        2.3.8 Coastal Barrier Resources Act [16 U.S.C. § 3501 through 3510] ..... 13

2.3.9	Magnuson-Stevens Fishery Conservation and Management Act [16 U.S.C. § 1801-1891d] .....	13
2.3.10	Marine Mammal Protection Act [16 USC §§ 1361-1407].....	13
2.3.11	Migratory Bird Treaty Act [16 U.S.C. §§ 703-712.] .....	14
2.3.12	National Historic Preservation Act [54 U.S.C. 300101 et seq.].....	14
2.3.13	National Flood Insurance Act of 1968 [42 U.S.C. § 4001 et seq.].....	14
Chapter 3 -	Coastal Highways: An Overview .....	17
3.1	What are Coastal Highways? .....	17
3.2	The Extent of Coastal Roads and Bridges .....	18
3.3	Societal Demand for Coastal Highways .....	18
3.4	Natural Processes Impacting Coastal Highways.....	19
3.4.1	Water Level Change .....	19
3.4.2	Sea Level Rise .....	19
3.4.3	Storm Surge .....	19
3.4.4	Major Weather Events .....	19
3.4.5	Waves.....	22
3.4.6	Shoreline Erosion and Barrier Island Breaches.....	22
3.4.7	Littoral Drift .....	22
3.4.8	Shoreline Recession.....	23
3.4.9	Tsunamis .....	23
3.4.10	Upland Runoff.....	24
3.4.11	High-Velocity Flows .....	24
3.4.12	Other Processes.....	24
3.5	Coastal Highway Planning and Design .....	24
3.6	Coastal Engineering as a Specialty Area .....	25
3.6.1	Education.....	25
3.6.2	State-of-Practice.....	26
3.6.3	Professional Specialty Certification as a Coastal Engineer .....	26
3.6.4	Resources .....	26
3.6.5	Coastal Engineering in the Highway Community .....	27
Part 2 –	Principles of Coastal Science for Highway Engineering.....	29
Chapter 4 -	Water Levels .....	31
4.1	Sea Level Rise .....	31
4.1.1	Causes of SLR and Terminology.....	31
4.1.2	Historical RSLR Data: Tide Gages .....	32

4.1.3	Historical SLR Data: Satellites.....	38
4.1.4	Historical SLR Data: Geologic Record .....	38
4.1.5	Discussion of Historical and Present-Day GMSLR.....	39
4.1.6	Projections of Future GMSLR.....	40
4.1.7	SLR Values for Planning and Design aligned with NCHRP 15-61 .....	44
4.1.8	Example Future RSLR Calculation: Atlantic City .....	50
4.2	Astronomical Tides.....	51
4.2.1	Characteristics of Astronomical Tides .....	52
4.2.2	Tidal and Survey Datums .....	53
4.3	Storm Surge .....	55
4.3.1	Characteristics of Storm Surge.....	55
4.3.2	Storm Surge Modeling.....	56
4.3.3	Wave Setup .....	63
4.3.4	Impacts of SLR on Storm Surge.....	63
4.4	Coastal-Riverine Flooding .....	64
4.5	Lake Water Level Fluctuations .....	66
4.6	Design Water Levels .....	68
Chapter 5	Waves .....	73
5.1	Definitions, Theories, and Properties of Waves .....	73
5.2	Wave Transformation and Breaking.....	80
5.3	Irregular Waves .....	88
5.4	Wave Generation and Modeling.....	91
5.5	Wave Runup.....	94
5.6	Ship Wakes .....	94
5.7	Tsunamis.....	95
Chapter 6	Coastal Sediment Processes.....	97
6.1	Overview of Coastal Geomorphology.....	97
6.2	Beach Terminology .....	100
6.3	Coastal Sediment Characteristics .....	106
6.4	Cross-Shore Sand Transport and Dune Erosion Modeling .....	108
6.5	Longshore Sand Transport and Shoreline Change Modeling .....	111
6.6	Tidal Inlets.....	113
6.7	Future Sea Level Rise Effects on Coastal Processes.....	118
6.8	Physical Models in Coastal Engineering .....	119

Part 3 – Issues and Applications in Coastal Highway Design.....	123
Chapter 7 - Coastal Revetments.....	125
7.1 Types of Revetments and Seawalls .....	125
7.2 Hudson’s Equation for Armor Stone Size.....	130
7.3 Design Wave Heights for Revetment Design .....	136
7.4 Other Issues for Coastal Revetment Design .....	138
7.4.1 Common Failure Mechanisms of Coastal Revetments .....	138
7.4.2 Alternative Revetment Concepts and Materials .....	141
7.5 Wave Runup and Overtopping – Coastal Structures .....	143
7.6 Design Example: Coastal Revetment.....	146
7.6.1 Example Situation.....	146
7.6.2 Design Steps .....	146
Chapter 8 - Roads in Areas of Receding Shorelines .....	153
8.1 Examples of Issues .....	153
8.2 Quantifying Shoreline Change Rates .....	156
8.3 Estimating Future Shoreline Positions .....	158
8.3.1 Shortcomings of Shoreline Change Assumptions .....	158
8.3.2 Sediment Budgets .....	161
8.4 Relocation/Abandonment Considerations .....	161
8.5 Shoreline Stabilization Options .....	161
8.6 The Functional Design of Coastal Structures.....	162
8.7 Beach Nourishment.....	164
8.8 Combining Beach Nourishment with Structures.....	167
8.9 Marsh Restoration/Creation .....	172
8.10 Unproven “Experimental” Shoreline Stabilization Approaches.....	176
Chapter 9 - Increased Flooding due to Relative Sea Level Rise .....	177
9.1 Description of the Problem .....	177
9.2 Assessing the Problem.....	182
9.2.1 Sweet <i>et al.</i> (2014)/Sweet and Park (2014).....	182
9.2.2 Kriebel and Henderson (2018) .....	183
9.2.3 Jacobs <i>et al.</i> (2018a) .....	188
9.3 Raising Roadway Elevation.....	188
Chapter 10 - Highway Overwashing .....	193
10.1 Description of Overwashing .....	193

10.2	The Coastal Weir-Flow Damage Mechanism.....	194
10.2.1	Coastal Weir-Flow Damage Mechanism Investigations .....	198
10.3	Strategies for Roads that Overwash .....	202
10.3.1	Road Location Considerations .....	202
10.3.2	Road Elevation Considerations .....	203
10.3.3	Construction of Sand Dunes.....	203
10.3.4	Armoring of Shoulders.....	205
Chapter 11 - Coastal Bridges.....		209
11.1	Coastal Bridge Settings.....	209
11.1.1	Bridges at Inlets.....	209
11.1.2	Bridges over Bays and Sounds .....	210
11.1.3	Bridges Spanning Tidal Embayments .....	210
11.1.4	Bridges Crossing Rivers .....	212
11.2	Wave Loads on Bridge Decks: Examples and Description .....	213
11.2.1	I-10 Escambia Bay (Hurricane Ivan).....	214
11.2.2	US 90 Biloxi Bay (Hurricane Katrina) .....	217
11.2.3	Description of the Wave Load Damage Mechanism .....	219
11.3	Wave Loads on Bridge Decks: Literature.....	221
11.4	Wave Loads on Bridge Decks: Method for Estimating .....	223
11.4.1	Equations for Estimating Wave Loads on Bridge Decks .....	223
11.4.2	Example Application of Wave Load Equations.....	225
11.4.3	Discussion of the Method .....	226
11.5	Wave Loads on Bridge Decks: Countermeasures .....	229
11.6	Bridge Deck Elevation to Avoid Wave Loads.....	229
11.6.1	Nominal Maximum Wave Height Approach.....	230
11.6.2	Depth-Limited Maximum Wave Height Approach.....	231
11.6.3	Estimating the Maximum Wave Crest Elevation.....	231
11.6.4	Freeboard Considerations .....	231
11.7	Other Coastal Bridge Issues .....	232
11.8	Selection of Design Storm Surge & Design Wave Heights .....	233
11.8.1	Design Storm Surge SWL .....	234
11.8.2	Design Wave Heights .....	234
11.8.3	Coastal Engineer Involvement.....	234

Chapter 12 - Coastal Scour .....	235
12.1 Introduction.....	235
12.1.1 Bridge Scour Policy, Guidance, and Reference Materials.....	236
12.2 Hydraulics for Coastal Bridge Locations & Crossings .....	237
12.2.1 Tidally-Influenced River Crossings.....	237
12.2.2 Tidally-Dominated River Crossings .....	239
12.2.3 Tidal Crossings.....	240
12.2.4 Non-Tidal Waters.....	240
12.2.5 Other Considerations.....	240
12.3 Types of Coastal Scour .....	241
12.3.1 Long-term Changes.....	241
12.3.2 Bedforms .....	244
12.3.3 Contraction Scour.....	245
12.3.4 Local Scour at Bridge Piers .....	247
12.3.5 Local Scour at Bridge Abutments .....	254
12.3.6 Wave-Induced Scour .....	256
12.3.7 Tsunami-Induced Scour .....	260
12.3.8 Time-Dependent Scour .....	262
12.3.9 Other Types of Coastal Scour .....	263
12.4 Bridge Scour Evaluation Methods .....	263
12.4.1 Tidally-Influenced Bridge Scour Evaluation.....	263
12.4.2 Tidally-Dominated Bridge Scour Evaluation .....	264
12.4.3 Tidal Bridge Scour Evaluation .....	265
12.4.4 Example of Tidal Bridge Scour Calculations .....	266
12.5 Scour Appraisal Methodologies.....	270
12.5.1 Low-Risk Crossings.....	270
12.5.2 Typical Crossings .....	270
12.5.3 Special Cases.....	270
12.6 Scour Countermeasures .....	271
Part 4 – Coastal Highway Vulnerability Assessment .....	275
Chapter 13 - Engineering Risk at the Coast .....	277
13.1 Return Period and Probability of Occurrence.....	277
13.2 Coastal Storm Flood Frequencies.....	279
13.2.1 Atlantic and Gulf Coast Surge Frequencies .....	279

13.3	Available Estimates of Storm Surge: SSIMs and FIRMs.....	281
13.4	Other Approaches to Quantifying Coastal Risk.....	282
Chapter 14 - Analysis Methods for Assessing Vulnerability to Extreme Coastal Events .....		285
14.1	Literature on Assessing the Impacts of Future Environmental Conditions.....	287
14.2	Levels of Effort in Assessments .....	290
14.2.1	Level of Effort 1: Use of Existing Data and Resources.....	290
14.2.2	Level of Effort 2: Modeling of Storm Surge and Waves.....	291
14.2.3	Level of Effort 3: Modeling in a Probabilistic Risk Framework.....	292
14.3	Gulf of Mexico and South Atlantic Coast.....	293
14.3.1	Level of Effort 1: Gulf of Mexico and South Atlantic Coast.....	293
14.3.2	Level of Effort 2: Gulf of Mexico and South Atlantic Coast.....	297
14.3.3	Level of Effort 3: Gulf of Mexico and South Atlantic Coast.....	300
14.4	Mid-Atlantic and New England Coast.....	302
14.4.1	Level of Effort 1: Mid-Atlantic and New England Coast.....	302
14.4.2	Level of Effort 2: Mid-Atlantic and New England Coast.....	303
14.4.3	Level of Effort 3: Mid-Atlantic and New England Coast.....	306
14.5	Great Lakes.....	307
14.5.1	Level of Effort 1: Great Lakes Coast .....	307
14.5.2	Level of Effort 2: Great Lakes Coast .....	310
14.5.3	Level of Effort 3: Great Lakes Coast .....	312
14.6	Pacific Coast & Islands – Storms .....	313
14.6.1	Level of Effort 1: Pacific Coast – Storms .....	314
14.6.2	Level of Effort 2: Pacific Coast – Storms .....	316
14.6.3	Level of Effort 3: Pacific Coast – Storms .....	317
14.7	Pacific Coast & Islands – Tsunamis.....	318
14.7.1	Level of Effort 1: Pacific Coast – Tsunamis.....	318
14.7.2	Level of Effort 2: Pacific Coast – Tsunamis.....	319
14.7.3	Level of Effort 3: Pacific Coast - Tsunamis.....	321
14.8	Vulnerability Assessment Case Studies.....	322
14.8.1	Level 1 Case Study: Adapting to Rising Tides - San Francisco Bay.....	323
14.8.2	Level 2 Case Study: The Gulf Coast 2 Study - Mobile, Alabama .....	328
14.8.3	Level 3 Case Study: Central Artery Project, Boston, Massachusetts.....	335
Chapter 15 - Adaptation Strategies for Coastal Highways.....		345
15.1	Typical Coastal Damage Mechanisms.....	345

15.1.1	Roadway Damage by Wave Attack .....	345
15.1.2	Roadway and Railway Damage by Coastal “Weir-Flow” .....	347
15.1.3	Roadway Damage by Bluff Erosion and Shoreline Recession .....	348
15.1.4	Bridge Deck Damage by Waves on Surge .....	349
15.1.5	Structure Damage by Wave Runup .....	351
15.1.6	Tunnel and Road Damage by Overtopping .....	351
15.1.7	Damage by Tsunamis .....	351
15.2	Adaptation Strategies for Coastal Highway Infrastructure .....	352
15.2.1	Manage and Maintain .....	352
15.2.2	Increase Redundancy .....	352
15.2.3	Protect .....	353
15.2.4	Accommodate .....	354
15.2.5	Relocate .....	355
	References .....	359
	Appendix – Workshop Participants .....	385

## List of Figures

Figure 1.1. A US coastal highway (Florida SH A1A in Ft. Lauderdale 2018).....	3
Figure 3.1. A local coastal road along an estuary (Shore Road along Mt. Sinai Harbor, Town of Brookhaven, New York).....	17
Figure 3.2. Big Creek Bridge on the Pacific Coast Highway (California SH 1) .....	18
Figure 3.3. Damage caused by surge and waves in Hurricane Michael (October 14, 2018; permission to use photograph provided by John Cleary) .....	21
Figure 3.4. US Highway 90 bridge across Biloxi Bay, Mississippi, after Hurricane Katrina. (photograph looking northeast from Biloxi September 21, 2005) .....	23
Figure 4.1. Relative sea level rise (RSLR) trend for New York City based on tide gage data (image downloaded from NOAA Tides and Currents website September 6, 2018) ...	33
Figure 4.2. Annual average sea level at Dauphin Island, Alabama .....	34
Figure 4.3. Sea levels along the US Atlantic and Gulf Coasts for the past century .....	35
Figure 4.4. Sea levels along the US Pacific Coast for the past century.....	36
Figure 4.5. Relative sea level rise (RSLR) rates measured at tide gages around the US (image downloaded from NOAA Tides and Currents website, Sept 5, 2018) .....	37
Figure 4.6. Map of sea level change as measured by satellites 1992-2017 (permission for use provided by CNES/LEGOS/CLS).....	38
Figure 4.7. Global Mean Sea Level Rise (GMSLR) 1993-2018 as measured by satellite altimetry (data from CNES/LEGOS/CLS 2018) .....	39
Figure 4.8. Projections of GMSLR in this century (relative to 2000) from Kopp <i>et al.</i> (2014) for a) RCP 8.5, b) RCP 4.5, and c) RCP 2.6 .....	42
Figure 4.9. GMSLR scenarios and process-based projections. The scenarios (dashed curves) are the SLR Interagency Task Force (Sweet <i>et al.</i> 2017b) scenarios and the projections (blue line for median and shading for 90% confidence interval) are the Kopp <i>et al.</i> (2014) scientific, process-based projections for RCP 8.5 (upper panel) and for RCP 4.5/6.0 (lower panel) .....	43
Figure 4.10. RSLR projections for four US cities corresponding to the GMSLR scenarios of the Interagency report (adapted from Sweet <i>et al.</i> 2017b) .....	45
Figure 4.11. Future SLR values for planning and design as per NCHRP 15-61: the RSLR corresponding with the GMSLR values shown by the circles on the lower panel are minimum values (see Table 4.1). The circles on the upper panel are higher values for more sensitive, or fragile, asset planning (see Table 4.2) (see Figure 4.9 caption for explanation of the other curves) .....	47
Figure 4.12. Relative sea level rise (RSLR) trend for Atlantic City, New Jersey (image downloaded from NOAA Tides and Currents website September 10, 2018) .....	50
Figure 4.13. Basic definitions of tides (image downloaded from <a href="http://tidesandcurrents.noaa.gov">http://tidesandcurrents.noaa.gov</a> ) .....	53
Figure 4.14. An example of the relationship between the survey and tidal datums .....	54

Figure 4.15. Approximate predicted change from NAVD 88 to the new vertical datum which will replace it in 2022 (adapted from NGS 2018).....	55
Figure 4.16. Storm surge at Galveston, Texas, from Hurricane Alicia in 1983 .....	56
Figure 4.17. When and where to apply riverine hydraulic and coastal hydrodynamic models as a function of distance from the coast and importance of infrastructure (Webb 2017) .....	58
Figure 4.18. Example of numerical mesh used for a storm surge model.....	60
Figure 4.19. Detail of a seamless topographic-bathymetric mesh surface used for modeling coastal storm surge flooding.....	61
Figure 4.20. Example of storm surge model output (with input winds) along the Alabama coast during Hurricane Katrina (2005).....	62
Figure 4.21. Water level measurements near Sabine, Texas (upper panel) and the path of Hurricane Harvey (lower panel).....	65
Figure 4.22. Example of seasonal lake level fluctuations (USACE-Detroit District 2018).....	67
Figure 4.23. Annual lake level fluctuations – Lakes Michigan and Huron (dashed line is the long-term average) .....	68
Figure 4.24. An example of water level, wave height and wave period values near San Luis Pass, Texas obtained from the USACE Coastal Hazards System database .....	70
Figure 5.1. Wave parameter definitions .....	74
Figure 5.2. Water particle paths under waves in deep water.....	77
Figure 5.3. Water particle paths under waves in shallow and intermediate water depths .....	77
Figure 5.4. Stokes 2 <sup>nd</sup> order wave theory water surface profile .....	78
Figure 5.5. Bending of wave crests as they approach the shore due to refraction (adapted from USACE 2002).....	81
Figure 5.6. Wave energy focused on headland by a wave refraction and diffraction (adapted from USACE 2002).....	82
Figure 5.7. Waves refracting, diffracting and breaking on the shallow-water reefs south of the Diamond Head Lighthouse, Honolulu, Hawaii.....	83
Figure 5.8. Depth-limited wave breaking in shallow water.....	84
Figure 5.9. Depth-limited wave breaking during storm surge (permission to use photograph provided by Happy Partridge).....	85
Figure 5.10. Wave breaker types.....	86
Figure 5.11. Example of a plunging breaker (from Douglass 2002) .....	87
Figure 5.12. Example of a spilling breaker (Huntington Beach, California, 2017) .....	87
Figure 5.13. Example of a collapsing breaker (Morro Bay, California) .....	88
Figure 5.14. A train of long-period swell approaching the Oregon coast.....	89
Figure 5.15. Irregular waves on San Francisco Bay, California.....	89
Figure 5.16. A storm-driven, irregular, sea state in the Gulf of Mexico (Florida SH 30E) .....	90

Figure 5.17. ADCIRC+SWAN wave model hindcast of maximum significant wave heights generated during Hurricane Ivan (2004) at the I-10 bridge across Escambia Bay, Pensacola, Florida.....	94
Figure 6.1. Sea cliff and pocket beach on the Oregon coast (Oswald West State Park).....	98
Figure 6.2. An example of a barrier island. Dauphin Island, Alabama (circa 2001, looking east with Gulf of Mexico to the right and Mississippi Sound to the left).....	99
Figure 6.3. Sea level rise curve for the past 20,000 years.....	100
Figure 6.4. Terminology used to describe processes of waves and currents in the surf zone..	101
Figure 6.5. Terminology used to describe the beach profile .....	102
Figure 6.6. Sand bar and trough exposed at low tide (Garden City Beach, South Carolina)....	102
Figure 6.7. A beach scarp (Los Angeles County, California) .....	103
Figure 6.8. A sand dune (St. George Island, Florida) .....	103
Figure 6.9. Beach profile surveying crew using a traditional level and rod .....	104
Figure 6.10. A CRAB (Coastal Research Amphibious Buggy) used to measure beach profiles during beach nourishment .....	105
Figure 6.11. Dean's equilibrium beach profile shape definition sketch .....	106
Figure 6.12. Examples of colors of US beach sands (from Douglass 2002, photograph used with permission of the author) .....	107
Figure 6.13. Example grain size distribution based on a sieve analysis for beach sand .....	108
Figure 6.14. Typical beach profile changes in response to cross-shore transport of sand.....	109
Figure 6.15. Dune erosion model results example .....	110
Figure 6.16. Definition sketch of wave angle at breaking .....	112
Figure 6.17. The CERC equation model for longshore sand transport rate plotted with field data (adapted from USACE 1984).....	113
Figure 6.18. Two tidal inlets on the southwest Florida coast (New Pass and Big Sarasota Pass, Lido Key is the barrier island between the two inlets) .....	115
Figure 6.19. Typical inlet morphology .....	116
Figure 6.20. Idealized ocean-inlet-bay system (adapted from USACE 1984) .....	116
Figure 6.21. Tidal prism versus minimum inlet throat area for all major inlets on the Atlantic, Gulf, and Pacific Coasts (USACE 1984) .....	117
Figure 6.22. Physical model experiment on wave loads on a bridge deck in a wave flume (University of South Alabama wave flume).....	121
Figure 6.23. A small-scale wave flume being used to model wave runup for professional development training in NHI Course #135082 Highways in the Coastal Environment .....	121
Figure 6.24. A movable-bed, physical model experiment on beach salient formation in a wave basin (University of South Alabama wave basin).....	122
Figure 7.1. A revetment protecting a coastal highway (Bayfront Road, Mobile, Alabama, 2019) .....	126

Figure 7.2. Types of shore protection walls .....	126
Figure 7.3. Galveston Seawall (Seawall Boulevard, 2018).....	127
Figure 7.4. San Francisco's Great Highway Seawall (California SH 35, 1991) .....	127
Figure 7.5. Seawall protecting a coastal highway (Venice, Florida, 2001) .....	128
Figure 7.6. Seawall protecting a coastal highway (Pacific Coast Highway, Pacific Palisades, California, 2003) .....	128
Figure 7.7. Seawall protecting a coastal highway (Florida SH A1A, Flagler Beach, 2002) .....	129
Figure 7.8. Seawall protecting a coastal highway (US 101, Curry County, Oregon, 2001) .....	129
Figure 7.9. Wave striking a seawall protecting Kaumuali'i Highway on Kauai (Hawaii SH 50, 2018) .....	130
Figure 7.10. Revetment protecting a highway along a bay shoreline (Florida SH 60 crossing Tampa Bay, 2003).....	131
Figure 7.11. Revetment protecting a highway along a bay shoreline (Washington SH 105, Willapa Bay, 2003) .....	132
Figure 7.12. Seawall protecting a local road (West Cliff Drive, Santa Cruz, California, 2001)..	132
Figure 7.13. Concrete seawall designed to look like the natural rock formation built on an eroding sea cliff to protect a local road (East Cliff Drive, Santa Cruz, California, 2001) .....	133
Figure 7.14. Typical coastal revetment design cross-section .....	133
Figure 7.15. Storm waves breaking on a rock, rubble-mound breakwater in a bay (Mobile Bay, Alabama).....	135
Figure 7.16. A revetment with rocks too small to withstand the wave attack at this location....	139
Figure 7.17. Example of a failed attempt at embankment protection (USACE archives photographs) .....	139
Figure 7.18. An example of splash damage behind seawall (circa 2004).....	140
Figure 7.19. Example of a splash apron (center of photograph) at the top of a coastal rock revetment protecting a local road along a bluff on Chesapeake Bay (Shore Road, Anne Arundel County, Maryland, 2017) .....	141
Figure 7.20. Example of rigid concrete-block revetment failure (Florida SH A1A, Delray Beach, circa 1972; University of Florida and USACE archive photos).....	142
Figure 7.21. Example of failed block revetment (Louisiana SH 82, circa 1980, USACE archives photos) .....	143
Figure 7.22. Wave runup on a structure definition sketch.....	144
Figure 7.23. Wave overtopping a seawall (Lihue, Hawaii, 2018).....	145
Figure 7.24. Critical values of average overtopping discharges (adapted from USACE 2002)	147
Figure 7.25. Eroding profile input to coastal revetment design example .....	148
Figure 7.26. Coastal revetment design example cross-section .....	151
Figure 8.1. A highway initially built inland now threatened by long-term shoreline erosion. Cape Shoalwater area of Washington SH 105 (2003) .....	154

Figure 8.2. A local road threatened by long-term shoreline recession (Ocean Drive, Whale Beach area of Cape May County Road 619, Ludlam Island, New Jersey 2003) .....	155
Figure 8.3. A local road being undermined by bluff erosion and long-term shoreline recession on the Great Lakes (Painesville, Ohio, 2001) .....	155
Figure 8.4. Road destroyed by shoreline recession: a) broken pavement on the beach at the old location; b) south end of the closed section; c) location map. (Texas SH 87, Jefferson County, circa 2002).....	156
Figure 8.5. An example of shoreline position changes through time. Stump Hole area of St. Joseph's Peninsula, Florida.....	158
Figure 8.6. An example of shoreline change rates along 30,000 ft of coast showing temporal and spatial variations but a significant recessional trend. Western-facing shoreline of St. Joseph's Peninsula, Florida.....	159
Figure 8.7. Example of projected future shoreline positions at Stump Hole .....	160
Figure 8.8. Groin field in Long Branch, New Jersey (2006) .....	163
Figure 8.9. A beach nourishment project under construction in Gulf Shores, Alabama (2001)	165
Figure 8.10. Beach nourishment project with constructed dune on top of old, failed revetment protecting Florida SH A1A (Delray Beach, 2001) .....	166
Figure 8.11. Beach nourishment seaward of a seawall protecting a road. (New Jersey SH 35, Sea Bright, 2001).....	166
Figure 8.12. Offshore segmented breakwaters with salients in beach nourishment protecting a highway (Louisiana SH 82, Holly Beach).....	167
Figure 8.13. Offshore segmented breakwaters with salients in beach nourishment (Presque Isle State Park, Pennsylvania, circa 1980, USACE archive photograph).....	168
Figure 8.14. Offshore segmented breakwater system at Presque Isle, Pennsylvania.....	169
Figure 8.15. Empirical relationships for shoreline effect of offshore segmented breakwaters. (after Pope and Dean 1986, and USACE 2002).....	170
Figure 8.16. Offshore segmented breakwaters with groins and beach nourishment on Corpus Christi Bay (Ocean Drive, Corpus Christi, Texas).....	170
Figure 8.17. Constructed pocket beach stabilized with a T-head groin breakwater system (Point Clear, Alabama, circa 2006).....	171
Figure 8.18. Beach nourishment project stabilized as pocket beaches with a headland breakwater system protecting a road (Water Street, Yorktown, Virginia, circa 2006) .....	172
Figure 8.19. Example of a constructed marsh stabilized with a nearshore breakwater (Little Bay, Bayou LaBatre, Alabama) .....	174
Figure 8.20. Example of a constructed marsh protected by nearshore rock breakwaters (Holts Landing State Park, Indian River Bay, Delaware, 2009).....	175
Figure 9.1. Flooding of the Tidal Basin in Washington, District of Columbia (June 2018; permission for use of photograph provided by Loic Pritchett) .....	178
Figure 9.2. Example of coastal flooding on an urban road (Honolulu, March 30, 2017).....	179

Figure 9.3. Example of coastal flooding on a primary road (Florida SH A1A, Hollywood Beach, October 21, 2017) .....	179
Figure 9.4. Example of coastal flooding on a local road that crosses a developed barrier island (Hollywood Beach, Florida, October 21, 2017) .....	180
Figure 9.5. Example of flooding of a coastal road which is affecting traffic and parking (Dock Street, Annapolis, Maryland, 2017 photograph provided by Joe Krolak) .....	180
Figure 9.6. The increased frequency of flooding occurs because the full distribution of tides rises with RSLR (from Sweet <i>et al.</i> 2014).....	183
Figure 9.7. Increased flooding due to RSLR including historical exceedances (orange), future projections through 2100 based upon the continuation of the historical trend (blue), and future projections under median RCP2.6, 4.5 and 8.5 conditions, for Charleston, South Carolina and San Francisco, California (from Sweet <i>et al.</i> 2017a adapted from Sweet and Park 2014) .....	184
Figure 9.8. Flooding of McNair Road, US Naval Academy, Annapolis, Maryland (permission for use of photograph provided by David Kriebel) .....	184
Figure 9.9. Probability distribution for high tides at Annapolis approximately follows a normal distribution (from Kriebel and Henderson 2018).....	185
Figure 9.10. Average annual flood events above threshold water levels at Annapolis, 2014-2017 (from Kriebel and Henderson 2018). .....	186
Figure 9.11. The effect of RSLR on annual flood events at Annapolis (from Kriebel and Henderson 2018).....	187
Figure 9.12. Applying the annual flood events curves to McNair Road, Annapolis (from Kriebel and Henderson 2018).....	188
Figure 9.13. Annual vehicle-hours of delay projected for major roads (principal arterials, minor arterials, and major collectors) due to increased flooding due to RSLR by state; year (2020, 2060, 2100), and RSLR scenario (Intermediate-Low, Intermediate, and Extreme) (from Jacobs <i>et al.</i> 2018a) .....	189
Figure 9.14. Example of a road which has been raised to reduce flooding due to RSLR (Sunset Harbour Drive, Miami Beach, 2017).....	190
Figure 9.15. Flooding of McNair Road due to RSLR without (left panel) and with (right panel) a 1 ft increase in road elevation (from Kriebel and Henderson 2018) .....	191
Figure 10.1. Example of pavement damage due to storm surge (Florida SH 292 on Perdido Key after Hurricane Ivan, September 2004). .....	193
Figure 10.2. Example of pavement damaged by hurricane (photograph looking west on Florida SH 399, Gulf Islands National Seashore, 2005).....	194
Figure 10.3. Flow regimes leading to failure of embankments in riverine flooding situations (after Clopper and Chen 1988).....	195
Figure 10.4. Embankment failure mechanisms (after Clopper and Chen 1988).....	196
Figure 10.5. Pavement destroyed by the weir-flow mechanism (Fort Pickens Road, Gulf Islands National Seashore, near Pensacola, Florida) .....	196
Figure 10.6. Weir-flow damage beginning (Fort Pickens Road, Gulf Islands National Seashore, Florida, July 2005; FHWA photograph).....	197

Figure 10.7. Weir-flow damage occurring. (Fort Pickens Road, Gulf Islands National Seashore, Florida, July 2005; FHWA photograph).....	197
Figure 10.8. USA/TAMU laboratory experiment model setup schematic.....	198
Figure 10.9. Schematic of results from USA/TAMU laboratory experiments test run one .....	199
Figure 10.10. Schematic of results from USA/TAMU laboratory experiments test run two.....	199
Figure 10.11. Laboratory tests of the weir-flow damage mechanism showing scour destroying the downstream shoulder and beginning to undermine the edge of pavement. (USA/TAMU flume tests, June 2005).....	200
Figure 10.12. Laboratory tests of the weir-flow damage mechanism showing scour has continued to the point of undermining failure of 3 sections (6 ft) of roadway surface. (USA/TAMU flume tests, June 2005).....	200
Figure 10.13. Pavement moved landward by overwash processes. (Florida SH 399, Gulf Islands National Seashore, Florida after Hurricane Ivan, 2004).....	201
Figure 10.14. Evidence of weir-flow damage to the seaward edge of pavement due to return flow late in the storm (Alabama SH 182, after Hurricane Ivan, Gulf Shores, 2004) .	202
Figure 10.15. Schematic of sand erosion and deposition on a barrier island resulting from overwash .....	203
Figure 10.16. Example of road buried by overwash sand after it was opened by plows .....	204
Figure 10.17. Artificial sand dune constructed seaward of a highway to protect the highway (North Carolina SH 12; looking north, the Atlantic Ocean is to the right and Pamlico Sound is to the left, 2002).....	204
Figure 10.18. Schematic summarizing three approaches (bayward location, low elevation, constructed sand dunes near road) to minimize damage to roads that overwash ...	205
Figure 10.19. Sheet pile, with buried gabions for scour protection, at edge of pavement to resist pavement damage due to coastal storm surge overwash. (Florida DOT figure) .....	206
Figure 10.20. Gabions at edge of pavement to resist pavement damage due to coastal storm surge overwash. (Florida DOT figure) .....	206
Figure 10.21. Highway shoulder which has been designed to withstand the weir-flow damage during overwashing events (US 98, Okaloosa Island, Florida, 2016).....	207
Figure 10.22. Conceptual design to resist pavement damage due to coastal storm surge overwash .....	208
Figure 11.1. Conceptual schematic of four typical bridge settings within the coastal environment.....	210
Figure 11.2. Bridge spanning a small inlet (Alabama SH 182 in Gulf Shores) .....	211
Figure 11.3. The F.J. Torras Causeway bridges between Brunswick and Saint Simons Island, Georgia .....	211
Figure 11.4. Interstate 10 bridge crossing Mobile Bay, Alabama .....	212
Figure 11.5. Pacific Coast river mouth crossings (clockwise from top left: Big Creek, Oregon; Pistol River, Oregon; Yachats River, Oregon, and Redwood Creek, California) .....	213

Figure 11.6. Location map of some of the highway bridges damaged by wave loads in hurricanes along the north-central Gulf Coast (from Douglass <i>et al.</i> 2006a) .....	214
Figure 11.7. Location map and damage overview for the I-10 bridge across Escambia Bay, Florida in Hurricane Katrina .....	215
Figure 11.8. Interstate-10 bridge across Escambia Bay, Florida, after Hurricane Ivan. Photograph looking northeast from Pensacola September 16, 2004 (photograph used with a license from AP Images) .....	216
Figure 11.9. US 90 bridge over Biloxi Bay, Mississippi showing the spans below a critical elevation were removed by Hurricane Katrina (photograph looking southwest from Ocean Springs, February 19, 2016) .....	218
Figure 11.10. Details of damage to US 90 bridge over Biloxi Bay caused by Hurricane Katrina .....	218
Figure 11.11. Schematic of resultant wave-induced load, with both uplift and lateral components, on a bridge deck .....	220
Figure 11.12. Schematic of typical time-history of wave loads on rigid structures.....	220
Figure 11.13. Horizontal and vertical wave-induced loads on bridge decks .....	224
Figure 11.14. Definition sketch for $\Delta z_h$ , $\Delta z_v$ , $A_h$ , $A_v$ , and $\eta_{max}$ in Equations 11.1 and 11.2 for estimating wave loads on elevated bridge decks) .....	225
Figure 11.15. Example of concave seaward face of a coastal bridge (I-10 bridge over Mobile Bay, Alabama) .....	228
Figure 11.16. Definition sketch of wave parameters and water levels for determining elevation of bridge deck for clearance from wave crests.....	230
Figure 12.1. Discharge record for a tidally-influenced location (image downloaded from USGS website May 2019) .....	238
Figure 12.2. Discharge record for a tidally-dominated location (image downloaded from USGS website May 2019) .....	239
Figure 12.3. Representation of recession-dominated flow following Hurricane Harvey.....	241
Figure 12.4. Aerial imagery of Oregon Inlet, North Carolina from 1993, March 2011, and August 2011 .....	243
Figure 12.5. Aerial imagery of Matanzas Inlet, Florida from 1995, 2012, and 2016 .....	243
Figure 12.6. Bathymetric elevations showing scour holes inside Indian River Inlet (circa 1999) .....	244
Figure 12.7. Definition sketch showing the representative variables used to estimate the height and length of orbital ripples.....	245
Figure 12.8. Examples of possible horizontal contractions at coastal bridges (thin lines denote possible streamlines, double-ended arrows denote the potential for flow reversals).....	246
Figure 12.9. Vertical contraction or pressure scour schematic (Arneson <i>et al.</i> 2012).....	247
Figure 12.10. Local scour depression at the terminus of a coastal structure.....	249
Figure 12.11. Complex pier components for Sheppard pier scour equations (FDOT 2005).....	250

Figure 12.12. Individual elements for Sheppard pier scour equations (FDOT 2005).....	251
Figure 12.13. Concept of effective diameter for complex piers in the Sheppard pier scour equations (FDOT 2005).....	251
Figure 12.14. Three cases for Sheppard pier scour equations (FDOT 2005).....	252
Figure 12.15. Johns Pass, Florida (2002).....	253
Figure 12.16. Location overview for Johns Pass, Florida .....	253
Figure 12.17. Typical scour profiles due to waves at the toe of a vertical wall (from USACE 2002) .....	254
Figure 12.18. Scour due to breaking waves at a vertical wall (USACE 2002) .....	255
Figure 12.19. Damage to bridge approach behind abutment due to wave action in a hurricane.....	256
Figure 12.20. Wave-induced local pier scour (Webb and Matthews 2014).....	258
Figure 12.21. Definition sketch for effective diameter of pile groups for wave-induced pier scour (Webb and Matthews 2014).....	259
Figure 12.22. Scour hole formed by Hurricane Katrina (permission to use photograph provided by Joe Krolak).....	259
Figure 12.23. Jensen Beach Causeway bridge .....	260
Figure 12.24. Jensen Beach Causeway bridge post-event scour bathymetry (2005).....	261
Figure 12.25. Proposed design scour analysis workflow for a tidally-influenced bridge crossing .....	264
Figure 12.26. Proposed design scour analyses workflow for a tidally-dominated bridge crossing .....	265
Figure 12.27. Proposed design scour analyses workflow for a tidal bridge crossing.....	266
Figure 12.28. Location overview for the Pensacola Bay Bridge scour example .....	267
Figure 12.29. Return period still water levels and corresponding event velocity magnitudes on Neches River, TX .....	267
Figure 12.30. Definition sketch for scour protection at the base of vertical walls.....	273
Figure 13.1. Probability of occurrence as a function of return period, $T$ , and years of service, $n$ .....	278
Figure 14.1. Vulnerability of highways in the coastal environment .....	285
Figure 14.2. FHWA's Vulnerability Assessment and Resilience "Framework" (FHWA 2017d). 286	
Figure 14.3. Deerfield Beach, Florida (2018).....	294
Figure 14.4. Portland Head Lighthouse, Maine (2016) .....	304
Figure 14.5. Chicago waterfront (2018) .....	309
Figure 14.6. Laguna Beach, California .....	315
Figure 14.7. Wainiha River, on the north shore of the island of Kauai, Hawaii, is an area with an extremely high tsunami hazard and a history of tsunami-induced bridge damage.....	320

Figure 14.8. Shoreline Drive, Alameda, California on San Francisco Bay (2018) .....	324
Figure 14.9. Inundation map of Alameda County for 100-year storm flood with 16 inches of sea level rise and additional elevation for wave effects (from ART 2011b).....	326
Figure 14.10. Detailed inundation map of the northern portion of Alameda County for the 100-year storm flood with 16 inches of sea level rise and additional elevation for wave effects (from ART 2011b).....	327
Figure 14.11. Modeled storm surge depths in Mobile County, Alabama for the scenario of Hurricane Georges conditions with 2.5 ft (75 cm) of future sea level rise (from Choate <i>et al.</i> 2012) .....	332
Figure 14.12. Validation of ADCIRC surge estimates by comparison with a tide gage at Dauphin Island, Alabama .....	333
Figure 14.13. Validation of ADCIRC storm surge estimates by comparison with measured high water marks .....	334
Figure 14.14. Modeled wave heights for the scenario of Hurricane Georges conditions with 2.5 ft (75 cm) of future sea level rise (from Choate <i>et al.</i> 2012) .....	336
Figure 14.15. Example of the fine, highly-resolved hydrodynamic model mesh used in the Boston Central Artery/Tunnel vulnerability assessment study (from Douglas 2015; permission to use image provided by MassDOT).....	339
Figure 14.16. Example of the inundation map products from the Boston Central Artery/Tunnel Vulnerability Study. The exceedance probability of coastal flooding in 2070/2100 (from Bosma <i>et al.</i> 2015; permission to use image provided by MassDOT) .....	341
Figure 14.17. Example of coastal flood mapping results from the Boston Central Artery/Tunnel vulnerability study focused on the area around Long Wharf and Christopher Columbus Park (from Bosma 2019; permission to use image provided by MassDOT).....	341
Figure 14.18. Model results showing depth for a 1% flooding probability in 2013 at the 93 Granite Ave. location, as well as residence time and local flood pathways (from Bosma <i>et al.</i> 2015; permission to use image provided by MassDOT).....	343
Figure 14.19. Model results showing depth for a 1% flooding probability in 2030 at the 93 Granite Ave. location, as well as residence time and local flood pathways (from Bosma <i>et al.</i> 2015; permission to use image provided by MassDOT).....	344
Figure 15.1. Partial embankment damage caused by waves on storm surge during Hurricane Ivan (Pensacola, Florida, 2004) .....	346
Figure 15.2. Example of the coastal weir-flow damage mechanism as it occurs (photograph provided by FDOT, circa 2005) .....	347
Figure 15.3. Railway embankment damage caused primarily by the coastal weir-flow damage mechanism during (Mississippi, 2005) .....	348
Figure 15.4. Pavement damage due to waves and surge in an extreme event (North Carolina SH 12, 2009; permission to use photograph provided by Dave Henderson).....	349
Figure 15.5. Two bridges destroyed by wave loads in Hurricane Katrina (Biloxi Bay, Mississippi).....	350

Figure 15.6. New, much higher, US 90 bridge across Bay St. Louis, Mississippi built after Hurricane Katrina (June 14, 2007) ..... 355

Figure 15.7. Example of coastal highway relocation in Florida (SH 399: the dashed line shows the previous highway location: permission to use image provided by the Gulf Islands National Seashore)..... 357

## List of Tables

Table 4.1 Minimum GMSLR estimates for use in planning and design as per NCHRP 15-61 (values are relative to 2000) .....	46
Table 4.2 Higher projections of GMSLR for consideration in the planning and design of high-value assets which are sensitive to SLR as per NCHRP 15-61 (See circles on upper panel of Figure 4.11, values are relative to 2000). .....	49
Table 4.3. Numerical coastal models cited in this manual .....	58
Table 5.1. Wave height statistics in irregular seas .....	91
Table 12.1. Tsunami-induced scour guidance from Dames and Moore (1980) and FEMA (2012). .....	262
Table 13.1. Probability of extreme event occurrence for various periods of time .....	279
Table 14.1. Exposure assessment steps for level of effort 1: Gulf of Mexico/South Atlantic Coast .....	295
Table 14.2. Exposure assessment steps for level of effort 2: Gulf of Mexico/South Atlantic Coast .....	298
Table 14.3. Exposure assessment steps for level of effort 3: Gulf of Mexico/South Atlantic Coast. ....	301
Table 14.4. Exposure assessment steps for level of effort 1: Mid-Atlantic/New England Coast .....	304
Table 14.5. Exposure assessment steps for level of effort 2: Mid-Atlantic/New England Coast. ....	305
Table 14.6. Exposure assessment steps for level of effort 3: Mid-Atlantic/New England Coast .....	307
Table 14.7. Exposure assessment steps for level of effort 1: Great Lakes Coast .....	308
Table 14.8. Exposure assessment steps for level of effort 2: Great Lakes Coast .....	310
Table 14.9. Exposure assessment steps for level of effort 3: Great Lakes Coast .....	312
Table 14.10. Exposure assessment steps for level of effort 1: Pacific Coast .....	314
Table 14.11. Exposure assessment steps for level of effort 2: Pacific Coast. ....	316
Table 14.12. Exposure assessment steps for level of effort 3: Pacific Coast. ....	317
Table 14.13. Exposure assessment steps for level of effort 1: tsunamis. ....	319
Table 14.14. Exposure assessment steps for level of effort 2: tsunamis .....	321
Table 14.15. Exposure assessment steps for level of effort 3: tsunamis .....	322
Table 14.16. Scenarios modeled in GC2 (modified from Choate <i>et al.</i> 2012) .....	330
Table 14.17. Validation analysis of ADCIRC model storm surge estimates .....	334

## List of Symbols

$A$	=	horizontal orbital semi-displacement
$A$	=	parameter in Dean's equilibrium profile shape
$A_h$	=	area of the projection of the bridge deck onto the vertical plane
$A_v$	=	area of the projection of the bridge deck onto the horizontal plane
$a_x$	=	horizontal component of water particle acceleration
$a_z$	=	vertical component of water particle acceleration
$C_r$	=	coefficient to account for horizontal loads due to bridge girders
$C$	=	wave celerity
$C_0$	=	wave celerity in deep water
$C_D$	=	drag coefficient
$C_g$	=	wave group velocity
$C_{gb}$	=	wave celerity at breaking
$C_h$	=	empirical coefficient for the horizontal, wave-induced loads on bridge decks
$C_M$	=	coefficient of mass or inertia
$C_r$	=	reflection coefficient
$C_v$	=	empirical coefficient for the vertical, wave-induced loads on bridge decks
$d$	=	water depth
$d_{50}$	=	median diameter of sand grains
$d_e$	=	depth of wall penetration below seabed
$d_s$	=	design flood depth
$D$	=	diameter
$D^*$	=	effective diameter of the complex pier
$D_e$	=	effective diameter of a pile group
$D_{col}^*$	=	effective diameter of the column
$D_{pc}^*$	=	effective diameter of the pile cap
$D_{pg}^*$	=	effective diameter of the pile group
$\bar{E}$	=	total energy in a wave train per unit area of sea averaged over one wavelength
$F$	=	Coriolis parameter
$F$	=	fetch length
$f_D$	=	drag force per unit length of pile in Morison's equation
$f_i$	=	inertial force per unit length of pile in Morison's equation
$f_p$	=	horizontal force per unit length of a vertical pile in Morison's equation
$(F_h)_{max}$	=	maximum of the horizontal wave-induced load
$F_s$	=	factor of safety
$(F_v)_{max}$	=	maximum of the vertical wave-induced load
$g$	=	gravitational constant having a value of 32.2 ft/s <sup>2</sup> (9.81 m/s <sup>2</sup> )
$H$	=	wave height
$H_{1\%}$	=	height exceeded by 1% of waves
$H_{10\%}$	=	height exceeded by 10% of waves
$\bar{H}_1$	=	average of the highest 1% of waves
$\bar{H}_{10}$	=	average of the highest 10% of waves
$\bar{H}_5$	=	average of the highest 5% of waves
$H_b$	=	maximum breaking wave height
$(H/d)_{max}$	=	maximum ratio of wave height to water depth
$H_i$	=	incident wave height
$H/L$	=	incident wave steepness

$H_{max}$	=	maximum wave height
$H_{m_0}$	=	spectral-based significant wave height
$H_o'$	=	unrefracted deepwater wave height
$H_r$	=	reflected wave height
$H_s$	=	significant wave height
$K$	=	an empirical coefficient in CERC equation for longshore sand transport rate
$k$	=	wave number = $2\pi/L$
$KC$	=	Keulegan-Carpenter number
$K_D$	=	empirical coefficient in Hudson's equation for revetment stone size for wave attack
$K_s$	=	shoaling coefficient
$L$	=	wavelength
$L_o$	=	deepwater wavelength
$L_p$	=	wavelength associated with the peak wave period
$n$	=	ratio of wave group velocity to wave celerity
$N$	=	the number of girders supporting the bridge span deck
$P$	=	probability
$\bar{P}$	=	wave power, wave energy flux
$P_{Is}$	=	wave energy flux factor
$Q$	=	longshore sand transport rate
$r$	=	a roughness coefficient ( $r = 0.55$ for the stone revetments)
$R$	=	roughness coefficient
$R_u$	=	vertical extent of wave runup
$R_{u,2\%}$	=	runup level exceeded by 2% of runups in an irregular sea
$S$	=	equilibrium scour depth
$S_m$	=	maximum scour depth
$S_r$	=	specific gravity of stone
$T$	=	return period of storm in years
$t$	=	time
$T$	=	wave period
$T_p$	=	wave period corresponding with the peak of the energy density spectrum
$u$	=	horizontal component of water particle velocity
$U_m$	=	maximum nearbed wave orbital velocity
$u_{rms}$	=	the root-mean-square of the horizontal nearbed wave orbital velocity
$w$	=	vertical component of water particle velocity
$W$	=	weight
$W$	=	pile group width
$W_{50}$	=	median weight of armor stone
$w_r$	=	unit weight of stone
$x$	=	horizontal position
$Y_{max}$	=	difference between the SWL elevation and wave crest elevation for the maximum wave in the design sea-state
$z$	=	vertical direction (coordinate measured from SWL)
$\alpha$	=	angle of the breaking wave crest with the shoreline
$\gamma$	=	specific weight of water
$\Delta z_h$	=	difference between the elevation of the crest of the maximum wave and the elevation of the centroid of $A_h$
$\Delta z_v$	=	difference between the elevation of the crest of the maximum wave and the elevation of the underside of the bridge deck
$\xi_{op}$	=	surf similarity parameter

$\eta$	=	water surface elevation
$\bar{\eta}$	=	water surface elevation with waves removed (used in hydrodynamic modeling)
$\eta_{\max}$	=	maximum elevation of wave crest
$\theta$	=	slope
$\lambda$	=	ripple length
$\rho$	=	density
$\sigma$	=	wave frequency = $2\pi/T$
$\varphi$	=	sediment angle of internal friction, sediment angle of repose

## Acknowledgements

The cover image is a mosaic showing (from the top):

- a coastal marsh in New York protecting a road (from Figure 13b of FHWA 2017c),
- global mean sea level rise projections for planning and design (see Figure 4.11, lower panel),
- an interstate highway bridge over coastal waters (see Figure 11.4),
- output from a numerical, hydrodynamic model of coastal storm surge in a hurricane (see Figure 4.20),
- storm waves striking a rubble-mound seawall protecting a coastal highway (see Figure 5.16), and
- the definition sketch for wave height,  $H$  (see Figure 5.1).

Unless noted otherwise, all photographs and graphics in this document were developed by the authors, who give permission for their use in this document.

In Figure 4.21, Figure 5.17, Figure 6.18, Figure 8.12, Figure 8.14, Figure 11.3, Figure 11.5, Figure 11.7, Figure 12.4, Figure 12.5, Figure 12.6, Figure 12.16, Figure 12.23, Figure 12.28, and Figure 14.15, the original maps are the copyright property of Google® Earth™ and can be accessed from <https://www.google.com/earth> (Google 2019, 2020). The authors developed the map overlays for this document.

## Notice

This document is disseminated under the sponsorship of the US Department of Transportation (USDOT) in the interest of information exchange. The US Government assumes no liability for the use of the information contained in this manual. This manual does not constitute a standard, specification, or policy.

The US Government does not endorse products or manufacturers. Trademarks or manufacturer's names appear in this manual only because the Government considers them essential to the objective of the document. The manual includes them for informational purposes only and the Government does not intend them to reflect a preference, approval, or endorsement of any one product or entity.

## Non-Binding Contents

The contents of this document do not have the force and effect of law and are not meant to bind the public in any way. This document is intended only to provide clarity to the public regarding existing requirements under the law or agency policies.

## Quality Assurance Statement

The Federal Highway Administration (FHWA) provides high-quality information to serve Government, industry, and the public in a manner that promotes public understanding. The FHWA uses standards and policies to ensure and maximize the quality, objectivity, utility, and integrity of its information. The FHWA periodically reviews quality issues and adjusts its programs and processes to ensure continuous quality improvement.

## Supporting Purpose

The FHWA developed this manual, in part, to support 23 U.S.C. § 503(b)(3)(B)(viii), that directs the Department of Transportation to "... carry out research and development activities ... to study the vulnerabilities of the transportation system to ... extreme events and methods to reduce those vulnerabilities" and the July 27, 2017 US Senate Report 115-138 for the "Transportation, and Housing and Urban Development, and Related Agencies Appropriations Bill, 2018" that directed FHWA to "... expand its technical assistance ... to help coastal States, MPOs, and cities to revise their practices in all phases of transportation planning and asset management, project planning and development, and operations with the goal of improving the resiliency of our coastal highways and reducing the life-cycle costs for these natural disaster-prone roadways."

## Glossary

**0.2-PERCENT-ANNUAL-CHANCE FLOOD:** The flood that has a 0.2-percent chance of being equaled or exceeded in any given year. See 500-year flood.

**1-PERCENT-ANNUAL-CHANCE FLOOD:** The flood that has a 1-percent chance of being equaled or exceeded in any given year. See 100-year flood.

**2-PERCENT-ANNUAL-CHANCE FLOOD:** The flood that has a 2-percent chance of being equaled or exceeded in any given year. See 50-year flood.

**10-PERCENT-ANNUAL-CHANCE FLOOD:** The flood that has a 10-percent chance of being equaled or exceeded in any given year. See 10-year flood.

**10-YEAR FLOOD:** Flood level which will recur on average once every 10 years. See 10-Percent-Annual-Chance Flood.

**50-YEAR FLOOD:** Flood level which will recur on average once every 50 years. See 2-Percent-Annual-Chance Flood.

**100-YEAR FLOOD:** Flood level which will recur on average once every 100 years. See 1-Percent-Annual-Chance Flood.

**500-YEAR FLOOD:** Flood level which will recur on average once every 500 years. See 0.2-Percent-Annual-Chance Flood.

**ACCRETION:** The extension of a beach out into the water by deposition of sand. Accretion is often used to refer to a net seaward movement of the shoreline over a specified time.

**ADAPTATION** – Adjustment in natural or human systems in anticipation of or response to a changing environment in a way that effectively uses beneficial opportunities or reduces negative effects.

**ADAPTIVE CAPACITY:** The degree to which the system containing the asset (road, bridge, etc.) can adjust or mitigate the potential for damage or service interruption by the hazards.

**ALONGSHORE:** Parallel to and near the shoreline; longshore.

**ARMOR LAYER:** Protective layer on the outside or top of a revetment or seawall composed of armor units.

**ASTRONOMICAL TIDE:** The tidal levels and character which would result from gravitational effects, e.g. of the Earth, Sun, and Moon, without any atmospheric influences.

**ATTENUATION:** A lessening of the height or amplitude of a wave with distance.

**A-ZONE:** FEMA zones which are estimated to be subject to inundation by the 1-percent-annual-chance flood event (the 100-yr storm). In a coastal setting, A-zones landward of a V-zone are considered to be subject to storm-related waves of up to 3 feet in wave height.

**BACKSHORE:** The zone of the shore or beach lying between the foreshore and the coastline comprising the berm or berms and acted upon by waves only during severe storms, especially when combined with exceptionally high water.

**BAR:** A submerged or emerged embankment of sand, gravel, or other unconsolidated material built on the sea floor in shallow water by waves and currents.

**BARRIER ISLAND:** An unconsolidated, elongated body of sand or gravel lying above the high-tide level and separated from the mainland by a lagoon or marsh. It is commonly between two

inlets, has dunes, vegetated areas, and swampy terrains extending from the beach into the lagoon.

**BATHYMETRY:** The depths of water in oceans, seas, and lakes.

**BAY:** 1) a body of water almost completely surrounded by land but open to some tidal flow communications with the sea. 2) a recess in the shore or an inlet of a sea between two capes or headlands, not so large as a gulf but larger than a cove.

**BEACH:** The zone of unconsolidated material, typically sand, that extends landward from closure depths where sand is moved by waves to the place where there is marked change in material or physiographic form, or to the line of permanent vegetation (usually the effective limit of storm waves).

**BEACH FILL:** Sand placed on a beach; beach nourishment

**BEACH BERM:** A nearly horizontal part of the beach or backshore formed by the deposit of material by wave action. Some beaches have no berms, others have one or several.

**BEACH EROSION:** The carrying away of beach materials by wave action, tidal currents, littoral currents, or wind.

**BEACH FACE** The section of the beach normally exposed to the action of the wave uprush. The foreshore of a beach. (Not synonymous with shoreface.)

**BEACH NOURISHMENT:** The direct placement of large amounts of good quality sand on the beach to widen the beach.

**BEACH PROFILE:** A cross-section taken perpendicular to a given beach contour; the profile may include the face of a dune or sea wall; extend over the backshore, across the foreshore, and seaward underwater into the nearshore zone.

**BEACH SCARP:** An almost vertical slope along the beach caused by erosion by wave action. It may vary in height from a few cm to a meter or so, depending on wave action and the nature and composition of the beach.

**BERM:** 1) On a beach: a nearly horizontal plateau on the beach face or backshore, formed by the deposition of beach material by wave action or by means of a mechanical plant as part of a beach renourishment scheme. Some natural beaches have no berm, others have several. 2) On a structure: a nearly horizontal area, often built to support or key-in an armor layer.

**BERM BREAKWATER:** Rubble mound structure with horizontal berm of armor stones at about sea level, which can be (re)shaped by the waves.

**BLUFF:** A high, steep bank or cliff.

**BORE:** A broken wave propagating across the surf zone characterized by turbulent white water.

**BOUNDARY CONDITIONS:** Environmental conditions, e.g. water levels, waves, currents, drifts, etc. used as boundary input to numerical models.

**BREACH:** Gap in a barrier island or spit or dune caused by a storm.

**BREAKER:** A wave breaking on a shore, over a reef, etc. Breakers may be classified into four types: collapsing, plunging, spilling, and surging.

**BREAKER ZONE:** The zone within which waves approaching the coastline commence breaking caused by the reduced depths.

**BREAKING:** Reduction in wave energy and height. In the surf zone breaking is due to limited water depth.

**BREAKWATER:** A structure protecting a shore area, harbor, anchorage, or basin from waves.

**BULKHEAD:** A structure or partition to retain or prevent sliding of the land. A secondary purpose is to protect the upland against damage from wave action.

**CAUSEWAY:** A raised road across wet or marshy ground, or across water.

**CAUSTIC:** In refraction of waves, the name given to a region of crossed orthogonals and high wave convergence.

**CELERITY:** Wave speed.

**CHANNEL:** 1) A natural or artificial waterway of perceptible extent which either periodically or continuously contains moving water, or which forms a connecting link between two bodies of water. 2) The part of a body of water deep enough to be used for navigation through an area otherwise too shallow for navigation. 3) A large strait, as the English Channel. 4) The deepest part of a stream, bay, or strait through which the main volume or current of water flows.

**CHART:** A special-purpose map, esp. one designed for navigation such as a bathymetric chart.

**CLIFF:** A high, steep face of rock; a precipice.

**CNOIDAL WAVE:** A type of wave in shallow water (i.e. where the depth of water is less than 1/8 to 1/10 the wavelength).

**COASTAL AREA:** The land and sea area bordering the shoreline.

**COASTAL ENGINEERING:** The planning, design, construction and operation of infrastructure in the wave, tide and sand environment that is unique to the coast. A well-established specialty area of civil engineering that focuses on the coastal zone and coastal processes.

**COASTAL PROCESSES:** Collective term covering the action of natural forces on the shoreline and nearshore seabed.

**COASTAL ZONE:** The transition zone where the land meets water, the region that is directly influenced by marine and lacustrine hydrodynamic processes. Extends offshore to the continental shelf break and onshore to the first major change in topography above the reach of major storm waves. On barrier coasts, includes the bays and lagoons between the barrier and the mainland.

**COASTLINE:** Commonly, the line that forms the boundary between the land and the water, esp. the water of a sea or ocean.

**COBBLE:** A rock fragment between 64 and 256 mm (2 to 10 inches) in diameter, usually rounded. Also called a cobblestone.

**COLLAPSING BREAKER:** A descriptive type of wave breaking characterized by the wave peaking up as if to break and then moving rapidly onto the structure or beach face including the lower half of wave, with no air pocket but with bubbles and foam present.

**CONTINENTAL SHELF:** 1) The zone bordering a continent extending from the line of permanent immersion to the depth, usually about 100 m to 200 m (300 ft to 600 ft), where there is a marked or rather steep descent toward the great depths of the ocean. 2) The area under active littoral processes during the Holocene period. 3) The region of the oceanic bottom that extends outward from the shoreline with an average slope of less than 1:100, to a line where the gradient begins to exceed 1:40 (the continental slope).

**CONTOUR:** A line on a map or chart representing points of equal elevation with relation to a datum. Also called depth contour.

**CORIOLIS:** Force due to the Earth's rotation, capable of generating currents. It causes moving bodies to be deflected to the right in the Northern Hemisphere and to the left in the Southern Hemisphere. The "force" is proportional to the speed and latitude of the moving object. It is zero at the equator and maximum at the poles.

**CRITICAL FLOW:** The flow condition where the specific energy of flow is at a minimum and the Froude number for the flow is one; term from open-channel flow hydraulics. Related terms are sub-critical flow and super-critical flow.

**CROSS-SHORE:** Perpendicular to the shoreline.

**CURRENT:** 1) The flowing of water, 2) That portion of a stream of water which is moving with a velocity much greater than the average or in which the progress of the water is principally concentrated. 3) Ocean currents can be classified in several different ways. Some important types include the following: A) Periodic – a result of the effect of the tides; such Currents may be rotating rather than having a simple back and forth motion. The currents accompanying tides are known as tidal currents; B) Temporary - due to seasonal winds; C) Permanent or ocean - constitute a part of the general ocean circulation. The term drift current is often applied to a slow broad movement of the oceanic water; D) Nearshore - caused principally by waves breaking along a shore.

**CYCLONE:** A system of winds that rotates about a center of low atmospheric pressure. Rotation is clockwise in the Southern Hemisphere and anti-clockwise in the Northern Hemisphere. In the Indian Ocean, the term refers to the powerful storms called hurricanes in the Atlantic.

**DATUM:** Any permanent line, plane, or surface used as a reference datum to which elevations are referred.

**DEEPWATER:** Water so deep that surface waves are little affected by the ocean bottom. Generally, water deeper than one-half the surface wavelength is considered deep water.

**DENSITY:** Mass per unit of volume of a substance. For pure water, the density is 1,000 kg/m<sup>3</sup> (62.4 lb/ft<sup>3</sup>). For seawater, the density is usually more. Density increases with increasing salinity, and decreases with increasing temperature.

**DEPTH-LIMITED:** Wave height is limited by the local depth of water.

**DESIGN STORM:** A hypothetical extreme storm whose wave's coastal protection structures will often be designed to withstand. The severity of the storm (i.e. return period) is chosen in view of the acceptable level of risk of damage or failure. A design storm consists of a design wave condition, a design water level and a duration.

**DESIGN WAVE:** In the design of harbors, harbor works, etc., the type or types of waves selected as having the characteristics against which protection is desired.

**DESIGN WAVE CONDITION:** Usually an extreme wave condition with a specified return period used in the design of coastal works.

**DIFFRACTION:** The phenomenon by which energy is transmitted laterally along a wave crest. When a part of a train of waves is interrupted by a barrier, such as a breakwater, the effect of diffraction is manifested by propagation of waves into the sheltered region within the barrier's geometric shadow.

**DIURNAL:** Having a period or cycle of approximately one tidal day.

**DIURNAL INEQUALITY:** The difference in height of the two high waters or of the two low waters of each day. Also the difference in velocity between the two daily flood or ebb currents of each day.

**DIURNAL TIDE:** A tide with one high water and one low water in a tidal day.

**DOWNDRIFT:** The direction of predominant movement of littoral materials.

**DREDGING:** Excavation or displacement of the bottom or shoreline of a water body. Dredging can be accomplished with mechanical or hydraulic machines. Most is done to maintain channel depths or berths for navigational purposes; other dredging is for shellfish harvesting, for cleanup of polluted sediments, and for placement of sand on beaches.

**DRIFT:** 1) Sometimes used as a short form for littoral drift. 2) The speed at which a current runs.

**DUNES:** 1) Ridges or mounds of loose, wind-blown material, usually sand.

**DURATION:** In wave forecasting, the length of time the wind blows in nearly the same direction over the fetch (generating area).

**DYNAMIC EQUILIBRIUM:** Short term morphological changes that do not affect the morphology over a long period.

**EBB:** Period when tide level is falling; often taken to mean the ebb current which occurs during this period.

**EBB TIDAL DELTA:** The sand shoals formed at the seaward mouth of tidal inlets as a result of interaction between tidal currents and waves. Also called outer bar.

**EBB TIDE:** The period of tide between high water and the succeeding low water; a falling tide.

**EL NIÑO:** A large scale weakening of the trade winds and warming of the surface layers in the eastern and central equatorial Pacific Ocean. El Niño events occur irregularly at intervals of 2-7 years, although the average is about once every 3-4 years. They typically last 12-18 months, and are accompanied by swings in the Southern Oscillation (SO), an interannual see-saw in tropical sea level pressure between the eastern and western hemispheres. During El Niño, unusually high atmospheric sea level pressures develop in the western tropical Pacific and Indian Ocean regions, and unusually low sea level pressures develop in the southeastern tropical Pacific. The SO tendencies for unusually low pressures west of the date line and high pressures east of the date line have also been linked to periods of anomalously cold equatorial Pacific sea surface temperatures (SSTs) sometimes referred to as La Niña.

**EL NIÑO SOUTHERN OSCILLATION (ENSO):** The atmospheric component of El Niño. See definition of El Niño.

**EMBAYMENT:** An indentation in the shoreline forming an open bay.

**EPOCH:** An extended period time with some consistent characteristic. A tidal epoch is about 19 years (18.6). A geological epoch, a subdivision of a period, can be many thousands of years

**EROSION:** The wearing away of land by the action of natural forces. On a beach, the carrying away of beach material by wave action, tidal currents, littoral currents, or by deflation.

**ESTUARY:** 1) The region near a river mouth in which the fresh water of the river mixes with the salt water of the sea and which received both fluvial and littoral sediment influx. 2) The part of a river that is affected by tides.

**EUSTATIC SEA LEVEL RISE:** Change in sea level due to change in the volume of the world's ocean basins and the total amount of ocean water. Vertical Land Movement (VLM) is not included. See Global Mean Sea Level Rise.

**EXPOSURE:** The degree to which a transportation asset (road, bridge, etc.) experiences a hazard.

**EXTRATROPICAL:** A term used in advisories and tropical summaries to indicate that a cyclone has lost its "tropical" characteristics. The term implies both poleward displacement of the cyclone and the conversion of the cyclone's primary energy source from the release of latent heat of condensation to baroclinic (the temperature contrast between warm and cold air masses) processes. It is important to note that cyclones can become extratropical and still retain winds of hurricane or tropical storm force.

**EXTREME EVENT:** Severe, rarely occurring event that usually causes damage, destruction or severe economic losses. Such events may include unseasonable weather, heavy precipitation, a storm surge, flooding, drought, windstorms (including hurricanes, tornadoes, and associated storm surges), extreme heat, extreme cold, earthquakes and tsunamis.

**FEMA 540 RULE:** Guidance FEMA uses to determine if a sand dune is large enough to survive a 100-year storm. If the cross-sectional area of the dune above the storm SWL surge level is greater than 540 square feet, the dune is assumed to be large enough to survive.

**FETCH:** The distance or area in which wind blows across the water forming waves. Sometimes used synonymously with fetch length and generating area.

**FETCH-LIMITED:** Situation in which wave energy (or wave height) is limited by the size of the wave generation area (fetch).

**FINITE-DIFFERENCE:** A general type of numerical method for approximating the solutions to boundary value problems with differential equations using finite-difference equations, algebraic equations across small distances, to approximate derivatives.

**FINITE ELEMENT:** a general type of numerical method for finding approximate solutions to boundary value problems of differential equations which discretizes the area, or domain, of interest into small, variable-sized, usually triangular, mesh elements.

**FLOOD:** A general and temporary condition of partial or complete inundation of normally dry land areas from 1) the overflow of inland or tidal waters or 2) the unusual and rapid accumulation or runoff of surface waters from any source.

**FLOOD CURRENT:** The tidal current toward shore or up a tidal stream. Usually associated with the increase in the height of the tide.

**FLOOD TIDAL DELTA:** The shoal of sand formed at the landward mouth of tidal inlets as a result of flow expansion.

**FLOOD TIDE:** The period of tide between low water and the succeeding high water; a rising tide; an incoming tide.

**FORESHORE:** The part of the shore, lying between the crest of the seaward berm (or upper limit of wave wash at high tide) and the ordinary low-water mark, that is ordinarily traversed by the uprush and backrush of the waves as the tides rise and fall.

**FREEBOARD:** 1) The vertical distance between the water level and the top of a coastal levee or dike. 2) The distance from the waterline to the low-chord of the bottom of a suspended deck such as a bridge deck or offshore platform. 3) The distance from the crest of the design wave to the low-chord of the bottom of a suspended deck such as a bridge deck or offshore platform.

**FROUDE NUMBER:** The dimensionless ratio of the inertial force to the force of gravity for a given fluid flow situation. It may be given as  $Fr = V/Lg$  where  $V$  is a characteristic velocity,  $L$  is a characteristic length, and  $g$  the acceleration of gravity - or as the square root of this number.

**FULLY-ARISEN SEA:** The waves that form when wind blows for a sufficient period of time across water. The waves of a fully developed sea have the maximum height possible for a given wind speed, fetch and duration of wind.

**GABION:** 1) Steel wire-mesh basket to hold stones or crushed rock to protect a bank or bottom from erosion. 2) Structures composed of masses of rocks, rubble or masonry held tightly together usually by wire mesh so as to form blocks or walls. Sometimes used on heavy erosion areas to retard wave action or as a foundation for breakwaters or jetties.

**GEOMORPHOLOGY:** 1) That branch of physical geography which deals with the form of the Earth, the general configuration of its surface, the distribution of the land, water, etc. 2) The investigation of the history of geologic changes through the interpretation of topographic forms.

**GEOTEXTILE:** A synthetic fabric which may be woven or non-woven used as a filter.

**GLACIER:** A large body of ice moving slowly down a slope of valley or spreading outward on a land surface (e.g. Greenland, Antarctica) and surviving from year to year.

**GLOBAL MEAN SEA LEVEL RISE:** The sea level rise averaged across the world's oceans. This is the average change in sea level due to a change in the volume of the world's ocean basins and the total amount of ocean water. Vertical land movement (VLM) is not included. See Eustatic Sea Level Change.

**GLOBAL POSITIONING SYSTEM:** Commonly called GPS. A navigational and positioning system by which the location of a position on or above the Earth can be determined by a special receiver at that point interpreting signals received simultaneously from several of a constellation of special satellites.

**GORGE:** 1) The deepest portion of an inlet, the throat. 2) A narrow, deep valley with nearly vertical rock walls.

**GRAVITY WAVE:** A wave whose velocity of propagation is controlled primarily by gravity because gravity is the restoring force. Most waves of importance in coastal engineering are gravity waves. Water waves more than 5 cm long are considered gravity waves. Waves longer than 2.5 cm and shorter than 5 cm are in an indeterminate zone between capillary and gravity waves.

**GRID POINT:** Location specified in the domain of a numerical model solution.

**GROIN:** Narrow, roughly shore-normal structure built to reduce longshore currents, and/or to trap and retain littoral material. Most groins are of timber or rock and extend from a seawall, or the backshore, well onto the foreshore and rarely even further offshore.

**GULF:** 1) A relatively large portion of the ocean or sea extending far into land; the largest of various forms of inlets of the sea. 2) The Gulf of Mexico.

**HEADLAND:** A promontory extending out into a body of water

**HEADLAND BREAKWATER:** A rock breakwater constructed to function as a headland by retaining an adjacent sandy pocket beach.

**HIGH TIDE:** The maximum elevation reached by each rising tide.

**HIGH WATER:** Maximum height reached by a rising tide. The height may be solely due to the periodic tidal forces or it may have superimposed upon it the effects of prevailing meteorological conditions. Nontechnically, also called the high tide.

**HIGHER HIGH WATER:** The higher of the two high waters of any tidal day. The single high water occurring daily during periods when the tide is diurnal is considered to be a higher high water.

**HINDCAST:** Application of a numerical model to simulate a past event. Often used in model validation to see how well the output matches known events.

**HOLOCENE:** An epoch of the quaternary period, from the end of the Pleistocene, about 12,000 to 20,000 years ago, to the present time. This is the geologic time period of the most recent rise in eustatic sea level.

**HURRICANE:** An intense tropical cyclone in which winds tend to spiral inward toward a core of low pressure, with maximum surface wind velocities that equal or exceed 33.5 m/sec (75 mph or 65 knots) for several minutes or longer at some points. Tropical storm is the term applied if maximum winds are less than 33.5 m/sec but greater than a whole gale (63 mph or 55 knots). Term is used in the Atlantic, Gulf of Mexico, and eastern Pacific.

**HYDRODYNAMIC:** Having to do with the science of moving water.

**HYDROGRAPH:** 1) a graph of the variation of SWL with time. 2) a graph of discharge with time.

**ICE AGE:** A loosely-used synonym of glacial epoch, or time of extensive glacial activity; specifically, of the latest period of widespread continental glaciers, the Pleistocene Epoch.

**INLET:** 1) A short, narrow waterway connecting a bay, lagoon, or similar body of water with a large parent body of water. 2) An arm of the sea (or other body of water) that is long compared to its width and may extend a considerable distance inland.

**IRREGULAR WAVES:** Waves with random wave periods (and in practice, also heights), which are typical for natural wind-induced waves.

**JETTY:** 1) (US coastal engineering usage) On open seacoasts, a structure extending into a body of water, which is designed to prevent shoaling of a channel by littoral materials and to direct and confine the stream or tidal flow. Jetties are built at the mouths of rivers or tidal inlets to help deepen and stabilize a channel. 2) (British usage) Wharf or pier.

**KEY:** Also "cay," one of the low, insular banks of sand, coral, and limestone off the southern coast of Florida or in the Caribbean Sea

**KINETIC ENERGY (OF WAVES):** In a progressive oscillatory wave, a summation of the energy of motion of the particles within the wave.

**KING TIDE:** Non-technical term for an extremely high tide level due to regular astronomical (interactions of the moon/earth/sun system) fluctuations. Photos of these high tide levels have been used to help visualize and understand the impacts of sea level rise along the Pacific coast.

**KNOT:** The unit of speed used in navigation equal to 1 nautical mile (6,076.115 ft or 1,852 m) per hour.

**LA NINA:** Is characterized by periods of below-average sea surface temperatures across the east-central Equatorial Pacific. Global La Niña impacts tend to be opposite those of El Niño impacts. In the tropics, ocean temperature variations in La Niña also tend to be opposite those of El Niño. During a La Niña year, winter temperatures are warmer than normal in the Southeast and cooler than normal in the Northwest.

**LAGOON:** A shallow body of water, like a pond or sound, partly or completely separated from the sea by a barrier island or reef. Sometimes connected to the sea via an inlet.

**LIFE CYCLE COST ANALYSIS:** An engineering economic analysis that allows officials to quantify the differential costs of alternative investment options for a given project.

**LITTORAL:** Of or pertaining to a shore, especially of the sea.

**LITTORAL ZONE:** In beach terminology, an indefinite zone extending seaward from the shoreline to just beyond the breaker zone. The zone of wave-induced sand movement.

**LONGSHORE:** Parallel to and near the shoreline; alongshore.

**LONGSHORE BAR:** A sand ridge or ridges, running roughly parallel to the shoreline and extending along the shore outside the trough, that may be exposed at low tide or may occur below the water level in the offshore.

**LONGSHORE CURRENT:** The littoral current in the breaker zone moving essentially parallel to the shore, usually generated by waves breaking at an angle to the shoreline.

**LONGSHORE SAND TRANSPORT:** Littoral drift; the movement of sand down the beach driven by breaking waves and longshore current.

**LOW TIDE:** The minimum elevation reached by each falling tide.

**LOW WATER:** The minimum height reached by each falling tide. Nontechnically, also called low tide.

**LOWER LOW WATER:** The lower of the two low waters of any tidal day. The single low water occurring daily during periods when the tide is diurnal is considered to be a lower low water.

**MARSH:** 1) A tract of soft, wet land, usually vegetated by reeds, grasses and occasionally small shrubs. 2) Soft, wet area periodically or continuously flooded to a shallow depth, usually characterized by a particular subclass of grasses, cattails and other low plants.

**MEAN HIGH WATER:** The average height of the high waters over a 19-year tidal epoch. For shorter periods of observations, corrections are applied to eliminate known variations and reduce the results to the equivalent of a mean 19-year value. All high water heights are included in the average where the type of tide is either semidiurnal or mixed. Only the higher high water heights are included in the average where the type of tide is diurnal. So determined, mean high water in the latter case is the same as mean higher high water.

**MEAN HIGHER HIGH WATER:** The average height of the higher high waters over a 19-year period. For shorter periods of observation, corrections are applied to eliminate known variations and reduce the result to the equivalent of a mean 19-year value.

**MEAN LOW WATER:** The average height of the low waters over a 19-year period. For shorter periods of observations, corrections are applied to eliminate known variations and reduce the results to the equivalent of a mean 19-year value. All low water heights are included in the average where the type of tide is either semidiurnal or mixed. Only lower low water heights are included in the average where the type of tide is diurnal. So determined, mean low water in the latter case is the same as mean lower low water.

**MEAN LOWER LOW WATER:** The average height of the lower low waters over a 19-year period. For shorter periods of observations, corrections are applied to eliminate known variations and reduce the results to the equivalent of a mean 19-year value. Frequently abbreviated to lower low water.

**MEAN SEA LEVEL:** The average height of the surface of the sea for all stages of the tide over a 19-year period, usually determined from hourly height readings.

**METEOTSUNAMI:** Long-wave motions principally caused by meteorologically-induced disturbances, including those associated with pressure jumps, frontal passages, and squalls.

**MIXED TIDE:** A type of tide in which the presence of a diurnal wave is conspicuous by a large inequality in either the high or low water heights, with two high waters and two low waters usually occurring each tidal day. In strictness, all tides are mixed, but the name is usually applied without

definite limits to the tide intermediate to those predominantly semidiurnal and those predominantly diurnal.

**MONOCHROMATIC WAVES:** A series of waves generated in a laboratory, each of which has the same length and period.

**MONTE CARLO:** A class of computational algorithms that use repeated random sampling to obtain risk estimates.

**MORPHOLOGY:** The form and structure, and the changes of form and structure of the earth's surface. Same as geomorphology.

**NATURE-BASED SOLUTIONS:** Options which mimic characteristics of natural features, but are created by human design, engineering, and construction. They include a spectrum of natural and nature-based features that serve as alternatives to or enhancements of traditional shoreline stabilization and infrastructure protection techniques.

**NEAP TIDE:** Tide of decreased range occurring semimonthly as the result of the moon being in quadrature. The neap range of the tide is the average semidiurnal range occurring at the time of neap tides and is most conveniently computed from the harmonic constants. The neap range is typically 10 to 30 percent smaller than the mean range where the type of tide is either semidiurnal or mixed. Where the type of tide is diurnal, the term is commonly used to refer to the portion of the lunar month with reduced tide range.

**NEARSHORE:** 1) In beach terminology, an indefinite zone extending seaward from the shoreline well beyond the breaker zone. 2) The zone which extends from the swash zone to the position marking the start of the offshore zone, typically at water depths of the order of 50 ft.

**NEARSHORE CURRENT:** A current in the nearshore zone.

**NONLINEAR:** Occurring as a result of a mathematical operation that is not linear.

**NOR'EASTER or NORTHEASTER:** Common storm type in the North Atlantic Ocean which produces northeast winds along the US Atlantic seaboard.

**NUMERICAL MODELING:** The analysis of natural processes including storm surge, tidal circulation, and wave generation using computational methods with computers.

**OCEANOGRAPHY:** The study of the sea, embracing and indicating all knowledge pertaining to the sea's physical boundaries, the chemistry and physics of seawater, marine biology, and marine geology.

**OFFSHORE:** 1) In beach terminology, the comparatively flat zone of variable width, extending from the shoreface to the edge of the continental shelf. It is continually submerged. 2) The direction seaward from the shore. 3) The zone beyond the nearshore zone where sediment motion induced by waves alone effectively ceases and where the influence of the sea bed on wave action is small in comparison with the effect of wind. 4) The breaker zone directly seaward of the low tide line.

**ONSHORE:** A direction landward from the sea.

**ORBITAL VELOCITY:** The flow of water accompanying the orbital movement, the back and forth movement, of the water particles in a wave. Not to be confused with wave-generated littoral currents.

**OSCILLATORY WAVE:** A wave in which each individual particle oscillates about a point with little or no permanent change in mean position. The term is commonly applied to progressive oscillatory waves in which only the form advances, the individual particles moving in closed or nearly closed orbits.

**OUTCROPPING:** A surface exposure of bare rock in the sea not covered by soil or vegetation.

**OVERTOPPING:** Passing of water over the top of a structure as a result of wave runup or surge action.

**OVERWASH:** 1) The part of the uprush that runs over the crest of a berm or structure or barrier island and does not flow directly back to the ocean or lake. 2) The effect of waves overtopping a coastal defense, often carrying sediment landwards which is then lost to the beach system.

**PACIFIC DECADEAL OSCILLATION:** A long-lived El Niño-like pattern of Pacific weather variability.

**PARTICLE VELOCITY:** The velocity induced by wave motion with which a specific water particle moves within a wave.

**PASS:** In hydrographic usage, a navigable channel through a bar, reef, or shoal, or between closely adjacent islands. On the Gulf of Mexico Coast, inlets are often known as passes.

**PEAK WAVE PERIOD:** The wave period determined by the inverse of the frequency at which the wave energy spectrum reaches its maximum. Most of the energy in an irregular sea state is at this wave period.

**PEBBLES:** Beach material usually well-rounded and between about 4 mm to 64 mm (1/8 in to 2 in) diameter.

**PENINSULA:** An elongated body of land nearly surrounded by water and connected to a larger body of land by a neck or isthmus.

**PHASE:** In surface wave motion, a point in the period to which the wave motion has advanced with respect to a given initial reference point, e.g. the crest of the wave is a phase of the wave.

**PHYSICAL MODELING:** Refers to the investigation of coastal or hydraulic processes using a scaled model.

**PIER:** A structure, usually of open construction, extending out into the water from the shore, to serve as a landing place, recreational facility, etc., rather than to afford coastal protection. In the Great Lakes, a term sometimes applied to jetties.

**PILE:** A long, heavy timber or section of concrete or metal that is driven or jetted into the earth or seabed to serve as a support or protection.

**PINEAPPLE EXPRESS:** A weather system characterized by a jet stream dip into the vicinity of Hawaii (thus the "pineapple") which carries a moisture-laden storm system to Washington, Oregon, or California. Unlike tropical events, these winter storms do not behave as cyclonic systems; instead they are characterized by high winds that drive waves onto coastal areas.

**PLEISTOCENE:** An epoch of the Quaternary Period characterized by several glacial ages.

**PLUNGING BREAKER:** A descriptive type of wave breaking characterized by the crest of the wave curling over an air pocket and forming a tube of air under a jet, or "lip," of water which falls, or "plunges," down on the face of the wave. This type of breaking can create extreme turbulent eddies at that location.

**POCKET BEACH:** A beach, usually small and curved, in a coastal embayment between two headland littoral barriers.

**POTENTIAL ENERGY OF WAVES:** In a progressive oscillatory wave, the energy resulting from the elevation or depression of the water surface from the undisturbed level.

**PROTOTYPE:** In laboratory usage, the full-scale structure, concept, or phenomenon used as a basis for constructing a scale model or copy.

**QUATERNARY PERIOD:** The most recent, current, period in the geologic time scale.

**RANDOM WAVES:** The irregular, non-monochromatic, sea states that occur in nature.

**RAYLEIGH DISTRIBUTION:** A model probability distribution, commonly used in analysis of waves because individual wave heights in naturally occurring, irregular, sea fits this distribution.

**RECESSION:** Landward movement of the shoreline. A net landward movement of the shoreline over a specified time.

**REEF:** Offshore consolidated rock. Often refers to coral fringing reefs in tropical waters.

**REFLECTED WAVE:** That part of an incident wave that is returned seaward when a wave impinges on a steep beach, barrier, or other reflecting surface.

**REFLECTION:** The process by which the energy of the wave is returned seaward.

**REFRACTION:** The process by which the direction of a wave moving in shallow water at an angle to the contours is changed: the part of the wave advancing in shallower water moves more slowly than that part still advancing in deeper water, causing the wave crest to bend toward alignment with the underwater contours.

**REFRACTION COEFFICIENT:** The ratio of the refracted wave height at any point to the deepwater wave height.

**REFRACTION DIAGRAM:** A drawing showing positions of wave crests and/or orthogonals in a given area for a specific deepwater wave period and direction.

**REGULAR WAVES:** Waves with a consistent height, period, and direction; monochromatic waves.

**RELATIVE SEA LEVEL RISE:** Sea level change at a coastal location relative to the land. This includes both the eustatic sea level rise component and the vertical land movement (VLM) component. This is the sea level change measured by long-term tide gages.

**RETURN PERIOD:** Average period of time between occurrences of a given event.

**REVTMENT:** A layer or layers of stone, concrete, etc., to protect an embankment, or shore structure, against erosion by wave action or currents.

**RIP CURRENT:** A strong surface current flowing seaward from the shore that is part of a nearshore circulation cell driven by incident wave energy. A rip current is often miscalled a rip tide.

**RIPRAP:** A protective layer or facing of quarrystone, usually well graded within a wide size limit, randomly placed to prevent erosion, scour, or sloughing of an embankment or bluff; also the stone so used.

**RISK:** Chance or probability of failure due to all possible environmental inputs and all possible mechanisms. The concept of flood risk typically captures both the probability of the flood event and the consequences of the flood event.

**ROCK:** An aggregate of one or more minerals.

**RUBBLE:** Rough, irregular fragments of broken rock.

**RUBBLE-MOUND STRUCTURE:** A mound of random-shaped and random-placed stones protected with a cover layer of selected stones.

**RUNUP:** The upper level reached by a wave on a beach or coastal structure, relative to still water level.

**SAFFIR-SIMPSON HURRICANE WIND SCALE:** A 1 to 5 rating based on a hurricane's sustained wind speed. Named for the originators of the scale.

**SALIENT:** Coastal formation of beach material developed by wave refraction and diffraction and littoral drift comprising of a bulge in the coastline towards an offshore island or breakwater, but not connected to it as in the case of a tombolo.

**SALINITY:** Number of grams of salt per thousand grams of sea water, usually expressed in parts per thousand.

**SAND:** Sediment particles, often largely composed of quartz, with a diameter of between 0.0024 inches and 0.079 inches (0.062 mm and 2 mm), generally classified as fine, medium, coarse or very coarse. Beach sand may sometimes be composed of organic sediments such as calcareous reef debris or shell fragments.

**SAND BAR:** A submerged or emerged embankment of sand built on the sea floor in shallow water by waves and currents.

**SAND BYPASSING:** Hydraulic or mechanical movement of sand from the accreting updrift side to the eroding downdrift side of an inlet or harbor entrance. The hydraulic movement may include natural movement as well as movement by man (which is sometimes referred to as artificial sand bypassing).

**SAND DUNE:** A hill formed of sand through wind-blown processes landward of the active beach and berm.

**SAND SPIT:** A narrow sand embankment, created by an excess of deposition at its seaward terminus, with its distal end (the end away from the point of origin) terminating in open water.

**SCOUR:** Removal of underwater material by waves and currents, especially at the base or toe of a structure.

**SCOUR PROTECTION:** Protection against erosion of the seabed.

**SEA:** 1) Waves caused by wind at the place and time of observation. 2) State of the ocean or lake surface, in regard to waves.

**SEA CLIFF:** A cliff situated at the seaward edge of the coast.

**SEA LEVEL RISE:** The long-term upward trend in mean sea level.

**SEA STATE:** Description of the sea surface with regard to wave action.

**SEAS:** Waves caused by wind at the place and time of observation.

**SEAWALL:** A structure, often concrete or stone, built along a portion of a coast to prevent erosion and other damage by wave action. Often it retains earth against its shoreward face. A seawall is typically more massive and capable of resisting greater wave forces than a bulkhead.

**SEDIMENT:** 1) Loose, fragments of rocks, minerals or organic material which are transported from their source for varying distances and deposited by air, wind, ice and water. Other sediments are precipitated from the overlying water or form chemically, in place. Sediment includes all the unconsolidated materials on the sea floor. 2) The fine-grained material deposited by water or wind.

**SEDIMENT TRANSPORT:** The main agencies by which sedimentary materials are moved are: gravity (gravity transport); running water (rivers and streams); ice (glaciers); wind; the sea (currents and littoral drift).

**SEICHING:** Wave oscillation of an enclosed or semi enclosed waterbody that continues, pendulum fashion, after the cessation of the originating force, which may have been seismic, atmospheric, or vessel-generated.

**SEMIDIURNAL:** Having a period or cycle of approximately one-half of a tidal day (12.4 hours). The predominating type of tide throughout the world is semidiurnal, with two high waters and two low waters each tidal day. The tidal current is said to be semidiurnal when there are two flood and two ebb periods each day.

**SENSITIVITY:** The degree to which an asset (road, bridge, etc.) is damaged or service is interrupted by the hazards.

**SHALLOW WATER:** 1) Commonly, water of such a depth that surface waves are noticeably affected by bottom topography. 2) More strictly, in hydrodynamics with regard to progressive gravity waves, water in which the depth is less than 1/25 the wavelength.

**SHALLOW WATER WAVE:** A progressive wave which is in water less than 1/25 the wave length in depth.

**SHINGLE:** flat or flattish pebbles common on some beaches.

**SHOAL:** 1) (noun) A detached area of any material like a sand deposit: The depths over it are a danger to surface navigation. 2) (verb) To become shallow gradually. 3) To cause to become shallow. 4) To proceed from a greater to a lesser depth of water.

**SHOALING:** Decrease in water depth. The transformation of wave profile as they propagate toward shore.

**SHOALING COEFFICIENT:** The ratio of the height of a wave in water of any depth to its height in deep water with the effects of refraction, friction, and percolation eliminated.

**SHORE:** The narrow strip of land in immediate contact with the sea, including the zone between high and low water lines. A shore of unconsolidated material is usually called a beach. Also used in a general sense to mean the coastal area (e.g. to live at the shore).

**SHOREFACE:** The narrow zone seaward from the low tide shoreline, covered by water, over which the beach sands and gravels actively oscillate with changing wave conditions.

**SHORELINE:** The intersection of a specified plane of water with the shore or beach (e.g. the high water shoreline would be the intersection of the plane of mean high water with the shore or beach). The line delineating the shoreline on National Ocean Service nautical charts and surveys approximates the mean high water line.

**SIGNIFICANT WAVE HEIGHT:** The primary measure of energy in a sea state. that is calculated either as the average height of the one-third highest waves or via energy density spectral analysis methods.

**SOLITARY WAVE:** A wave consisting of a single elevation (above the original water surface), whose height is not necessarily small compared to the depth, and neither followed nor preceded by another elevation or depression of the water surfaces.

**SORTING:** Process of selection and separation of sediment grains according to their grain size (or grain shape or specific gravity).

**SPILLING BREAKER:** A descriptive type of wave breaking characterized by the presence of air bubbles and turbulent white-water falling, or "spilling," down front face of the wave. Breaking generally occurs relatively slowly over a distance across the surf zone.

**SPIT:** A small point of land or a narrow shoal projecting into a body of water from the shore.

**SPRING TIDE:** A tide that occurs at or near the time of new or full moon (syzygy) and which rises highest and falls lowest from the mean sea level.

**STACK:** An isolated, pillar-like rocky island isolated from a nearby headland by wave erosion; a needle or chimney rock.

**STILLWATER LEVEL:** Commonly abbreviated to SWL. The surface of the water if all wave and wind action were to cease.

**STONE:** Quarried or artificially-broken rock for use in construction.

**STORM SURGE:** A rise in average (typically over several minutes) water level above the normal astronomical tide level due to the action of a storm. Storm surge results from wind stress, atmospheric pressure reduction, and wave setup.

**STORM SURGE HYDROGRAPH:** Graph of the variation in the rise in SWL with time due to a storm.

**SUBSIDENCE:** Sinking or downwarping of a part of the earth's surface.

**SURF:** 1) Collective term for breakers. 2) The wave activity in the area between the shoreline and the outermost limit of breakers. 3) In literature, the term surf usually refers to the breaking waves on shore and on reefs when accompanied by a roaring noise caused by the larger waves breaking. 4) the recreational riding of waves.

**SURF ZONE:** The zone of wave action extending from the water line (which varies with tide, surge, set-up, etc.) out to the most seaward point of the zone (breaker zone) at which waves approaching the coastline commence breaking.

**SURGING BREAKER:** A descriptive type of wave breaking characterized by the wave peaking up as if to break, but bottom rushes forward from under wave, and wave slides up beach or structure face with little or no bubble production.

**SWASH:** The rush of water up onto the beach face following the breaking of a wave.

**SWASH ZONE:** The zone of wave action on the beach, which moves as water levels vary, extending from the limit of run-down to the limit of runup.

**SWELL:** Wind-generated waves that have traveled out of their generating area. Swell characteristically exhibits a more regular and longer period and has flatter crests than waves within their generating fetch (seas).

**T-HEAD GROIN:** A groin built in the general shape of a letter "T" with the trunk section connected to land.

**TECTONICS:** Forces generated from within the earth that result in uplift, movement, or deformation of part of the earth's crust.

**TIDAL CURRENT:** The alternating horizontal movement of water associated with the rise and fall of the tide caused by the astronomical tide-producing forces.

**TIDAL EPOCH:** An 18.6-year time period used to calculate sea levels.

**TIDALLY-INFLUENCED:** A river location where the discharge and stage are modulated by the astronomical tides but where the flow does not reverse under normal tidal conditions.

**TIDAL INLET:** 1) An inlet maintained by tidal flow. 2) Loosely, any inlet in which the tide ebbs and flows.

**TIDAL PERIOD:** The interval of time between two consecutive, similar, phases of the tide.

**TIDAL PRISM:** 1) The total amount of water that flows into a bay or out again with movement of the tide, excluding any fresh water flow. 2) The volume of water between mean low and mean high tide.

**TIDAL RANGE:** The difference in height between consecutive high and low (or higher high and lower low) waters. The mean range is the difference between mean high water and mean low water. The great diurnal range or diurnal range is the difference in height between mean higher high water and mean lower low water. Where the type of tide is diurnal, the mean range is the same as the diurnal range.

**TIDAL SHOALS:** Sand shoals that accumulate near inlets due to the transport of sediments by tidal currents associated with the inlet.

**TIDAL WAVE:** 1) The wave motion of the tides. 2) In popular usage, any unusually high and destructive water level along a shore. It usually refers to storm surge or tsunamis.

**TIDE:** The periodic rising and falling of the water that results from gravitational attraction of the Moon and Sun and other astronomical bodies acting upon the rotating Earth. Although the accompanying horizontal movement of the water resulting from the same cause is also sometimes called the tide, it is preferable to designate the latter as tidal current, reserving the name tide for the vertical movement.

**TOE:** Lowest part of a revetment or seawall slope, generally forming the transition to the seabed.

**TOMBOLO:** A bar or spit that connects or "ties" an island to the mainland or to another island. Also applied to sand accumulation between land and a detached breakwater.

**TROPICAL STORM:** A tropical cyclone with maximum winds less than 34 m/sec (75 miles per hour). Less strength when compared with hurricane or typhoon (winds greater than 75 miles per hour).

**TROUGH:** A long and broad submarine depression with gently sloping sides. Often used to describe the deeper water between the beach face and an offshore sand bar.

**TSUNAMI:** A long-period wave caused by an underwater disturbance such as a volcanic eruption or earthquake. Commonly miscalled "tidal wave."

**UPDRIFT:** The direction opposite that of the predominant movement of littoral materials.

**VALIDATION:** The process of determining the degree to which a model is an accurate representation of the real world from the perspective of the intended uses of the model.

**VULNERABILITY:** The extent to which a transportation asset or system is susceptible to sustaining damage from hazards during extreme events. Vulnerability is a function of the extent to which an asset or system is exposed to damaging forces; its sensitivity to those forces; and its adaptive capacity.

**V-ZONE/VE-ZONE:** FEMA zones subject to inundation by the 1-percent-annual-chance flood event (the 100-yr storm) with additional hazards due to storm-induced velocity wave action (waves higher than 3 feet).

**WAVE:** A ridge, deformation, or undulation of the surface of a liquid.

**WAVE AMPLITUDE:** The magnitude of the displacement of a wave from a mean value. An ocean wave has an amplitude equal to the vertical distance from still water level to wave crest. For a sinusoidal wave, the amplitude is one-half the wave height.

**WAVE CELERITY:** The speed of individual wave propagation.

**WAVE CLIMATE:** The seasonal and annual distribution of wave height, period and direction.

**WAVE CREST:** 1) The highest part of a wave. 2) That part of the wave above still water level.

**WAVE DIRECTION:** The direction toward, or from, which a wave is moving.

**WAVE FORECASTING:** The theoretical determination of future wave characteristics, usually from observed or predicted meteorological phenomena (winds).

**WAVE FREQUENCY:** The inverse of wave period.

**WAVE GROUP:** A series of waves in which the wave direction, wavelength, and wave height vary only slightly.

**WAVE HEIGHT:** The vertical distance between a crest and the preceding trough.

**WAVE PERIOD:** The time for a wave crest to traverse a distance equal to one wavelength. The time for two successive wave crests to pass a fixed point.

**WAVE RAY:** On a wave-refraction diagram, a line drawn perpendicularly to the wave crests; also known as orthogonals.

**WAVE RUNUP:** The upper level, elevation, reached by a wave on a beach or coastal structure, relative to still water level.

**WAVE SETUP:** Superelevation of the water surface over normal surge elevation due to onshore mass transport of the water by wave action alone.

**WAVE SPECTRUM:** In ocean wave studies, a graph, table, or mathematical equation showing the distribution of wave energy as a function of wave frequency. The spectrum may be based on observations or theoretical considerations.

**WAVE STEEPNESS:** The ratio of wave height to wavelength.

**WAVE TRAIN:** A series of waves from the same direction.

**WAVE TRANSFORMATION:** Change in wave energy due to the action of physical processes.

**WAVE TROUGH:** The lowest part of a wave form between successive crests. Also that part of a wave below still water level.

**WAVE VELOCITY:** The speed at which an individual wave advances. See also wave celerity.

**WAVELENGTH:** The horizontal distance between similar points on two successive waves measured perpendicular to the crest.

**WEIR:** A low dam or wall across a stream to raise the upstream water level.

**WELL-SORTED:** Clastic sediment or rock that consists of particles all having approximately the same size. Example: sand dunes.

**WETLANDS:** Lands whose saturation with water is a dominant factor determining the nature of soil development and the types of plant and animal communities that live in the soil and on its surface (e.g. mangrove forests).

**WHITECAP:** On the crest of a wave, the white froth caused by wind-induced spilling breaking.

**WIND SEA:** Wave conditions directly attributable to recent winds, as opposed to swell.

**WIND SETUP:** On reservoirs and smaller bodies of water: 1) the vertical rise in the still water level on the leeward side of a body of water caused by wind stresses on the surface of the water; 2) the difference in still water levels on the windward and the leeward sides of a body of water caused by wind stresses on the surface of the water.

**WIND STRESS:** The way in which wind transfers energy to the sea surface.

**WIND WAVES:** 1) Waves being formed and built up by the wind. 2) Loosely, any wave generated by wind.

## List of Acronyms

AASHTO	American Association of State Highway and Transportation Officials
ABFE	Advisory Base Flood Elevation (FEMA acronym)
ACOPNE	Academy of Coastal, Ocean, Ports and Navigation Engineers
ADCIRC	ADvanced CIRCulation model
AEP	annual exceedance probability
ASCE	American Society of Civil Engineers
BFE	Base Flood Elevation (FEMA acronym)
CFD	computational fluid dynamics
CEM	Coastal Engineering Manual
CERA	Coastal Emergency Risks Assessment
CERC	Coastal Engineering Research Center
CH3D	Curvilinear Hydrodynamics Three Dimensional
CMS	Coastal Modeling System
COMCOT	Cornell Multi-grid Coupled Tsunami
CO-OPS	Center for Operational Oceanographic Products and Services
CRAB	Coastal Research Amphibious Buggy
CSSR	Climate Science Special Report
CU	US Customary Units
DCE	Diplomate of Coastal Engineering. A specialty certification by ACOPNE
DOT	Department of Transportation
EST	Empirical Simulation Technique
FDEP	Florida Department of Environmental Protection
FDOT	Florida Department of Transportation
FEMA	Federal Emergency Management Agency
FHWA	Federal Highway Administration
FIS	Flood Insurance Study (FEMA acronym)
FIRM	Flood Insurance Rate Map (FEMA acronym)
FVCOM	Finite Volume Coastal Ocean Model
GIS	geographical information system
GPS	global positioning system
GMSLR	global mean sea level rise
HEC-RAS	Hydrologic Engineering Center's River Analysis System
HICE	Highways in the Coastal Environment

HURDAT	HURricane DATabases
IPCC	Intergovernmental Panel on Climate Change
JONSWAP	Joint North Sea Wave Project
JPM	joint probability method
MassDOT	Massachusetts Department of Transportation
MEOW	maximum envelope of water
MHHW	mean higher high water
MHW	mean high water
MLLW	mean lower low water
MLW	mean low water
MOST	Method of Splitting Tsunami
MPO	metropolitan planning organization
MSL	mean sea level
NAVD 88	North American Vertical Datum of 1988
NAVFAC	Naval Facilities Engineering Command
NCA	National Climate Assessment
NCDOT	North Carolina Department of Transportation
NCEP	National Center for Environmental Prediction
NGVD 92	National Geodetic Vertical Datum of 1929
NHC	National Hurricane Center
NOAA	National Oceanic and Atmospheric Administration
NOS	National Ocean Service.
NRC	National Research Council
NTHMP	National Tsunami Hazard Mitigation Program
NTR	non-tidal residual
RCP	representative concentration pathway
REF/DIF	REFraction/DIFfraction model
Risk MAP	Risk Management, Assessment, and Planning
ROW	right of way
RSLR	relative sea level rise
SH	State Highway
SI	International System of Units
SDOT	State Departments of Transportation
SLOSH	Sea, Lake, and Overland Surges from Hurricanes

SLR	sea level rise
SMB	Sverdrup, Munk and Bretschneider
SPM	Shore Protection Manual
SRH-2D	Sedimentation and River Hydraulics - Two-Dimensional
SSIM	Storm Surge Inundation Map (FEMA acronym)
STWAVE	Steady State Spectral Wave
SWAN	Simulating WAVes Nearshore
SWL	still water level
TAMU	Texas A&M University
TxDOT	Texas Department of Transportation
US	United States
USA	University of South Alabama
USACE	US Army Corps of Engineers
USC&GS	US Coast and Geodetic Survey
USEPA	US Environmental Protection Agency
USGS	US Geological Survey
USDOT	US Department of Transportation
VLM	vertical land movement
WAM	Wave Analysis Model
WIS	Wave Information Study

## **Part 1 – Background & Context**

*Page Intentionally Left Blank*

## Chapter 1 - Introduction

Two of the United States' (US) most storied love affairs are with the coast and with roads. Where these two intersect, coastal highways, there is a need for wise engineering planning and design. Americans began migrating to the coast decades ago and sea levels are rising. Thus, coastal highways are experiencing both increasing societal pressures and increasing physical stresses.

Coastal roads and bridges are exposed to unique extreme events and are in unique ecosystems. The Federal Highway Administration (FHWA) has developed this manual, HEC-25: Highways in the Coastal Environment (HICE), to assist the transportation professional working in the coastal environment.



Figure 1.1. A US coastal highway (Florida SH A1A in Ft. Lauderdale 2018)

This introductory chapter describes the purpose and scope, organization, target audience, and the units of this manual on highways in the coastal environment.

### **1.1 Purpose and Scope**

This 3<sup>rd</sup> edition of HEC-25: Highways in the Coastal Environment creates one comprehensive document including the latest research for the analysis, planning, design and operation of these highways. The focus is on roads and bridges (highways) near the coast that are always, or occasionally during storms, influenced by coastal tides and waves.

The 1<sup>st</sup> edition of HEC-25 summarized a pooled-fund study of the hydraulics of coastal bridge scour. The 2<sup>nd</sup> edition of HEC-25 was a much more comprehensive discussion of issues with HICE (Douglass and Krolak 2008). A supplemental edition, HEC-25: Volume 2, was released in 2014 with methods for assessing the vulnerability of HICE to extreme events (Douglass *et al.* 2014). This 3<sup>rd</sup> edition combines the material in those two latter HICE documents.

This new edition also includes:

- improvements in our understanding of the relevant coastal sciences,
- improvements in accepted, related coastal engineering practice tools,
- updated analysis on sea level rise projections and how to incorporate these projections in highway engineering planning and design (Section 4.1),
- new information on increased flooding due to sea level rise (Chapter 9),
- a revision to the method for estimating wave loads on bridge decks (Section 11.4),
- new information on coastal scour (Chapter 12), and
- new information on nature-based solutions; such as restoration or construction of wetlands, beaches, dunes, and reefs; that reduce coastal damage as an alternative to, or in conjunction with, more traditional engineering approaches. This new material draws from FHWA's "Nature-based Solutions for Coastal Highways Resilience: An Implementation Guide" (Webb, *et al.* 2019) (Chapter 8)).

This edition of HEC-25 supersedes the previous editions. This edition provides the best available and actionable engineering and science on coastal resilience within a framework that is adaptable to future improvements. The pace of research and application in some of these areas (e.g. sea level rise projections and response) will rapidly evolve. This document is intended as a reference document for the FHWA, State Departments of Transportation (SDOT), the American Association of State Highway and Transportation Officials (AASHTO), consultants to these organizations, and others.

This document focuses on tools directly applicable to coastal highways and does not address other aspects of coastal engineering more closely related to the maritime industry. For information on assessing the vulnerability of highways in the riverine environment, see HEC-17 "Highways in the River Environment," 2<sup>nd</sup> ed. (Kilgore *et al.* 2016).

## 1.2 Organization

This HICE document is organized into four major parts with 15 chapters:

**Part 1** discusses the background and context of highways in the coastal environment:

- **Chapter 1** introduces this document and explains the rationale for its necessity,
- **Chapter 2** outlines federal requirements and policies that may affect HICE, and
- **Chapter 3** very briefly introduces some of the societal and natural processes that make the planning, design and operation of HICE unique and challenging. It also includes a description and explanation of the specialty field of coastal engineering.

**Part 2** briefly summarizes some of the science that is unique to the coast and is used in engineering of HICE:

- **Chapter 4** discusses tides and water levels including tidal datums, storm surge, and sea level rise. Water level controls the location of wave attack on the shoreline. Sea level rise, which is already causing problems for HICE, is projected to increase significantly,
- **Chapter 5** discusses water waves and engineering models of water waves. Waves are often the primary hydraulic force of interest in coastal engineering and clearly have the potential to cause significant damage to HICE, and
- **Chapter 6** introduces some of the coastal sediment processes including an overview of coastal geology, coastal sediment characteristics and transport, tidal inlet dynamics, and the role of physical models in coastal engineering.

**Part 3** discusses some of the common planning and design issues for highways and bridges that are unique to the coastal environment:

- **Chapter 7** addresses one of the most common HICE issues - the design of revetments to resist wave attack. Coastal rubble-mound revetment design principles are different than those of typical rock revetments in the riverine environment,
- **Chapter 8** describes HICE threatened by shoreline recession; providing examples on how the HICE community has evaluated such issues and have developed a spectrum of mitigation plans and options ranging from walls to nature-based solutions like beaches and marshes,
- **Chapter 9** describes more frequent and more extensive flooding of coastal areas including roads. Long-term sea level rise has been recently recognized as a significant contributing factor to flooding problems in almost every coastal state,
- **Chapter 10** presents engineering strategies for coastal roads that are occasionally overwashed by storms because of their location and elevation,
- **Chapter 11** discusses bridges near the coast and the hydrodynamic loads on them due to coastal storms, and
- **Chapter 12** summarizes coastal scour information of value to highway engineers including scour at coastal bridges.

**Part 4** presents methods for assessing the vulnerability of HICE to extreme events with future sea level rise:

- **Chapter 13** summarizes tools available for the quantitative evaluation of probability of flooding of HICE. This includes fundamental concepts like the risk of a 100-year storm occurring,
- **Chapter 14** presents some existing approaches and methods for assessing the vulnerability, particularly the exposure component of vulnerability, of HICE to extreme events. The methodologies include the effects of future sea level rise and outlines how others have engaged in varying levels of effort for each region of the US, and
- **Chapter 15** briefly summarizes typical damage mechanisms and corresponding strategies to improve the resilience of HICE.

Other materials in this document include a glossary of terms, list of acronyms, references cited, and an appendix acknowledging workshop participants.

### **1.3 Target Audience**

This manual is written for a wide cross-section of users with varying backgrounds and expertise. The target audience is civil engineers, hydraulic engineers, roadway designers, planners, environmental staff, field inspectors, construction supervisors, scientists, coastal engineers, and other personnel involved in the analysis, planning, design and operation of HICE.

This manual should help those with little experience in coastal engineering to understand and, as appropriate, to apply scientific methods and engineering approaches that are unique to the coast. For experienced coastal engineers, this manual should serve as a reference document in providing specific highway-oriented assistance and consultation for FHWA and SDOT projects.

The coastal engineering design environment is complex and unique. Staff in a typical FHWA or SDOT engineering or planning unit often do not have a formal education in the processes and principles of coastal science and engineering. Part 2 of this HICE document is not meant as a substitute for more in-depth study of these sciences but rather as a basic, entry-level primer for someone with a general civil engineering background. Also some tools outlined throughout this manual are presently undergoing significant research and development resulting in changes to accepted practices.

This manual does not attempt to “simplify” this complex practice into mechanistic, “one-size-fits-all” approaches. Rather it provides the transportation community with an overview and awareness of good practice in coastal engineering for HICE. The result of this awareness will allow practitioners to seek appropriate technical documentation and expertise for specific projects. Other references, summary manuals, textbooks, and original sources in the coastal sciences and engineering fields, are cited for further details.

Within this framework, this manual does not have the force and effect of law and it is not meant to bind the public in any way. The FHWA intends any descriptions of processes and approaches to provide illustrative insights into the underlying scientific and engineering concepts and practices rather than any proscribed guidance or requirements.

### **1.4 Units in this Manual**

US Customary (English) units consistent with FHWA policy are used with a few exceptions. In limited situations, both customary (English) units and SI units are used, or only SI units are used because these are the predominant metrics nationwide and globally for these topics. In these situations, this manual provides the rationale for the use of units.

## Chapter 2 - Federal Policy for Coastal Highways

Federal policy for coastal highways is at the nexus, essentially the geographic overlap, of two broad federal policy arenas:

- highway engineering and
- coastal management.

Each of these has its own evolving history which influences the road system along our coasts. This Chapter provides some background on these policy arenas, provides some FHWA specific statutes and regulations applicable to the coastal environment, and then provides an overview of other Federal statutes and regulations that may affect a coastal highway project.

### **2.1 Federal Highway and the Coast: National Overview**

The FHWA has the primary responsibility for US federal policy on highways. Legislation for the federal road system dates back over a century. The Federal-Aid Road Act of 1916 created the Federal-Aid Highway Program which funded state highway agencies so they could make road improvements “to get the farmers out of the mud.” This 1916 Act charged the Bureau of Public Roads with implementing the program. The growth of the Federal highway system, including the addition of the Interstate Highway System and concerns about how these highways affected the environment, city development, and the ability to provide public mass transit, led to the 1966 establishment of the US Department of Transportation (USDOT). The same enabling legislation renamed the Bureau of Public Roads to the FHWA. Currently, the FHWA continues to administer US federal policy on highways, but also coordinates extensively with other federal agencies on environmental policies and permits, floodplains, and other compliance issues related to highway program and project delivery.

In contrast, US federal policy on coastal management is not entirely concentrated in any one agency but dispersed over several according to their historical missions. Agency policy responsibilities often began as scientific responsibilities. For example, President Thomas Jefferson established the Survey of the Coast in 1807. That agency evolved to become the US Coast and Geodetic Survey and today is the National Geodetic Service within the National Oceanic and Atmospheric Administration (NOAA) within the US Department of Commerce. The NOAA also administers the most comprehensive, modern coastal management legislation, the Coastal Zone Management Act of 1972. Similarly, the US Army Corps of Engineers (USACE) has had a beach erosion research mission dating back to the Beach Erosion Board established in 1930. The USACE has both coastal regulatory and civil works missions today.

### **2.2 FHWA Statutes & Regulations**

The FHWA provides financial and technical assistance to State and local governments to ensure that US roads and highways continue to be among the safest and most technologically sound in the world. The FHWA authority for the subject matter of this manual on coastal highways includes the following statutes and regulations. The section below provides a synopsis of these various authorities as well as pertinent Congressional findings and statements, policy, and guidance.

#### **2.2.1 FHWA Statute**

The FHWA operates under the statutory authority of Title 23 (Highways) of the United States Code (U.S.C.). For the purposes of this manual, relevant sections include:

- **Standards [23 U.S.C. § 109].** It is the intent of Congress that federally funded projects for resurfacing, restoring, rehabilitating highways shall “be constructed in accordance with standards to preserve and extend the service life of highways and enhance highway safety.” [23 U.S.C. § 109(n)]. Designs for new, reconstructed, resurfaced, restored, or rehabilitated highways on the National Highway System must consider, among other criteria, the “constructed and natural environment of the area.” [Id. at (c)(1)(a)].
- **Maintenance [23 U.S.C. § 116].** Preventive maintenance is eligible for Federal assistance under Title 23 if a State Departments of Transportation (SDOT) can demonstrate that it is a “cost-effective means of extending the useful life of a Federal-aid highway.” [23 U.S.C. § 116(e).]
- **National highway performance program [NHPP] [23 U.S.C. § 119].** The NHPP allows FHWA to provide Federal-aid funds for “[c]onstruction, replacement ..., rehabilitation, preservation, and protection (including ... protection against extreme events) of bridges on the National Highway System.” [23 USC § 119(d)(2)(B)]. The NHPP also allows Federal-aid funds for “[c]onstruction, replacement ..., rehabilitation, preservation, and protection (including ... protection against extreme events) of tunnels on the National Highway System.” [Id. at (d)(2)(C)].
- **Surface transportation block grant [STBG] program [23 U.S.C. § 133].** The STBG program allows FHWA to provide Federal-aid funds for protection of “bridges (including approaches to bridges and other elevated structures) and tunnels on public roads” including “painting, scour countermeasures, seismic retrofits, impact protection measures, security countermeasures, and protection against extreme events.” [23 U.S.C. § 133(b)(9)]. The STBG program also allows Federal-aid funds for “inspection and evaluation of bridges and tunnels and other highway assets.” [Id.]
- **Metropolitan transportation planning [23 U.S.C. § 134].** In the context of metropolitan transportation planning, Congress has found that it “is in the national interest ... to encourage and promote the safe and efficient management, operation, and development of surface transportation systems ... within and between States and urbanized areas” including taking “resiliency needs” into consideration. [23 U.S.C. § 134(a)(1)].
- **National bridge and tunnel inventory and inspection standards [23 U.S.C. § 144].** Congress has found that “continued improvement to bridge conditions is essential to protect the safety of the traveling public.” [23 U.S.C. § 144(a)(1)(A)]. Congress has further found that “the systematic preventative maintenance of bridges, and replacement and rehabilitation of deficient bridges, should be undertaken.” [Id. at (a)(1)(B)]. In addition, Congress has also declared that “it is in the vital national interest” to use a “data-driven, risk-based approach” toward meeting these ends.” [Id. at (a)(2)(B)]. Considering these findings and declarations, Section 144 requires FHWA to maintain an inventory of bridges and tunnels on public roads both “on and off Federal-aid highways.” [Id. at (b)]. The FHWA is also required to “establish and maintain inspection standards for the proper inspection and evaluation of all highway bridges and tunnels for safety and serviceability.” [Id. at (h)(1)(A).] Section 144 also provides an exception to the requirement to obtain a bridge permit from the US Coast Guard for certain bridges over a limited subset of navigable waters. [Id. at (c)(2)].
- **National goals and performance management measures [23 U.S.C. § 150].** Congress has declared that it is “in the interest” of the US to focus the Federal-aid highway program on certain national transportation goals including Infrastructure Condition, or the objective to “maintain ... highway infrastructure in a state of good repair;” and System Reliability, or

the objective to “improve the efficiency of the surface transportation system.” [23 U.S.C. § 144(b)].

- **Research and technology development and deployment [23 U.S.C. § 503].** In carrying out certain highway and bridge infrastructure and research and development activities, FHWA must “study vulnerabilities of the transportation system to ... extreme events and methods to reduce those vulnerabilities.” [23 U.S.C. § 503(b)(3)(B)(viii)].

### 2.2.2 Appropriation Language

The July 27, 2017 US Senate Report 115-138 for the “Transportation, and Housing and Urban Development, and Related Agencies Appropriations Bill, 2018” included direction from the Committee on Appropriations to the FHWA on “Resilient Infrastructure.” The Committee directed FHWA to “expand its technical assistance and training workshops to help coastal States, MPOs, and cities to revise their practices in all phases of transportation planning and asset management, project planning and development, and operations with the goal of improving the resiliency of our coastal highways and reducing the life-cycle costs for these natural disaster-prone roadways.” [US Senate Report 115-138, at 52-53]

The FHWA considers this HEC-25 “Highways in the Coastal Environment (3<sup>rd</sup> edition) to support the FHWA’s technical assistance to help coastal States.

**Congress directs FHWA to expand its technical assistance to help coastal SDOTs, MPOs and cities “with the goal of improving the resiliency of US coastal highways.”**

### 2.2.3 FHWA Regulations

The FHWA’s regulations are found within the Code of Federal Regulations (CFR), Title 23, Highways (23 CFR). The FHWA requires compliance with Federal law and the regulations in Chapter I, Subchapter A, Part 1 of 23 CFR for a project to be eligible for Federal-aid or other FHWA participation or assistance. 23 CFR § 1.36.

The following FHWA regulations apply to highway projects and actions interacting with and within coastal waterways and floodplains (paraphrased for brevity):

**Scope of the statewide and nonmetropolitan transportation planning process [23 CFR § 450.206].** SDOTs must “carry out a continuing, cooperative, and comprehensive statewide transportation planning process that provides for consideration and implementation of projects, strategies, and services that will ... improve the resiliency and reliability of the transportation system. [23 CFR § 450.206(a)].

**Asset Management Plans [23 CFR § 515].** Part 515 establishes processes that a SDOT must use to develop an asset management plan. Two notable sections include:

- Section 515.7(b).** “A State DOT shall establish a process for conducting life-cycle planning for an asset class or asset sub-group at the network level (network to be defined by the State DOT). As a State DOT develops its life-cycle planning process, the State DOT should include future changes in demand; information on current and future environmental conditions including extreme weather events, climate change, and seismic activity; and other factors that could impact whole of life costs of assets.”
- Section 515.7(c).** “A State DOT shall establish a process for developing a risk management plan. This process shall, at a minimum, produce the following information:

(1) Identification of risks that can affect condition of NHS pavements and bridges and the performance of the NHS, including risks associated with current and future environmental conditions, such as extreme weather events, climate change, seismic activity, and risks related to recurring damage and costs as identified through the evaluation of facilities repeated damaged by emergency events carried out under part 667 of this title.”

**Design Standards [23 CFR § 625].** Part 625 describes structural and geometric design standards.

- a. **Section 625.3(a)(1) and § 625.4(b)(3).** The FHWA, in cooperation with SDOTs, has approved the American Association of State Highway and Transportation Officials (AASHTO) Load and Resistance Factor Design (LRFD) Bridge Design Specifications. Based on FHWA’s approval, certain National Highway System (NHS) projects must follow those Specifications including sections related to hydrology, hydraulics, and bridge scour.
- b. **Section 625.3(a)(2).** Non-NHS projects must follow SDOT standard(s) and specifications on drainage, bridges, and other topics.

**Location and Hydraulic Design of Encroachments on Flood Plains [23 CFR Part 650, Subpart A].** One of the FHWA’s most important coastal related regulations, 23 CFR Part 650, Subpart A sets forth policies and procedures for location and hydraulic design of highway encroachments in base (1-percent chance) floodplains. Section 650.111 sets forth requirements for location hydraulic studies to identify the potential impact of the highway alternatives on the base floodplain; these studies are commonly used during NEPA. The regulations prohibit significant encroachments on base floodplains unless FHWA determines that such impacts are the only practicable alternative. [23 CFR § 650.113(a)]. This finding must be included in the NEPA documents for a project and supported information including the reasons for the finding and considered alternatives. [Id]. The procedures also provide minimum standards for Interstate Highways, set freeboard requirements to account for debris and scour, and require highway encroachments to be consistent with certain established design flood standards for hydraulic structures, including standards from FEMA and State and local governments related to administration of the National Flood Insurance Program (NFIP). [23 CFR § 650.115(a)]. Notably, the policies and procedures in this Subpart apply to encroachments in all base floodplains, not just the floodplains regulated by the Federal Emergency Management Agency (FEMA) in the NFIP. [23 CFR § 650.107]. Additionally, the Subpart incorporates a requirement for project-by-project risk assessments or analyses. [23 CFR § 650.115(a)(1)]. Two notable sections include:

- a. **Section 650.115 [Hydraulic Design Standards].** This regulation applies to all Federal-aid projects, whether on the NHS or Non-NHS. Federal, State, local, and AASHTO standards may not change or override the design standards set forth under § 650.115 — although certain State and local standards must also be satisfied under that section. That section requires development of a “Design Study” for each highway project involving an encroachment on a floodplain. [23 CFR § 650.115(a)].
- b. **Section 650.117 [Content of Design Studies].** This regulation requires studies to contain the “hydrologic and hydraulic data and design computations.” [23 CFR § 650.117(b)]. As both hydrologic and hydraulic factors and characteristics lead to scour formation, data and computations applicable to scour should be provided as well. Project

plans must show the water surface elevations of the overtopping flood and base flood (i.e., 100-year flood) if larger than the overtopping flood. [23 CFR §650.117(c)].

**National Bridge Inspection Standards [23 CFR § 650 Subpart C].** This regulation implements requirements of 23 U.S.C. § 144. In addition to the inspection and inventory requirements, the regulation specifically focuses on scour at bridges.

**Mitigation of Impacts to Wetlands and Natural Habitat [23 CFR § 777].** This regulation provides policy and procedures for the evaluation and mitigation of adverse environmental impacts to wetlands and natural habitat resulting from Federal-aid funded projects.

## **2.3 Other Federal Agency Coastal Statutes & Regulations**

Civil engineering projects in the coastal environment are subject to numerous federal laws, policies, and regulations. This section describes some of the most common federal statutes, regulations, and other authoritative guidance that may govern coastal highway projects.

### **2.3.1 Rivers and Harbors Act of 1899 [33 U.S.C. § 401 and § 403]**

Coastal highway engineering projects are subject to Section 9 [33 U.S.C. § 401] and Section 10 [33 U.S.C. § 403] of the Rivers and Harbors Act of 1899. Section 9 of this act restricts the construction of any bridge, dam, dike, or causeway over or in US navigable waterways. Section 10 of this act restricts the building of any wharf, pier, jetty, breakwater, bulkhead, or other structure, as well as excavation or fill within navigable waterways. With the exception of bridges and causeways under Section 9 [33 U.S.C. § 401], the USACE is responsible for maintaining the standards set by and for issuing permits under the Rivers and Harbors Act.

Authority to administer Section 9, applying to bridges and causeways, was redelegated to the US Coast Guard under the provisions of the Department of Transportation Act of 1966 (as discussed below).

### **2.3.2 General Bridge Act of 1946 [33 U.S.C. § 525 through 533]**

The General Bridge Act of 1946 requires the location and plans of bridges and causeways across the navigable waters of the United States be submitted to and approved by the US Coast Guard prior to construction. [33 U.S.C. § 525]. The USACE may also impose conditions relating to maintenance and operation of the structure. [Id]. The General Bridge Act of 1946 is cited as the legislative authority for bridge construction in most cases. Although the General Bridge Act of 1946 originally provided authority for issuing bridge permits to the USACE, subsequent legislation transferred these responsibilities from the USACE to the US Coast Guard.

### **2.3.3 Transportation Act of 1966 [Public Law 89-670]**

The Transportation Act of 1966 transferred the US Coast Guard (USCG) to USDOT. One of USCG's newly assigned duties was to issue bridge permits. This, along with the Rivers and Harbors Act and General Bridge Act, made the USCG responsible for ensuring that bridges and other waterway obstructions do not interfere with the navigability of waters of the United States without express permission of the United States Government. Subsequent legislation amended 23 U.S.C. § 144 to provide certain exceptions to USGC's authority under 33 U.S.C. § 401 and 33 U.S.C. § 525 for bridges constructed, reconstructed, rehabilitated, or replaced using Federal-aid funds. [23 U.S.C. § 144(c)(2)].

### 2.3.4 Coastal Zone Management Act [16 U.S.C. § 1451-1466]

Coastal highway engineering projects are often subject to the Coastal Zone Management Act (CZMA) of 1972. The NOAA is responsible for programmatic administration of the CZMA at the national level but relies on its 34 Coastal Zone Management Programs in participating coastal states for ensuring project compliance with CZMA consistency requirements at the state level. [16 U.S.C. § 1456(c)]. The CZMA consistency requirements incorporate certain relevant state and local requirements related to coastal management into the coastal construction permit process for federal agency actions and provides for participation by state and local agencies. *Id.* The CZMA encourages coastal states to develop and implement coastal zone management plans, which are used in the “consistency determination” process. This Act was established as a US national policy to preserve, protect, develop, and where possible, restore or enhance, the resources of the nation's coastal zone for “this and succeeding generations.” [16 U.S.C. § 1452]. The Office for Coastal Management within NOAA administers the CZMA and its amendments (<https://coast.noaa.gov>). NOAA administers some grant programs that distribute limited funds to the states with approved plans.

**The “federal consistency” provision of the CZMA brings relevant state and local agencies into the coastal permitting process for federal agency actions.**

### 2.3.5 National Environmental Policy Act [42 U.S.C. § 4321, et seq.]

The National Environmental Policy Act of 1969 (NEPA) establishes the continuing policy of the Federal government to use all practicable means and measures “to foster and promote the general welfare, ... create and maintain conditions under which man and nature can exist in productive harmony, and fulfill the social, economic, and other requirements of present and future generations of Americans. [42 U.S.C. § 4331]. To achieve this goal, NEPA creates a requirement for Federal agencies to consider the environmental impacts of their actions before undertaking them. [42 U.S.C. § 4332(C)].

Section 102(2)(C) of NEPA requires Federal agencies develop a detailed statement on proposals for major Federal actions significantly affecting the quality of the human environment. [42 U.S.C. § 4332(C)]. Environmental impact statements address items including “the environmental impact of” and “alternatives to” the proposed action.” [*Id.*] FHWA implements NEPA according to the Council on Environmental Quality (CEQ) NEPA regulations at 40 CFR Part 1500 et seq. and the FHWA-FRA-FTA joint regulations at 23 CFR Part 771.

### 2.3.6 Clean Water Act [33 U.S.C. § 1251-1387]

Almost every project involving work or activities in coastal areas is subject to the Clean Water Act (CWA) of 1972, which is administered by the US Environmental Protection Agency (USEPA) in coordination with state governments. The CWA is the primary federal statute governing protection of the Nation's surface waters. Engineering of highways in the coastal environment is often subject to Section 404 of the CWA, which regulates the discharge of dredged or fill material in waters of the US, including wetlands. [33 U.S.C. § 1344]. This includes the use of dredged or fill material for development, water resource projects, and infrastructure development (e.g., roads, bridges, etc.). The USACE handles the day-to-day administration and enforcement of the Section 404 program, including issuing permits. In circumstances where Section 404 is triggered, permit applicants must also obtain a Section 401 certification from the state in which the discharge of dredged or fill material originates. [13 U.S.C. § 1341]. The Section 401 certification assures that

materials discharged to waters of the US will comply with relevant provisions of the CWA, including water quality standards.

### 2.3.7 Endangered Species Act [16 U.S.C. § 1531-1544]

Coastal highway engineering projects have the potential to impact federally listed fish, wildlife, plants, and marine mammals. The purposes of the Endangered Species Act of 1973 (ESA) include conserving “the ecosystems upon which endangered species and threatened species depend may be conserved” and providing “a program for the conservation of such endangered species and threatened species.” [16 U.S.C. § 1531]. It is the policy of Congress that all Federal agencies shall seek to conserve endangered and threatened species and shall utilize their authorities in furtherance of the purposes of the ESA. [16 U.S.C. § 1531]. The US Fish and Wildlife Service (USFWS) and the NOAA National Marine Fisheries Service (NMFS) administer the ESA. The USFWS and NMFS conduct consultations with the lead federal agency when a proposed project may affect federally endangered or threatened species. USFWS or NMFS involvement in a project depends on the affected species and the nature and extent of anticipated impacts (direct and indirect) to that species and its designated critical habitat. If anticipating a “take” of a federally-listed species, USFWS or NMFS will issue a biological opinion, the terms and conditions of which are binding on the lead federal agency. [16 U.S.C. § 1536.]

### 2.3.8 Coastal Barrier Resources Act [16 U.S.C. § 3501 through 3510]

The Coastal Barrier Resources Act (CBRA) of 1982, and subsequent amendments, designated specific portions of relatively undeveloped coastal barriers along the Atlantic, Gulf of Mexico, Great Lakes, U.S. Virgin Islands, and Puerto Rico coasts as part of the John H. Chafee Coastal Barrier Resources System (CBRS). These undeveloped areas became ineligible for most new federal expenditures and financial assistance. The primary reason for the landmark legislation was to protect and conserve the fish, wildlife, and other resources unique to the coastal barrier islands. [16 U.S.C. § 3501]. One of the original exceptions in the CBRA is the maintenance, replacement, reconstruction, or repair, but not the expansion, of publicly-owned or publicly-operated roads, structures, or facilities that are essential links in a larger network or system. [16 U.S.C. § 3505].

### 2.3.9 Magnuson-Stevens Fishery Conservation and Management Act [16 U.S.C. § 1801-1891d]

The Magnuson-Stevens Fishery Conservation and Management Act of 1976, or more simply the Magnuson-Stevens Act (MSA), governs commercial and recreational fisheries in US territorial waters. The MSA may apply to coastal highway engineering projects because they have the potential to negatively affect Essential Fish Habitat (EFH). Similar to administration of the ESA, NMFS reviews public notices and environmental documents for compliance with the MSA and conducts consultations with the lead federal agency when a proposed project may adversely affect EFH. [16 U.S.C. § 1855(b)(2)].

### 2.3.10 Marine Mammal Protection Act [16 USC §§ 1361-1407]

The Marine Mammal Protection Act (MMPA) may apply to coastal engineering projects that have the potential to harm or impair marine mammal species. [16 USC §§ 1361-1407]. The MMPA prohibits, with certain exceptions, the “take” of marine mammals in US waters and by US citizens on the high seas, and the importation of marine mammals and marine mammal products into the United States. [16 U.S.C.A. § 1372]. This means people may not harass, hunt, capture, or kill any marine mammal unless authorized or exempted. [16 U.S.C. § 1362]. The MMPA also include

other prohibitions related to marine mammals. [16 U.S.C.A. § 1372]. Implementation of MMPA is jointly shared by NMFS, USFWS, and the Marine Mammal Commission, which provides independent oversight of federal agencies under the MMPA (<https://www.mmc.gov/about-the-commission/our-mission/#duties-under-the-mmpa>).

### 2.3.11 Migratory Bird Treaty Act [16 U.S.C. §§ 703-712.].

The protection of all migratory birds is governed by the Migratory Bird Treaty Act (MBTA). [16 U.S.C. 703-712]. The MBTA generally prohibits the “take” of any migratory bird or any part, nest, or eggs of any such bird. [16 U.S.C. § 703(a)]. Under the MBTA, it is illegal to “take, kill, possess, transport, or import migratory birds or any part, nest, or egg of any such bird” unless authorized by a valid permit from the USFWS. [Id.]. Regulation 50 CFR § 10.13A includes a list of migratory birds protected by the Migratory Bird Treaty Act (MBTA).

### 2.3.12 National Historic Preservation Act [54 U.S.C. 300101 et seq.]

Coastal highway engineering projects are commonly subject to the National Historic Preservation Act of 1966 (NHPA). Section 106 of the National Historic Preservation Act (NHPA) (commonly called “Section 106”) requires Federal agencies to consider the impacts on historic properties of projects that they carry out, approve, or fund. [54 U.S.C. § 306108]. The implementing regulations for the Section 106 process are found in 36 CFR part 800. Those regulations provide that Federal agencies, in consultation with the Advisory Council on Historic Preservation, the State Historic Preservation Officers (SHPO) and certain other interested parties, must identify and assess adverse effects to historic properties and seek ways to avoid, minimize, or mitigate those effects. [36 C.F.R. § 800.4-800.6]. Under Section 106, “historic property” is defined as any prehistoric or historic district, site, building, structure, or object included in, or eligible to be included in, the National Register of Historic Places [36 CFR 800.16(l)(1); see also 54 U.S.C. 300311 and 302102]. The responsibilities of SHPOs are set forth at 54 U.S.C. § 302303.

In addition to Section 106, Section 4(f) of the U.S. Department of Transportation Act of 1966 [23 U.S.C. 138 and 49 U.S.C. 303] requires that FHWA not approve the use of historic sites for a project unless there is no prudent and feasible alternative and the project incorporates all possible planning to minimize harm, or any impacts to historic sites are determined to be de minimis. The FHWA’s regulations for implementation of Section 4(f) are found at 23 CFR part 774.

### 2.3.13 National Flood Insurance Act of 1968 [42 U.S.C. § 4001 et seq.]

The National Flood Insurance Act of 1968 instituted the National Flood Insurance Program (NFIP) to help indemnify and reduce impacts associated with floods. The NFIP adopted the area subject to a one percent chance or greater of being flooded on any given year (also known as the 100-year flood) as the standard, or base flood, for mapping US floodplains. See, e.g., 44 CFR § 9.4). The area inundated by the 100-year flood determines the Special Flood Hazard Area (SFHA) on Flood Insurance Rate Maps (FIRMs) developed by FEMA and used to determine flood insurance rates for structures. See, e.g. 44 CFR § 59.1 (defining “area of special flood hazard). See also Section 13.1 below for a discussion of the 100-year flood. FEMA implements the NFIP using its regulations found in 44 CFR.

The FHWA’s policies require projects to be consistent with the Standards and Criteria in the NFIP, where appropriate. 23 CFR § 650.115(a)(5). To assist SDOTs in complying with this policy, FHWA developed coordination procedures for Federal-aid highway projects with encroachments in NFIP regulated floodplains. FEMA agreed to these procedures by signing a 1982 Memorandum of Understanding with FHWA. Coastal floodplain practices delineate the 100-year coastal floodplain using very different engineering analysis tools than the riverine floodplain. And, unlike the riverine

system, encroachments in coastal floodplains often have little or no negative impacts due to the nature of coastal flooding. See HICE Section 4.6, Chapter 13, and Chapter 14 below for discussions of coastal flooding and mapping.

*Page Intentionally Left Blank*

## Chapter 3 - Coastal Highways: An Overview

Thousands of miles of US highways are influenced by the unique challenges in the coastal environment. This chapter is a brief overview of the extent of these highways, the natural processes affecting these highways, and the unique issues faced in planning and engineering these highways. The specialty area of civil engineering called “coastal engineering” is described in Section 3.6.

### 3.1 *What are Coastal Highways?*

Coastal highways are those roads influenced by their presence in or near the water level, wave, and sand transport environment unique to a coast. While normally associated with the oceans, the coastal environment includes the Great Lakes and any other water bodies affected by coastal storms and waves. Every coastal state has highways that are flooded and damaged in coastal storms. Some of these roads are perpendicular to the coast and serve as access and evacuation routes. Some of these roads are parallel to the coast either right along (Figure 3.1) or inland from the shore. Some of these roads are major highways that run across or along bays or estuaries.



Figure 3.1. A local coastal road along an estuary (Shore Road along Mt. Sinai Harbor, Town of Brookhaven, New York)

Many of our coastal roads are literally part of the culture. Examples include Florida’s A1A (see Figure 1.1) and California’s Pacific Coast Highway (Figure 3.2). Americans drive their cars to the beach on coastal highways, and these same highways can influence the quality of the beach

itself. Highways along receding shoreline are often protected by walls resulting in the loss of intertidal beach or wetland habitat. The full spectrum of possible engineering solutions, including nature-based solutions that mimic natural ecosystems, should be considered along the coast.



Figure 3.2. Big Creek Bridge on the Pacific Coast Highway (California SH 1)

### **3.2 The Extent of Coastal Roads and Bridges**

Roughly 60,000 road miles in the US are occasionally exposed to coastal waves and surge. Road miles in flood zones near the coast were measured to generate this rough national estimate (Douglass and Krolak 2008). After Hurricane Katrina, the FHWA assessed coastal bridges potentially vulnerable to failure from coastal storm events. Using very broad criteria, over 36,000 bridges are within 15 nautical miles of coasts. Of these, over 1,000 bridges may be vulnerable to the same failure modes as those associated with damaging coastal storms (FHWA 2005/2007). Some coastal states have assessed the vulnerability of their highways and bridges to coastal storms (e.g. Mertz and Hayes 2009, Sheppard and Dompe 2013; Bosma *et al.* 2015) and some of those results are included in asset management and GIS systems (Snead 2018).

### **3.3 Societal Demand for Coastal Highways**

Millions of Americans live near the coast and millions more want to vacation there. The primary way that we get to the beach is by car. In 2010, about 39% of the US population lived in the 452 coastal counties, those with shorelines on the major coasts and the Great Lakes (NOAA 2013). Population density in the coastal counties is six times greater than the inland counties. Because much of the actual "beachfront" property is already developed in the US, much of the growth and new development is in the area near the coast but some miles inland from the water. The

implication is that these people use the roads to get to the shoreline. Only a few beaches are regularly reached by transit in a few major urban centers (e.g. Coney Island, New York).

One of the largest industries in the US, travel and tourism, lists beaches as the leading tourist destination (Houston 2018). The travel and tourism industry employs over 15 million people (US Department of Labor 2017, US Travel Association 2017).

### **3.4 Natural Processes Impacting Coastal Highways**

Many different natural processes and forces impact roads and bridges near the coast. The natural stresses on the coast are challenging today and are increasing in a number of ways. This document focuses on the natural processes that are not typically experienced by inland roads. The unique challenges for coastal roads are briefly listed here with expanded discussions in Part 2: Principles of Coastal Science for Highway Engineering.

#### **3.4.1 Water Level Change**

Water levels are constantly changing along the coast. Tides rise and fall daily along all the ocean coasts. The range of tides varies dramatically along the US coast. Near Anchorage, Alaska, the tide range is often over 20 ft. Near Pensacola, Florida, the tide range can be essentially zero during some days of the month. The Great Lakes have fluctuations in average water level throughout the year in response to seasonal rainfall differences that can approach 2 ft. Multi-year fluctuations in response to drought cycles can approach 5 ft in elevation. And the Great Lakes can have fluctuations, called seiches, that raise and lower the water level several feet in several hours during major storms.

#### **3.4.2 Sea Level Rise**

Sea level has been rising along most US ocean coasts (relative sea level rise) for the past century. Projections suggest that the rate of this rise will increase significantly this century. Sea level rise (SLR) is progressively making coastal roads and bridges more vulnerable and less reliable (Jacobs *et al.* 2018b).

#### **3.4.3 Storm Surge**

Storm surge can cause significant changes in the water level along the coast in addition to the tides. Storm surge is an increase in water level along the coast in response to the storm winds and pressures. Storm surge in Hurricane Katrina (2005) along the Mississippi coast exceeded 27 ft (Douglass 2005). The Great Lakes can experience water level changes of up to 8 ft in response to a severe storm.

#### **3.4.4 Major Weather Events**

Major weather patterns cause high storm surge and waves. The great coastal storms of the southeast include tropical storms and hurricanes. The major coastal storms of the northeast include those as well as extra-tropical storms including “Nor'easters.” The great coastal storms of the West Coast include the El Niño related storms and the “pineapple expresses.” The major storms of the Great Lakes include the winter north winds associated with arctic high-pressure systems and their related weather fronts.

### 3.4.4.1 Tropical Storms and Hurricanes

A hurricane is a type of tropical cyclone, the general term for all rotating weather systems (counterclockwise in the Northern Hemisphere) over tropical waters. Tropical cyclones are classified as follows:

- Tropical Depression - an organized system of clouds and thunderstorms with a defined circulation and maximum sustained winds of up to 38 miles per hour (mph)
- Tropical Storm - an organized system of strong thunderstorms with a defined circulation and maximum sustained winds of 39 to 73 mph
- Hurricane - an intense tropical weather system with a well-defined circulation and maximum sustained winds of greater than 74 mph

The term "sustained wind" refers to surface wind speeds (10 m above the surface) that persist for durations of one minute.

Hurricanes form in the tropical oceans, frequently in the eastern Atlantic Ocean (or the eastern Pacific) and are powered by heat from the sea. Many hurricanes are steered westward by easterly trade winds. The Coriolis effect provides the characteristic cyclonic spin of these storms. Around their core, winds grow with great velocity, generating violent seas. As the fierce winds accompanied by the low pressure move ashore, the storm surge grows and creates extensive flooding. In addition, the hurricane carries with it torrential rains and can produce tornadoes.

The well-known Saffir-Simpson scale classifies hurricanes according to wind speed:

- Category 1 - winds 74-95 mph
- Category 2 - winds 96-110 mph
- Category 3 - winds 111-129 mph
- Category 4 - winds 130-156 mph
- Category 5 - winds > 156 mph

Use of the Saffir-Simpson scale as the basis for coastal engineering design decisions about infrastructure can be problematic because the scale ignores the important, damaging phenomena of storm surge and waves (e.g. see Figure 3.3). There is little correlation of the scale with surge and waves: two Category 2 events may result in quite different storm surge still water elevations and wave conditions at different locations.

**The Saffir-Simpson Hurricane Scale is not usually used for planning and design in coastal engineering because it is a wind scale... and waves on storm surge (not wind) cause most of the damage to roads and bridges in hurricanes.**

Damage from hurricanes extends well inland. Frequently, the most noted or newsworthy aspect of hurricane damage results from flooding along the coastal area. This is particularly important in low-lying areas such as the coastal barrier islands. The coastal flooding will continue upstream through every inlet open to the ocean including urban drainage systems.



Figure 3.3. Damage caused by surge and waves in Hurricane Michael (October 14, 2018; permission to use photograph provided by John Cleary)

#### 3.4.4.2 Extratropical and Nor'easter Events

Cyclonic events such as extratropical storms form when unstable air produces significant temperature and pressure differences. At times, such systems may stall off the coast and produce long (i.e. several days) periods of high winds and inland rainfall. Although these events rarely obtain hurricane level wind speeds, they can cause significant coastal surge effects and wave damage.

Many historically significant coastal flood events on the Mid-Atlantic and New England coasts are northeasters, or nor'easters. The "Ash Wednesday" storm of March 1962 was formed by the combination of several slow moving coastal low-pressure systems along the Atlantic seaboard. This storm resulted in hurricane force winds and water levels 9 ft or more above mean low water level in areas of Maryland and Delaware over a period of several days. Likewise, the popularized "All Hallows Eve" or "Perfect Storm" of 1991 produced 5 days of high wave action, coastal erosion, and washover (USGS 2003). A northeaster called a "bomb cyclone" developed and moved up the eastern seaboard in early January 2018 which generated wave heights similar to, and in some cases exceeding, the largest hurricane waves generated the previous year (Behrens *et al.* 2018). That previous year of 2017 included three major hurricanes in September: Irma, Jose, and Maria. These extratropical events extend beyond the Atlantic Coast. For example, Florida's west coast, its Gulf of Mexico Coast, experiences severe flooding from such events.

During one March 1993 event, at a location north of Tampa Bay, the resulting inundation and damage was similar to those predicted to occur from a Category 1 hurricane (Citrus County 2000, Good 2018). Likewise, the Great Lakes coastal regions endure wave damage during winter extratropical events (USGS 2003).

#### 3.4.4.3 Long-term Fluctuations

Mean sea level along the coast also fluctuates on longer timescales in response to weather systems. The frequency and intensity of damaging coastal storms are influenced by El Niño episodes, the Pacific Decadal Oscillation (PDO), the Atlantic Multidecadal Oscillation (AMO), and El Niño Southern Oscillation (ENSO).

El Niño is a weather pattern characterized by a large-scale weakening of the trade winds and warming of the surface layers in the eastern and central equatorial Pacific Ocean. El Niño events occur irregularly at intervals of 2 to 7 years, although the average is about once every 3 to 4 years. They typically last 12 to 18 months and are accompanied by swings in the Southern Oscillation (SO); an inter-annual see-saw in tropical sea level pressure between the eastern and western hemispheres.

During El Niño, high sea levels and very high waves can strike the Pacific Coast of the US. Wave-driven processes of importance include wave runup and wave setup. The mean sea level along the Pacific Coast can be over six inches higher, when averaged over an entire year, during El Niño years.

#### 3.4.5 Waves

Waves are one of the major forces affecting coastal systems including roads and bridges. Large, damaging waves occur during the great coastal storms previously mentioned. Waves can generate tremendous forces and cause considerable damage when they are riding on top of storm surge and are able to strike roads and bridges that are not typically designed for such forces. For example, the waves in the Gulf Coast hurricanes of 2004 and 2005 caused billions in damage to bridges, even moving bridge deck spans that weighed over 340,000 lb each (see Figure 3.4).

#### 3.4.6 Shoreline Erosion and Barrier Island Breaches

Storm waves can erode coastal dunes and bluffs, potentially damaging roads in the process. Storm surge contributes greatly to this erosion by allowing the waves to attack the dunes or bluff at higher elevations than normal. The combination of storm surge and waves can cause overtopping and overwash on some low elevation roads. Overwash in Hurricane Isabel (2002) caused portions of the barrier island west of Cape Hatteras, North Carolina (Pea Island), to breach and form a new inlet. This overwash and breach completely removed a stretch of road, North Carolina SH 12, which could not be repaired until the barrier island was artificially rebuilt by beach nourishment techniques. Similar vulnerable areas exist on other barrier islands.

#### 3.4.7 Littoral Drift

Waves can also move tremendous amounts of sand down the coast in longshore sand transport, also called “littoral drift.” Thus, our shorelines are always changing location in response to changes in wave conditions and local sand supplies. Barrier spits, islands, and inlets migrate. Shorelines accrete or recede over the long-term in response to changes in the longshore sand transport.



Figure 3.4. US Highway 90 bridge across Biloxi Bay, Mississippi, after Hurricane Katrina. (photograph looking northeast from Biloxi September 21, 2005)

### 3.4.8 Shoreline Recession

Most of the US coast is experiencing long-term shoreline recession. Causes are both natural, e.g. responding to sea level rise, and man-made, e.g. interruptions in sand movement along the coast by ship channels (Douglass 2002). This coastal erosion can often threaten or even destroy roads located near the shoreline. For example, a 20-mile long portion of Texas SH 87 has remained closed for decades due to coastal erosion.

### 3.4.9 Tsunamis

Tsunamis (“tidal waves”) normally result from an underwater disturbance (usually an earthquake) that triggers a series of water waves that can travel many hundreds or thousands of miles. The “Boxing Day” tsunami of December 26, 2004 in the Indian Ocean was one of the worst natural disasters of the past century. The tsunami waves reached up to 100 ft high on land, killed over 220,000 people and destroyed entire cities and villages. The 2011 Japanese tsunami generated waves which reached even higher, up to 130 ft, and damaged a nuclear power plant. In the US, tsunamis in 1946 and 1957 damaged bridges on the north coast of the Hawaiian island of Kauai. The 1958 Lituya Bay tsunami in southeast Alaska caused wave runup over 1,700 ft above sea level (Griggs 2011). The 1964 Alaskan earthquake sent tsunami waves between 10 and 20 ft high along the coasts of Washington, Oregon, and California. Tsunamis can hit any US coast but 95% of them hit the Pacific states and territories (NTHMP 2018). Many US coastal communities in these states have tsunami evacuation routes with signs that have been coordinated with the SDOT.

### 3.4.10 Upland Runoff

Upland runoff can affect storm surge heights and flow conditions in tidal waterways if significant runoff discharges occur during the surge. Hurricanes can produce significant amounts of rainfall and extreme flooding in river systems much farther inland than the flooding caused by the surge. Runoff from watersheds near the coast can interact with coastal storm surge to exacerbate this flooding (e.g. Hurricane Harvey in 2017). During Harvey, rainfall drained more slowly from the coastal watersheds from Houston to Sabine because the coastal Gulf of Mexico storm surge was high in the bays and acting as a very high tailwater condition in the river systems that drain to those bays.

### 3.4.11 High-Velocity Flows

Floodwaters moving at high velocities can lead to hydrodynamic forces on structural elements in the water column, including drag forces in the direction of flow and lift forces perpendicular to the direction of flow. Oscillations in lift forces correspond to the repeated shedding of vortices from alternate sides of the structural element (for example, these vortices are often visible in the wakes behind bridge pilings in rapidly moving water). High-velocity flows can also move large quantities of sediment and debris.

### 3.4.12 Other Processes

Other coastal processes that can affect coastal roads include common coastal ice problems in northern climates, wave overtopping, flooding (Chapter 9), and wave spray (e.g. salt water on reinforced concrete).

Ice can prohibit wave generation. Increases in the “ice-free” durations in northern latitudes, including the Arctic Ocean and the Great Lakes, are causing more erosion, recession and damage. Native American communities on the north slope of Alaska have suffered losses of historical and cultural sites due to increased waves (Jones *et al.* 2008).

Ice can also remove sediment from beaches as it moves offshore into deeper water since beach ice can include sediment (Hampton *et al.* 1999). Similarly, ice flows can remove armor stones from rock revetments through a process called “ice picking.” Ice picking occurs when a layer of thick ice collects on large armor stones and then cantilevered portions of the ice pull the stones down the revetment slope when they thaw (Smith and Carter 2011).

## **3.5 Coastal Highway Planning and Design**

Some highway planning and design issues are unique to the coast. For example, the design of revetments exposed to wave attack bears additional considerations beyond those in non-coastal situations. These revetments can provide embankment protection along roads or at approaches to bridges.

The possible relocation of roads in response to erosion is another common coastal planning issue: Historically, some coastal roads have been abandoned or relocated landward due to shoreline migrations. Coastal engineering options can stabilize shorelines when a road is threatened by erosion. Manipulating the elevation of coastal roads and bridges can avoid some of the unique coastal forces. For example, the bridges destroyed by Hurricanes Ivan and Katrina are now at much higher elevations. A related issue is the vulnerability of existing bridges that might be exposed to similar conditions. Also increasing flooding referred to as “nuisance flooding” has become a problem in almost every coastal state. Later chapters in this document discuss each of these issues.

The coast presents many challenges for roads including some environmental and aesthetic issues. Coastal roads traverse bays, estuaries, beaches, dunes and bluffs. These are some of the most unique and treasured habitats for humans as well as a variety of plants and animals. The list of endangered species requiring these coastal habitats for survival includes numerous sea turtles, birds, mammals, rodents, amphibians and fishes. The preservation of natural resources has value in itself; natural and nature-based features can be valuable tools for transportation engineers and planners. Careful application of nature-based solutions can accomplish many of the goals traditionally associated with hard engineering solutions, such as shoreline stabilization and erosion control.

### **3.6 Coastal Engineering as a Specialty Area**

This document provides State Departments of Transportation (SDOT) and FHWA hydraulics units with sufficient information for them to understand issues in the coastal environment. However, coastal engineering projects – those in the wave, tide, and sand transport environment unique to the coast - should be done by trained, experienced coastal engineers.

**Coastal engineering is a well-established specialty area of civil engineering. It is the planning, design, construction and operation of infrastructure in the unique wave, water level and sand transport climate along the coast.** Coastal engineering makes extensive use of the sciences of nearshore oceanography and coastal geomorphology as well as geotechnical, environmental, structural and hydraulic engineering principles. Traditional coastal engineering projects involve solving maritime navigation or shoreline erosion problems. Over time, the scope of coastal engineering projects has broadened to include new beaches for recreational and resilience purposes and many projects to improve coastal water quality and coastal habitats. The focus of this manual is coastal engineering related to highways.

The design environment - the coastal water level, wave and sand environment - is the primary distinguishing factor of coastal engineering from other civil engineering disciplines. The coastal design environment is very challenging since design conditions are often affected by storms that contain much more energy and induce very different loadings from those normally experienced.

#### **3.6.1 Education**

Coastal engineering is primarily taught at the graduate level in the US. A few US universities have undergraduate coastal engineering programs. A formal education in coastal engineering, like any other specialty area of civil engineering, is unique and extensive. In other words, the formal education of coastal engineers differs significantly from the education of most civil engineers.

Most coastal engineering graduate programs include:

- two or more graduate courses in wave mechanics,
- two or more courses in other coastal hydrodynamics such as tidal circulation and modeling,
- two or more courses in coastal sediment transport, and
- several courses in the functional and structural design of infrastructure in this environment.

Many coastal engineering programs also include coastal ecology, geology, and oceanography science courses.

Roughly two dozen US universities have some formal graduate level coastal engineering program with a few faculty members teaching in the field. Most of these programs are affiliated with civil engineering departments. The American Shore and Beach Preservation Association (ASBPA)

periodically surveys and summarizes the breadth of the coastal engineering university community (e.g. ASBPA 2018).

### 3.6.2 State-of-Practice

The practice of coastal engineering is still much of an art because the physical processes are often too complex for adequate theoretical description and the design level of risk is often high. Consequently, practitioners should have a broad base of practical coastal engineering experience and should exercise sound judgment based on that experience. There is no substitute for the judgment that comes from coastal engineering experience.

Some distinction can be drawn between coastal engineers and coastal modelers. Coastal numerical models simulate the complex physical processes along the coast (see Webb 2017). This necessitates a distinct, highly-specialized, set of computer skills. But numerical models are only one tool available to coastal engineers and are not a substitute for engineering judgment. Experienced modelers often perform the modeling and experienced coastal engineering design professionals oversee the application of the modeling results.

### 3.6.3 Professional Specialty Certification as a Coastal Engineer

Coastal engineers can obtain a specialty certification from the Academy of Coastal, Ocean, Ports and Navigation Engineers (ACOPNE) as Diplomates of Coastal Engineering (DCE). ACOPNE is affiliated with the American Society of Civil Engineers (ASCE). The ASCE is the US's oldest engineering society and represents more than 150,000 members of the civil engineering profession in 177 countries. A DCE is a board certified professional with at least twelve years of progressive coastal engineering experience after earning their first engineering degree, has achieved a master's degree in the field, and has passed a specialized board examination (ACOPNE 2018). The inclusion of a DCE on the professional team is encouraged for complex coastal projects.

**A board-certified Diplomate, Coastal Engineer can be included on the planning/design team for major coastal planning and engineering projects.**

### 3.6.4 Resources

The field of coastal engineering is summarized in textbooks such as Kamphuis (2010) and Sorensen (2006). Other summary references are mentioned throughout this manual. The USACE's Coastal Engineering Manual (CEM) attempts to summarize the aspects of the field that are of most importance to that agency's mission. Over 2,500 pages long, the CEM was originally published in 2002. It replaced the Shore Protection Manual (SPM) which was often called the "bible of coastal engineering" (USACE 1984). Other coastal engineering manuals and handbooks include Herbich (2000) and Kim (2018).

The breadth and the changes in the field of coastal engineering are best captured by professional specialty conferences and journals. The International Conference on Coastal Engineering takes place every two years and typically has hundreds of highly-technical presentations. Most of these proceedings are available as open access, on-line resources with a keyword searchable database (Coastal Engineering Research Council 2018).

Several series of ASCE sponsored specialty conferences include the "Coastal Sediments" conferences, the "Coastal Structures" conferences, the "Solutions to Coastal Disasters" conferences, the "Ports" conferences, and the "Coastal Zone" conferences. Each of these

conference series has a longer, formal title that is more explanatory, but these are the commonly used names. These conference series have hundreds of presentations and most publish written proceedings. The American Shore and Beach Preservation Association has an annual National Beach Conference which is held at different venues around the US. The Florida Shore and Beach Preservation Association has an annual National Beach Preservation Technology Conference (that is usually held in Florida). The *ASCE Journal of Waterway, Port, Coastal and Ocean Engineering* is published six times per year. Other journals with coastal engineering research results include the *Journal of Coastal Engineering, Shore and Beach*, and the *Journal of Coastal Research*.

### 3.6.5 Coastal Engineering in the Highway Community

**A goal of this document is to encourage the better integration of coastal engineering principles and practices in the planning and design of roads along the coast.** As society continues its great migration to the coasts in the face of changing natural stresses on the coast, opportunities for fruitful integration of coastal engineering in the transportation engineering process will continue to arise.

AASHTO (2008) recommends early input from a coastal engineer to clarify issues and scope for any bridge vulnerable to coastal storms and specifies criteria for qualification as a coastal engineer. At the time of the development of AASHTO (2008), no specialty certification for coastal engineers existed. Now however (see Section 3.6.3), the DCE specialty certification by ACOPNE has similar but more quantified criteria as those specified in AASHTO (2008).

Some coastal states are already encouraging, and even requiring, the inclusion of coastal engineers in multi-disciplinary teams addressing highway and bridge projects near the coast. Florida DOT has required coastal engineers be involved in coastal engineering projects for years. Texas DOT has developed a new coastal precertification requirement for consultants along these lines (TxDOT 2019). This document should aid the transportation professional in understanding when input from a trained coastal engineer would be helpful to the planning or design team.

Most transportation agencies do not have any coastal engineers on staff. However, since these agencies are planning, designing, constructing and operating projects that are, in reality, coastal engineering projects, they often hire consulting coastal engineering expertise. Coastal engineers are vital to transportation planning and decision-making processes in coastal environments.

*Page Intentionally Left Blank*

## **Part 2 – Principles of Coastal Science for Highway Engineering**

*Page Intentionally Left Blank*

## Chapter 4 - Water Levels

Coastal water levels fluctuate because of astronomical tides, storm surges, riverine discharges, and long-term sea level rise (SLR). Water level determines where waves act and still water level (SWL) is an important input assumption for coastal infrastructure design. The “still” in SWL is essentially a convenient construct for engineering design that includes all the contributions to coastal water level except the waves themselves.

### 4.1 Sea Level Rise

Sea levels (the long-term average ocean levels) are slowly rising along most of the US coast and the rate of this rise is projected to increase significantly this century. The effects of SLR on coastal highways includes increased flooding (Chapter 9) and more vulnerability during storms (Chapter 14).

This section discusses the causes of SLR, historical measurements of it, and projections for its future rates. Section 4.1.7 presents specific values of SLR for engineering design. Section 4.2.2 discusses the impact of ongoing SLR on the relationship between surveying and tidal datums.

**SLR values for design are presented in Section 4.1.7 (see Figure 4.11).**

#### 4.1.1 Causes of SLR and Terminology

Causes of global SLR include thermal expansion, melting glaciers and to some extent, reservoir storage and groundwater manipulations. Increased heat in the ocean causes thermal expansion of the water. Sea level is also rising as glaciers melt. The projected increasing rate of SLR is primarily due to increasing contributions of water from major land-based glacial ice sheets including those of Antarctica and Greenland. Changes in reservoir storage and groundwater manipulations contribute minimally.

**“Relative” sea level rise (RSLR) and “global mean” sea level rise (GMSLR) are important, but distinct, terms.**

RSLR is the combined effect of ocean water elevation and land elevation change at a location. The RSLR is the sea level rise any coastal engineering project location is experiencing. RSLR includes any vertical land movement (VLM). Three common types of VLM are subsidence, post-glacial rebound, and tectonics. Some of the US land-mass near the coast is subsiding due to a variety of natural geologic factors including compaction and man-induced factors such as groundwater or oil and gas extraction (e.g. coastal Louisiana). Some of the US, particularly at northern latitudes, however, is rebounding or emerging, due to glacial retreat (post-glacial rebound). A significant VLM on parts of the US Pacific Coast is regional tectonic movement.

Global mean sea level rise (GMSLR), or “eustatic” sea level rise, is the average SLR across all the ocean basins. Coastal engineers have traditionally assumed that the difference between the RSLR and the GMSLR is due exclusively to the VLM at a location. However, other physical processes contribute to this difference because GMSLR is not evenly distributed across all the ocean basins. The oceans are not a static bathtub; they have ever-changing winds, tides, and currents. The long-term sea level at any location is a function of those currents and the related Coriolis forces and this is one reason GMSLR is not evenly distributed across the oceans. Also, sea level is a function of the overall gravitational field of the earth which includes the mass of the major ice sheets. As those major ice sheets melt, their effect on the overall gravitational field

changes. Interestingly, the loss of ice sheet mass in Antarctica leads to increased sea levels in the northern latitudes of the northern hemisphere as the gravitational attraction decreases. This idea that the loss of ice sheet mass leads to greater SLR on the other side of the earth is sometimes termed “fingerprinting” in the scientific literature. See Sweet, *et al.* (2017a) for more discussion on the physics of the causes of GMSLR and RSLR.

**RSLR is the sea level rise that coastal highways will experience and should be accounted for in planning and design.**

#### 4.1.2 Historical RSLR Data: Tide Gages

The historical RSLR data are summarized in this section and the next two sections. Sea levels have been rising not only in the past century but for the past 20,000 years. US tide gage measurements vary in length by location but generally started in the late 1800’s or early 1900’s. Satellites started measuring worldwide sea levels in 1993. Geologic records can estimate prehistoric sea levels.

**US tide gage records provide a wealth of data and analyses which can be readily obtained online at the NOAA “Tides and Currents” website** (NOAA 2019). An example of long-term tide gage data for The Battery in lower Manhattan, New York City is shown in Figure 4.1. Monthly average sea levels at that tide gage are shown. The vertical axis, the y-axis, is the sea level where the zero value is the average sea level from 1983 to 2001. This is the most recent National Tidal Datum Epoch (see Section 4.2 for discussion of tidal epochs). This New York City gage record extends back to the 1850’s (with a gap in the data in the 1870-1890’s). Seasonal fluctuations have been removed.

Figure 4.1 shows an obvious long-term trend in the data that is positive, i.e. sea level has been rising. The average annual rate of rise is 2.84 mm/yr which is equivalent to 0.93 ft per century. The 95% confidence interval about that linear trend rate is 0.09 mm.

The plot also shows the monthly-average “noise” about that long-term trend. Significant fluctuations in average sea level month to month appear as the “spikiness” of the data plot. Yearly and multi-year periods have visibly different trends, but the long-term trend is one of RSLR at a fairly constant rate.

Similar plots of the tide gage records are available at the NOAA website for many other locations around the US. **Engineers can obtain the NOAA plot and analysis from the tide gages nearest to their project site to begin to understand the historical RSLR rates.**

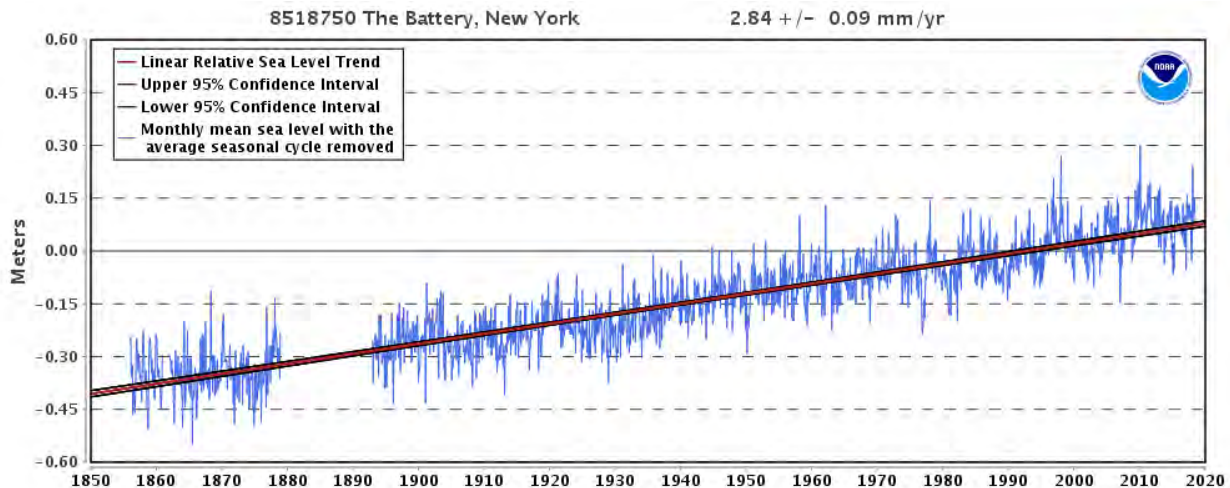


Figure 4.1. Relative sea level rise (RSLR) trend for New York City based on tide gage data (image downloaded from NOAA Tides and Currents website September 6, 2018)

Other data visualizations such as smoothing and the use of different averaging periods can improve the understanding of these tide gage RSLR data. This is a time-honored way to understand a variety of engineering time series data (Bendat and Piersol 2010). The monthly average sea level data are available for download for further analysis from the same NOAA website (NOAA 2019).

As an example, Figure 4.2 shows annual average sea levels for Dauphin Island, Alabama. Similar to Figure 4.1, the vertical axis in Figure 4.2 is the average sea level and the zero value is the average sea level from 1983 to 2001. Thus, in 1967, the average sea level was about 3 inches lower than the 1983-2001 average but in 2017 it was about 6 inches higher than that average and 9 inches higher than the average in 1967. The Dauphin Island tide gage has only been operational since 1967 and the plot excludes years with significant data gaps. The important point is that viewing the data this way provides some interesting observations for that location:

- The annual average sea levels along the Alabama coast in 2016 and 2017 were the highest ever on record,
- The average Alabama sea levels in 2016 and 2017 were roughly 6 inches higher than the average in the 1980's and 1990's and 8 inches higher than the average in the 1960's and 1970's,
- The 2016 Alabama record was 2.5 inches higher than the previous record high year, and
- Seven of the highest years in history for average sea level along the Alabama coast have occurred in the last 9 years.

Although the data do not change with the averaging period, these characterizations of the data are not as obvious with NOAA's monthly average plot. The relatively high sea level shown for Alabama in 2016 and 2017 is generally consistent with other gages along this portion of the northern Gulf of Mexico Coast and is partly the result of the regional weather patterns those two years. **Engineers can download these data for the tide gages nearest to their project site and plot the historical statistics with a variety of techniques to better understand the historical RSLR rates.**

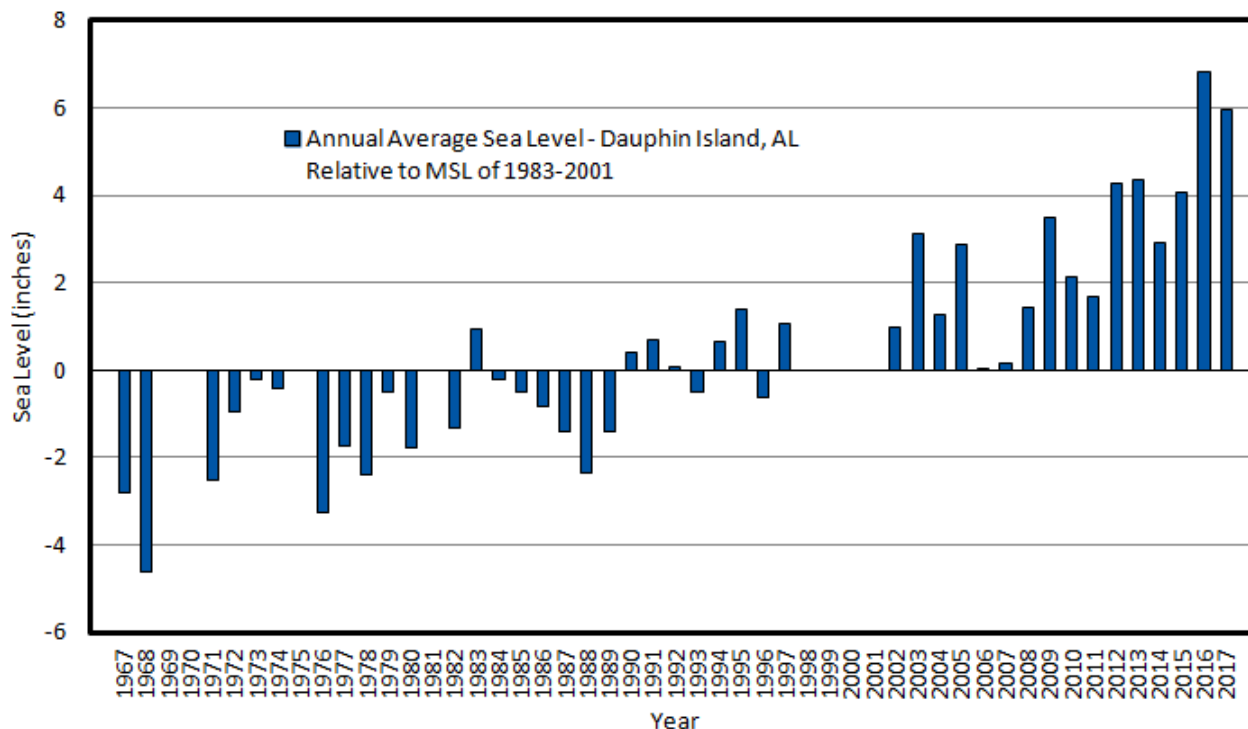


Figure 4.2. Annual average sea level at Dauphin Island, Alabama

Tide gages have measured RSLR around the US for the last century or so depending on location. Figure 4.3 (Atlantic and Gulf Coasts) and Figure 4.4 (Pacific Coast) show some of the variation in the average annual mean sea level (MSL). The values shown are relative to the latest local MSL datum (see explanation of tidal datums in Section 4.2). The relative sea level change rates shown in Figure 4.3 and Figure 4.4 indicate a clear upward trend, i.e. RSLR, along much of the US coast.

**Sea levels have been slowly rising around most of the US for the past century.**

The rate of RSLR shown is fairly constant at the locations in Figure 4.3 and Figure 4.4. Sea levels have risen roughly 1 ft since the 1920's at the Pensacola, Florida gage. But, at the Galveston, Texas gage the RSLR this century is approximately 3 ft. The difference is due to the unique rates of VLM at those two locations. In much of southeastern coastal Texas, land is subsiding due to groundwater and fossil fuel extraction (Kafalenos *et al.* 2008).

Some places in the US exhibit lower rates or a negative trend. For example, Juneau, Alaska has a negative rate of RSLR. In much of Alaska, the sea level is falling: the vertical land movement (VLM) is an upward post-glacial rebound, in response to glacial retreat in the past millennia, at a rate that exceeds the GMSLR rate.

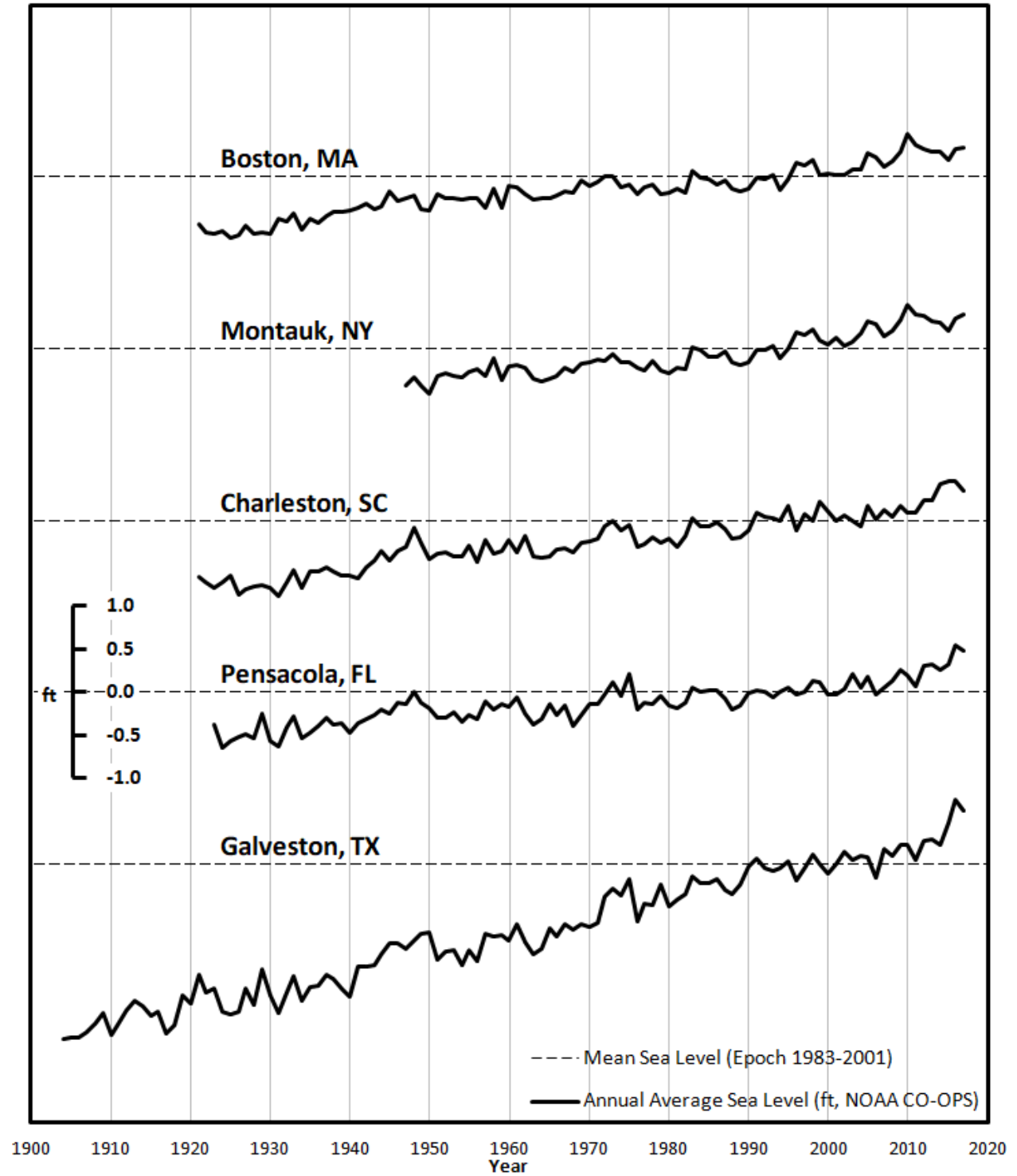


Figure 4.3. Sea levels along the US Atlantic and Gulf Coasts for the past century

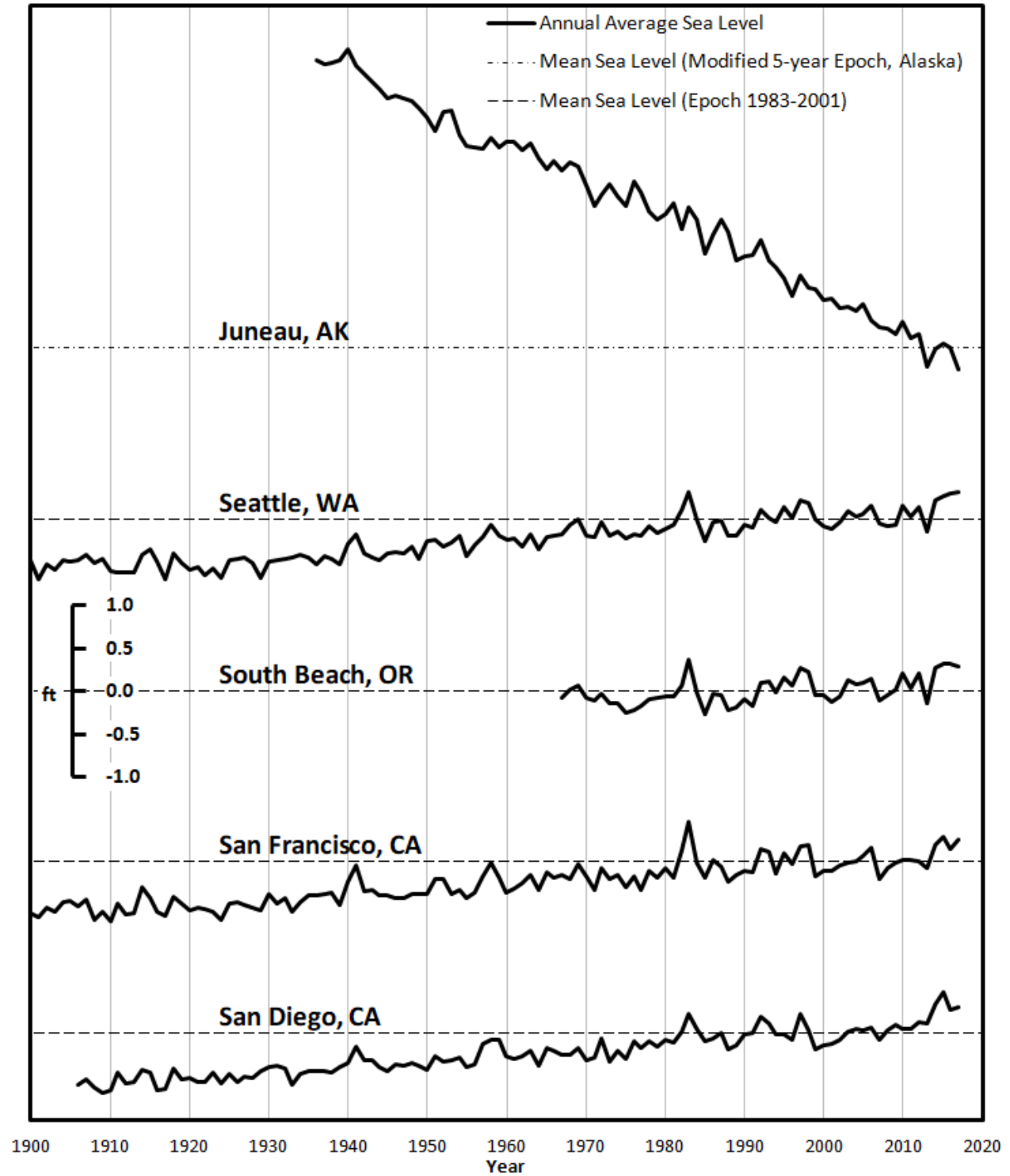


Figure 4.4. Sea levels along the US Pacific Coast for the past century

Figure 4.5 summarizes the long-term RSLR trends, as measured by tide gages, around the US. **The relative sea level is rising along most of the US coast.** The rates of rise vary by location primarily due to regional variability in VLM and other physical phenomenon including oceanic circulation patterns.

Along most of the Atlantic and Gulf Coasts, the rate of rise is between 0 and 1 ft/century or between 1 and 2 ft/century. More precise values are available on-line for each location as shown in Figure 4.1 for New York City. The largest positive rates of RSLR in the US shown on Figure 4.5 are those near the mouth of the Mississippi River in Louisiana where the VLM rates are very high due to marsh subsidence (note: these are the red, upward-pointing arrows on the northern Gulf of Mexico Coast). Chapter 9 - Increased Flooding Due to Relative Sea Level Rise discusses problems in areas with large regional subsidence rates.

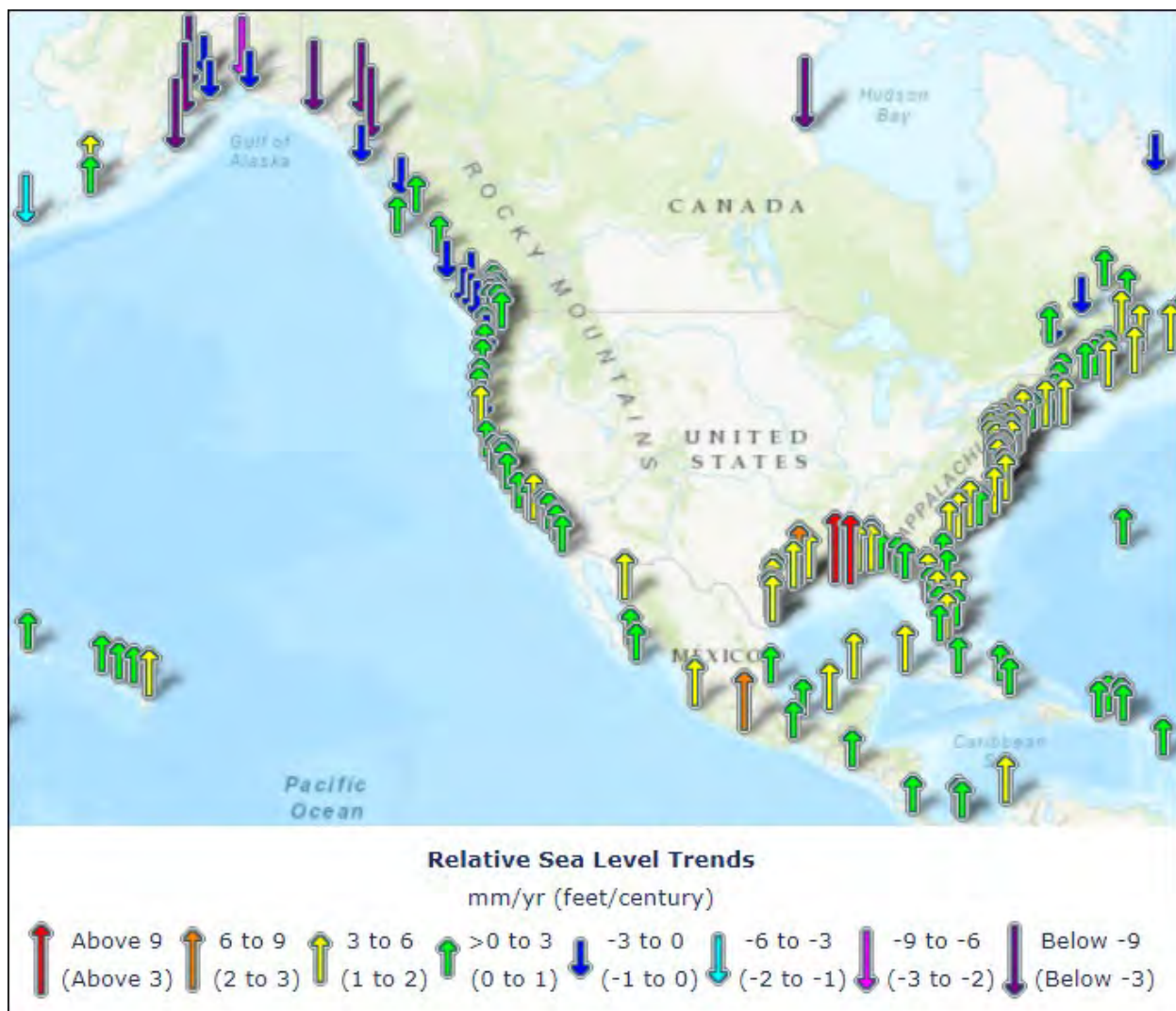


Figure 4.5. Relative sea level rise (RSLR) rates measured at tide gages around the US (image downloaded from NOAA Tides and Currents website, Sept 5, 2018)

For the past century, **the worldwide average rate of SLR based on tide gage records, the GMSLR rate, is most commonly estimated to be 1.7 mm/yr (0.067 in/yr) (IPCC 2007).** This corresponds to about a 0.6 ft rise in GMSLR during the past century. The US Atlantic and Gulf coasts have experienced more RSLR in general.

### 4.1.3 Historical SLR Data: Satellites

Satellite altimetry can also measure sea levels (Leuliette *et al.* 2004; JPL 2013). Satellites have mapped the sea surface several times per month since 1993, measuring sea level across large portions of the earth's oceans. The measurements are not limited to the locations of the long-term tide gages that are all on the coast and mostly in the northern hemisphere. Figure 4.6 shows the sea level trends as measured by satellites (CNES/LEGOS/CLS 2018). One interesting aspect of this sea level change data measured by satellites is its spatial, or regional, variability across the oceans. The values shown range from much higher rates in portions of the western tropical Pacific to near zero values in portions of the north Pacific to negative values (i.e. sea level has fallen) in a few portions of the south Pacific. **Based on satellite data, the average rate of GMSLR has been 3.32 mm/yr (0.13 in/yr) since 1993** (see Figure 4.7).

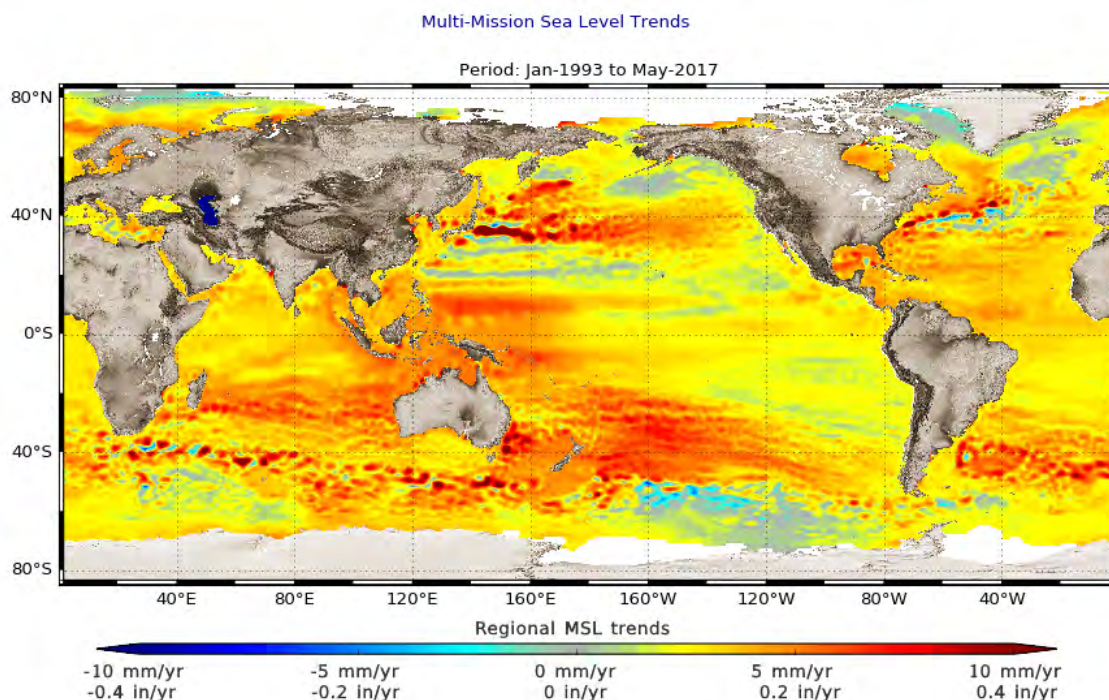


Figure 4.6. Map of sea level change as measured by satellites 1992-2017 (permission for use provided by CNES/LEGOS/CLS)

### 4.1.4 Historical SLR Data: Geologic Record

The geologic record predates tide gages and satellites. Coastal geologists estimate past sea levels using a variety of sediment analysis techniques including radiocarbon dating. These so-called “proxy” data, combined with other geological evidence, are useful for estimating ancient sea levels. Twenty thousand (20,000) years ago, the global eustatic sea level was probably 300 ft to 400 ft lower than it is today (see Section 6.1 - Coastal Geomorphology). The past 12,000 to 20,000 years is the Holocene Epoch, characterized by the rise of global sea level in response to the melting of the last of the Wisconsin ice-age glaciers (Davis and Fitzgerald 2009). The Holocene SLR is divisible into two distinct time periods (see Figure 6.3). Prior to about 6,000 years ago, sea level rose at a much faster rate of 10 mm/yr (0.39 in/yr) or about 3 ft per century. The rate of rise slowed significantly about 6,000 years ago. The SLR rate may have been only 0.1 to 0.2 mm/yr or about 0.5 ft per century when averaged over the last 3,000 years (Church *et al.* 2001).

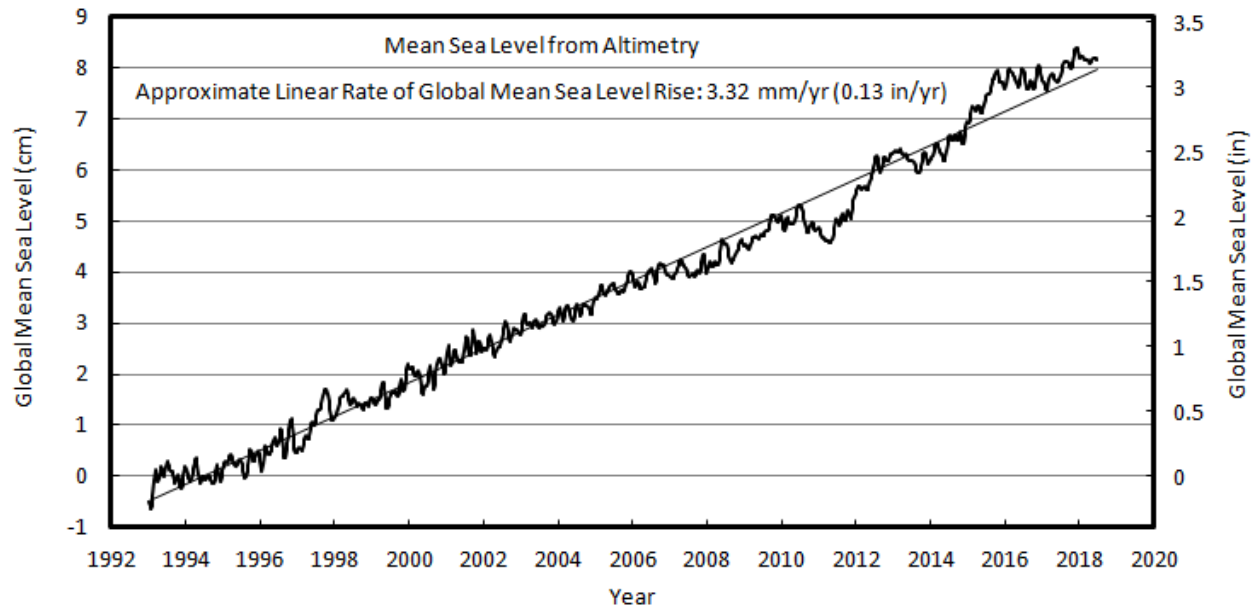


Figure 4.7. Global Mean Sea Level Rise (GMSLR) 1993-2018 as measured by satellite altimetry (data from CNES/LEGOS/CLS 2018)

#### 4.1.5 Discussion of Historical and Present-Day GMSLR

Sea levels are rising in all the data discussed. Whether GMSLR rates are accelerating is a subject of debate in the scientific literature. A number of investigations have suggested that SLR has been accelerating in recent decades (Merrifield *et al.* 2009; Church and White 2006; Church and White 2011; Hamlington *et al.* 2011). Comparing the GMSLR rate as measured by tide gages over the past century (1.7 mm/yr) with the satellite rate since 1993 (3.3 mm/yr) suggests acceleration. Sweet *et al.* (2017b) show acceleration by considering an amalgamation of all three types of historical SLR data with future SLR scenarios.

Confidence in a present-day acceleration conclusion would be higher if accelerations were measurable within the same data set, either the tide gage data or the satellite data, or within both. Church and White (2011) found a very small acceleration rate in tide gage data,  $0.009 \text{ mm/yr}^2$  ( $0.00035 \text{ in/yr}^2$ ), which would add less than 100 mm (3 inches) of sea level change in the next century. This is significantly below most of the future SLR projections/scenarios discussed in Section 4.1.6 and less than the contribution from the historic, global, eustatic, “linear” rate (1.7 mm/yr). Boon *et al.* (2018) find a rate acceleration by only considering the most recent decades in the tide gage data. Nerem *et al.* (2018) find an acceleration rate of  $0.084 \text{ mm/yr}^2$  in an adjusted form of the satellite data, which implies 2.2 ft of GMSLR by 2100. That level of rise is consistent with the projections for future SLR projections discussed in Section 4.1.6.

Other investigators have found that historical SLR rates measured by tide gage data have not been accelerating (Houston and Dean 2011, Douglas 1992). This finding is consistent with casual observation of the full record as shown in Figure 4.1, Figure 4.3, Figure 4.4, and any figure from NOAA’s Tides and Currents web-site for tide gage data around the US. An upturn in RSLR rate is not clearly obvious in the last several decades. Some of the gage plots shown in these figures may show an upturn for the most recent few years, perhaps indicating an upward, accelerating trend that is just not yet statistically significant.

The implication is that while sea level is rising, the rate of rise is not increasing at the locations of US tide gages, at least not yet at a statistically significant level. A synthesis report that focused

on sea levels, prepared by a large, interagency science group specifically for input to the 3<sup>rd</sup> National Climate Assessment (NCA), discussed the Houston and Dean (2011) findings and reasonably concluded that, “the presence or absence of accelerations in sea level rise and the causal mechanisms remain an area of scientific debate (Parris *et al.* 2012).”

The tide gages, of course, only measure past rates and do not forecast future RSLR rates. And for design, planning and operation of coastal transportation infrastructure, the future sea levels will be important.

#### 4.1.6 Projections of Future GMSLR

All of the projections of future GMSLR in the scientific literature are for increasing rates this century. A range of GMSLR projections is available and the science of these projections will likely continue to evolve and improve rapidly.

The National Cooperative Highway Research Project (NCHRP)<sup>1</sup> 15-61 “Applying Climate Change Information to Hydrologic and Hydraulic Design of Transportation Infrastructure” investigated these GMSLR and RSLR future projections. The objectives of NCHRP 15-61 were to review the literature for tools and techniques that represent the state of the art for actionable hydrologic design of transportation infrastructure accounting for the potential effects of climate change. In addition to the Final Report (Kilgore *et al.* 2019a), the study produced a Design Practices manual (Kilgore *et al.* 2019b) to provide practitioners with information to consider GMSLR. Aligned with other literature, both the “Design Practices” and “Final Report” describe two broad types of SLR projections:

- process-based, scientific estimates of the physical processes controlling SLR such as IPCC (2013) and Kopp *et al.* (2014) and
- “scenarios” for planning that are based on the range of scientifically possible sea levels, but are arbitrarily selected values within that range, such as Sweet *et al.* (2017b).

Both are valuable for practical coastal planning and engineering. Section 4.1.6.1 discusses the process-based, scientific estimates, Section 4.1.6.2 discusses the “scenarios” of SLR.

##### 4.1.6.1 Process-Based, Scientific Estimates

The first broad type is exemplified in Figure 4.8, a process-based, scientific estimate of future GMSLR following Kopp *et al.* (2014). These projections are based on a sum of the best available estimates of each of the physical components contributing to sea level rise including thermal expansion of the ocean water and ice-sheet melt contributions to the volume of ocean water.

**Sea levels are rising along most US coasts and the rate of rise is projected to increase significantly.**

The SLR projections in Figure 4.8 are developed for each of the common “representative concentration pathways,” RCPs, following the Intergovernmental Panel on Climate Change (IPCC). The RCPs are a set of standard emission scenarios that are the basis for most of the atmosphere-ocean global climate model numerical experiments. They are based on a range of projections of future population growth, technological development, and societal responses. RCP 8.5 is a “high” global emissions scenario, RCP 4.5 and RCP 6.0 are “intermediate” scenarios

---

<sup>1</sup> NCHRP operates under the auspices of the Transportation Research Board of the National Academies of Sciences, Engineering and Medicine.

consistent with midrange mitigation of future emissions, and RCP 2.6 is a scenario consistent with a high level of future emissions reduction. The reader is referred to Fletcher (2013), Kilgore *et al.* (2016), Taylor *et al.* (2012), or IPCC (2013) for more description of the RCPs and to USGCRP (2017) and USGCRP (2018) for discussion about how present-day emissions compare with the RCPs.

Figure 4.8 depicts three plots of the GMSLR projections corresponding to RCP's with a) RCP 8.5, b) RCP 4.5 (and RCP 6.0), and, c) RCP 2.6, respectively. Kopp, *et al.* (2014) did not model RCP 6.0, because the GMSLR projections of RCP 6.0 are nearly identical to those of RCP 4.5 through 2100. The plots show the median values of GMSLR from 2000 as well as estimates of the probability distribution about those median values. The solid blue line is the median projection, and the blue shaded areas represent the 90% confidence interval about that median projection. The RCP 8.5 values shown in Figure 4.8 are higher than those of RCP 4.5/6.0, and the RCP 2.6 values are lower, as expected.

For example, for RCP 4.5 as shown in Figure 4.8b, the GMSLR projection by 2050 is 0.85 ft at the median probability, with 90% confidence that it will be between 0.6 ft and 1.15 ft (relative to the 2000 mean sea level). In other words, the GMSLR is expected to be 0.85 ft. More specifically, there is a 50% chance that the increase in GMSLR between 2000 and 2050 will be less than 0.85 ft and a 95% chance that it will be less 1.15 ft.

#### 4.1.6.2 Planning “Scenarios” of Future GMSLR and RSLR

The literature describes the second broad type of informative future SLR projections as the use of “scenarios” (e.g., Sweet *et al.* 2017b). Because of the uncertainty ranges for the process-based scientific projections, including the significant overlap within the probabilistic ranges of those projections, “scenarios” of SLR are often used for planning.

Scenarios are recommended by the NOAA Technical Report from the Sea Level Rise and Coastal Flood Hazard Scenarios and Tools Interagency Task Force jointly convened by the US Global Change Research Program (USGCRP) and the National Ocean Council (Sweet *et al.* 2017b). The “SLR Interagency Task Force” charge was to develop and disseminate, through interagency coordination and collaboration, future RSLR and associated coastal flood hazard scenarios and tools for the entire US.

The effort developed RSLR projections for six GMSLR “scenarios” of 0.3, 0.5, 1.0, 1.5, 2.0, and 2.5 m of GMSLR between 2000 and 2100 using the same process models of Kopp *et al.* 2014. These scenarios are named Low, Intermediate-Low, Intermediate, Intermediate-High, High, and Extreme respectively. The SLR Interagency Task Force increased the lower bound suggested by Parris *et al.* (2012) and used in the 3<sup>rd</sup> NCA by 0.1 m to 0.3 m (to 1 ft) and increased the upper bound by 0.5 m to 2.5 m (to 8 ft). Thus, the range of scientifically plausible projections for GMSLR is 1 to 8 ft by 2100. The half meter increments of the four mid-range scenarios are arbitrary within that range.

**Figure 4.9 shows how the “scenarios” compare with the projections of Figure 4.8.** This is how the full range of scientifically-plausible planning scenarios from the SLR Interagency Task Force (Sweet, *et al.* 2017b) compare with the process-based scientific projections (Kopp, *et al.* 2014). The figure has two panels and each panel has both types of curves of GMSLR projections:

- The dashed curves are the scenarios from the SLR Interagency Task Force (Sweet, *et al.* 2017b). These six scenarios are labeled Low, Intermediate-Low, Intermediate, Intermediate-High, High, and Extreme.

- The blue curves are the process-based science projections from Kopp *et al.* (2014). The upper panel shows the Kopp projections for RCP 8.5 (the most extreme RCP). The lower panel shows the Kopp projections for RCP 4.5/6.0.

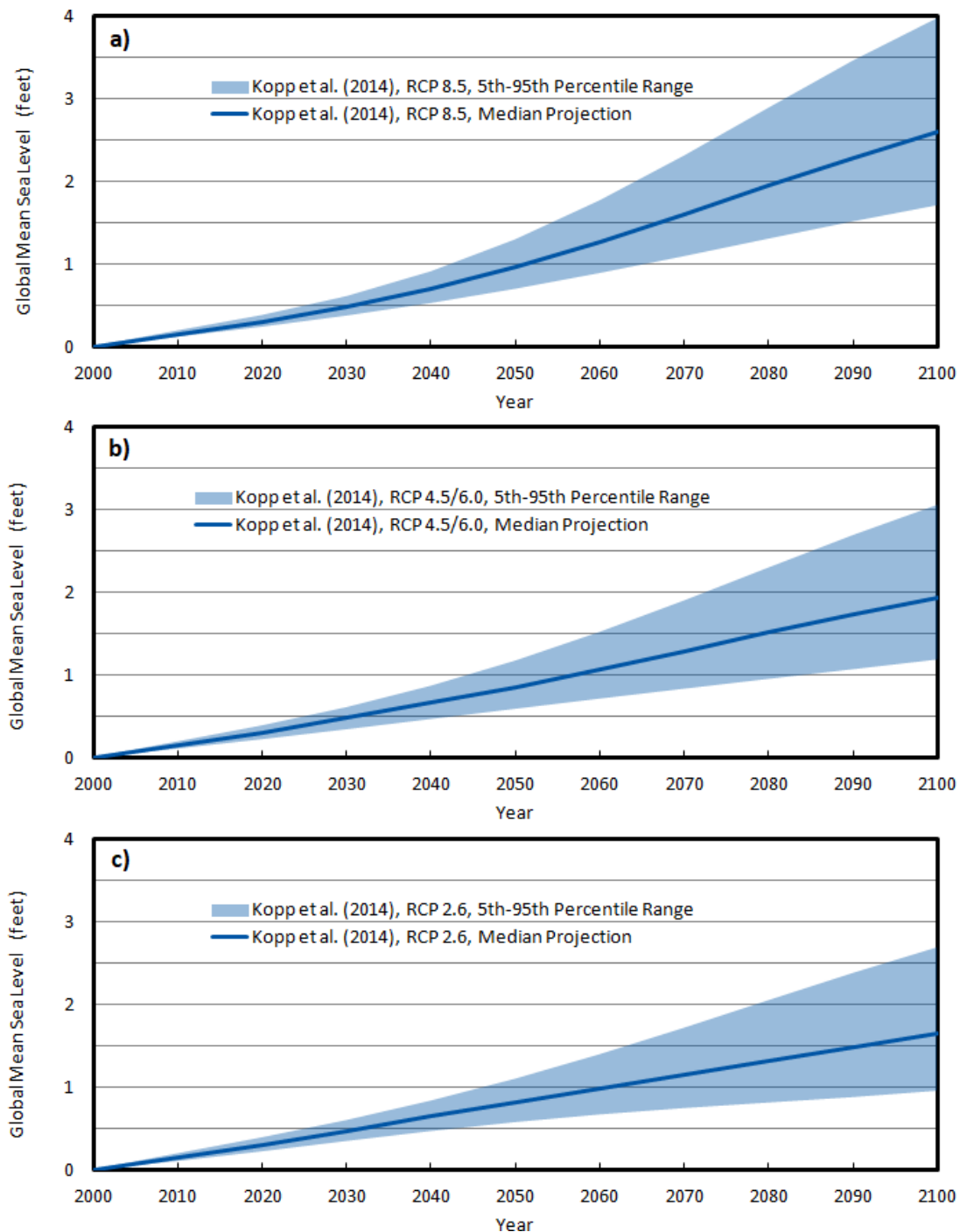


Figure 4.8. Projections of GMSLR in this century (relative to 2000) from Kopp *et al.* (2014) for a) RCP 8.5, b) RCP 4.5, and c) RCP 2.6

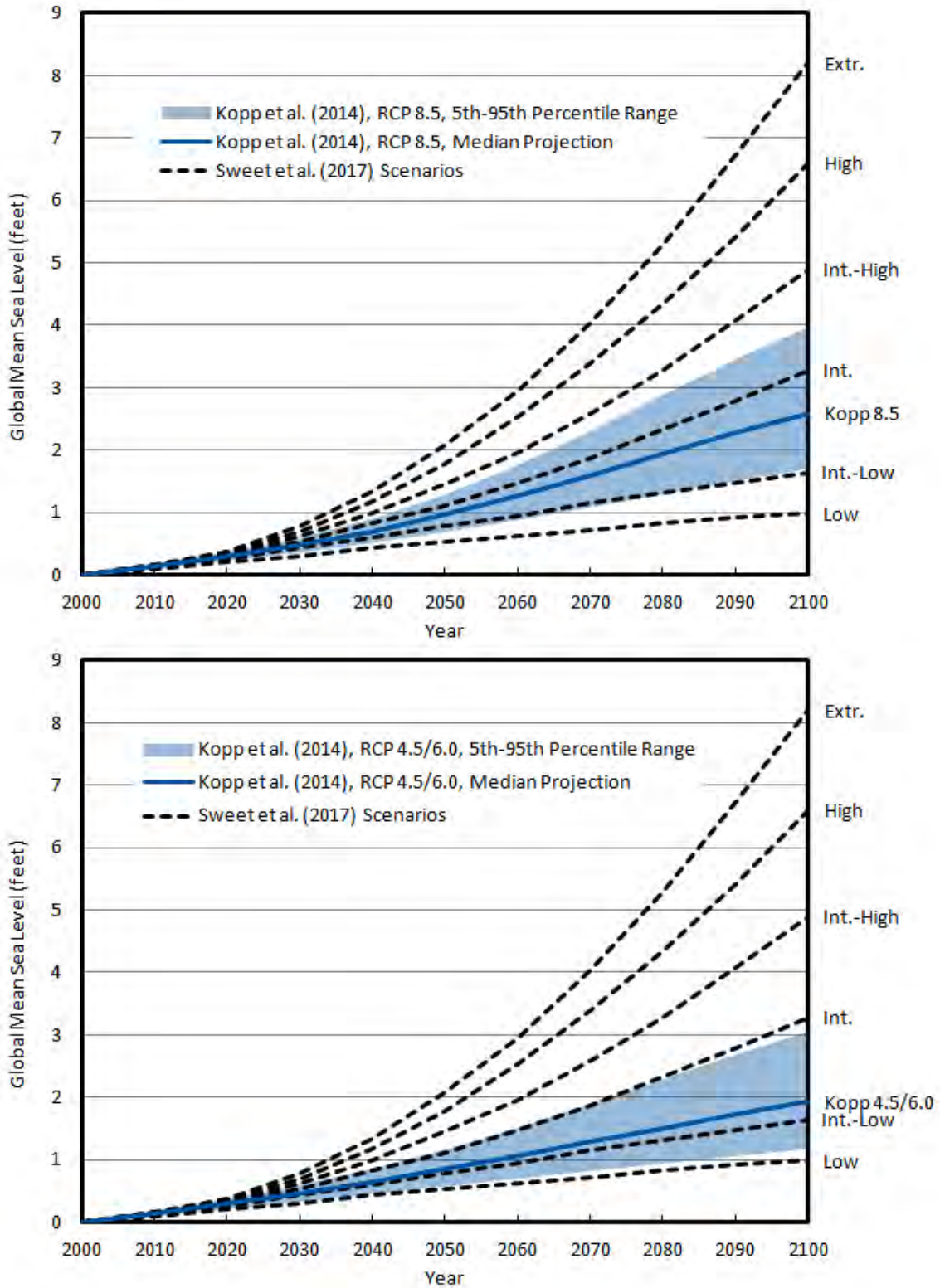


Figure 4.9. GMSLR scenarios and process-based projections. The scenarios (dashed curves) are the SLR Interagency Task Force (Sweet *et al.* 2017b) scenarios and the projections (blue line for median and shading for 90% confidence interval) are the Kopp *et al.* (2014) scientific, process-based projections for RCP 8.5 (upper panel) and for RCP 4.5/6.0 (lower panel)

These two panels show essentially “how bad GMSLR could be” (the higher scenarios shown with the dashed curves) and “what we think GMSLR likely will be” (the blue curves). The median process-based GMSLR projection curves are between the Intermediate-Low and the Intermediate scenarios. The full range of the 90% confidence intervals for the process-based GMSLR projection curves are between the Low and the Intermediate-High scenarios.

**The SLR Interagency Task Force report provides detailed projections of RSLR at many coastal locations**, including at all the tide gages around the US coast (Sweet *et al.* 2017b). These projections are powerful new tools for the coastal engineer and planner. The report essentially answers the question, “if the GMSLR is 0.5 m (or 1.0 m, 1.5 m, etc.), what will the RSLR be at my specific location?”

**The site-specific RSLR estimates from the SLR Interagency Task Force are powerful new tools for the coastal engineer and planner.**

A companion table to the report with all the detailed projection outputs is available at the NOAA website for the report (Sweet, *et al.* 2017c). The projections include the RSLR that corresponds with the GMSLR scenarios. All the physical process components discussed in Section 4.1.1 are included in these RSLR projections (VLM, thermal expansion, ocean circulation, ice sheet contributions including the regional variations due to fingerprinting, etc.). Engineers can evaluate these scenario-based data, for the locations nearest to their project site, to develop site-specific RSLR projections for planning and design of coastal transportation projects.

Figure 4.10 shows RSLR at four US locations for each of the SLR Interagency Task Force GMSLR scenarios. For example, at New York City, the Low scenario projects a RSLR of about 1 ft by 2060 and the Intermediate-High scenario projects a RSLR of about 3 ft by 2060. Corresponding values are higher for Galveston and lower for San Francisco due to the other factors effecting RSLR (primarily VLM).

#### 4.1.7 SLR Values for Planning and Design aligned with NCHRP 15-61

The NCHRP 15-61 report recommended that the planning and design of successful coastal transportation infrastructure include three considerations:

1. Include future RSLR projections in planning and design.
2. Use minimum projections of RSLR throughout the remainder of this century, corresponding to the GMSLR values of Table 4.1, for design
3. Encourage engineers to be aware of the uncertainty in future RSLR projections and account for it appropriately in design. To illustrate, consider higher projections of RSLR when overall project performance is very sensitive (i.e. fragile) to design sea levels and/or when designing long-lived or expensive infrastructure (see Table 4.2).

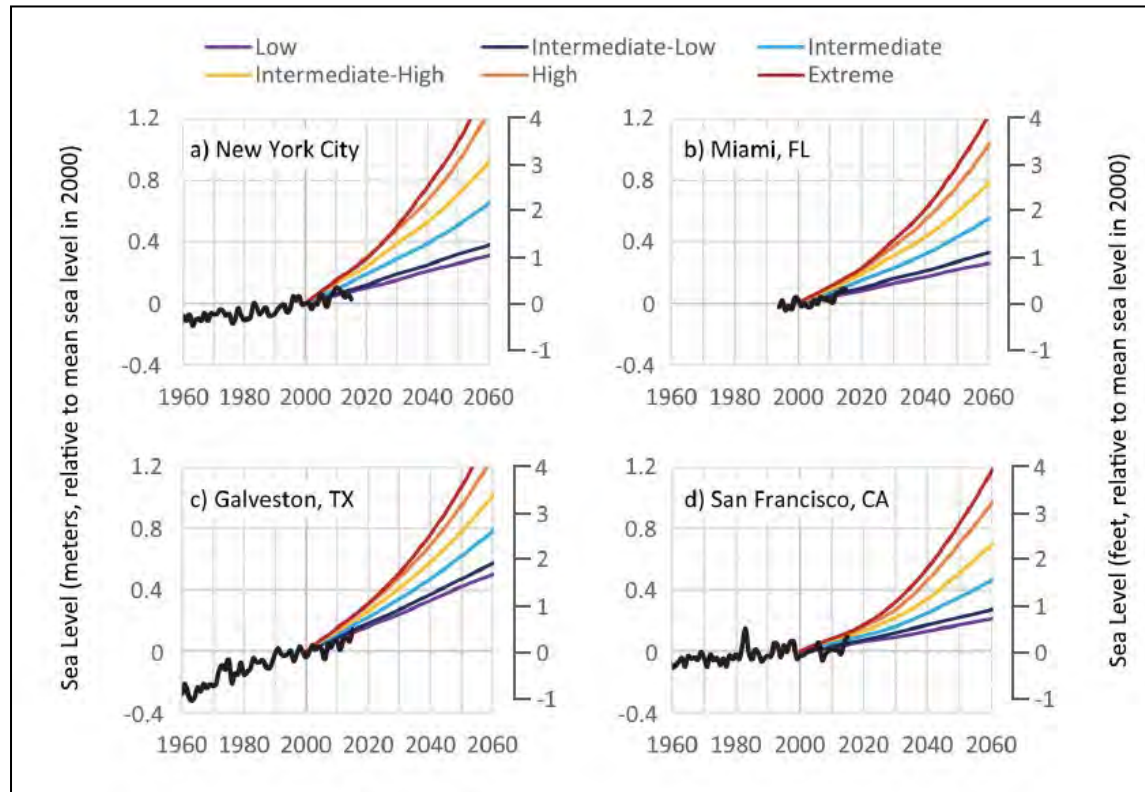


Figure 4.10. RSLR projections for four US cities corresponding to the GMSLR scenarios of the Interagency report (adapted from Sweet et al. 2017b)

In providing these three considerations within this document, it is important to accept that these are not legally binding to HICEs and compliance is voluntary. Additionally, there are many possible RSLR choices; nothing in this section should be interpreted as countervailing existing Federal, State or (as appropriate) local requirements or guidance. For example, many coastal states and local governments may have already developed their own regulations, ordinances, or guidance on incorporating RSLR for use in planning (e.g. California, California 2018; Washington, Miller *et al.* 2018; and Broward and Miami-Dade Counties, Southeast Florida 2015). Much of this existing State and local planning material is in terms of the probability of different levels of RSLR occurring for varying planning horizons. Therefore, with a proper understanding of this context, the next paragraphs will more fully describe these three considerations.

#### 4.1.7.1 Consideration 1: Include Future RSLR projection in planning and design

The first consideration recognizes that prudent **coastal transportation infrastructure planning and design should account for future RSLR projections**. Coastal engineering practice has evolved over the past several decades toward inclusion of RSLR in design and planning as the long-term effects of the process have become more obvious and the scientific projections have improved. RSLR projections now are frequently used in both government and private practice for coastal engineering. This is true for both the design of traditional infrastructure (seawalls, jetties, etc.) as well as the nature-based solutions (e.g. beach nourishment and living shorelines). USACE guidance has evolved from limited recommendations to use RSLR based on projections of the historical linear rate (USACE 1984, USACE 2002) to explicit guidance to include RSLR for planning and design reflecting the best available science (e.g. USACE 2014, Hall *et al.* 2016).

**Projections of future RSLR should be considered in design of coastal highways.**

Within FHWA literature the consideration of SLR has similarly evolved. HEC-25 2<sup>nd</sup> edition discussed SLR but did not provide specific guidance (Douglass and Krolak 2008). HEC-25 Volume 2 recommended that SLR projections be used in vulnerability assessments of coastal transportation infrastructure (Douglass *et al.* 2014). That recommendation was to consider a range of RLSR corresponding to GMSLR of between 1 and 4 ft this century, following the 3<sup>rd</sup> NCA (Melillo *et al.* 2014). HEC-25: Volume 2 did not provide more specific values within that range because of the uncertainties in the science and the need to allow the engineer/decision maker flexibility in determining the appropriate level of risk tolerance for any specific project.

#### 4.1.7.2 Consideration 2: Apply minimum projected RSLR aligned to asset service life

The second consideration is that the **design of coastal infrastructure apply some minimum RSLR, commensurate to the service life of the asset.** Table 4.1 depicts NCHRP 15-61 aligned GMSLR estimates with corresponding decadal values. For example, for an asset with a service life extending to the end of this century, the design RSLR corresponds to a GMSLR of about 2 ft. Figure 4.11 plots these GMSLR versus decadal values as well (circles in lower panel).

Table 4.1 Minimum GMSLR estimates for use in planning and design as per NCHRP 15-61 (values are relative to 2000)

Units	2020	2030	2040	2050	2060	2070	2080	2090	2100
m	0.09	0.14	0.20	0.26	0.33	0.39	0.46	0.52	0.58
ft	0.31	0.46	0.66	0.85	1.07	1.29	1.50	1.72	1.94

The estimates in Table 4.1 are the 19-year averages centered on the decade relative to that of 2000. In order to obtain a RSLR estimate, one would adjust these values for local factors (e.g. VLM and other processes). In refining the NCHRP 15-61 information, the Table 4.1 values used a second-order polynomial equation (following NRC 1987 and USACE 2014) to model the GMSLR throughout the century to reach the target GMSLR by 2100. The second-order polynomial equation is:

$$R(t) = at + bt^2 \quad (4.1)$$

where:

R(t)	=	GMSLR since 2000
t	=	time in years after 2000
a	=	0.0109 ft/yr
b	=	0.000085 ft/yr <sup>2</sup>

The initial rate parameter, a, matches the satellite GMSLR estimate since 1993 (3.32 mm/yr = 0.0109 ft/yr) and the acceleration term, b, is set to match the 2000 to 2100 projected median GMSLR value of 1.94 ft of Kopp *et al.* (2014) for RCP 4.5/6.0 (see Figure 4.11). The polynomial equation produces results that are within 0.07 ft (2 cm) of the median RCP 4.5 projection of Kopp *et al.* (2014) throughout the century.

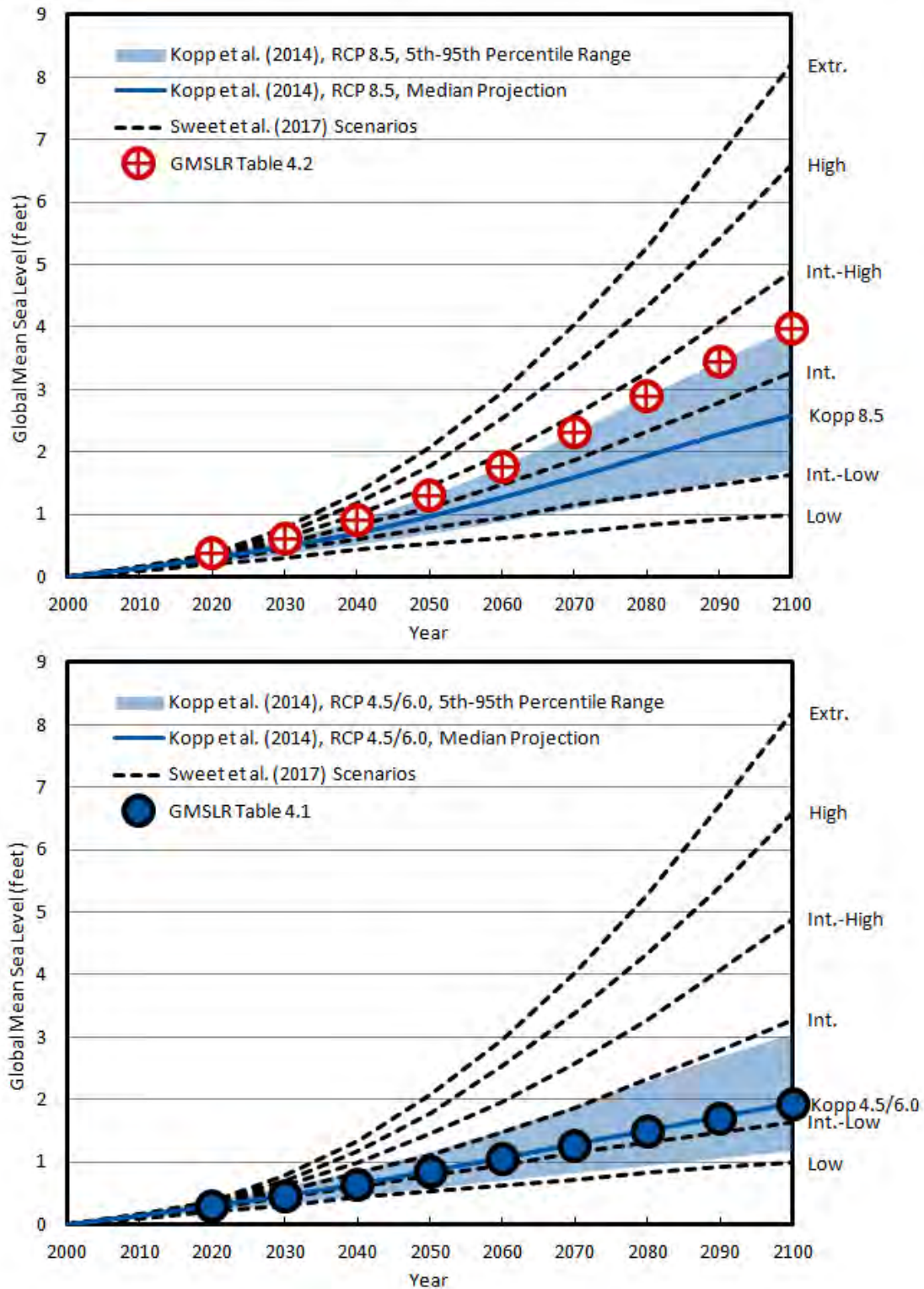


Figure 4.11. Future SLR values for planning and design as per NCHRP 15-61: the RSLR corresponding with the GMSLR values shown by the circles on the lower panel are minimum values (see Table 4.1). The circles on the upper panel are higher values for more sensitive, or fragile, asset planning (see Table 4.2) (see Figure 4.9 caption for explanation of the other curves)

The estimated values in Table 4.1 are consistent with the literature, including NCHRP 15-61 recommendations and USACE guidance, and provide a simple, reasonable estimate of GMSLR for the design of most transportation facilities in the coastal environment. Use of such values aligns with asset management life-cycle planning and risk management planning requirements of 23 CFR § 515.7(b) and 23 CFR § 515.7(c). Projects for which this minimum approach are appropriate may include parking lots and roadways for which the consequences of flooding are low or moderate as determined by the design team.

**RSLR values that correspond to the GMSLR values in Table 4.1 (and the lower panel of Figure 4.11) are the minimum suggested values for design.**

Using the GMSLR values in Table 4.1 to estimate RSLR will result in higher values than the present-day rates from historical data. This assumption of a significant increase in RSLR this century is justified as use of the “best available science” at this time. The Kopp *et al.* (2014) projections are based on models that are similar to those of the IPCC which have shown some skill in modeling the SLR of the past century (Church *et al.* 2013). This science is expected to continue to evolve and improve rapidly over the next decade. Thus, the numerical values in this recommendation may change within this general logical framework.

#### 4.1.7.3 Consideration 3: Scientific and Engineering Uncertainties

**The third consideration is that practitioners should be aware of, and account for appropriately, the magnitude of the overall uncertainty in SLR projections.** Figure 4.8 shows the uncertainty within all the Kopp *et al.* (2014) projections, at the 90% confidence level, to be roughly between 1 and 4 ft of GMSLR by 2100. This range, 1 to 4 ft, corresponds with the recommendations of Douglass *et al.* (2014) and USGCRP (2017). The significant spread of all the GMSLR curves shown in Figure 4.11 indicates the uncertainty range that should be considered in planning and design. This uncertainty is both scenario uncertainty, e.g. unknown future emissions levels, and scientific uncertainty, e.g. the variation shown by the extent of the scenarios shown by the dashed lines on Figure 4.11.

Engineers who fully appreciate this uncertainty should be able to account for it appropriately for their particular decision and situation. Civil engineers commonly deal with uncertainty in methods and models in a variety of other situations (e.g. Manning’s equation, the rational method, flood regression equations) and have developed a level of understanding of the scientific principles and the engineering science models of those processes.

Traditionally, water resources engineers have used median estimates of flood statistics and developed appropriately conservative designs through an awareness of the level of uncertainty in those values. Also, coastal engineers typically use analysis tools and inputs which are not “conservative” by themselves. It is incumbent on the engineer to address the appropriate factor of safety at some point in the design process.

Specific approaches for handling the uncertainty in RSLR projection include robust decision frameworks and/or adaptive management frameworks appropriate for deeply uncertain contexts:

- evaluating the impacts of a full range of SLR scenarios,
- adopting a “minimize regret” viewpoint that uses higher SLR values such as the 95<sup>th</sup> percentile for more expensive facilities that might be sensitive (i.e. fragile) to SLR-dependent process (e.g. depth-limited waves),
- analyzing the full life cycle cost,

- using higher scenarios similar to the use of larger storms as design “check events” are used for bridge scour calculations, and
- designing systems that can be adapted in the future to higher sea levels.

Projections which reach about 4 ft of GMSLR this century are recommended as higher values to be considered for planning and design of high-value assets which are sensitive (i.e. fragile) to RSLR. The corresponding decadal values are shown in Table 4.2 and are plotted in Figure 4.11 (circles in upper panel). The values in Table 4.2 are developed using Equation 4.1 with the acceleration term,  $b$ , is set to match the 2000 to 2100 projected 95<sup>th</sup>-percentile GMSLR value of 3.97 ft of Kopp *et al.* (2014) for RCP 8.5 (see Figure 4.11). There is a 95% chance that GMSLR will be less than these values even if society follows the more extreme emissions scenario of RCP 8.5.

Table 4.2 Higher projections of GMSLR for consideration in the planning and design of high-value assets which are sensitive to SLR as per NCHRP 15-61 (See circles on upper panel of Figure 4.11, values are relative to 2000).

Units	2020	2030	2040	2050	2060	2070	2080	2090	2100
m	0.10	0.18	0.27	0.38	0.51	0.66	0.83	1.01	1.21
ft	0.33	0.58	0.89	1.26	1.69	2.17	2.71	3.31	3.97

In alignment with establishing a risk management plan under 23 CFR § 515.7(c)(1) [i.e., risk to bridges on the National Highway System (NHS) from current and future conditions], a SDOT may consider this higher range of GMSLR estimates as a logical element of their life-cycle analyses. For example, the design team may consider NHS bridges that will be damaged by wave loads or NHS pavement damages from storm surge and overtopping. However, as described earlier, the use of these Table 4.2 values are voluntary for purposes of compliance.

“A rise of as much as 8 ft by 2100 cannot be ruled out” (USGCRP 2017). Investigators have long recognized the possibility of higher rates (Church *et al.* 2013, Parris *et al.* 2012, Melillo *et al.* 2014). A variety of other projections suggest higher upper limits to the projected GMSLR by 2100 (e.g. Vermeer and Rahmstorf 2009). In particular, DeConto and Pollard (2016) added a new model of the physics of ice sheet melting processes to the process-based approach of Kopp *et al.* (2014). They found the potential for increases in GMSLR over the next century. Some of the assumptions inherent in these ice sheet dynamics models and their use in determining “best estimates” are an open scientific question (see Kopp *et al.* 2017).

The engineer and planner should consider all the higher, scientifically plausible, GMSLR rates but this may raise other related infrastructure issues which may be beyond the typical responsibility of the transportation engineer. These planning issues may include changes in land use, inhabitability, and the overall need for transportation services. Elevations of the surrounding area and infrastructure should also be considered in the context of RSLR. It may do limited good to elevate a highway asset beyond some threshold unless the adjacent system of roads is also elevated or otherwise adapted. Planning decisions often consider the region or corridor. Therefore, a prudent approach may be to consider RSLR early in the planning process, well before project development or final design.

All investigators conclude that the values of SLR projections through the mid-century, 2050, are very similar. For example, Figure 4.8 shows that the median expected value by 2050 for the three RCPs only varies from 0.82 ft to 0.95 ft, a total of 1½ inches. Even the higher projections of DeConto and Pollard (2016) only add up to another 1½ inches to those 2050 values. Thus, **the**

engineer and planner tasked with making assumptions about future SLR can have confidence that the uncertainty in projections is minimal through the mid-century. Likewise, these projections for design past mid-century should be used with care since the scientific uncertainty is very large.

The FHWA expects that future editions of HICE will update these SLR considerations over time in accordance with the best available science. See Kilgore *et al.* (2019a and 2019b) for more background on these SLR design recommendations.

#### 4.1.8 Example Future RSLR Calculation: Atlantic City

This section presents an example calculation of projected future sea level for a specific project location near Atlantic City, New Jersey. The planning horizon for the project is mid-century (2050) and the asset is assumed to be somewhat insensitive to water level, e.g. exceedance of the RSLR estimate will not destroy the asset.

Two similar methods for this RSLR example calculation are presented here. The first uses Table 4.1 with location-specific data available from the NOAA Tides and Currents website to account for the difference between GMSLR and RSLR. The second uses one of the SLR Interagency Task Force scenarios and the corresponding RSLR listed directly in that data report (these values are also available in the online USACE 2017 SLR Calculator).

For the example location, the historical RSLR data are inspected first. Figure 4.12 shows the monthly average sea levels at the Atlantic City tide gage. The vertical axis, the y-axis, on the NOAA plot is the sea level with the zero value the average sea level from 1983 to 2001. This is the most recent National Tidal Datum Epoch (see Section 4.2 for discussion of tidal epochs). Figure 4.12 shows the long-term, historical linear RSLR rate at the Atlantic City tide gage has been 4.08 mm/yr (1.34 ft/century).

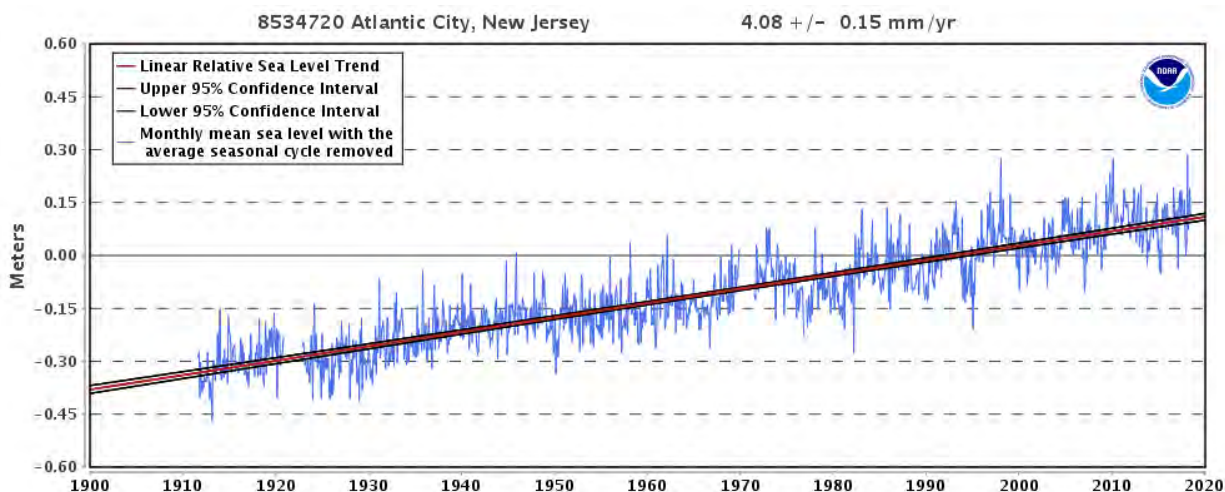


Figure 4.12. Relative sea level rise (RSLR) trend for Atlantic City, New Jersey (image downloaded from NOAA Tides and Currents website September 10, 2018)

Since GMSLR is projected to increase this century, the RSLR rates will increase from this value. The commonly assumed GMSLR for the period of record of tide gages in the US is 1.7 mm/yr (IPCC 2007). This value can be used to estimate the “local” component of SLR that includes the VLM at Atlantic City (and all “local” or regional oceanic SLR components) as:

$$4.08 \text{ mm/yr} - 1.7 \text{ mm/yr} = 2.38 \text{ mm/yr} \quad (7.8 \times 10^{-3} \text{ ft/yr})$$

Using this value gives a total of the “local” component of RSLR for the 50-year planning horizon (from 2000) of:

$$(50 \text{ yr}) (7.8 \times 10^{-3} \text{ ft/yr}) = 0.39 \text{ ft}$$

Adding the projected GMSLR from Table 4.1, which is 0.85 ft for 2050, the total RSLR projection is:

$$0.39 \text{ ft} + 0.85 \text{ ft} = 1.24 \text{ ft.}$$

This final result is the projected RSLR at a location near Atlantic City between 2000 and 2050. In summary, the first method in this RSLR example projects the average annual sea level near Atlantic City will be 1.2 ft higher in 2050 than it was in 2000 (rounding off to 2 significant digits).

The SLR Interagency Task Force scenarios can be used as an alternative method. Since the facility is assumed not to be particularly sensitive to water level, the RSLR corresponding to the Intermediate-Low scenario will be used. This Intermediate-Low scenario has GMSLR values close to those of the Kopp RCP 4.5/6.0 median projection values, and close to the values of Table 4.1 (see Figure 4.11). There are two equivalent ways to find the Intermediate-Low scenario RSLR values for Atlantic City.

One way is to use the tabular data released with the SLR Interagency Task Force report (Sweet *et al.* 2017c). The output data table from that report can be downloaded into a spreadsheet for easy viewing. It presents RSLR for every tide gage location in the US with the “MED,” “LOW,” and “HIGH” values corresponding to each of the six GMSLR scenarios (0.3, 0.5, 1.0, 1.5, 2.0, and 2.5 m by 2100) where the “MED” value is the median of the projection. The “LOW” and “HIGH” values are the +/- one standard deviation or 17<sup>th</sup> and 83<sup>rd</sup> percentiles of the spread about the “MED” value. The “0.5 – MED” value for Atlantic City for RSLR in 2050 in that data table is 36 cm (1.18 ft).

A second but equivalent way to find this value is with the USACE Sea-Level Change Curve Calculator (USACE 2019). Selecting the Atlantic City, NJ gage and the “NOAA *et al.* 2017” as the Scenarios Source, produces a table with the RSLR at that location for all the SLR Interagency Task Force scenarios for every 10 years in this century. For 2050, the “NOAA-2017 Int-Low” value is 1.18 ft.

This result, 1.18 ft, is the projected RSLR at a location near Atlantic City between 2000 and 2050 using the second approach for this example calculation.

The difference between the results of the two alternative methods, 0.06 ft, less than  $\frac{3}{4}$  of an inch, is well within the uncertainty of the methods and well within the natural variability of sea level from year to year. The difference is primarily because the values in Table 4.1 are slightly higher than the Intermediate-Low scenario (see Figure 4.11). Section 4.2 discusses how to relate these RSLR estimates to survey datums and how to relate them to different MSL time periods.

This RSLR by 2050, 1.2 ft, may cause significant increases in frequency of flooding as well as depth of flooding in Atlantic City (see Chapter 9). Note that this value should not be considered a “high” or “conservative” projection since it is based on Table 4.1. It is the median RSLR estimate of the mid-range scenarios.

## 4.2 Astronomical Tides

The tide is the slow rise and fall of the ocean waters in response to the gravitational pull of the moon and the sun. The tide is essentially a very long ocean wave with a wave period (or tidal period) of 12.4 hours. The usual interval between successive high tides is 12.4 hours as the arrival

of the crests of these waves represent high tide. The moon exerts a greater influence on the tides than does the sun.

The astronomical tide can be predicted for any time at many locations. Tidal predictions are well understood even by most coastal residents and are often included in local daily newspapers and weather forecasts. NOAA provides on-line tidal forecasts as well as other information sea levels around the nation on their Tides and Currents web-site (NOAA 2019). Along most coasts the astronomical tide forecasts are within 1 ft of the actual tide elevation 90% of the time. The difference between the forecasts and actual water elevation measurements is normally a result of weather-related phenomena (e.g. wind blowing from same direction over some period, i.e. a storm surge). Understanding some of the characteristics of tides is helpful in understanding some of the terminology used to define tides and tidal datums.

#### 4.2.1 Characteristics of Astronomical Tides

In most locations in the US, two high tides and two low tides occur every “tidal day” (24.8 hours). **These are called “semidiurnal” tides** (see Figure 4.13). At many locations, the two high tides that occur each day are roughly of the same elevation. But at many other locations, there is a “mixed tide” with a clear “diurnal inequality” in the high tides as one is significantly higher than the other. Some places, like portions of the Gulf of Mexico, have only one high tide and one low tide per day. These tides are called “diurnal” tides.

Large differences in tide range occur at the same location throughout the month. The highest tides which occur at intervals of half a lunar month are called “spring tides.” A lunar month is roughly 29.5 days. They occur at or near the time when the moon is new or full, i.e. when the sun, moon and earth fall in-line, and the tide generation forces of the moon and sun are additive. When the tide range is at its lowest during the lunar month, the “neap tides” occur.

**Most of the US coast has “semi-diurnal” tides... two highs and two lows a day.**

Large differences in the magnitude of the daily tide range occur at different locations in the US. Interactions of the oceanic tidal motions with the continental land mass, as well as the depths and shape of coastal bays and shelves, cause these differences. At Anchorage, Alaska, the tide range can vary up to almost 30 ft between high and low tide. At Pensacola, Florida, however the range can be less than 2 ft throughout a day. These differences in tidal range can occur within short distances along the coast and up bays. For example, the average tide range at Sandy Hook, New Jersey is about 5 ft but just 125 miles away at Montauk Point, New York, it is only 2 ft.

The basic astronomical tide producing forces go through a “tidal epoch,” a cycle that lasts approximately 18.6 years. Thus, water level statistics related to tides, such as mean sea level, are computed by averaging over a complete epoch.

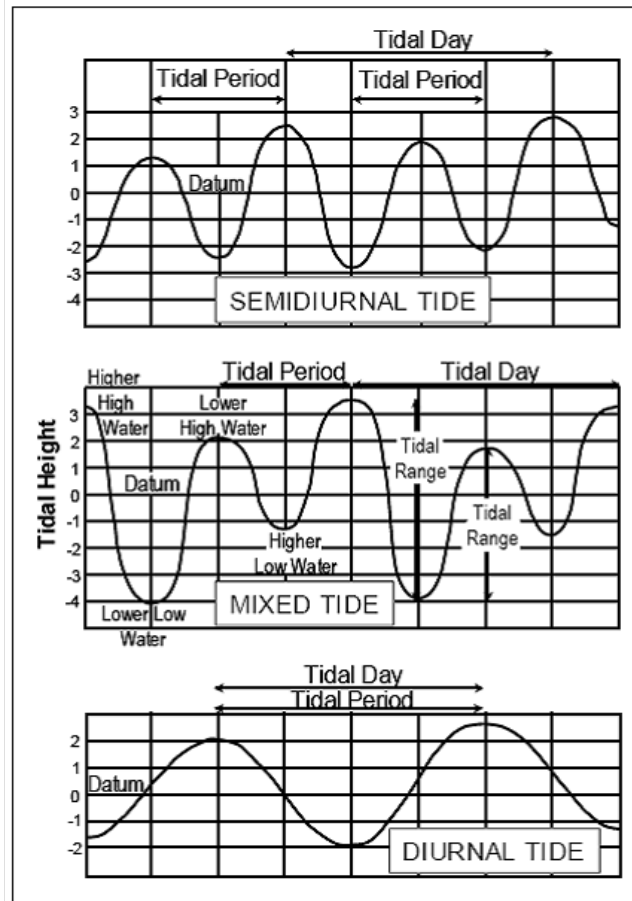


Figure 4.13. Basic definitions of tides (image downloaded from <http://tidesandcurrents.noaa.gov>)

#### 4.2.2 Tidal and Survey Datums

The distinction between tidal datums and surveying datums can be important in the design, construction, and operation of engineering works near the coast. Tidal datums are vertical datums based on the epoch-averaged tide levels at a specific location. Tidal datums are based on actual measurements at a specific tide gage. Since sea level is changing over the long-term, the tidal datums are re-established after every tidal epoch. The most recent, complete tidal epoch ended in 2001 and NOAA's National Ocean Survey established the tidal datums for most of the US tide gage locations for that 1983-2001 tidal epoch (called the National Tidal Datum Epoch). Presumably, they will be revising the tidal datums sometime after 2020.

There are a number of tidal datums. The mean high water datum (MHW) is the average, over an 18.6-year tidal epoch, of the high water elevations at a specific location. The mean higher high water datum (MHHW) is the average of the higher high water elevations. The difference between these two datums, MHW and MHHW, is greatest at locations with the greatest "diurnal inequality" in high tides during a typical day. Likewise, the mean low water datum (MLW) is an average of the low tide elevations and the mean lower low water datum (MLLW) is an average of the lower low tide elevations. MLLW is the basis for most navigation charts because it provides mariners with a consistent, somewhat conservative, estimate of the depth. The local mean sea level datum (MSL) is the average of all the observations of water level over a tidal epoch.

Survey datums are specified for geodetic surveying and set by the NOAA's National Geodetic Survey. The National Geodetic Vertical Datum of 1929 (NGVD 29) and the North American

Vertical Datum of 1988 (NAVD 88) are two primary vertical survey datums used in the US. The older NGVD 29 geodetic datum was originally established using estimates of mean sea level at 26 tide gages around the nation. Thus, it was often referred to as just “mean sea level.”

**NAVD 88 is a fixed survey datum that is not MSL. It is generally near MSL, and the relationship is always changing because of RSLR.**

However, it has long been recognized that it was not actually the MSL because **MSL changes gradually through time and survey datums do not**. The National Geodetic Survey has not called NGVD 29 the “mean sea level” for decades. NAVD 88 was an improvement to the NVGD 29 and has now replaced it as the primary vertical datum for surveying. It normally will be *near* the MSL at the open coast but it is *not* the MSL.

The relationship between the survey datum, NAVD 88, and the tidal datums, e.g. MSL or MLLW, has been calculated by the NOAA National Ocean Service for many of the tide gages around the US. An example is shown in Figure 4.14 using the values for Charleston, South Carolina. The mean sea level (1983 to 2001) at Charleston, SC is -0.22 ft NAVD 88. This relationship is not the same at other locations around the nation. NOAA provides and supports VDATUM, software for converting between all datums at locations around the US.<sup>2</sup>

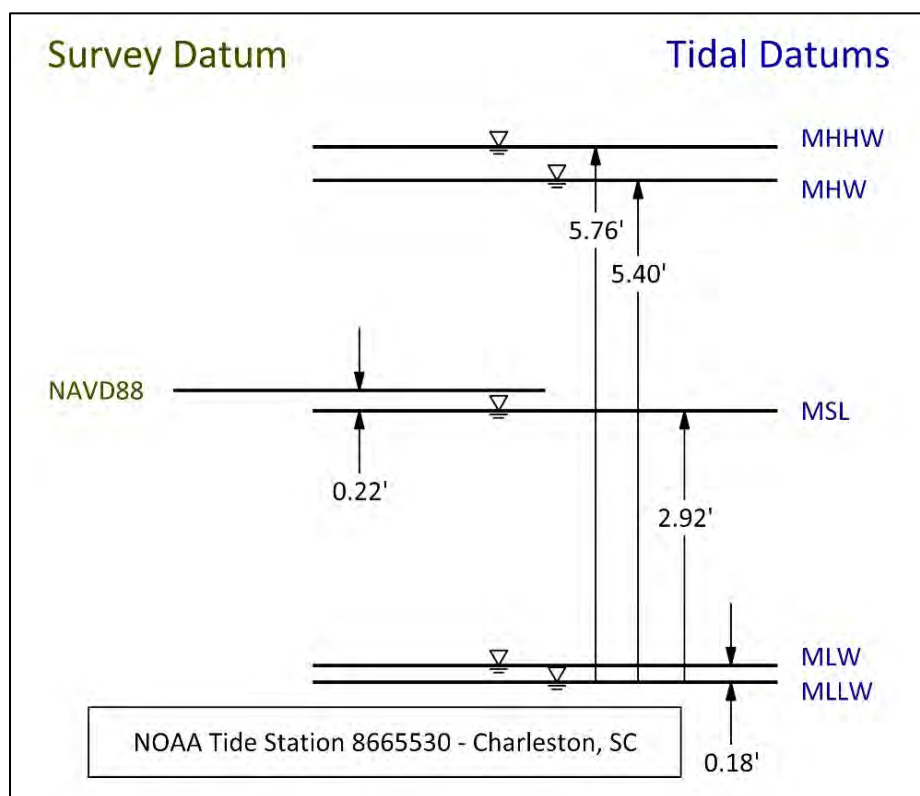


Figure 4.14. An example of the relationship between the survey and tidal datums

Beginning in 2022 a new vertical datum will replace NAVD88 (NGS 2018). NOAA’s National Geodetic Survey plans on replacing NAVD88 with the North American-Pacific Geopotential

<sup>2</sup> <https://vdatum.noaa.gov/> (accessed September 12, 2018)

Datum of 2022, NAPGD2022, to address shortcomings in the existing datum system. The new datum will be easier to access with modern Global Positioning Systems (GPS). Figure 4.15 summarizes the numerical differences between the two vertical datums. They will vary significantly across the US, with only a slight difference in elevation in portions of the Southern US and up to 4 ft of difference in some areas of the Pacific Northwest. More information about the progress toward replacing switching this datum can be found on the National Geodetic Survey website (NGS 2018).

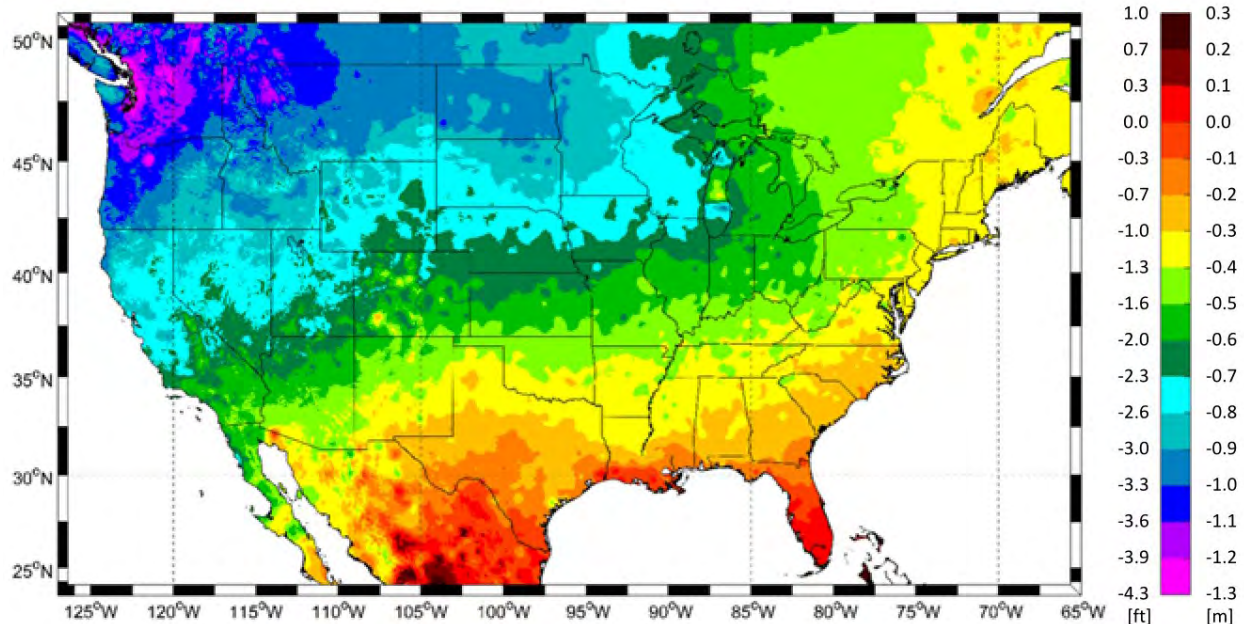


Figure 4.15. Approximate predicted change from NAVD 88 to the new vertical datum which will replace it in 2022 (adapted from NGS 2018)

### 4.3 Storm Surge

Storm surge is the rise of the water level above the astronomical tide as a result of weather. This is primarily wind but also includes the barometric pressure and rainfall runoff. Storm surge, also sometimes called storm tide, can be negative, i.e. winds can decrease water levels (but that is typically not a problem for highways in the coastal environment). Storm surge is highly influenced by geography including the shape of the coast and its bays, the nearshore bathymetry, and the flooded topography. High storm surges occur along the coast where the landmass stops the hydrodynamic movements in areas with broad shallow nearshore bathymetry. The highest storm surge can occur in bays. Wind affects storm surge by placing a stress on the water surface, by generating oceanic currents and by generating waves. Breaking waves can contribute to storm surge by adding a component of mean water surface elevation called wave setup. Storm surge is an important coastal process for the design of coastal infrastructure primarily because it increases the design still water level (SWL) and allows waves to attack higher elevations. Surge also can be an important component in tidal inlet hydrodynamics.

#### 4.3.1 Characteristics of Storm Surge

Figure 4.16 is an example of hurricane storm surge. The predicted tide is plotted along with measurements from a tide gage located on a pier in the Gulf of Mexico during passage of a hurricane. The surge, the difference between the predicted and actual water level, extends for several days with a very dramatic peak of over 7 ft above the predicted high tide early on August

18. That high peak corresponds with the time that the hurricane made landfall with its eye just to the southwest of the tide gage. The tide gage was on the right side of the hurricane's circulation where winds are highest and onshore.

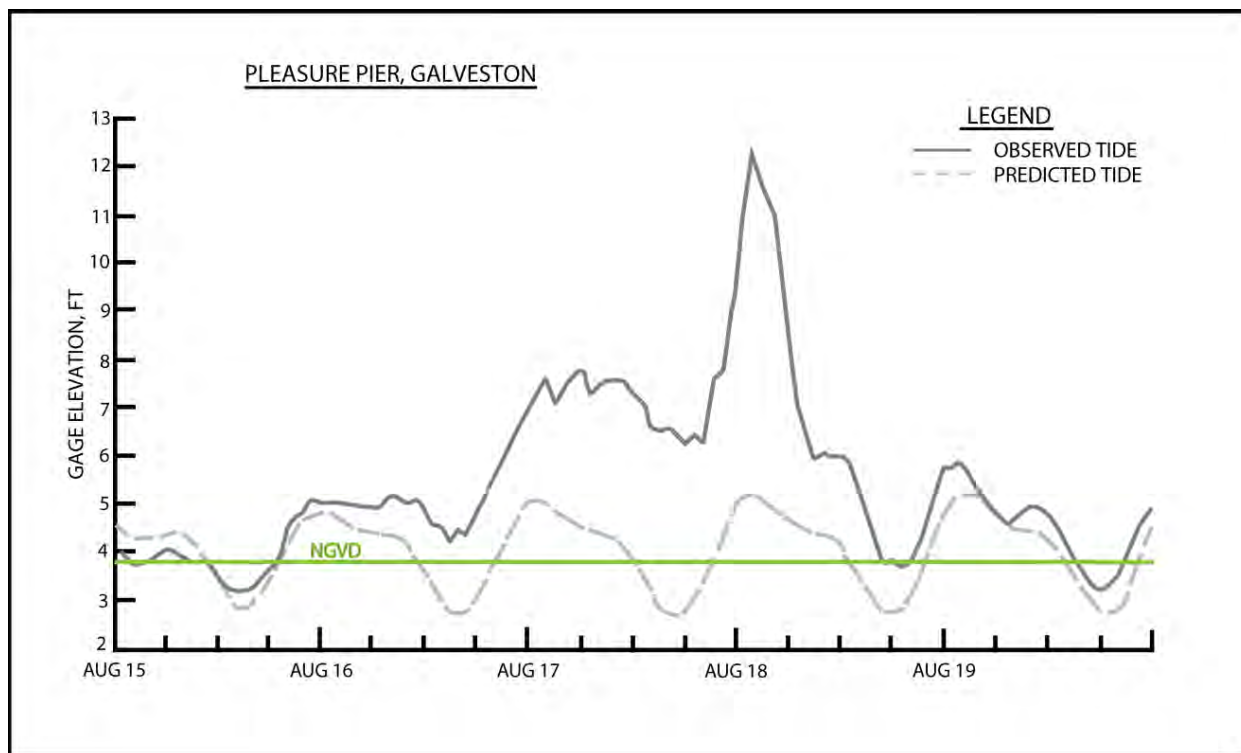


Figure 4.16. Storm surge at Galveston, Texas, from Hurricane Alicia in 1983

The hydrograph of a coastal storm surge is usually considered as the time variation of water surface elevation at a specific location (Figure 4.16). Both the magnitude and duration of a coastal storm surge can be important. During Hurricane Katrina in 2005, storm surge along much of the coast near Bay St. Louis, Mississippi resulted in a rise of water level 27 ft higher than the predicted tide elevation (Douglass *et al.* 2006a; FEMA 2006). This storm surge was unprecedented in US history. This storm surge water level exceeded the previous record level of 21 ft, a result of Hurricane Camille in 1969 along this same stretch of coast.

Another of the most destructive storms in US history, the Nor'easter Ash Wednesday Storm of 1962, caused much of its damage due to its relatively long duration. The storm surge lasted for 2½ days over five semi-diurnal high tides, or “five high-tides.” This long duration allowed beach storm erosional processes to act that long and cause extensive property damage along the Atlantic Coast.

#### 4.3.2 Storm Surge Modeling

Storm surge can be modeled well with modern coastal hydrodynamic modeling techniques. **Webb (2017) is an introductory “primer” on the broader field of coastal hydrodynamic modeling specifically written for transportation engineering professionals.** It explains when, why, and at what level use of coastal models is beneficial in the planning and design of coastal highways as well as when it is appropriate to solicit the expertise of a coastal engineer. It provides transportation professionals with the information needed to determine scopes of work, prepare requests for professional services, communicate with consultants, and evaluate modeling approaches and results. Topics include modeling basics, preparing model input, interpreting input

and output, calibration and validation, model coupling, and the use of models in coastal vulnerability assessments. Written for the layperson, it is an introduction to the broader field of coastal modeling, i.e. not just storm surge.

Webb (2017) includes detailed information on the selection and use of riverine hydraulic and coastal hydrodynamic models. These two types of models are related and generally solve the same types of equations that describe fluid motion, but they are not all applicable to the same conditions and locations. The decision to employ coastal hydrodynamic modeling, riverine hydraulic modeling, or some combination of the two is complex, constrained in part by the proximity of the subject site to the coast and the criticality of the asset. Figure 4.17 graphically describes the function of a site's coastal proximity and criticality. The closer a site is to the coast (and by extension, coastal hazards such as storm surge and wave attack) and the more important the infrastructure or roadway is, the more likely coastal hydrodynamic modeling will be needed in analysis and design.

The numerical modeling of coastal hydrodynamics is based on solving the fundamental fluid mechanics of motion, the continuity equation and the momentum equation, in a manner that is most efficient and appropriate for the problem. A rich history of this modeling has developed over the past forty years in both the nearshore physical oceanography and coastal engineering research communities. Different formulations of the equations and different solution algorithms have been applied. Much of the research and development of these models was done with funding from federal agencies with coastal interests including NOAA, FEMA, and USACE.

**Storm surge can be simulated well with modern coastal hydrodynamic models.**

Table 4.3 lists models discussed in this manual, along with a brief comment as to the type of possible application/use in the design and planning of coastal infrastructure. Engineers and scientists with specialized training in these coastal models should be included in teams applying them to assess transportation infrastructure. The specific use of some of these models is discussed throughout this manual.

**One of the more commonly used models which can estimate storm surge well is the ADvanced CIRCulation model (ADCIRC).** ADCIRC was originally developed for the USACE as a hydrodynamic circulation model for coastal waters (Luettich *et al.* 1992; Westerink *et al.* 1994). It now has an active research and application community in academia, agencies, and consulting. The ADCIRC program is actually a collection of numerical models that can be used to simulate tidal flows, water levels, and constituent transport (e.g. salt, larvae, contaminants, etc.) in two or three dimensions throughout the water column. However, its two-dimensional version is used most commonly for storm surge. These programs utilize the finite element method in space allowing the use of highly flexible, unstructured, high-resolution grids. Because of its skill and ability to provide excellent results at a high resolution, ADCIRC is sometimes referred to as a “high fidelity” model (see Webb 2017 for more explanation of modeling terminology).

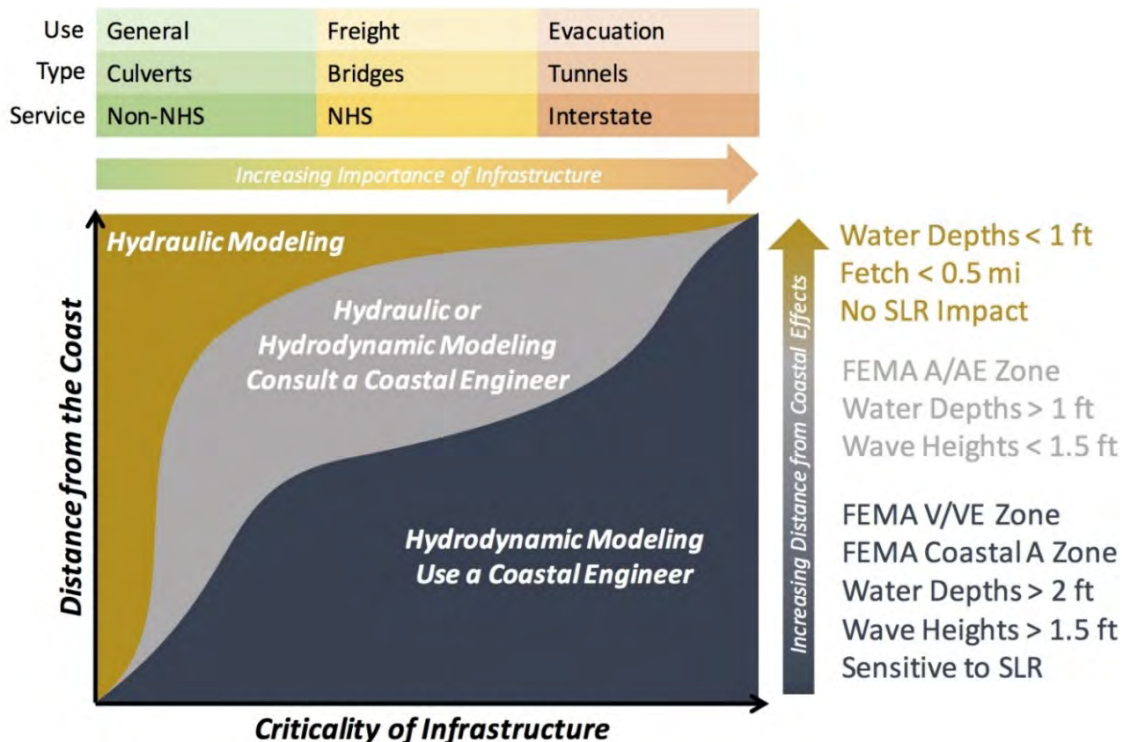


Figure 4.17. When and where to apply riverine hydraulic and coastal hydrodynamic models as a function of distance from the coast and importance of infrastructure (Webb 2017)

Table 4.3. Numerical coastal models cited in this manual

Model/Program	Comments
ADCIRC	Hydrodynamic model (often used to model storm surge)
SLOSH	Storm surge model
ET-SURGE	Storm surge forecasting model
DELFT-3D	Hydrodynamics, waves, and morphology model
MIKE-21	Hydrodynamics, waves, and morphology model
FVCOM	Hydrodynamic model
WAM	Wave model
STWAVE	Wave model
CMS	Hydrodynamics, waves, and morphology model
SWAN	Wave model
CH3D	Hydrodynamic model
EDUNE	Dune erosion model
SBEACH	Cross-shore morphology model
XBEACH	Hydrodynamics, waves, and morphology model
CSHORE	Cross-shore wave and morphology model
CHAMPS	Cross-shore wave and morphology model

Although ADCIRC does not explicitly model wind waves, it can incorporate their effects on storm surge. Gradients in wave momentum can be specified as additional model inputs which are obtained from a separate wave model. Appropriate coupling between ADCIRC and a numerical wave model yields accurate storm surge elevations which include wave setup effects (Dietrich *et al.* 2011). Central to its use in modeling storm surge, the ADCIRC model includes Holland-type (Holland 1980) parameterization of tropical storms based on general storm characteristics like central pressure, maximum wind speed, radius to maximum winds, etc. These models, including some significant enhancements inherent to ADCIRC, make it a particularly useful tool for simulating peak storm water levels in tropical storms. At the time of producing this manual, typical practice of the USACE and other entities is to apply ADCIRC in many coastal surge modeling efforts (USACE 2011b, 2015, FEMA 2011, Webb 2017, CERA 2018). Aligning with such efforts (and being able to readily use available model inputs and outputs) makes the ADCIRC model a strong candidate for the higher levels of effort in vulnerability assessments (as discussed in Chapter 14: Analysis Methods for Assessing Vulnerability to Coastal Storms).

Numerous hydrodynamic models can be used to estimate storm surge water levels. While their details vary, they all typically solve some similar set of governing conservation equations for mass and momentum, accept similar types of boundary conditions and forcing, and do not explicitly model the waves. One well-known example, the Sea, Lake, and Overland Surges from Hurricanes (SLOSH) model, was developed by the National Weather Service (Jelesnianski *et al.* 1992; Glahn *et al.* 2009). The SLOSH model has been used for years to develop coastal Storm Surge Inundation Maps (SSIMs) primarily for input to emergency evacuation decisions. Inherent limitations in SLOSH have led many investigators toward other models like ADCIRC for detailed mapping of coastal flooding. The SLOSH model accounts for a local balance between the sea surface slope induced by the wind stress and the restorative forces of gravity and Coriolis and bottom drag, but it does not include some of the governing physics explicitly such as momentum acceleration effects and wave setup effects. These can be important components of storm surge. Other issues relate to the ability of SLOSH grids to highly resolve large areas adequately.

Other storm surge models include the extratropical storm surge model ET-SURGE (or ETSS) developed by NOAA as an operational forecast tool providing surge guidance for extratropical storms like nor'easters. The ET-SURGE model is a variation of SLOSH forced by real-time output of winds and pressures from NOAA's National Centers for Environmental Prediction's Global Forecast System (Kim *et al.* 1996; Glahn *et al.* 2009). Other hydrodynamic models which can be used for storm surge modeling include the Curvilinear Hydrodynamics Three-Dimensional (CH3D) model (Sheng 1990; Johnson *et al.* 1991), the DELFT3D model (Vatvani *et al.* 2012), the MIKE-21 Model (Savioli *et al.* 2003) and the Finite Volume Coastal Ocean Model (FVCOM; Chen *et al.* 2006). These models offer fully three-dimensional results of extended coastal ocean processes. Others, like the USACE Coastal Modeling System (CMS) strictly provide two dimensional (depth-integrated) solutions (Buttolph *et al.* 2006).

An example of a numerical mesh used for estimating storm surge in the Atlantic basin is shown in Figure 4.18. It has over 400,000 nodes and covers the entire Gulf of Mexico, Caribbean Sea, and much of the western North Atlantic Ocean. The spacing of the nodes is very large in the open ocean and so small near the coast that they can't be seen in Figure 4.18 except as solid blue. The extensive coverage is considered necessary to adequately capture the large-scale aspects of hurricane storm surge.

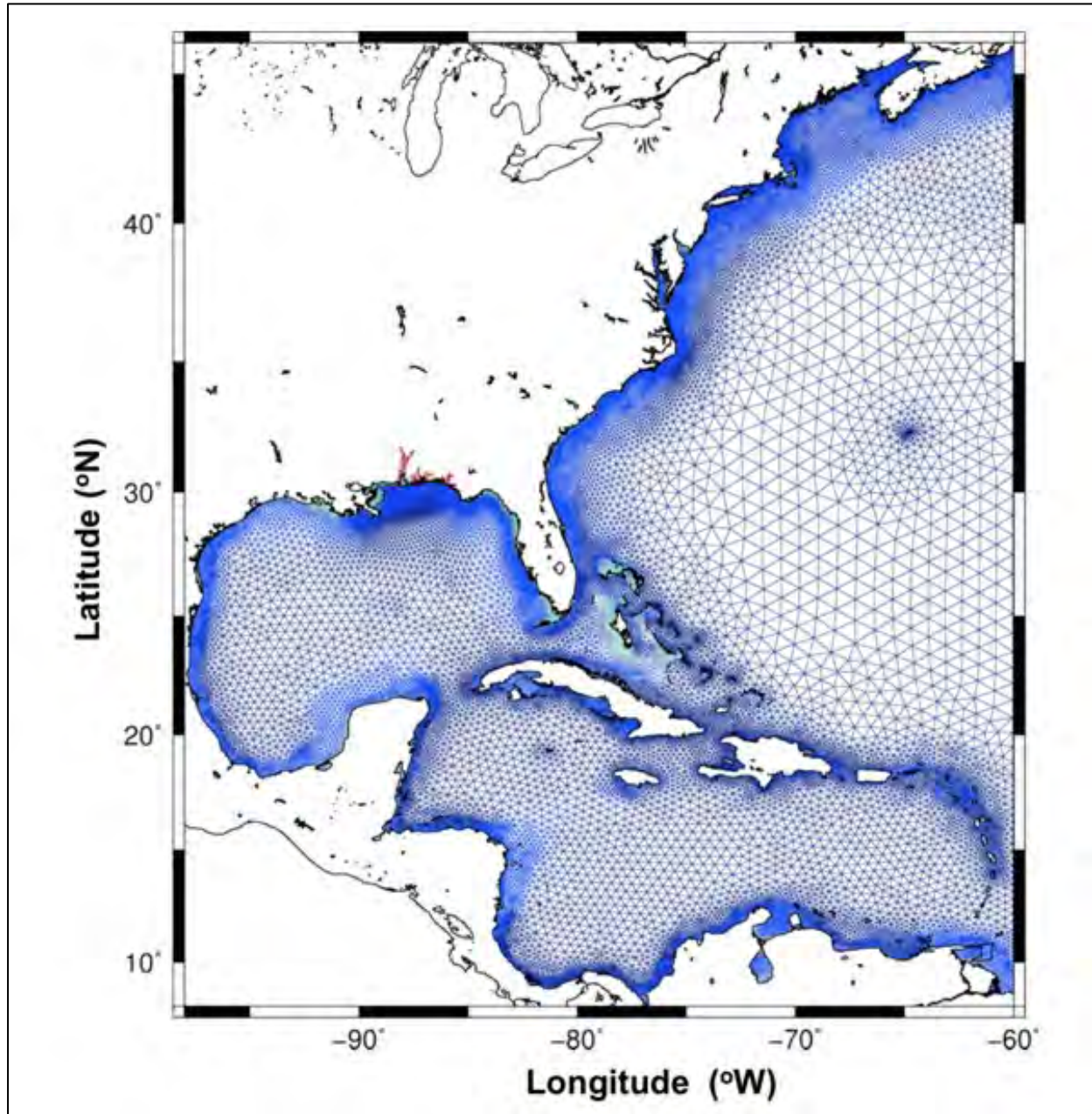


Figure 4.18. Example of numerical mesh used for a storm surge model

Along the coast, the numerical storm surge model mesh should include upland areas to account for flooding. An example topographic-bathymetric mesh surface for a storm surge model of Mobile Bay, Alabama is shown in Figure 4.19. It includes both the water and the low-lying lands adjacent to the water. The topography shown includes all the areas with elevations below 50 ft. The extensive area in Figure 4.19 to the north of Mobile is the Mobile Delta area which is the historical river deltas of the Tombigbee and Alabama Rivers.

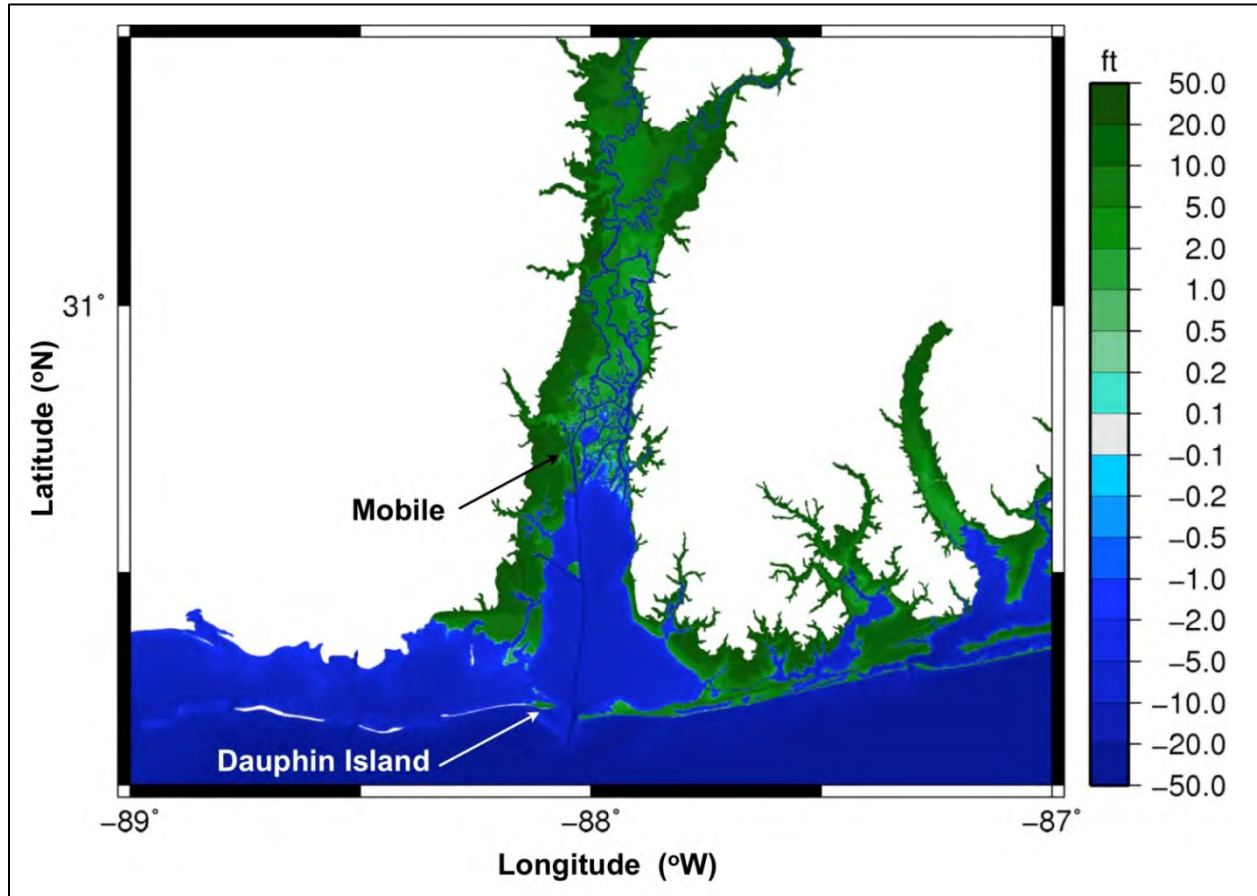


Figure 4.19. Detail of a seamless topographic-bathymetric mesh surface used for modeling coastal storm surge flooding

An example of output from a storm surge model is shown in Figure 4.20. This output is from a “hindcast” of Hurricane Katrina (2005) for the Alabama coast. **Hindcasting is the use of a model to simulate a past time period and is often used to validate that a model is working.** The colors represent the maximum water surface elevation during the passage of the storm. Modelled surge elevations exceeded 12 ft in the northern end of Mobile Bay but much less at the southern end of the bay. These values are consistent with the actual surge values in the bay during passage of the storm. The strong south winds were causing significant wind setup of the water surface in the bay, and the numerical model captures that well. The highest surge values shown are at the western boundary of this hindcast in coastal Mississippi. Hurricane Katrina was making landfall near the Mississippi-Louisiana border, roughly 100 miles to the west of the mouth of Mobile Bay at this time.

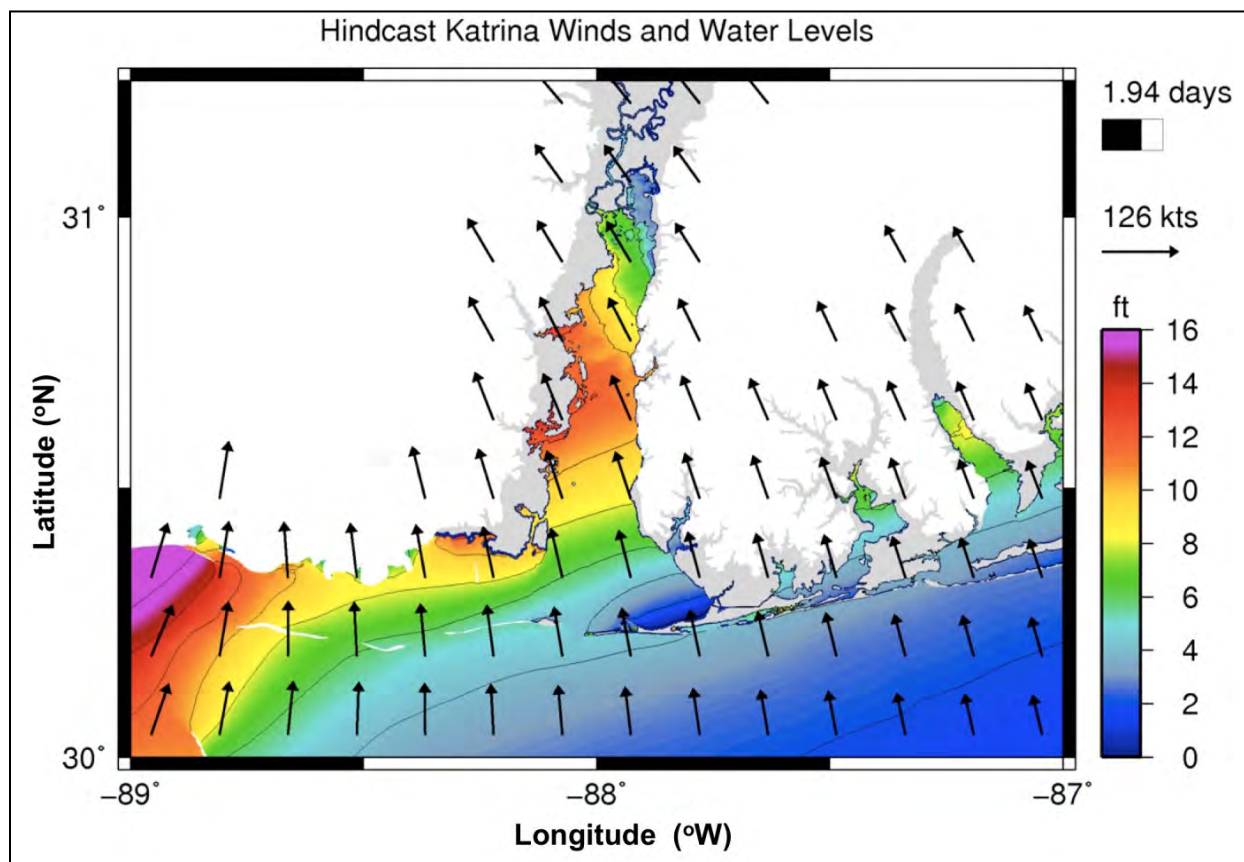


Figure 4.20. Example of storm surge model output (with input winds) along the Alabama coast during Hurricane Katrina (2005)

**ADCIRC also produces good storm surge forecasts.** The Coastal Emergency Risks Assessment system provides on-line storm surge forecasts at a high resolution whenever a hurricane is approaching the US.<sup>3</sup> Forecast exposure of individual coastal transportation facility locations, roads and bridges, can be evaluated. The storm forecast (track, windspeed, forward speed, size, etc.) from the National Hurricane Center (NHC) is the primary input to the model. The surge forecasts change as the NHC storm track and strength forecasts change. The surge forecasts are limited by the uncertainty in the input storm parameter forecasts with additional scientific uncertainty inherent in the model. However, the surge forecasts provide good results due to their high resolution (CERA 2018). North Carolina DOT has integrated the on-line forecasts from CERA with their internal GIS-based asset management database and can visualize and quantify which facilities are at risk as hurricanes approach (NCDOT 2018).

One promising approach for both developing risk-based design storm data and for forecasting storms is the general approach called a “**surrogate model.**” Essentially, a high-fidelity model for storm surge, with coupled models for waves and runup, are run for the full range of possible storm characteristics with the results placed in a matrix. Queries of that matrix are a surrogate to actually running the models. The big advantage is run time. Thousands of hours of computational time for

<sup>3</sup> <https://cera.coastalrisk.live/> website for the Coastal Emergency Risk Assessment program which is affiliated with LSU and UNC (accessed September 12, 2018)

the real models are reduced to seconds in the surrogate model. Smith *et al.* (2012) and Taflanidis *et al.* (2013) describe the approach with a surrogate model developed for coastal storms in Hawaii.

Most of the available storm surge models compute the velocity of flow in the incoming and outgoing surge. Thus, the velocity of flow, usually depth averaged, is a part of the output. These flow values can be important in some damage mechanisms including hydrodynamic forces on structures and bridge scour. However, the resolution and detail in the velocity estimates from these models depends on the resolution and detail in the numerical grid/mesh of the model. Individual building edges and road embankments can be appropriately accounted for in these models.

#### 4.3.3 Wave Setup

A phenomenon called wave setup is also a component of storm surge at some locations. Wave setup occurs primarily in the surf zone and landward of the surf zone such as on a flooding barrier island or behind a reef. **Wave setup is an increase in mean (time-averaged) water level at a location due to the presence of the waves.** For example, average water levels on a beach can be higher than those at the end of a beach pier due to wave setup. Wave setup is due to the momentum flux of the water by wave action and is greatest when waves are breaking (Dean and Walton 2018). Wave setup increases with wave height and the magnitude of the contribution of wave setup to storm surge can be up to several feet at some locations during major coastal storms.

Some models, including ADCIRC, DELFT3D and MIKE 21, are capable of dynamically incorporating wave contributions to storm surge through momentum transfer and wave setup. Such models are said to be dynamically coupled passing the circulation and wave model results back and forth in order to model the effects of waves on storm surge and currents, as well as the effects of storm surge and currents on wave generation, transformation and breaking.

#### 4.3.4 Impacts of SLR on Storm Surge

This section discusses the likely effects of SLR on storm surges and other factors that could influence the strength, frequency and damage of coastal storms in future environmental conditions.

Sea level rise can clearly increase flood depths along the coast due to storm surge. However, this is not a “one-to-one” or linear relationship. A one-foot rise in sea level will not necessarily produce a one-foot rise in storm surge elevation at most coastal locations. This is because of the complex physics of coastal storm surge inundation and wave propagation. Storm surge at any location for a specific storm is a complex function of the storm’s interaction with the ground elevations around that location. Those interactions will likely change somewhat as different areas will be flooded at different depths. A significant portion of onshore storm surge is due to wave setup which is very sensitive to local depth and ground slope. There will also, likely, be geomorphological changes along the coast, such as wetland changes. These will also affect the relationship between sea level rise and increased storm surge elevations.

**One foot of future sea level rise can increase storm flood levels more than one foot! There is a nonlinear relationship between sea level and flood level.**

Detailed methods for incorporating future sea levels into quantitative storm surge modeling are outlined in Chapter 14. Several recent, numerical, hydrodynamic model studies of storm surge under different sea level rise scenarios have demonstrated this “nonlinear” response of storm

surge (and also waves) to increased water levels (Smith *et al.* 2010; Choate *et al.* 2012; Hagen and Bacopoulos 2012; Atkinson *et al.* 2013). In some cases, and locations, particularly in shallow water near the coast, the incremental change in storm surge can be greater than the corresponding sea level rise. In other words, the storm surge increase will be amplified compared with the sea level rise. In other cases, and locations, the storm surge increase will be less than the sea level rise increment but still greater than a similar storm surge on present-day sea levels.

There has been a substantial increase in hurricane activity in the Atlantic since the 1970s and these increases have been linked, in part, to higher sea surface temperatures (Melillo *et al.* 2014). There have long been concerns about increases in the strength of individual coastal storms as well as the frequency of, and damage produced by, coastal storms. However, in spite of these logical linkages, research on coastal storms provides varied conclusions. There are significant issues with the historical data record and other factors (Church *et al.* 2001; IPCC 2007; Knutson *et al.* 2010).

Knutson *et al.* (2010) summarizes the research into each of these aspects (strength, frequency, damage) related to tropical storms in the future. Bender *et al.* (2010) have suggested, based on atmosphere-ocean models, that there may be an increase in the number of large hurricanes but a slight decrease in the overall frequency of all tropical storms in the north Atlantic.

#### **4.4 Coastal-Riverine Flooding**

Some extreme flooding is related to the interaction of coastal storm surge and runoff from rainfall on watersheds near the coast. Combined hydraulic and hydrodynamic simulations of flow and water levels reveal that rainfall-runoff can significantly affect coastal water levels and that the presence of storm surge generally results in higher flood levels upstream. Important to these results are the topography of the watershed and an associated time lag between the rainfall event and the storm surge (Blumberg *et al.* 2015, Klerk *et al.* 2015, McGuigan *et al.* 2015, Torres *et al.* 2015).

Coastal flooding can exacerbate upstream flooding, subsequently impacting bridges some distance from the coast. The elevated coastal water levels act as a downstream control for storm related rainfall runoff within coastal watersheds. Until the surge recedes, this runoff does not have anywhere else to go, increasing the backwater and flooding effects. This flooding may occur over some time, possibly more time than the storm surge duration. Additionally, the probability of exceedance of the resulting flood level may be much greater than the frequency of either the storm surge event or the rainfall event. In other words, a storm with a 10-year return period storm surge and a 15-year return period rainfall might combine to produce a 100-year return period flood event at a specific location.

Consider the following example from the Texas coast during Hurricane Harvey in 2017. Figure 4.21 shows measured water level heights from a NOAA tide gage located at Sabine Pass on the Texas Coast and from a USGS stream gage located on the Sabine River near Orange, TX. The USGS gage is approximately 30 miles from the coast. In order to aid in their comparison, the predicted tidal signal was removed from the measured water levels at Sabine Pass, resulting in a time-series of the non-tidal residual (NTR) water levels (NTR = Measured Water Level – Predicted Tide). In this manner, the NTR (gray line) represents all non-tidal contributions to measured water levels at the coast. A 24-hour moving average applied to the NTR, shown by the black dashed line, shows the slowly-varying behavior of water levels at the coast. Note how the coastal surge peaks just before August 30, 2017 as Hurricane Harvey makes its second and final landfall along the Texas coast. Flooding at the USGS gage closely mimics the behavior of the downstream coastal stage.

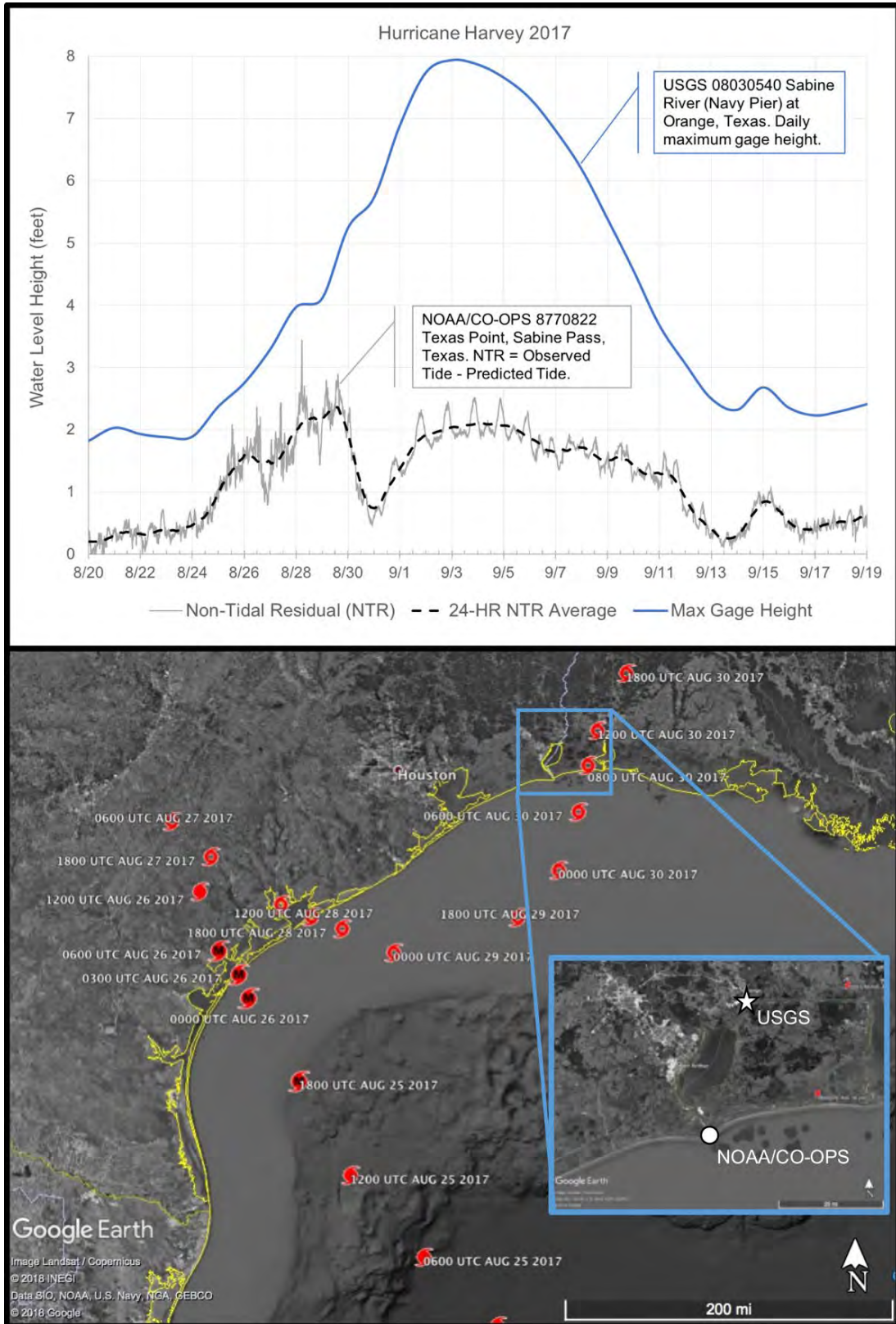


Figure 4.21. Water level measurements near Sabine, Texas (upper panel) and the path of Hurricane Harvey (lower panel)

As the storm passes to the east of the NOAA tide gage at Sabine Pass, north winds on the west side of the eye push the surge offshore resulting in a lowering of the coastal water levels at the tide gage. However, water levels at the USGS gage on Sabine River continue to increase until September 3, 2017. This fluvial flooding drives an increase in the coastal stage that persists over a nearly two-week period from 9/1/17 to 9/13/17. This example demonstrates well how coastal flooding contributes to backwater effects and how fluvial discharge can impact downstream coastal flooding.

When considered individually or as components, the peak flow resulting from storm surge tends to be much higher than that from rainfall-runoff, owing to the intense flood and ebb of storm surge during a short duration storm event. However, the total flood volume draining toward the coast tends to be dominated by rainfall-runoff (Torres *et al.* 2015).

Hydraulic design associated with peak flow (e.g. bridge foundation, culvert, drain, etc.) would likely be sensitive to the increased flows associated with the rushing flood or ebb of storm surge. Design that is most concerned with flow volumes (e.g. detention basins, routing reservoirs, stormwater wetlands, etc.) would be more sensitive to long-lasting or delayed drainage due to combined rainfall-runoff and storm surge.

Because this compound flooding is so dependent on location-specific characteristics, the joint probability of rainfall-runoff and storm surge bears consideration. Sea level rise is one major cause of increased coastal flooding, but sea level effects will likely increase the probability of compound events (surge and heavy precipitation), augmenting flooding potential in some areas (Wahl *et al.* 2015).

#### **4.5 Lake Water Level Fluctuations**

The Great Lakes, the Great Salt Lake, and other very large inland lakes are tideless. They are completely separated from the oceans and are too small for any astronomical tides of their own. Water levels in these large inland lakes have significant fluctuations however in response to rainfall/snowmelt in their drainage basins and winds associated with major weather events.

Many of these very large lakes have their own local lake level datums that are used for science and engineering related to the water level. A bulletin describing lake levels for the Great Lakes is available from the Detroit District of the USACE on-line (USACE – Detroit District 2018).

Figure 4.22 shows an example of seasonal fluctuations of Lakes Michigan and Huron. The lake levels generally rise in the spring and fall in the fall. Also shown is the 6-month forecast lake levels at the time this graphic was downloaded (September 2018). The lake levels for 2017 and 2018 shown in Figure 4.22 are higher than the long-term average. However, some of the historical water level lows occurred as recently as 2012 and 2013.

Figure 4.23 shows a much longer historical record of average annual lake levels. The dashed, horizontal line is the average for the entire period of record. There have been 5 to 6 ft of maximum lake level change in the past century. A 15-year period of low lake levels prior to 2013 was followed by an increase in lake levels that was unprecedented (Gronewold *et al.* 2015).

High lake levels cause increased bluff erosion as waves strike higher elevations. Interestingly though, there are erosion issues related to the historically low water levels, too. The lower levels expose the base of seawalls to different levels of air, ice and waves.

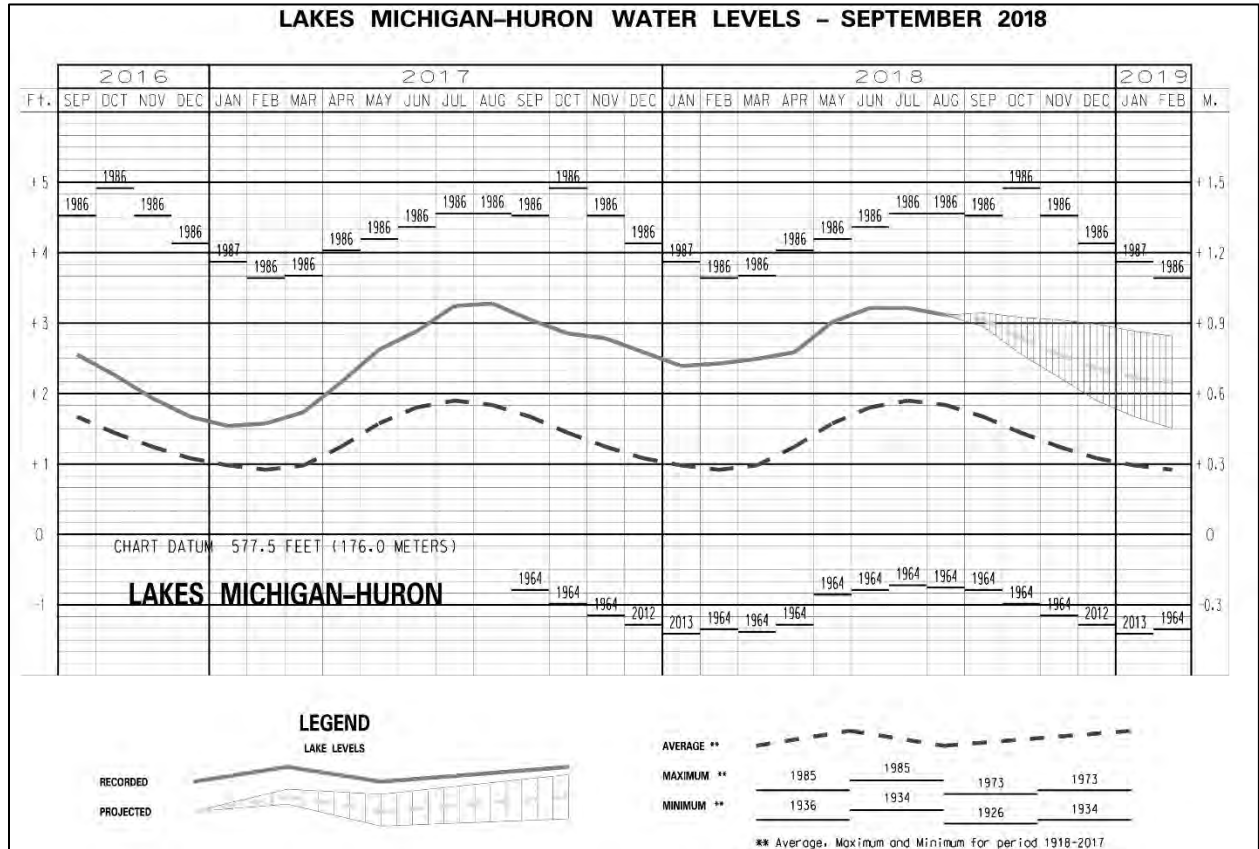


Figure 4.22. Example of seasonal lake level fluctuations (USACE-Detroit District 2018)

Lake levels depend on the hydrologic balance, including precipitation, runoff, evaporation and outflow. Most studies conclude that lake levels will fall (Hayhoe *et al.* 2010, Angel and Krunkel 2010) but some question the level of reduction (Lofgren *et al.* 2011). Mackey (2012) presents a range of possible scenarios with reductions of 0.66 ft (0.2 m) to about 3.3 ft (1 m) by the end of the century. An interactive, on-line “Great Lakes Water Level Dashboard,” Smith *et al.* (2016), allows for graphical presentations/comparisons of the long-term lake level forecasts. The magnitude of the range in fluctuations is similar to long-term water-level changes in the lakes (e.g. 33-yr, 60-yr, 160-yr fluctuations), making it difficult to differentiate between change and variability (Baedke and Thompson 2000; Baedke *et al.* 2004).

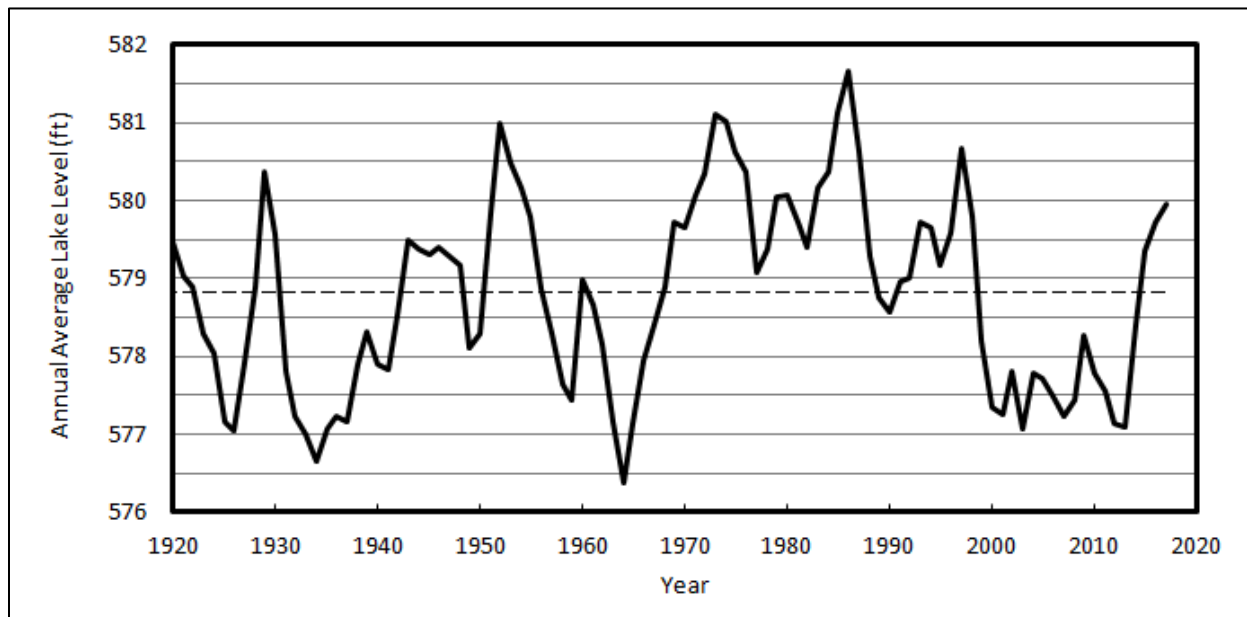


Figure 4.23. Annual lake level fluctuations – Lakes Michigan and Huron (dashed line is the long-term average)

One interesting phenomenon is the “seiching” of the lakes. A **seich** is a long-period (several hours duration in the lakes) oscillation of the water levels after passage of a weather front. Lake Erie and Lake Ontario are particularly susceptible to these extreme storm surge levels and subsequent seiching motions. A storm in 1985 caused so much wind stress across Lake Erie that the water level at Toledo dropped 4 ft while the water level at Buffalo rose 4 ft. After passage of the front to the east, the lake levels oscillated back and forth for several days. The water levels rose and fell at opposite ends of the lake while the water level in the middle of the lake, near Cleveland, remained nearly constant. Investigations of seiching in Lakes Michigan and Huron reveal that the two systems are coupled and cannot be considered separately.

One phenomenon that occurs in the Great Lakes, as well as in all water bodies, is the **meteotsunami**. Barometric pressure fluctuations can combine with wind fields to cause wave oscillations that can propagate alongshore in response to the distant forcing. For tsunamis, the distant forcing is a submarine landslide and for meteotsunamis the forcing is a meteorological disturbance on the water surface such as very quick increases in winds or a pressure disturbance-anomaly related to a weather front (Monserrat *et al.* 2006). These can explain freak wave occurrences that have occurred in the Great Lakes (Anderson *et al.* 2012) and along the Atlantic Coast where they are also called squall line surges (Dean and Dalrymple 2002).

## 4.6 Design Water Levels

The selection of a design water level can be one of the most important coastal engineering decisions for the designs and structures discussed in Part 3 of this document. For example, the design still water level (SWL) often controls the design wave height, stone size and extent of armoring on coastal revetments. Also, wave loads on elevated bridge decks are extremely sensitive to water level. Essentially, the water level dictates the reach and the power of waves.

Typical practice in hydraulic engineering addresses design water level decisions using the traditional, risk-based approach of a “design return period.” To illustrate, the FHWA regulation 23 CFR § 650.105(b) defines the “base flood” as “mean the flood or tide having a 1-percent chance of being exceeded in any given year.” As “tide” indicates the storm tide (or storm surge), for HICE,

the "100-year storm surge level" is the surge elevation with a 1%-annual probability of exceedance. Each year, there is a 1% chance that a storm surge of this magnitude (or greater) will occur. Some coastal designs may justify a lower return period (e.g. 25- year or 50-year) in certain areas – balancing the greater risks affiliated with such design with engineering and economic considerations. Chapter 13 Engineering Risk at the Coast discusses these fundamental risk-based design concepts.

The many potential sources of coastal water level data include federal agencies, state agencies, universities, and private consultants. This section describes only a limited subset of potential data sources.

Obtaining water level data for the purpose of engineering design has long been a challenge especially in coastal regions. These existing sources of measured and analyzed data tend to be far from where they are needed for transportation design. Some form of modeling, ranging from simple to complex, is typically needed in order to overcome the geographic gap between where data exist and where they are needed. In recent years, the availability of coastal hazard data, including storm surge water levels, has improved greatly.

**The USACE Coastal Hazards System is a useful online source for design water level information.**

The USACE's Coastal Hazards System is an online database for water levels and other "hazards" including waves. As a component of the North Atlantic Coast Comprehensive Study funded in the aftermath of Hurricane Sandy, the USACE initiated development of this system which contains high resolution hazard data in coastal regions around the US including the Great Lakes (USACE 2019). This Coastal Hazards System database contains densely spaced points of hydrodynamic "data" along the coast in open water and on the coastal floodplain. These data are the output from hydrodynamic models. The density, location, and data available at each point make this dataset useful for coastal transportation projects. Most data points provide water level, depth-averaged water velocity, wave height, wave period, wave direction, wind velocity, and atmospheric pressure time-series and/or representative statistics for each of the synthetic storms (hundreds or thousands) simulated with storm surge and wave models. Annual exceedance probabilities (AEPs) for water levels, wave height, and wave period ranging from 0.1 percent to 10 percent (10-, 20-, 50-, 100-, 200-, 500-, and 1,000-yr return periods) are available. In addition to the expected value AEP for each parameter, the 68 percent, 85 percent, 95 percent, and 98 percent confidence limits are also given.

Consider an example from the Texas coast shown in Figure 4.24. That figure shows the expected AEP and associated 98 percent confidence interval for water level, significant wave height, and peak wave period for a point near the CR 257 bridge that crosses San Luis Pass between Galveston and Follets Islands. For example, the 50-year return period water level is slightly higher than 3 m (10 ft).

FEMA, as part of their flood insurance mapping mission, has estimated 100-year flood levels and areas of subsequent inundation along much of the US coast. However, the techniques used to develop these coastal FEMA products are constantly evolving. The accuracy of the FEMA results can be limited and should be evaluated carefully before use in design and planning of coastal transportation facilities.

Some of the more recent FEMA coastal modeling efforts related to mapping have used state-of-the-art surge models including high resolution ADCIRC modeling. FEMA documentation specifies these coastal products are for flood mapping for insurance purposes only. While similar FEMA

products are commonly used for upland riverine flood engineering analysis and flood plain regulation by local government, those riverine products are based on the same basic technologies (regression analysis for runoff and the standard back-step model for backwater computations) that have been used successfully for riverine flooding for decades.

Many emergency management agencies have coastal inundation maps that are based on results from hydrodynamic models. The SLOSH model is usually used to estimate the worst possible flood level for each of the Saffir-Simpson scale storm categories. These may provide an estimate of extremely rare storms but do not provide risk-based information for design. Some USACE Districts have developed their own water level-return period relationship for design at many coastal locations. Some State resource management agencies, e.g. Florida's Department of Environmental Protection, have developed estimates of surge-return period relationships along the coast.

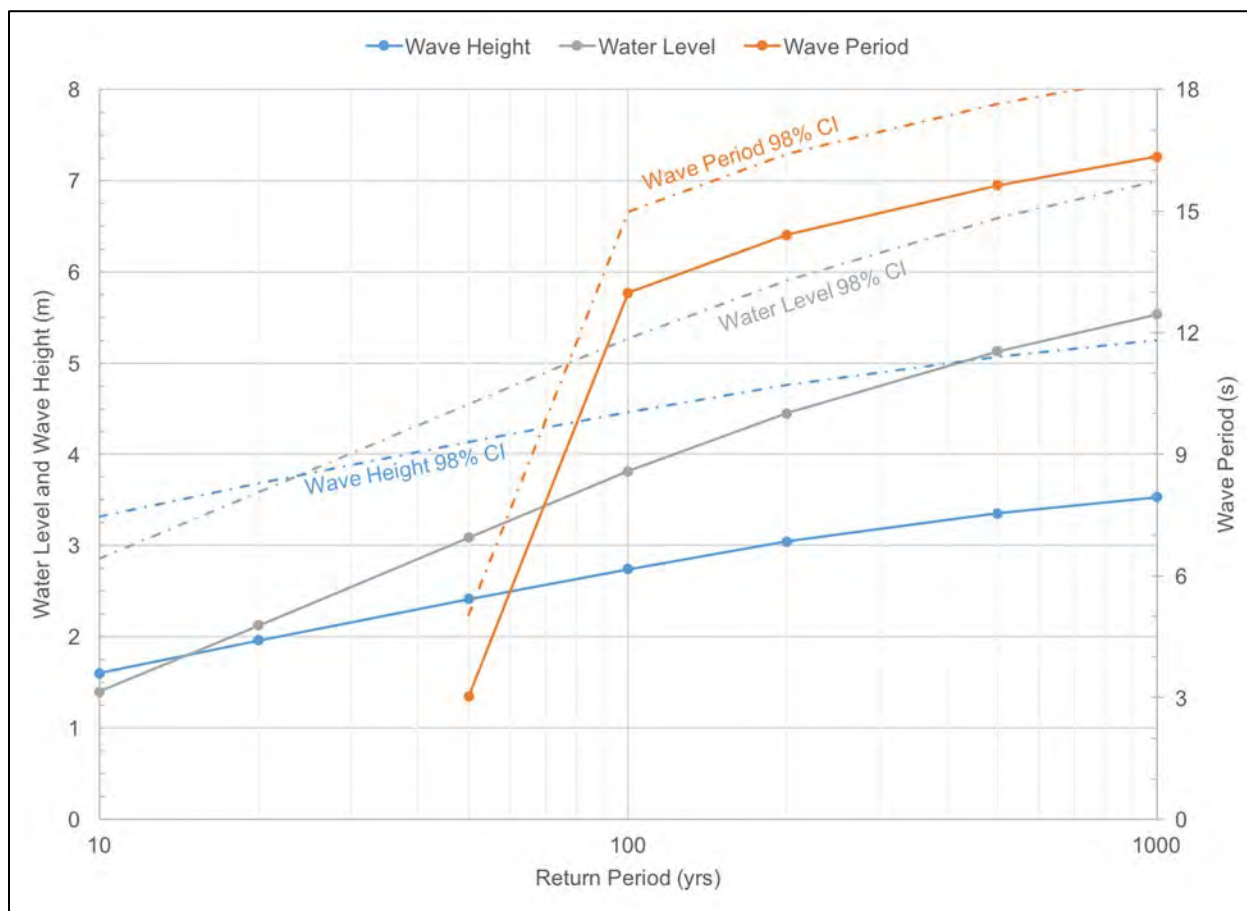


Figure 4.24. An example of water level, wave height and wave period values near San Luis Pass, Texas obtained from the USACE Coastal Hazards System database

All available estimates of the surge-return period relationship should be collocated and evaluated carefully before use in design. Available estimates are often not adequate for design of site-specific coastal works and the judgment/review of an experienced, qualified coastal engineer can be valuable. The Florida DOT has researched application of such analyses and developed a protocol that may be useful for others to review and adopt (Sheppard and Miller 2003).

The literature provides examples of a probabilistic, numerical approach; using a hydrodynamic model for storm surge simulations and historical storm information; for application at major

infrastructure studies and projects (e.g. USACE 2015, Bosma *et al.* 2015). The model should be calibrated appropriately. Input storm conditions for historical hurricanes for the past 150 years are available from the NOAA HURDAT database. There are two general approaches to assigning the proper probability to historical storms and other "hypothetical storms;" 1) the Joint Probability Method (JPM) which is typically used by FEMA in their coastal flood studies (now usually with an optimal sampling scheme), and 2) the Empirical Simulation Technique (EST) which was developed by the USACE to develop site-specific water level-return period relationships (USACE 2002). This type of analysis likely necessitates the integration of a qualified, coastal engineer or scientist into the design team.

**None of the available data for determining design water levels mentioned above includes the effects of future sea level rise (SLR).** Chapter 14 – “Analysis Methods for Assessing Vulnerability to Extreme Coastal Events” presents techniques for including future SLR in design water levels.

*Page Intentionally Left Blank*

## Chapter 5 - Waves

Waves, one of the primary hydraulic forces affecting our coasts, are caused by a disturbance of the water surface. The original disturbance may be caused by winds, boats or ships (wakes), or other disturbances such as underwater landslides due to earthquakes (tsunamis). But wind generates most of the waves that strike our coasts. After waves are formed, they can propagate across the surface of the sea for thousands of miles. When waves break on a shoreline or coastal structure, they have fluid velocities and accelerations that can impart tremendous forces. When riding on top of storm surge, waves can strike roads and bridges that are typically not designed for such forces.

Practical wave mechanics is a blend of theories and empirical evidence. Several wave theories, including the small-amplitude wave theory, and Stokes 2<sup>nd</sup> order wave theory developed in the late 1800s, are still used today. Much of the practical scientific study of coastal waves changed during World War II. Plans for amphibious landings such as at Normandy on D-Day and on the Pacific Islands later in the war needed the highest possible quality predictions of the surf conditions that the landing craft could expect. Research led to equations for forecasting wave heights based on wind speeds as well as equations for estimating how waves break in shallow water. That research revolutionized nearshore oceanography and led to predecessors of the coastal engineering tools still used today and that this manual briefly summarizes below.

### 5.1 *Definitions, Theories, and Properties of Waves*

This section introduces the basic definitions used in wave mechanics, some of the more useful engineering properties of waves, and in brief, several of the most important wave theories. Many engineering applications of wave theories rely on the small-amplitude wave theory. However, several important engineering properties can only be explained by more complex theories or by empirical methods.

Figure 5.1 depicts the basic parameter definitions in the simplest model of water waves. The wave in Figure 5.1 is assumed to be progressing toward the right and the individual waves are long-crested (such that the 2-dimensional plane shown in Figure 5.1 is sufficient) and part of an infinite train of repeating waves. The basic length scales used to define the wave are the wavelength ( $L$ ) defined as the distance between wave crests, and the wave height ( $H$ ) defined as the difference between the elevation of the crest and the trough of an individual wave. Waves are called monochromatic waves in this simplest model since the waves are all the same wavelength. The water depth ( $d$ ) is defined as measured to the still water level (SWL), the level of the water if the waves were not present. Wave period ( $T$ ) is the time a wave takes to travel one wavelength.

Small amplitude wave theory provides estimates of many of the basic engineering properties of the monochromatic wave train on a fixed water depth. The result is a progressive, monochromatic wave solution to the boundary value problem consisting of the governing equations of motion for irrotational motion of an inviscid fluid (Laplace's equation) and the appropriate boundary conditions.

A fundamental assumption in the theoretical development of the theory is that the wave amplitude is small. Coastal engineers define amplitude ( $a$ ) as  $\frac{1}{2}$  of wave height ( $H$ ) or  $a = H/2$ . The small-amplitude wave theory is often called "linear wave theory" because the small-amplitude assumption allows for the boundary conditions to be mathematically "linearized" and thus solved.

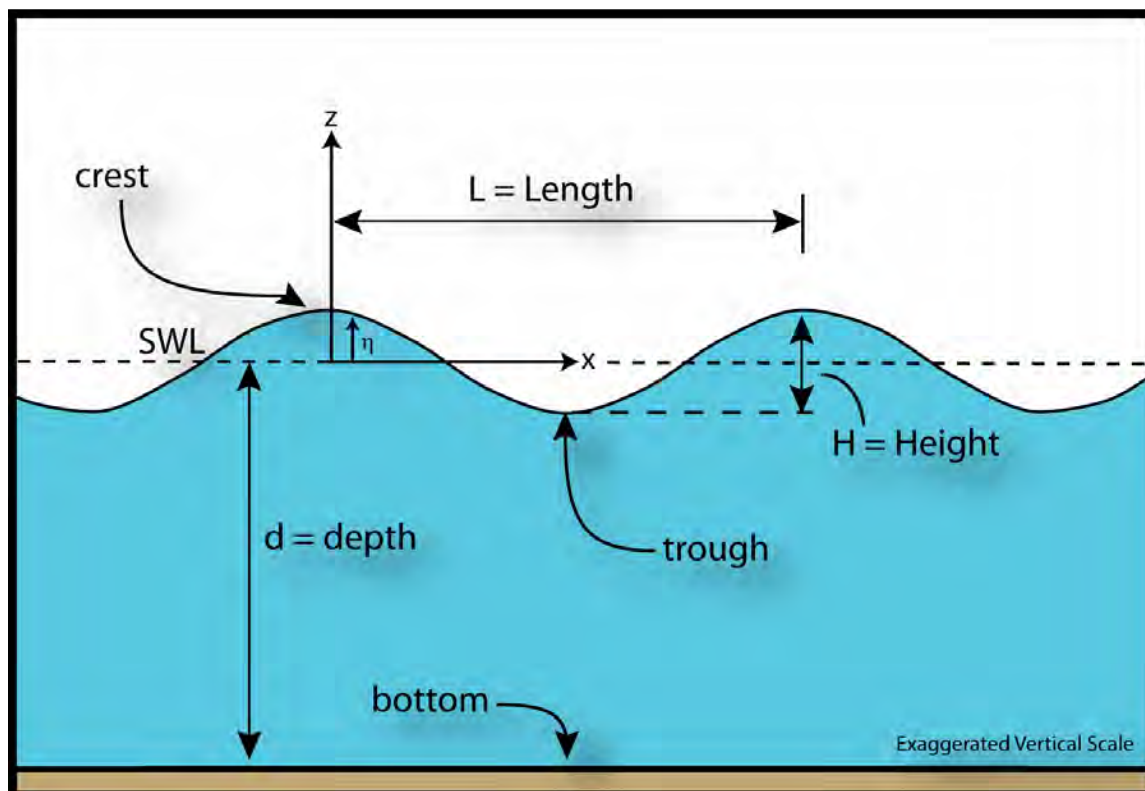


Figure 5.1. Wave parameter definitions

In spite of the seemingly limiting assumption of small waves, **small-amplitude wave theory estimates many of the basic properties of waves very well.** For more information on the theoretical basis and results of small-amplitude wave theory, see Dean and Dalrymple (1991) or Sorensen (1993).

The primary small-amplitude theory solution for the water surface elevation ( $\eta$ ) is a cosine wave (as shown in Figure 5.1) described by Equation 5.1.

$$\eta = \frac{H}{2} \cos\left(\frac{2\pi x}{L} - \frac{2\pi t}{T}\right) \quad (5.1)$$

where:

$\eta$	=	water surface elevation (as measured from the SWL)
$H$	=	wave height
$x$	=	horizontal position
$t$	=	time
$L$	=	wavelength
$T$	=	wave period

Small-amplitude wave theory indicates that three of the four basic parameters describing the basic wave model are not independent. Specifically, the wavelength ( $L$ ) is a function of water depth and wave period ( $T$ ) (Equation 5.2):

$$L = \frac{gT^2}{2\pi} \tanh\left(\frac{2\pi d}{L}\right) \quad (5.2)$$

where:

$g$	=	acceleration due to gravity
-----	---	-----------------------------

d = water depth  
 tanh = hyperbolic tangent function

In deepwater, where the depth is greater than one-half the wavelength ( $d > L/2$ ), Equation 5.2 reduces to:

$$L_0 = \frac{gT^2}{2\pi} \quad (5.3)$$

where:

$L_0$  = wavelength in deepwater

Wave speed, or celerity (C), is the speed at which the wave form moves across the ocean surface. Based on the parameters above, this is:

$$C = L/T \quad (5.4)$$

where:

C = wave celerity

In deepwater, Equation 5.4 becomes:

$$C_0 = \frac{gT}{2\pi} \quad (5.5)$$

where:

$C_0$  = wave celerity in deep water

Note that Equation 5.5 suggests that waves of different periods move at different speeds in deep water.

In shallow water, where depth is less than one-twentieth of the wavelength (i.e.  $d < L/20$ ), Equation 5.4 becomes:

$$C = \sqrt{gd} \quad (5.6)$$

Equation 5.6 indicates that **all waves move at the same speed in shallow water** regardless of wave period and that waves slow down as they move into shallower water.

Equation 5.2 is an implicit equation for L. One explicit approximation to Equation 5.2 is Eckart's approximation:

$$L \approx L_0 \sqrt{\tanh\left(\frac{2\pi d}{L_0}\right)} \quad (5.7)$$

Equation 5.7 gives results within 5% of those from Equation 5.2. Given the lack of precision of input conditions in many coastal design situations as well as the uncertainty inherent in the analytical methods this accuracy is often acceptable for engineering purposes.

Instantaneous water particle velocities in waves are given by the small-amplitude wave theory, as:

$$u = \frac{\pi H}{T} \left( \frac{\cosh[k(d+z)]}{\cosh[kd]} \right) \cos(kx - \sigma t) \quad (5.8)$$

and

$$w = \pi H / T \left( \frac{\sinh[k(d+z)]}{\cosh[kd]} \right) \sin(kx - \sigma t) \quad (5.9)$$

where:

u	=	horizontal component of water particle velocity
w	=	vertical component of water particle velocity
k	=	wave number = $2\pi/L$
$\sigma$	=	wave frequency = $2\pi/T$
z	=	vertical direction (measured from the SWL, see Figure 5.1)
cosh	=	hyperbolic cosine function
sinh	=	hyperbolic sine function

Note that the velocity field in waves is oscillatory or orbital, with respect to the wave phase or the position of the wave crest. The velocity equations have essentially three parts: (1) an oscillatory term with the sine or cosine function, (2) a hyperbolic function of z which is an exponential decrease in velocity with distance below the free surface, and (3) a magnitude term,  $\pi H/T$ .

Maximum velocities occur when the phase is such that the sine or cosine term equals 1.0, e.g. when  $\cos(kx - \sigma t) = 1$  for Equation 5.8. Considering the vertical variation in velocity, maximum velocity occurs at the free surface ( $z = 0$ ).

Note that, based on the assumptions inherent in the small amplitude theory, the free-surface is taken as  $z = 0$  instead of at some higher elevation such as  $z = \eta$ . The maximum forward water particle velocity occurs on the free surface of the crest of the wave and is:

$$u_{\max, z=0} = \pi H / T \quad (5.10)$$

The wave-induced horizontal velocity on the bottom ( $z = -d$ ), which can control sediment movement on the bottom, becomes:

$$u_{z=-d} = \pi H / T \left( \frac{1}{\cosh[kd]} \right) \cos(kx - \sigma t) \quad (5.11)$$

with a maximum value, where  $\cos(kx - \sigma t) = 1$ , is

$$u_{\max, z=-d} = \pi H / T \left( \frac{1}{\cosh[kd]} \right) \quad (5.12)$$

The instantaneous water particle accelerations in a wave field are given by:

$$a_x = g\pi H / L \left( \frac{\cosh[k(d+z)]}{\cosh[kd]} \right) \sin(kx - \sigma t) \quad (5.13)$$

and

$$a_z = g\pi H / L \left( \frac{\sinh[k(d+z)]}{\cosh[kd]} \right) \cos(kx - \sigma t) \quad (5.14)$$

where:

$a_x$	=	horizontal component of water particle acceleration.
$a_z$	=	vertical component of water particle acceleration.

Water particle displacements or the paths of individual water particles in water waves can be estimated by small-amplitude wave theory. In deepwater the paths are circular with the magnitude of the circular motion decreasing with distance below the free surface (Figure 5.2). At a depth of about one-half the wavelength the wave-induced orbital movements die out (see Dean and

Dalrymple 1991, Sorensen 1993, or USACE 2002 for the particle equations). Below that depth,  $d=L/2$ , no surface wave motion is felt.

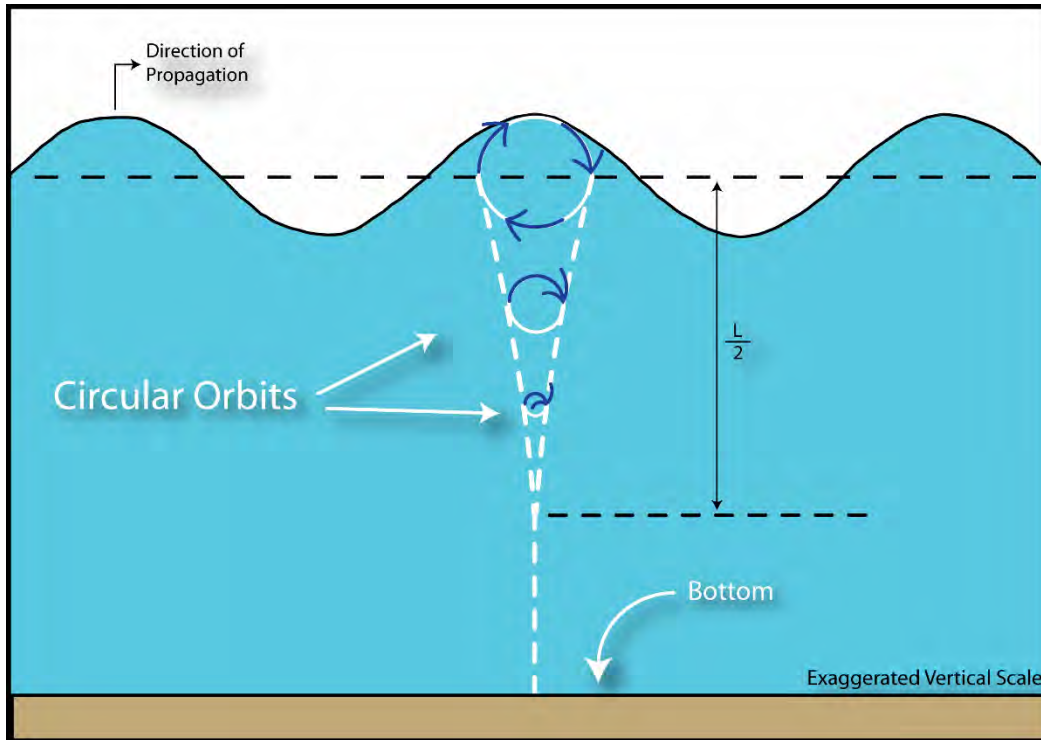


Figure 5.2. Water particle paths under waves in deep water

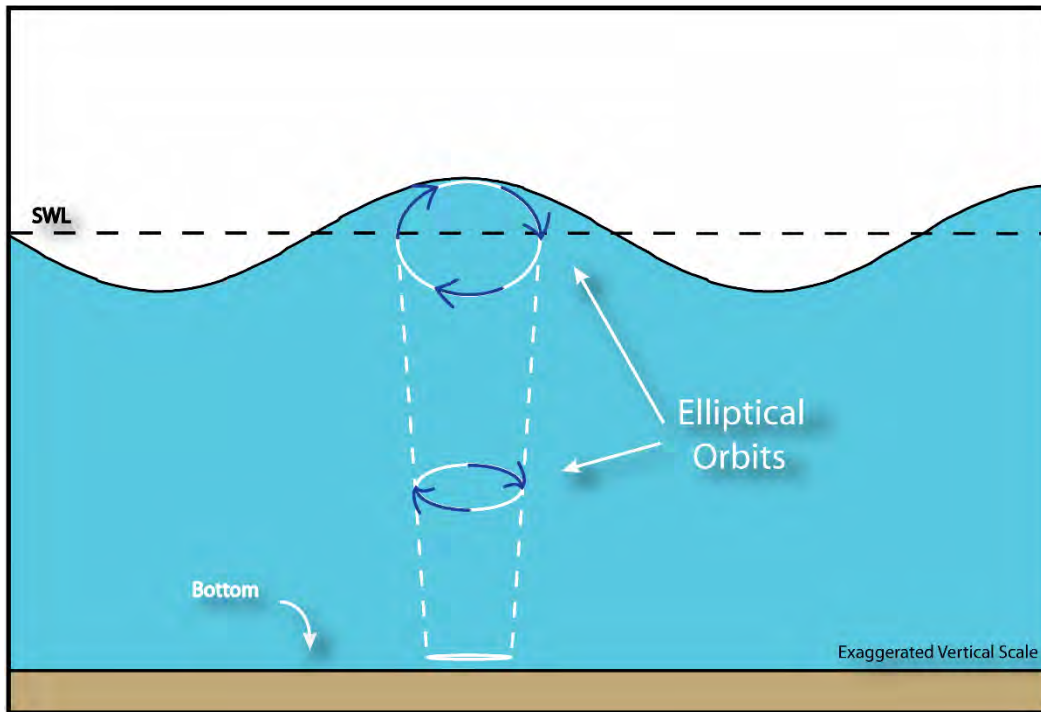


Figure 5.3. Water particle paths under waves in shallow and intermediate water depths

Water particle paths are elliptical in intermediate and shallow depths (Figure 5.3). The vertical amplitude of the elliptical motion decreases with increasing depth. At the bottom, the water particles move back and forth along the bottom. Scuba divers in shallow water are familiar with this back and forth motion and often refer to it as “wave surge.” The magnitude of the motion can cause difficult working conditions for divers as the corresponding accelerations can make for nauseous conditions.

The small-amplitude wave theory provides adequate approximations of the kinematics of wave motion for many engineering applications. However, when waves are very large or in very shallow water, small-amplitude theory results may not be adequate. Higher-order wave theories, such as higher order Stokes wave theories, cnoidal wave theory, and solitary wave theory address these important situations more appropriately. Numerical wave theories, however, have the broadest range of applicability.

Small-amplitude wave theory may not adequately predict the distortion of the water surface profile for large waves or for shallow water waves. The sinusoidal shape of the free surface of a water wave (shown in Figure 5.1) is a reasonable engineering model of the free surface of smaller waves in deepwater.

However, larger waves are known to have water surface profiles that are more like those shown in Figure 5.4. Stokes 2<sup>nd</sup> order theory predicts water surface profiles that are the sum of two phase-locked sinusoidal waves with the smaller having half the wavelength of the first. The resulting water surface profile has more sharply peaked crests and flatter troughs than the sinusoidal profile from small-amplitude theory. The elevation of the crest of the wave is higher, for the same  $H$ , which can be important for bridge clearance.

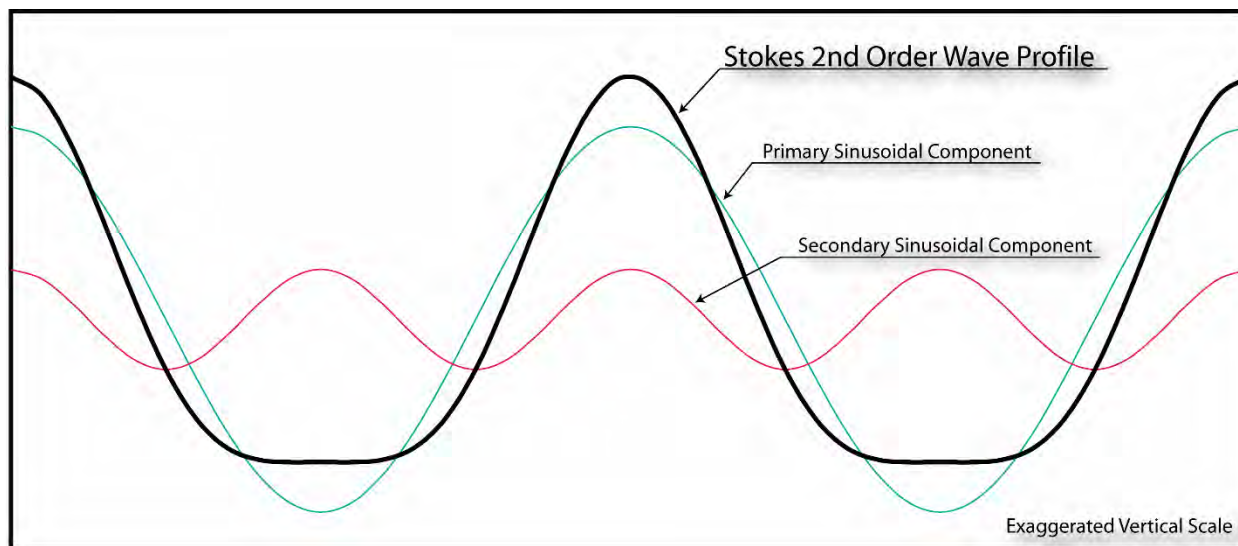


Figure 5.4. Stokes 2<sup>nd</sup> order wave theory water surface profile

Numerical wave theories can predict water surface shape and kinematics for large waves in deep or shallow water to any level of accuracy. The iterative power of the computer is used to more precisely solve the governing equations and appropriate boundary conditions. The most commonly available numerical wave theories are Dean’s stream function wave theory (Dean 1965, Dean 1973) and Rienecker and Fenton’s potential theory (Rienecker and Fenton 1981).

Two shallow water wave theories are the solitary wave theory and the cnoidal wave theory. These are both analytical theories for waves in very shallow water. The solitary wave considers a single wave. The cnoidal wave is part of a train of monochromatic waves.

The phenomenon of a non-sinusoidal shape of the water surface profile can become obvious for swell in shallow water. Cnoidal waves or the numerical theories can model this phenomenon well.

The wave kinematics, including orbital velocities and accelerations, predicted by higher-order wave theories vary from those predicted by the small-amplitude theory. The velocities and accelerations under the crests of the waves will be larger but of shorter duration than those predicted by linear theory. However, the variation from the small-amplitude theory is often less than 20-30%.

**Wave height is a surrogate for energy in the sea state. Larger waves have much more energy.**

The total wave energy of a wave train is the sum of its kinetic energy and its potential energy. The kinetic energy is that part of the total energy due to water particle velocities associated with the orbital wave-induced motion discussed above. Potential energy is that part of the energy resulting from part of the fluid mass in the wave crest being above the wave trough. The total energy density (energy per unit surface area) in a wave train is given by small-amplitude wave theory as:

$$\bar{E} = \gamma H^2 / 8 \quad (5.15)$$

where:

$\bar{E}$	=	total energy in a wave train per unit area of sea averaged over one wavelength
$H$	=	wave height
$\gamma$	=	specific weight of water

The implication of Equation 5.15 is that energy in a sea state is directly related to the square of the wave height. Wave height can be used as a measure of energy in a sea-state. Energy is very sensitive to wave height and doubling the wave height increases the energy in the sea-state four-fold.

Waves propagate energy across the sea by moving in wave groups. Interestingly, the groups of waves, and thus the energy in the waves, can move at different speeds than the individual waves. The wave group velocity ( $C_g$ ), or the velocity at which energy is propagated, is related to the individual wave celerity as:

$$C_g = nC \quad (5.16)$$

where:

$n$	=	ratio of wave group velocity to wave celerity (given by Equation 5.17 below)
$C$	=	wave celerity (defined by Equation 5.4)

$$n = \frac{1}{2} \left( 1 + \frac{(4\pi d/L)}{\sinh(4\pi d/L)} \right) \quad (5.17)$$

The value  $n$  varies from  $\frac{1}{2}$  to 1. In deepwater, it approaches  $n = \frac{1}{2}$ . In shallow water, it approaches  $n = 1$ . Thus, in deepwater, the wave energy is propagated at about one-half ( $\frac{1}{2}$ ) of the individual wave celerity.

However, in shallow water the energy moves at the individual wave celerity:

$$C_g = C \approx \sqrt{gd} \quad (5.18)$$

The wave power, or wave energy flux in a wave train, is given by:

$$\bar{P} = \bar{E} C_g \quad (5.19)$$

where:

$$\begin{aligned} \bar{P} &= \text{wave power} \\ \bar{E} &= \text{total wave energy density (defined in Equation 5.15)} \\ C_g &= \text{wave group velocity (defined in Equation 5.16)} \end{aligned}$$

Wave energy flux entering the surf zone has been related to the longshore sediment transport rate, wave setup in the surf zone, and other surf zone dynamics as discussed in Chapter 6.

## 5.2 Wave Transformation and Breaking

As waves move toward the coast into shallower water depths, they undergo transformations and ultimately break. The wave period of individual waves remains constant through the transformations until breaking but the direction of propagation and the wave height can change significantly. Transformations include shoaling, refraction, diffraction, attenuation and reflection. Waves break in different ways when they hit a shoreline or structure. The concept of a depth-limited wave height in shallow water can be very valuable in some coastal engineering applications.

As a wave moves into shallower water the wavelength decreases (recall Equation 5.2) and the wave height increases. For two-dimensional propagation, i.e. straight toward shore, the increase in wave height can be theoretically shown, by conservation of wave energy considerations:

$$K_s = H/H_0' = \sqrt{2n/\tanh(2\pi d/L)} \quad (5.20)$$

where:

$$\begin{aligned} K_s &= \text{shoaling coefficient} \\ H &= \text{wave height} \\ H_0' &= \text{deepwater wave height} \end{aligned}$$

The shoaling coefficient increases from  $K_s = 1.0$  up to perhaps as much as  $K_s = 1.5$  as the individual wave moves into shallower water until the wave breaks via the depth-limited mechanism discussed below.

Wave crests bend as they move into shallower water via refraction. As waves approach the beach at an angle, a portion of the wave is in shallower water and moving more slowly than the rest of the wave. Viewed from above (Figure 5.5) the wave crest begins to bend and the direction of wave propagation changes. Refraction changes the height of waves as well as the direction of propagation.

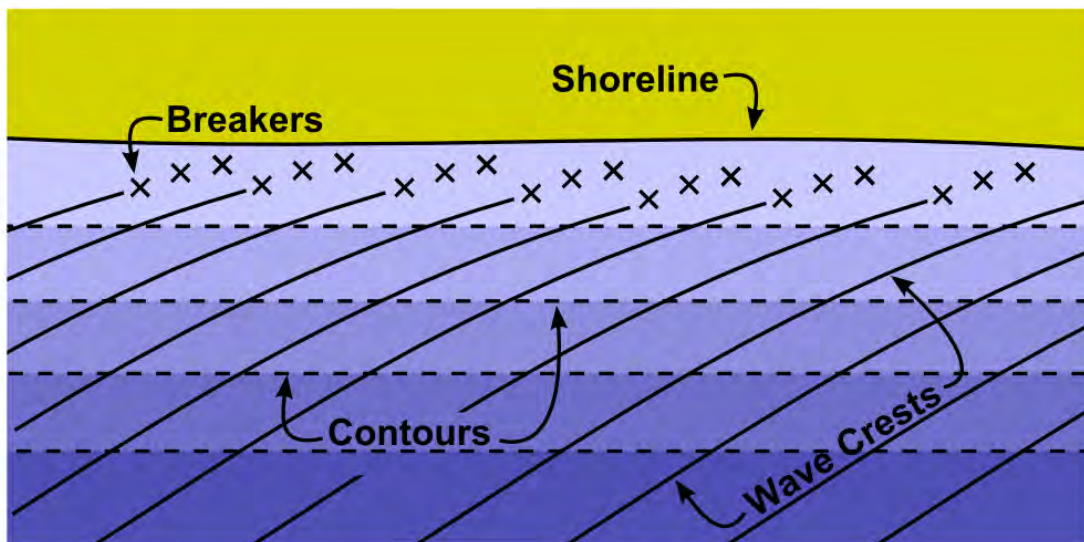


Figure 5.5. Bending of wave crests as they approach the shore due to refraction (adapted from USACE 2002)

There are two general types of models for monochromatic wave refraction: wave-ray models and grid-based refraction models. Wave-ray models, the older type, estimate the path of wave rays, lines perpendicular to the wave crests. These wave ray models are based on Snell's Law. They can provide reasonable estimates of refraction but have problems with crossing wave rays or "caustics." These caustics are physically impossible since they imply an infinite wave height. Grid-based refraction models solve some form of governing differential equation for the wave height field across arbitrary bottom contours and avoid this "caustic" problem.

Diffraction is the bending of wave crests as they spread out into quieter waters. An example of wave diffraction is the spreading of wave energy around the tip of a breakwater into the lee of the breakwater. The wave crest, as viewed from above, can wrap itself around the tip of the breakwater and appears to be propagating from that tip location into the quieter water. Diffraction also occurs in open water as waves propagate across varying depths. Thus, wave diffraction and refraction often occur together and any separation of the two mechanisms can be problematic in engineering modeling.

The combination of wave refraction and diffraction can cause wave energy to be focused on headlands or reefs and de-focused in embayments as shown in Figure 5.6. Thus, wave heights can be increased on headlands and decreased in embayments. Figure 5.7 shows combined wave refraction, diffraction, and breaking occurring across the shallow reefs offshore of the Diamond Head Lighthouse.

Numerical wave refraction models are often combined with diffraction models. One such combined model is the REF/DIF model originally developed by Kirby and Dalrymple (1983). Modern numerical wave generation models (see Section 5.4) typically include some form of refraction and diffraction in the wave propagation algorithm.

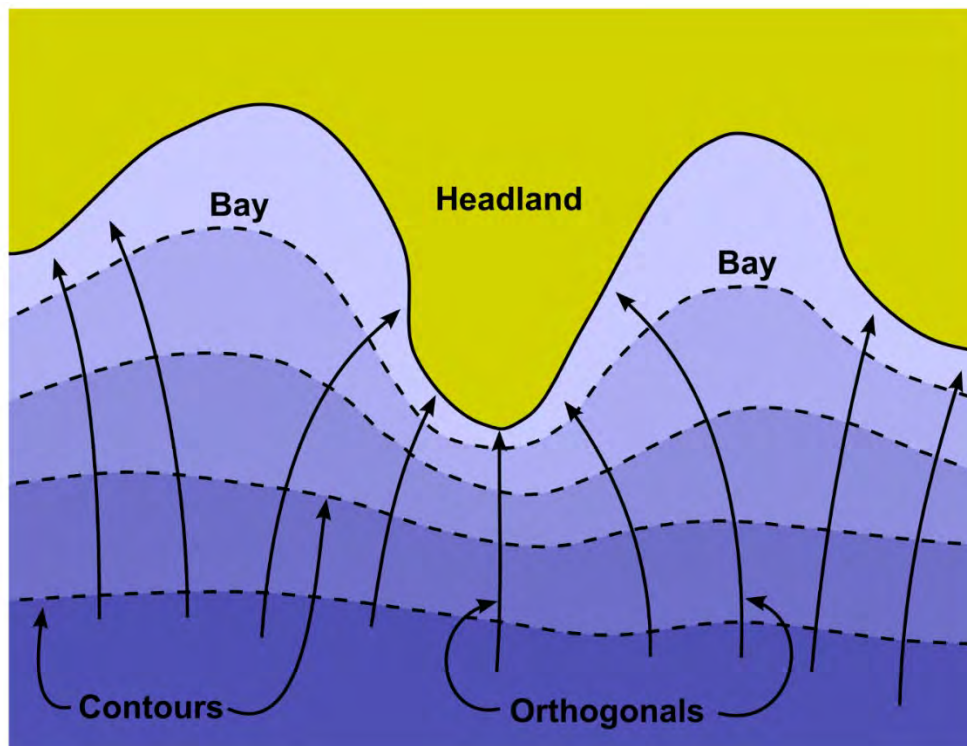


Figure 5.6. Wave energy focused on headland by a wave refraction and diffraction (adapted from USACE 2002)

Wave energy can propagate very long distances across the ocean with very little loss of energy. However, wave height can decrease as a wave propagates across flat bottoms in shallow water. Energy can be lost due to bottom friction and other processes. These energy losses, or attenuation, can significantly reduce wave heights. Wave breaking across a shallow bar or reef is also sometimes referred to as wave attenuation.

$$C_r = H_r / H_i \quad (5.21)$$

where:

$C_r$	=	reflection coefficient
$H_r$	=	reflected wave height
$H_i$	=	incident wave height

The reflection coefficient can vary from  $0 < C_r < 1$  depending on the shoreline or structure type. Smooth, vertical walls have reflection coefficients of  $0.9 < C_r < 1.0$ . Reflection from sloping walls, revetments and beaches is very sensitive to slope and can vary from 0.05 to 0.9 for different smooth slopes. The lower values are for very flat slopes. Typical values of reflection coefficient for sandy beaches and rubble-mound structures are  $0 < C_r < 0.45$  and  $0 < C_r < 0.55$  respectively (USACE 1984).

Waves break at two general limits:

- In deepwater, waves can become too steep and break when the wave steepness defined as,  $H/L$ , approaches  $1/7$ .
- In shallow water, waves break when they reach a limiting depth (see Figure 5.8 and Figure 5.9.).

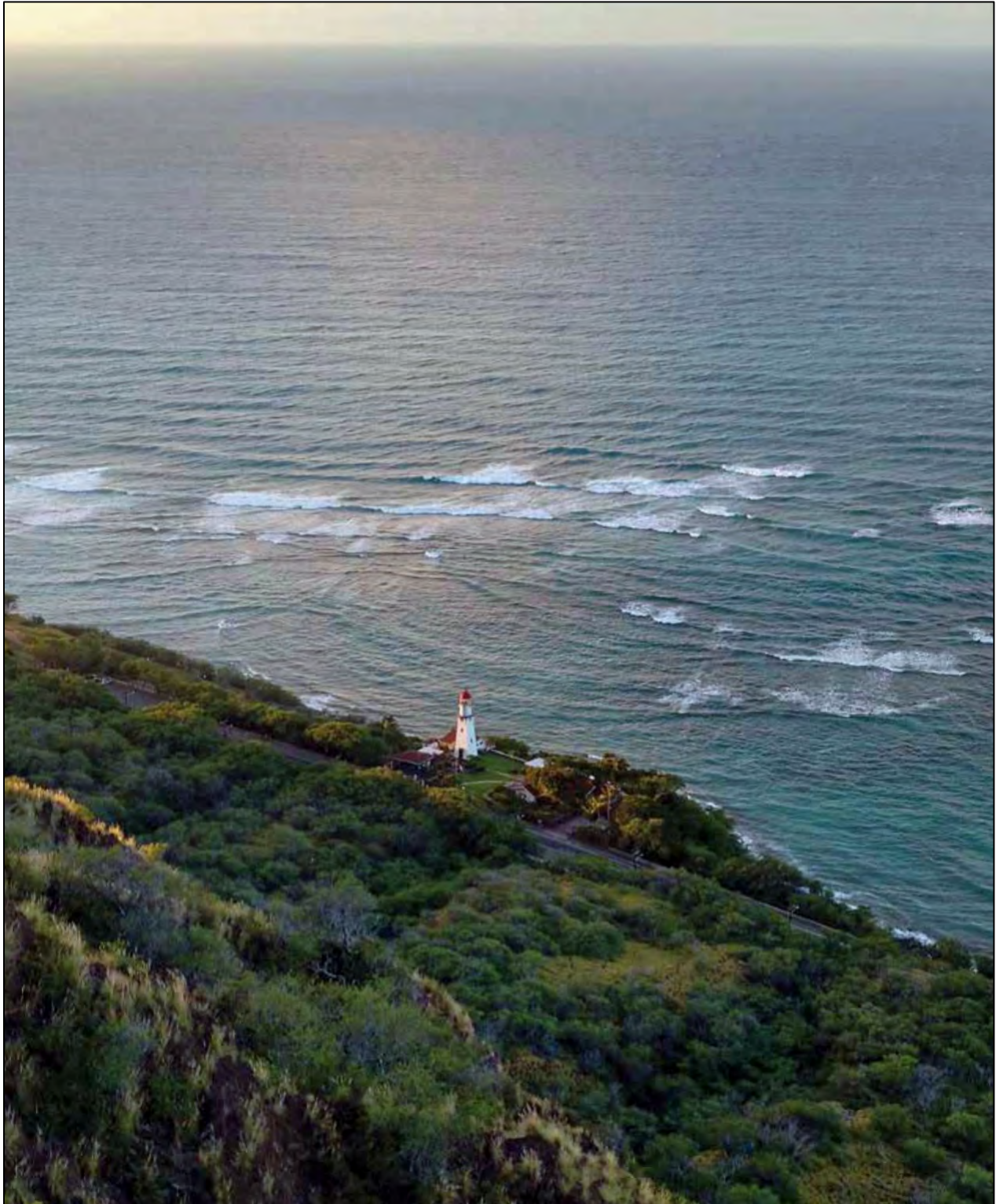


Figure 5.7. Waves refracting, diffracting and breaking on the shallow-water reefs south of the Diamond Head Lighthouse, Honolulu, Hawaii

Wave energy is usually partially reflected when it hits a shoreline or structure. The reflection coefficient is defined as the ratio of the reflected wave height to the incident wave height:

The photograph in Figure 5.9. shows depth-limited wave breaking across an area that is normally dry land near the shore of Mobile Bay. The surge and winds are from Hurricane Katrina which had made landfall about 100 mi west of this location several hours earlier. These waves were generated by those winds in Mobile Bay, which is on the right side of the photograph. The storm surge was inundating a low coastal bluff along the bay allowing waves to propagate into these trees.

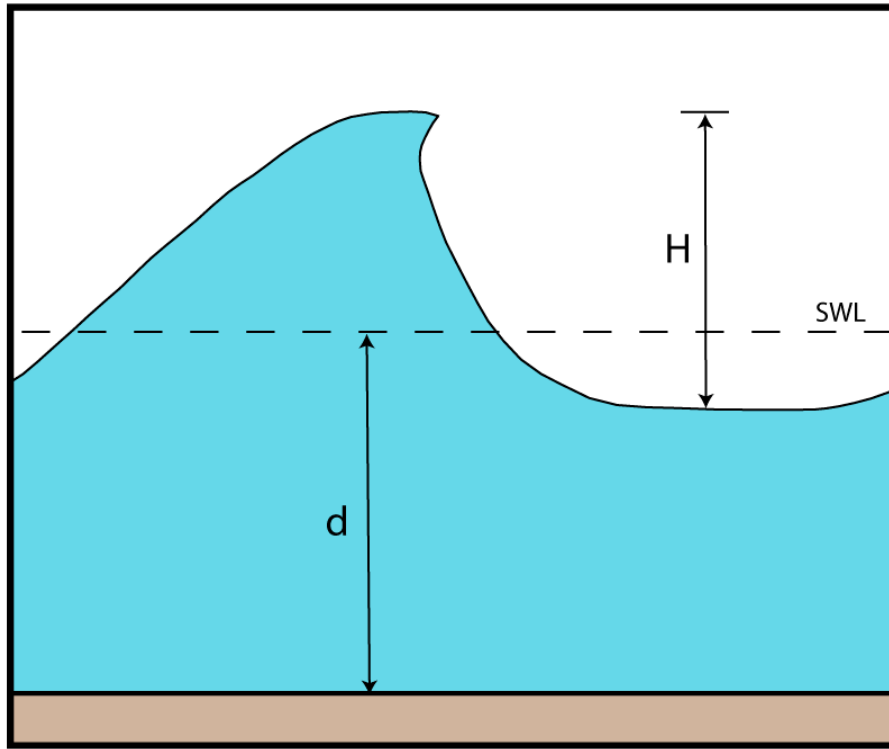


Figure 5.8. Depth-limited wave breaking in shallow water

This depth-limited breaking can be very important in the design of coastal revetments protecting highways. For an individual wave, the limiting depth is roughly equal to the wave height and lies in the practical range:

$$0.8 < \left(\frac{H}{d}\right)_{\max} < 1.2 \quad (5.22)$$

where:

$$\left(\frac{H}{d}\right)_{\max} = \text{maximum ratio of wave height to water depth.}$$

The variation expressed in Equation 5.22 is due to nearshore slope and incident wave steepness,  $H/L$ .

Steeper nearshore slopes result in higher values of  $\left(\frac{H}{d}\right)_{\max}$ .



Figure 5.9. Depth-limited wave breaking during storm surge (permission to use photograph provided by Happy Partridge)

A practical value when there is a mild slope offshore of the structure is:

$$\left(\frac{H}{d}\right)_{\max} = 0.8 \quad (5.23)$$

Which corresponds with a theoretical limit from solitary wave theory of:

$$\left(\frac{H}{d}\right)_{\max} = 0.78 \quad (5.24)$$

The **depth-limited wave height** can be expressed as:

$$H_{\max} \approx 0.8d \quad (5.25)$$

where:

$$\begin{aligned} H_{\max} &= \text{maximum wave height} \\ d &= \text{depth of water (as shown in Figure 5.8)} \end{aligned}$$

Equation 5.25 is often useful in selecting an upper limit for a design wave height for coastal structures in shallow water. Given an estimate of the water depth at the structure location, the maximum wave height  $H_{\max}$  that can exist in that depth of water is known. Any larger waves would have broken farther offshore and been reduced to this  $H_{\max}$ . Equation 5.25 is a nominal limit and

is not conservative on sloped bottoms. Note that depth,  $d$ , is the total water depth, including tides and design surge levels, and allowances for scour if applicable.

**The depth-limited wave height is often used as the design wave height in coastal engineering design.**

Waves striking built coastal infrastructure are often depth-limited, i.e. their height at a specific location is controlled by the water depth at and around that location. The depth-limited wave concept is part of numerous FEMA regulations, methods and guidance (e.g. FEMA 2011); USACE guidance in many situations (USACE 2002); and guidance in the ASCE-7 building code (ASCE 2016). Numerical wave generation and propagation models use a similar concept when estimating wave breaking in shallow water. This rather simple concept plays a significant role in the final results of many analyses, vulnerability assessments, risk-based coastal flood elevations, insurance rate maps, and engineering designs.

There are four different types of breaking waves: spilling, plunging, surging and collapsing breakers. Typical water surface profiles for these breaker types are shown in Figure 5.10. Breaker type is controlled by wave steepness ( $H/L$ ), beach or structure slope, and local wind direction.

Spilling and plunging are the most common breaker types on sandy beaches. The spilling breaker begins gradually at the top of wave crest with some tumbling white-water. The tumbling water increases until the entire wave face is tumbling white-water. An example of a plunging wave is shown in Figure 5.11. When waves plunge, the wave form stands up in vertical face that then plunges over often forming a “tube” of the sort that good surfers like. Local wind direction at the time of breaking can change the breaker type between spilling and plunging (Douglass and Weggel 1988).

If a breaking wave plunges onto a rigid structure such as a seawall or highway bridge deck, a pocket of air can be trapped between the water and the structure. The air pocket can be compressed and produce extremely large, short duration loads on the vertical structure (see Figure 11.12).

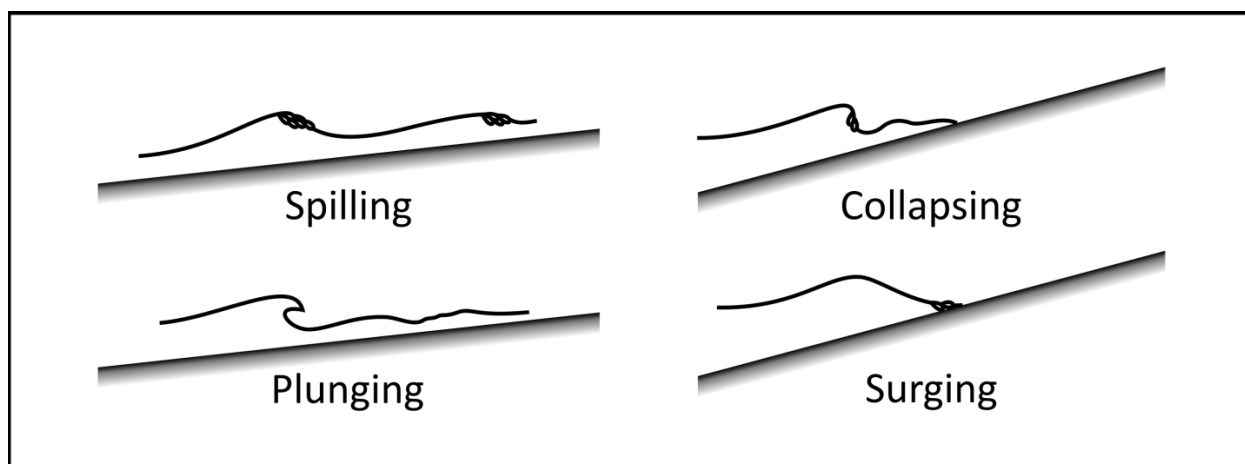


Figure 5.10. Wave breaker types



Figure 5.11. Example of a plunging breaker (from Douglass 2002)



Figure 5.12. Example of a spilling breaker (Huntington Beach, California, 2017)



Figure 5.13. Example of a collapsing breaker (Morro Bay, California)

Surging breakers occur on very steeply sloped beaches and on coastal structures. The surging breaker type is really just a form of wave reflection. The collapsing breaker is intermediate between the plunging and surging types. Collapsing breakers are often the most damaging to coastal structures, particularly rubble-mound structures, because the entire wave front collapses on the structure generating extremely high wave particle velocities and accelerations. Figure 5.13 shows a rock breakwater being struck by a collapsing wave.

### **5.3 Irregular Waves**

The smooth water surfaces of monochromatic wave theories are not often realistic representations of the sea state on real ocean or bay surfaces. Figure 5.14 shows a long period swell approaching the Pacific Coast. For long-period swell situations such as this one, the monochromatic theories are appropriate. Note in the background a continuous train of waves that are of almost the same height with long, straight wave crests (except where they begin to refract and break). The wave profiles show some of the behavior of sharp crests and flat troughs discussed above for Stokes 2<sup>nd</sup> order wave and cnoidal wave theories.

Another, more typical, water surface is shown in Figure 5.15. Individual smooth wave trains are not obvious and the sea state in the bay looks much more chaotic with short-crested waves. Figure 5.16 shows waves breaking in the nearshore and on a highway rock, rubble-mound seawall. This photograph was taken when there was a strong onshore wind generating waves in the Gulf of Mexico. The more typical storm sea-states, like those shown in Figure 5.15 and Figure 5.16, can be referred to as “irregular waves,” or random waves, since they do not have the smooth, repeating shapes of monochromatic theories.



Figure 5.14. A train of long-period swell approaching the Oregon coast



Figure 5.15. Irregular waves on San Francisco Bay, California



Figure 5.16. A storm-driven, irregular, sea state in the Gulf of Mexico (Florida SH 30E)

“Significant wave height,”  $H_s$ , is a term with a long history of use in oceanography and coastal engineering. Oceanographers have developed two different sets of tools to describe realistic sea states and significant wave height. One is a statistical representation of the individual wave heights in a sea state. This leads to a primary wave height definition called a “significant wave height”, the average height of the one-third highest waves. The other, an energy-frequency spectrum representation of the water surface elevation, leads to a primary wave height definition that is also called the “significant wave height.” See Dean and Dalrymple (1991) or other text for more on wave spectral analysis. The notation for the statistically-based  $H_s$  is often:

$$H_s = \overline{H_{1/3}} \quad (5.26)$$

and the notation used for the spectral significant wave height is:

$$H_s = H_{m_0} \quad (5.27)$$

The two definitions lead to values of significant wave height ( $H_s$ ) that are approximately equal in deepwater seas. However, in shallow water, and especially in the surf zone, the two parameters diverge. The term “significant wave height” probably arose as a way for ship-board observers to estimate the wave height. Some argue that there is nothing truly “significant” about either definition since very few individual waves in an irregular sea will be of the same height as the significant wave height. The significant wave height ( $H_s$ ) for a sea state is a statistical artifact. However,  $H_s$  (with either definition) provides a consistent, meaningful measurement of the energy in a given sea state. Most modern engineering methods use the spectral significant wave height definition.

Individual wave heights vary in an irregular sea state. The distribution of individual wave heights follows a Rayleigh probability distribution (see USACE 2002). This one-parameter distribution allows for estimation of other wave heights that are sometimes used in design. Table 5.1 provides the relation of some of these other wave heights to  $H_s$ . Table 5.1 shows two types of statistics:

- the average of waves with heights above a certain level ( $\overline{H}_{10}$ ,  $\overline{H}_5$ ,  $\overline{H}_1$ )
- the wave height exceeded by a given percentage of waves in the irregular sea state ( $H_{10\%}$ ,  $H_{1\%}$ ).

Table 5.1. Wave height statistics in irregular seas.

Wave statistic	Description	Multiple of $H_s = \overline{H}_{1/3}$
$\overline{H}_{10}$	average of the highest 10% of waves	1.27
$\overline{H}_5$	average of the highest 5% of waves	1.38
$\overline{H}_1$	average of the highest 1% of waves	1.67
$H_{10\%}$	height exceeded by 10% of waves	1.07
$H_{1\%}$	height exceeded by 1% of waves	1.52

Individual wave periods also vary in an irregular sea. The peak wave period,  $T_p$ , is the wave period corresponding to the peak of the energy density spectrum. That is the period of most of the energy in the irregular sea state. Peak wave period,  $T_p$ , is the output of almost all wave generation models discussed in the next section.

Each of the wave transformations discussed above for the simpler monochromatic wave train model occur in irregular seas. This includes refraction, diffraction, shoaling, attenuation, and depth-limited breaking. Several numerical approaches have been developed to model these wave transformations.

## 5.4 Wave Generation and Modeling

Almost all water waves in the ocean and on bays are caused by winds. Wind first ripples the water surface and then begins to increase the heights of the ripples until they become small waves that propagate on their own. Wave heights continue to increase as the wind blows farther or harder across the water surface. This includes energy transfer from the wind and complex hydrodynamics of nonlinear transfers of energy between waves. If the water body is large enough, eventually the wave heights will stop growing unless the wind speed increases more. Once they are generated, waves often propagate for hundreds or thousands of miles across the ocean. They travel beyond the storm that generated them. Most waves that hit the shoreline were generated far out at sea. Waves that have traveled out of the winds that generated them are called “swell.” See Figure 5.14 for a photograph of swell waves. Waves that are still being acted upon by the winds that created them are called “sea.” See Figure 5.15 and Figure 5.16 for photographs of sea waves.

Fetch ( $F$ ) is the distance across the water that a wind blows to generate waves. For enclosed bays, this is the maximum distance across the water body in the direction of the wind. Duration is the time that a wind blows. Waves are called “fetch-limited” if their height is limited by the available fetch distance. Waves are called “duration-limited” if their height is limited by the duration that the wind has blown. If winds blow long enough, until the sea state is no longer duration-limited, the sea is considered “fully-arisen.”

One of the products that came out of the World War II efforts to forecast surf and wave conditions for amphibious landings was an empirical method for estimating wave generation (Sverdrup and Munk 1947). Bretschneider improved it to form the method now known as the SMB method after those investigators. The USACE Shore Protection Manual (USACE 1984) replaced the SMB method with a similar method based on results from JONSWAP experiments (Hasselmann *et al.* 1980) and adjusted for depth-limited conditions. These equations are listed in Section 6.2.2.4 of AASHTO (2008) and also in Appendix C of Douglass and Krolak (2008). The equations can estimate design wave height and period for bays and lakes. These situations are “fetch-limited” in that the fetch is limited by the size of the bay or lake.

On the open ocean, waves are almost never fetch-limited and they continue to move after the wind ceases or changes. Swell wave energy can propagate very long distances and into other storms. Waves striking the shore at any moment in time may include swells from several different locations plus a local wind sea. Modern wave modeling can numerically solve wave generation and propagation equations using a grid across the entire ocean. These models can include wave generation as well as the transformations of refraction and depth-limited breaking. The appropriate selection of a model will depend on the scale of the process being simulated, as well as the nature of the problem being evaluated.

A number of available wave models include the Steady-state Spectral Wave (STWAVE) model (Smith *et al.* 2001), the Wave Analysis Model (WAM) (Komen *et al.* 1994) and the Simulating Waves Nearshore (SWAN) model (Booij *et al.* 1999). See Table 4.3 for a list of modern coastal engineering models. Wave generation and transformation modeling is an active area of research and the technology is still being developed and debated in the oceanography community. However, throughout the world, these and other models are used daily to forecast waves and aid in engineering analysis for design.

The prediction of storm surge and waves at the local scale (i.e. barrier island) often relies on a definition of wave characteristics at the basin scale (i.e. ocean). The Global Ocean Wave Prediction Model (WAM) is commonly used to provide wave boundary conditions for nearshore wave models (Group 1988). The model predicts the growth of wind waves from sea surface roughness and wind characteristics, and simulates nonlinear wave-wave interactions as well as the dissipation of short waves. WAM provides wave conditions at each model grid point at chosen times. While WAM is effective at simulating basin-scale wave propagation it should not be used to simulate the propagation and transformation of waves close to shore.

**Wave modeling is an excellent tool in coastal engineering. The techniques simulate wave heights and wave periods across the oceans and into shallow coastal locations.**

Wave models account for the wave transformations that occur in intermediate to shallow water depths (when the local depth is less than one-half of the wavelength). Such processes include wave refraction and shoaling, current-induced refraction and shoaling, wave diffraction, and wave breaking (see Section 5.2). Appropriate treatment of these wave transformations becomes increasingly important during storm surge events as coastal topography is inundated. The Steady-State Spectral Wave (STWAVE) model provides steady-state solutions of wave transformation-propagation over variable bathymetry in two dimensions. The STWAVE model is also a wind-wave generation model and accepts depth-averaged currents from a circulation model to simulate current-induced wave shoaling and refraction (Smith *et al.* 2001). STWAVE is capable of simulating most nearshore wave transformations of interest on a rectangular, Cartesian grid. The model simplifies the treatment of wave diffraction and does not consider wave reflections.

STWAVE has been used on a number of engineering project studies (Smith and Smith, 2001). STWAVE is a finite-difference model designed to simulate the nearshore transformation of a directional spectrum of wave energy. A typical application is to take known offshore wave conditions, such as those measured by a NOAA buoy, and transform them over complex nearshore bathymetry, often to the point of nearshore breaking. Typical coverage areas are 10-20 km in the offshore direction and 20-40 km along the shore, with grid cell sizes ranging from 25 to 100 m.

The USACE CMS model has a stand-alone wave model, CMS-Wave, whose capabilities are similar to those of STWAVE with some enhancements (Lin *et al.* 2008). CMS-Wave is a two-dimensional wave transformation model. Similar to STWAVE, the CMS-Wave model is capable of wind-wave generation and propagation over variable bathymetry, and includes nearshore wave transformations including shoaling, refraction, diffraction, reflection, and breaking.

The Simulating Waves Nearshore (SWAN) model has been adapted for coupling with many different types of general circulation models. The SWAN model is capable of simulating two-dimensional (horizontal) wave propagation in time and space in Cartesian or spherical coordinate systems. The SWAN model simulates random, short-crested wind-wave generation and propagation in coastal and inland waters (Booij *et al.* 1999; Ris *et al.* 1999). The wave model is capable of simulating nearshore wave transformations as well as transmission and reflection. It can be successfully coupled with ADCIRC (Dietrich *et al.* 2011) and CH3D (Sheng *et al.* 2006) as part of tightly coupled hindcast and forecast simulations of storm surge and waves.

The same models used for wave forecasting can be used for wave “hindcasting.” **Hindcasting is the application of the model to estimate wave conditions that occurred in the past.** This can be done for historical storms or for long-term simulations.

Figure 5.17 shows results from a hindcast of Hurricane Ivan (2004) using the SWAN model. It shows the maximum wave heights in the vicinity of the I-10 bridge across Escambia Bay in Pensacola, Florida. The model results are overlain on the Google Earth image and the diagonal line across the bay in the middle of the graphic shows the bridge location. The colors refer to estimated significant wave heights for each location and the arrows indicate wave direction at that maximum. The storm surge, about 11 ft at its peak, flooded the low-elevation land to the east of the bay. The wave heights on top of that flooded land are the blues to the right of the plot. The land to the west of the bay is much higher and did not flood. Wave heights at the bridge in the middle of the bay exceeded 8 ft but near the shoreline of the bay, they were lower. This reduction in wave heights near the shoreline of the bay effected the pattern of damage experienced by the bridge (see Figure 11.7). The modelled wave height distribution shown in Figure 5.17 explains the damage pattern well. Where the waves were lower, the damage was less severe.

The USACE Wave Information Study (WIS) has developed a hindcast database of wave conditions around the US coastline. Ocean wave generation models were used with decades of wind estimates generated from historical barometric pressure fields. The results are numerical modeling estimates of wave conditions;  $H_s$ ,  $T_p$  and wave direction at thousands of locations around the US coast. The resulting data and summaries are available on-line at the USACE Coastal Hydraulics Laboratory web-site.<sup>4</sup> These hindcast WIS data are used to develop estimates of long-term wave statistics for engineering design and estimating longshore sand transport rates. Care should be taken in using these hindcast wave statistics for design since these results are not based on actual measurements but rather computer simulations.

---

<sup>4</sup> <http://www.frf.usace.army.mil/> (accessed September 25, 2018)

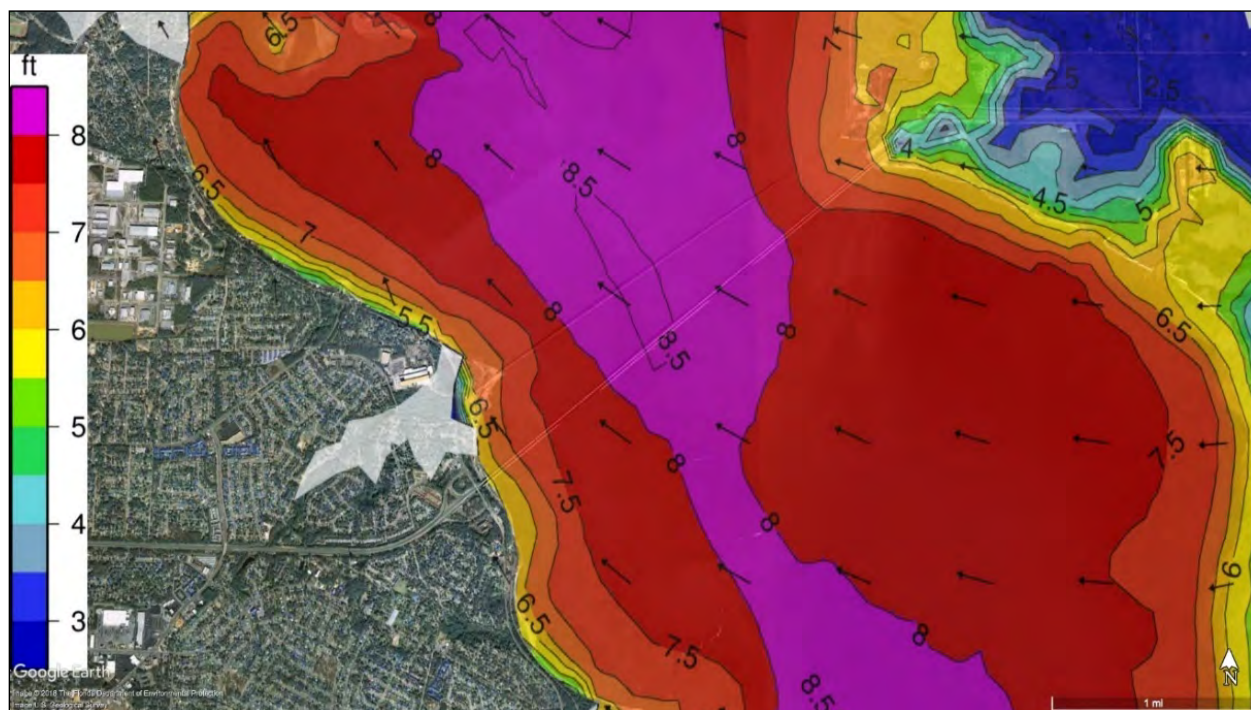


Figure 5.17. ADCIRC+SWAN wave model hindcast of maximum significant wave heights generated during Hurricane Ivan (2004) at the I-10 bridge across Escambia Bay, Pensacola, Florida

The WIS data have been incorporated into USACE Coastal Hazards System discussed in Section 4.6 Design Water Levels (see Figure 4.24 for an example). The Coastal Hazards System is an excellent source for design wave height information which includes exceedance probabilities corresponding to 10-, 20-, 50-, 100-, 200-, 500-, and 1,000-yr return periods.

## 5.5 Wave Runup

Wave runup is the rush of water up a beach, or other slope, as the wave breaks. The limit of runup defines what gets wet on a beach above the still water level due to waves. Wave runup on a natural beach during storms is a fairly complex hydrodynamic process in that there are several components beyond the swash (runup and rundown) of any single wave. Wave setup raises the water level in the surf zone. Sometimes oscillations of water level in the surf zone, called “surf beat” or infragravity energy, cause fluctuations, with periods of 30 sec to 3 min, in the water level in the surf zone.

Runup is typically defined as the elevation difference between the upper limit of runup and the still water level (see Figure 7.22 for a definition sketch). One commonly used empirical equation to estimate runup on sandy beaches is Stockdon *et al.* (2006). Poate *et al.* (2016) propose a similar empirical equation for runup on cobble beaches.

## 5.6 Ship Wakes

Ship wakes are sometimes the largest waves that occur at sheltered locations and thus can be the design waves for some revetments or other structures. Large ships can generate wakes with

wave heights exceeding  $H=10$  ft and smaller vessels (including tugboats) can generate wakes of  $H=5$  ft.

The wake depends on the size, hull shape, speed of the vessel and distance from the sailing line. Engineering judgment based on observations can be used to establish a reasonable upper limit on wake size if the maximum speeds from all possible vessels are considered. Several methodologies for estimating ship wakes are available including Weggel and Sorensen (1986) and Kriebel *et al.* (2003) for large vessels and Bottin *et al.* (1993) for some smaller recreational watercraft.

## 5.7 Tsunamis

Tsunamis are a series of waves resulting from a rapid, large-scale disturbance in a body of water caused by earthquakes, landslides, volcanic eruptions, and meteorite impacts. Many of the tsunamis have generated broad area destruction and fatalities. Tsunamis are some of the world's most powerful water waves because they have extremely long wavelengths that transform significantly as they propagate into shallow water. They are often called “tidal waves” even though they have nothing to do with the tides. Tsunami is a Japanese word which loosely translates to “harbor wave” (“wave” directly translates as “nami”). Tsunami has been adopted in the worldwide oceanography community to avoid the term “tidal wave.”

**Tsunamis are a rare, but potentially deadly and damaging, natural hazard that influences civil engineering designs along the US Pacific Coasts and Islands.**

The generation and propagation of tsunamis is an active area of oceanography research and the flow dynamics of a tsunami runup, including how it interacts with infrastructure such as buildings and roads, can be very complex and is an active area of civil engineering research. The destructive flows due to tsunami wave breaking and runup can vary greatly from location to location for the same tsunami based on local bathymetry and topography.

The deadly 2004 “Boxing Day” tsunami in the Indian Ocean struck an area that had previously been thought to be unlikely for major tsunamis. It was caused by a magnitude-9.3 underwater earthquake and devastated coastal areas around the northern Indian Ocean. It killed over 220,000 and displaced over 1.5 million people. The Tohoku Japan Tsunami of 2011 was generated by a magnitude-9.0 earthquake and ran up to inundation heights in that region that exceeded all historical records. It killed over 19,000 people and caused extensive damage to ports, buildings, bridges and other coastal infrastructure (FEMA 2012).

Tsunamis in 1946 and 1957 damaged bridges on the north coast of the Hawaiian island of Kauai. The 1964 Alaskan earthquake tsunami caused coastal infrastructure damage along the coasts of Washington, Oregon, and California.

Tsunamis can hit any US coast but 95% of reported tsunamis in the US hit the Pacific states and territories (NTHMP 2018). Large portions of the US Pacific Coast and Hawaii have tsunami warning systems in place in recognition of the threat. Many US coastal communities have tsunami evacuation routes with signs that have been coordinated with the SDOT. Tsunamis can occur along the Atlantic and Gulf Coasts but the probability is extremely low.

Analysis tools for assessing the vulnerability of coastal highways to tsunamis are presented in Section 14.7 and tsunami-induced scour is discussed in Section 12.3.7.

*Page Intentionally Left Blank*

## Chapter 6 - Coastal Sediment Processes

Sediments along the coast are constantly being reshaped by waves and currents. These processes, primarily sand movement, can have significant implications for engineers tasked with working in this environment. The study of coastal sediment processes includes several specialty areas of coastal geology including “coastal geomorphology,” the study of coastal landforms and features, and “coastal sedimentology,” the study of the properties of beach sands.

**A good understanding of the terminology and concepts of coastal geology is valuable for coastal engineering** because it is an underpinning science. The design function of many coastal engineering projects is to positively affect coastal sediment processes. Many coastal engineering projects which have improved navigation, such as inlet or harbor jetties and dredging, have caused nearby beach erosion. Inlet jetties can trap sand that was otherwise moving across the inlet naturally to the downdrift beaches. This trapping can cause beach erosion for miles downdrift. Many ship channels are dredged through a sand bar that is part of the beach’s littoral, sand-sharing system. If the dredged sand is not placed back into the littoral system appropriately, downdrift beaches can be starved and recede. Thus, the engineering works themselves can cause erosion problems. A clear understanding of the coastal processes and the geological framework at work at each project location is needed for comprehensive coastal engineering projects.

This chapter provides a brief introduction to some coastal sediment processes including an overview of coastal geology, beach terminology, coastal sediment characteristics and transport, and tidal inlets. Just a few of the other textbooks and references with much more detail on these topics include Komar (1998) and Dean & Dalrymple (2002) for coastal sediment processes; Davis (1994), Davis & FitzGerald (2009), and Davis (2014) for coastal geology; and the SPM (USACE 1984), the CEM (USACE 2002), and Kamphuis (2010) for some of the coastal engineering and management applications.

### 6.1 Overview of Coastal Geomorphology

This section is a very brief introduction to some of the coastal geomorphology concepts that are valuable in understanding the underlying geologic framework for some coastal road situations.

Coastlines in the US include the extensive barrier islands systems of the south Atlantic and Gulf Coast as well as the coastal bluffs of New England, the Pacific, and the Great Lakes. A few ocean coasts are muddy shorelines (the “big bend” of Florida) or vegetated shorelines (mangroves of southwestern Florida) but these are the exceptions. Some coasts are rock cliffs that extend into the sea and are pounded by relentless ocean waves. Marsh shorelines are common on small bays with small waves. Most of America’s coasts have some form of sandy shoreline.

Beaches, the accumulations of loose sediments along the shoreline can either be barrier islands or just short pocket beaches between two rock headlands. The type of coast and beach at each location is partially controlled by the “geologic framework” that created it. This framework includes the local geologic formations and the interplay between plate tectonics, sea-level changes and waves that have created each beach.

**Coastal geomorphology is the study of coastal landforms.** Many of the most obvious coastal landforms are products of either erosional processes or depositional processes. Sea cliffs, stacks, arches, caves and wave cut terraces are some erosional features found on retreating rocky coasts (see Komar 1998).



Figure 6.1. Sea cliff and pocket beach on the Oregon coast (Oswald West State Park)

Figure 6.1 shows a sea cliff on the Pacific Coast. Note a small beach at the base of the cliff. This is a pocket beach that forms from sand eroded out of the cliff and from a nearby creek. The beach is held in place by the headlands where the cliffs extend to the sea at the ends of the beach.

Barrier islands, sand spits, bays and lagoons are some large-scale depositional features found along much of the US sandy coast. Figure 6.2 shows a barrier island on the Gulf of Mexico. The US barrier island system, that generally extends along much of the coast between New York and Texas, is the longest such system in the world.

One of the fundamental geologic controls on shoreline position and characteristics is sea level. Sea level has fluctuated tremendously throughout the past two million years. Section 4.1 discusses the sea level change experienced along the US shorelines during the past century. However, the history of sea level changes over the past 2 million years, and particularly the past 20,000 years has had an impact on the coastlines we have today. During the ice ages, sea level fell as glaciations increased and rose as the glaciers receded.

According to geologists' estimates, 20,000 years ago, the global, eustatic (with land elevation changes removed), sea level was probably 300 ft lower than it is today. One estimate of the rate of sea level rise in the past 20,000 years is shown in Figure 6.3. This time period, particularly the past 12,000 to 20,000 years, is the Holocene Epoch at the end of the Quaternary Period. It is characterized by the rise of global sea level in response to the melting of the last of the Wisconsin ice-age glaciers (Davis and FitzGerald 2009).



Figure 6.2. An example of a barrier island. Dauphin Island, Alabama (circa 2001, looking east with Gulf of Mexico to the right and Mississippi Sound to the left)

The Holocene rise in sea level (Figure 6.3) has two distinct portions. Prior to about 5,000 to 7,000 years ago, sea level rose at a much faster rate: about 3 ft/century. This fast rate potentially caused the coastline to move so rapidly that mature barrier islands did not have time to form. The rate of rise slowed significantly about 6,000 years ago. The slower rate allowed the shorelines to become more stable and wave-driven longshore sand movement to create the barrier island systems along many of our shores today.

The question marks shown on Figure 6.3 represent the uncertainty about the way that the Holocene rise in sea level occurred. Although some investigators postulate that there was significant fluctuation and others do not, most agree with the general shape of the curve shown (Davis 1994).

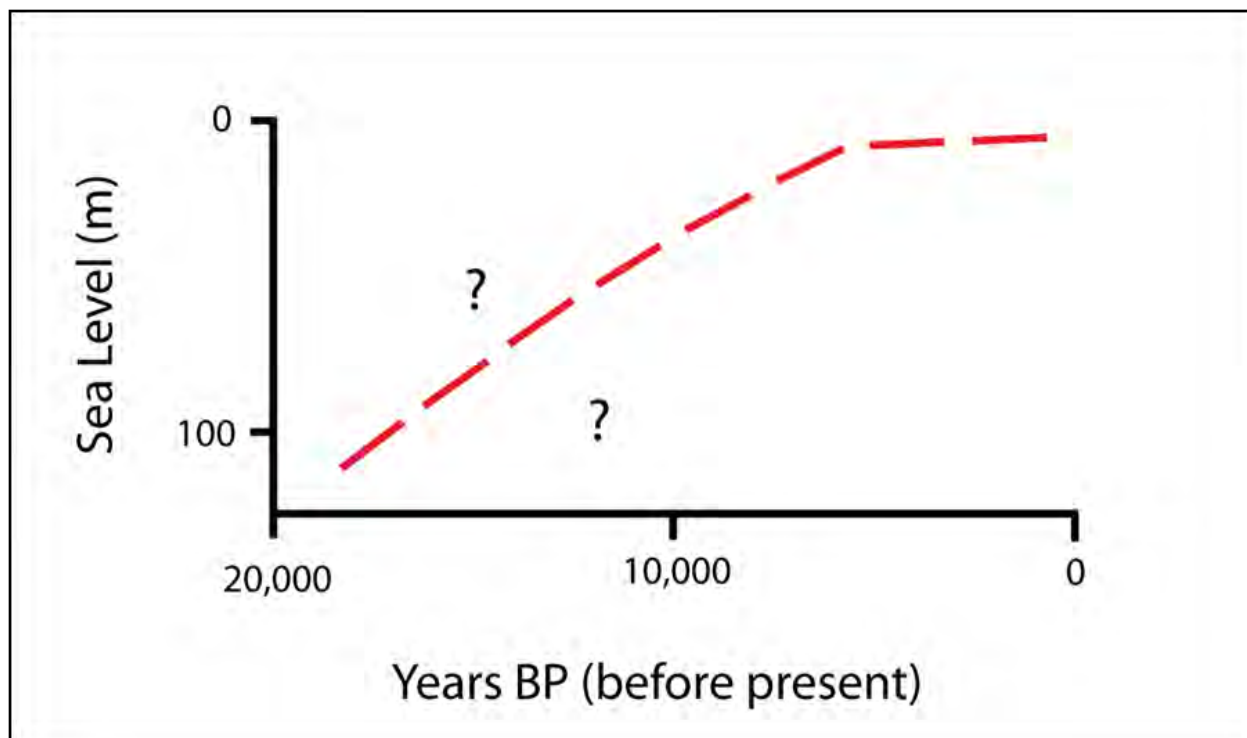


Figure 6.3. Sea level rise curve for the past 20,000 years

The position and characteristics of shorelines are partially controlled by global plate tectonics (Inman and Nordstrom 1971). The Pacific Coast of the US is on the “leading” edge (the edge of the plate that is in the front of the plate’s movement) of the North American plate and the Atlantic Coast is on the “trailing” edge. The difference explains some of the general differences in shoreline characteristics including the presence of mountain ranges and a narrow continental shelf near the Pacific Coast but not the Atlantic Coast (Davis 1994). These are contributing factors to the lack of barrier island systems on the Pacific Coast and their extensive presence on the Atlantic Coast.

## 6.2 Beach Terminology

The beach can be defined as the accumulation of unconsolidated sediment (sand, gravel, and/or cobbles) extending from some upland location, such as a sea cliff or sand dune or vegetation line, to the water line and extending out below the water to a depth where the sediment is not moved by wave action. The beach is commonly synonymous with the term “littoral” referring to this same area where waves can move sand (Komar 1998). The offshore limit of the littoral zone can be very deep during large storms but is often just assumed to be a depth of 20 to 60 ft depending on the wave climate.

Terminology used to describe the processes of waves and currents in the nearshore is shown in Figure 6.4. The nearshore zone extends from the upper limit of wave runup on the beach to just beyond where the waves are breaking. The breaker zone or line is the portion of the nearshore region in which waves arriving from offshore become unstable and break (see Section 5.2 Wave Transformation and Breaking). The swash zone is the portion where the beach face is alternately covered by the run-up of the wave swash and then exposed by the backwash. The surf zone is the portion of the nearshore between the breaker line and swash zone. The surf zone can have bore-like, breaking or broken waves propagating across it. The field of “surf zone dynamics” is an

active area of research that focuses on the hydrodynamic motions of waves and currents as well as the sediment response to those motions in the surf zone.

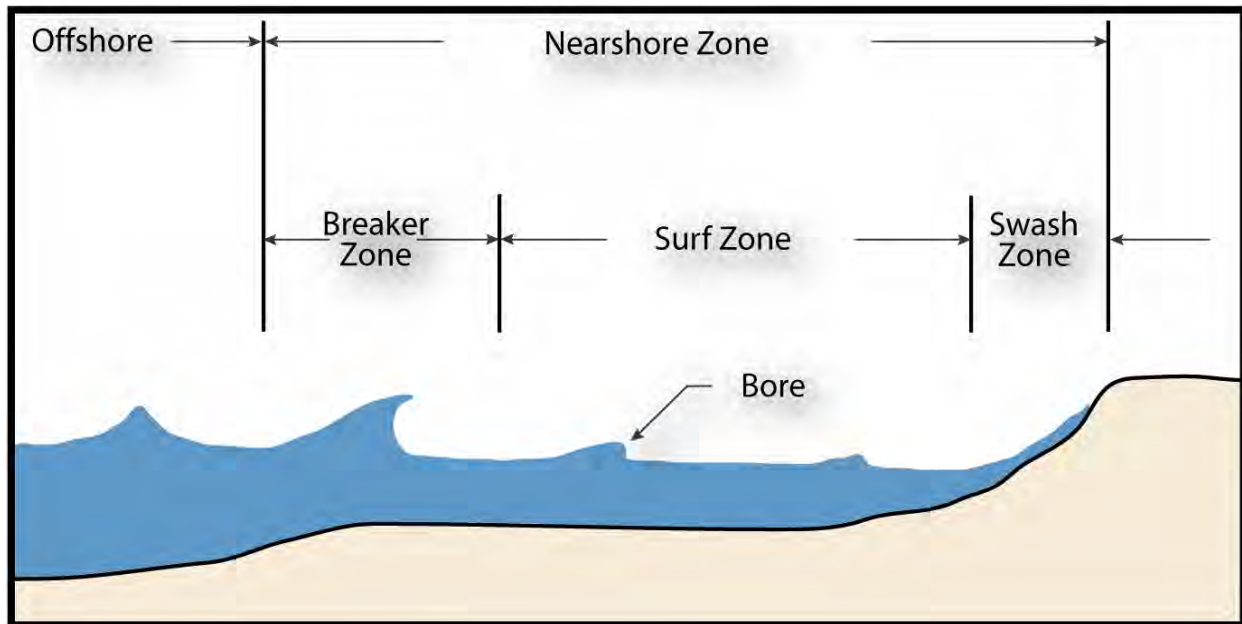


Figure 6.4. Terminology used to describe processes of waves and currents in the surf zone

The shape of a beach profile, or transect or cross-section, has some typical features. The terminology used to describe the beach profile is shown in Figure 6.5. A longshore bar, or sand bar, is an underwater ridge of sand running roughly parallel to the shore. Sand bars can be exposed at low tide in areas with large tide ranges. Figure 6.6 shows a sand bar exposed at low tide at a location on a South Carolina coast where the tide range is about 7 ft. Because of the beach slope, the intertidal area here is several hundred feet wide. A longshore trough is a depression inside of a sand bar. The beach face is the area of the swash zone. The beach berm is the nearly horizontal portion of the beach formed by the deposition of sediments by waves. Some beaches have more than one berm at slightly different levels separated by a scarp. A scarp is a nearly vertical cut into the berm portion of the beach profile by wave erosion. Scarps are often at the top of the beach face when erosion is occurring. A scarp along a southern California beach is shown in Figure 6.7. Waves were actively eroding the berm at the time the photograph was taken.

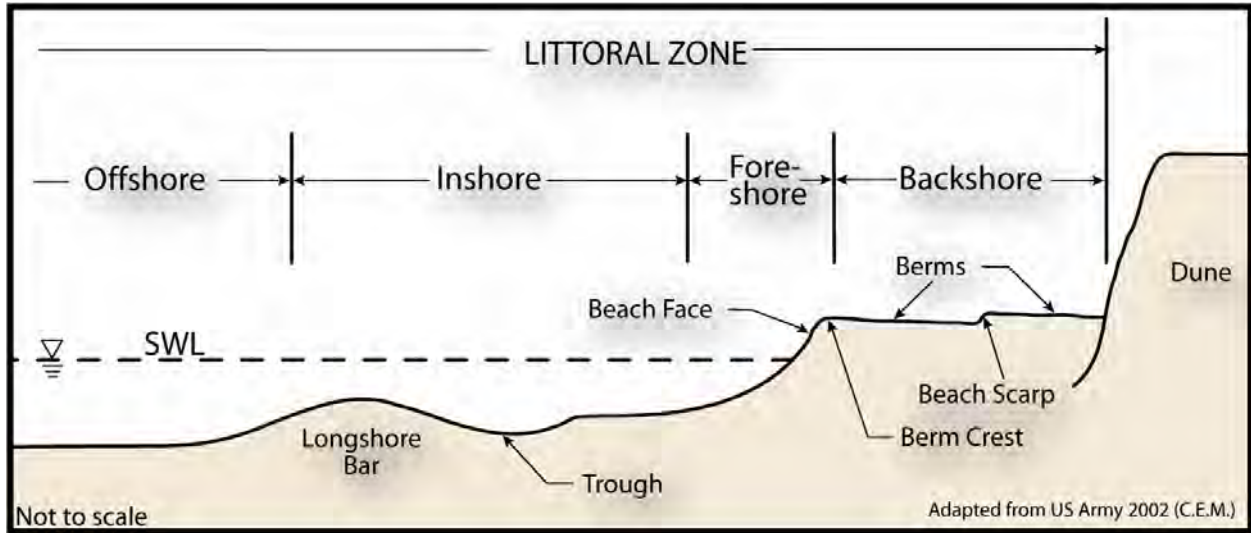


Figure 6.5. Terminology used to describe the beach profile



Figure 6.6. Sand bar and trough exposed at low tide (Garden City Beach, South Carolina)



Figure 6.7. A beach scarp (Los Angeles County, California)



Figure 6.8. A sand dune (St. George Island, Florida)

Sand dunes are natural features behind many sandy beaches in the US (see Figure 6.8). Dunes are a unique type of habitat and host some endangered and threatened species of mice. Sand dunes also provide protective benefits during storm events by blocking or reducing storm surge flooding and wave action. Dunes function as sacrificial volumes of sand that minimize storm impacts until the dunes are eroded by waves or overtopped by storm surge. Dunes with sand fencing and vegetation trap and stabilize sand, leading to increases in dune volume and dune height over time.

Repetitive measurements of beach profiles are a common tool in quantifying erosion and other coastal processes. Elevation of sand surface, both above and below the waterline, is measured. A variety of techniques have evolved over the years for obtaining these measurements. The problem is that neither traditional land surveying techniques nor traditional marine surveying techniques can easily span the offshore, the surf zone, and the upland portions of the beach profile. So, overlapping coverage with different techniques is necessary.

Figure 6.9 shows a beach surveying crew using a traditional land surveyor's level to measure the profile. The person holding the rod has to wade and swim in the surf zone and this can become problematic in large surf. One highly specialized modification of this approach is shown in the left side of the photograph in Figure 6.10 where a staff gage or total reflector station is attached to a CRAB (Coastal Research Amphibious Buggy) that drives out through the surf zone while measurements are made. The CRAB shown in Figure 6.10 is privately owned and used exclusively for measuring beach profiles in beach nourishment projects.



Figure 6.9. Beach profile surveying crew using a traditional level and rod



Figure 6.10. A CRAB (Coastal Research Amphibious Buggy) used to measure beach profiles during beach nourishment

Marine surveying techniques have been adapted for the surf zone by placing fathometers and GPS or total stations on jet-skis (personal watercraft). This can improve the ability of the vessel to obtain data in very shallow water.

A common method for measuring land elevations is airborne LIDAR, laser-based elevation measurements, from an airplane. LIDAR technology has the capability of measuring the dry beach elevation and the underwater portion of the profile at the same time with the same equipment. The water depth measuring LIDAR has some operational limitations related to water clarity and surf zone breaking. The laser can only penetrate water if it is clear enough: the air bubbles in white-capping in the surf zone can cause problems. However, the ability of LIDAR to collect large amounts of precise measurements over large distances in short periods of time is a significant advance for beach profile surveying.

**LIDAR can measure water depths in some locations (clear water).**

Many beach profiles have similar shapes. If the sand bar is ignored, many beach profiles are concave upward with slopes that are much milder than the angle of repose of the same sands on dry land. This shape is a response to the wave energy present in the surf zone. A useful concept is that of an “equilibrium beach profile” where the shape of the profile is in equilibrium with the wave energy. The shape of the offshore portion of the profile has been modeled with a variety of different expressions. One is shown in Figure 6.11. This simple relationship between depth and distance offshore fits many sandy beach profiles at different locations and has some physical

meaning related to the dissipation of energy in the surf zone (Dean 1974, Dean and Dalrymple 2002). The addition of more parameters, including the use of a variable exponent in place of  $2/3$ , can improve the fit of the relationship to any particular profile or set of profiles. The value of the “A” parameter has been shown to be a function of the sand grain size (typically between  $0.1 < A < 0.2$ ).

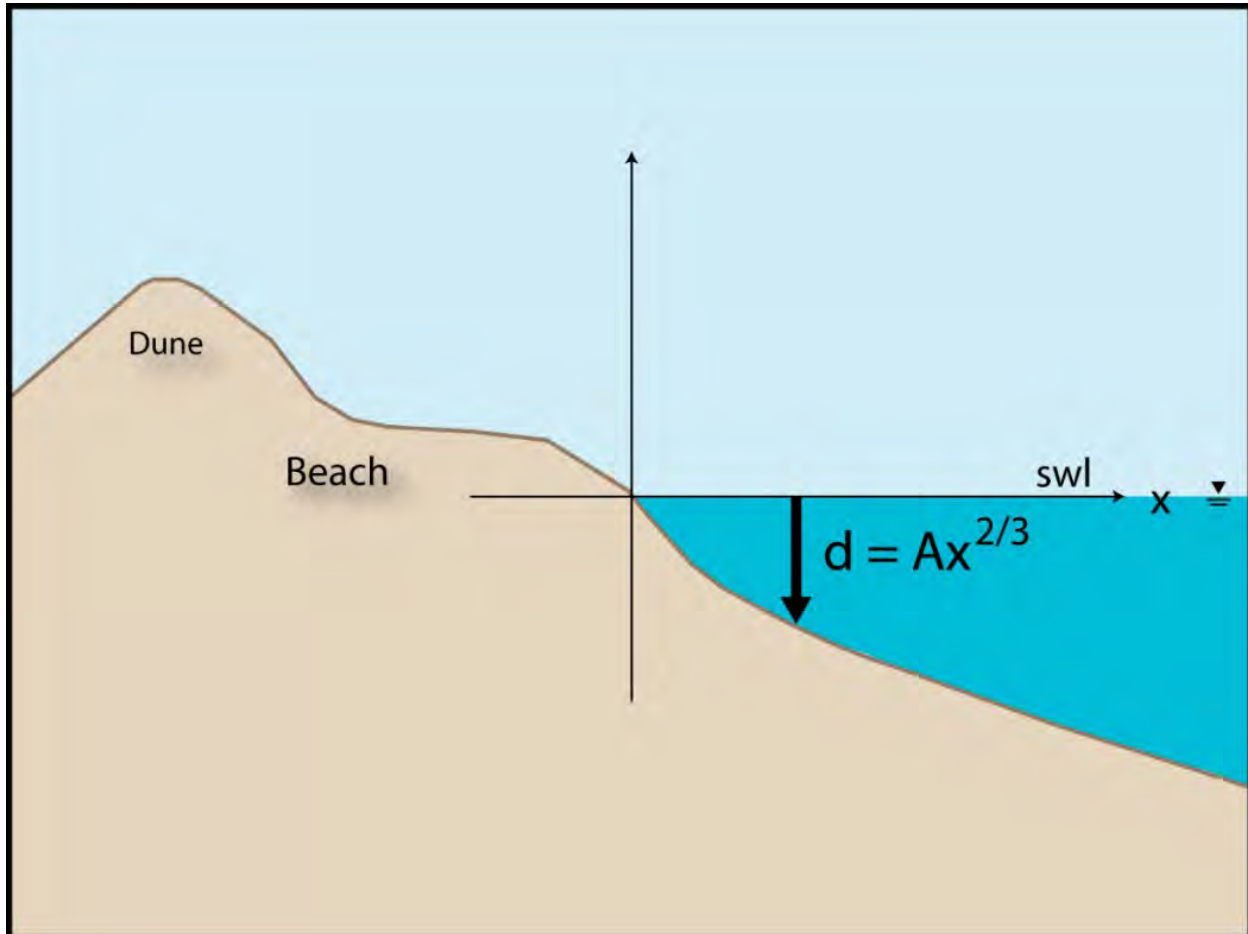


Figure 6.11. Dean's equilibrium beach profile shape definition sketch

### 6.3 Coastal Sediment Characteristics

The sediments on most American beaches are whatever hard, loose sediments are available, based on the local geology. The majority of coastal sediments are sands. Exceptions include the many cobble beaches of the Pacific, New England, and the Great Lakes. Cobbles and pebbles are round stones, and shingles are flatter stones.

Most sand-size sediments on American beaches are quartz or some other hard mineral. Exceptions to this general rule are the many beaches consisting of shell hash, ground up coral reefs, or other carbonate materials that exist in Florida, Hawaii, and to a lesser extent, along many other beaches. The mineral composition of the sand grains depends on the local geologic framework. Figure 6.12 shows the variation in color of beach sands throughout the nation.

The size of the sand grains influences the way a beach behaves and is very important in beach nourishment engineering. Beach sand grain size can vary significantly. Beach sediment grain size can be evaluated with a sieve analysis much like grain size in other civil geotechnical engineering

analyses. The median diameter ( $D_{50}$ ) is the most common measure of sand grain size. Typical median grain sizes for American beaches are 0.15 to 0.60 mm.



Figure 6.12. Examples of colors of US beach sands (from Douglass 2002, photograph used with permission of the author)

The results of a grain size analysis on beach sand are shown in Figure 6.13. The median diameter is about  $D_{50} = 0.25$  mm. Figure 6.13 shows an important characteristic of beach sand grain size distribution - they can be extremely well-sorted. Essentially, waves can winnow all the other grain sizes away. Since almost all the grains are of the same size, care should be taken to include the full complement of available sieve sizes in order to adequately differentiate beach sand grain sizes with sieve analysis.

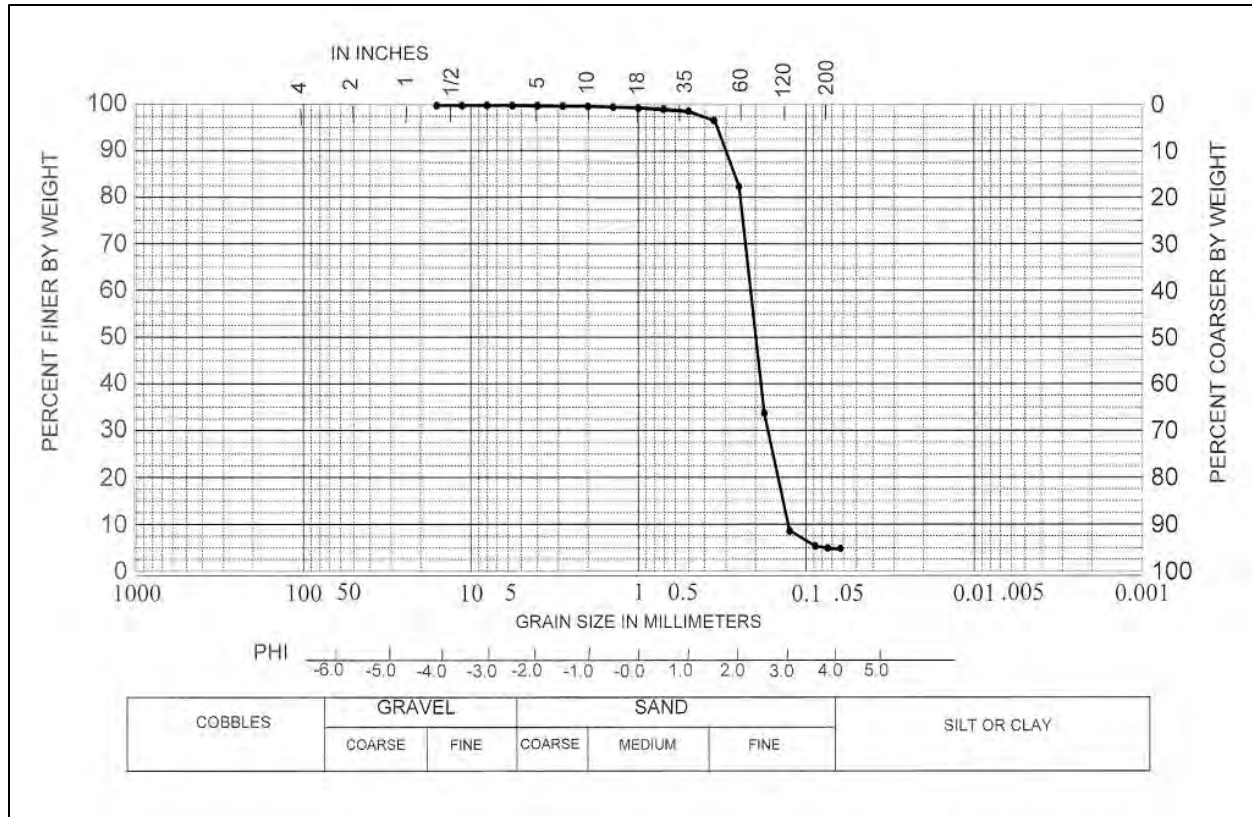


Figure 6.13. Example grain size distribution based on a sieve analysis for beach sand

#### 6.4 Cross-Shore Sand Transport and Dune Erosion Modeling

Waves have the capacity to move tremendous amounts of sand in the surf zone. This sand movement on beaches can be conveniently considered as either longshore or cross-shore sand transport. This distinction, cross-shore vs. longshore transport, is somewhat artificial, in that the individual grains of sand may be moved both in the cross-shore and longshore directions at the same time. The movement of individual sand grains in response to wave motion and currents in the surf zone is extremely complex. Movement is related to instantaneous near-bottom water velocities under breaking irregular waves, the resulting shear stress on the bottom sand grains, and the subsequent transport of sand including the rich variations in transport mechanisms (bedload, suspended load, ripple and other bedform effects, bed ventilation effects). The complexities of surf zone dynamics and sediment transport processes preclude any meaningful analytic approaches. Thus, coastal engineers and scientists typically look for simplifications of the dynamics of the processes that can be modeled and compared with empirical results. One of the simplifications adopted is the separation of transport into the cross-shore and longshore directions.

Coastal practitioners have long understood that sand moves back and forth across a beach profile in response to changes in incident wave energy. This is shown schematically in Figure 6.14.

Wave steepness, the ratio of wave height to wave length,  $H/L$ , has a significant impact on whether sand bars are moving onshore or offshore. When the wave steepness is low, such as with swell, sand bars typically migrate to the shore. The sand bars sometimes can move all the way into the dry beach and build up the berm making the dry portion of the beach wider. These low steepness wave conditions typically occur in the summer on the US Atlantic and Pacific Coasts and thus this

profile shape, with a wide beach berm, is called a “summer profile.” When waves are steep, such as with a locally generated short period wind sea, sand is eroded out of the berm and the sand bars form or are pulled farther offshore. These sea wave conditions typically occur in the winter and thus, this profile shape is called a “winter profile.” The beach is narrower than for the summer profile. Essentially, the beach profile shape is just moving toward a new equilibrium with the incoming waves. Since incoming waves are always changing steepness through time, the beach may never really reach an equilibrium shape but is always approaching one.

These seasonal shifts of sand on the beach profile, which cause a narrowing of the dry, visible beach are not typically the cause of real beach erosion and long-term shoreline change. However, shoreline recession along a coast which is eroding because of a longshore deficit of sand will appear most obviously after storms. Furthermore, in very large storms, sand can be moved out into sand bar formations and take several years to return to the nearshore system.

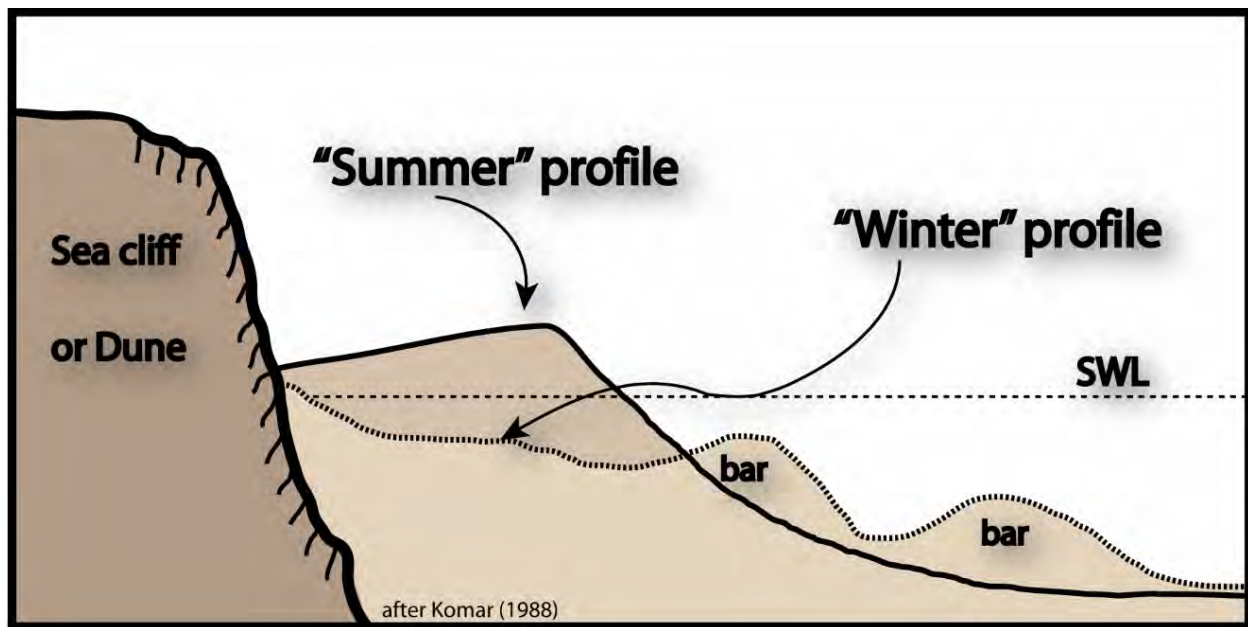


Figure 6.14. Typical beach profile changes in response to cross-shore transport of sand

Sand in the berm and dune can be moved out to sea into sand bars when storm surge temporarily raises the still water level. This storm-induced dune erosion can destroy large dune fields in a single major storm. Several models simulate storm-induced dune erosion.

Two examples of simple cross-shore morphology (i.e. dune erosion) models are EDUNE (Kriebel and Dean, 1985; Kriebel, 1986) and SBEACH (Larson and Kraus, 1989, Larson *et al.* 1990). These models require a definition of the initial beach profile, or bathymetric profile, as well as storm wave and water level characteristics. The models seek to describe a modified beach profile that is in equilibrium with the storm conditions. While the models typically capture the dune erosion and overwashing events well, the simple cross-shore morphology models are not as capable of accurately predicting the redistribution of sediments to deeper portions of the profile. In most cases this would not present a limitation when considering impacts to infrastructure along the coast. Figure 6.15 shows some an example of modeled dune face erosion.

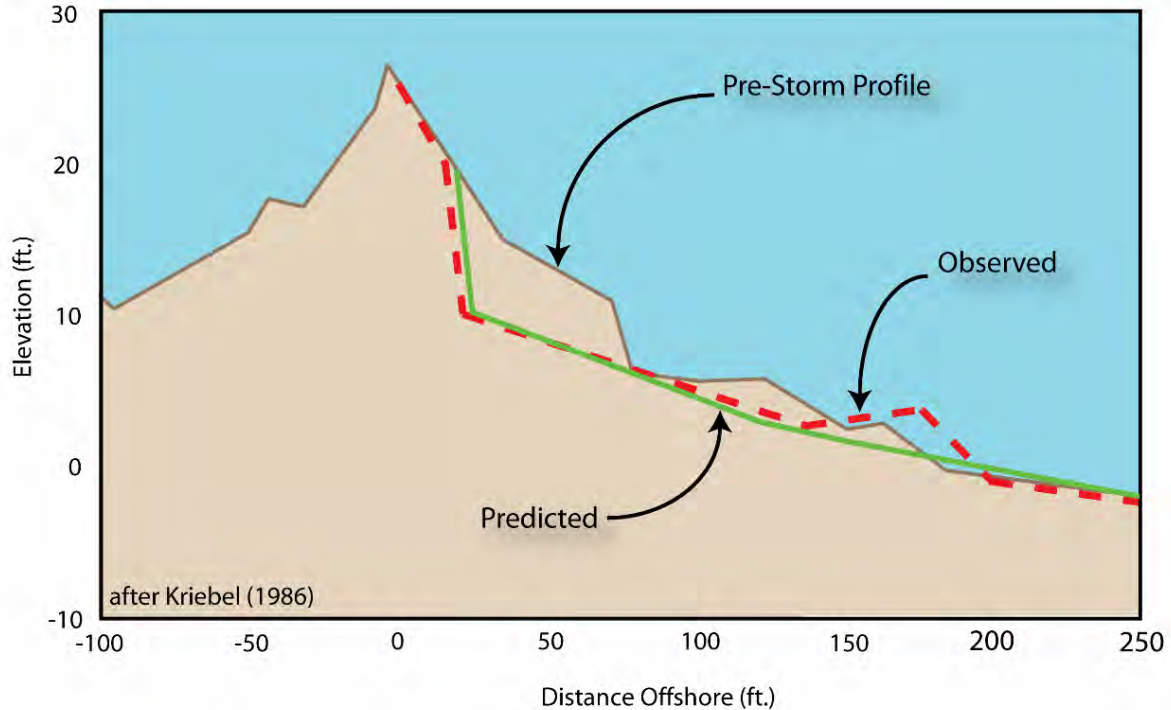


Figure 6.15. Dune erosion model results example

FEMA has adopted a simpler, parametric model for storm-induced dune erosion for the purposes of mapping coastal flood plains. FEMA's model empirically relates the volume of sand eroded from the dune directly to the storm return period (Hallermeier and Rhodes 1988):

$$(Vol) = cT^{0.4} \quad (6.1)$$

where:

- (Vol) = volume of erosion from the sand dune above the storm surge elevation per unit length of shoreline
- T = return period of storm in years
- C = empirical coefficient:  $c = 86$  when (Vol) is in  $ft^2$ ;  $c = 8$  when (Vol) is in  $m^2$

Equation 6.1 estimates the volume of erosion for the 100-year and 5-year storm levels as  $20 \text{ yd}^3$  and  $6 \text{ yd}^3$  of sand per foot of shoreline, respectively. These values are for the volume of sand above the storm surge elevation (which of course can be much higher for the 100-year storm). This dune erosion model has been incorporated into FEMA's Coastal Hazard Analysis Model (CHAMP) model that is available on-line.

Equation 6.1 can be used to design sand dunes as nature-based solutions. Since there is no factor-of-safety in the parametric model, engineering judgment is needed in nature-based solution design applications. Dunes can be constructed as integral parts of larger beach nourishment projects or as stand-alone barriers to overwash. Small, FEMA funded dunes (erroneously termed "berms") are often designed using Equation 6.1 and built as emergency projects after major hurricanes to "jump-start" the dune recovery process and reduce overwashing.

Numerical models of coupled waves, flow, and morphology are being used in the coastal engineering research community. These models simulate both cross-shore sand transport and longshore sand transport (see Section 6.5). The XBEACH (Roelvink *et al.* 2009) and CMS (Buttolph *et al.* 2006) models are both two-dimensional models capable of simulating the coupling

between waves, currents, sediment transport and morphology in a time-dependent fashion. Typically, sediment transport modeling, by its very nature, is not as well understood as hydrodynamic modeling. Even more complex, the modeling suite DELFT3D can estimate morphologic change (Roelvink *et al.* 1998). Although the EDUNE and SBEACH models are relatively easy to apply, they do not provide a time history of morphologic response during storm events, nor do they seek to describe morphologic change in a direction parallel to the coast. The XBEACH, CMS, DELFT3D, and MIKE 21 models, by comparison, provide estimates of the temporal and spatial morphologic change including dune erosion, overwashing, and breaching. Less complex, coupled, one-dimensional (transect) models are CSHORE (Johnson *et al.* 2012) and CHAMPS (FEMA 2007).

## 6.5 Longshore Sand Transport and Shoreline Change Modeling

Waves have the ability to move tremendous amounts of sand down the coast in longshore sand transport. As wave energy enters the surf zone, some of the energy is transformed into nearshore currents and expended in sand movement. The nearshore current field is driven by the incident wave energy and the local winds. The largest currents, in terms of absolute magnitude, are the oscillatory currents associated with the waves. However, several forms of mean currents are important to sediment transport: the longshore current, rip currents associated with nearshore circulation cells, and downwelling or upwelling associated with winds.

**If longshore sand transport is interrupted by engineering works, downdrift erosion can be extensive.**

Longshore current is the mean current along the shore between the breaker line and the beach that is driven by an oblique angle of wave approach (see Figure 6.16). The waves provide the power for the mean current and also provide the wave-by-wave agitation to suspend sand in the longshore current. The resulting movement of sand down the beach is littoral drift or longshore sand transport. This process has been likened to a “river of sand” that flows along all our sandy shorelines. The amount or rate of longshore sand transport can be tremendous during large storms. When averaged over a year, it can exceed a million cubic yards per year moving down the beach along some parts of the US coast. Longshore sand transport, unlike rivers, reverses direction frequently in response to changes in the direction of wave approach. Thus, the net longshore transport rate is significantly less than the gross rate. If longshore sand transport is interrupted by a ship channel or other engineering works like a jetty system to stabilize an inlet for shipping, erosion can occur for many miles downdrift.

The most common equation for estimating longshore sand transport rate is the so-called “CERC Equation” or energy-flux method (USACE 2002). It estimates the sand transport rate based on the longshore component of energy flux or wave power entering the surf zone. Using the expressions for wave power (Equation 5.19), the wave-energy flux factor evaluated at breaking can be derived as:

$$P_{ls} = \frac{\gamma H_b^2 C_{gb} \sin(2\alpha)}{16} \quad (6.2)$$

where:

- $P_{ls}$  = wave energy flux factor
- $H_b$  = wave height at breaking
- $C_{gb}$  = wave celerity at breaking
- $\alpha$  = angle of the breaking wave crest with the shoreline

$\gamma$  = specific weight of water

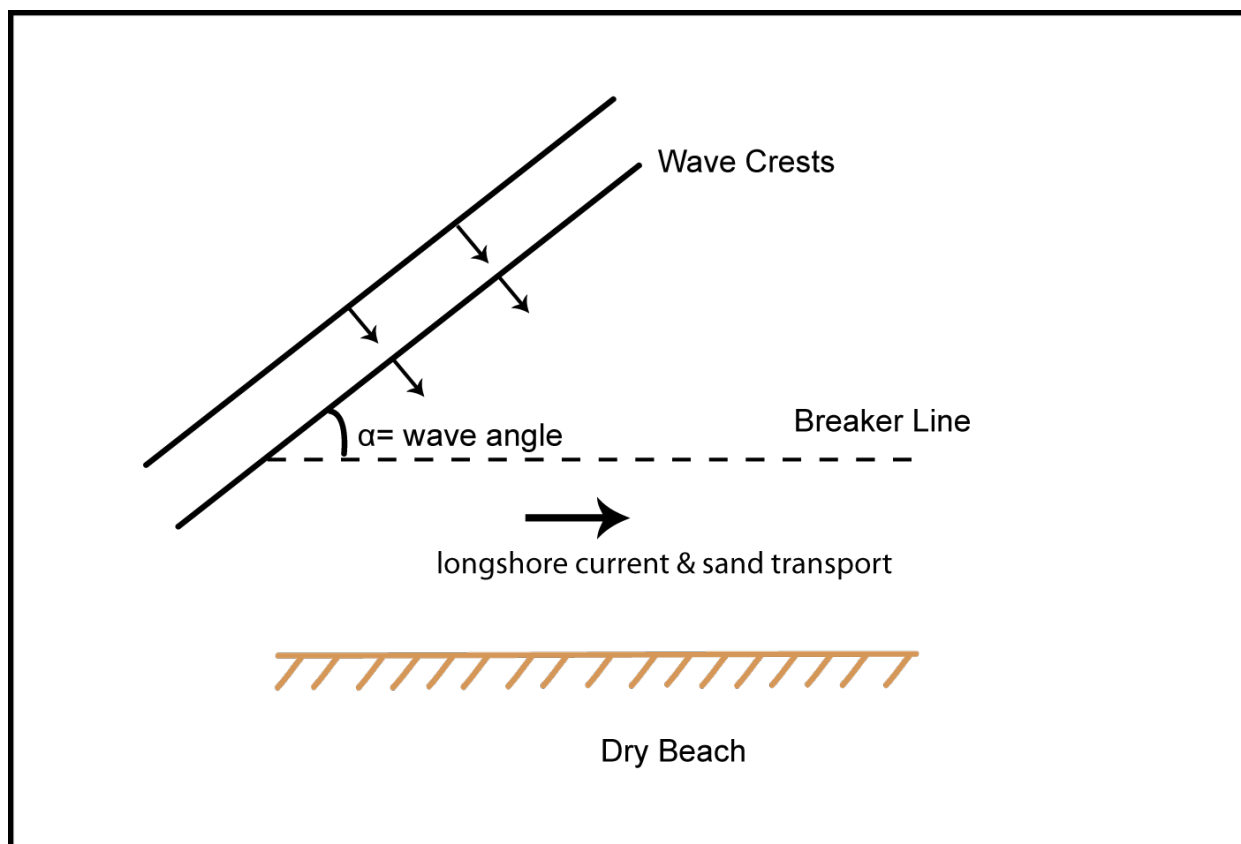


Figure 6.16. Definition sketch of wave angle at breaking

The CERC equation relating this to longshore sand transport can be written as:

$$Q = K P_{ls} \quad (6.3)$$

where:

- $Q$  = longshore sand transport
- $K$  = Empirical coefficient ( $K=7,500$  when  $Q$  is expressed in  $yd^3/year$  and  $P_{ls}$  in  $lb/s$ )

The relationship between transport rate and energy flux factor is not a precise relationship as shown in Figure 6.17 with prototype, field data. Also, there is often uncertainty in estimating the input wave parameters, such as  $H_b$  in the CERC equation. In many situations, the CERC equation can be considered as a good order of magnitude estimate of transport.

Shoreline change models simulate the temporal change in shoreline position, i.e. the movement of the shoreline. The CERC equation, or some derivative of it, often is used to estimate the longshore sand transport rate at all locations along the shoreline. Then conservation of sand down the coast is modeled. The equations are solved repetitively in time for a discretized shoreline. Wave refraction and diffraction have been incorporated into most shoreline change models. The results of shoreline change models are estimates of the changes in shoreline position due to the construction of engineering works such as groins or beach nourishments. Several shoreline change models are available: Perlin and Dean (1983), GENESIS (Hanson and Kraus 1989), and ONELINE (Dabees and Kamphuis 1998) for example. Since shoreline change models are essentially multiple applications of a form of the CERC equation or some other longshore sand

transport model, their results include all the uncertainties inherent in such modeling. Thus, shoreline change models need to be adequately validated and judgment is needed in applications. The inherent uncertainties in coastal sediment modeling are much greater than those in coastal hydrodynamic and wave modeling.

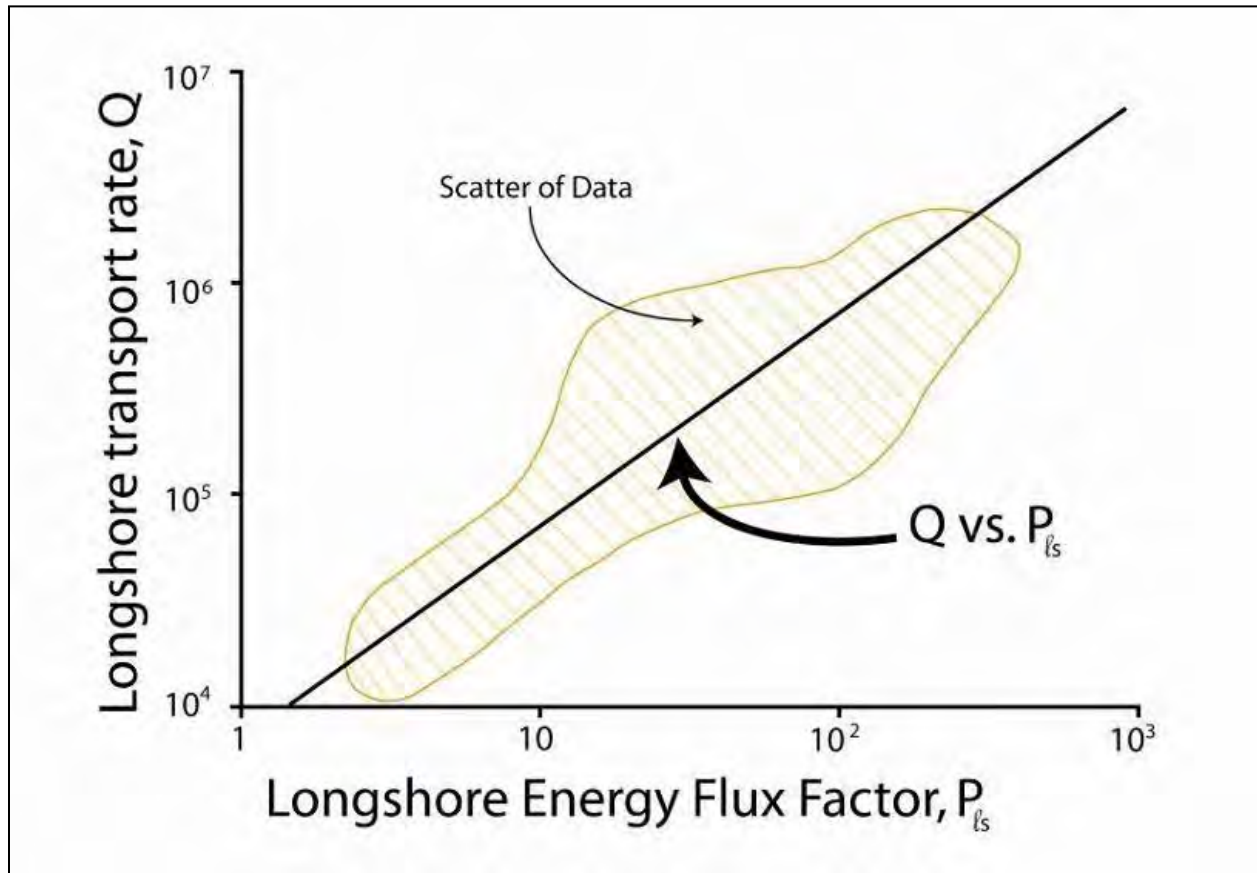


Figure 6.17. The CERC equation model for longshore sand transport rate plotted with field data (adapted from USACE 1984)

The more complex models mentioned in Section 6.5, XBEACH, CMS, DELFT3D, and MIKE 21, are numerical models of coupled waves, flow, and morphology being used in the coastal engineering research community. These models simulate both cross-shore sand transport and longshore sand transport.

## 6.6 Tidal Inlets

Tidal inlets allow water to flow from the ocean to the bay and back. Two tidal inlets are shown in Figure 6.18. There are about 600 tidal inlets of various sizes in the US. Oregon Inlet, North Carolina, is an example of a large, unstabilized inlet. Tidal inlets are dynamic parts of the barrier island system that have important influences on the bays and the nearby beaches.

While every inlet is unique, Figure 6.19 shows some common geomorphological features. The flood tide is the movement of water into the inlet and the ebb-tide is the flow of water out of the bay back to the ocean. Typical patterns of the strongest ebb-tide and flood-tide flows are shown by the flow arrows in Figure 6.19. The shoal, or bulge of sand, formed just seaward of an inlet is called the ebb-tidal delta or ebb-tidal shoal. Likewise, a shoal just inside of an inlet is called the flood-tidal delta or shoal. The outer bar of the ebb-tidal delta permits longshore sand transport to

naturally bypass an inlet to the downdrift beaches. There are often other shoals inside the outer bar of the ebb-tidal shoal.

The gorge or throat section of the inlet is the main flow channel. It is typically the deepest part of the inlet with the highest, most concentrated ebb- and flood-tidal flows. Tidal inlets can exhibit significant migratory tendencies. These can be problematic for highway infrastructure.

Tidal inlets are essentially in some dynamic equilibrium between the longshore sand transport system of the adjacent barrier island system and the tidal currents (Bruun 1966). The wave-driven longshore sand transport would seal off the inlet if not for the tidal currents scouring the sand out of the throat and depositing it on the inlet shoals. Most inlets are not symmetrical about their throat like that shown schematically in Figure 6.19 but rather skewed in the direction of net longshore sand transport. For example, the tidal channels and shoals in Figure 6.18 are skewed to the south by the dominant southerly direction of longshore sand transport along that portion of the coast.

**Many tidal inlets naturally migrate and this can cause transportation infrastructure problems.**

The hydraulics of tidal flows through inlets can be extremely complex due to the shoals, waves and currents. The primary tidal flows can be idealized as shown in Figure 6.20. Water flows into the inlet when the tide in the ocean has risen to a level that exceeds the elevation of the water surface in the bay. This vertical difference in elevation, the head difference, between the ocean and the bay drives the flow much as the downslope gradient in river elevation drives the flow in rivers. The flow in the inlet will continue to “flood” until the tide level in the ocean falls to an elevation below that in the bay. Thus, the bay tide always “lags” the ocean tide. The tidal lag can vary significantly depending on the shape of the bay and inlet.

Tidal hydraulics can be simulated well with numerical hydrodynamic models like ADCIRC. These models usually provide depth-averaged water velocities but some can estimate 3-dimensional flows. See Section 4.3.2 and Webb (2017) for discussions of coastal hydrodynamic modeling.

The amplitude, or range, of the tide in the bay can also be much smaller than in the ocean. This results in an **attenuation of the tide range**. This is common when the inlet is constricted to a level that does not allow enough time for the bay to completely fill up during the rising ocean tide before the ocean tide begins to fall. In many cases, the tide range can actually increase farther up an estuary due to inertial effects. There are a number of quasi-analytical parametric models of the solutions to the idealized ocean-inlet-bay system including solutions for maximum velocity in the inlet and bay tidal range amplitude (USACE 1984). Other parametric models relate to the stability of inlet systems.

Beaches adjacent to and near tidal inlets are part of the dynamic littoral system of the inlet and exhibit much more shoreline change than beaches farther from inlets. Sometimes the shoreline movement is recession and sometimes it is accretion. The beaches near inlets can increase dramatically in width as some of the shoals migrate onshore. Inlet geometry can change dramatically in both the short-term and the long-term. A single storm can move hundreds of thousands of cubic yards of sand shoals into or out of an inlet. Some inlets have a tendency to migrate along the coast. Some migrate in the direction of net longshore sand transport and some migrate in the other direction.



Figure 6.18. Two tidal inlets on the southwest Florida coast (New Pass and Big Sarasota Pass, Lido Key is the barrier island between the two inlets)

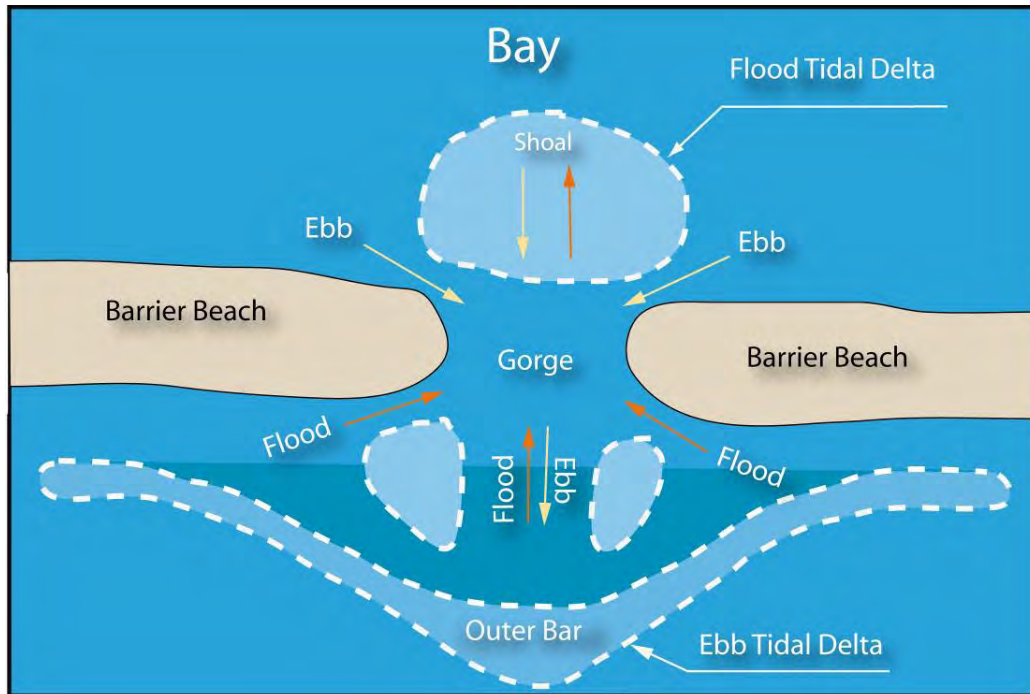


Figure 6.19. Typical inlet morphology

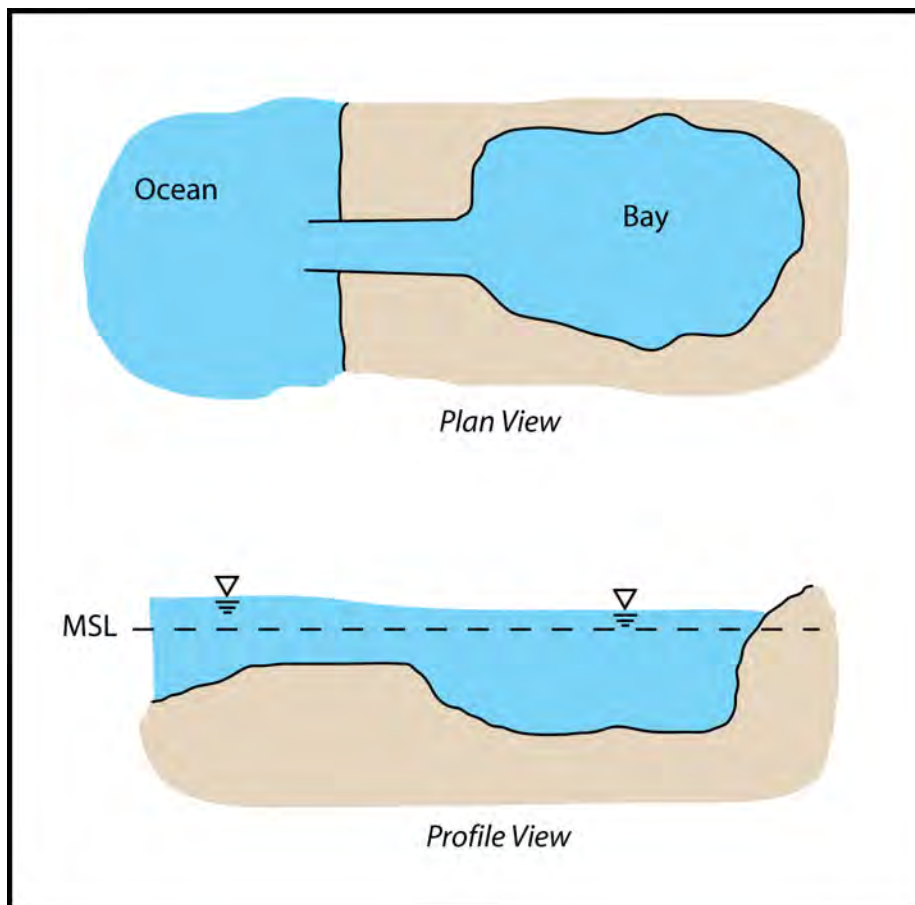


Figure 6.20. Idealized ocean-inlet-bay system (adapted from USACE 1984)

Empirical relationships have been recognized between the components of tidal inlet systems. Figure 6.21 shows one empirical relationship between tidal prism and inlet throat area. Tidal prism is defined as the amount of water that moves into and out of a tidal inlet during a tidal cycle. It is essentially the area of the bay multiplied by the bay tide range.

All tidal inlets are evolving and changing over the long-term. This evolution is in response to many changing factors including sea level rise, changes in longshore sand transport rate and changes in tidal prisms. These factors change naturally but also can be changed by engineering. Engineered changes to the ocean-inlet-bay system include the stabilization of the inlet with jetties or the dredging of the inlet or bay for navigation.

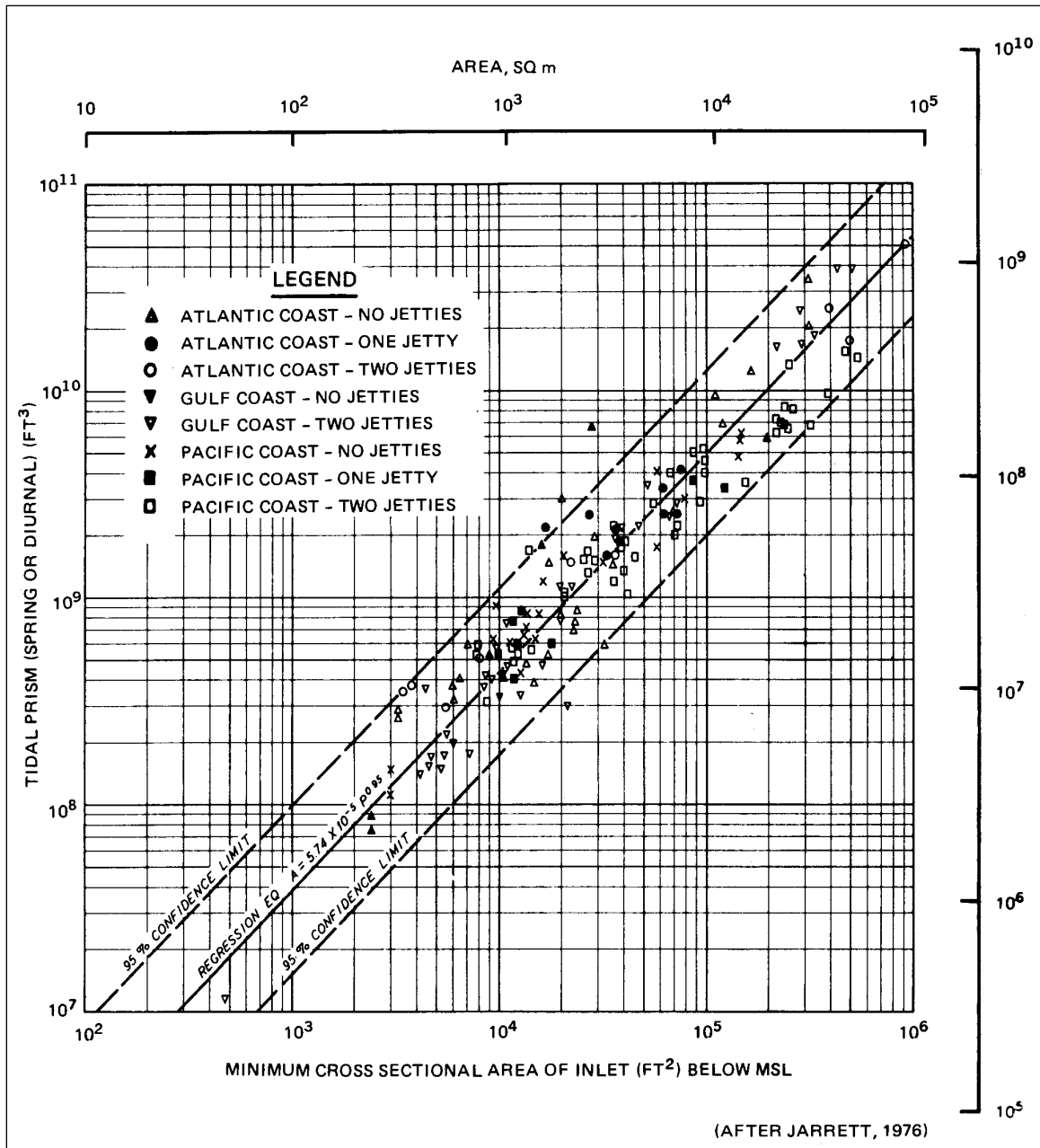


Figure 6.21. Tidal prism versus minimum inlet throat area for all major inlets on the Atlantic, Gulf, and Pacific Coasts (USACE 1984)

Less obvious changes include the impact of engineering works in the bay that affect the tidal prism. This impact can be caused by the filling of wetlands or the construction of causeways in the bay. The implication of the relationship shown in Figure 6.21 is two-fold: any change in the tidal prism of a bay can affect the inlet and, any change in the inlet including shoaling, scour, dredging and engineered structures can affect the tidal flow.

The two inlets shown in Figure 6.18 are evolving in response to a number of factors including the original creation of Lido Key by filling many decades ago and the construction of causeways not shown inside the bay. Another factor in the evolution of those two inlets is the complexities added to the tidal hydraulics by the interconnectedness of the multiple inlets to the bay. Multiple inlet systems can evolve as one inlet captures more of the tidal prism and expands while allowing others to close.

## 6.7 Future Sea Level Rise Effects on Coastal Processes

Sea level is an important component of coastal geology. The type of coast and beach at each location is partially controlled by the “geologic framework” that created it. This framework includes the local geologic formations and the interplay between vertical land movements, sediments, sea level changes and waves which have shaped our coasts over the past millennia.

As sea levels rise, wave-driven erosional forces will act farther up on coastal bluffs and cause increased erosion (Hampton *et al.* 1999). Furthermore, as the timing, duration, and volumes of precipitation within a watershed, and as temperature modifies the state of precipitation (snow/rain/runoff), the quantities of water and sediment delivered to the coast in the form of fluvial discharge will undoubtedly affect some of these coastal processes.

**Barrier islands and beaches have some natural mechanisms to survive relative sea level rise... they move.**

The long-term fate of some of the presently low-lying barrier islands as sea levels rise has been questioned. Is it reasonable to assume that a specific barrier island will still be in place in 2100 if sea levels have risen by 2 ft? by 4 ft? In response, some literature suggests this is probably a reasonable assumption at many barrier island locations in the US (FitzGerald *et al.* 2008, Moore *et al.* 2010, Miselis and Lorenzo-Truebas 2017, USGS 2018).

Barrier islands have a number of natural migration mechanisms that have allowed them to move and survive the sea level rise of the past several millennia (Davis 1994). These mechanisms include barrier island rollover processes related to storm overwash processes (see Chapter 10), inlet migration and the movement of sand from the ocean to the bay in flood tidal shoals, longshore sand transport onto spits at the ends of barrier islands, and wind-blown sand transport. Some former barrier islands off the Louisiana coast have now become underwater sand shoals but those are areas which have suffered both from substantial natural subsidence and loss of all new sands due to the Mississippi River mouth migrations of the past several thousand years. US barrier islands will likely be able to survive the projected rates of future sea level rise except in areas where the natural sand sharing system is interrupted by natural or man-made reasons (e.g. see Douglass 2002).

One complicating factor is the human response or adaptation. Within the past several centuries, human modifications have had significant impacts on our coasts. Human efforts, including dredging of navigation channels and trapping of sand by coastal structures, have removed over one billion cubic yards of beach sands from US beaches and caused many of the most severe beach erosion and shoreline recession problems in the past century (Douglass *et al.* 2003).

However, most of those issues related to erosion caused by blocking of the natural littoral drift have been addressed with improved artificial sand bypassing during the past few decades. Artificial sand bypassing is the use of mechanical dredging equipment to place sand dredged from navigation channels or trapped by coastal structures on the downdrift beaches. Where artificial bypassing is not happening adequately, barrier islands might disappear.

One of the primary responses to beach erosion and shoreline recession today is beach nourishment, the direct placement of large amounts of good quality sand on the beach to widen the beach (see Section 8.7). Beach nourishment has ceased and reversed recessional shoreline change trends along many of our highly-developed US coastal communities (Douglass 2002, Houston and Dean 2013). It appears that beach nourishment will be able to keep pace with the projections for future sea level rise (Houston 2019). Coastal wetlands will respond to future sea levels in different ways. The stability of a coastal wetland depends on sea and land levels, the biological production of the salt marsh, and the deposition of sediments that maintain the marsh surface in a dynamic equilibrium with the local mean sea level (Morris *et al.* 2002). Many present-day coastal wetlands have adjusted to the historical rate of sea level rise already. Protected coastal wetlands have the ability to vertically grow and adjust to some increments of rise. However, large areas of coastal wetlands in some locations, including coastal Louisiana and southern Dorchester County Maryland, are being converted from marsh to shallow open water habitat due to land subsidence (essentially an increased rate of relative sea level rise, RSLR), reduced sediment influx due to river engineering, and/or dredged canals. This process can be important in some of the modeling discussed in Chapter 14. For example, Smith *et al.* (2010) have adjusted Manning's "n" values (the empirical coefficient quantifying surface roughness in most storm surge models) to account for changes, including conversion from marsh to open water, in coastal wetlands due to higher sea levels. Chapter 14 describes how to quantify the impacts of sea level rise on coastal highway infrastructure. The FHWA "Nature-based Solutions for Coastal Highway Resilience: An Implementation Guide" (Webb *et al.* 2019) addresses the issue of coastal marsh response to future sea level rise in more detail.

## **6.8 Physical Models in Coastal Engineering**

Coastal engineering, like the broader field of hydraulic engineering, relies on three complementary techniques to deal with the complex fluid flows typical of many projects:

- field measurements and observations,
- laboratory measurements and observations, and
- mathematical and numerical calculations.

Laboratory studies are generally termed physical models because they are miniature reproductions of a physical system. In parallel to the physical model is the numerical model, which is a mathematical representation of a physical system based on assumed governing equations and solved using a computer (Hughes 1993).

The use of physical models in coastal engineering has evolved in response to the development of numerical models. For example, in the mid-1900s, large physical models of tidal estuary systems were used to understand the complex flows and analyze the influence of major engineering works. However, "large physical models of tidal estuary systems have now been almost totally replaced with numerical models that can predict flows with a good degree of success" (Hughes 1993).

Physical models are still important for coastal engineering to address other types of problems (beyond the estuary tidal circulation problem). They are particularly important for understanding

complex flows around structures where wave and current-induced turbulence issues reduce the usefulness of mathematical-numerical approaches. They are important for newer fluid-structure-sediment-interaction problems that have not been tested extensively.

This evolution from physical models to numerical models is similar to that in river hydraulics engineering and research. For example, the J. Sterling Jones Hydraulics Laboratory at the FHWA Turner Fairbank Highway Research Center often applies numerical models to complex river flow problems but also maintains physical models to validate the numerical methods (FHWA 2019a). Physical model tests are often performed to calibrate empirical coefficients in the numerical model or to validate the results of the numerical models. “Hybrid modeling” is the use of both physical and numerical models to complement each technique (Hughes 1993).

**NHI Course No. 135082: Highways in the Coastal Environment is an opportunity for transportation professionals to learn coastal engineering principles while using a small, portable coastal wave flume model.**

Physical models have a role in coastal engineering applications to highways for both reasons: the complex flows and the newer problems. For example, the problem of wave loads on bridge decks (Section 11.4) has been investigated with physical models in several different laboratories.

Figure 6.22 shows a 1:20 scale physical model of a bridge deck subjected to waves in a laboratory. The tests are being conducted in a glass-sided wave flume which is 5 ft wide (and 75 ft long) and the model bridge deck is the horizontal white object in the middle of the photograph. The model bridge deck is partially obscured by an aluminum hanger which is instrumented to measure loads and deflections. A single wave is visible at the left side of the photograph. It is propagating to the right and is about to impact the model bridge deck. This problem of wave loads on bridge decks involves extremely complex flows, including extreme turbulence levels and air entrainment, and thus the physical model tests are justified to validate the engineering analysis models used in design.

The use of physical models in coastal engineering is very much of an art as well as a science. Model to prototype similarity issues are extremely complex. Hughes (1993) summarizes the issues and capabilities of physical models and laboratory techniques in coastal engineering.

Physical laboratory models of waves can be very useful for education and training. Figure 6.23 shows a small-scale, portable, wave flume being used to wave model runoff on a smooth slope. This flume is used in the FHWA’s National Highway Institute (NHI) Course No. 135082 Highways in the Coastal Environment. The participants making the measurements in the photograph are primarily SDOT professionals enrolled in the course (and their counterparts from some US Territories). Other coastal phenomena which course participants model in this small flume include wave properties, rock revetment stability in waves, wave loads on bridge decks, and road overwashing.

The physical models shown in Figure 6.22 and Figure 6.23 only have fluids (including the air/water interface) and the structure. They do not include any sediment. So-called “movable-bed” models include sediments. The inclusion of sediments in physical modeling adds significant complexities because of the addition of new scaling issues.

Figure 6.24. shows a moveable-bed physical model of an offshore breakwater system. The wave basin is 20 ft wide and the wave generator is behind the camera location. The progression of times shows the development of a salient, or bulge in the shoreline, in the lee of the middle breakwater.



Figure 6.22. Physical model experiment on wave loads on a bridge deck in a wave flume (University of South Alabama wave flume)



Figure 6.23. A small-scale wave flume being used to model wave runup for professional development training in NHI Course #135082 Highways in the Coastal Environment

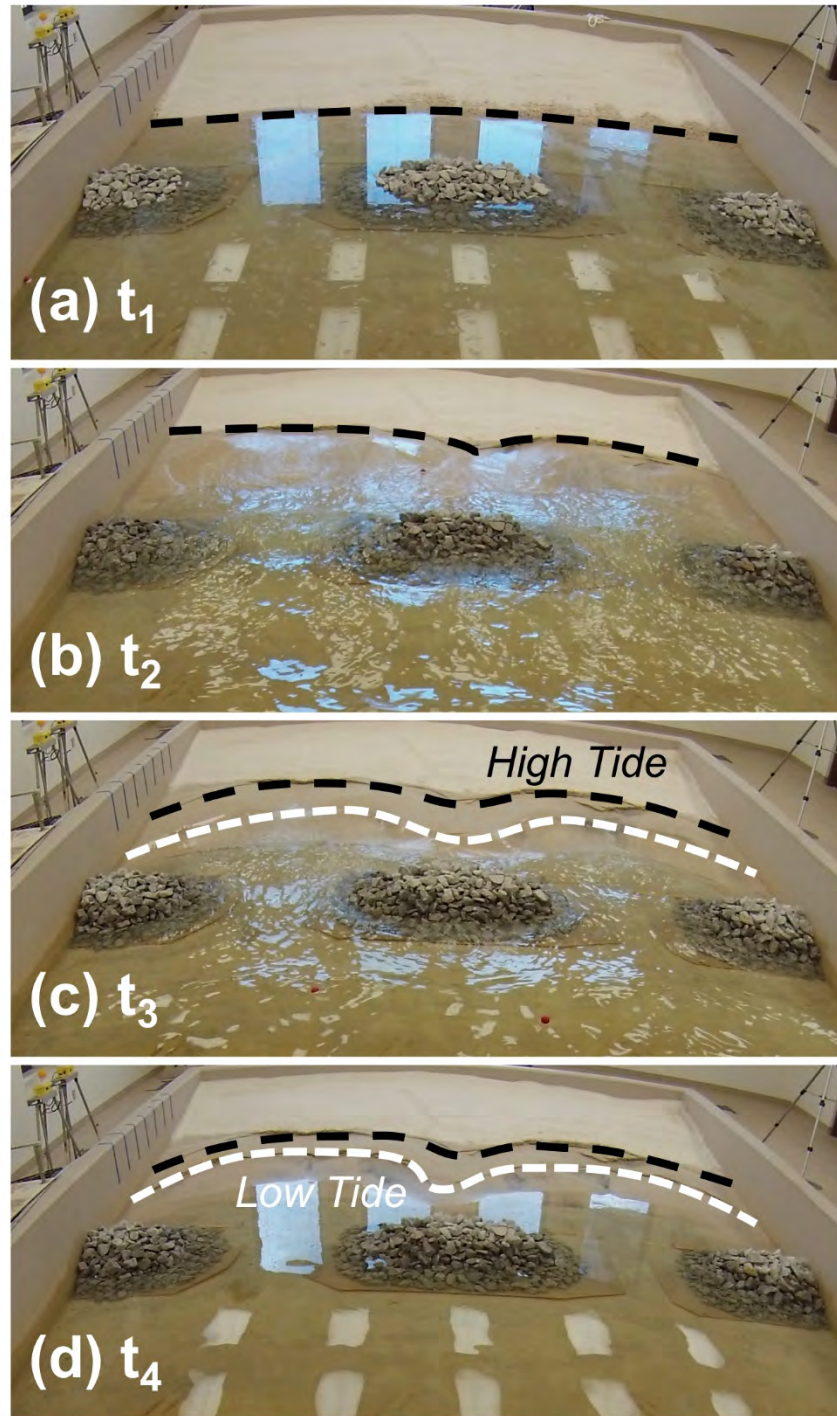


Figure 6.24. A movable-bed, physical model experiment on beach salient formation in a wave basin (University of South Alabama wave basin)

The initial condition,  $t_1$ , is a straight beach with parallel bottom contours of sand. The subsequent times,  $t_2$  and  $t_3$ , show laboratory waves diffracting through the breakwater gaps. The final time,  $t_4$ , shows a salient (bulge in the shoreline) has formed on the beach in the lee of the breakwater. Nearshore breakwaters with beach nourishment are discussed as a nature-based engineering solution in Section 8.8.

## **Part 3 – Issues and Applications in Coastal Highway Design**

*Page Intentionally Left Blank*

## Chapter 7 - Coastal Revetments

Rubble-mound revetments are often used as slope protection from waves for coastal highways. Revetments can be used for protection from four broad hydraulic situations: direct rainfall impacts, overland flow, stream or river currents, and waves. Only waves are addressed here. HEC-23 (Lagasse *et al.* 2009) provides procedures for the design of riprap revetments for channel bank protection on streams and rivers.

Consistent with USACE, AASHTO, and other practices, this chapter describes an approach for coastal revetments designed for waves based on determining a design wave and using Hudson's equation to size the stones in the outermost, armor, layer (USACE 1984, USACE 2002, Lagasse *et al.* 2009, AASHTO 2014). This approach considers the nature of the higher forces caused by waves and can lead to designs with larger stones and narrower stone gradations than designs for non-wave situations. The chapter also discusses practical issues and common failure mechanisms of coastal revetments as well as wave runup and overtopping of structures. The chapter concludes with a detailed design example of a coastal revetment.

### 7.1 Types of Revetments and Seawalls

This section describes some applications of coastal structures for embankment protection along the coast. Figure 7.1 shows a revetment along a Gulf of Mexico bay shoreline designed to protect a local road from erosion by waves during storms. This design has a stone revetment extending from below the water surface up to a sheet pile wall and pile cap near the roadway shoulder. Storm surges can exceed the pavement elevation at this location.

Revetments, seawalls, and bulkheads are distinguished by their function (USACE 1984). Revetments are layers of protection on the top of a sloped surface to protect the underlying soil. Seawalls are walls designed to protect against large wave forces. Bulkheads are designed primarily to retain the soil behind a vertical wall in locations with less wave action. Design issues such as tie-backs and depth of sheets are primarily controlled by geotechnical issues. Figure 7.2 provides a conceptual distinction between the three types of coastal protection based on the relationship between wave height and fetch (distance across the water body). Bulkheads are most common where fetches and wave heights are very small. Seawalls are most common where fetches and wave heights are very large. Revetments are often common in intermediate situations such as on bay or lake shorelines.

Seawalls can be rigid structures or rubble-mound structures specifically designed to withstand large waves. Two very large, rigid, concrete seawalls with recurved tops to minimize overtopping are the Galveston Seawall (Figure 7.3) and San Francisco's Great Highway Seawall (Figure 7.4). Sand has buried much of both seawalls in these photographs. Such massive structures are not commonly constructed in the US. Vertical sheet pile seawalls with concrete caps are common but require extensive marine structural design. A more common seawall design type in the US is a rubble-mound that looks very much like a revetment with larger stones to withstand the design wave height. Thus, the two terms, seawalls and revetments, can be used interchangeably with the former typically used for the larger wave environments. Figure 7.5, Figure 7.6, Figure 7.7, Figure 7.8 and Figure 7.9 are examples of rubble-mound seawalls protecting coastal roads exposed to open-coast storm waves.



Figure 7.1. A revetment protecting a coastal highway (Bayfront Road, Mobile, Alabama, 2019)

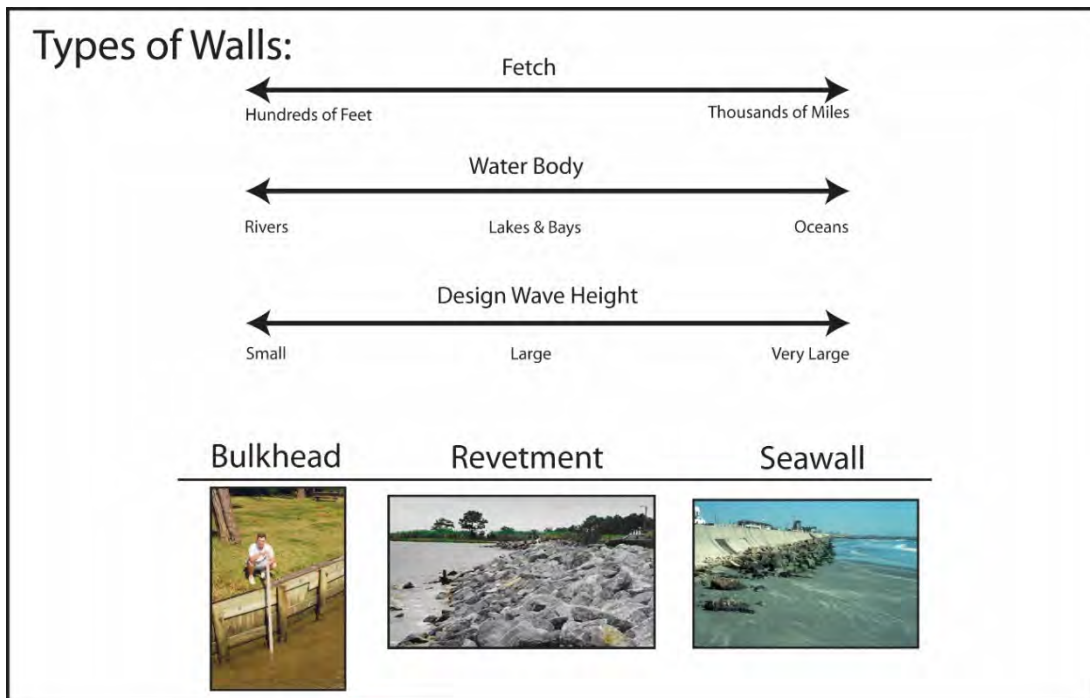


Figure 7.2. Types of shore protection walls



Figure 7.3. Galveston Seawall (Seawall Boulevard, 2018)



Figure 7.4. San Francisco's Great Highway Seawall (California SH 35, 1991)



Figure 7.5. Seawall protecting a coastal highway (Venice, Florida, 2001)



Figure 7.6. Seawall protecting a coastal highway (Pacific Coast Highway, Pacific Palisades, California, 2003)



Figure 7.7. Seawall protecting a coastal highway (Florida SH A1A, Flagler Beach, 2002)



Figure 7.8. Seawall protecting a coastal highway (US 101, Curry County, Oregon, 2001)



Figure 7.9. Wave striking a seawall protecting Kaumuali'i Highway on Kauai (Hawaii SH 50, 2018)

Figure 7.10 and Figure 7.11 (as well as Figure 7.1) are examples of rubble-mound revetments protecting highways along coastal bays. Revetments are common on bay or lake shorelines where design waves are short-period, fetch-limited, locally-generated storm waves (see OWaves).

Revetments are criticized for a variety of reasons, including their aesthetics. Figure 7.12 and Figure 7.13 show two different types of protection designed for local roads that were threatened by bluff erosion. Figure 7.12 shows a rock revetment and Figure 7.13 shows a concrete wall that has been designed to look much like the natural bluff. The engineered seawall is in the middle of the Figure 7.13 image. The aesthetically pleasing seawall (Figure 7.13) was designed more recently than the rock revetment. This is an example of the evolving nature of seawall design in the US.

## **7.2 Hudson's Equation for Armor Stone Size**

A well-designed and well-constructed rubble-mound revetment can protect embankments from waves. The underlying philosophy of the rubble-mound is that a pile of stones is efficient at absorbing wave energy and that it is robust enough to avoid catastrophic damage. It also can be relatively inexpensive. Some of the oldest coastal structures in the world are rubble-mounds. They have the inherent ability to survive storms in excess of their design storm. In the words of an old advertisement for a brand of watches, rubble-mound revetments “can take a licking and keep on ticking.” This ability to continue to provide some function even after experiencing storms that are more severe than their design storm is valuable in a coastal environment where costs often preclude selection of extremely rare design storms.



Figure 7.10. Revetment protecting a highway along a bay shoreline (Florida SH 60 crossing Tampa Bay, 2003)



Figure 7.11. Revetment protecting a highway along a bay shoreline (Washington SH 105, Willapa Bay, 2003)



Figure 7.12. Seawall protecting a local road (West Cliff Drive, Santa Cruz, California, 2001)



Figure 7.13. Concrete seawall designed to look like the natural rock formation built on an eroding sea cliff to protect a local road (East Cliff Drive, Santa Cruz, California, 2001)

Figure 7.14 illustrates the important elements of a typical coastal revetment. An outer, armor, layer of larger stones is placed on a slope to absorb breaking wave energy. Hudson’s equation can be used to determine the appropriate size of the stones in the armor layer to withstand the wave-induced loads. There may be an underlayer of stones and usually a geotextile of some kind to prevent the underlying soils from being removed by wave action or rainfall. Both a toe at the bottom and a splash apron at the top are often included.

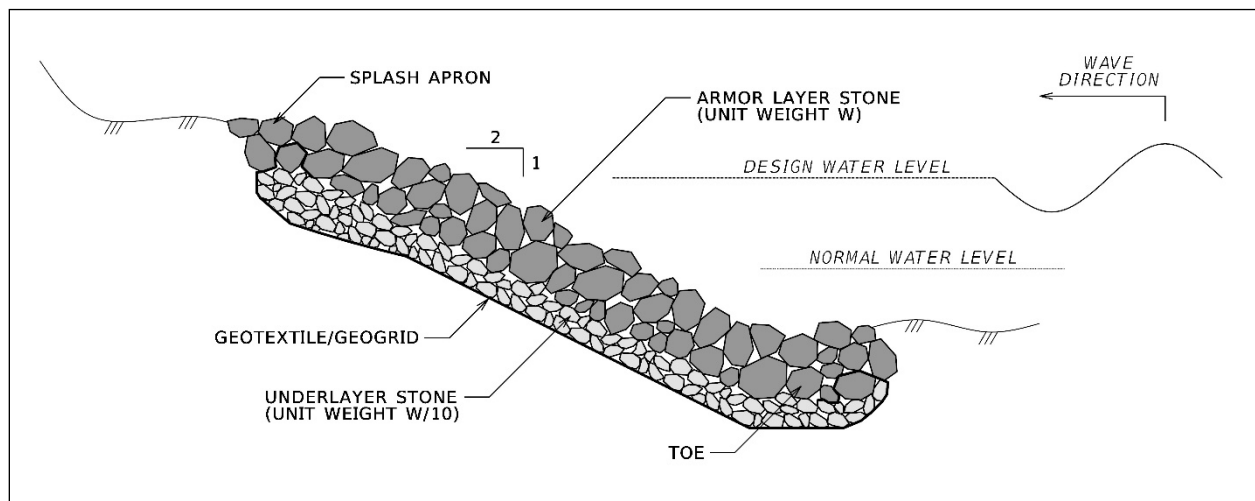


Figure 7.14. Typical coastal revetment design cross-section

Hudson's equation (USACE 1984) provides a basis for estimating the appropriate stone size in a sloped revetment that is struck by waves (e.g. Figure 7.15). It accounts for the most important variables, including design wave height, structure slope, and stone density and angularity. The appropriate median weight for the outer, or armor layer, stones is:

$$W_{50} = \frac{w_r H^3}{K_D (S_r - 1)^3 \cot \theta} \quad (7.1)$$

where:

$W_{50}$	=	median weight of armor stone
$w_r$	=	unit weight of stone (~165 lb/ft <sup>3</sup> for granite)
$H$	=	design wave height
$K_D$	=	empirical stability coefficient (= 2.2 for rip-rap gradations)
$S_r$	=	specific gravity of stone (~2.65 for granite)
$\theta$	=	slope

Note that Hudson's equation relates the armor stone weight to the cube of wave height. Therefore, careful consideration of the design wave height is needed (see Section 7.3).

**Coastal revetment rock size to survive waves is based on Hudson's equation.**

Also, revetment armor stones are generally more stable if placed on a milder slope and this is reflected in Hudson's equation. Steeper slopes call for larger, heavier stones. The range of recommended slopes here is up to 2:1 (horizontal: vertical). Note that, by definition, the  $\cot \theta = 2$  for a 2:1 slope and  $\cot \theta = 3$  for a 3:1 slope, etc. Engineering practice does not recommend revetment structure slopes steeper than 1½:1 (horizontal: vertical) (USACE 1984). Hudson's equation also includes the influence of density of the rock and therefore the armor layer can use other rocks besides granite.

The empirical coefficient in Hudson's equation,  $K_D$ , is based on laboratory tests and varies to include the effect of stone angularity/roundness, number of layers of armor stone, distribution of individual stone sizes about the median size, and interlocking characteristics. The value suggested here,  $K_D = 2.2$ , for rip-rap is for a layer of rough-angular quarrystone at least two stones thick with a gradation of weights that varies between

$$0.125 W_{50} < W < 4 W_{50} \quad (7.2)$$

where:

$W_{50}$	=	median weight of armor stone
$W$	=	weight of all the armor stones in the revetment

The gradation of the individual stones should be relatively uniform between the upper and lower limit of Equation 7.2. USACE (1984) and USACE (2002) discuss values of  $K_D$  for a variety of other situations.



Figure 7.15. Storm waves breaking on a rock, rubble-mound breakwater in a bay (Mobile Bay, Alabama)

The equivalent diameter of the median stone weight can be found using a number of different empirical formulations. The CEM (USACE 2002) provides an approximate empirical equation for the typical diameter of an angular armor layer stone (using sieves at the quarry) as:

$$D = 1.15 (W/w_r)^{1/3} \quad (7.3)$$

where:

- D = typical size, diameter, of a stone
- W = weight of the stone
- $w_r$  = unit weight of stone (~165 lb/ft<sup>3</sup> for granite)

An armor layer thickness of at least two stones is typical as a rule of thumb in all coastal design situations and the thickness,  $t$ , of the armor layer (and any underlayer) can be calculated using

$$t = n (W_{50}/w_r)^{1/3} \quad (7.4)$$

where:

- $t$  = thickness of armor layer (or underlayer)
- $n$  = number of stones per layer (at least 2)
- $W_{50}$  = median weight of armor stone
- $w_r$  = unit weight of stone (~165 lb/ft<sup>3</sup> for granite)

Caution should be exercised when using standard specification language in coastal designs. **The stone gradations recommended for coastal revetment rip-rap are narrower than those typically called for in highway specifications for other purposes.** For example, the FHWA's Standard Specifications for Roads and Bridges on Federal Highway Projects calls for Class 5 rip-rap to have a median weight of  $W_{50} = 525$  lb, with 15% of the stones weighing between 0 to 190 lb and including spalls and rock fragments to provide a stable, dense mass (FHWA 2014). However, the gradation recommended above for Hudson's equation for a coastal revetment for the same median weight calls for all stones to weigh between 65 and 2100 lb. Thus, the recommended coastal revetment gradation precludes the smaller stones in that FHWA specification. These smaller stones are typically not included in coastal revetments for two reasons. One, smaller stones work against one of the fundamental purposes of a rock revetment under wave attack which is to have large open voids in the armor layer to cause turbulence that removes the incident wave energy most effectively. Two, they have more tendency to move in response to wave action. Thus, while there may be reasons to "chock" the larger stones with the smaller stones in a revetment designed for the riverine environment, there are reasons not to do so in a revetment designed for the coastal environment.

A properly designed coastal revetment usually needs specially ordered armor stone. This is not unusual and most quarries understand these USACE coastal rock gradations. Most SDOTs have rip-rap gradation specifications for revetments which were primarily developed for the riverine environment yet may state that they are for "wave protection for causeways and shoreline roadway embankments" and for different levels of "waves." But, some of these standard specification statements are not consistent with the coastal revetment design concept outlined in this chapter. A few SDOTs have special coastal revetment design material which is consistent with sound coastal engineering practice and with this chapter.

The use of an underlayer of rocks under the armor layer is common except when the stone size is less than 200 lb. The underlayer should have a median weight no smaller than one-tenth that of the armor layer stones (USACE 1984):

$$W_{50, \text{underlayer}} = 1/10 W_{50, \text{armorlayer}} \quad (7.5)$$

Undersized underlayer stones might be pulled out between the gaps of the armor stones. The underlayer should have a thickness of at least two underlayer stones.

Engineering practice recognizes that one component of a coastal revetment design cross-section shown in Figure 7.14 is use of a filter layer of geotextile or composite geotextile/geogrid between the rocks and the underlying soil (Lagasse *et al.* 2009, AASHTO 2014). The geotextile should provide rapid transfer of water through the material while holding soil particles, and it should be strong enough to survive the construction process without the overlying rocks puncturing it. The modern use of a plastic grid integrally welded to the geotextile can provide some additional strength to soft underlying soils. The geotextile should not allow the rocks to slide down the surface. The geotextile should be wrapped up and back under some of the armor stones at the seaward end so it does not "wave" in the waves when some scour occurs. This will protect the soil under the toe and protect the entire slope better.

### 7.3 Design Wave Heights for Revetment Design

Hudson's equation is sensitive to wave height. The proper wave height for Hudson's equation above for coastal revetment design is either the depth-limited maximum wave height or the average of the highest 10% of all wave heights in the design sea-state ( $\bar{H}_{10}$ ) whichever is lesser (USACE 1984).

The basis of using this wave height value within Hudson's equation is engineering judgment and interpretation considering the origin of the equation (USACE 1984). Hudson's equation was originally derived based on monochromatic laboratory tests. Thus, the proper selection of a corresponding wave height statistic from an irregular sea-state is not obvious. Experience has found that the use of the significant wave height,  $H_s$ , in Hudson's equation is not conservative and can lead to undesired levels of damage to the revetment.

Some researchers have suggested that the proper irregular wave height statistic for use in Hudson's equation is  $\bar{H}_{10}$ . To be more conservative, some engineers use the average of the highest 5% of all wave heights in the design sea-state ( $\bar{H}_5$ ). The relationships between significant wave height and these other statistics are  $\bar{H}_{10} = 1.27 H_s$  and  $\bar{H}_5 = 1.38 H_s$  (see Table 5.1).

Coastal revetments are often located where the design sea-state is depth-limited (see Section 5.2), i.e. the depths are so shallow immediately offshore of the location of the revetment that the largest storm waves have broken and the largest waves remaining are,

$$H_b = 0.8 d_s \quad (7.6)$$

where:

$H_b$  = maximum breaking wave height  
 $d_s$  = design depth at the toe of the structure

To account for the distance over which waves travel as they break, a depth some distance offshore of the toe (say one wavelength) sometimes is used in Equation 7.6. For steep nearshore slopes see USACE (1984) and USACE (2002) for guidance on depth-limited breaking.

**Hudson's equation has no inherent factor of safety, so appropriate engineering judgment should be used for design applications.**

A depth-limited design wave height used in Hudson's equation should account for any long-term erosion that may change the depths immediately offshore. The construction of a revetment, while it protects the upland, does not address the underlying cause of erosion. The depths at the toe of the revetment will likely increase if the erosion process continues. Also, the revetment or seawall does not allow the material in the bluff to naturally nourish the beach at the toe of the bluff. And, the presence of a revetment or seawall can increase the vertical erosion at its base by increasing wave scour (see Chapter 12).

Hudson's equation has no factor of safety. The  $K_D$  values suppose that armor layer will sustain some small level of damage, represented as a percentage of the armor layer stones that moved under the design wave condition. The  $K_D$  values represent 0-5% damage. Thus, it is entirely appropriate to add some conservatism or factor of safety to the design process based on engineering judgment. Selection of a conservative design wave height used (such as  $\bar{H}_5$ ) in Hudson's equation or increasing the specified design median rock weight could provide this factor of safety.

Fetch and depth limitations result in a design wave height for many revetments being less than  $H = 5$  ft. Designs for larger wave heights use a narrower gradation of armor stone than specified in Section 7.2 above (see USACE 2002). When design wave heights get very large and the design water depths get very large, problems with the performance of rubble-mound structures can occur. These problems relate in part to wave groupiness (back to back large waves), design sea-state specification, constructability and other issues. Seawalls with design wave heights much greater than  $H = 5$  ft need more judgment, more experience, and input from a trained, experienced

coastal engineer. Other details about the design of rubble-mound revetments are discussed in the CEM (USACE 2002).

## **7.4 Other Issues for Coastal Revetment Design**

This section discusses other related issues for coastal revetment design: common failure mechanisms and alternative design approaches.

### **7.4.1 Common Failure Mechanisms of Coastal Revetments**

Understanding common failure mechanisms is valuable when designing coastal revetments. This section briefly discusses those mechanisms and approaches to avoid them. Each can be prevented by an experienced, knowledgeable engineer. Common failure mechanisms are:

1. inadequate armor layer,
2. inadequate underlayer,
3. flanking,
4. toe scour, and
5. overtopping splash.

The first failure mechanism, inadequate armor layer, can be avoided by using Hudson's equation to size the armor layer. Sections 7.2 and 7.3 outline the best proven way to design revetments for wave attack. Revetment failures have occurred because the rocks were just too small for the site-specific wave conditions.

Also, careful engineering judgment based on experience should be used when the design cross-section varies from the typical cross-section shown in Figure 7.14. Figure 7.16 shows a revetment protecting a highway that has a small, vertical bulkhead with stones on the seaward side and an almost flat stone section landward. This cross-section design essentially "trips" breaking waves when storm surge raises the water level and begins to inundate the highway. Thus, breaking waves plunge directly on the small stones behind the wall and move them onto and across the roadway during major storms. For very mild slopes approaching horizontal, Hudson's equation estimates very small armor stones. However, sound coastal engineering judgment would suggest a larger stone weight should be used to prevent this type of failure.

The second failure mechanism, inadequate underlayer, can be avoided with a design as outlined in Section 7.2. The use of a proper underlayer helps to ensure the stability of the soil underlying a revetment. Figure 7.17 shows a failed attempt to protect an embankment. The slope protection, used concrete slab panels, were available from some other project and were set on the surface of the eroding bluff. Although the panels were heavy enough to withstand the wave action itself, wave action during storms likely pulled, or pumped, the underlying soil out from between the gaps in the slabs. Consequently, the panels collapsed. The second photograph shows the panels after collapse. A rock revetment was subsequently placed farther back on the bluff. The original panel design did not adequately protect the underlying soil and did not have the flexibility of a rubble-mound revetment.



Figure 7.16. A revetment with rocks too small to withstand the wave attack at this location



Figure 7.17. Example of a failed attempt at embankment protection (USACE archives photographs)

The third failure mechanism, flanking, can be avoided with careful consideration of the ends of the revetment. Flanking occurs when adjacent, unprotected shorelines continue to recede. Erosion at the end of the wall allows wave action to remove the soil from behind the wall starting at the ends, then progressing along the walls as they fail. Flanking can be avoided by extending the revetment or wall to meet an existing revetment, a wall, or a natural rock outcropping. It can also be avoided by using a return wall. A return wall is aligned perpendicular to the shoreline. The length of the return wall should exceed the expected long-term and storm-induced recession of the adjacent shorelines.

**Typical coastal revetment failure mechanisms can be avoided with engineering judgment.**

The fourth failure mechanism, toe scour, can be avoided with the use of an adequate toe scour apron. Vertical scour at the toe of a revetment or seawall can cause the underlying soil to be exposed to waves. One solution to toe scour problems is shown in the recommended revetment cross-section in Figure 7.14. A significant volume of stones is placed at the toe. This toe is

designed to collapse into any toe scour hole that develops without loss of the stones on the slope. For very erosive areas, more stones can be used in the toe (see USACE 2002).

The fifth failure mechanism, overtopping splash, can be avoided with careful consideration in design. Overtopping splash at the top of a revetment or seawall can lead to failure by exposing the underlying soil to waves, resulting in its removal. If the wall does not extend to a high enough elevation, waves will overtop the wall. Figure 7.18 shows indications of overtopping splash damage at the top of rock seawall. A solution to overtopping splash problems is to provide a splash apron as shown in the revetment cross-section in Figure 7.14. The rocks extend some distance back from the break in slope. The width of the splash apron varies depending on the severity of the expected overtopping. A minimal splash apron width is 5 to 10 ft. An example of a splash apron is shown at the top of the rock revetment in Figure 7.19. Splash aprons can raise issues with overall space limitations and with highway clear zones.



Figure 7.18. An example of splash damage behind seawall (circa 2004)



Figure 7.19. Example of a splash apron (center of photograph) at the top of a coastal rock revetment protecting a local road along a bluff on Chesapeake Bay (Shore Road, Anne Arundel County, Maryland, 2017)

#### 7.4.2 Alternative Revetment Concepts and Materials

Revetments come in all shapes and sizes, widely varying in form and material. Although the layered armor stone revetment is a proven, robust design in coastal situations, other approaches are often employed. The USACE CEM discusses and summarizes methods to quantify the stability of revetments in wave attack beyond the Hudson's equation approach outlined above (2002). Most of that USACE discussion is in terms of a "stability number;" likely necessitating services of a trained coastal engineer for design using these other methods.

**A "dynamic revetment" (or "berm revetment") which contains a significantly larger volume of smaller stones with a wider gradation is one alternative to the traditional design** of Figure 7.14. The general design philosophy of a dynamic revetment is to allow the rocks to move in response to storm waves into an equilibrium shape much like a cobble or sand beach. This approach has the advantage of allowing a higher percentage of the stones from the quarry to be used in the breakwater than the traditional design approach (Baird and Hall 1984). The equilibrium cross-section shape is similar to the equilibrium shape for sandy beaches (see Figure 6.11) where the rocks act, essentially, as much larger grain sediments than sands and develop a concave upward shape. Stones at the location and elevation where the largest waves are striking the structure during design conditions get pulled offshore a short way and change the shape of the face of the structure.

There has to be enough rock material so that the underlying soils are not exposed and the upland feature (roadway) is not attacked by the recession of the structure face during the design storm. This recession can be significant (see Andersen *et al.* 2014). Berm breakwater revetments thus typically have a much wider footprint than traditional rubble-mound revetments. Many practical design examples of this approach around the world (see van der Meer and Sigurdarson 2017)

are for harbor breakwaters exposed to very energetic seas, i.e. not typical of shallow water revetments along most US coastal highways. However, the general concept extends to cobble beaches and several of those have been included in recent designs to protect US coastal highways as nature-based solutions (Surfers Point Managed Retreat Project in Ventura, CA and Cardiff Beach, CA).

Concrete armor units provide an alternative to using extremely large stones in the armor layer of a traditional revetment design. These typically are lighter since they interlock better than quarrystone and thus have higher  $K_D$  values. They are made of reinforced concrete and can be cast on site. A common reason for their use is that the wave energy is too energetic and thus the extremely large armor stones that could be used are extremely expensive. A number of shapes of artificial concrete armor units are available, including several patented shapes that may involve licensing to use (thus augmenting cost). Concrete armor units are typically used for harbor breakwaters, not coastal highway revetments.

Concrete block revetments, however, are problematic alternatives to rubble mound revetments. Some of these have some physical interlocking between individual blocks and others do not. The performance of interlocking blocks in severe coastal environments has not been good. One problem is that minor damage can lead to failure of a large portion of the revetment. Two examples are shown in Figure 7.20 and Figure 7.21.

The failed revetment in Figure 7.20 has subsequently been covered by a sand beach through beach nourishment (see Figure 8.10). The failed revetment in Figure 7.21 has been covered by a sand beach through beach nourishment stabilized with offshore segmented breakwaters (see Figure 8.12).

Problems with concrete block revetments in coastal situations often develop at the ends of the revetment where the blocks abut a more rigid structure. Even a small amount of settlement can affect the performance and aesthetics of block revetments.



Figure 7.20. Example of rigid concrete-block revetment failure (Florida SH A1A, Delray Beach, circa 1972; University of Florida and USACE archive photos)



Figure 7.21. Example of failed block revetment (Louisiana SH 82, circa 1980, USACE archives photos)

Other revetment systems include articulated concrete mats, flexible rock-filled marine mattresses, gabions, and sand-filled geotextile tubes or bags. Articulated concrete mats have concrete blocks interconnected by cables. The size and weight of the blocks should be a function of the wave height, slope, currents, etc. Proper installation includes adequate filtration material and secure anchoring at the top of the slope. The toe is sometimes unsecured to allow it to settle (scour). Flexible rock-filled marine mattresses are used as foundations and for scour control underneath marine structures like nearshore breakwaters; but they are not generally recommended for slope protection by themselves. Gabions are rock-filled "baskets" composed of steel wire or polypropylene grid which are stacked for embankment protection but their performance in coastal waves has been "poor" (Jackson *et al.* 2006).

Sand-filled geotextile containers (tubes or bags) are typically only used for temporary revetment protection in the coastal zone. They can be buried within the existing grade and designed to become exposed only during storm erosion (an example is illustrated in Figure 8.2). The structures are prone to damage or failure by vandalism, rolling, and natural deterioration when exposed.

## 7.5 Wave Runup and Overtopping – Coastal Structures

Waves breaking on a sloping structure like a revetment or seawall cause water to run up the structure, potentially overtopping it. For situations where the embankment elevation is much higher than the expected level of wave runup during design conditions, a decision regarding the height of the revetment is needed. The height of wave runup ( $R_u$ ) is shown in Figure 7.22. It can be estimated using:

$$R_{u,2\%} / H_s = 1.6 r \xi_{op} \quad \text{with a maximum of } 3.2 r \quad (7.7)$$

where:

- $R_{u,2\%}$  = runup level exceeded by 2% of the runups in an irregular sea
- $H_s$  = significant wave height near the toe of slope
- $r$  = a roughness coefficient ( $r = 0.55$  for the stone revetments)
- $\xi_{op}$  = the surf similarity parameter as defined below

$$\xi_{op} = \tan \theta / \sqrt{2 \pi H_s / g T_p^2} \quad (7.8)$$

where:

- $\theta$  = angle of slope of structure (see Figure 7.22)
- $H_s$  = significant wave height
- $T_p$  = wave period, peak period
- $g$  = acceleration of gravity

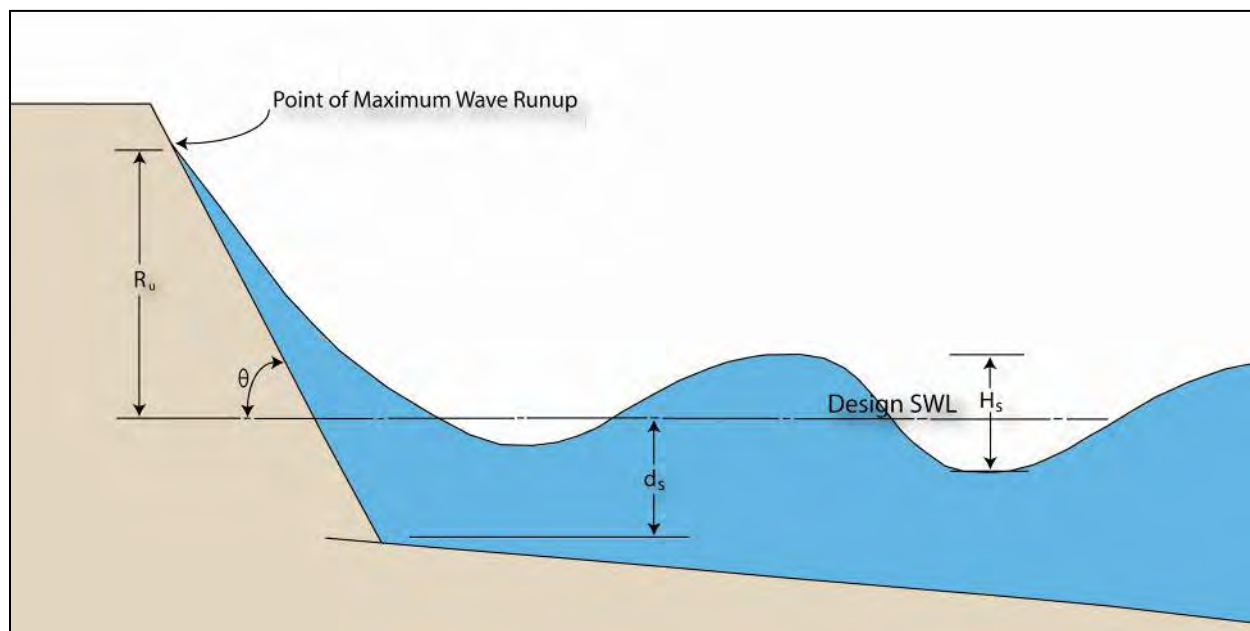


Figure 7.22. Wave runup on a structure definition sketch

Note that  $R$  is defined as the vertical difference in elevation between the SWL and the peak of the wave runup. The level given by Equation 7.7 is for the 2% runup level - the runup level exceeded by 2% of the incoming waves. Thus, 2% of the waves will run up higher than this level.

The roughness coefficient ( $r$ ) accounts for the roughness of the surface of the revetment with  $r = 1$  for smooth slopes. For rock revetments, such as shown in Figure 7.14, the recommended value for  $r$  is 0.55, and Equation 7.7 has an upper limit of  $3.2 r = 1.76$ . Thus, the 2% level of runup is  $\leq 1.76H_s$ . Equation 7.7 is adapted from a methodology developed by van der Meer and summarized by Pilarczyk (1999). More detail including other structure geometries can be found in that reference.

Wave overtopping of revetments and seawalls occurs when runup exceeds the top or crest of the structure. Wave overtopping onto coastal roads is fairly common in some parts of the United States. Figure 7.23 shows a wave overtopping a seawall protecting a local road in Lihue, Hawaii. The wave is moving from left to right striking the vertical wall in the foreground and some of the splash from the wave is landing landward of the wall. Overtopping splash from larger waves on high tide often splash so far that it lands on the other side of the second vertical wall by the road on the far right-hand side of the photograph. Local drainage systems channel the overtopped water back to the sea to the left from both the area between the two walls and the road. Local drainage is often designed, like this, to return overtopped water to the sea. Building seawalls high enough to completely prevent overtopping is often unacceptable because of aesthetics and costs.

Two aspects of overtopping which can be of interest to the highway engineer are the time-averaged volumetric rate of overtopping and the tolerable limits of intensity or force of a single wave overtopping event. Accurately estimating volumetric overtopping rates can be vital to design of seawall crest elevations if inland flooding is caused. Unfortunately, accurately estimating overtopping rates can be very difficult for many situations. Many of the tools available for estimating overtopping rates are empirical results from physical model testing and are only valid for very specific circumstances (including structure type, material, and sea state). Guidance on estimating overtopping can be found in Goda (1985), USACE (2002), EurOtop (2007) and EurOtop (2016).



Figure 7.23. Wave overtopping a seawall (Lihue, Hawaii, 2018)

The EurOtop model has been used to estimate the volumetric rate of flooding due to waves overtopping the entrance walls at the western portal to the I-10 tunnel near Mobile Bay. That analysis found that significant levels of tunnel flooding will occur when the storm surge elevation is 2 to 3 ft below the crest of the tunnel entrance walls due to wave overtopping (Douglass 2010). Interestingly, the entrance walls at that tunnel portal are 3 ft higher than the other portal of that tunnel which is in downtown Mobile and will not have any wave attack or wave overtopping (clearly the original tunnel designers understood the overtopping risk at the western portal well enough to raise those elevations an appropriate amount!).

USACE (2002) condenses a number of field studies regarding tolerable limits and critical values of overtopping discharge as shown in Figure 7.24. Some rough guidelines of the critical overtopping values for various asset types are presented. The overtopping discharge rates shown

are in terms of  $q$ , the time averaged flowrate over the wall per unit length of the wall since this is a typical result from overtopping equations like the EurOtop model. It should be recognized that the overtopping discharge is very unevenly distributed in space and in time because it varies considerably from wave to wave. Most of the overtopping is due to a small fraction of the waves, the largest waves in the sea state. The intensity of overtopping from one wave can be more than 100 times the average overtopping rate. The true critical values for any given site are extremely site dependent. What constitutes a "critical" value is itself very subjective, depending on individual opinion, local custom, and other factors.

## **7.6 Design Example: Coastal Revetment**

This section presents an example procedure for the design of a rubble-mound revetment exposed to waves. The example applies and follows the engineering principles within this chapter.

### **7.6.1 Example Situation**

Consider the scenario of a coastal highway running along the top of an eroding bluff on a bay shoreline. Shoreline and bluff erosion presently threaten to undermine the roadway. Figure 7.25 shows the eroding bluff and roadway shoulder in cross-section. The design SWL (including tide, storm surge) has been estimated as +8 ft NAVD. The design wave height ( $H_s$ ) has been estimated as 5 ft with a wave period ( $T_p$ ) equal to 5 s (using a wave generation model for this fetch-limited bay location) (see Section 5.4).

### **7.6.2 Design Steps**

Hudson's equation (Equation 7.1) is used to determine the armor layer stone weights needed to withstand the wave loads. The content and discussions outlined above reduces to the following steps:

#### **Step 1 – Determine proper H to use in Hudson's Equation, $H_{10}$ :**

Following Section 7.3 and using Table 5.1, the proper H to use in Hudson's equation is  $H_{10}$ , which is the average of the highest 10% of the waves in the sea state:

$$H_{10} = 1.27 H_s = 1.27 (5) = 6.35 \text{ ft}$$

#### **Step 2 – Specify slope, specific gravity and weight of stone**

The slope of the revetment will be set at 2:1 (horizontal: vertical) to follow the recommendation of Section 7.2. This slope also generally matches the assumed existing slope shown in Figure 7.25.

There may be issues related to width of right-of-way restrictions and encroachment into adjacent water bottoms that are site-specific. Milder slopes need more space and more, but smaller/lighter, stones. Cut and fill to match the desired revetment slope is often a consideration also.

Assume that the stone used for construction of the revetment is granite having a specific gravity of  $S_r = 2.65$  and a specific weight of  $w_r = 165 \text{ lb/ft}^3$  (typical values for granite).

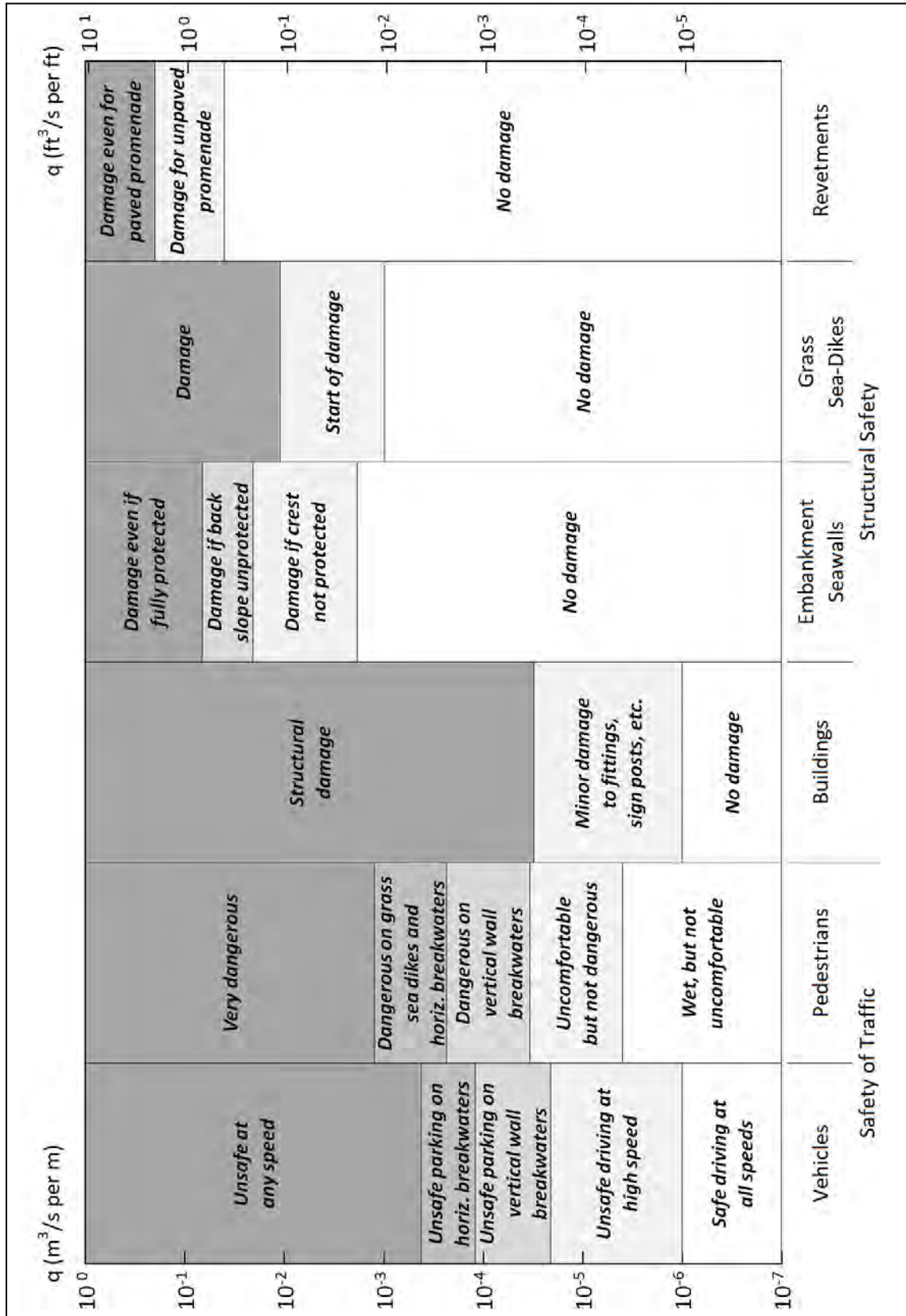


Figure 7.24. Critical values of average overtopping discharges (adapted from USACE 2002)

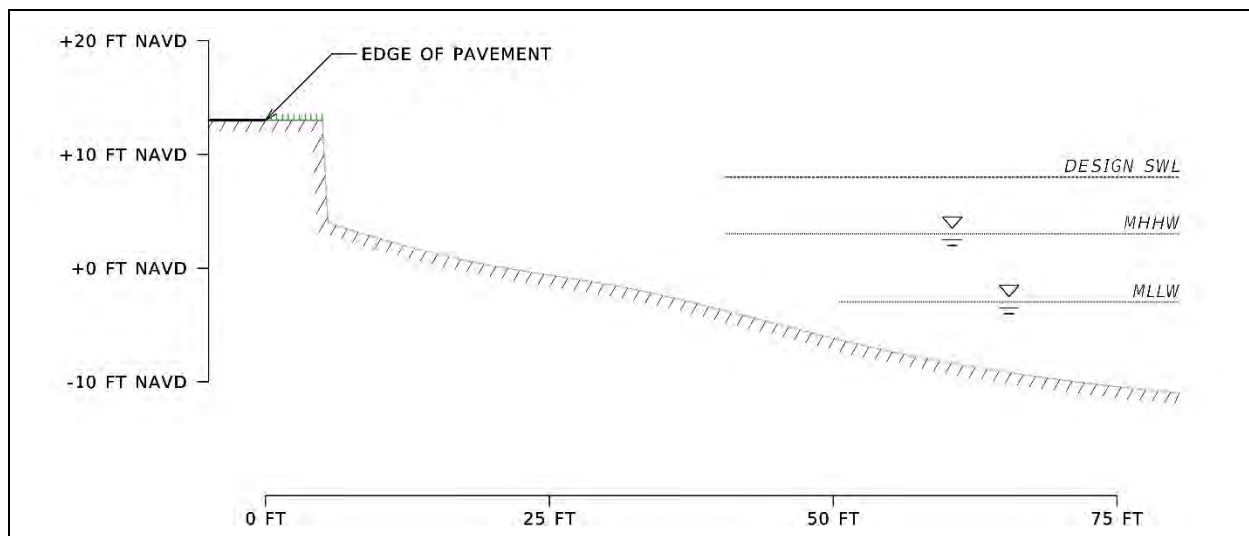


Figure 7.25. Eroding profile input to coastal revetment design example

### Step 3 – Apply Hudson's Equation to determine design armor stone median weight, $W_{50}$

Next, determine the median weight of armor stone needed for stability given the design wave height and other specified parameters by applying Hudson's equation (Equation 7.1):

$$W_{50} = \frac{w_r H^3}{K_D (S_r - 1)^3 \cot \theta} = \frac{(165 \text{ lb/ft}^3)(6.35 \text{ ft})^3}{(2.2)(2.65-1)^3(2)} = 2,138 \text{ lb}$$

This value can be rounded up to 2,500 lb. A Hudson's stability coefficient of  $K_D = 2.2$  is used following Section 7.2 for rough, angular quarystone. Since no factor of safety is inherent in the Hudson's equation calculation, one way to make the design more conservative is to increase the median weight by some rounding up of the median weight, say to  $W_{50} = 2,500$  lb, with a corresponding increase in the full gradation. Another way to make the design more conservative would have been to round up the input  $H$ .

### Step 4 – Specify armor stone weight gradation

The standard USACE coastal riprap gradation used with Hudson's equation (see Equation 7.2) is  $0.125 W_{50} < W < 4 W_{50}$ . Thus, the lower and upper bounds of the riprap gradation for use in the revetment are:

$$0.125 W_{50} = 312 \text{ lb (round to 300 lb)}$$

$$4 W_{50} = 10,000 \text{ lb} = 5 \text{ tons}$$

Thus, all the stones in the revetment armor layer should weigh between  $300 \text{ lb} < W < 5 \text{ tons}$ . Alternatives which would reduce the armor stone median weights include using milder slopes or using a dynamic revetment (see Section 7.4).

### Step 5 – Determine corresponding design armor stone median size, $d_{50}$

The equivalent diameter of the median stone weight can be estimated with Equation 7.3:

$$D_{50} = 1.15 (W_{50}/w_r)^{1/3} = 1.15 (2,500 / 165)^{1/3} = 2.8 \text{ ft}$$

and the armor sizes will range from

$$D_{\min} = 1.15 (W_{\min}/w_r)^{1/3} = 1.15 (300 / 165)^{1/3} = 1.4 \text{ ft}$$

to

$$D_{\max} = 1.15 (W_{\max}/w_r)^{1/3} = 1.15 (10,000 / 165)^{1/3} = 4.5 \text{ ft}$$

Thus, the size of the individual stones in the armor layer will range from 1.4 to 4.5 ft with a median, or typical, of 2.8 ft.

### Step 6 – Specify armor layer thickness

The armor layer of the cross-section should be at least two stone widths thick. Using Equation 7.4 this thickness is:

$$t = n (W_{50}/w_r)^{1/3} = 2 (2,500/165)^{1/3} = 5 \text{ ft}$$

### Step 7 – Determine the level of runup

Given the low elevation of the top of the bluff, relative to the design SWL, as shown in Figure 7.25, runup will likely exceed the elevation of the road pavement. This can be checked with the runup equation given above, Equation 7.7:

$$R_{u,2\%}/H_s = 1.6 r \xi_{op}$$

$$\xi_{op} = \tan \theta / \sqrt{2 \pi H_s/g T_p^2} = \tan(26.6) / \sqrt{2 \pi (5)/32.2 (5)^2} = 2.5$$

$$R_{u,2\%} = 1.6 r \xi_{op} H_s = 1.6 (0.55) (2.5) (5) = 11 \text{ ft}$$

Thus, wave runup from the largest (2%) waves in the sea state could be expected to reach the design storm surge elevation plus this value, 8 + 11 = 19 ft NAVD if the revetment extended up that high. Since it does not, severe overtopping and overwashing of the road is expected during design conditions. Thus, a splash apron as part of the design cross-section is needed and care should be taken during construction at the location where the rocks meet the pavement shoulder.

### Step 8 – Specify splash apron

The splash apron serves to armor the top of the coastal revetment embankment to prevent failure due to wave overtopping. Given the proximity of the highway to the eroding bluff, the splash apron can reach all the way to the edge of the pavement and it should include the armor layer with the large stones to survive design conditions.

### Step 9 – Specify toe protection

Toe protection is necessary at the foot of the revetment. As a rule of thumb, the maximum wave height is a conservative upper limit of scour depth at the toe of the structure (see Chapter 12). Thus, a toe depth of 6.5 ft should be adequate. This is between 2 and 3 of the median stone widths. Construction of a toe often involves excavation.

### Step 10 – Specify underlayer and geogrid/textile

The design cross-section should include an underlayer that consists of large enough stones that they do not get pulled out of the holes in the armor layer. The median rock weight of the underlayer should be, using Equation 7.5,

$$W_{50, \text{underlayer}} = 1/10 W_{50, \text{armorlayer}} = 1/10 (2,500 \text{ lb}) = 250 \text{ lb}$$

This is the median weight of the underlayer. The underlayer can also follow a riprap gradation with minimum and maximum weights of:

$$0.125 W_{50} / 10 = 30 \text{ lb}$$

$$4 W_{50} / 10 = 1,000 \text{ lb}$$

Thus, all the stones in the revetment's underlayer should weigh between  $30 \text{ lb} < W < 1,000 \text{ lb}$ . A geogrid is included under that and a layer of gravel is often included above the geogrid to avoid damage to the geotextile during construction.

The diameter of the underlayer stones will range from (using Equation 7.3)

$$D_{\text{underlayer, min}} = 1.15 (W_{\text{min}}/w_r)^{1/3} = 1.15 (30 / 165)^{1/3} = 0.65 \text{ ft}$$

to,

$$D_{\text{underlayer, max}} = 1.15 (W_{\text{max}}/w_r)^{1/3} = 1.15 (1,000 / 165)^{1/3} = 2.1 \text{ ft}$$

with a median, or typical, size of,

$$D_{\text{underlayer, 50}} = 1.15 (W_{50}/w_r)^{1/3} = 1.15 (250 / 165)^{1/3} = 1.3 \text{ ft}$$

The underlayer thickness (also set two stones thick) using Equation 7.4 will be:

$$t = n (W_{50}/w_r)^{1/3} = 2 (250/165)^{1/3} = 2.3 \text{ ft}$$

So, the armor layer will be 5 ft thick and the underlayer will be about 2.3 ft thick.

### Step 11– Sketch design cross-section

The design cross-section (Figure 7.26) of the revetment will have armor stones weighing between 300 lb and 10,000 lb with a median stone weight of 2,500 lb. The slope of the armor layer will be 2:1 (H: V), and the armor layer will be 5 ft thick. The armor layer will include a flat splash apron reaching to the edge of the pavement and toe protection reaching down about 6.5 ft below the original grade. The cross-section will include an underlayer of rocks weighing between 30 lb and 1,000 lb with a median weight of 250 lb, 2.3 ft thick. Below the underlayer is filter layer of geotextile or geogrid. Given that this design extends to the edge of pavement, a guardrail is likely needed (not shown) for driver safety concerns.

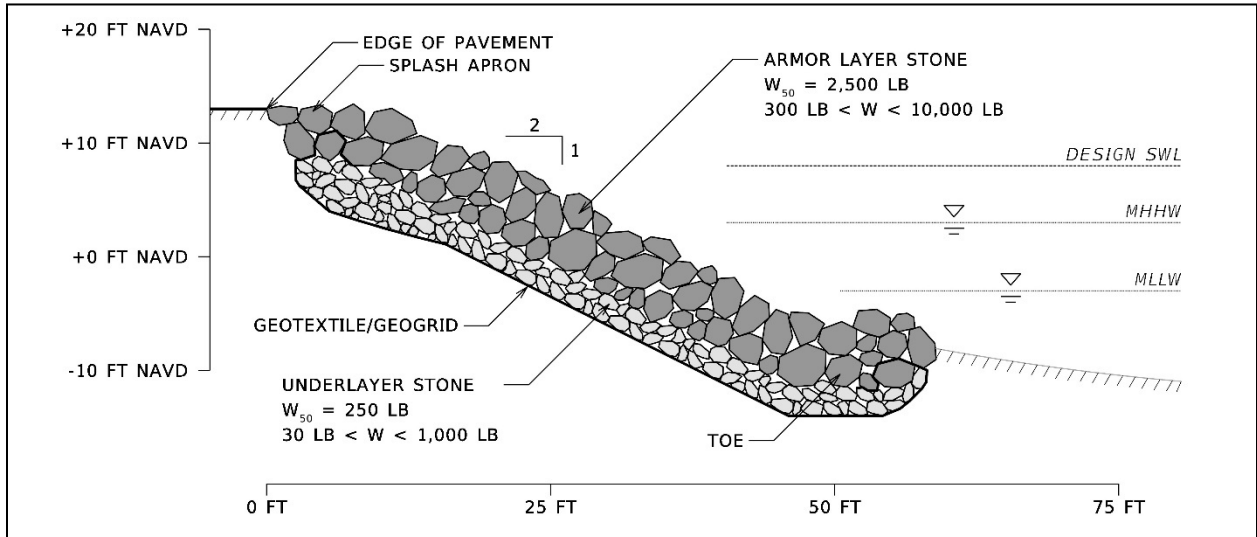


Figure 7.26. Coastal revetment design example cross-section

*Page Intentionally Left Blank*

## Chapter 8 - Roads in Areas of Receding Shorelines

Many roads in the US near the coast are exposed to waves on a daily basis, and many more are occasionally exposed to waves during storms. Also, much of the US coastline is experiencing long-term recession (erosion) due to sea level rise and other factors. Consequently, roads near these receding shorelines will eventually be subjected to waves. While this chapter does not present any FHWA requirement, it does attempt to provide an understanding of receding shorelines and associated issues faced in HICE by transportation officials. Therefore, this chapter outlines a potential process for how to assess and design for roads in areas of receding shorelines. It covers how long-term shoreline changes can be quantified and used to estimate future shoreline positions. It describes the general engineering options available for highways exposed to coastal waves and erosion including relocation/abandonment, and the alternative shoreline stabilization techniques available for protecting a highway in place. These alternatives include a spectrum of solutions from seawalls, revetments, and bulkheads to nature-based solutions like beaches and marshes.

### 8.1 *Examples of Issues*

The “Stump Hole” area of Cape San Blas, Florida has a roadway with a rubble mound revetment seawall protecting it from waves (see Figure 5.16). In the 1970s the road was located over 300 ft landward of the shoreline. The beach here is eroding at a high rate so that the shoreline has been moving toward the road at an average rate of 15 ft per year for the past 35 years. Shoreline recession progressively narrowed the beach until an emergency rock revetment/seawall was constructed. The revetment has not slowed the recession of the adjacent beaches. Tree stumps are exposed in the surf and on the beach face as a result of the recession. Shoreline recession has continued on both sides of the revetment and the road is extending farther out into the sea. The seawall is now protecting the road and functioning like an artificial headland.

Figure 8.1 shows the Cape Shoalwater area of Washington SH 105 built along another rapidly receding shoreline. At the time of this photograph (April 2003) there was a rock revetment at the base of the bluff and a groin in the background. There had been some limited beach nourishment. The shoreline recession has continued in this general location and now there is a rock revetment along more of this shoreline (2018). Figure 8.2 shows a road on a narrow, low-lying barrier island in New Jersey. The road parallels the beach on one side and a back-bay wetland on the other. The shoreline here has been receding for decades and the road is threatened. Several shoreline stabilization and roadway protection projects have been attempted. A sand-filled geotextile tube was built and covered with a sand dune to protect the highway but was being repaired after a small storm in 2003 and is visible here. This beach and dune system were restored with a major beach nourishment project in 2016 which was a joint effort of the USACE and the New Jersey Department of Environmental Protection.



Figure 8.1. A highway initially built inland now threatened by long-term shoreline erosion. Cape Shoalwater area of Washington SH 105 (2003)

This location is typical of coastal road problems in two ways. One, the problem areas often remain problem areas for the transportation entity for a long time. Two, many former road problem areas are no longer problem areas because of beach nourishment by non-transportation organizations. Figure 8.3 shows a local road undermined by bluff erosion on Lake Erie. This road used to continue straight ahead until bluff erosion undermined the pavement. The bluff erosion has been exacerbated by sand starvation of the beaches at the base of the bluff by an updrift jetty system. Figure 8.4 shows Texas SH 87 along the east Texas coast of the Gulf of Mexico destroyed by shoreline recession. A twenty-mile stretch of this highway along the coast has been closed since 1989 when a storm caused significant pavement damage.



Figure 8.2. A local road threatened by long-term shoreline recession (Ocean Drive, Whale Beach area of Cape May County Road 619, Ludlam Island, New Jersey 2003)



Figure 8.3. A local road being undermined by bluff erosion and long-term shoreline recession on the Great Lakes (Painesville, Ohio, 2001)



Figure 8.4. Road destroyed by shoreline recession: a) broken pavement on the beach at the old location; b) south end of the closed section; c) location map. (Texas SH 87, Jefferson County, circa 2002)

## 8.2 Quantifying Shoreline Change Rates

This section describes a potential process (1) to quantify shoreline change rates and (2) to estimate future shoreline positions. It also describes the shortcomings of such estimates, and the concept and role of sediment budgets.

Coastal erosion rates are often given in terms of the change in average annual shoreline position with time, e.g. 2 ft per year. These are actually shoreline change rates rather than erosion rates. **The terms “recession” and “accretion” are typically used to describe the direction of shoreline movements.** A beach that is widening in response to sand deposition has an accreting shoreline. A beach that is narrowing in response to erosion has a receding shoreline.

Shoreline change rates typically vary with location and time. Shoreline change rates should be evaluated over as long a time period as possible with as many observations as possible. “Long-term” shoreline change usually refers to multi-decadal time scales. Many observations in a single year can give some estimate of the seasonal variability in shoreline position as sand moves cross-shore on the profile. However, these data are typically not useful for developing “long-term” shoreline change trends.

Historical shoreline data are available from a variety of sources. The USGS has significant shoreline change databases covering all US coasts. **Often a state resource agency, such as the State of Florida’s Department of Environmental Protection, has the most comprehensive shoreline change information.**

No accepted national standard exists for shoreline change analyses. The quantity and quality of shoreline change data vary significantly. Each location has different types of historical data and

analyses. New analysis of existing data may be needed to develop a clear understanding of historical shoreline changes for a project.

Historical shoreline positions can be measured by repetitive surveys or by remote sensing such as air photograph interpretation. Historical and current vertical air photographs can provide the basis for shoreline location data with proper interpretation and positioning analysis. One source for estimates of older historical shoreline locations is NOAA's National Ocean Survey surveys and the surveys of their predecessor organization, the US Coast & Geodetic Survey (USC&GS). High-quality estimates of shoreline position can extend as far back as the 1850s. The USC&GS significantly improved the accuracy of coastal surveys at about that time. Pre-1840 estimates of shoreline position are not as accurate as those done after 1850. USC&GS "t-sheets" and "h-sheets" are the summary plots of specific surveys and correspond with the dates of the actual survey. Navigation charts, however, are updated continuously and the date of the chart does not correspond with the date of all of the information shown on it. Accuracy of these historical shoreline estimates often can be adequate for the purpose of shoreline change analysis (Crowell *et al.* 1991).

**US Coast & Geodetic Survey maps of historical shorelines became very accurate due to changes in land surveying techniques in the 1850s.**

An example of a shoreline change analysis is shown in Figure 8.5. The plot is for five locations, spaced 1,000 ft apart, centered on the location where the road in Figure 5.16 extends into the sea. The plot shows the measured shoreline locations through time and the lines are splines fit to the data for visual convenience. A recessional (negative) trend is obvious at all five locations and is very consistent at four of the five locations. Some variability in the overall trend at station R-106 may be explained by effect of the revetment protecting the road. The nomenclature and designations of the stations are those of the Florida Department of Environmental Protection (FDEP). Given the natural temporal variability of shoreline location, the strong trends shown in Figure 8.5 are not typical. Similar plots often show much more variability through time and the trend is not always clear. The site analyzed in Figure 8.5 has a very clearly recessional shoreline. Figure 8.5 shows a nonlinear trend in shoreline position through time. The recession rate appears to be greatest in the most recent years. A relatively large number of major storms have impacted this coast since 1997.

More results from the same shoreline change analysis are shown in Figure 8.6. The average annual recession rate along 30,000 ft of shoreline on the west-facing shoreline of St. Joseph Peninsula is shown. The average annual rate depends on location and the time period over which the average is taken. Clearly the recession rate is much greater to the south (higher R-monument numbers).

Recession rates shown in Figure 8.6 have been calculated by the "end-point method" which averages the change in shoreline position from the beginning to the end of the time period. An alternative to the end-point method is linear regression (Crowell *et al.* 1997). Linear regression is typically preferred to the end-point method because it uses all the available data and is less sensitive to one spurious or aberrant value.

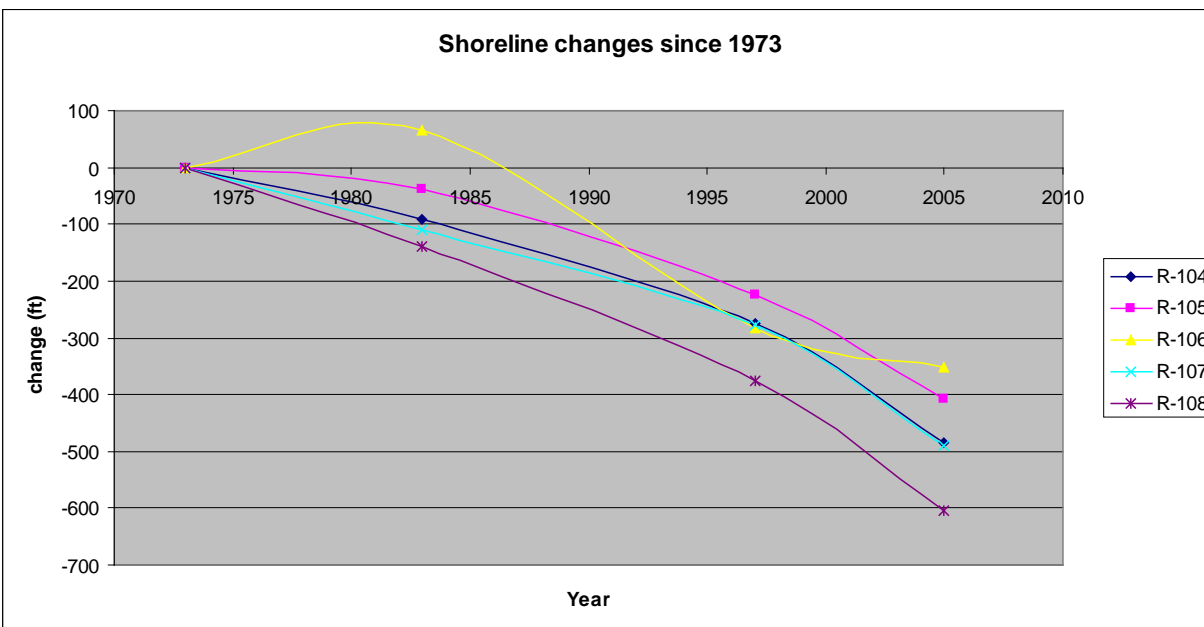


Figure 8.5. An example of shoreline position changes through time. Stump Hole area of St. Joseph's Peninsula, Florida

### 8.3 Estimating Future Shoreline Positions

An estimate of future shoreline locations can be valuable in planning highways near areas of receding shorelines. The most common method for estimating future shoreline positions is direct extrapolation of historical shoreline change rates to the present shoreline (Crowell *et al.* 1997). Figure 8.7 shows some historical shoreline positions as well as projected future positions at one location. The historical shoreline data were obtained from the FDEP on-line database. Florida originally obtained the older (1868 and 1934) data from the USC&GS, made appropriate datum corrections and added their own data from beach profile surveys. The projected shorelines are extrapolations from the 2005 shoreline location, at 1,000-foot intervals along the coast based on the average annual rate of shoreline recession. The average annual rate of shoreline recession was based on the most recent 32 years (1973 to 2005). The result shows that more and more of the highway will be threatened by recession in the coming decades. Such projections with graphical presentations can be valuable in planning alternative responses.

#### 8.3.1 Shortcomings of Shoreline Change Assumptions

From a coastal science perspective, shortcomings exist in the underlying assumptions inherent in using historical shoreline change rates to estimate future shoreline position:

- Natural shoreline change processes are often not linear in time,
- Engineering may have influenced historical shoreline changes, and
- Engineering may influence future shoreline changes.

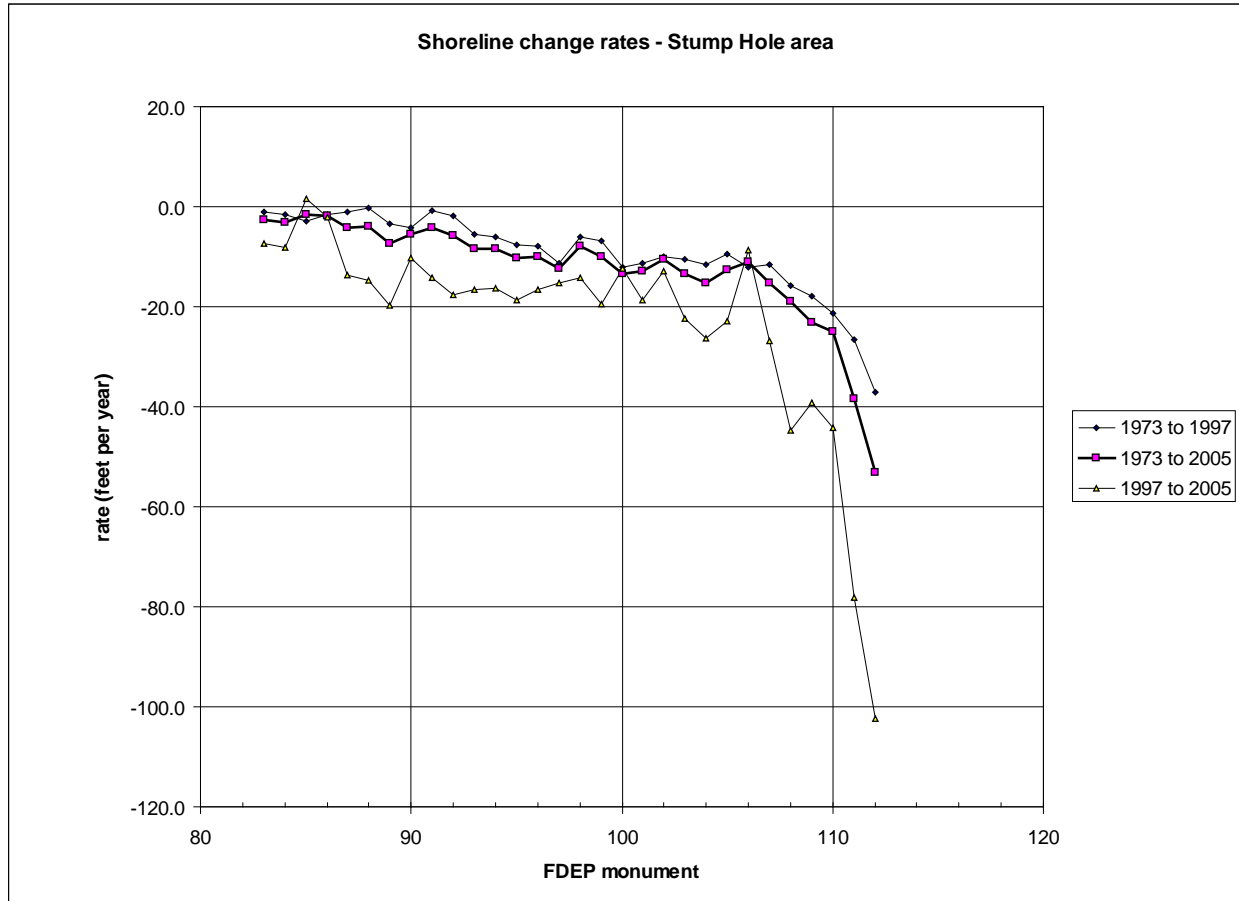


Figure 8.6. An example of shoreline change rates along 30,000 ft of coast showing temporal and spatial variations but a significant recession trend. Western-facing shoreline of St. Joseph's Peninsula, Florida

It has long been recognized that shoreline change can be episodic. An individual storm may cause significant erosion or even trigger the beginning of an erosional period. The natural dynamic equilibrium on some beaches involves years of recovery after major storms. Large storms on low-lying barrier islands can cause island rollover and migration. Large storms on some coasts may remove large amounts of sand from the beach, via longshore and cross-shore sand transport resulting in bluff erosion. Subsequent times of lesser storm activity can result in the replacement of much of that sand by similar processes.

Shoreline position in many US locations has been influenced either positively or negatively by engineering works. Engineering works can include seawalls, groins, breakwaters, inlet jetties, dams (on the US West Coast), dredging of ship channels, and beach nourishment. For example, a groin that traps sand will often widen an updrift beach while narrowing a downdrift beach. Over 1 billion cubic yards of sand have been trapped or removed from US beaches by such projects (Douglass *et al.* 2003). Beach nourishment projects can widen beaches significantly.

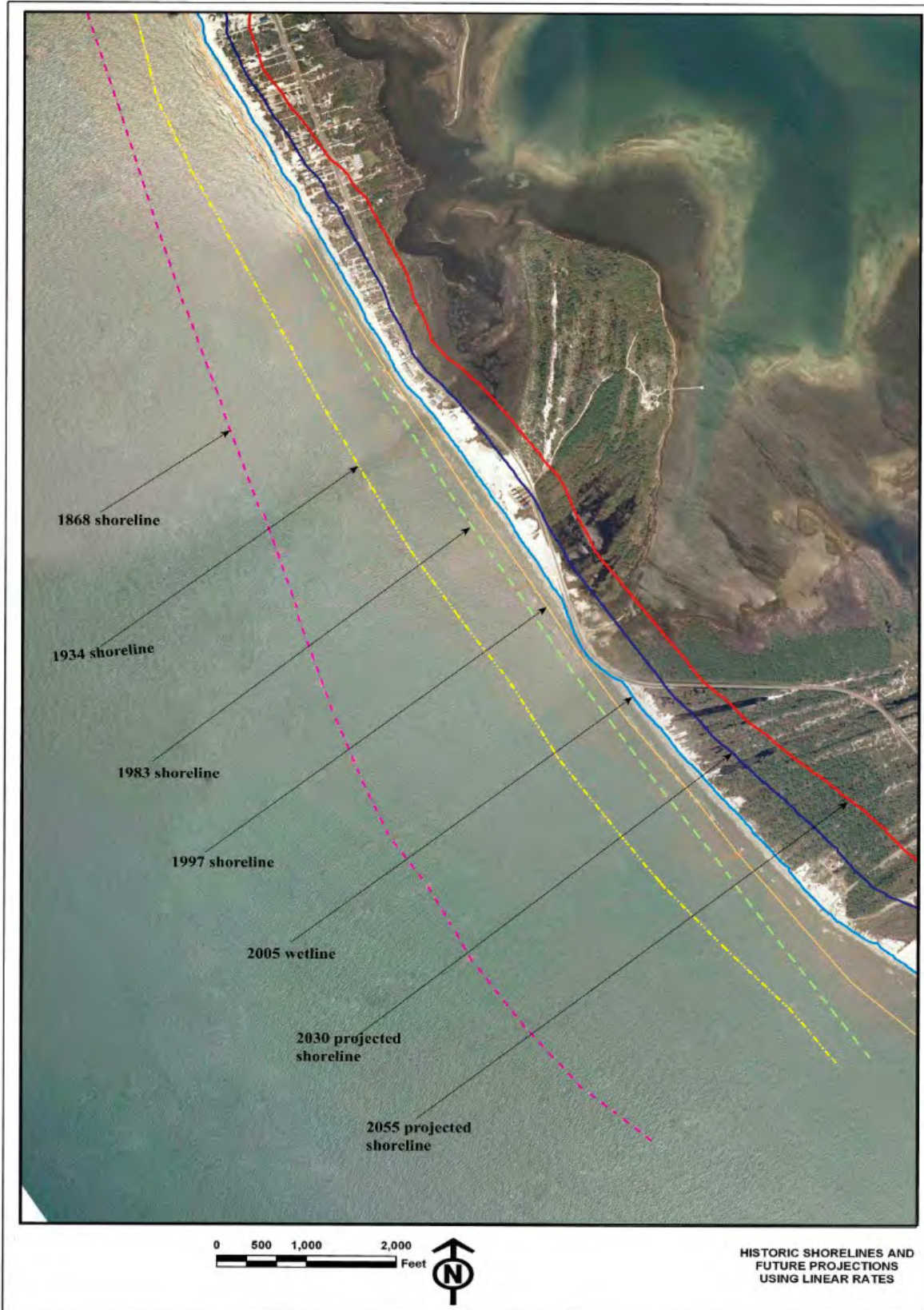


Figure 8.7. Example of projected future shoreline positions at Stump Hole

### 8.3.2 Sediment Budgets

Sediment budgets are one tool to estimate future shoreline positions. Sediment budgets are estimates of the rate at which sand is entering and leaving a specific reach along the coast. The difference between the volume entering and the volume leaving an area yields the volume gained or lost by that area. Sediment budgets typically make use of much more data and analysis than simple shoreline change extrapolation.

## 8.4 Relocation/Abandonment Considerations

One obvious solution to the problem of a roadway threatened by shoreline recession is to relocate the road. Roads have been moved or abandoned at different locations along the US coast for decades. One example is Washington SH 105 in the Cape Shoalwater area (see Figure 8.1). This road was moved several times because this area has experienced some of the highest, long-term shoreline recession rates in the nation. By 1998 however, a series of coastal structures has been employed to protect the existing highway. Relocation of the road had again been considered but not selected as the preferred alternative.

One example of an abandoned road is Texas SH 87 between High Island and Sabine (see Figure 8.4). The road was closed indefinitely due to damage by Hurricane Jerry in 1989. Prior to that, the road had been damaged repeatedly by coastal storms. A road in that location had been there for over a century.

A primary issue when considering road relocation is the new route. The logical location is farther inland from a receding shoreline. However, those areas are often already occupied by private property or wetlands. Developing private property is extremely expensive due to its location near the coast. Wetlands are protected for their habitat value.

The stretch of Texas SH 87 that is closed today is in front of wetlands that are part of the McFadden National Wildlife Refuge. Relocating the road landward would involve filling the wetlands. Likewise, relocation of CR 30E in the Stump Hole area of Cape San Blas (see Figure 8.7) would involve the filling of wetlands currently managed by the state as an outstanding aquatic preserve. Alternative relocation options considered for Washington SH 105 in the Cape Shoalwater area include private cranberry bog farms.

Abandoning even small section of local roads may cause significant legal issues. More discussion of the issues with coastal road abandonment is included in Section 15.2.5.

## 8.5 Shoreline Stabilization Options

Some form of shore “stabilization” is a popular option to protect a road along a receding shoreline. Stabilization is essentially holding the line and resisting the recession. The shore protection generally is in one of two forms. One could be some form of traditional “hard” structural shoreline protection such as a seawall or revetment (e.g. Chapter 7). Two could be some form of “soft” sand shoreline protection such as beach nourishment, marsh, or other nature-based solution.

**Nature-based solutions are options which mimic characteristics of natural features, but are created by human design, engineering, and construction** (Webb *et al.* 2019). They include a range of features that serve as alternatives to, or ecological enhancements of, traditional shoreline stabilization and infrastructure protection techniques. A wide variety of terminology describes nature-based approaches, some of which are listed in the text box. The common thread connecting these approaches is the desire to protect or improve the built environment while maximizing the ecological function of the overall system. Because they address a specific ecological or ecosystem function, nature-based solutions are often site-specific and their design

requires a cross-section of expertise drawing on the fields of coastal ecology, coastal geology, coastal oceanography, and coastal engineering.

#### Names for Nature-Based Solutions:

- Coastal green infrastructure
- Nature-based infrastructure
- Living shoreline
- Natural and nature-based features (NNBF)
- Engineering With Nature (EWN)
- Building with Nature (BwN)
- Working with Nature (WwN)

In 2019, the FHWA developed the “Nature-Based Solutions for Coastal Highway Resilience: An Implementation Guide” (Webb *et al.* 2019) in parallel with the development of this HEC-25 3<sup>rd</sup> edition revision. Some of the information in that implementation guide has been incorporated here.

The FHWA developed this implementation guide to help transportation practitioners understand how and where nature-based solutions can be used to improve the resilience of coastal roads and bridges. Upfront, it summarizes the potential flood reduction benefits and co-benefits of these strategies. From there, the implementation guide follows the steps in the design process:

- how to consider nature-based solutions in the planning process,
- how to conduct a site assessment to determine if nature-based solutions are appropriate,
- what engineering and ecological design considerations are crucial,
- what permitting approaches to use,
- what to consider for construction, and
- what monitoring and maintenance strategies to incorporate.

The implementation guide also includes examples of nature-based solutions, a site characterization questionnaire, an evaluation tool, performance metrics, additional tools and resources, and technical fact sheets. Another product from that FHWA study is a detailed “white paper” that summarizes the literature on nature-based solutions (Webb *et al.* 2018).

## 8.6 The Functional Design of Coastal Structures

Similar to other concepts within science and engineering, coastal “functional design” refers to how a structure behaves, or “functions,” within the coastal environment (USACE 2002). Coastal structures can be categorized in terms of their primary function as follows:

- seawalls, revetments, bulkheads – shore-parallel structures on the shoreline designed to protect upland property from waves (Chapter 7),
- groins – shore perpendicular structures designed to control longshore sand transport,
- breakwaters – shore-parallel structures located seaward of the shoreline to reduce the wave energy in their lee and to control longshore sand transport,
- hybrid structures – some functional combination of groins and breakwaters including “t-head groins” or “headland breakwaters”

**“Functional design” refers to how the coastal structure functions in influencing coastal hydrodynamics, sediments, and habitats.**

Groins were probably the most common shoreline stabilization technique in the first half of the 20<sup>th</sup> century. Figure 8.8 shows a groin field. Groins are typically placed as shown in groups or “fields.” They are often called “jetties” by laypersons but that term is typically reserved by the US coastal engineering community for structures that stabilize inlets.



Figure 8.8. Groin field in Long Branch, New Jersey (2006)

Groins can stabilize a shoreline via two mechanisms if there is adequate sand in the littoral system:

- Groins can locally realign the shoreline to reduce the longshore sand transport rate.
- Groins can shelter the area adjacent to them from the wave energy especially when waves approach the shore at an angle.

Groins can trap sand on one side while causing erosion on the other. The shoreline on the updrift side of a groin accretes while the shoreline on the downdrift side recedes. Thus, groins are often built in groin fields so the one just downdrift stabilizes the next portion of the shore. Shoreline recession downdrift of the last groin at the end of a groin field can be severe.

Groins are much less acceptable today as a shoreline stabilization technique than they were prior to the 1960s. New groins were discouraged or prohibited in many states for years because of their potential downdrift negative impacts. However, in the past decade their use is becoming acceptable when modern coastal engineering principles adequately address the downdrift impacts.

## 8.7 Beach Nourishment

**Beach nourishment is the placement of large volumes of good quality sand on a beach to widen the beach.** Sand dunes can be constructed at the back of a nourished beach. Beach nourishment is a viable engineering alternative for shore protection and has become the principal technique for beach restoration (NRC 1995). Beach nourishment is a “nature-based solution.”

Figure 8.9 shows a beach nourishment project under construction. Sand is being pumped from an offshore dredge (not shown) to the beach and then down the beach to where the sand-water slurry discharges from the pipe. The beach is then shaped by bulldozers. As the new beach extends farther down the beach, the dredge pipe is extended.

Beach nourishment projects usually need to be maintained through subsequent renourishment as the sand moves out of the project limits. Many of the policy, management, and engineering issues related to beach nourishment projects are qualitatively described in Douglass (2002). Many of the quantitative engineering tools used in beach nourishment planning and design are presented in Dean (2002). The quantitative tools for beach nourishment for shoreline stabilization include methods for evaluating the performance of potential nourishment sands, estimating the short-term performance and the long-term renourishment intervals, and evaluating the ability of structures (if desired) to extend the renourishment interval. Each of these can be important aspects of beach nourishment planning and design.

Beach nourishment projects protect a number of roads in the US. Two examples are shown in Figure 8.10 and Figure 8.11. The beach and dune in Figure 8.10 were constructed by the City of Delray Beach on top of the failed seawall shown in Figure 7.20. The sidewalk and parapet wall on the crest of the seawall in Figure 7.20 is the same as the sidewalk and bench shown in Figure 8.10. Since originally constructed in 1973 this beach nourishment project has protected the road while providing a beach. The site has been renourished five times since 1973. The protective and aesthetic benefits of the beach outweigh the costs of renourishment.

**Beach nourishment is a nature-based engineering solution that protects many coastal highways.**

The nourishment project at Sea Bright, New Jersey, shown in Figure 8.11 is a federal shore protection project funded through the USACE's shore protection authority. The beach was initially constructed in 1994 directly seaward of the seawall. Nourishment was the preferred alternative to further seawall repairs. It has been renourished after passage of Hurricane Sandy.

Proponents for beach nourishment projects have typically not been DOTs, even when the project protects a state highway. Rather, local government, a state resource management or economic development agency, the USACE, or a private entity typically sponsors beach nourishment. However, SDOTs have sponsored or co-sponsored several beach nourishment projects.



Figure 8.9. A beach nourishment project under construction in Gulf Shores, Alabama (2001)



Figure 8.10. Beach nourishment project with constructed dune on top of old, failed revetment protecting Florida SH A1A (Delray Beach, 2001)



Figure 8.11. Beach nourishment seaward of a seawall protecting a road. (New Jersey SH 35, Sea Bright, 2001)

The USACE shore protection program has the authority to consider and build either beach nourishment or seawalls to protect upland property. Almost all the USACE's federally authorized beach nourishment projects require a matching cost contribution from a non-federal sponsor. The USACE shore protection program typically has an annual budget of around \$100 million, and the program has not grown significantly during the past several decades.

Sand dunes are often part of major beach nourishment projects because they provide protective benefits during storm events by blocking or reducing storm surge flooding and wave action. Dunes function as sacrificial volumes of sand that minimize storm impacts until the dunes are eroded by

waves or overtopped by storm surge. Post-Sandy assessments demonstrate that the presence of dunes contributed substantially to reductions in storm damage (Tomiczek *et al.* 2017) and flooding (Walling *et al.* 2014). Dunes with sand fencing and vegetation trap and stabilize sand, leading to increases in dune volume and dune height over time.

Beach nourishment has proven effectiveness and broader societal benefits of aesthetics, recreation and environmental enhancement. It should be considered by transportation engineers where a road is threatened by a receding shoreline.

### **8.8 Combining Beach Nourishment with Structures**

Modern nature-based coastal engineering shoreline stabilization solutions often combine beach nourishment with coastal structures. The purpose of the structures is to extend the interval between periodic renourishment. Some of these “hybrid” soft-hard solutions attempt to emulate natural geomorphological features such as pocket beaches and tombolos. The names of these “hybrid” solutions are evolving.

Figure 8.12 shows some nearshore segmented breakwaters with beach nourishment protecting a highway in Louisiana. This system extends over 7 mi along the coast with 85 nearshore breakwaters. This is the same general area of the highway once protected by the failed interlocking concrete block revetment in Figure 7.21.

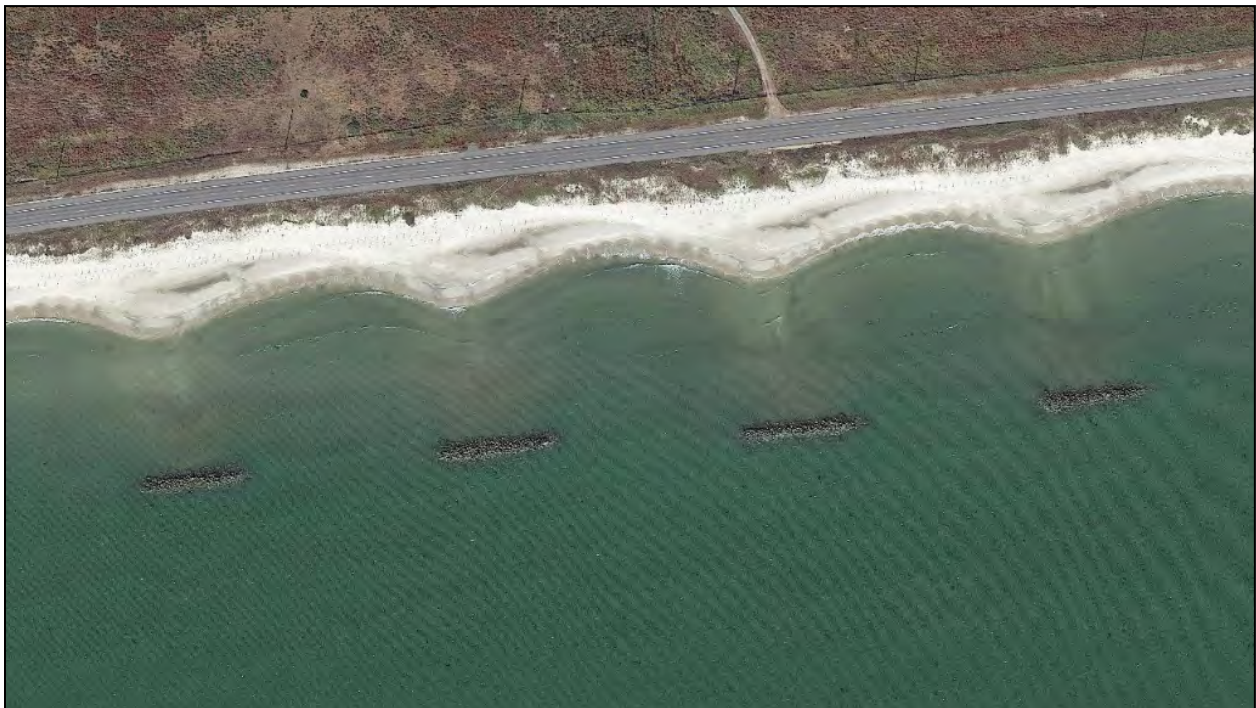


Figure 8.12. Offshore segmented breakwaters with salients in beach nourishment protecting a highway (Louisiana SH 82, Holly Beach)

Figure 8.13 and Figure 8.14 show a portion of another extensive system of offshore segmented breakwaters and nourishment sand to protect a road and other infrastructure. In the system at Presque Isle, Pennsylvania (on Lake Erie), there are 58 breakwaters with nourishment along over 5 mi of shoreline. Tombolos do not form (that is by design), i.e. the beach does not extend out to the breakwaters. The bulges in the shoreline in the lee of the breakwaters are called “salients.” This system reduces longshore sand transport in the lee of the breakwaters. Figure 8.13 is an

historical photograph showing the initial three breakwaters and beach nourishment at a popular beach in the state park. This project was built as a “proof-of-concept” demonstration project which was so successful that the other 55 breakwaters were added in the 1980s.



Figure 8.13. Offshore segmented breakwaters with salients in beach nourishment (Presque Isle State Park, Pennsylvania, circa 1980, USACE archive photograph)

The formation of salients or tombolos is controlled by the geometry of the breakwater system as shown in Figure 8.15. The Coastal Engineering Manual (USACE 2002) provides more guidance on the functional design of nearshore segmented breakwaters.

**Coastal structures are often designed to extend the life of the beach nourishment.**

Figure 8.16 shows a nearshore segmented breakwater system with terminal groins used to build a small recreation beach. The beach was created with nourishment on the bay side of a long seawall that protected a road but did not have any sandy beach. The breakwater and groin structure system were designed to retain the nourishment sand. The beach was built to provide access to the bay for wind surfers and others.



Figure 8.14. Offshore segmented breakwater system at Presque Isle, Pennsylvania

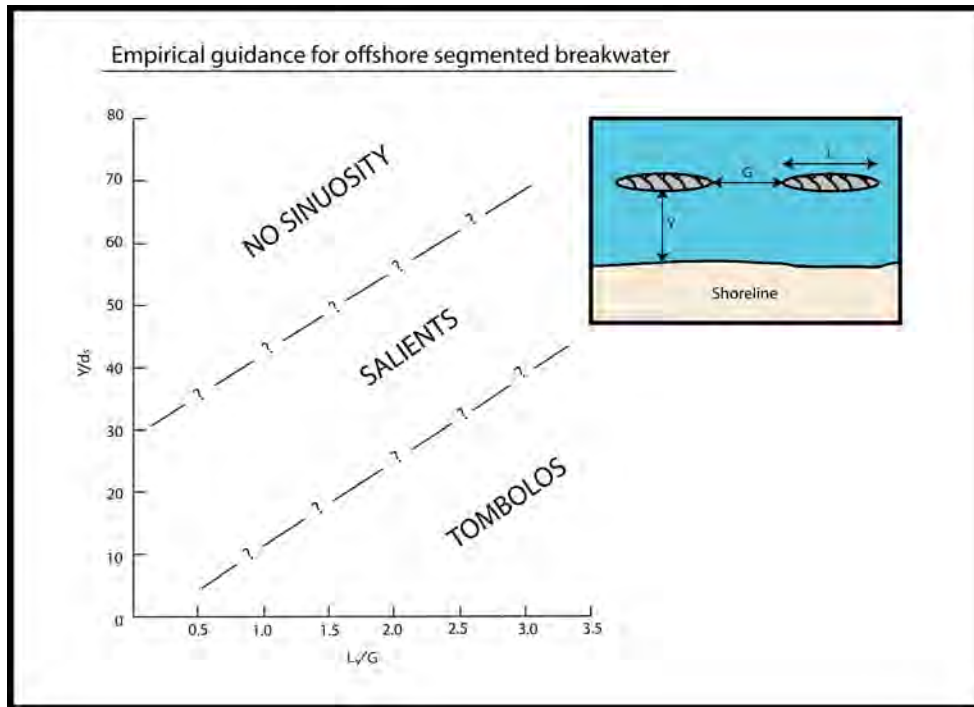


Figure 8.15. Empirical relationships for shoreline effect of offshore segmented breakwaters. (after Pope and Dean 1986, and USACE 2002)



Figure 8.16. Offshore segmented breakwaters with groins and beach nourishment on Corpus Christi Bay (Ocean Drive, Corpus Christi, Texas)

Figure 8.17 and Figure 8.18 show headland breakwater-pocket beach systems designed to retain beach nourishment sands on bay shorelines. Both were constructed in front of seawalls that had previously been damaged by erosion. These headland breakwater-pocket beach systems use structures to retain sand by providing artificial headlands. Figure 8.17 shows a headland breakwater that incorporates a “T-head groin” in the middle. The structures in Figure 8.18 do not include the stem of the “T” because tombolos were expected to form. The Virginia DOT was a partial sponsor of the project in Figure 8.18 since the system protected a short stretch of road.

Functional design parameters for the design of headland breakwater-pocket beach systems include the distance offshore as well as the gap spacing. The goal is the creation of a pocket beach with the sand fill. The shorelines as shown in Figure 8.17 and Figure 8.18 are curved because they have responded to the wave energy coming through the gaps in the artificial headland structures. Wave heights and directions are modified as waves diffract through the gaps. **The structure layout can essentially be “tuned” to the local, site-specific wave climate to produce a beach with a desired curved shape and width** (Bodge 1998). More guidance for the design of these systems including methods for estimating the final equilibrium shoreline shape and location are given in Silvester and Hsu (1993) and Hardaway and Gunn (2000). The potential complexity associated with design of solutions which combine nourishment and structures may necessitate involvement by an experienced, qualified coastal engineer during project delivery process.



Figure 8.17. Constructed pocket beach stabilized with a T-head groin breakwater system (Point Clear, Alabama, circa 2006)



Figure 8.18. Beach nourishment project stabilized as pocket beaches with a headland breakwater system protecting a road (Water Street, Yorktown, Virginia, circa 2006)

### 8.9 Marsh Restoration/Creation

Coastal marshes protect many roads along bay shorelines in the US. Restoration of natural marshes, or construction of new marshes, can be a nature-based solution to protect these roads. Coastal marshes, mangroves, and even coral reefs in some locations can reduce wave heights, erosion of roadway embankments, and vulnerability to shoreline retreat (Webb, *et al.* 2018). Keeping a healthy fringe marsh between a coastal roadway and bay waters provides habitat value as well as protective services. When thinking about any nature-based solution, perhaps consider the adage “it is best to let nature be your guide.” Most successful engineered nature-based solutions mimic some nearby natural feature (beach, dune, marsh, mangroves, etc.) with some additional coastal engineering.

Hybrid approaches are common in bay settings. The combination of marsh with breakwaters enhances the resilience of both the infrastructure and the ecosystem. The structural features serve at least three purposes: first, they improve the reliability of the system; second, they improve the performance of the system; and, third, they provide the specific hazard reduction benefits that a nature-based solution, on its own, may not. Examples of some common, proven hybrid approaches along bay shorelines are:

- Constructed marsh with a stone or timber sill structure,
- Marsh/mangrove with breakwaters or reefs, and
- Beach nourishment with breakwaters and/or groins (Section 8.8).

Figure 8.19. and Figure 8.20 show constructed marshes built with nearshore breakwaters. The primary value of this type of solution is its habitat. Note the horseshoe crab on the sandy pocket beach in the foreground of Figure 8.20. The constructed interface between the land and bay functions much more naturally, in terms of connectivity, than a bulkhead or revetment. The horseshoe crab is able to climb directly up on a sandy beach as its ancestors have done in this bay for millennia.

**“Nothing is invented, for it’s written in nature first.”  
- Antonio Gaudi (1852-1926)**

Some form of structure to attenuate waves and/or stabilize shorelines in addition to marsh grass plantings are common in medium-to-high energy bay wave environments (e.g. fetch greater than 1 mile). Meeting project objectives dictates the design of the size, characteristics, and location of the structure (e.g. rock breakwaters or sills, timber structures, or complex habitat-type devices). Common mistakes include the following:

- Under- or over-designing structures for their intended application,
- Using non-traditional structures (e.g. alternatives to rock or timber breakwaters) where their performance is not well understood, and
- Placing structures in sites where they that may exacerbate shoreline erosion.

The project shown in Figure 8.19. uses a breakwater composed of multiple small concrete units arranged as breakwaters with gaps. The project shown in Figure 8.20 uses more traditional rock breakwaters with gaps (see Section 8.8). The layout of the breakwaters and gaps for both projects were designed to reduce the wave energy to a tolerable level for the marsh grass to thrive. A rule of thumb is that marsh grasses cannot tolerate storm wave heights of  $H > 1$  ft. See Webb, *et al.* (2018) for more information on the design of bay marshes.

As allowed under FHWA regulation 23 CFR § 777 (Mitigation of Impacts to Wetlands and Natural Habitat), **transportation officials may consider constructed marshes as an alternative where receding bay shoreline threatens a road.** In addition to their effectiveness in mitigation, they may also serve the broader societal benefits of environmental habitat enhancement. This type of solution will typically need engineering beyond the width of the normal highway right of way. FHWA regulation 23 CFR § 777 also allows a project to consider partnering with other entities, such as the state resource agency.

Figure 3.1 depicted a typical situation where a constructed marsh system would be an effective nature-based solution. Shoreline recession threatens a local road on a small bay. However, other parts of the road nearby are well-protected by natural marshes. Construction of a new marsh with some small breakwaters is a solution that will protect the threatened road while mimicking the habitat value of a marsh (FHWA 2017c).

See the “Nature-Based Solutions for Coastal Highway Resilience: An Implementation Guide” (Webb *et al.* 2019) for more implementation guidance about nature-based solutions for coastal highways.



Figure 8.19. Example of a constructed marsh stabilized with a nearshore breakwater (Little Bay, Bayou LaBatre, Alabama)



Figure 8.20. Example of a constructed marsh protected by nearshore rock breakwaters (Holts Landing State Park, Indian River Bay, Delaware, 2009)

### **8.10 Unproven “Experimental” Shoreline Stabilization Approaches**

This section briefly discusses the many so-called “experimental, or “innovative,” shoreline stabilization techniques which have been suggested for decades. SDOTs may not even have these techniques within their design and construction standards and specifications (FHWA, 2012a). When such techniques do not conform to criteria or specifications, on a project basis, FHWA may approve such experimental features using its authority under 23 CFR § 625.3(f)(i) (Exceptions). Proposed solutions have included artificial seaweed, used tire breakwaters, different types and shapes of rigid submerged and emergent devices, and beach dewatering. Many rely on expensive, patented devices and systems. The marketing of these systems often argues that they function differently than more traditional approaches. But all follow the same general principles of physics including mass (sand) conservation. Some of these systems have survivability problems in large surf conditions. The USACE (2002) describes new or innovative coastal project design concepts as being more susceptible to failure due to lack of experience with similar designs.

If the wave attenuation characteristics of rigid breakwater units are adequately quantifiable, and the design level of wave attenuation will clearly be beneficial at that location, some coastal structures can be designed to function very similarly to the more traditional rock structures. If the placement of a device or apparatus in the surf causes beach sands to deposit, it functions much like the more traditional structures described above (and has the capability of causing downdrift erosion).

Sometimes, so-called “innovative” approaches are marketed based on questionable coastal science such as a linkage between calmer waves and the presence of submerged aquatic vegetation (SAV). However, SAV health is often more closely tied to broader water clarity issues than those related to wave action level.

Most innovative solutions are serious attempts to address a challenging problem. But unproven shore protection solutions for highway applications should be pursued judiciously if not recognized as typical practice. The broader research and development community should continue to evaluate all potential solutions to beach erosion problems. Meanwhile, **prudent highway engineering planning and design should focus on proven solutions: relocation, nourishment or other proven nature-based approaches, structures, or some combination of these approaches.**

## Chapter 9 - Increased Flooding due to Relative Sea Level Rise

Communities in almost every coastal state are experiencing problems with more frequent, and more severe, road flooding at high tide and during small storms. This problem has only recently become apparent and recognized. Previous editions of this document did not address it.

Figure 9.1 shows a poignant example of the problem: the sidewalk around the Tidal Basin is under a foot or two of water because of an abnormally high tide exacerbated by moderate flooding in the Potomac River. The construction of waterfront infrastructure in most US cities involved filling wetlands decades or centuries ago. The perceived local flood stage at the time of construction was likely the controlling factor for the height of fill. Sea levels have risen at almost all US waterfront locations, and the old local flood stage is now exceeded more frequently.

This chapter briefly describes the problem, how the transportation community has begun to assess the problem, and one of the mitigation countermeasure options being used to address the problem (i.e., raising the road). Typically, the choice is to raise local flood thresholds or experience more flooding.

### 9.1 Description of the Problem

This section describes the issues of increased flooding due to relative sea level rise (RSLR) with a focus on road examples. Since sea levels are rising along most US coasts and the rate of this rise is projected to increase significantly this century (see Figure 4.11), this flooding will become progressively more problematic. As a result, SDOT's and local transportation agencies will face a need to address these issues more in the coming decades.

Figure 9.2 is a typical example of this flooding on a local street. This intersection floods with salt water from a tidal lagoon about 2,000 ft away flowing up through the storm sewer system at high tide. Local citizens often detour around this area to avoid driving in salt water. Similar situations occur in hundreds of coastal communities in Florida (see Figure 9.3 and Figure 9.4), Maryland (see Figure 9.5), South Carolina, North Carolina, Washington, Texas, Alabama, Massachusetts, Hawaii, New Jersey, Georgia, Virginia, California, and New Hampshire.

**“Increased flooding due to relative sea level rise” is the term used in this document for this issue.**

Figure 9.3 shows similar flooding of a primary road in the Miami area. The salt water on the road to the right in the photograph has backed up through the storm sewer system into the traffic lane. The Atlantic Intracoastal Waterway is visible on the right side of the photograph. The flooding is not restricted to the road immediately adjacent to the waterway: Figure 9.4 shows a local street to the east on the barrier island flooding the same day (the Atlantic Ocean is at the far end of that local cross-street). The flooding is also due to salt water from the waterway backing up through the local storm drainage system.

Figure 9.5 shows similar flooding of a local road which is affecting traffic flow and parking in Annapolis, Maryland. Flooding in this block has extended into the businesses on the left of the photograph (and at least one business, a coffee shop, has relocated from this area to a nearby, higher location to avoid the repeated flooding).



Figure 9.1. Flooding of the Tidal Basin in Washington, District of Columbia (June 2018; permission for use of photograph provided by Loic Pritchett)

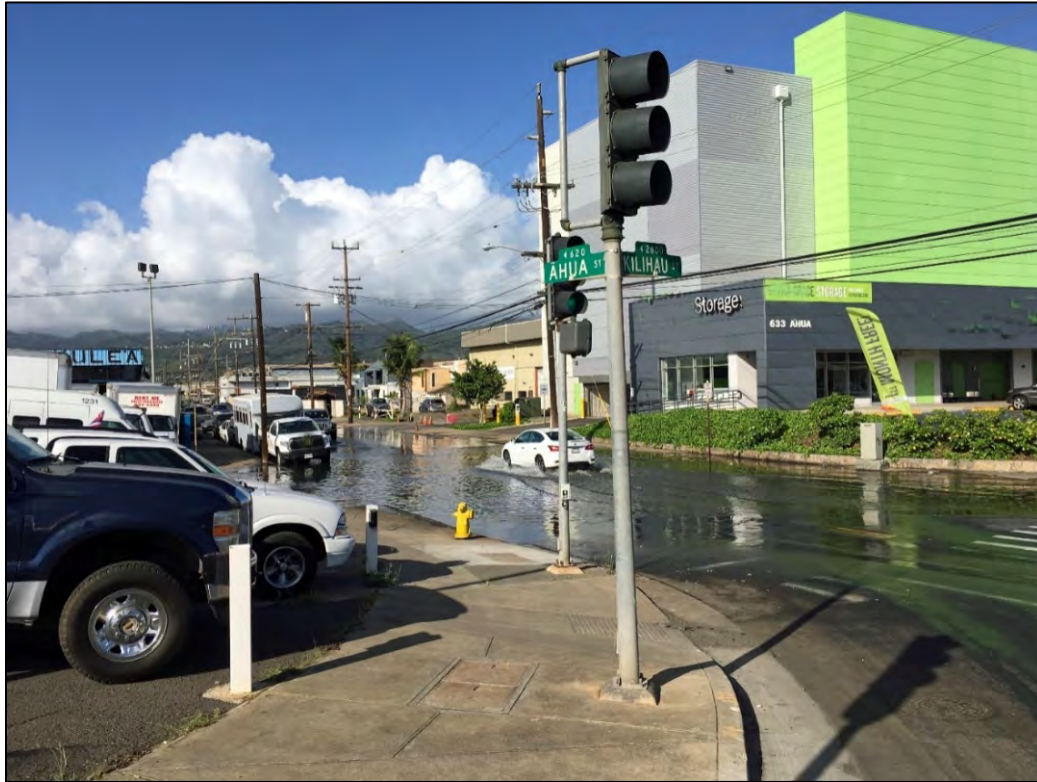


Figure 9.2. Example of coastal flooding on an urban road (Honolulu, March 30, 2017)



Figure 9.3. Example of coastal flooding on a primary road (Florida SH A1A, Hollywood Beach, October 21, 2017)



Figure 9.4. Example of coastal flooding on a local road that crosses a developed barrier island (Hollywood Beach, Florida, October 21, 2017)



Figure 9.5. Example of flooding of a coastal road which is affecting traffic and parking (Dock Street, Annapolis, Maryland, 2017 photograph provided by Joe Krolak)

This type of flooding has been called “nuisance flooding,” “sunny-day flooding,” “high-tide flooding,” “more flooding,” “storm-tide flooding,” “chronic flooding,” “recurrent flooding,” and “king-tide flooding.” It is associated with either weather or tidal conditions, or both, including the following:

- the peak of the high tide for the day,
- periods of the year when the astronomical high tides are above average,
- wind blowing across coastal waters and bays that causes a local increase in mean water level (wind setup),
- local rainfall runoff,
- storms (although it can occur on sunny days), or
- some combination of the above.

In this document, **this type of flooding is called “increased flooding due to relative sea level rise (RSLR).”** Both depths and the frequency of flooding are higher as a result of RSLR. While flooding happened before, the gradual RSLR over the past decades has brought the sea levels closer to the infrastructure levels. Areas that once flooded only every few years during major storms may be flooding several times per year. Areas that once flooded only during the most extreme storm tides may be flooding during any high tide when the position of moon makes the tide higher than the usual daily high tide. And areas that once flooded an inch deep now flood several inches deep and for longer durations.

RSLR has broader societal impacts than coastal highways. Increased frequency of coastal flooding is a reason for people to move out of low-elevation neighborhoods (e.g. Norfolk, Miami, and Tampa). Keenan *et al.* (2018) finds a correlation between housing prices in the Miami area, since 2000, and increased flooding due to RSLR. Lower elevation areas have a lower rate of property value appreciation. Increased flooding due to RSLR may have already contributed to real estate value losses in the Miami area and other coastal areas (McAlpine and Porter 2018, First Street Foundation 2019). These concerns have been discussed in the common press extensively (e.g. Smith 2018, Kusisto and Campo-Flores 2018).

As mentioned, coastal highway surface flooding is often caused by bay waters essentially backing up through the culverts and storm drains in the local surface water drainage system. The coastal bay water surface is higher than the road surface. Flood water on the road surface is problematic for drivers until the water levels recede off the pavement. The driver can either drive more slowly through the standing water or take alternative routes around the lower portions of road. Drivers often avoid these areas because of the known effects of saltwater corrosion on vehicle undercarriages. This type of flooding often recedes a few hours after the peak of the high tide or when the wind changes speed or direction. The effect of increased flooding to RSLR on vehicle travel times has been quantified by Jacobs *et al.* (2018a, see Section 9.2.3).

Knott *et al.* (2017) discusses how increased flooding due to RSLR can affect the service life of pavements in coastal roads. Coastal groundwater tables are expected to rise with RSLR and will intersect the unbound layers of road base. This can lead to pavement service life reductions related to fatigue and rutting.

The FHWA held a small workshop on the coastal flooding issue in 2017 and a series of regional peer workshops around the US in early 2018. Those workshops informed this chapter. The Appendix of this manual lists workshop participants.

## 9.2 Assessing the Problem

This section discusses some potential approaches for quantitatively accessing increased flooding due to RSLR. Three examples from the literature are presented:

- Sweet *et al.* (2014)/Sweet and Park (2014) – quantitative examples of the historical problem and the future problem (considering sea level rise projections),
- Kriebel and Henderson (2018) - an expanded example that presents a **simplified method for evaluating the increase in flooding due to future RSLR at a specific transportation asset**, and
- Jacobs *et al.* (2018a) - an analysis of vehicle delay increases over a multi-state area due to the problem.

All three examples estimate how exposure to this problem will increase in the coming decades.

Much of the work on increased flooding due to RSLR follows landmark papers by Sweet *et al.* (2014) and Sweet and Park (2014). Others who have described and quantified this type of flooding well include Kriebel and Geiman (2014), Kriebel *et al.* (2015), Moftakhari *et al.* (2015), Sweet *et al.* (2018), and Kriebel and Henderson (2018).

### 9.2.1 Sweet *et al.* (2014)/Sweet and Park (2014)

The Sweet *et al.* (2014) report cover has a photograph of a flooded public park and statue at the City Dock in Annapolis that illustrates the issues facing communities. The report presents results by region, explores the seasonality of the phenomenon, and concludes that flood frequencies will increase dramatically at many US locations.

Sweet *et al.* (2014) explain the increased flooding due to RSLR in a straight-forward way - by considering the local NOAA tide gage data. Because sea levels have risen, the hourly water levels have shifted upward as shown in Figure 9.6. The figure shows hourly water level observation data at the NOAA gage at Sewells Point (Norfolk), Virginia for (a) 1950 and (b) 2012 and those (c) yearly water level distributions. All the elevations in Figure 9.6 are relative to the 1980-2001 MSL datum. Panels (a) and (b) show a monthly spring-tide influence and a few discrete storm events. Readily apparent in panel (c) is a shift of the distribution.

The shift of the distribution to the right in panel (c) of Figure 9.6 is due to the RSLR between 1950 and 2012 at that location. Also shown is the MHHW elevation of the 1983-2001 epoch. The plot shows that MHHW elevation was exceeded in several hundred hourly observations in 1950. But it was exceeded in several thousand hourly observations in 2012. The dashed, pink-yellow lines in all three panels represent the elevation (about +1 m) of a local nuisance flood elevation threshold in that area. Although that elevation was not exceeded in 1950 it was exceeded several times in 2012. The threshold is exceeded more often now due to RSLR.

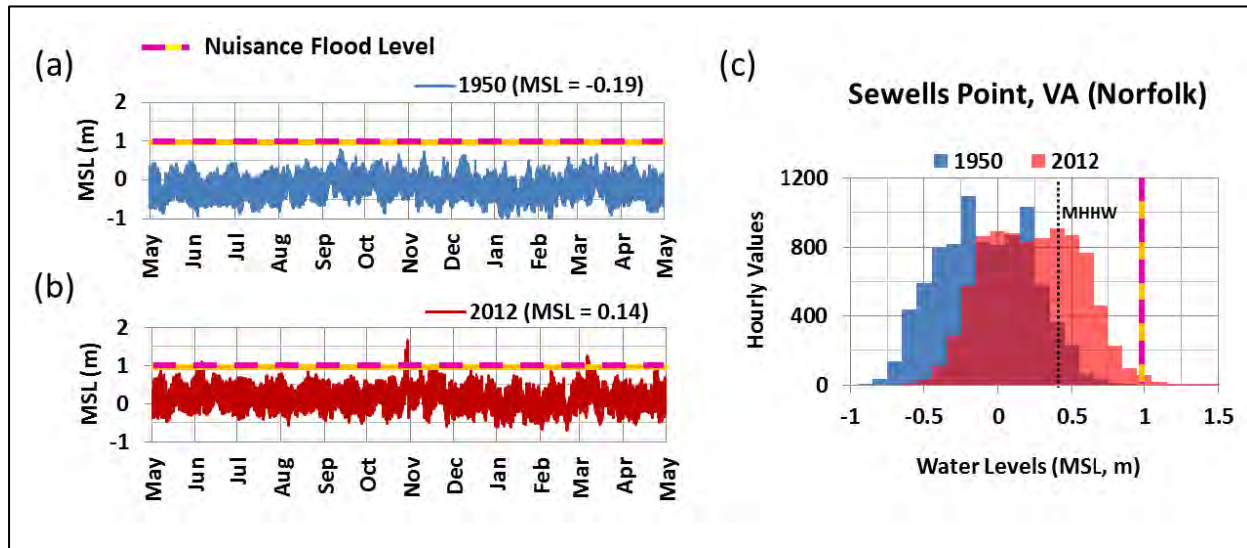


Figure 9.6. The increased frequency of flooding occurs because the full distribution of tides rises with RSLR (from Sweet *et al.* 2014)

Figure 9.7 shows the projected future increase in frequency of flooding with RSLR at two US coastal cities. The number of “minor tidal floods” in a year will increase rapidly this century to near or over 100 days per year by mid-century and almost every day by 2100 regardless of the assumption of future RSLR (see Section 4.1.6 for an explanation of RCPs and sea level rise projections). Minor tidal floods are those above the NOAA “minor” threshold. NOAA has established coastal flood severity thresholds for use when that agency issues coastal flood advisories and warnings. The thresholds are based upon water level heights empirically calibrated to tide gage measurements from years of impact monitoring by NOAA local Weather Forecast Offices and emergency managers. The threshold elevations differ around the US due to the extent of infrastructure vulnerabilities, which vary by topography and relief, land-cover types or existing flood defenses. Sweet *et al.* (2018) describes these thresholds and the patterns and projections of increased flooding due to RSLR in terms of them.

### 9.2.2 Kriebel and Henderson (2018)

Kriebel and Henderson (2018) present a straight-forward, effective, way to quantify the increase in flooding due to RSLR at any roadway location. This type of analysis can be applied at any location experiencing problems with increased flooding due to RSLR. It can inform the evaluation of engineering countermeasures (e.g. see Figure 9.15).

Kriebel and Henderson (2018) consider McNair Road on the US Naval Academy, Annapolis, Maryland. A portion of the road floods occasionally and these occasions are becoming more frequent. Figure 9.8 shows that portion of McNair Road flooded. The water in the foreground is a tidal creek connected to the Severn River and Chesapeake Bay.

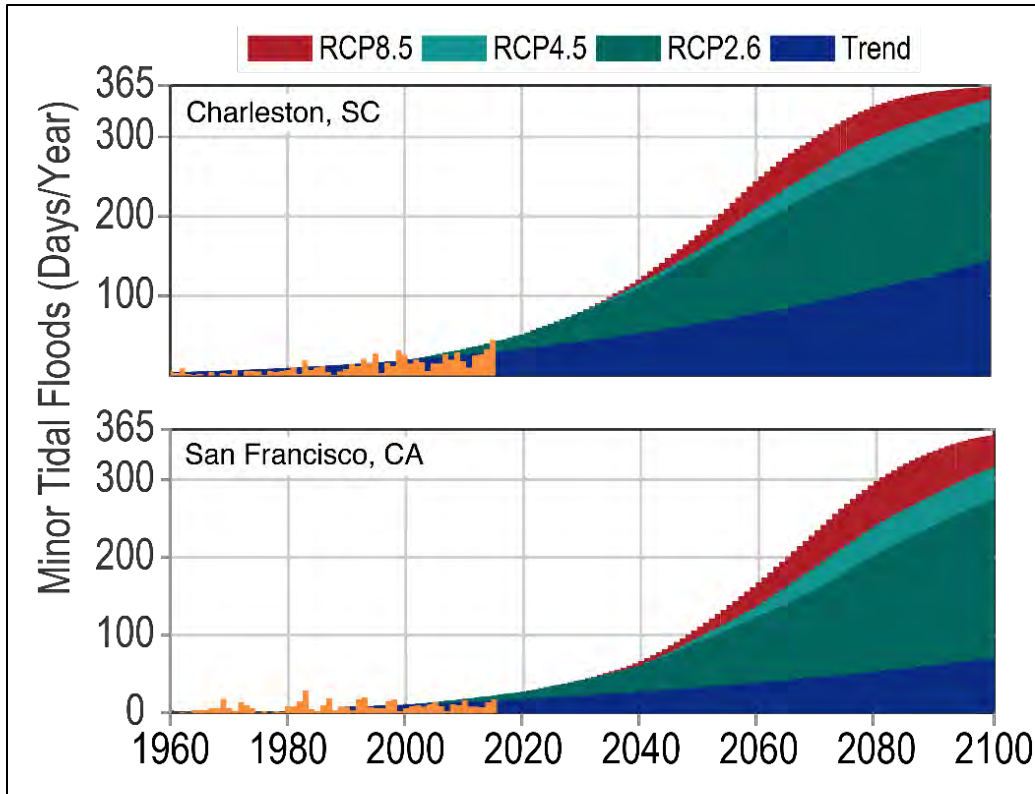


Figure 9.7. Increased flooding due to RSLR including historical exceedances (orange), future projections through 2100 based upon the continuation of the historical trend (blue), and future projections under median RCP2.6, 4.5 and 8.5 conditions, for Charleston, South Carolina and San Francisco, California (from Sweet *et al.* 2017a adapted from Sweet and Park 2014)



Figure 9.8. Flooding of McNair Road, US Naval Academy, Annapolis, Maryland (permission for use of photograph provided by David Kriebel)

Kriebel and Henderson (2018) find that the distribution of high tides fairly closely follows a normal, or Gaussian, distribution at many eastern US locations. Figure 9.9 shows the cumulative exceedance probability of the high tides at the nearby Annapolis NOAA tide station. The blue line represents the data points and the red line (which is obscured because it overlays the wider blue line) represents the normal distribution. The median value of high tide is about 0.5 ft above MSL. Several major floods in the high tide data are the blue circles towards the right side of the plot. A plot like Figure 9.9 shows the relationship between the tides and any specific elevation. For, example, roughly 20% of high tides exceed +1 ft (MSL).

**Transportation officials could choose to apply a Kriebel and Henderson (2018) type analysis to any road location to inform planning and design decisions related to increased flooding due to RSLR.**

To apply to coastal infrastructure, the tidal elevation data are usually converted from the tidal datum (MSL) to the survey datum (NAVD88). See Section 4.2.2 Tidal and Survey Datums for a discussion of this conversion. The surface of McNair Road begins to flood when the tide elevation is +1.98 ft (NAVD88).

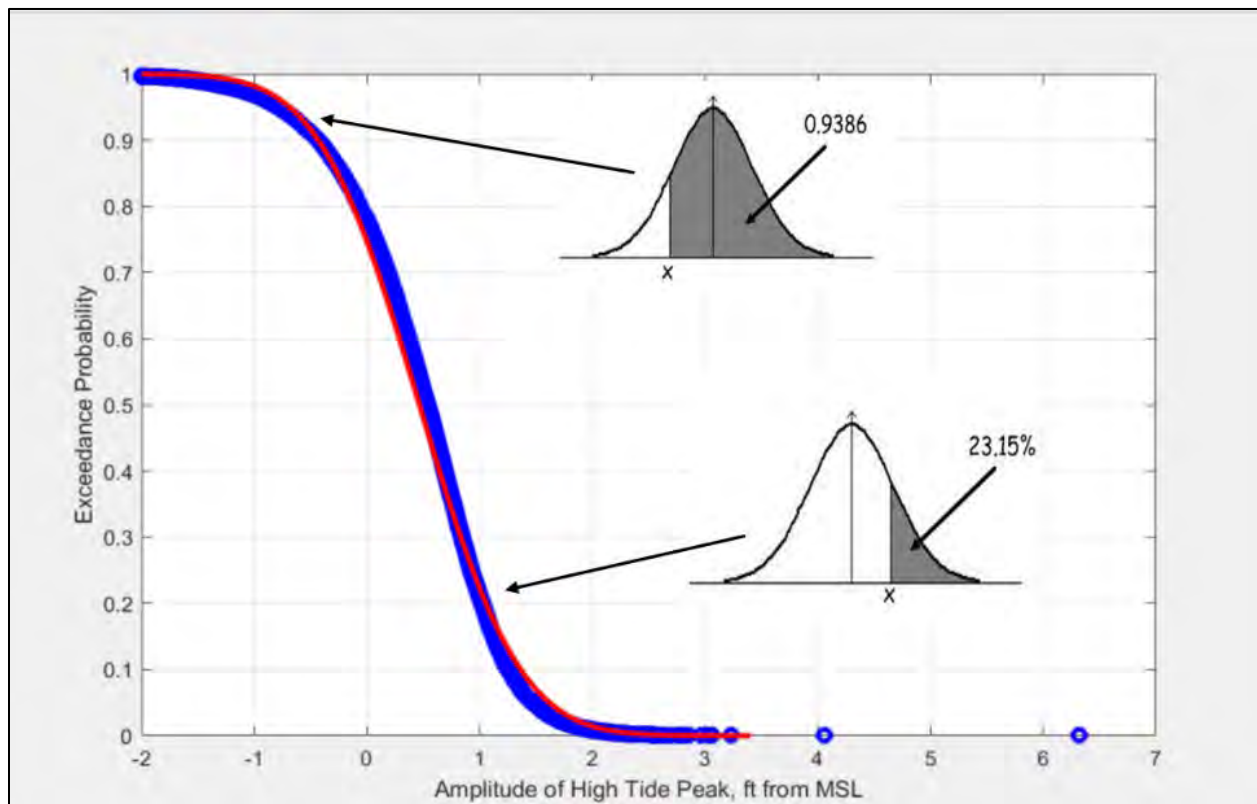


Figure 9.9. Probability distribution for high tides at Annapolis approximately follows a normal distribution (from Kriebel and Henderson 2018)

The lower, right side of the exceedance probability distribution curve in Figure 9.9 is where most of the problem with increased flooding due to RSLR is being experienced in the US with today's sea levels. That portion of the distribution can be evaluated with a more focused graphic that changes the cumulative probability scale to an "average number of floods per year" scale as shown in Figure 9.10 for the Annapolis data. The black circle on the graphic highlights the

elevation at which McNair Road floods (+1.98 ft NAVD88). With today's sea levels, McNair Road floods 21 times per year on average. The other circles on the graphic highlight the elevations at which other infrastructure in downtown Annapolis begin to flood:

- Dock Street storm drain = 1.90 ft (see Figure 9.5)
- City Dock storm drain = 1.71 ft
- Compromise Street storm drain = 1.67 ft
- Newman Street storm drain = 1.44 ft

The Newman Street storm drain floods almost 90 times per year. Figure 9.10 shows that the number of annual flooding events changes dramatically with just a few inches of elevation.

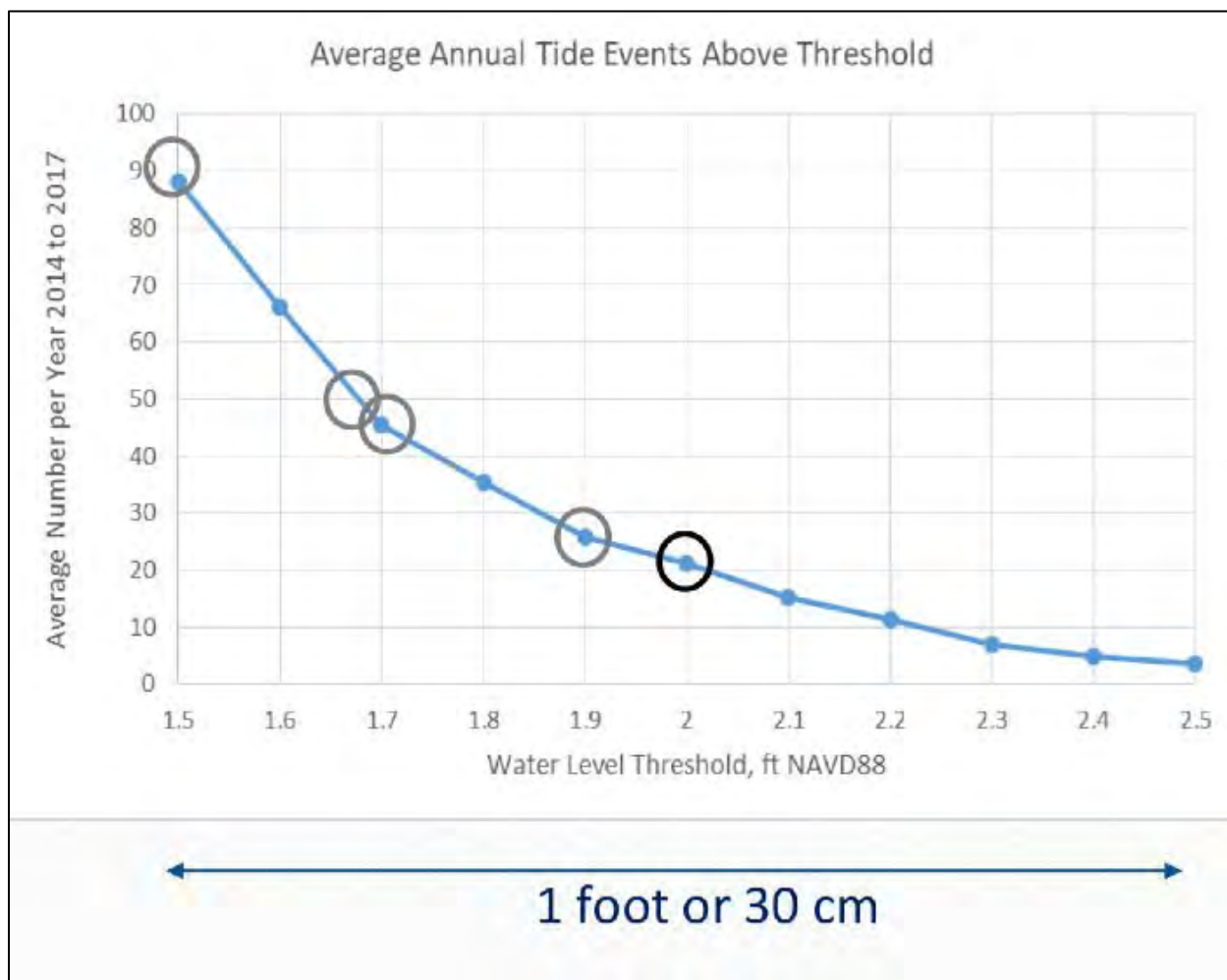


Figure 9.10. Average annual flood events above threshold water levels at Annapolis, 2014-2017 (from Kriebel and Henderson 2018).

Future RSLR projections can be added to the analysis by shifting the distribution as shown in Figure 9.11. The annual number of flood events is shown for today's sea level and 0.5 ft, 1.0 ft, 1.5 ft, and 2.0 ft of future RSLR. Note that the upper end of vertical scale is near 730 high tide events because Annapolis has a semi-diurnal tide, and thus, two high tides per day. This analysis assumes that the shape of the probability curve does not change with future SLR (which seems like a reasonable initial assumption for engineering).

Figure 9.12 shows how this information can be used to quantify the increase in flood frequency of a specific asset with RSLR. The right panel is specific to the +1.98 ft (NAVD88) elevation. The number of times that the McNair Road is flooded will increase from an average of 21 times per year, with today's sea level, to about 80 times per year with 0.5 ft of RSLR, to about 280 times per year with 1 ft of RSLR.

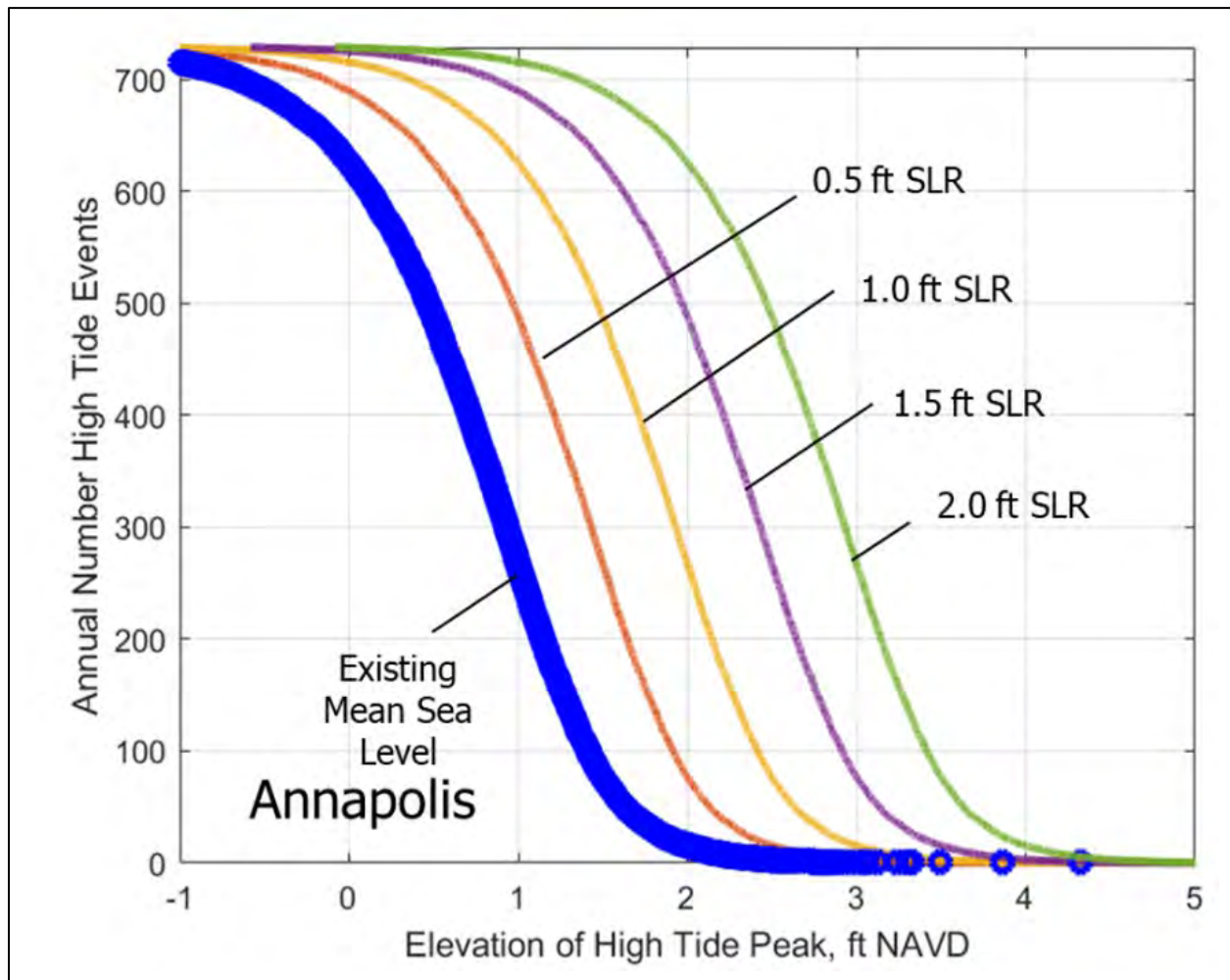


Figure 9.11. The effect of RSLR on annual flood events at Annapolis (from Kriebel and Henderson 2018)

**This extreme sensitivity to less than 1 ft of RSLR in this example may be indicative of the seriousness of the problem the US will face with RSLR in the coming decades.** With site-specific information like this, the transportation planning entity can consider the effects of a range of RSLR scenarios and the expected timing of that much RSLR (see Section 4.1 Sea Levels). Further analysis of this McNair Road example is presented in Section 9.3 Raising Roadway Elevation (see Figure 9.15).

The left panel in Figure 9.12 shows two other elevations along with the McNair Road elevation. The “NOAA Minor” and “NOAA Moderate” elevations refer to NOAA’s coastal flood severity thresholds (see discussion of these thresholds in Section 9.2.1 above or see Sweet *et al.* 2018).

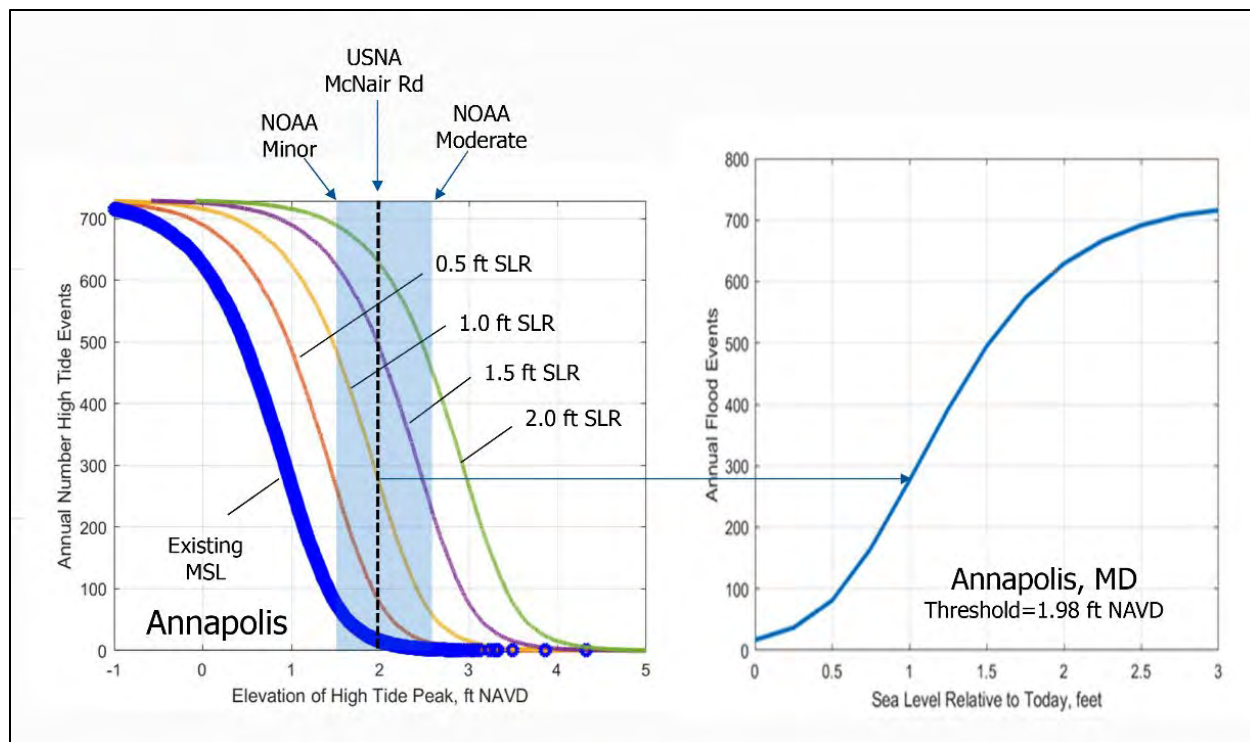


Figure 9.12. Applying the annual flood events curves to McNair Road, Annapolis (from Kriebel and Henderson 2018)

### 9.2.3 Jacobs *et al.* (2018a)

Jacobs *et al.* (2018a) analyze vehicle delay increases over a multi-state area caused by increased flooding due to RSLR. The study identifies vulnerable roads and quantifies the risk from increased flooding due to RSLR in the eastern US by combining public road information from the FHWA's Highway Performance Monitoring System with flood frequency maps, tide gage data, and future projections of annual minor tidal flood frequencies and durations. This is a form of an inundation mapping approach (see Section 14.1). Jacobs *et al.* (2018a) find that increased flooding due to RSLR threatens 7,500 miles (12,000 km) of roadways including over 400 miles (644 km) of interstate roadways in the eastern US. Vehicle-hour delays induced by this flooding are estimated to exceed 100 million vehicle-hours annually and that value is estimated to increase to 160 million vehicle-hours of delay across the eastern US by 2020 (85% increase from 2010). Figure 9.13 summarizes state-by-state vehicle-hour delay findings.

## 9.3 Raising Roadway Elevation

This section discusses a constructed solution to the problem of increased flooding due to RSLR – raising the elevation of the road. A broader discussion of mitigation approaches is in Chapter 15.

Figure 9.14 shows a Miami Beach road raised to address the problem of increased flooding due to RSLR. The road to the right of the photograph was raised several feet, and the retail businesses at the left of the photograph (see the café tables) are at the original road elevation. Biscayne Bay is a block away in the far background of this photograph (not visible). Prior to construction, the road and these businesses suffered from increased flooding due to RSLR. The local stormwater drainage system was re-engineered as part of the road elevation project. Pumps move rainfall stormwater runoff up and out of the area behind the raised road.

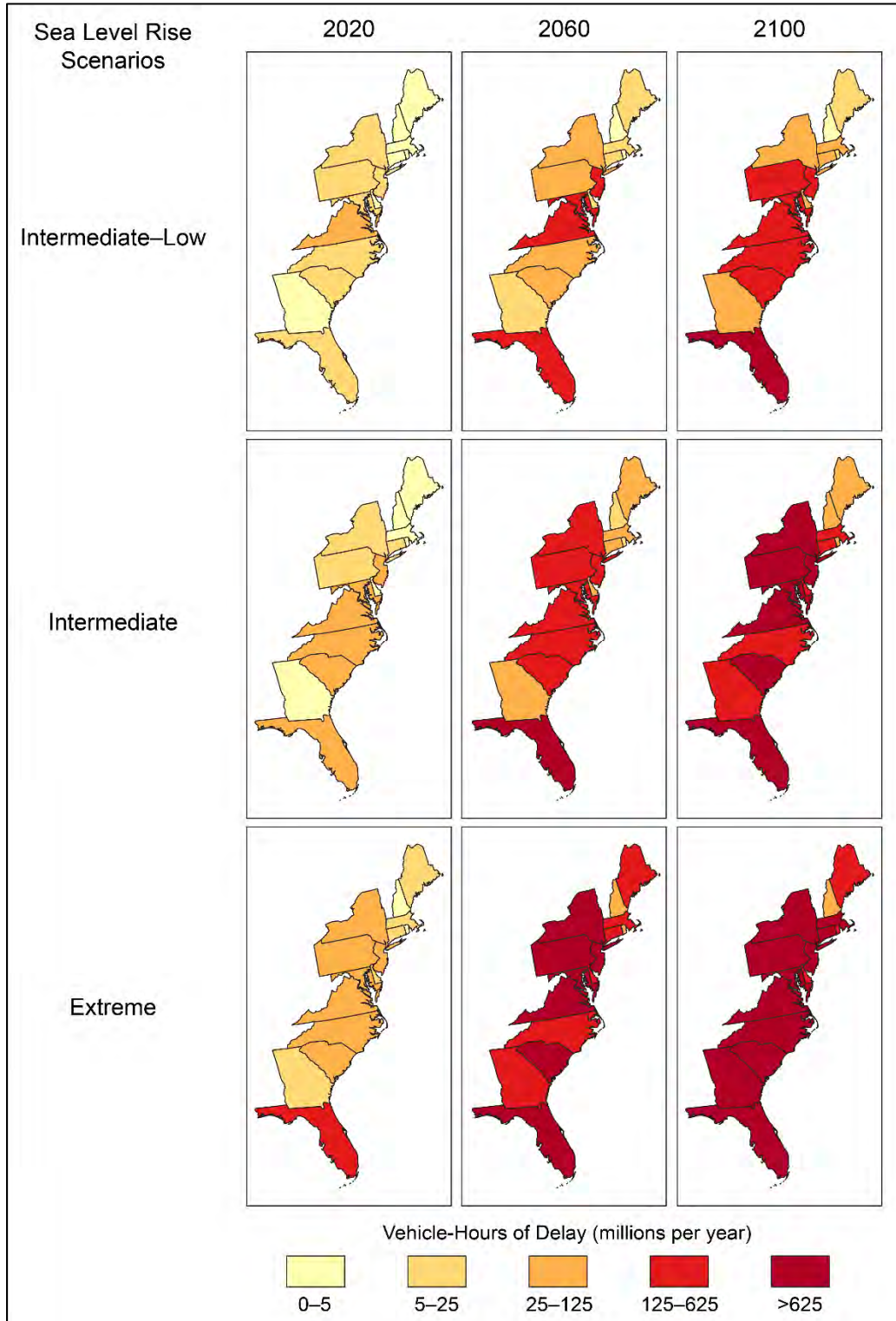


Figure 9.13. Annual vehicle-hours of delay projected for major roads (principal arterials, minor arterials, and major collectors) due to increased flooding due to RSLR by state; year (2020, 2060, 2100), and RSLR scenario (Intermediate-Low, Intermediate, and Extreme) (from Jacobs *et al.* 2018a)

A significant portion, sometimes more than half, of the roads in southern Dorchester County, Maryland are flooded on some high tides. Many yards are flooded more frequently also. The residents of parts of the county have adjusted to this reality though lifestyle changes (e.g. realizing that on some days they cannot drive to the city, buying vehicles with higher clearance, etc.). The southern portion of Dorchester County is an area with a high regional subsidence rate (VLM). The high rates of RSLR combined with the low elevations raise other land use planning issues that are related to the transportation issues (e.g. see discussion near the end of Section 4.1.7).

The analysis methods outlined in this chapter may provide transportation officials with potential approaches for planning and design of countermeasures and adaptations for the problem of increased flooding due to RSLR (e.g., raising the road). For example, Kriebel and Henderson (2018) relate how an engineer could extend the McNair Road analysis to consider the reductions in future flood frequency afforded by raising the road.



Figure 9.14. Example of a road which has been raised to reduce flooding due to RSLR (Sunset Harbour Drive, Miami Beach, 2017)

The left panel of Figure 9.15 shows the increase in the number of annual flood events with four future RSLR assumptions. The bottom (blue) curve is the existing, historic, linear rate of RSLR (at Annapolis this is 3.61 mm/yr, which is about one ft above today's level by 2100). The other three curves are for an additional +1, +2, and +3 ft of RSLR by the end of the century above that existing linear rate. All the values on the left-hand panel are likely to be problematic in reality. For example, if RSLR increases at the existing, historic, linear rate; the roadway will be flooded about 80 times per year by 2060. Note that sea level is projected to rise faster than the historical rate

(e.g. see Figure 4.11). The number of annual flood events on McNair Road is estimated to increase to 170, 300 or 430 times per year by 2060 if RSLR follows the other curves shown on Figure 9.15.

The right panel of Figure 9.15 shows the reductions in flooding of McNair Road if it were to be raised 1 ft. Such an adaptation-countermeasure would essentially “turn back the flooding clock.” The annual number of floods would reduce to just a few initially. However, with time, the number of floods across the road would begin to increase as shown in the panel to the right. The elevated road would flood as frequently as it is now by about 2065 to 2070 about 2 ft of RSLR this century (that is the orange line of +1 ft above the Existing Trend). While each transportation entity and project has their own potential approaches and constraints, **this type of information can still inform planning and design decisions related to engineering adaptations.**

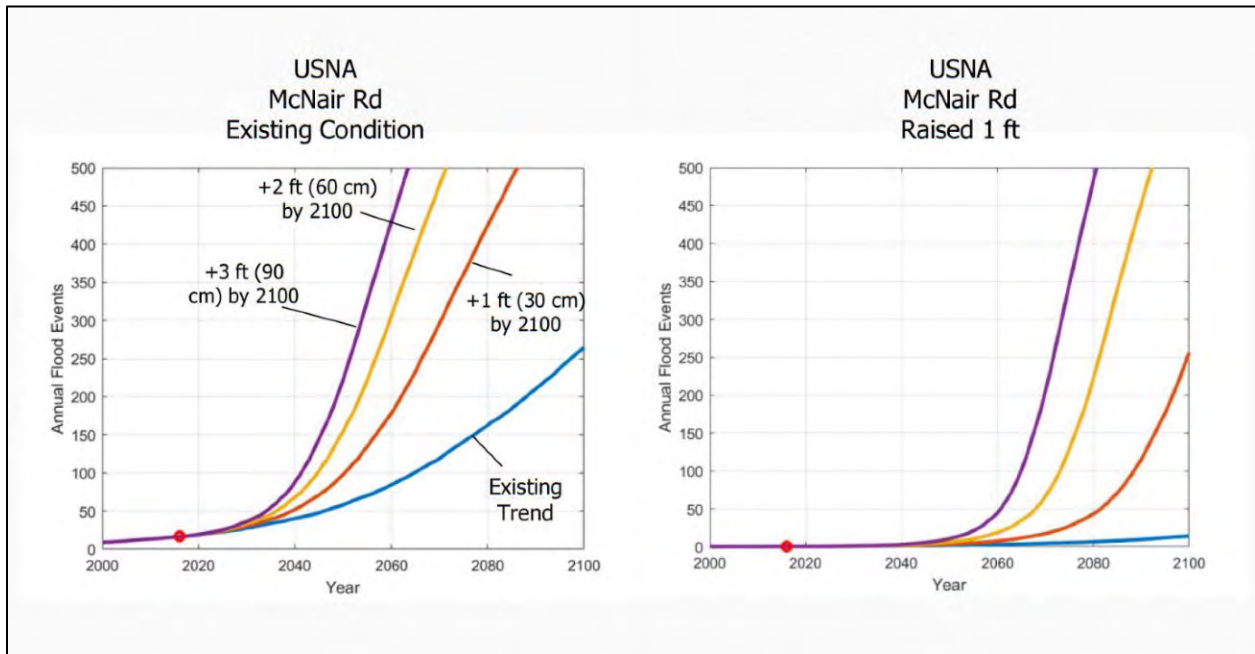


Figure 9.15. Flooding of McNair Road due to RSLR without (left panel) and with (right panel) a 1 ft increase in road elevation (from Kriebel and Henderson 2018)

*Page Intentionally Left Blank*

## Chapter 10 - Highway Overwashing

Coastal highways are vulnerable to storm damage during overwashing during storms. In some cases, overwashing leads to complete damage of the roadway surface through a process termed the “coastal weir-flow damage mechanism.” This chapter provides an overview of the issues associated with this type of damage.

### 10.1 Description of Overwashing

Coastal highway overwashing occurs when coastal storm surge elevations with wave runup exceed those of the roadway and water flows across the pavement with velocities high enough to cause embankment erosion.

Figure 10.1 shows an example of post-storm damage from overwashing. Hurricane Ivan (2004) caused this damage along the Gulf of Mexico Coast near the Florida/Alabama border. The road pavement elevation was about +8 ft (NAVD) and the storm surge peak from Hurricane Ivan here was roughly +11 ft (NAVD). Figure 3.3 shows overwashing damage caused by Hurricane Michael in 2018.



Figure 10.1. Example of pavement damage due to storm surge (Florida SH 292 on Perdido Key after Hurricane Ivan, September 2004).

## 10.2 The Coastal Weir-Flow Damage Mechanism

This section describes the coastal weir-flow damage mechanism in detail, including the use of diagrams and figures that draw on common hydraulic engineering concepts of weir flow mechanics.

Pavements subject to overwash can be damaged primarily by three mechanisms: direct wave attack on the seaward shoulder of the road, flow across the road and down the landward shoulder (“weir-flow” damage mechanism), and flow parallel to the road as water moves to “breaches” or lower spots in the road as the storm surge recedes.

Paradoxically, much of the damage to road pavements observed after Hurricane Ivan (2004) was on the landward side of the road. The Gulf of Mexico is to the right side of Figure 10.1 (behind the buildings). Figure 10.2 shows another example of similar damage, partial pavement undermining on the landward side of the road. Hurricane Ivan damaged over 50 miles of roads with partial damage as shown or complete damage. Weir-flow was likely the primary cause of the failure mode with contributions from parallel flow. This is based on post-storm damage assessments. The barrier islands were evacuated during the hurricane.



Figure 10.2. Example of pavement damaged by hurricane (photograph looking west on Florida SH 399, Gulf Islands National Seashore, 2005)

**Road embankments can act like broad-crested weirs during incoming and outgoing storm surge flooding.**

The specifics of the damage mechanism are as follows: **the road embankment acts like a broad-crested weir to the incoming storm surge** and the pavement is essentially the crest of

the broad-crested weir. As the surge elevation exceeds the elevation of the crown of the road, water flows across the road. Flow across a broad-crested weir passes through the critical flow condition (Chow 1959). In particular, flow down the landward shoulder is super-critical (high speed) and erodes the shoulder material. If the scour reaches the edge of the pavement, water continuing to flow over the edge of the pavement forms a hydraulic jump and undermines the pavement. The same mechanism can scour the seaward shoulder later in the storm as the surge returns to the sea.

A similar mechanism is responsible for damage to road embankments in a riverine environment (Chen and Anderson 1987, Clopper and Chen 1988). Figure 10.3 shows the general flow regimes that are established when a roadway embankment is overtopped. Damage can occur with or without tailwater (see Figure 10.4).

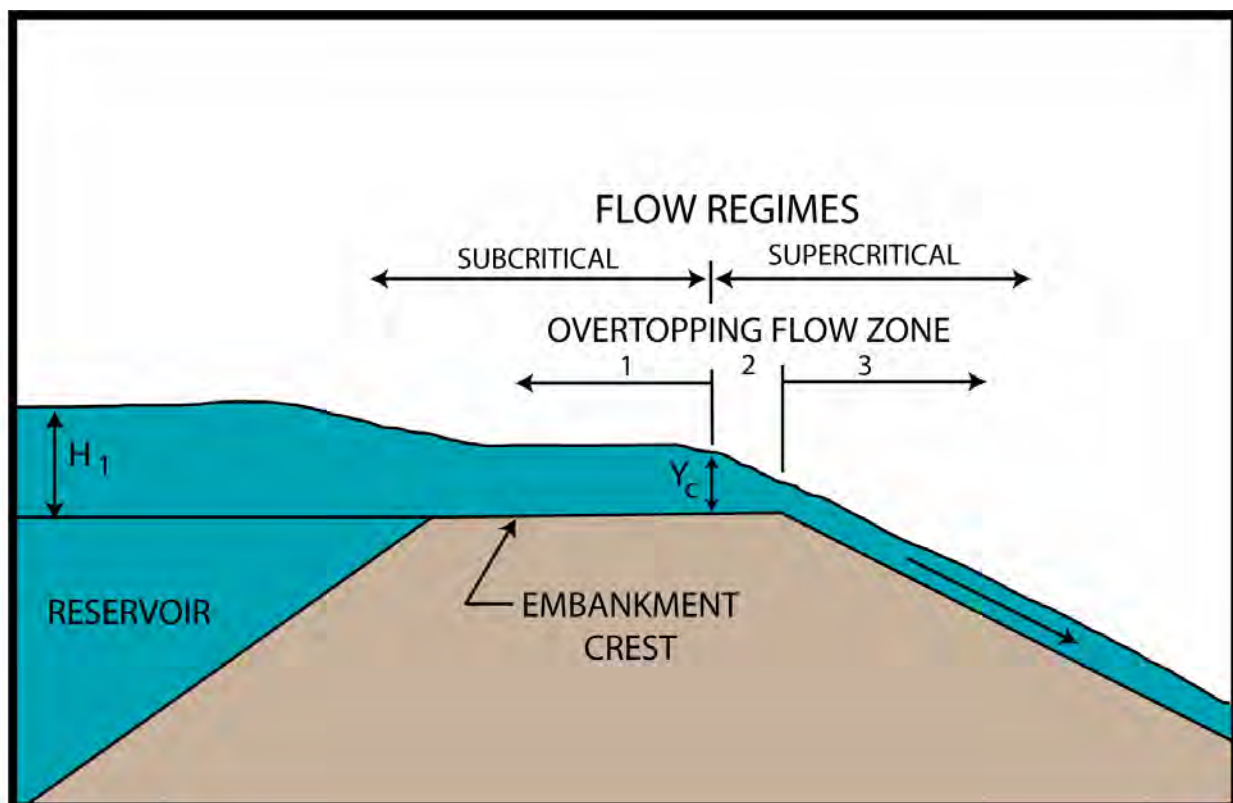


Figure 10.3. Flow regimes leading to failure of embankments in riverine flooding situations (after Clopper and Chen 1988)

Figure 10.5 shows a road destroyed during Tropical Storm Arlene (June 2005). This road was under construction after having been destroyed the previous year by Hurricane Ivan (September 2004). Hurricane Ivan removed all the sand dunes and allowed this portion of the barrier island to overwash during smaller storms.

During several small storms in 2005, coastal weir-flow damage was observed. Prior to those storms, the barrier islands were typically evacuated during major storms and the islands had sand dunes that prevented overwash during minor storms. Figure 10.6 and Figure 10.7 show the mechanism, as it was occurring, at two different locations during Tropical Storm Cindy (July 2005). The storm surge flow direction is from the ocean to a bay in both pictures. Flow is from right to left across the pavement in Figure 10.6 and from left to right in Figure 10.7. A small hydraulic jump is visible on the downstream side in each picture due to the elevation drop across the edge of the pavement.

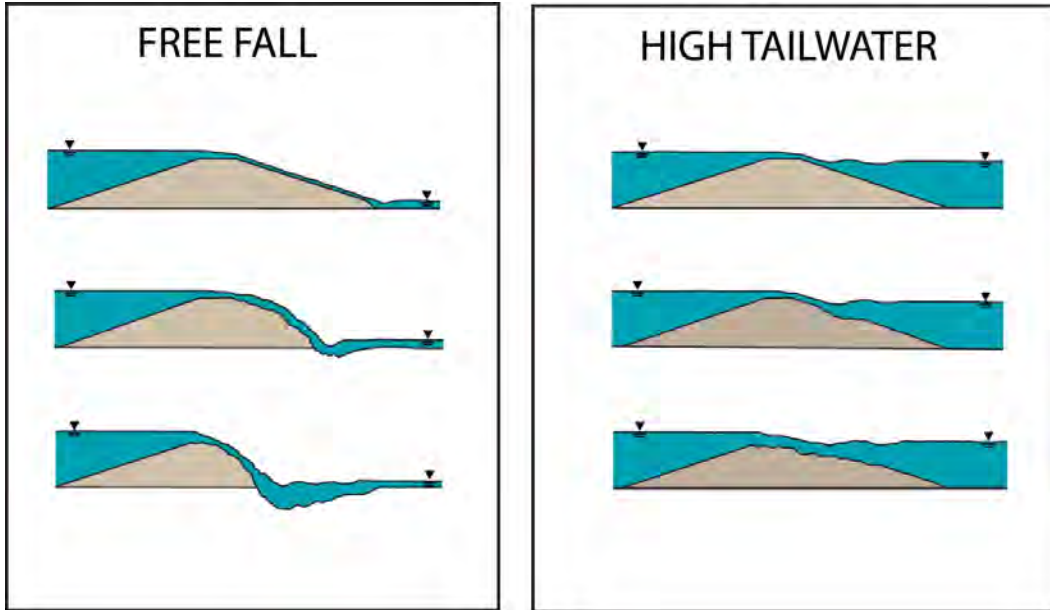


Figure 10.4. Embankment failure mechanisms (after Clopper and Chen 1988)



Figure 10.5. Pavement destroyed by the weir-flow mechanism (Fort Pickens Road, Gulf Islands National Seashore, near Pensacola, Florida)



Figure 10.6. Weir-flow damage beginning (Fort Pickens Road, Gulf Islands National Seashore, Florida, July 2005; FHWA photograph)



Figure 10.7. Weir-flow damage occurring. (Fort Pickens Road, Gulf Islands National Seashore, Florida, July 2005; FHWA photograph)

### 10.2.1 Coastal Weir-Flow Damage Mechanism Investigations

An FHWA-funded study conducted jointly by the University of South Alabama (USA) and Texas A&M University (TAMU) investigated the coastal weir-flow damage mechanism prototype-scale in a laboratory in early 2005. Figure 10.8 shows a schematic of the laboratory set-up and Figure 10.9 and Figure 10.10 show schematics of the results. The experiment was conducted in a 12-foot wide and 10-foot deep flume. The flume contained a constructed, sandy road embankment with a roadway on its crest consisting of 12, 2-foot wide concrete slabs. The sand shoulders were unconsolidated as is typical of many coastal highways. Water was pumped across the road section until failure as shown in Figure 10.9 and Figure 10.10. Figure 10.11 and Figure 10.12 show the failure. The USA/TAMU tests showed that the weir-flow is the likely cause of pavement damage observed in post-storm damage assessments. The damage can occur with only a little depth of water flowing across the road.

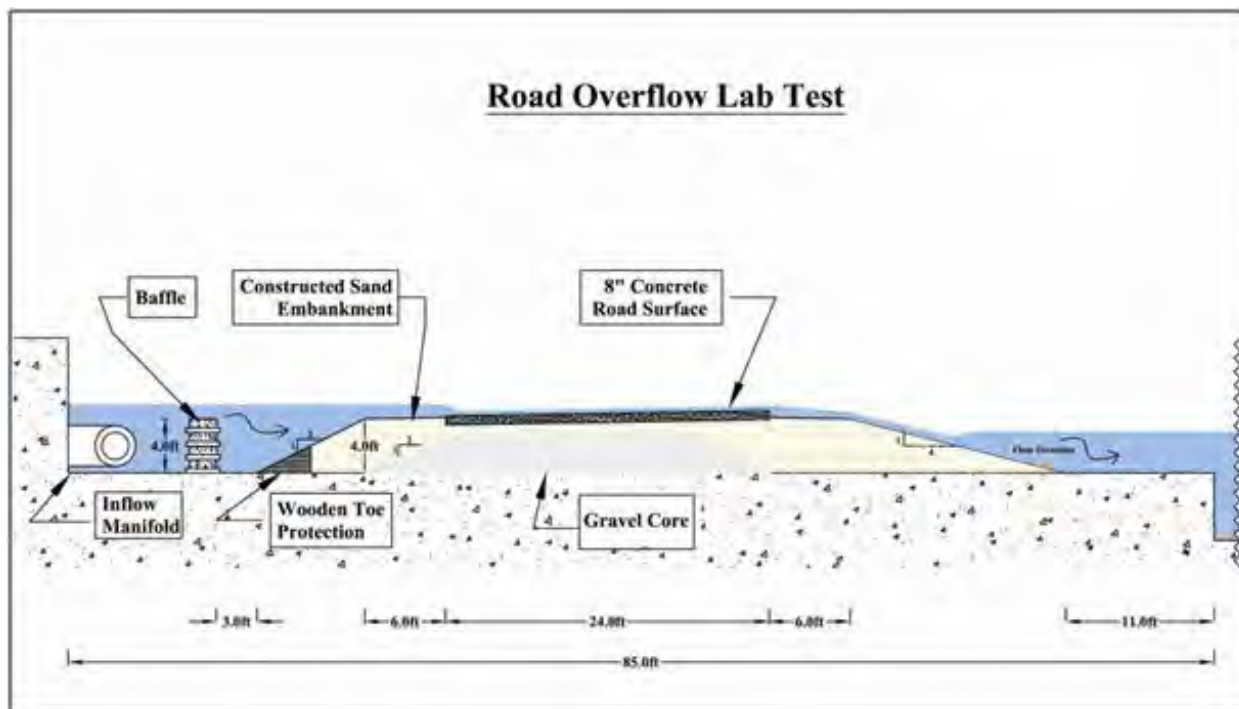


Figure 10.8. USA/TAMU laboratory experiment model setup schematic

Waves likely exacerbate the weir-flow damage mechanism. Waves moving across the pavement on the storm surge will increase the instantaneous flow velocities on the downstream shoulder which lead to more scour. Some levee failures in the greater New Orleans area during Hurricane Katrina were also due to downstream side erosion due to overtopping waves.

Clopper and Chen (1988) discuss uplift on overtopped pavements on a riverine embankment. Uplifting may be an even greater problem in the coastal environment because of the easier transmittal of pore-pressure under the pavement due to the sandy nature of the coastal road bases and the accelerations in water waves. There was some evidence of pavement lifting during Hurricane Ivan as shown in Figure 10.13.



Figure 10.9. Schematic of results from USA/TAMU laboratory experiments test run one



Figure 10.10. Schematic of results from USA/TAMU laboratory experiments test run two

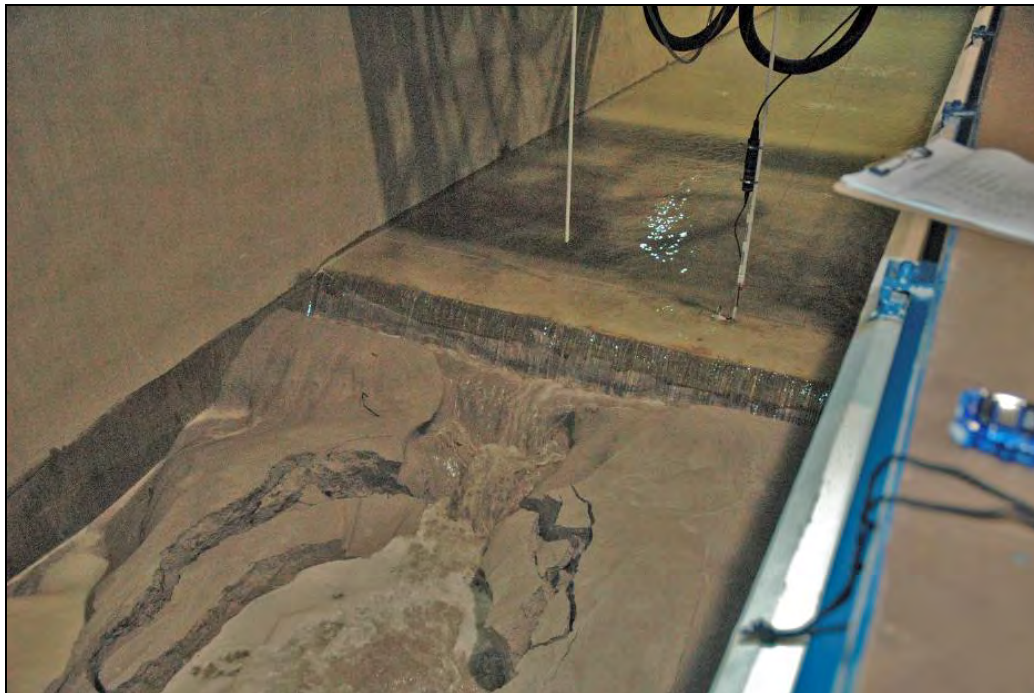


Figure 10.11. Laboratory tests of the weir-flow damage mechanism showing scour destroying the downstream shoulder and beginning to undermine the edge of pavement. (USA/TAMU flume tests, June 2005)



Figure 10.12. Laboratory tests of the weir-flow damage mechanism showing scour has continued to the point of undermining failure of 3 sections (6 ft) of roadway surface. (USA/TAMU flume tests, June 2005)



Figure 10.13. Pavement moved landward by overwash processes. (Florida SH 399, Gulf Islands National Seashore, Florida after Hurricane Ivan, 2004)

The same weir-flow mechanism that can damage the landward shoulder of a coastal road can damage the seaward shoulder too. Later in the storm, as the storm surge recedes, the water elevation on the landward side of the road embankment may be higher than the elevation on the seaward side. Flow is back to the sea and the downstream shoulder is now the seaward shoulder. Figure 10.14 shows pavement damage likely due to this return flow. The Gulf of Mexico is to the right in Figure 10.14. The damage looks more like it is due to the weir-flow damage than direct wave attack. Notice the background showing the pavement edge buried in sand (the buried pavement was not damaged); in the foreground, the pavement is exposed and damaged. This damaged section was at a slightly lower elevation than the undamaged section in the background. It appears that the water flowed back to sea over this lower pavement late in the receding surge hydrograph.

Another related damage mechanism is parallel flow (parallel to the road direction) along the landward side of the coastal highway embankment as the storm surge recedes. Late in the storm, the embankment can begin to act like a dam holding the flood waters on the barrier island. If a portion of the embankment is lower due to failure or breaching, then water will flow laterally toward the low spot in the embankment. This flow scours the foundation material along the shoulder and contributes to its damage or failure. Lateral flow along the shoulders during coastal storms has been observed by Florida DOT personnel at US 98 near Destin, Florida. There is post-storm evidence of this flow in many locations (including the location shown in Figure 10.1).



Figure 10.14. Evidence of weir-flow damage to the seaward edge of pavement due to return flow late in the storm (Alabama SH 182, after Hurricane Ivan, Gulf Shores, 2004)

### **10.3 Strategies for Roads that Overwash**

This section presents some potential strategies for reducing or preventing the roadway damage commonly encountered during coastal overwashing events. Four strategies for minimizing pavement damage due to overwash have been successful for coast-parallel roads on barrier islands. They can be used in combination with each other:

- re-locating the road to a portion of the barrier island farther from the ocean,
- lowering the elevation of the road to be at or below much of the existing grade to encourage burial by sand during overwash,
- constructing a sand dune seaward of the road to reduce the likelihood of overwashing and to provide a reservoir of sand to bury the pavement when overwashing occurs, and
- armoring of the shoulders of the road to resist erosion during overwashing.

#### **10.3.1 Road Location Considerations**

Storm overwash on barrier islands often naturally erodes elevation from the front portion of the island and deposits sand on the landward portion of the island, shown schematically in Figure 10.15. This geological process is one of the primary mechanisms for barrier island migration (see Chapter 6). This process, called barrier island “rollover,” has been likened to the tread of a tank in that the sand from the front is thrown to the back and then gets rolled over by more sand from the front in later storms.

Frontal dunes are often the highest elevations on a barrier island. These dunes and the beach berm seaward of them often erode in major storms through dune erosion and overwash processes. Sand is pulled offshore until the dune crest is breached or overtopped by the storm surge. Then sand moves landward and is deposited in lower elevations on the back of the island. These deposits, called overwash fans, can extend back into the bay.

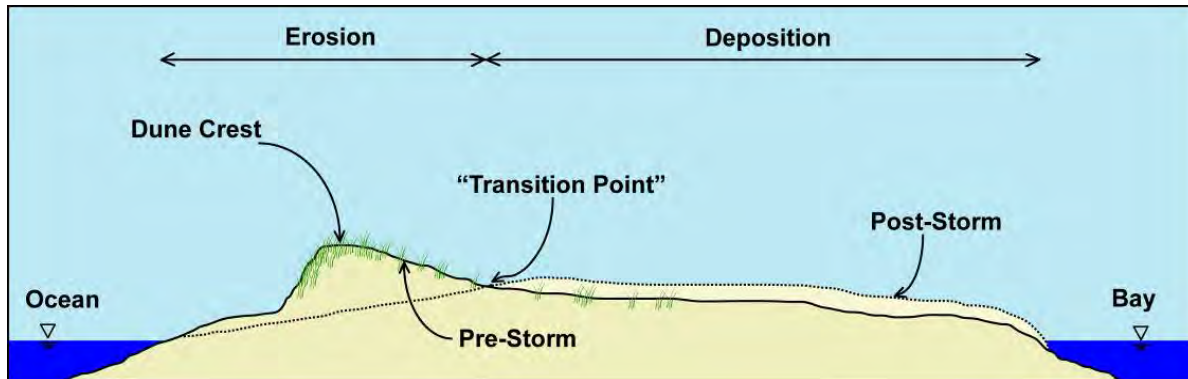


Figure 10.15. Schematic of sand erosion and deposition on a barrier island resulting from overwash

If the roadway is located where a cross-section erodes, it will be subject to severe wave attack and scour. If, however, it is located in the deposition zone, it can be buried by sand early in the overwashing event. Some roads, found under this layer of sand after a coastal storm, have been undamaged. A highway scraper or plow can scrape the sand off the road and the road can be opened to traffic shortly after the storm. Roadway relocation away from the ocean has been done on low barrier islands susceptible to overwash in Florida, North Carolina and elsewhere to work with the natural process depicted in Figure 10.15 (see Section 15.2.5).

### 10.3.2 Road Elevation Considerations

Another approach to reducing damage due to the coastal weir-flow damage mechanism is to lower the elevation of the road to near adjacent ground elevations. This lower elevation can prevent the weir flow from occurring since the crest of the pavement is not the highest portion of the grade. Figure 10.16 shows a road buried by overwash sand that survived a major hurricane. The piles of sand along the road were scraped off the road as part of the post-storm maintenance. Some practical limits to lowering the road depend on drainage and safety. Lower roads may also need more maintenance such as sand sweeping. Installation of sand fencing and vegetation can reduce drifting sand and the frequency of sweeping. Experience in west Florida suggests that constructing a typical road embankment elevated above the adjacent ground elevations can result in significant damage even if the road is relocated away from the ocean.

### 10.3.3 Construction of Sand Dunes

Sand dunes seaward of the road, either facilitated through sand fencing and vegetation plantings or through construction, reduce the likelihood of overwashing and provide a reservoir of sand to bury the pavement when overwashing occurs. Many states and local government have attempted to construct sand dunes seaward of roads to protect against storm surge and waves. North Carolina has used this approach to protect portions of North Carolina SH 12 along the Outer Banks. Figure 10.17 shows a portion of that highway north of Buxton, North Carolina, where a large, artificial sand dune has been constructed on the seaward side of the highway.



Figure 10.16. Example of road buried by overwash sand after it was opened by plows



Figure 10.17. Artificial sand dune constructed seaward of a highway to protect the highway (North Carolina SH 12; looking north, the Atlantic Ocean is to the right and Pamlico Sound is to the left, 2002)

Dune erosion analysis and modeling tools can be used to design the size and shape of the dune (see Section 6.4 Cross-Shore Sand Transport and Dune Erosion Modeling). Construction of a healthy sand dune usually involves vegetative plantings to stabilize the dune and to establish a dune that functions like a natural dune.

All three of the above approaches to reducing damage to pavements during overwashing can be implemented together. The schematic of Figure 10.18 shows a new road located as far from the ocean as practical, built at a low elevation, with small dunes constructed near it. The dune vegetation also acts to reduce wind-blown sand from covering the road during normal (non-storm) conditions.

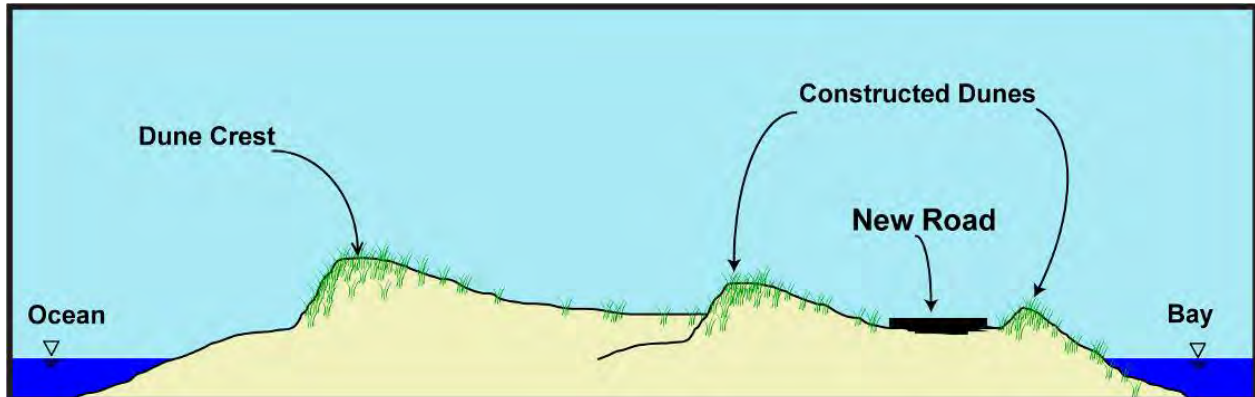


Figure 10.18. Schematic summarizing three approaches (bayward location, low elevation, constructed sand dunes near road) to minimize damage to roads that overwash

#### 10.3.4 Armoring of Shoulders

The downstream shoulder of roads that experience overwashing damage can be armored to withstand high velocity flows. This approach has been adopted to protect a section of US 98 on Okaloosa Island, Florida. The armoring includes sheet piling (Figure 10.19) and gabions (Figure 10.20). The sheet piling is located on the shoulder of the pavement farthest from the sea. This is the edge of pavement that has suffered the most damage due to the weir-flow damage mechanism in past hurricanes. The top of the concrete sheet pile wall cap section is visible in the photograph of Figure 10.21. Most of the engineering is not visible since it is buried under sand to the right of the roadway in that photograph. The bay is shown at the right-hand side of the photograph and the incoming surge flow is from left to right. Buried gabions are used elsewhere where the overwashing flow may be lower but flow parallel to the road during the storm is expected to be strong enough to cause damage. This design was constructed in 2005, after Hurricane Ivan, and had not been tested by a major overwashing event as of 2018.

This US 98 design was evaluated recently as a case study of an engineering adaptation to increase coastal highway resilience to rising sea levels (FHWA 2017b). The evaluation included a range of future relative sea level rise scenarios and the effect of that sea level rise on storm surge return period elevations. **Engineering economic analysis conducted under this evaluation concluded that the cost of this design was justified with today's sea level and that the economic justification becomes much stronger as sea levels rise.**

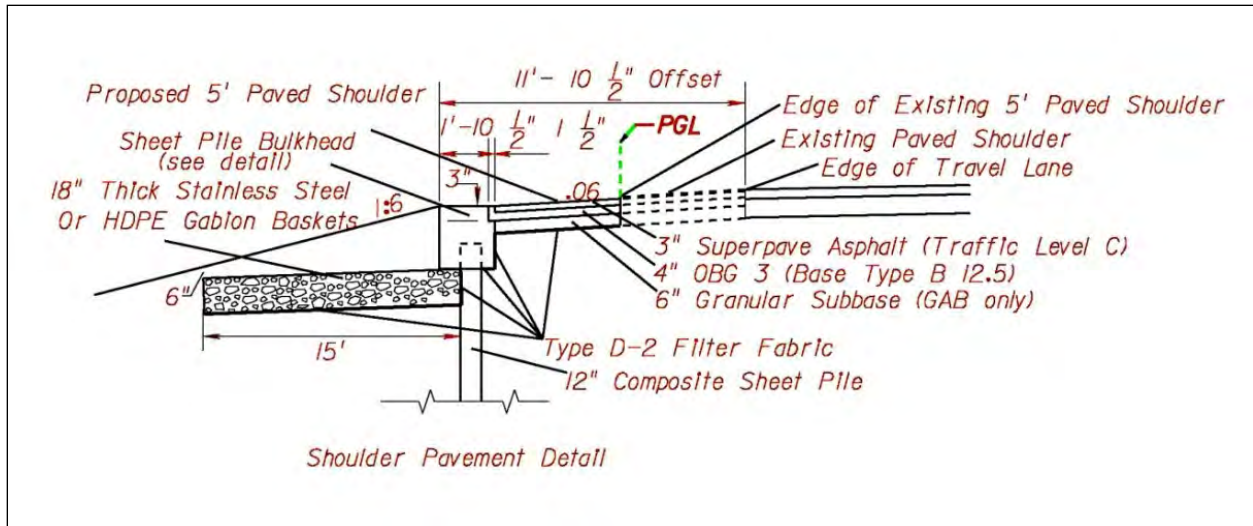


Figure 10.19. Sheet pile, with buried gabions for scour protection, at edge of pavement to resist pavement damage due to coastal storm surge overwash. (Florida DOT figure)

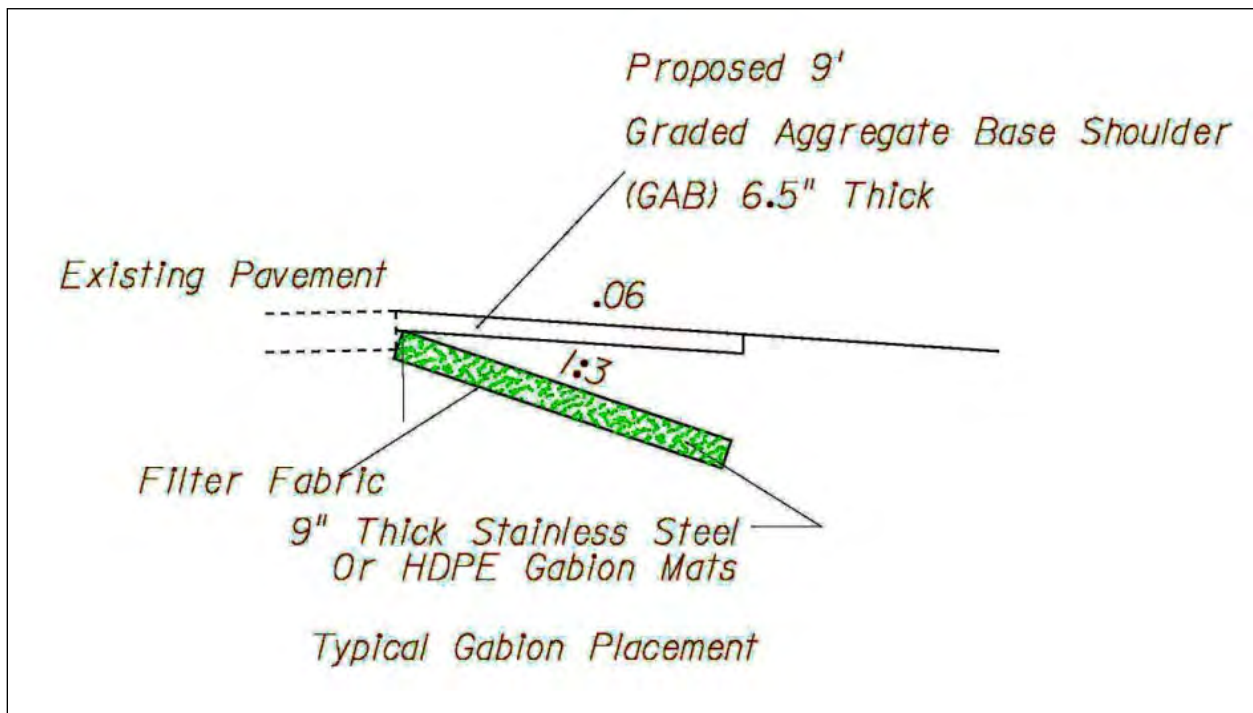


Figure 10.20. Gabions at edge of pavement to resist pavement damage due to coastal storm surge overwash. (Florida DOT figure)



Figure 10.21. Highway shoulder which has been designed to withstand the weir-flow damage during overwashing events (US 98, Okaloosa Island, Florida, 2016)

**A buried wall was built under the shoulder of the highway to reduce damage in future storms.**

Clopper and Chen (1988) provide results of research into armoring shoulders that might be applicable to the coastal problem. They conducted laboratory experiments on different possible countermeasures to resist the flow of water across a highway embankment. Their tests were based on riverine overflow situations and focused on soil types not as sandy as those typically found at the coast. They only considered current flow forces and not wave forces. However, Clopper and Chen (1988) found that a concrete block revetment system with relatively heavy blocks, horizontal and vertical interlocking cables, and anchors was able to resist the hydraulic forces due to overtopping better than a number of other alternatives. They tested flow rates generated by up to 4 ft of differential head over the embankment which is probably more than is typical in coastal storms. However, the addition of waves in coastal storms likely increases turbulence, shear stresses, and erosion significantly. Figure 10.22 is a sketch of how that concept could be implemented as a retrofit to protect a coastal highway. The capabilities of interlocking

blocks to withstand the overtopping condition was confirmed by laboratory tests by Clopper (1989).

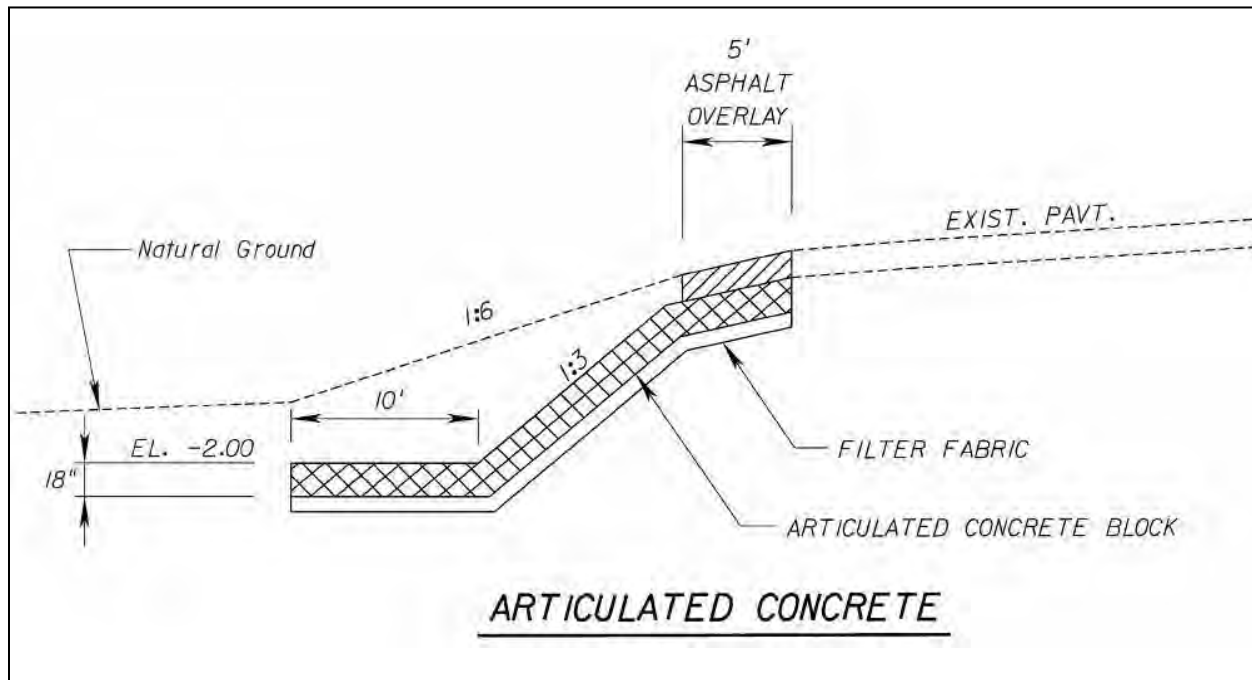


Figure 10.22. Conceptual design to resist pavement damage due to coastal storm surge overwash

## Chapter 11 - Coastal Bridges

Engineering of coastal bridges involves consideration of forces and processes unique to the coastal environment including loads from waves. Over 36,000 bridges are within 15 miles of coast in the US. But as this is only 6% of the approximately 600,000 bridges contained within the National Bridge Inventory, riverine-based hydraulic design approaches are often applied to these coastal bridges. This chapter provides an overview of some of the unique aspects of bridges in the coastal environment including:

- Bridge settings within the coastal floodplain,
- wave loads on bridge decks (with examples of damage, a description of the problem, a review of the technical literature, a revised method for estimating wave loads on bridge decks, and estimating bridge deck elevation needed to avoid wave loads),
- possible countermeasures for wave loads (and problems with them), and
- selection of design storm surge and wave heights.

The method of estimating wave loads on bridge decks presented below (Section 11.4) is revised from the previous edition of this manual. The limited research on countermeasures or retrofits that have been proposed to mitigate coastal bridge damage is summarized in Section 11.5. The important conclusion is that attempts to resist wave loads can lead to damage of some other bridge component later in the storm. Chapter 12 addresses the related issues of coastal scour.

**A revised method for estimating wave loads on bridge decks is presented in this Chapter (see Section 11.4).**

### 11.1 Coastal Bridge Settings

Coastal bridges are found at a variety of general types of location settings within the coastal environment including inlets, open-water bays or sounds, tidal embayments or arms, and river crossings (Figure 11.1). Each presents different issues and challenges for the coastal practitioner. These issues and challenges are described here to better orient the reader to subsequent descriptions of wave and hydrodynamic loads on bridges and coastal bridge scour (Chapter 12).

#### 11.1.1 Bridges at Inlets

Tides move between the ocean and a bay through inlets (see Section 6.6 Tidal Inlets). They are the entrance to many estuaries and other water bodies of ecological importance. These interior bays and estuaries can store significant volumes of water. Inlets experience complex hydrodynamics, some with extremely intricate interactions between currents and sands. Most shoreline change occurs near inlets and many inlets are “evolving” geologically in response to engineering and natural changes. There can be multiple inlets to the interior water body (bay, sound, etc., e.g. see Figure 6.18)

The US has over 600 tidal inlets, many with bridges across their throat. These can range from very large structures (e.g. Golden Gate Bridge) to relatively small spans (Figure 11.2).

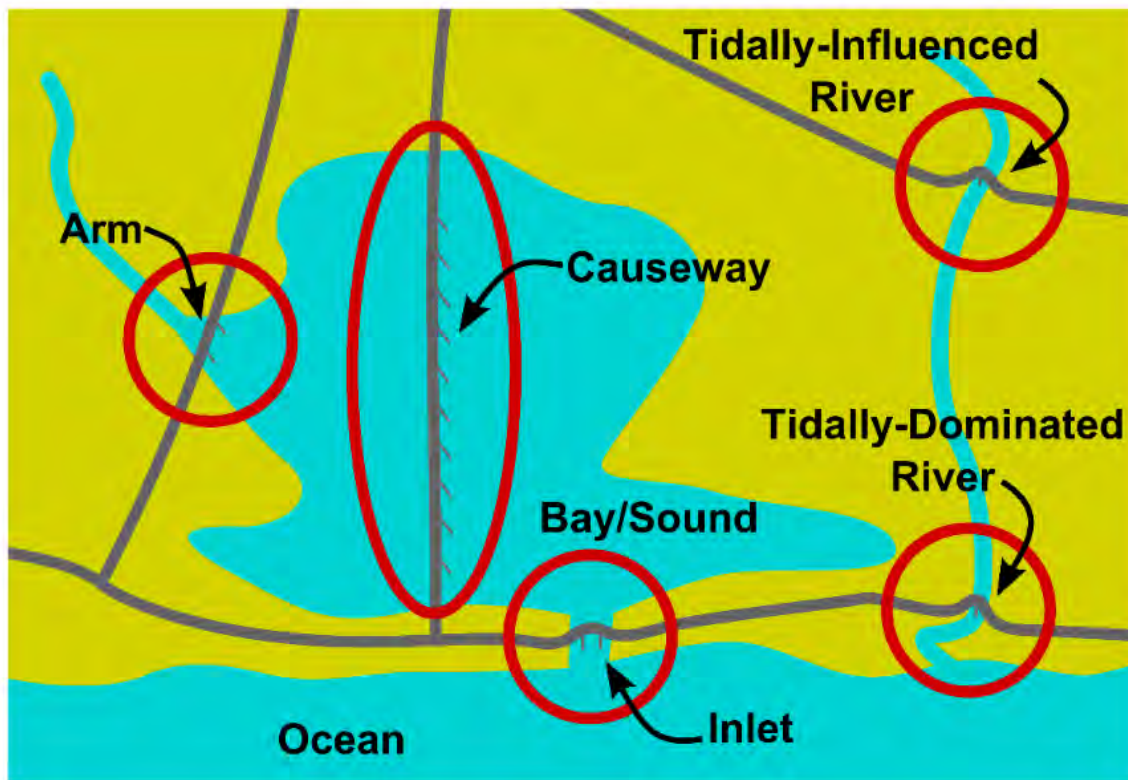


Figure 11.1. Conceptual schematic of four typical bridge settings within the coastal environment

### 11.1.2 Bridges over Bays and Sounds

Bridges link coastal barrier islands and peninsulas to the mainland. They are bridges or a combination of bridges and elevated causeway embankments. The floodplain crossing can be some combination of open water and wetlands. For example, Figure 11.3 shows the F.J. Torras Causeway between Brunswick and Saint Simons Island, Georgia. The causeway bridge, like many such structures, serves as an evacuation route during storm events. The total causeway length is over 21,000 ft and contains five bridges crossing tidal creeks and rivers. The total length of bridge structures, however, is less than 6,000 ft. The remaining 15,000 ft of the causeway is a roadway on a constructed embankment.

### 11.1.3 Bridges Spanning Tidal Embayments

Another common location for coastal bridge crossings is a tidal embayment. As opposed to inlet bridges, these bridges are located in interior water bodies or a distance “upstream” on an open bay or estuary. Bridges at these locations can vary in width and span length: from two-lane, 20-foot spans over tidal creeks to multi-mile interstate spans.

Bridges spanning tidal embayments are distinct from causeway bridges in that they are in open waters. Examples range from a small tidally influenced creek to large tidally influenced waterbodies such as Mobile Bay (Figure 11.4); Knik Arm, Alaska; or Chesapeake Bay.



Figure 11.2. Bridge spanning a small inlet (Alabama SH 182 in Gulf Shores)

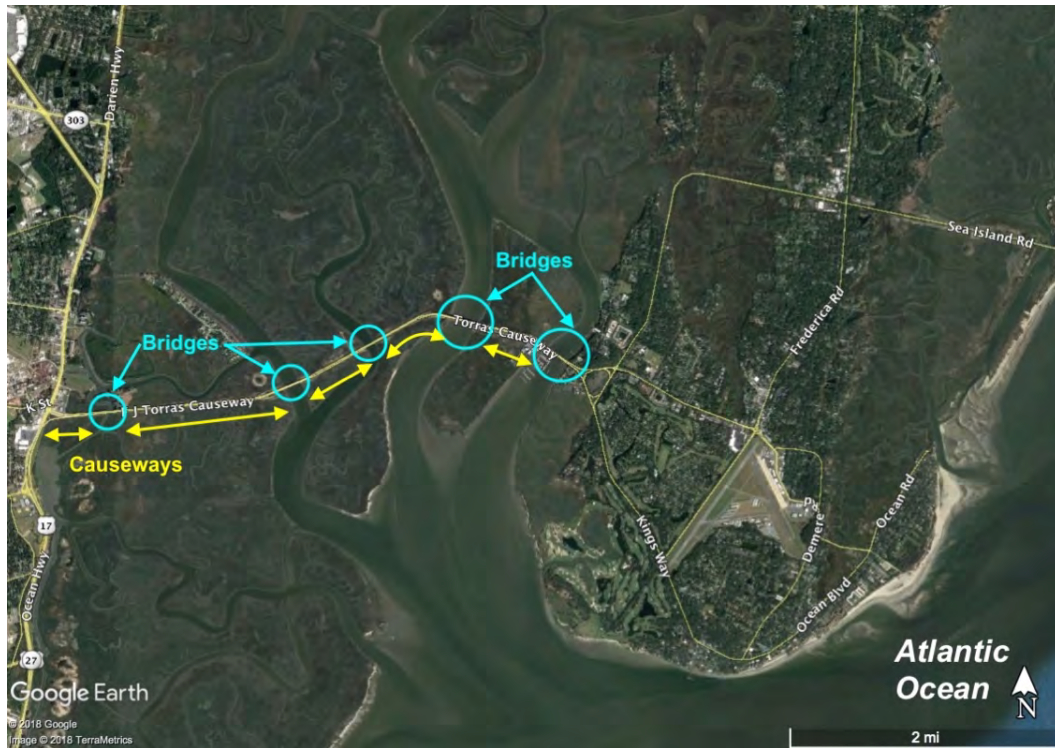


Figure 11.3. The F.J. Torras Causeway bridges between Brunswick and Saint Simons Island, Georgia



Figure 11.4. Interstate 10 bridge crossing Mobile Bay, Alabama

#### 11.1.4 Bridges Crossing Rivers

Bridges also cross rivers in the coastal setting. The locations of these crossings and the influence of tides, sea level rise, and coastal storm impacts are unique to their location. Such bridges may be located a short distance upstream from a tidal embayment on a bay, sound, or estuary, or perhaps even a considerable distance upstream, and still exhibit some tidal influence on hydraulic processes.

A distinction can be made between “tidally-dominated” and “tidally-influenced” areas of coastal rivers. Tidally-dominated areas have reversals in flow direction due to the tide. “Tidally-influenced” areas have unidirectional river flow with fluctuations in discharge controlled by the tide (by tailwater control). Examples of major rivers with miles of both types of flow are the Columbia River, Hudson River, and Cooper River.

Bridges also cross river mouths near the open ocean. Numerous such bridge crossings are along the Pacific Coast and on some Pacific Islands. Many of these crossings are over smaller rivers and creeks. Figure 11.5 shows four of these crossings.



Figure 11.5. Pacific Coast river mouth crossings (clockwise from top left: Big Creek, Oregon; Pistol River, Oregon; Yachats River, Oregon, and Redwood Creek, California)

These river bridge crossings differ from other locations described above in several ways. First, the local geographical features, such as hills and mountains extending to the shoreline, often result in a narrower floodplain. Second, the long-term geomorphological changes and shorter-term interactions between fluvial discharge and coastal processes, namely wave-driven longshore sand transport, result in a complex setting that may impact bridge hydraulics over time. Third, some of these rivers carry a notable sediment load to the littoral zone. Severe lateral channel migration may occur especially within the backshore beach zone. Thus, the shoals shown in Figure 11.5 change significantly in time.

## ***11.2 Wave Loads on Bridge Decks: Examples and Description***

Highway bridges along the north-central Gulf coast were damaged during landfall of Hurricanes Ivan (2004) and Katrina (2005). These include the Interstate-10 (I-10) bridge across Escambia Bay in Florida, the I-10 bridge across Lake Pontchartrain in Louisiana, the US 90 bridges across Biloxi Bay and Bay St. Louis in Mississippi, and an on-ramp to the I-10 bridge across Mobile Bay in Alabama (see Figure 11.6). The bridge to Dauphin Island, Alabama, that now carries Alabama SH 193, was destroyed by Hurricane Frederic in 1979. The two US 90 bridges in Mississippi bridges damaged in Hurricane Katrina had previously been damaged by Hurricane Camille in 1969. The replacement bridges built after Hurricane Camille (1969) were built at the same elevation. After they were damaged in Hurricane Katrina (2005), they were rebuilt at much higher elevations to avoid future storm surge and wave loads.



Figure 11.6. Location map of some of the highway bridges damaged by wave loads in hurricanes along the north-central Gulf Coast (from Douglass *et al.* 2006a)

Other bridges in the region suffered damage during Hurricane Katrina when vessels that had broken their moorings collided with them. A comprehensive listing of bridges damaged by Hurricane Katrina can be found in the ASCE Technical Council on Lifeline Earthquake Engineering (TCLEE) report (2006) and discussion of the overall civil engineering damage issues can be found in Robertson *et al.* (2007).

Reviewing information related to several of these damaged bridges reveals potential failure modes and commonalities. This section describes some of the forensic observations of two of the case studies of bridge damage in 2004-2005 and concludes with a description of the damage mechanism – waves on storm surge striking the bridge decks. The investigations and lessons taken from these two bridges could similarly describe many of other wave load impacted bridges.

### 11.2.1 I-10 Escambia Bay (Hurricane Ivan)

Interstate 10 (I-10) crosses Escambia Bay just east of Pensacola, Florida on elevated twin span bridges. The bridge was severely damaged both west and east of the high-span portions during passage of Hurricane Ivan September 15-16, 2004 (see Figure 11.7). The hurricane made landfall on the Gulf Coast west of this bay and generated extreme storm surge and large waves propagating up the bay toward the bridge as shown. Like many other bridges, the decks were simply supported spans atop pile caps (bent beams) with very minimal structural connections between the deck girders and pile caps. Waves riding on top of the elevated storm water levels

displaced the bridge decks. Higher elevation twin spans replaced this bridge following Hurricane Ivan.



Figure 11.7. Location map and damage overview for the I-10 bridge across Escambia Bay, Florida in Hurricane Katrina

Figure 11.8 shows a photograph of damage on the west side of the high span as a result of Hurricane Ivan (the area identified as “Damage W” on Figure 11.7). At the time of this photograph, the evening after landfall the previous night, the storm surge elevation had already receded below its maximum and the wave heights had also diminished significantly.

Note that the spans in the right of the photograph have moved to the left (in the direction of wave propagation) and some have fallen off the pile caps (bent beams). The spans in the foreground of the photograph have not moved even though they are at the same elevation as the spans that have moved. This implies that wave heights were slightly lower due to the partial sheltering of the shore and slightly shallower water near the shore. Numerical model hindcasts of the storm surge and wave fields which occurred during passage of Hurricane Ivan confirm this (see Figure 5.17).

The spans in the background of the photograph have not moved because they are elevated higher above the bay for the high-span for navigational clearance.

The connections between the decks and the pile caps were small steel clips (angles) with bolts embedded only a few inches into the concrete. The repeated extreme loads from individual waves broke the bolts out of the concrete.

The spans on the westbound bridge (left side of photograph) were less damaged than the ones on the eastbound bridge because the eastbound bridge provided shelter during the peak of the storm and reduced wave heights, and thus loads, on the westbound bridge. The large storm

waves were propagating from the right to the left during the peak of the storm (see wave travel direction indicated in Figure 11.7). The photographic evidence indicates that the wave-induced loads were just large enough to begin to move the decks at the peak of the storm surge. Some shifted a short distance but some moved far enough to topple off the pile caps. As the storm surge receded from its peak that night, wave loads on the bridge decks diminished.

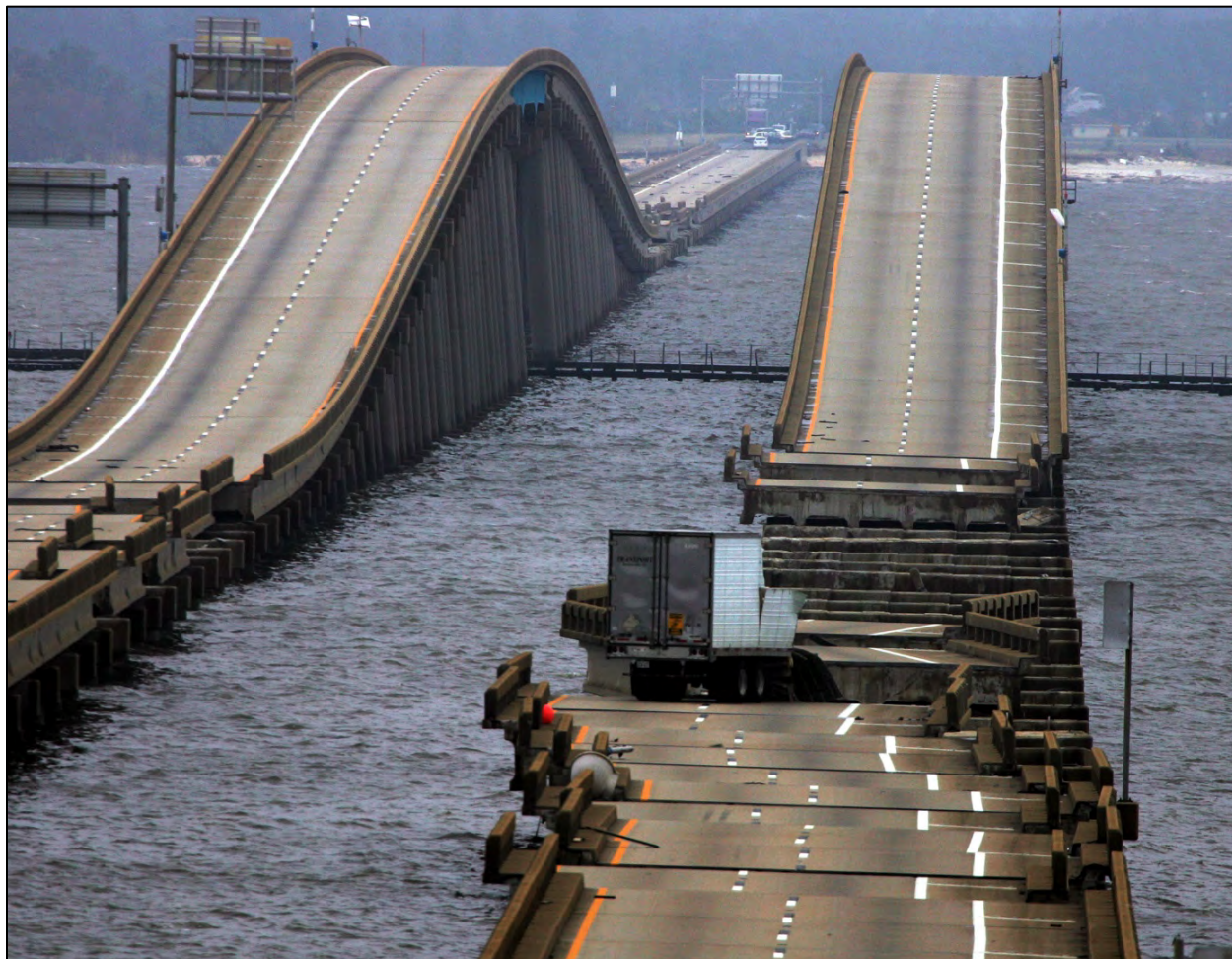


Figure 11.8. Interstate-10 bridge across Escambia Bay, Florida, after Hurricane Ivan. Photograph looking northeast from Pensacola September 16, 2004 (photograph used with a license from AP Images)

**Wave loads on bridge decks are extremely sensitive to water levels when the water level is near the deck elevation.** This sensitivity is clear in forensic investigations and in the methods for estimating these loads (see Section 11.4).

Recent forensic modeling of the storm surge and waves in Escambia Bay during Hurricane Katrina shows that long-term relative sea level rise (RSLR) likely contributed to the damage which occurred in Hurricane Ivan (Kilgore *et al.* 2019a). The magnitude of wave loads in 2004 when the bridge was actually damaged and those which would have occurred if a storm with the exact same characteristics had occurred with sea levels reflective of those 30 to 40 years prior, when the bridge was designed, are compared. ADCIRC and SWAN for both sea levels are used in the hindcasts.

The Pensacola NOAA tide gage records indicate that the MSL for the year 1970 was about 0.33 ft lower than in 2004 (annual average sea level). After performing the 2004 hindcast of Hurricane Ivan, a second simulation applied a water surface that was offset 0.33 ft lower in the models (1970 condition). The models capture all of the potential nonlinear effects that lead to changes in storm surge between the two different time periods (see Section 4.3.4 Impacts of SLR on Storm Surge).

The Douglass *et al.* (2006a) method is used to estimate the maximum vertical wave loads for both the 1970 and 2004 condition simulations. The only variable in the method that changes between the two simulations is the elevation of the maximum wave crest (since the bridge elevation was fixed). The resultant wave loads on the bridge decks would have been 70,000 lb less in 1970 due to the lower MSL at the start of the storm.

**RSLR has already contributed to damage of one major US bridge during a hurricane.**

In other words, RSLR, which occurred in the three to four decades between the design of the bridge and Hurricane Ivan, caused an increase in wave-induced loads on the bridge of about 70,000 lb. This is within the range of the resistance of the minimal connections between the deck girders and pile caps (bent beams).

Also, the higher elevation MSL and maximum wave crest elevations, due to the RSLR, caused a prolonged duration of wave attack during the storm event. The increased exposure time of the bridge to very large waves in the storm would have been about 2 more hours. Using the peak wave period values extracted from the model simulations at the bridge (~6 s), that extended 2-hour duration would have been equivalent to the bridge being hit by an additional 1,200 waves. In summary, this bridge may not have been damaged, or would not have experienced as much damage, if MSL had not risen because of RSLR in between the time of design and the landfall of Hurricane Ivan.

### 11.2.2 US 90 Biloxi Bay (Hurricane Katrina)

Figure 11.9 (and Figure 3.4) shows the US 90 bridge across Biloxi Bay, Mississippi after Hurricane Katrina. The extreme storm surge during the hurricane raised the water level to an elevation where waves could impact and inundate the bridge decks (superstructure). The simply supported-span bridge decks moved landward off the pile caps (the Gulf of Mexico is to the left in Figure 11.9). However, no bridge deck movement occurred at higher deck elevations (i.e. the approach to a ship channel - shown between the deckless pile caps and an open drawbridge across that channel). The forensic evidence is entirely consistent with the fact that these bridges were damaged by storm waves on the storm surge striking the decks.

Some of the details of the damage are visible in Figure 11.10. Inspection of the damage revealed three consistent observations. One, there was damage to the bearing pad assemblies with the exception of the seaward side of the seaward-most bearing pads with only seaward bolts surviving (see upper left inset). Two, there was more damage to the concrete surface of the pile caps on the landward side than on the seaward side. Three, some of the bridge decks flipped over during the storm and are visible to the right of the bridge in the shallow water.



Figure 11.9. US 90 bridge over Biloxi Bay, Mississippi showing the spans below a critical elevation were removed by Hurricane Katrina (photograph looking southwest from Ocean Springs, February 19, 2016)



Figure 11.10. Details of damage to US 90 bridge over Biloxi Bay caused by Hurricane Katrina

### 11.2.3 Description of the Wave Load Damage Mechanism

Wave loads were the primary force causing much of the damage to coastal bridges in the north, central Gulf coast due to Hurricanes Ivan (2004) and Katrina (2005). The damage occurs as the storm surge raises the water level to an elevation where larger waves can strike the bridge superstructure. The individual waves produce a force on the deck with a vertical (uplift) component and a horizontal component (see Figure 11.11). The magnitude of wave uplift force from individual waves can exceed the weight of the simple span bridge decks (Douglass *et al.* 2007). The total resultant wave force is able to overcome any resistance provided by the (typically small) connections. The decks begin to progressively slide, “bump,” or “hop” across the pile caps in the direction of wave propagation in response to individual waves. This condition can occur before the storm surge elevation exceeds the bridge deck elevation.

**Wave loads were the primary force causing much of the damage to coastal bridges in 2004 and 2005.**

The buoyancy of the bridge decks is a secondary influence. This includes any additional buoyancy produced by air pockets trapped under the bridge decks. The buoyancy contributes to the total force on the individual bridge decks when the deck is submerged, i.e. when the storm surge elevation exceeds the bridge decks. However, bridge decks that were elevated above the storm surge still water elevation were damaged in both Hurricanes Ivan and Katrina (Douglass *et al.* 2006a).

Due to the nature of hurricane hazards and evacuations, there are no videos of the prototype damage occurring. But post-storm forensic inspections indicate a similar pattern in every case. Physical model laboratory experiments subsequently confirmed this damage mechanism (e.g. see video of Douglass *et al.* 2006b). The laboratory results have remarkable qualitative and quantitative similarities with the prototype forensic damage. For example, some of the bridge decks flipped over in the laboratory experiments as seen in the prototype (Figure 11.10).

Figure 11.12 shows a schematic of the typical time-history of one component (either vertical or horizontal) of wave-induced loads on a rigid structure like a bridge deck. Such loading is consistent with measured laboratory loads reported in the literature by numerous investigators.

One part of the wave-induced force is a longer-duration slowly “varying” force. This “varying” force changes magnitude and direction with the phase (crest or trough) of the wave as the wave passes under or across the structure. This part of the wave-induced load has been called “quasi-static,” or simply “wave” force by others in the coastal engineering literature (Section 11.3). The duration of the “varying” load corresponds with the period of the incident waves that is typically on the order of 3 to 15 seconds. The horizontal slowly varying loads are in the landward direction (based on direction of wave propagation) for the wave crest but can reverse to the seaward direction in the wave trough. Likewise, the vertical slowly varying loads are directed up (i.e. lift) for part of the wave but can be downward for part of the wave. The downward-directed wave load can be due to both the mass and downward momentum of the portion of the wave crest above the bridge deck. The uplift loads appear to be typically greater than the downward-directed loads.

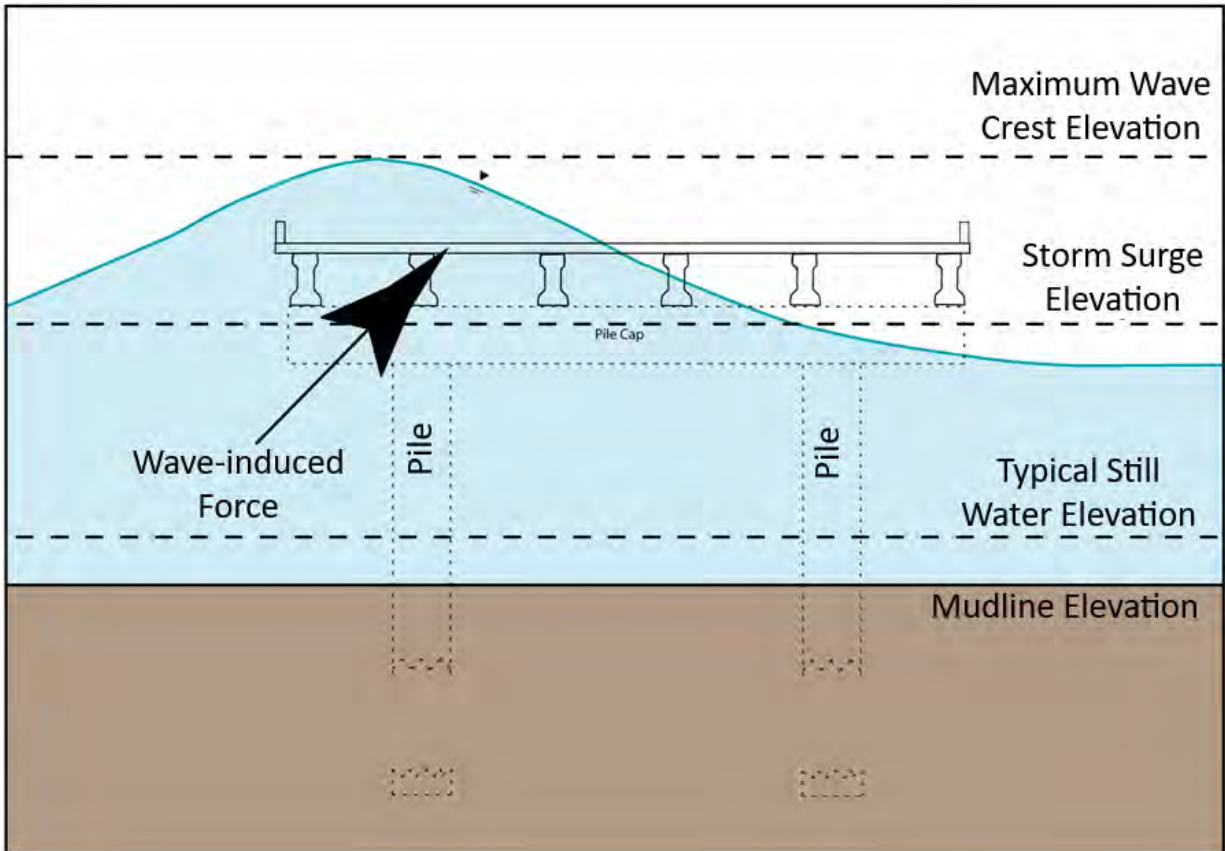


Figure 11.11. Schematic of resultant wave-induced load, with both uplift and lateral components, on a bridge deck

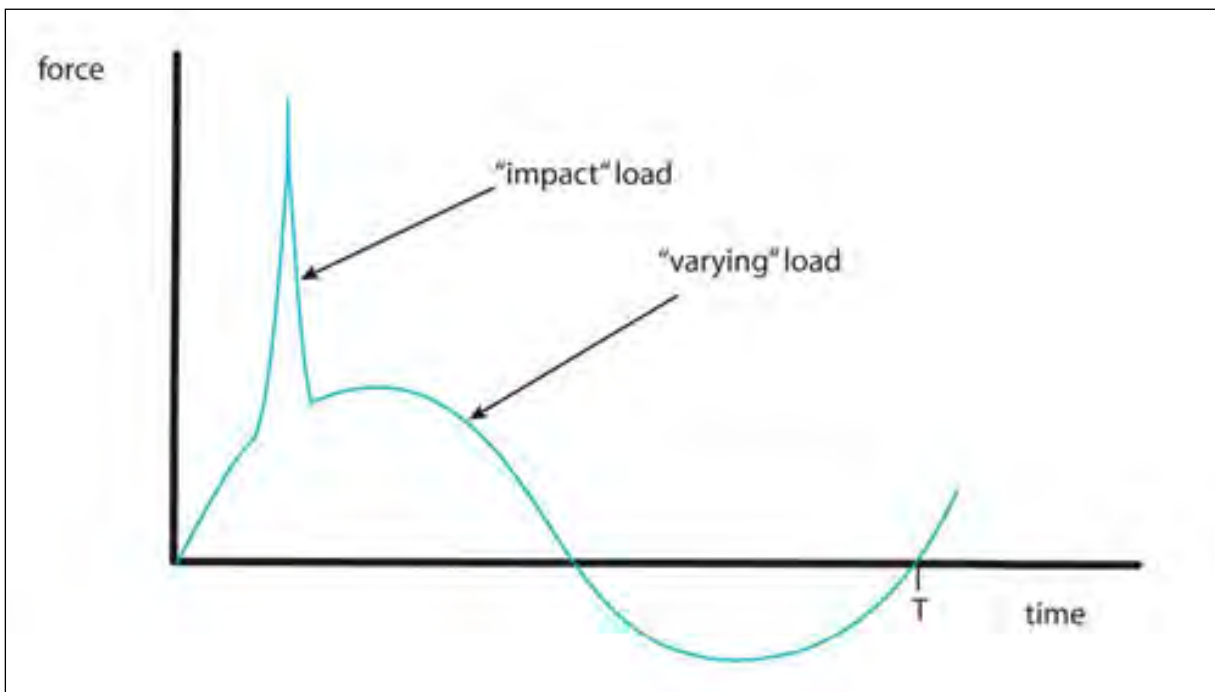


Figure 11.12. Schematic of typical time-history of wave loads on rigid structures

The other part of the wave-induced load shown in Figure 11.12 is a very short-duration (maybe less than 0.1 to 0.001 seconds long) “impact” force as the wave crest first begins to hit the deck. This force is directed in the horizontal direction of wave propagation and in the upward vertical direction. This impact force does not typically reverse direction. The impact force is often associated with the trapping of a small pocket of air between the structure and the wave face, and is sometimes referred to as the ‘slamming’ force. Wave impact loads have been studied most for horizontal loads on vertical walls. The duration of the “impact” and the magnitude of the peak “impact” force are inversely proportional for this type of wave load (Weggel 1997). Whether or not this extremely short impact load should be considered in the design of coastal bridges subjected to wave impacts is not clear and likely best left to the structural engineer. The large mass of the bridge decks may make these extremely short-duration loads less important than the “varying” loads due to structural dynamic response times as discussed in the next section.

### **11.3 Wave Loads on Bridge Decks: Literature**

The engineering literature on wave loads on bridge decks has expanded significantly since 2004-2005. Douglass *et al.* (2006a) provided a comprehensive literature review at that time. Hayatdavoodi and Ertekin (2016) is an excellent update to the literature review of the field which includes tsunami wave loads. Most of the literature prior to 2004-2005 was on the more general problem of piers and other horizontal decks subjected to wave loads and not specific to typical US bridge deck geometries. That is still a shortcoming in the available literature as discussed below.

A number of investigators measured wave uplift loads on flat, horizontal decks (not bridge deck geometry) subjected to monochromatic waves in physical models (e.g. El Ghamry 1963; Wang 1970; French 1970; Isaacson and Bhat 1996). A number of investigators presented methods for estimating wave loads on decks (not highway bridge decks) with significant clearance above the SWL which is typical of the offshore oil and gas industry (Kaplan *et al.* 1995; Bea *et al.* 1999; and McConnell *et al.* 2004). McConnell *et al.* (2004) also measured wave-induced loads on decks in the laboratory with irregular waves.

The US Naval Facilities Engineering Command (NAVFAC) has design memorandum with a simple equation for vertical uplift loads due to waves on bulkhead whalers, horizontal timbers as support structures on the seaward side of vertical walls (NAVFAC 1982). The NAVFAC equation is similar to ones considered by French (1970), Wang (1970), and a “practical design formula” used by Overbeek and Klabbers (2001) to explain wave uplift damage to a pier in the Caribbean.

Physical laboratory model tests of wave loads with models of more realistic highway bridge geometries have been reported by Denson (1978), Denson (1980), Cruz-Castro *et al.* (2006), Douglass *et al.* (2007), and Sheppard and Marin (2009).

McPherson (2008) conducted 1:20 scale physical model tests with simplistic girders and diaphragms to trap air under the deck like highway bridges. He used a range of monochromatic waves and, based on his observations and results, suggested modifications to improve the Douglass *et al.* (2006a) method for estimating wave loads on bridge decks.

Bradner *et al.* (2011) conducted very large-scale (1:5) physical model tests, with simplistic girders and diaphragms, and allowed the model decks to move to evaluate the structural dynamic response to the wave loads. Seiffert *et al.* (2014) conducted small-scale laboratory tests (1:35) and found that diaphragms, or “end caps,” between girders can cause a significant increase in wave-induced uplift loads. Douglass *et al.* (2007) reported a similar effect but Seiffert *et al.* (2016) suggest the intentional design of “air-relief-openings” to reduce wave loads. Hayatdavoodi *et al.* (2015) conducted extremely small-scale tests using nonlinear, cnoidal waves which may be representative of very-long period waves and tsunami wave loads on bridge decks.

Some of the literature addresses the magnitude and importance of the “impact” loads. It has long been suggested that structural engineers can ignore this component due to the extremely short duration relative to the dynamic response of the structure. Bradner *et al.* (2011) found these very high amplitude, but very short-duration, pressure spikes in some of their large-scale laboratory experiments. However, the “impact” spikes did not transfer to similar loads in the pile cap (bent beam) connections because of the structural dynamics of the overall deck system.

**Guo *et al.* (2015) recommends modifications, which are adopted here, to the Douglass *et al.* (2006a) equations for wave loads on bridge decks.**

Guo *et al.* (2015) conducted large-scale (1:10) physical laboratory tests with decks with simplistic girders and diaphragms. They found that the Douglass *et al.* (2006a) method for estimating wave loads on bridge decks generally agreed well with their experimental results. Specifically, they found that their vertical force data were bracketed (below and above) by the varying load estimate ( $C=1$ ) and the sum of the varying load estimate and the impact load estimate ( $C=1+3=4$ ). Guo *et al.* (2015) recommended combining the two portions (varying and impact) of the Douglass *et al.* (2006a) method for vertical loads and setting the combined coefficient to  $C=2$  to better match their data for all situations except total submergence. **As an example of such approaches, Section 11.4.1 (below) adopts and presents this revision of the method.**

Probabilistic bridge fragility, or damage, models for coastal bridges exposed to storm surge and waves are described in Ataei and Padgett (2013a), Ataei and Padgett (2013b), Ataei and Padgett (2013c), Ataei and Padgett (2015), Ataei *et al.* (2010), and Padgett *et al.* (2012). Bridge fragility curves conditioned on wind speed and water depth are provided in Chorzepa *et al.* (2016) as part of a study on the vulnerability of coastal bridges in the state of Georgia.

There is also a growing body of published literature addressing tsunami impacts on coastal bridges. Recent published literature addresses reliability assessments and fragility models, describes experiments and methods for estimating tsunami-induced forces, and describes damage from tsunamis. For example, studies by Akiyama *et al.* (2012) and Akiyama and Frangopol (2014) describe probabilistic estimation of reliability based on the development and application of probabilistic seismic hazard data combined with tsunami fragility curves, like those described in Gidaris *et al.* (2017). Numerous publications describe numerical or physical simulations of tsunami loads on bridges. A comprehensive overview of existing studies is given in Hayatdavoodi and Ertekin (2016). More specific information related to the numerical simulation of tsunamis and their resulting loads on bridges is found in Azadbakht and Yim (2014), Bricker and Nakayama (2014), Wei *et al.* (2015), Wei and Dalrymple (2016), Salem *et al.* (2016), and Winter *et al.* (2018). There are comparatively fewer physical studies, but descriptions of tsunami-induced loads on bridge superstructures are given in Shoji *et al.* (2011), Shijo *et al.* (2015), and Maruyama *et al.* (2017), the latter also included detailed observations of the Great East Japan earthquake of 2011. Detailed post-tsunami assessments of bridge damage are provided in Chock *et al.* (2013) and Kawashima and Buckle (2013).

At the time of the preparation of this document, a multi-state and federal study is developing bridge design guidelines for the estimation of tsunami loads on highway bridges (Transportation Pooled Fund Program 2019).

Cuomo *et al.* (2007) developed empirical equations for wave loads that are fairly similar to those of Douglass and Krolak (2008) but include wave height directly in the dimensional parameters.

AASHTO (2008) presents a method of estimating wave loads on bridge decks which is fundamentally different than the method presented in this chapter. Practitioners use both methods

with one sometimes being a check on the other. Independent laboratory test investigations have found that the method of estimating wave loads on bridge decks in AASHTO (2008) overestimates loads for some conditions and underestimates loads for other conditions (Hayatdavoodi *et al.* 2015, Guo *et al.* 2015). The laboratory data used to develop and calibrate the wave loads equation in AASHTO (2008) are not available for independent verification or use because Sheppard and Marin (2009) has a flawed printout of the data table (Appendix B: Table B-2 Significant Force Value for All Model Tests).

### 11.4 Wave Loads on Bridge Decks: Method for Estimating

This method for estimating wave loads on typical US bridge decks is a revision to the method originally suggested in Douglass *et al.* (2006a) and included as Appendix E of the previous edition of this manual (Douglass and Krolak 2008). The revision is based on some of the subsequently-published, independent laboratory experiments discussed above.

The following sections present the revised wave load equations, a brief example calculation, and an explanation of the basis of the method and it how ties into the expanded body of knowledge and literature in more detail.

#### 11.4.1 Equations for Estimating Wave Loads on Bridge Decks

The wave-induced loads imparted on elevated highway bridge decks by waves are estimated in terms of their vertical and horizontal components (see Figure 11.13) as:

$$(F_v)_{\max} = C_v \gamma (\Delta z_v) A_v \quad (11.1)$$

and

$$(F_h)_{\max} = [1 + c_r (N-1)] C_h \gamma (\Delta z_h) A_h \quad (11.2)$$

where:

- $(F_v)_{\max}$  = maximum of the vertical wave-induced load
- $(F_h)_{\max}$  = maximum of the horizontal wave-induced load
- $C_v$  = an empirical coefficient for the vertical load (recommended value is  $C_v=2$ )
- $C_h$  = an empirical coefficient for the horizontal load (recommended value is  $C_h = 2$ )
- $c_r$  = a reduction coefficient for reduced horizontal load on the internal (i.e. not the seaward-most) girders (recommended value is  $c_r = 0.4$ )
- $N$  = the number of girders supporting the bridge span deck
- $A_v$  = the area of the bridge contributing to vertical uplift, i.e. the projection of the bridge deck onto the horizontal plane (width of the deck times the length of the deck)
- $\Delta z_v$  = difference between the elevation of the crest of the maximum wave and the elevation of the underside of the bridge deck or the low-chord of the diaphragms under the deck if diaphragms are present (see Figure 11.14 for definition sketch)
- $\gamma$  = unit weight of water (64 lb/ft<sup>3</sup> for salt water)
- $A_h$  = the area of the seaward side of the bridge contributing to horizontal loads, i.e. the projection of the bridge deck onto the vertical plane (height of the deck, including girders and solid rails, times the length of the deck)
- $\Delta z_h$  = difference between the elevation of the crest of the maximum wave and the elevation of the centroid of  $A_h$  (see Figure 11.14 for definition sketch).

Note that  $A_v$  and  $A_h$  are shown in the definition sketch of Figure 11.13 as the deck width and height. Thus, the lengths shown on the sketch are multiplied by the span length to get the areas applied in Equations 11.1 and 11.2.

When the wave crest elevation does not exceed the top of the bridge (solid rail elevation), a reduced area and lowered centroid corresponding to the area below the wave crest elevation can be used to define  $A_h$  and  $\Delta z_h$ .

The wave crest elevation used in  $\Delta z_v$  and  $\Delta z_h$  should be that corresponding to a very large wave height estimated in the design sea state,  $\eta_{max}$ . Given a design sea state with a significant wave height ( $H_s$ ), this elevation can be estimated as (see Section 11.6):

$$\eta_{max} \approx (0.75)(1.7)H_s = 1.3H_s \quad (11.3)$$

The design sea state is typically computed using the design storm surge elevation (see Figure 11.14).

The recommended value of both empirical coefficients, in Equation 11.1 and 11.2, is 2 (i.e.  $C_v = 2$  and  $C_h = 2$ ). The selection of these recommended values is discussed below. They are not intended to be conservative. Thus, they should be increased for conservative design values. Given the uncertainties involved in the application of the available methods for estimating wave loads on US highway bridges, the load factor of 1.75 required by AASHTO (2008) may be appropriate (see Section 11.4.3 Discussion of the Method).

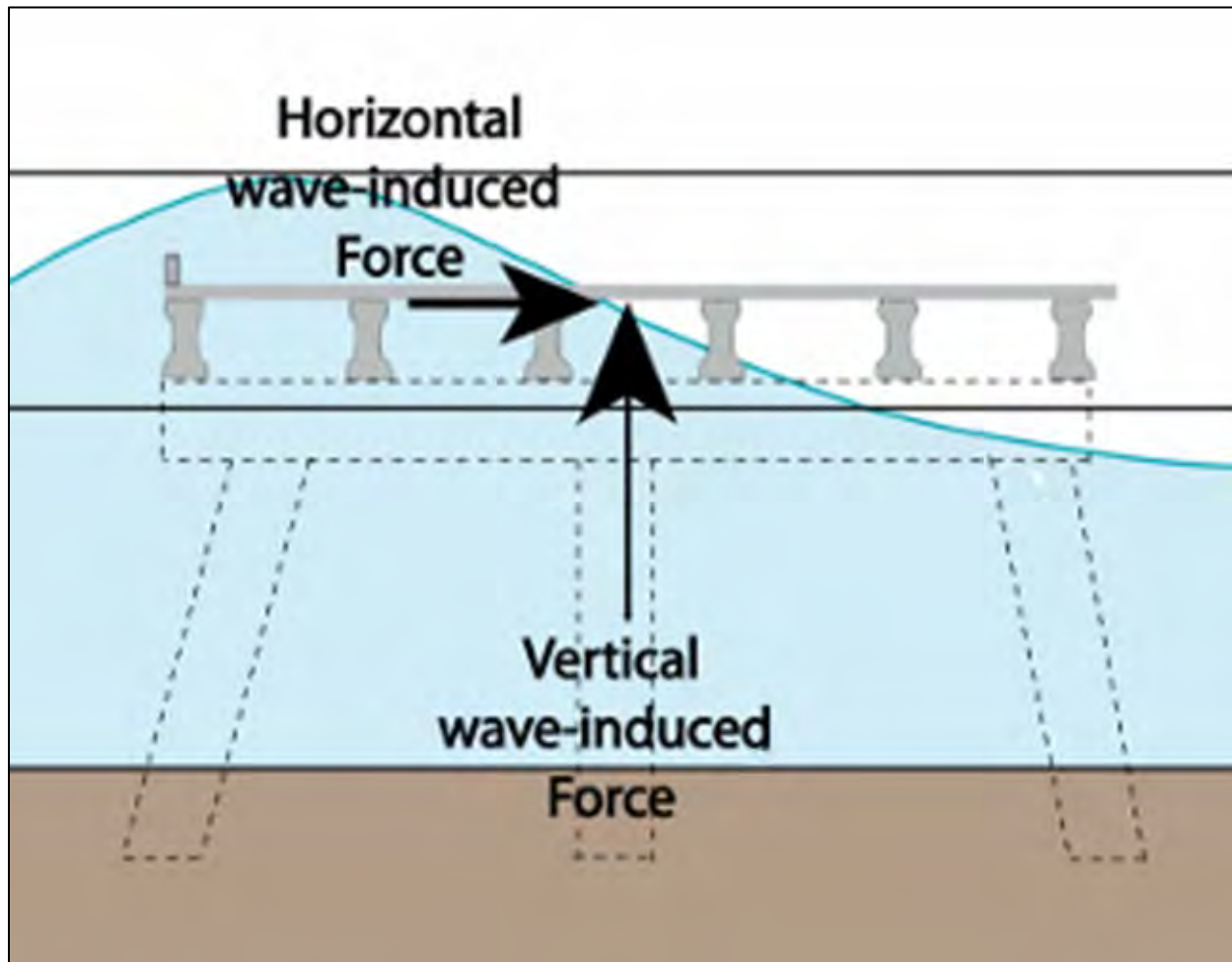


Figure 11.13. Horizontal and vertical wave-induced loads on bridge decks

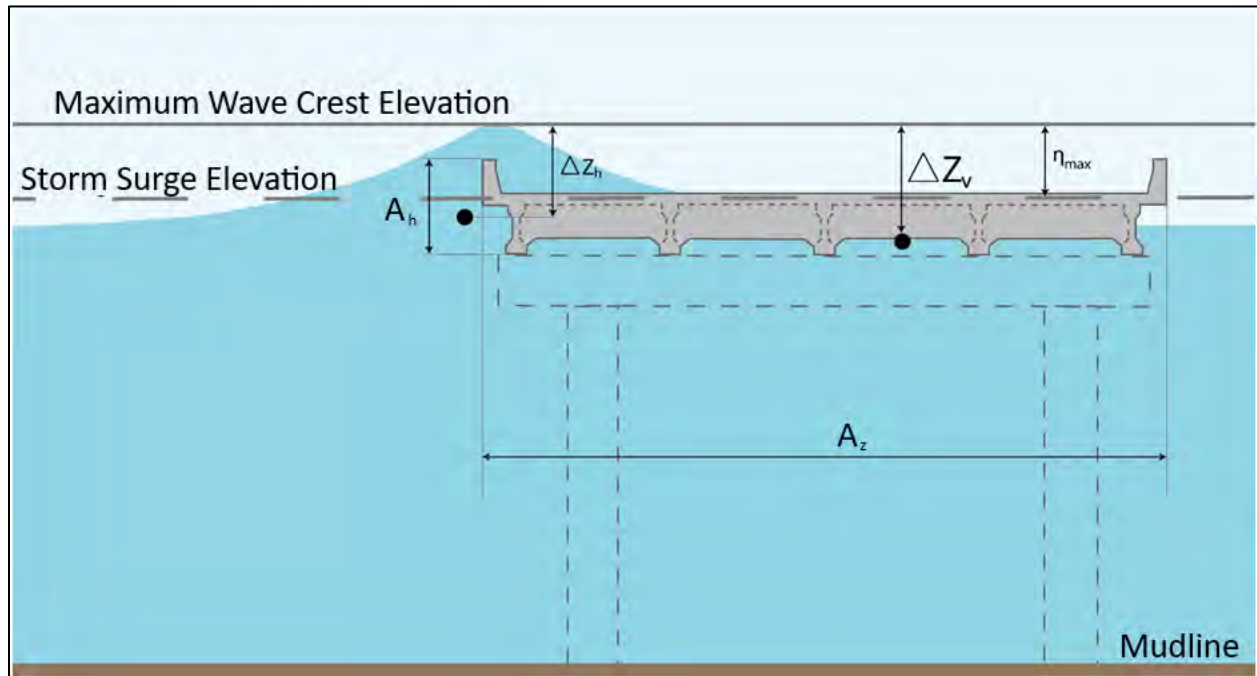


Figure 11.14. Definition sketch for  $\Delta Z_h$ ,  $\Delta Z_v$ ,  $A_h$ ,  $A_z$ , and  $\eta_{max}$  in Equations 11.1 and 11.2 for estimating wave loads on elevated bridge decks)

The method assumes that the two components (horizontal and vertical) of the wave-induced loads act in phase, i.e. their maximums at the same instant, to resolve the maximum resultant load. The two components will likely not be completely in phase but this is a reasonable initial approximation for engineering.

Equations 11.1 and 11.2 are for the maximum of the total loads. They include the magnitude of varying load and the impact load. Separate equations for the two types of loads were dropped in this revision following the recommendation in Guo *et al.* (2015).

#### 11.4.2 Example Application of Wave Load Equations

Application of the method is demonstrated using values which correspond to the US 90 bridge across Biloxi Bay, Mississippi during Hurricane Katrina. For the purposes of this example, a specific span has been selected as representative. This span is roughly in the middle of the western side of the bridge (see Figure 3.4). The low-chord elevation of the span (bottom of girders) was about +13 ft NGVD with the bottom of the diaphragms at +14 ft, top of the bridge deck at +16.5 ft, and the bottom of the deck at +16 ft. In this portion of the bay, the depth is fairly shallow, and the bottom, mud-line elevation is assumed to be about -4 ft NGVD. The decks were 33.4 ft wide and 52 ft long.

Storm surge and wave hindcast modeling results indicate that at 8:00 a.m. CDT on August 29, 2005, the mean water level had risen to an elevation of  $\bar{\eta} = 11.9$  ft and there was a significant wave height at the bridge location of  $H_s = 6.2$  ft (Douglass *et al.* 2006a). Thus, the waves were striking the span by that time in the storm.

The wave loads on the deck at that time are estimated as follows:

$$\text{elevation of maximum wave crest} = \bar{\eta} + \eta_{max} = 11.9 + 1.3(6.2) = 20 \text{ ft}$$

$$\Delta Z_v = (\text{elev. maximum crest}) - (\text{elev. bottom of diaphragms}) = 20 - 14 = 6 \text{ ft}$$

$$(F_v)_{\max} = C_v \gamma (\Delta z_v) A_v = 2(64 \text{ lb/ft}^3)(6 \text{ ft})[(52)(33.4)\text{ft}^2] = 1,300,000 \text{ lb} = 1,300 \text{ kips}$$

$$\Delta z_h = (\text{elevation maximum crest}) - (\text{elevation centroid of } A_h) = 20 - 15.7 = 4.3 \text{ ft}$$

$$(F_h)_{\max} = [1 + c_r (N-1)] C_h \gamma (\Delta z_h) A_h = [1+0.4(6-1)] (2)(64 \text{ lb/ft}^3)(4.3 \text{ ft})(286 \text{ ft}^2) = 470 \text{ kips}$$

In this example,  $A_h$  is 286 ft<sup>2</sup> with a centroid elevation of +15.7 ft. These values are obtained by accounting for the design of the rail based on engineering plans obtained from Mississippi DOT for the old Biloxi bridge. There were 6 girders.

So, in summary, at 8:00 a.m. the wave-induced loads on this span are estimated as being cyclical with maximum “varying” loads of 1,300 kips of vertical uplift and 470 kips of horizontal landward force.

These bridge decks weighed about 340 kips, and their connections provided essentially no resistance to uplift. Thus, these example calculations imply that the uplift from some of the largest waves in the sea state at this time was enough to exceed the weight of the bridge span at the same time it was experiencing large lateral loads. Thus, these spans had likely already been bumped, by individual large waves, up and over on the pile caps by this time in the storm. Such behavior is consistent with the evidence. Katrina’s storm surge (and wave heights) continued to increase to a peak SWL of about +21.5 ft at around 10:30 a.m. CDT.

### 11.4.3 Discussion of the Method

As mentioned above, Equations 11.1 and 11.2 are relatively simple to apply, can be applied in a conservative manner, are consistent with the available literature, and can be used to provide estimates of wave loads on bridge decks. These equations are slightly revised from the way this method was originally suggested in Douglass *et al.* (2006a) and included as Appendix E of the previous edition of this manual (Douglass and Krolak 2008).

The primary revisions are the combining of the two aspects of the typical load signature, “varying” and “impact;” and the new coefficient values. These changes are based primarily on the recommendation of Guo *et al.* (2015). That recommendation was for the vertical load component only. However, there is still tremendous uncertainty surrounding the horizontal component of these wave loads (see discussions below about trapped air potential below).

The older method did a good job of explaining the prototype 2004-2005 damage to bridges (see Douglass *et al.* 2006a) and these revisions do not change that. The older method was intended, at that time, to be tested and improved upon relatively easily in the future as independent laboratory and prototype experimental data become available.

The fundamental concept behind Equations 11.1 and 11.2 (that these loads are proportional to the relative relationship between wave crest elevation and deck elevation) is consistent with most of the literature including McConnell *et al.* (2004), Wang (1970), French (1970), Overbeek and Klabbers (2001), and NAVFAC (1982). When the coefficient is set to one, this method is identical to the method for estimating wave uplift loads on horizontal whalers on the front of vertical walls presented in NAVFAC (1982).

Inputs for the approach outlined above include the basic bridge deck cross-section and elevation information and estimates of storm surge elevation and wave height.

This approach is not necessarily conservative. These revisions likely reduce the overall conservativeness for the vertical loads. But this reduction seems appropriate given the much greater availability of more appropriate laboratory data than existed in 2006.

**These new equations for estimating wave loads can be conservatively applied with an appropriate factor of safety.**

The method can be conservatively applied with an appropriate factor of safety. A factor of safety can be applied for design by increasing the two coefficients. This is justified based on the complexities of the process, the uncertainties in estimating design wave conditions, the limited available lab-scale load data, the lack of bridge-specific lab results, and the relatively small scales of the available lab data. A similar load factor of two (2) has been adopted in ASCE Standard No. 7: Minimum Design Loads for Buildings and Other Structures for wave loads on buildings for similar reasons (ASCE 2005). AASHTO (2008) requires a load factor of 1.75 for coastal hydrodynamic loads. Either of those values is appropriate.

The method only provides an estimate of the total overall load without information concerning where that load is applied on the structure. Essentially, it thus implicitly assumes the load is applied through centroid of the cross-sectional area of the bridge. This is not particularly realistic. Also not considered are the details of wave phase and the fact that the down-wave width of bridge decks will likely cause spatially-varying loads, particularly uplift, that will impart a moment. These moments may be important aspects of bridge deck response.

The approach outlined above should be used primarily for the case where storm surge elevation is roughly near the bridge deck elevation. Analyses indicate that this was the case during Hurricanes Ivan and Katrina. However, there are two other situational cases for bridge decks:

- The deck is much higher than the storm surge such that only the crests of a very few waves in the storm sea state hit the girders (and loads are low),
- The surge is so high that the bridge deck is completely inundated. The method here likely overestimates that condition significantly.

More research on wave loads on bridge decks is justified by the magnitudes of the estimated wave loads, the seriousness of the implications of them for design, the significant uncertainty in the available methods for estimating the loads, and the likelihood that the uncertainty can be reduced with more research. This research need includes quantitative laboratory force measurements for the cross-sectional geometry typical of simple-span bridge decks used in US highways across coastal waters for different levels of relative inundation (particularly the submerged bridges).



Figure 11.15. Example of concave seaward face of a coastal bridge (I-10 bridge over Mobile Bay, Alabama)

A number of investigators have suggested that, while the vertical loads estimated by the method of Douglass *et al.* (2006a) are conservative but reasonable, the horizontal loads estimated are too high (i.e. too conservative). The revision outlined above effectively reduces the level of conservatism for the vertical loads. Also, none of the other investigators have used model geometries which are fully representative of one of the most important aspects of the geometry of US coastal highway bridges. Specifically, this is the likelihood of waves striking concave portions of the seaward side of the prototype structures. Figure 11.15 shows a typical seaward face of a prototype bridge deck. The combination of the seaward-most girder (which has a concave surface) and the overhanging deck has the potential to “catch” significant momentum in waves as well as allowing air pockets to form for an instant between the wave and the structure when storm surge is high enough. Whenever air is trapped against a rigid structure by waves, very high “impact” forces can be generated. Also, the coefficient for the individual girders,  $c_r = 0.4$ , is based solely on judgment and not on any analysis or experiments. Research with more realistic geometries is needed to better understand the coefficients in Equation 11.2.

McPherson (2008) suggested a logical, simple modification of the Douglass *et al.* (2006a) method which adds the weight of water on top of the bridge decks to the vertical load equation. The addition of this term improved the agreement of the method with the McPherson data. This is a promising approach that has not been adopted in this revision but should be considered in future revisions.

The needed research is both physical laboratory model tests and numerical “laboratory” model tests. Recent computational fluid dynamics (CFD) investigations show promise (e.g. Hayatdavoodi *et al.* 2019).

### **11.5 Wave Loads on Bridge Decks: Countermeasures**

A wide variety of engineering adaptations, or countermeasures, to withstand the extreme wave loads occasionally placed on highway bridge decks during storms and tsunamis have been suggested. However, there is no evidence that any of them will work (except elevation to avoid the loads).

Lehrman *et al.* (2011) found that none of the connections, between bridge deck girders and the pile caps (i.e. between the bridge superstructure and substructure), which are commonly used along the northern Gulf coast of the US are capable of resisting the extreme loads generated by hurricane waves on storm surge.

**Strengthening the connections between bridge decks and the substructure will lead to another failure mechanism – “negative bending” of the deck and girders.**

FHWA (2017a) and Cleary *et al.* (2018) considered four potential engineering adaptations-countermeasures to the I-10 bridge across Mobile Bay:

- strengthening the connections (two options were evaluated),
- increasing span continuity,
- modifying the shape of the bridge deck to reduce lateral wave-induced loads, and
- increasing the deck elevation in combination with other retrofit options.

This work followed the load path through the structure, traditional structural engineering practice, and found that none of the adaptations by themselves, with the exception of increasing the deck elevation, will ensure the survival of the structure in a reasonable, but severe, storm scenario.

If the existing connections between the bottom of the girders and the pile caps (bent beam) were reinforced adequately to transfer those extreme loads to other structural components, the structure would fail under the wave-induced loads due to negative bending in the girders and deck (FHWA 2017a). Failure of the substructure could eventually occur if the other bridge components could be reinforced to resist the loads.

It should be possible to design a highway bridge structure that can survive the most extreme wave-induced loads. One oft-mentioned approach is to build it at a lower elevation with the idea that this will avoid more severe wave loads in depth-limited situations. Unfortunately, our understanding of wave loads on submerged structures is limited. More research is needed for this submerged situation.

Design-specific laboratory tests of wave loads may be justified in the design of any high-cost asset that is expected to be subjected to extreme wave loads.

### **11.6 Bridge Deck Elevation to Avoid Wave Loads**

The most common design approach is to avoid superstructure wave forces by elevating the bridge so that the storm waves crests pass under the low-chord of the bridge. This elevation is shown schematically in Figure 11.16.

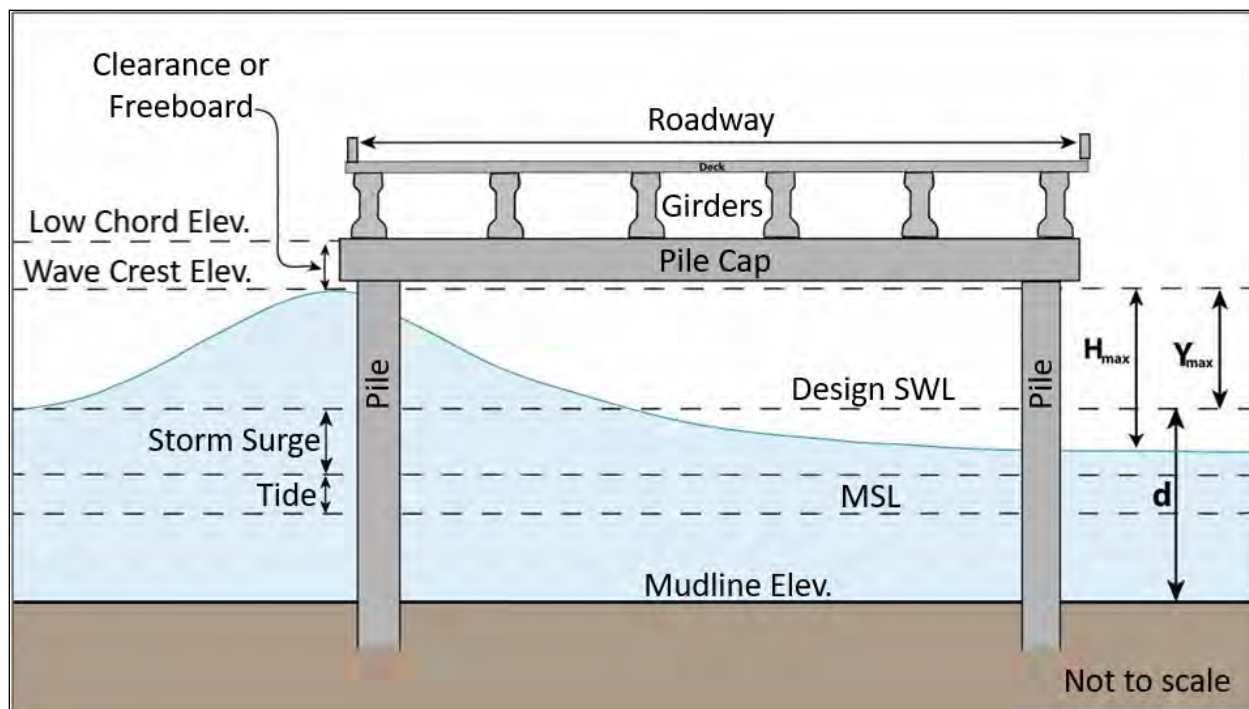


Figure 11.16. Definition sketch of wave parameters and water levels for determining elevation of bridge deck for clearance from wave crests

The elevation can be set by adding some additional clearance or freeboard above the crest of the largest wave in the design sea state:

$$(\text{low chord elevation}) = (\text{wave crest elevation})_{\text{max}} + \text{freeboard} \quad (11.4)$$

The low chord elevation is taken as the elevation of the bottom of the girders (see Figure 11.16). The maximum wave crest elevation can be calculated as:

$$(\text{wave crest elevation})_{\text{max}} = (\text{design storm surge SWL}) + Y_{\text{max}} \quad (11.5)$$

where:

- SWL = design still water level
- $Y_{\text{max}}$  = difference between the SWL elevation and wave crest elevation for the maximum wave in the design sea-state (defined below)

In general, the value for  $Y$  is the portion of the wave height,  $H$ , above the SWL. A useful engineering estimate of  $Y$  for this purpose is 75% of  $H$ . Thus,  $Y_{\text{max}}$  above can be estimated as:

$$Y_{\text{max}} = 0.75 H_{\text{max}} \quad (11.6)$$

where:

- $H_{\text{max}}$  = design maximum wave height (defined below)

### 11.6.1 Nominal Maximum Wave Height Approach

The design maximum wave height ( $H_{\text{max}}$ ) depends on the site-specific conditions. The design sea-state can be estimated using a wave generation model applied to that site for specific wind and water level conditions. Given a design significant wave height ( $H_s$ ), the design maximum wave height can reasonably be set as:

$$H_{\max} = 1.7 H_s \quad (11.7)$$

The value of 1.7 given in Equation 11.7 corresponds with a wave height statistic on the Rayleigh Distribution (see Table 5.1) that is slightly higher than the average of the highest 1% of wave heights ( $\bar{H}_1$ ). This 1.7 value corresponds with the probable maximum wave height for 200 waves. This is a reasonable number of waves for the typical durations of the peak of a storm surge and average wave periods in storm surges.

Combining Equations 11.6 and 11.7 yields:

$$Y_{\max} = 1.3 H_s \quad (11.8)$$

### 11.6.2 Depth-Limited Maximum Wave Height Approach

In some cases, however, the maximum wave height might be depth-limited, i.e. very large waves in very shallow water. Larger waves in the design sea state may break farther offshore of the bridge and the largest waves will not reach the bridge. In this case, check the depth-induced breaking criterion (or similar criteria):

$$\left(\frac{H}{d}\right)_{\max} \approx 0.8 \quad (11.9)$$

This can be written as:

$$H_{\max} = 0.8 d_s \quad (11.10)$$

where:

$d_s$  = depth at bridge structure during design conditions (i.e. including the storm surge)

For the depth-limited case, combining Equations 11.6 and 11.10 yields:

$$Y_{\max} = 0.6 d_s \quad (11.11)$$

### 11.6.3 Estimating the Maximum Wave Crest Elevation

The difference between the SWL elevation and wave crest elevation for the maximum wave in the design sea-state ( $Y_{\max}$ ) used in Equation 11.5 should be the lesser of the values yielded from Equation 11.8 and Equation 11.11. Therefore, considering the potential for non-depth-limited and depth-limited maximum wave heights, the primary equation estimating the elevation of the maximum wave crest (see Figure 11.16) becomes:

$$(\text{wave crest elevation})_{\max} = (\text{design storm surge SWL}) + (1.3 H_s \text{ or } 0.6 d_s)_{\min} \quad (11.12)$$

This equation can be used to set the elevation of the low-chord of bridge decks that span coastal waters. The next section discusses the use of additional freeboard above this elevation.

### 11.6.4 Freeboard Considerations

“Freeboard” can be added to the maximum wave crest elevation. The approach outlined above does not provide “freeboard” above the wave crests. In riverine systems, SDOTs may require one or two ft of “freeboard” to be added above the design water surface elevation to account for wave action or debris as well as for uncertainty in the analysis. This freeboard, if added in the coastal situation, will also account for higher waves in the sea-state. The uncertainties involved in coastal surge SWL analysis are likely at least as great as those in the riverine situation (if not significantly greater). Thus, some additional freeboard for the low-chord elevation of coastal bridges may be appropriate.

AASHTO (2008) sets a required vertical clearance to avoid wave loads for coastal bridges as 1 ft above the maximum wave crest elevation in the 100-year return period sea state at that location accounting for storm surge. Bridges with less clearance should be designed to withstand the wave loads.

However, complete clearance from all wave forces may not be needed to ensure bridge integrity during major coastal storms. Post-storm inspections of damage to bridge decks along the north-central Gulf coast in 2004 and 2005 indicate that some bridge decks survived that were exposed to some wave loads. Apparently, the loads were small enough that they did not cause damage. This is likely due to resistance to wave forces provided by the weight of the bridge spans and the limited connections. The damage pattern suggests that there was a critical elevation at each location for that specific bridge deck design and those site-specific and storm-specific surge and wave conditions. Spans below that elevation were displaced off the pile caps; spans above that elevation were not. The critical elevation was below the elevation for complete wave clearance given by Equation 11.12.

**The proven way to handle wave loads on bridge decks is to avoid them with elevation.**

For example, Figure 11.9 shows some simply-supported spans on the US 90 bridge across Biloxi Bay, Mississippi still in-place even after removal of lower spans by Hurricane Katrina. These remaining spans had a higher low chord elevation than those displaced. The maximum wave crest elevation was +34 ft at the peak of the storm (based on hindcast modeling and Equation 11.12), yet a bridge span as low as +24.5 ft “survived.” Thus, a bridge span with a low-chord elevation almost 10 ft lower than the maximum wave crest elevation apparently did not move.

Chen *et al.* (2009) found that the Biloxi Bay bridge damage level corresponded with the crest of the significant wave height (not the maximum wave height in the sea state). This would suggest the  $Y_{\max}$  could be set to  $0.75H_s$  without any additional freeboard. A preferable approach is to set the deck elevations of new bridges based on an improved understanding of the wave loads.

Projections of future relative sea level rise (RSLR) can be considered in freeboard design (see Figure 4.11).

## **11.7 Other Coastal Bridge Issues**

This section very briefly discusses other design and maintenance issues related to coastal bridges including increased concrete spalling due to wave splash, and lateral loads on pilings.

Some low-elevation coastal bridges have suffered increased concrete damage near their landward end just above vertical retaining walls. Wave splash during storms sprays salt water on the underside of the bridge deck concrete and, over time, these areas can become areas of concern for bridge inspectors. The use of reinforced concrete in the marine environment typically calls for additional considerations, including the use of air entrainment admixtures and increased minimum thickness of specified concrete cover over reinforcing bars. Newer bridges, with higher clearances and longer, higher approach sections, often avoid this problem by elevating all of the bridge deck well above the elevation of splash. Wave runup and splash on existing low bridges could be reduced by placing rip-rap on the vertical walls. Clearance issues for coastal bridges over navigation channels are primarily controlled by the US Coast Guard.

Waves can produce lateral loads on bridge pilings and pile groups. These loads in riverine situations are well modeled by the traditional fluid mechanics approach of estimating drag as a function of the water velocity squared and an empirical drag coefficient. However, the nature of

wave motion produces loads beyond those due only to drag. The oscillatory water particle motion below waves can impart significant forces on structures due to the fluid accelerations as well as the velocities. Thus, it is neither adequate nor appropriate to simply increase the velocity used in the drag equations to account for the maximum wave orbital velocity. The acceleration generated forces, also called inertia forces, bear consideration.

Morison's equation from ocean engineering estimates the horizontal force per unit length of a vertical pile in waves as:

$$f_p = f_i + f_D = C_M \rho \frac{\pi D^2}{4} a_x + C_D \rho D u |u| \quad (11.13)$$

where:

$f_p$	=	horizontal force per unit length of a vertical pile
$f_i$	=	inertial force per unit length of pile
$f_D$	=	drag force per unit length of pile
$D$	=	diameter of pile
$\rho$	=	density of water (1,025 kg/m <sup>3</sup> for seawater)
$u$	=	horizontal water particle velocity at the axis of the pile (as if the pile were not there)
$a_x$	=	horizontal water particle acceleration at the axis of the pile (as if the pile were not there)
$C_D$	=	drag coefficient
$C_M$	=	inertia or mass coefficient

The first term in Morison's equation, the inertia term, accounts for the dynamic force on the structure due to the acceleration in the waves. The second term is the drag term and it is analogous to the drag load on a piling in unidirectional flow. The absolute value is used in the drag term because the load reverses direction with wave phase. In a wave, the water particle velocity, direction and acceleration at different points are constantly changing with phase. They also vary with depth below the surface and the total force on the pile is the depth-integrated sum of these changing loads. The two terms are out of phase and thus not maximum at the same time.

More information, including values for the coefficients and appropriate applications, on Morison's equation can be found in other references (Sarpkaya and Isaacson 1981; USACE 1984).

An inherent assumption in Morison's equation is the "thin piling" assumption that velocity and acceleration do not vary over the structure in the direction of wave propagation and that the piling is thin enough to not cause much of an effect on the wave. Because of the complexities involved in applications of Morison's equation, a coastal or ocean engineer should be included in the design or analysis team for estimating wave loads on pilings. Empirical consideration of these forces is described in Wiegel (1964) and NAVFAC (1982). In cases of shallow water and/or wave breaking, where water particle velocities and accelerations will be significantly under-predicted by simple linear wave theory, higher-order theories are used (see Section 5.1). Dean's stream-function approach is a nonlinear wave theory that was developed to predict wave kinematics and forces on structures in deep and shallow water settings (Dean 1973).

## **11.8 Selection of Design Storm Surge & Design Wave Heights**

This section very briefly describes the process by which an engineer determines design water level and wave characteristics for resilient coastal bridge design.

### 11.8.1 Design Storm Surge SWL

The selection of the design storm surge SWL (still water level) can be based on an analysis of historical storm surge elevations at the specific site or on an analysis that incorporates site-specific modeling of historical (hindcast) storm surges (see Section 4.6 Design Water Levels). Projections of future relative sea level rise (RSLR) can be included (e.g. Figure 4.11).

USACE Coastal Hazard System, FEMA FISs and FIRMs provide SWL for many coastal areas. These may be suitable sources for these data, as long as study and methodological caveats are well understood. A nearby tide gage may not provide a reasonable first approximation of surge at a site. Storm surge elevations can vary significantly from location to location.

Site-specific, probabilistic modeling of storm surge (and waves) is appropriate for the design of major new bridges and decisions concerning modifications to existing bridges. The potential damage justifies a comprehensive hydrodynamic surge analysis. Developing a probabilistic basis for this design storm surge elevation is consistent with the process for riverine bridge design considerations, risk-based flood maps for coastal management done by FEMA (and other agencies), and our modern understanding of future sea level rise. The historical gage analysis can be used as a check on the reasonableness of the results of the modeling approach.

### 11.8.2 Design Wave Heights

The design wave height ( $H_s$ ) used in Equation 11.12 is the significant wave height at the bridge location during design conditions. Chapter 5 outlines appropriate ways for determining significant wave height. For fetch-limited situations, the parametric wind-wave generation modeling method may be adequate (see AASHTO 2008). For some situations in shallow water without much storm-surge, depth-limited wave conditions may apply (see Equation 5.25). Many situations, including those exposed to open ocean storm waves, may call for probabilistic oceanic wave modeling (see Section 5.4).

Some USACE Coastal Hazards System data are available. As a check, FEMA FISs contain wave height estimates. However, these may not report  $H_s$ , but some other wave height statistic. Apply such estimates with knowledge of these and other study caveats.

### 11.8.3 Coastal Engineer Involvement

Given the importance and complexity of these considerations to the integrity of the highway structure, the FHWA suggests transportation officials might consider involving a qualified coastal engineer in the bridge project's planning, design, and pre-construction review (see Section 3.6 Coastal Engineering as a Specialty Area).

## Chapter 12 - Coastal Scour

This chapter addresses coastal scour issues relevant to highway engineers working in the coastal environment. Coastal scour is the erosion/removal of granular bed material by hydrodynamic forces or processes in the vicinity of a coastal structure. This description of coastal scour, borrowed from the Coastal Engineering Manual (USACE 2002), specifically distinguishes it from a much broader interpretation of scour as simply erosion. Structures in the coastal environment—bridge foundations, abutment walls, revetments—often cause scour by their very presence. Their presence modifies the flow of water thereby resulting in a change in sediment transport behavior. However, coastal structures are also subjected to scour resulting from geomorphological processes that are much larger both spatially and temporally. Geomorphological processes such as tidal inlet migration, barrier island retreat, and others, are less impacted by the presence of transportation infrastructure in the coastal environment, but interactions between the two are often problematic (see example Section 8.1).

**Experience and sound engineering judgment should be relied upon when evaluating the scour predictions for coastal bridges.**

The FHWA's National Bridge Inspection Standards (23 CFR part 650 subpart C) requires an appraisal of scour criticality for all bridges over water. In coastal environments, these bridges range in complexity from small, local roads crossing tidal creeks to limited access highways (e.g., interstate and toll roads) along the open coast. The practitioner should account for the potential range of hydraulic conditions at a bridge crossing, then select the set of conditions that govern scour for the purpose of design. It is important to note that the combination of flow velocity and depth ultimately drive the formation of scour around bridge foundations. Similar combinations of flow velocity and depth, and subsequent scour estimates, may exist for many different bridge crossings and hydraulic settings. However, the practitioner should apply the appropriate evaluation methods and tools to obtain those values for their given bridge setting and hydraulic conditions.

This chapter covers a range of typical coastal scour issues and provides some potential processes and examples for their evaluation and estimation of interest to transportation professionals. The material begins with an overview of hydraulic conditions for coastal bridge locations and crossings. That discussion, and much of the discussion in this chapter, makes reference to Section 11.1 and the four general types of coastal bridge settings summarized there: tidal inlets, bays and sounds, tidal embayments, and rivers. Since scour depths are determined by parameter values (e.g., water depth and velocity), this chapter further categorizes bridges by their hydraulic setting and their exposure to tidal and/or other coastal processes that make those parameter values unique. The text then describes the various types of coastal scour. The chapter also includes pertinent examples of coastal scour and describes relevant applications of methods and tools for its estimation. The text briefly describes some scour countermeasures with the understanding that many strategies used in the riverine environment are transferable to coastal settings with appropriate modifications that account for wave attack and other coastal processes.

### 12.1 Introduction

Coastal hydraulics and hydrodynamics impacts many US bridges. Depending on the region of the US and the coastal setting, design conditions may be related to tides, tsunamis, hurricanes,

nor'easters, or strong frontal systems (i.e. Great Lakes region). The stability of bridges is dependent upon an appropriate foundation design, which uses knowledge of both the long-term and single event-driven scour based on the in-situ soil properties within the waterway crossing. Coastal bridge scour occurs when bridge foundations, decks, abutments, and/or causeway islands interact with currents and waves in a way that alters sediment mobility and transport.

The basic mechanisms driving scour are similar in both the riverine and coastal environments: flow velocity and flow depth. However, the coastal scour response to design events is often unique for at least four reasons:

1. No distinct flow from an “upstream” source of sediment exists,
2. Flows are unsteady and multi-directional,
3. The presence of waves complicates the scour processes, and
4. Large surge/stage events do not always produce large velocities.

No distinct “upstream” source of sediment exists in the coastal environment. Rather, net sediment transport initiates from either side of a bridge due to the presence of flood and ebb tidal currents, incoming and outgoing surge or tsunami flows, and wind-generated waves. Coastal bridge foundations are also subject to geomorphologic changes that occur in estuaries, bays, sounds, and at tidal inlets along the coast. These long-term changes in sediment transport and bed elevation impact foundation design as noted in Section 12.3.1.

Flows in the coastal environment are unsteady and multi-directional. There is no single “upstream” condition for coastal bridges. Existing methods for estimating equilibrium scour depths are almost universally based on two assumptions of the flow field: that it is steady, and that it is unidirectional. Tides are a type of “quasi-steady” flow. Their velocities persist over multiple hours of the day during the flood and ebb phases of the tide. The persistent direction of tidal currents during the flood and ebb phases means that the unidirectional assumption is not overly limiting. During design storm events, the currents associated with the rising and falling limb of a storm hydrograph may overwhelm the quasi-steady and unidirectional characteristics of tides. Further complicating matters, the orientation between flow velocity and the bridge foundation is also potentially unique for a given design event. Section 12.2.3 provides additional information regarding the complexity of coastal hydraulics at tidal bridge crossings.

The presence of waves further complicates the scour processes. Waves are much shorter in period than the timescales of other coastal flows yet mobilize sediment and produce scour depressions at bridge foundations. Existing engineering practice clearly supports the concept of a maximum scour depth based on foundation parameters for pier scour (see Section 12.3.6), and on wave parameters for abutment scour (see Section 12.3.5). This is due to the nature of wave interactions with each foundation element where wave reflection from abutment walls drives the scour process but plays little role in scour at the base of a pier or pile.

Large discharge events do not always yield large velocities. During a coastal flood event, lateral expansion of the floodplain often leads to exceptionally large cross-sectional flow areas. This expanded flow area yields comparatively smaller velocities and, therefore, smaller estimates of scour. Accordingly, evaluating scour potential for lower and higher exceedance probability events (longer and shorter return periods, respectively) is good practice.

### 12.1.1 Bridge Scour Policy, Guidance, and Reference Materials

An established body of knowledge, products, and tools exist for the evaluation of scour at bridges crossing rivers and streams. The FHWA uses these products to develop and provide national

scour policy and guidance. As described in Chapter 2, the National Bridge Inspection Standards<sup>5</sup> (NBIS) serve as one of the current policies for the inspection of bridges and the appraisal of scour. Other relevant and/or related policies include 23 CFR § 625, 23 CFR § 650 subpart A, and 23 CFR § 650 subpart C, and (via 23 CFR § 625.4) relevant chapters of the AASHTO LRFD Bridge Design Specifications (namely chapters 2, 3, 10, 11, and 12).

The FHWA currently has four reference documents containing information relevant to the topic of bridge scour in general:

- HEC-18 “Evaluating Scour at Bridges” (5<sup>th</sup> edition, Arneson *et al.* 2012)
- HEC-20 “Stream Stability at Highway Bridges” (4<sup>th</sup> edition, Lagasse *et al.* 2012)
- HEC-23 “Bridge Scour and Stream Instability Countermeasures: Experience, Selection, and Design Guidance” (3<sup>rd</sup> edition, Lagasse *et al.* 2009)
- Hydraulic Considerations for Shallow Abutment Foundations Technical Brief (FHWA 2019b)

Taken together, these documents provide information pertinent to the design of new bridges to resist scour impacts, for evaluating the vulnerability of existing bridges to scour, and for the design of countermeasures to mitigate scour. These reference materials provide important contextual information related to scour processes but do not specifically address most coastal scour issues. With some appropriate modifications, some of the tools developed for riverine scour are transferable to the coastal environment. This chapter identifies those opportunities, as are other methods, resources, and tools needed to develop estimates of the key hydrodynamic parameters (depth and velocity) that drive coastal scour formation.

The NBIS, and other regulatory requirements described above, make no distinctions between riverine and coastal scour situations. However, as a result of the complex hydrodynamics, sediment processes, and other coastal features, the FHWA cautions that in the coastal environment, the “hydraulic” expertise brought to bear on interdisciplinary teams should consider the inclusion of coastal engineering expertise, where appropriate.

## **12.2 Hydraulics for Coastal Bridge Locations & Crossings**

Waves, tides, storm surges, sediment transport, inlet dynamics and stability, and other coastal processes determine the hydrology and hydraulics that are most applicable for coastal bridges. Some bridges near the coast also experience varying levels of tidal influence. For those bridges, the practitioner should consider a combination of fluvial and coastal processes in order to determine the processes that govern bridge hydraulics. The following subsections describe many of these processes based on the degree of tidal influence on a bridge. The following text categorizes these bridges, in order of increasing tidal/coastal impacts, as tidally-influenced, tidally-dominated, and simply tidal bridges. The text also includes in its description of coastal bridges those that cross non-tidal waters but experience significant coastal processes. For example, bridges found throughout the Great Lakes. Section 12.4. provides suggestions for scour evaluation for each type of bridge crossing.

### **12.2.1 Tidally-Influenced River Crossings**

A tidally-influenced bridge is one that crosses a river or stream where astronomical tides modulate the fluvial discharge and stage, but where the flow does not reverse under normal tidal conditions.

---

<sup>5</sup> 23 CFR part 650 subpart C

These bridges often cross rivers, streams, or tributaries within coastal watersheds (see Figure 11.1 for a graphical example). Figure 12.1 shows a tidally-influenced discharge record taken from the Suwannee River near Wilcox, Florida. The influence of the mixed, semi-diurnal tidal signal characteristic of this part of the Gulf of Mexico is evident in the record of discharge shown (see Section 4.2 for more information on astronomical tides).

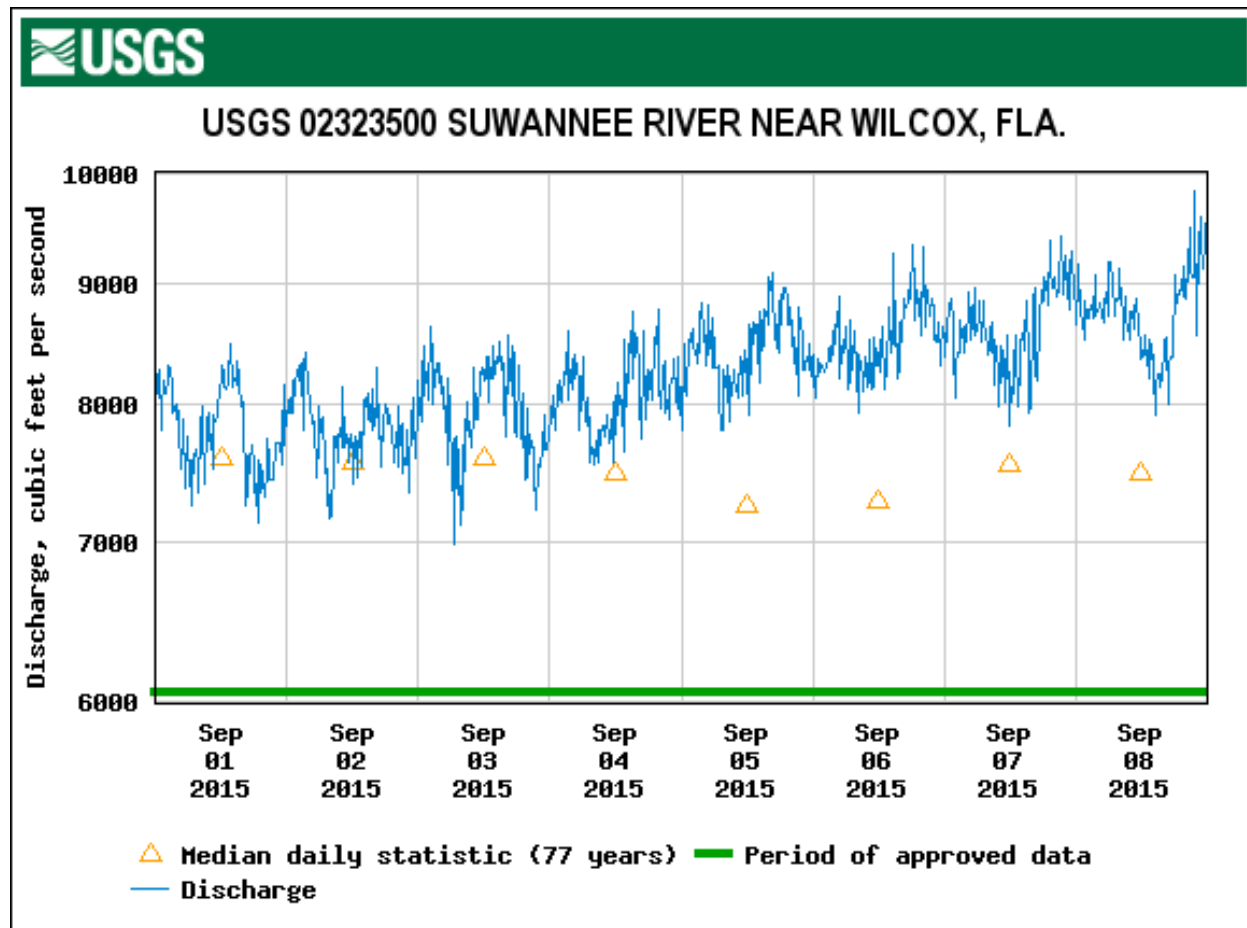


Figure 12.1. Discharge record for a tidally-influenced location (image downloaded from USGS website May 2019)

The flow at tidally-influenced bridges moves downstream with a magnitude that may slightly diminish during the flood tide. On the other hand, an ebbing tide enhances the downstream flow. At these bridges, the flow does not reverse direction during the flood tide. If the tidally-influenced bridge is well outside of the coastal floodplain, a typical hydraulic analysis of the bridge, using tools and equations typical of the riverine environment, is likely adequate.

**Three categories of coastal bridges are (in order of increasing tidal/coastal impacts): 1) tidally-influenced, 2) tidally-dominated, and 3) (simply) tidal bridges.**

Coastal processes may impact a tidally-influenced bridge during major storm events. The degree to which a tidally-influenced bridge experiences coastal impacts depends on the bridge's location, the characteristics of the coastal floodplain, and the magnitude of the coastal storm event. As

noted in Sections 12.4 and 12.5, one may need to evaluate the fluvial and coastal events in order to determine the hydraulics that govern the design of bridges in these settings.

### 12.2.2 Tidally-Dominated River Crossings

Tidally-dominated bridges cross clearly definable rivers or streams where flow reverses during the astronomical flood tide. Like tidally-influenced crossings, these bridge crossings exist in coastal watersheds but are closer to the tidal source (see Figure 11.1 for a graphical example). At these locations, the flooding tide overwhelms the fluvial discharge and the mean (i.e. time-averaged) flow is in the upstream direction for some period of the incoming tide. Figure 12.2 shows the discharge record for a gage closer to its tidal source than the one shown previously for the Suwannee River (Figure 12.1). The periods of negative discharge, appearing twice daily with unequal magnitudes, correspond to the mixed, semi-diurnal tides from the Gulf of Mexico. Note that periods of high river discharge and/or weak tides may temporarily suspend flow reversals. One such period corresponds to the weak, neap tidal forcing on September 5 – 6, 2015 in that gage record.

Tidally-dominated bridges are often in the coastal floodplain and, therefore, vulnerable to coastal storm surge and waves. In these cases, either the riverine flood event or the coastal flood event may govern bridge hydraulics. The practitioner should evaluate both conditions to determine which event leads to more scour and/or less freeboard (see Section 12.4.1 for a suggested approach).

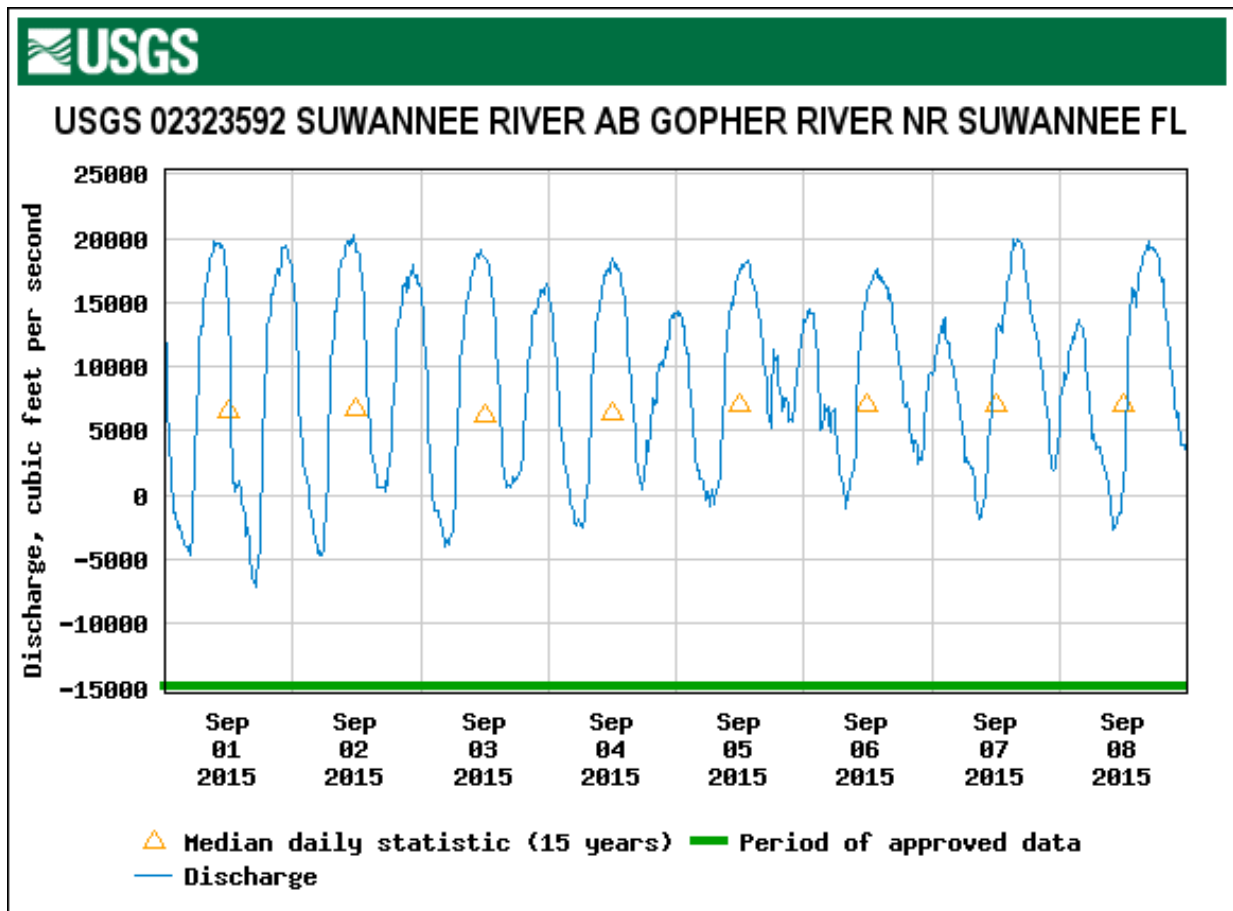


Figure 12.2. Discharge record for a tidally-dominated location (image downloaded from USGS website May 2019)

### 12.2.3 Tidal Crossings

Tidal bridge crossings cross open bodies of water such as estuaries, sounds, bays, bayous, and tidal inlets (see Figure 11.1 for examples). In these situations, the crossings are continuously elevated bridges with approach embankments on either side of the water body, or a series of elevated bridges connected by causeway islands. The physical coastal processes impacting tidal bridge crossings include relative sea level rise (RSLR), daily astronomical tides, storm surge, waves and wave processes, and potentially tsunamis, with all but the first producing combinations of flow velocity and flow depth that lead to scour. The influence of fluvial discharge on tidal bridge crossings is not always obvious. Depending on the characteristics of the fluvial discharge and the tidal water body, the watershed contributions may contribute only minimally to flow velocity, discharge, and depth.

Coastal processes over timescales ranging from short to long, often dominate scour at tidal bridge crossings. Tidal crossings are subject to two different flow events during coastal storms and tsunamis: the first associated with the initial flood-directed surge or tsunami propagation (i.e., the rising limb of a hydrograph), and the second associated with the ebb-directed return flow or tsunami drawdown (i.e., the receding limb of a hydrograph). Each of these events has the potential to produce unique, time-dependent depth and velocity combinations that impact the scour formation process.

### 12.2.4 Non-Tidal Waters

Bridge crossings over non-tidal waters may experience many of the coastal processes mentioned previously except for sea level rise and astronomical tides. Such bridges are located within the Great Lakes region. Bridges near the primary lake shorelines are vulnerable to significant seasonal or decadal lake level fluctuations. During storm events, these bridges often experience large waves, increased lake levels, and long-period lake level fluctuations (i.e. seiching). Methods and tools for evaluating scour at tidally-dominated bridge crossings are applicable to this category of bridges as well.

### 12.2.5 Other Considerations

The combination of fluvial and coastal flood events, or compound flooding, was addressed earlier in Section 4.4. These types of maximal flooding conditions, while certainly complex, may not necessarily be the same conditions as those that would produce the worst scour. This is because when comparing the effects of depth and velocity, the two primary hydraulic variables associated with scour, velocity plays a greater role. In addition to stage, the practitioner should consider relationships between stage and discharge or stage and velocity to determine the conditions that lead to larger scour estimates.

In the coastal environment, the maximum velocity and maximum storm tide elevation typically occur at different times. Maximal coastal scour formation conditions likely occur when the velocity is the greatest value. Such conditions arise during two scenarios: first, when surge is entering a tidal inlet or embayment on the rising limb of a storm hydrograph. The second occurs during the recessional period, when combined surge and the storm-derived rainfall flows back to the ocean. Consider Figure 12.3 as an illustrative example of this concept from a USGS gaging station on the Neches River near Beaumont, Texas. For the same stage value of 2.7 feet occurring before and after Hurricane Harvey on August 25, 2017 and September 19, 2017, respectively, the discharge and velocity are almost twice as large during the recessional period as they are preceding the storm.

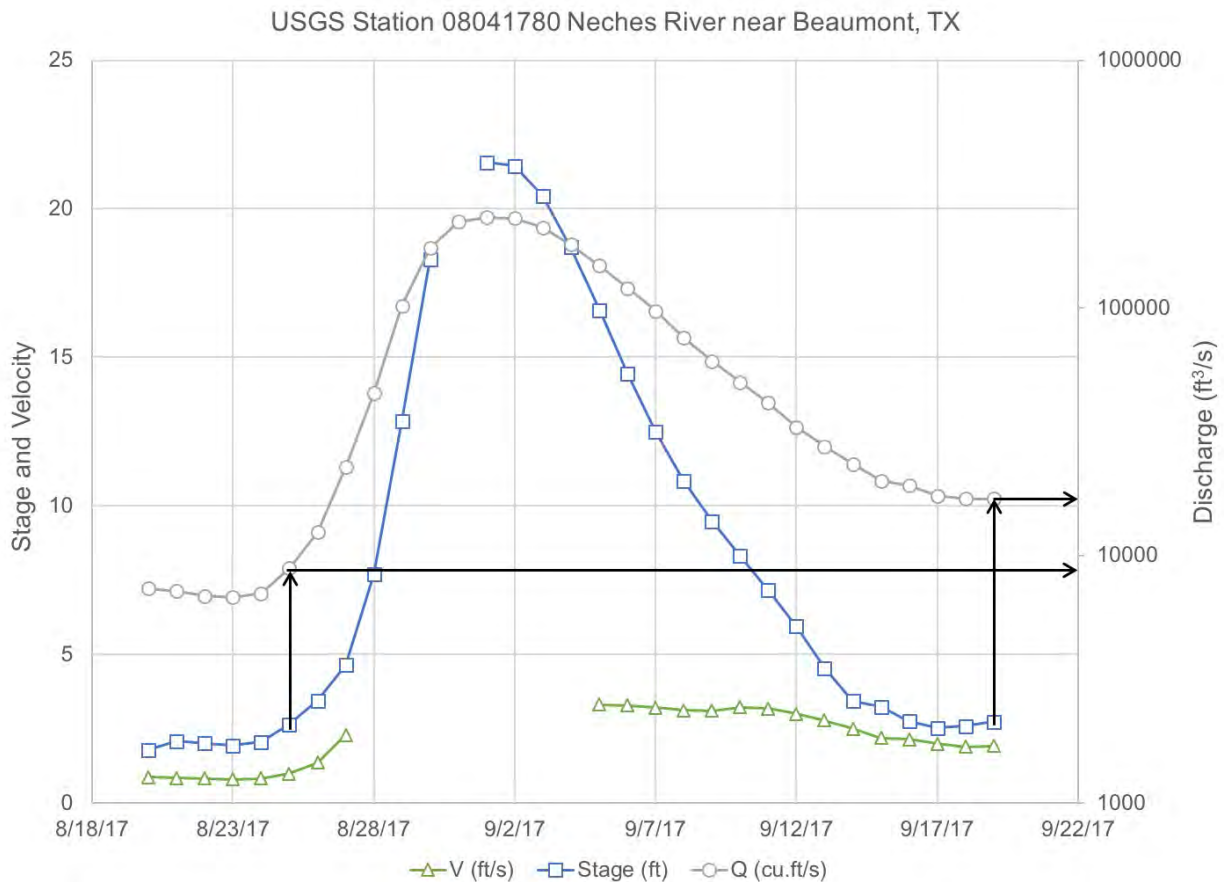


Figure 12.3. Representation of recession-dominated flow following Hurricane Harvey

## 12.3 Types of Coastal Scour

The types of scour that occur at bridges in the coastal environment include the same general categories (long-term change, contraction scour, and local scour) as found at riverine bridges. Additionally, coastal bridges can experience scour as a result of wave action (wave scour) and localized areas of high velocity associated with wave-current interactions. Coastal bridges, including tidally-influenced bridges located some distance from the coast, are experiencing sea level rise. Engineers can consider, as part of their bridge hydraulics evaluation, the effects that sea level rise will have on coastal bridge scour and freeboard requirements. See Section 4.1.6 for more information and discussions on projections of sea level rise for coastal transportation design.

Important caveats and differences are associated with scour in the coastal environment. One is geomorphologic changes that impact deposition and erosion at a coastal bridge. Others include the potential impact of bedforms on scour depressions; the influence of abutments and causeway islands on contraction scour; alternative methods for estimating local pier scour in coastal environments; and wave-induced scour at piers and abutments.

### 12.3.1 Long-term Changes

Long-term changes influencing scour at tidal bridge crossings include deposition and erosion of the bed, lateral migration of the channel thalweg (i.e. the deepest part of the channel) and/or shoals, shoreline recession, and tidal inlet migration. Changes in river or stream bank position are

also important considerations for tidally-influenced and tidally-dominated bridge crossings. Analyzing the effects of these long-term changes is important for two reasons. First, long-term changes alter hydrodynamic conditions including flow speed and direction, as well as wave height and direction which affect scour estimates. Second, these long-term changes may lead to undermining of bridge foundations even in the absence of the design scour event. Understanding and considering the impacts of long-term coastal change on bridge foundations are within the coastal engineer's area of expertise.

Deposition (aggradation) and erosion (degradation) refer to the long-term changes in bed elevation along a reach of a stream, channel, or water body. In the riverine environment, changes in upstream and downstream sediment supply, flow characteristics, and/or changes in the downstream hydraulic conditions drive the deposition and erosion that lead to bed elevation changes over time. For coastal bridges, deposition and erosion are often associated with changes in net sediment transport volumes, rates, or patterns. In the coastal environment, such changes occur over timescales ranging from short (i.e. hours) to long (i.e. centuries). Coastal storms and sea level rise, respectively, are the driving factors at each end of this scale. In addition to these natural processes, construction of jetties, groins, seawalls, bulkheads, causeway islands, and other works of man, alter the natural sediment delivery processes within the coastal environment.

Evaluations of deposition and erosion at coastal bridges rely on measurements of bed elevation over time. These data are typically available as part of routine bridge inspection surveys. The engineer uses the change in bed elevation between bridge inspection surveys to determine rates of deposition or erosion for their scour appraisal.

Bridges at or along the coast may not have foundations in well-defined stream or river banks and channels, but they are nevertheless vulnerable to lateral migration of the channel thalweg, as well as migration of the channel shoals. Some of the general techniques for evaluating stream stability mentioned in HEC-20 (Lagasse *et al.* 2012) apply here. One major exception is the use of aerial imagery, which by itself is not enough to determine channel stability. This analysis also uses historical hydrographic survey data. Hydrographic survey data are available in the form of historical nautical charts and, more recently, high-resolution side-scan sonar bathymetric mapping data.

Shoreline recession represents an important form of long-term change (see Section 8.2). Bridge approaches or foundations near receding shorelines are subject to undermining as the shoreline retreats and erodes in response to long-term changes in net sediment transport and sea level rise. While the bridge approaches, abutments, and foundations may withstand some amount of scour, complete undermining and/or flanking of protection is possible as shorelines retreat over long periods of time.

In the coastal environment, navigation channels often have a clearly defined cross-section where the deepest portion is usually at the channel thalweg. Typically submerged, the shallow areas adjacent to the channel are referred to as "shoals" instead of banks, since the latter often indicates emergence above the water. Federally managed navigation channels typically have well-defined and maintained alignments but, like natural channels, may shift in response to changes in hydrodynamic conditions and net sediment transport. This is particularly true in estuaries and natural tidal inlets.

Tidal inlets are in a dynamic equilibrium. Wave-driven longshore sand transport leads to lateral migration of the inlet throat, whereas ebb/flood tidal flows try to scour these deposits to maintain channel depths (see Section 6.6). Tidal inlets, even those stabilized by jetties, groins, or seawalls, can exhibit substantial morphologic changes in response to the net longshore sand transport, sea level rise, and changes to the back bay, sound, or estuary. Some, like Oregon Inlet in North Carolina, are extremely dynamic and change dramatically even over relatively short time periods,

as shown in Figure 12.4. Substantial lateral migration of the channel thalweg at this bridge contributed to significant local pier scour and even temporary closures during inspection and response efforts (Krolak and Henderson 2016).

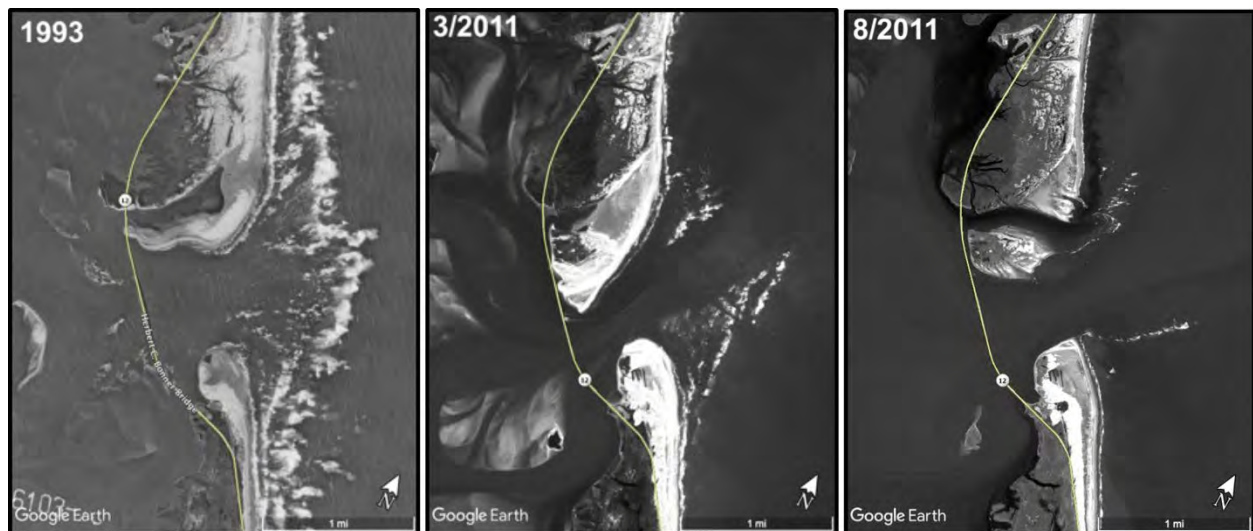


Figure 12.4. Aerial imagery of Oregon Inlet, North Carolina from 1993, March 2011, and August 2011

A much smaller tidal inlet, Matanzas Inlet near St. Augustine, Florida illustrates well the potential for tidal inlets, shoals, and channels to change over time as shown in Figure 12.5. The substantial changes in morphology, channel position, and channel depth attributed to natural tidal inlets can undermine and/or flank bridge foundations. Engineering of tidal inlets and/or modification of the tidal prism are known to impact scour as well (see Section 12.3.1.1 for one such example).

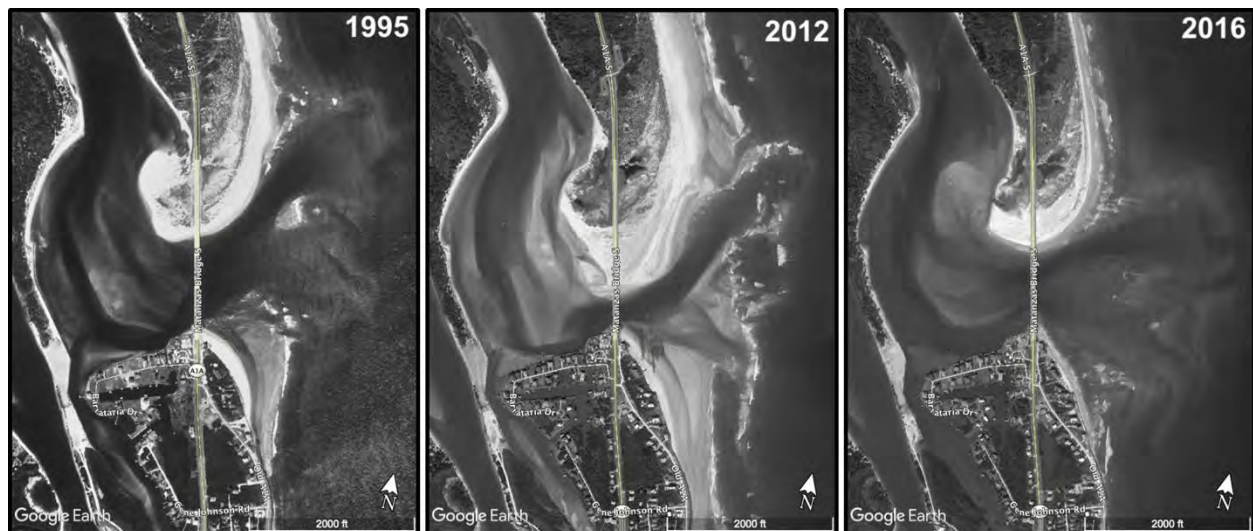


Figure 12.5. Aerial imagery of Matanzas Inlet, Florida from 1995, 2012, and 2016

#### 12.3.1.1 Example: Indian River Inlet (Delaware)

Indian River Inlet, Delaware (see Figure 12.6) has experienced progressive scour since it was originally dredged and stabilized with jetties in the 1930's. Scour holes near the bridge piers exceeded depths of 100 ft in 2000. As the inlet has deepened and its minimum cross-sectional throat area increased, more tidal flow has moved through it. Thus, its tidal prism has increased.

And as the tidal prism has increased, it has continued to scour out the throat area. Essentially, the artificially constructed and stabilized inlet has not reached its evolutionary equilibrium since its original opening in the 1930's. Placing large very large riprap around the bridge piers as scour countermeasures only exasperated the issue, as the resulting mounds (see "red" areas on the roadway alignment in Figure 12.6) reduced throat area until the tidal prism again worked to reestablish equilibrium; unfortunately, resulting in further scour.

Ultimately, scour concerns led to the construction of an entirely new cable-stayed bridge that spanned the entire inlet. However, even this new bridge had approach sections and piers within the locations of storm surge and tides.

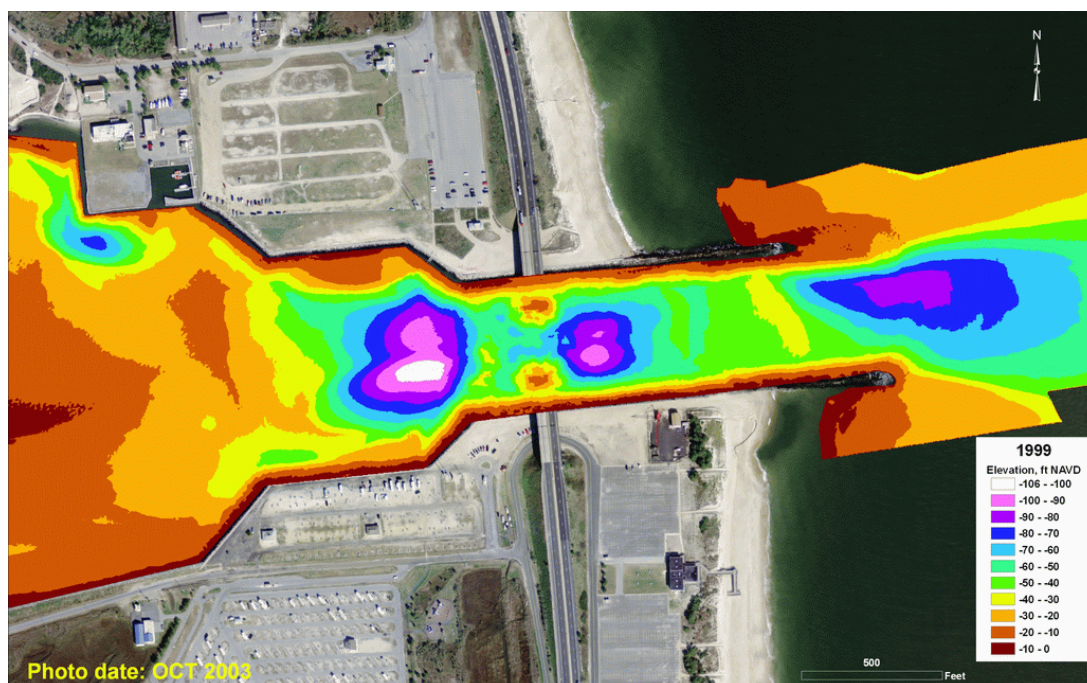


Figure 12.6. Bathymetric elevations showing scour holes inside Indian River Inlet (circa 1999)

### 12.3.2 Bedforms

Waves and currents lead to the development of bedforms in the coastal environment. Bedform lengths and amplitudes, while often small, contribute to the total scour at bridge foundations and abutments. Sand wave shoaling in navigation channels can generate very large bedforms, called megaripples, having heights up to 6 ft and lengths over 15 ft (Levin *et al.* 1992). Wave-generated bedforms, often termed "vortex or orbital ripples" because of their genesis, form by the interaction of wave orbital velocities with bed sediments. Characterizing the bedform dimensions of length and amplitude under field conditions is difficult. The Coastal Engineering Manual (USACE 2002) and some textbooks (e.g., Nielsen 1992) provide equations for predicting bedform dimensions over a range of sediment and hydrodynamic conditions. These reference materials provide equations for predicting bedform characteristics under regular and irregular wave conditions. In many cases, general equations represent the bedform length (Equation 12.1) and amplitude (Equation 12.2) with some amount of conservatism (see Figure 12.7 for definition sketch):

$$\lambda/A \approx 1.33 \quad (12.1)$$

$$A = (H L_o) / (2 L \cosh(2\pi d / L)) \quad (12.2)$$

$$\eta_{\max} \leq 0.32 \lambda \tan(\phi) \quad (12.3)$$

where:

- $\lambda$  = ripple length;
- $A$  = horizontal orbital semi-displacement;
- $\eta_{\max}$  = maximum ripple amplitude (one-half the ripple height); and
- $\phi$  = sediment angle of repose.

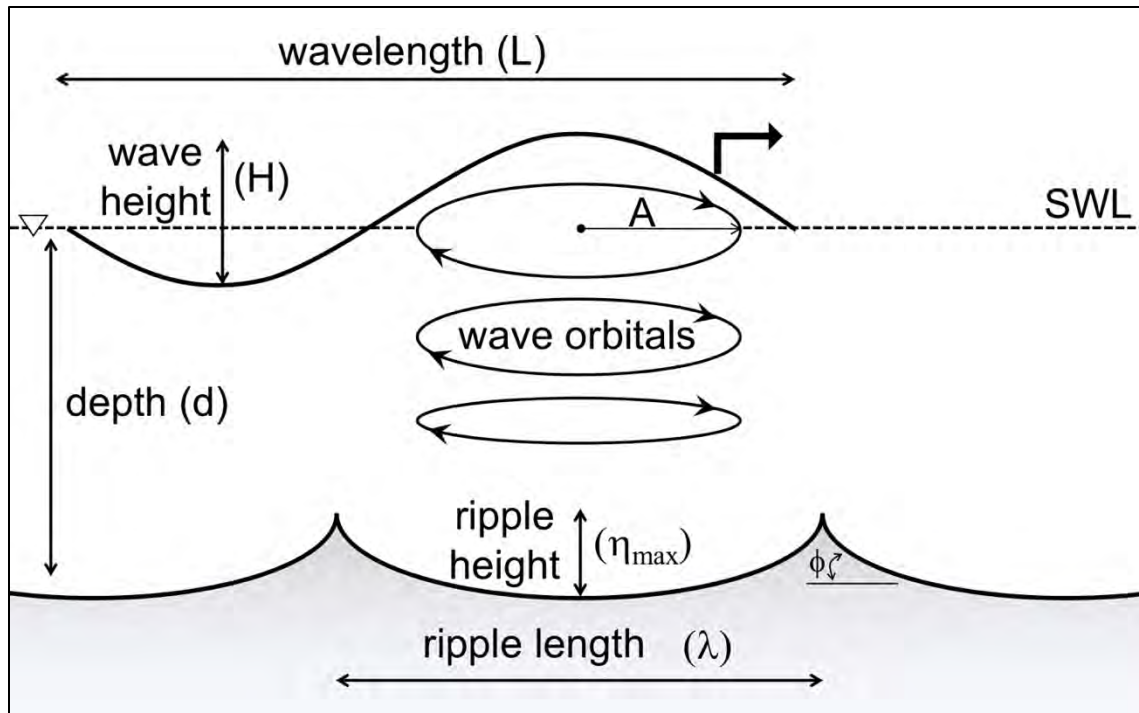


Figure 12.7. Definition sketch showing the representative variables used to estimate the height and length of orbital ripples

### 12.3.3 Contraction Scour

Contraction scour refers to the removal of bed, channel, bank, and shoreline sediment resulting from the contraction of flow due to physical obstructions. The localized increase in velocity within the contraction leads to enhancements in bed shear stress that mobilize and entrain bed sediments. Sediment transported out of the region of the bridge by currents and waves passing through the contraction result in an overall lowering of the bed elevation throughout the cross-section. In the coastal environment, natural channel narrowing, causeway islands, bridge abutments, bridge approach embankments, or any encroachment of the bridge structure lead to contraction of flow during normal and storm conditions (Figure 12.8).

The severity of contraction scour in the coastal environment depends greatly on the setting, the orientation between the obstruction and the flow, and the relative elevations between the obstruction and the adjacent terrain. For example, causeway islands may completely inundate under storm conditions, diminishing the severity of the contraction. Bridges crossing tidal inlets may experience similar conditions. In such cases, the portion of the embankment above the coastal flood elevation constitutes the only remaining obstruction that constricts the flow. The next two subsections include methods for estimating horizontal and vertical contraction scour.

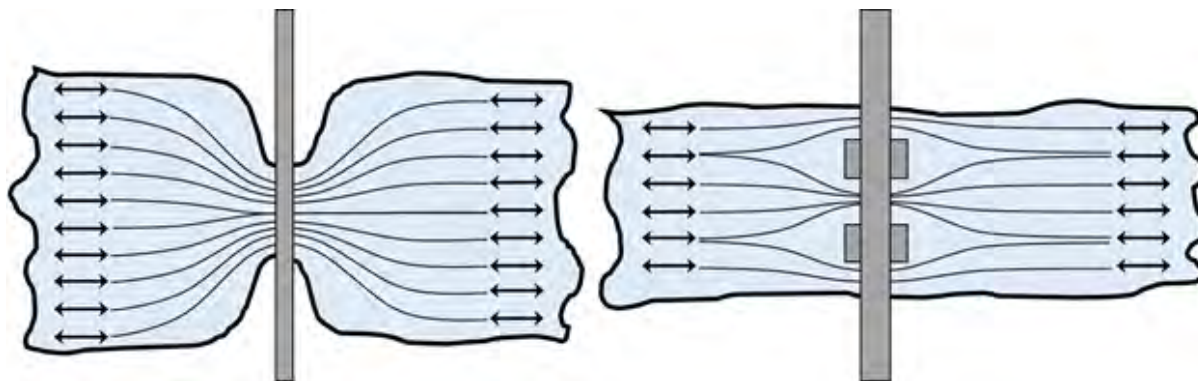


Figure 12.8. Examples of possible horizontal contractions at coastal bridges (thin lines denote possible streamlines, double-ended arrows denote the potential for flow reversals)

### 12.3.3.1 General Approach for Contraction Scour

The methods presented in HEC-18 (Arneson *et al.* 2012) for estimating contraction scour are applicable to coastal bridges, with some special considerations. Contraction scour at coastal bridges is most often like the Case 1 examples shown on page 6.2 in HEC-18. Contraction scour may occur under clear-water or live-bed conditions at coastal bridges. In order to determine the appropriate set of equations to apply, compare the critical velocity for sediment mobilization to the design flow velocity. During clear-water conditions localized increases in velocity within the contraction mobilize sediment and carry it away from the bridge crossing. During live-bed conditions the design velocity upstream of the bridge crossing is greater than the critical velocity, and sediment is moving toward the bridge crossing. HEC-18 describes both scenarios and provides the necessary equations for estimating contraction scour under either condition.

Selection of an upstream section needs special consideration in coastal contraction scour analyses. During a coastal storm surge event, velocities may approach the contraction from one side early in the event storm event, and from the opposite side as the storm surge recedes. It is important to evaluate contraction scour resulting from both “upstream” conditions. Receding storm surge flows may combine with watershed contributions resulting in flow velocities larger than those estimated during the initial surge propagation. A similar situation occurs during daily tidal exchange at each bridge, where the flood- and ebb-directed velocities approach the contraction from opposite sides during either phase of the tidal cycle.

Engineering judgment is needed in the selection of an upstream cross-section location for scour calculations. The most appropriate upstream cross-section locations are free from major constrictions or other changes in channel/flow alignment. In other words, the most appropriate section aligns perpendicular to the flow field, and the upstream flow streamlines are straight and parallel.

The HEC-18 contraction scour equations, originally based on a form of Laursen’s (1960) equations, may be overly conservative for coastal storm surge conditions. Steady, uniform flows are the assumed conditions leading to the ultimate scour condition. Coastal storms can produce extremely large velocities. However, the high velocity condition may not persist for long enough to attain the ultimate scour condition. This is also true of tidal velocities that persist either in the flood or ebb phases for no more than six to twelve hours per day. Performing two- or three-dimensional hydrodynamic and sediment transport numerical modeling is a viable alternative for overly conservative estimates. Physical modeling is another alternative, but geometric scaling considerations often make these experiments cumbersome to perform in most laboratories (see Section 6.8).

### 12.3.3.2 Vertical Contraction Scour

Partially or fully submerged bridge superstructures during flood events may contribute to another form of contraction scour. Vertical contraction scour, often termed “pressure scour,” develops due to the vertical contraction of flow below the bridge deck and girders/beams (see Figure 12.9). Note that vertical and horizontal contraction scour occur simultaneously when bridge superstructures are overtopped. HEC-18 presents a methodology for estimating the vertical contraction scour for partial or complete bridge submergence (see also FHWA 2019b for related information). The primary consideration when applying these equations to coastal bridges is that the vertical contraction may occur both early and late in the storm event on the rising and falling stages of the storm surge hydrograph. This may also apply during tsunami events as well. Low, at-grade, bridge crossings and bridge approach spans are most susceptible to vertical contraction scour.

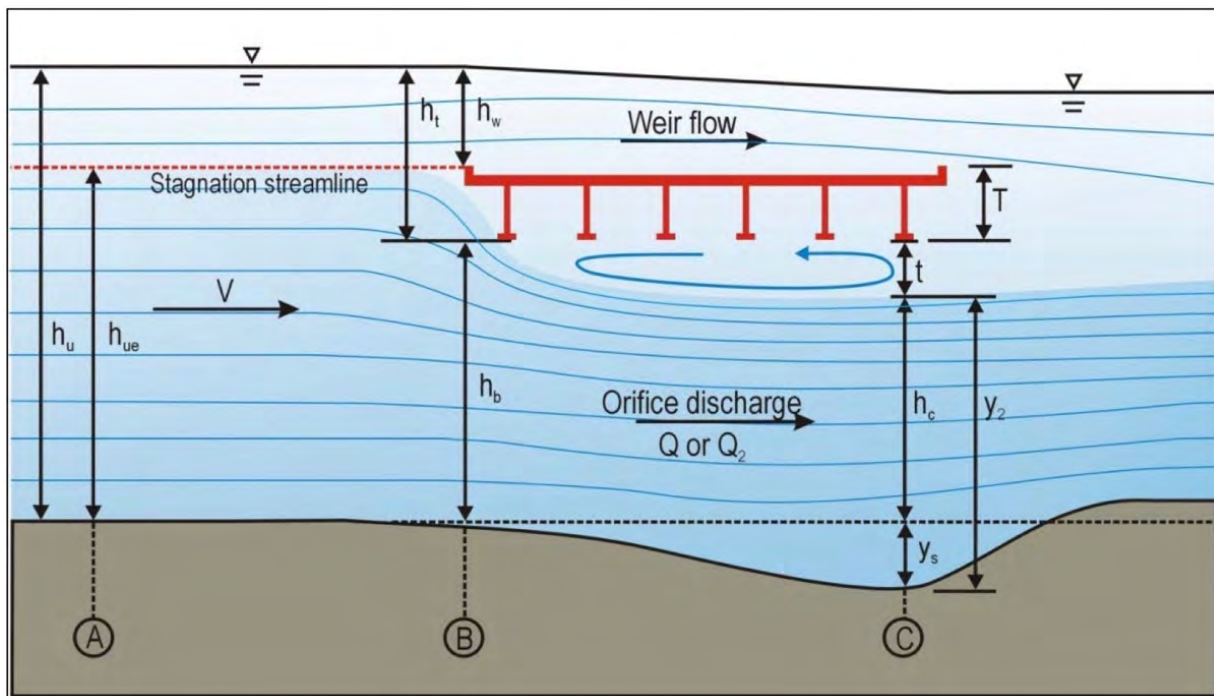


Figure 12.9. Vertical contraction or pressure scour schematic (Arneson *et al.* 2012)

### 12.3.4 Local Scour at Bridge Piers

Local scour describes the scour that forms when flows interact with piers, piles, caissons, or other similar vertical, surface piercing structures. Section 12.3.5 addresses abutment scour, which is another type of local scour. Local scour develops around the base of the structure. Unlike in the riverine environment where the scour hole primarily develops on one side of the pier or pile, the multi-directional characteristics of coastal flows yield scour holes that develop on either side and often coalesce into one complete scour depression at the base of the structure (see Figure 12.10 for example).

The following processes affect local pier scour:

- Increased mean flow velocities and pressure gradients near the structure,
- Development of secondary flows in the form of vortices, and
- Increased turbulence near the structure.

The development of secondary flows near the structure are known to influence the scour development process as a result of two specific flow mechanisms. First, separation of the flow around the structure produces wake vortices downstream of the structure. Second, horseshoe vortices, wrapping around the structure near the bed and free surface, develop due to the variation in stagnation pressure along the upstream face of the structure as well as flow separation at the limit of the scour depression (FDOT 2012). This discussion of local pier scour focuses on scour processes initiated by tidal or non-tidal currents. Waves also produce their own type of local pier scour (see Section 12.3.6). The mechanisms described above are generally responsible for scour development in both cases, the difference being the time scale of wave-induced effects on the mean flow field is much shorter in duration than that attributed to the tidal or non-tidal currents.

Like contraction scour, local pier scour happens during clear-water and live-bed conditions. If sediment is in motion upstream of the bridge, live-bed scour occurs. If sediment is not in motion upstream of the bridge and sediment mobilization only occurs near, and due to, the structure, then clear-water scour occurs. Recall that “upstream” conditions occur on both sides of the bridge during tidal and storm conditions and that the ebb tidal flows and receding storm flows can combine with fluvial discharge resulting in larger velocities.

#### 12.3.4.1 General Approach

Existing local pier scour equations were developed specifically for use in riverine conditions under the assumption of steady and uniform flow. However, they are based upon fundamental hydraulic processes and sediment characteristics that are transferable to the coastal environment. For example, a design velocity and mobilization velocity for sediment are definable in both the riverine and coastal settings. Still, their application in the coastal environment uses some special considerations and sound judgment.

This document describes two general approaches for estimating local pier scour at coastal bridges. They include the methods presented in HEC-18 and an alternative set of scour equations, originally developed by Sheppard *et al.* (1995) and described in the FDOT Bridge Scour Manual (FDOT 2005). Both documents provide local scour equations for clear-water and live-bed conditions. When the total estimated scour (i.e. the sum of long-term, contraction, and local scour) is greater than 5 feet, the FDOT Bridge Scour Manual recommends using the Sheppard Pier Scour Equations over the HEC-18 equations for coastal bridges.

#### 12.3.4.2 Wide and Complex Pier Geometry

Coastal bridge foundations are composed of multiple elements between the soil and the superstructure: bent beams, columns or piers, pile caps or platforms, and multiple piles. The elements that interact with currents and waves modify the flow field in ways that lead to local pier scour. The combination of these elements often results in complex shapes and geometries. In the case of bascule piers, the geometry of the foundation is very large compared to the flow field. However, existing scour equations were developed based on the formation of a scour hole around an individual obstruction. A correction factor or an effective diameter account for the geometry of complex piers in existing scour equations.



Figure 12.10. Local scour depression at the terminus of a coastal structure

HEC-18 includes methods to compute pier scour for standard and complex pier geometries. The HEC-18 equations include wide pier correction factors that may be applicable to bascule piers when the pier is wide in comparison to the flow depth. HEC-18 also outlines a procedure for evaluating scour at complex piers consisting of a combination of pile groups, pile caps, and piers. Hoffman and Verheij (1997), Melville and Coleman (2000), and Sheppard (2001) present alternative local pier scour equations that are infrequently used in practice.

The Sheppard pier scour equations from FDOT (2005) use an alternative definition of pier diameter. The complex pier method consists of developing an effective diameter, taken as the sum of the effective diameters of each component as shown in Figure 12.11:

$$D^* = D_{col}^* + D_{pc}^* + D_{pg}^* \quad (12.4)$$

where:

$D^*$  = effective diameter of the complex pier,

- $D_{col}^*$  = effective diameter of the column,  
 $D_{pc}^*$  = effective diameter of the pile cap, and  
 $D_{pg}^*$  = effective diameter of the pile group.

This effective diameter methodology, described fully in FDOT (2005), assumes that each individual complex pier element can be modeled as a simple surface piercing pile with its own unique effective diameter. The pier elements are shown graphically in Figure 12.12. The basic concept is that the scour produced by the complex pier element and the scour produced by its effective diameter are equal in magnitude. However, the scour depth for the complex pier geometry is not simply the combination of each scour depth associated with an element. The total scour depth for the complex pier geometry is estimated using the total effective diameter, because there is a nonlinear relationship between scour depth and effective diameter in the general local scour equations (FDOT 2005) (see Figure 12.13).

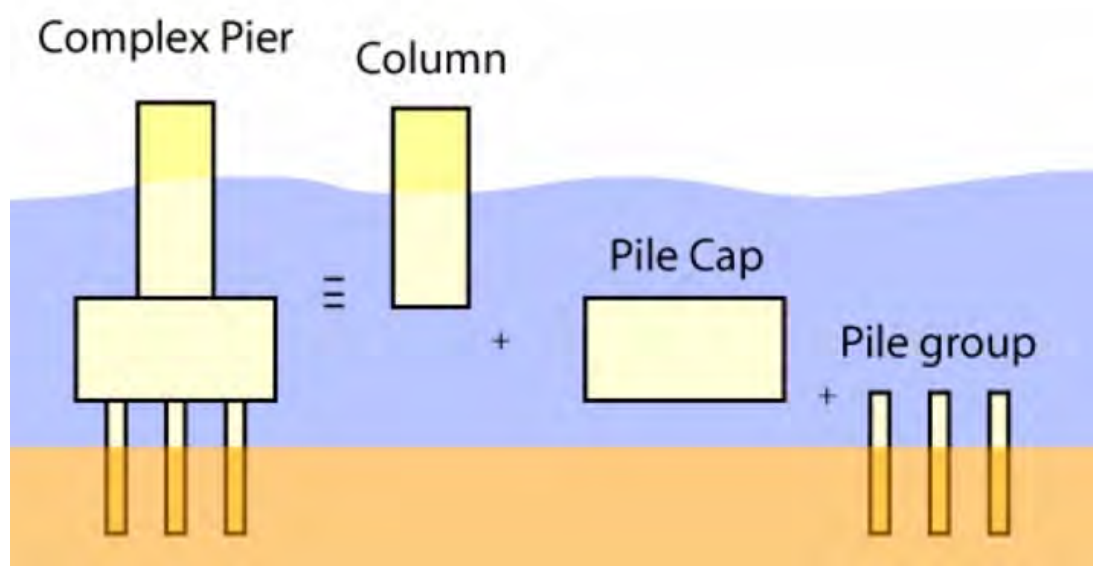


Figure 12.11. Complex pier components for Sheppard pier scour equations (FDOT 2005)

Complex pier geometries may consist of elements that become exposed during local scour. In these cases, the shape of the structure and its effective diameter change as scour progresses. Estimation of the equilibrium scour depth is an iterative process that accounts for changes in the effective diameter, flow, and/or sediment characteristics. This is a much more complex process. Therefore, the procedure is presented in terms of three specific cases (Figure 12.14) where the only difference is the location of the pile cap relative to the bed elevation prior to initiation of the local scour process. Note that the bed elevation used in this procedure should already account for the types of scour mentioned previously: long-term scour, bedform height, and contraction scour. The three cases are as follows:

- Case 1: for situations where the complex pier shape does not change as local scour progresses (the pile cap is above the eroded bed elevation);
- Case 2: for partially buried pile caps; and
- Case 3: for completely buried pile caps.

The FDOT Bridge Scour Manual (FDOT 2005) fully describes these methodologies for estimating effective pier diameters.

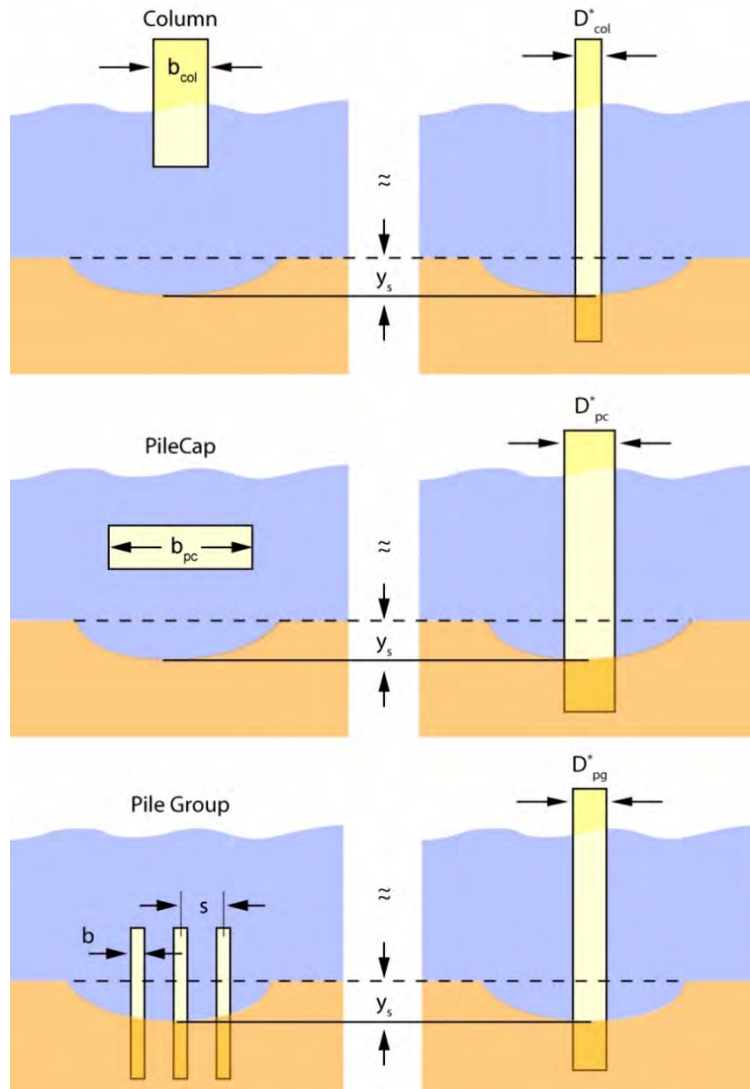


Figure 12.12. Individual elements for Sheppard pier scour equations (FDOT 2005)

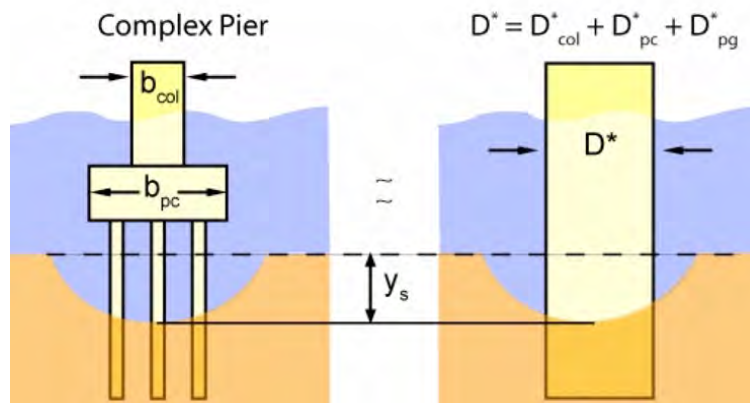


Figure 12.13. Concept of effective diameter for complex piers in the Sheppard pier scour equations (FDOT 2005)

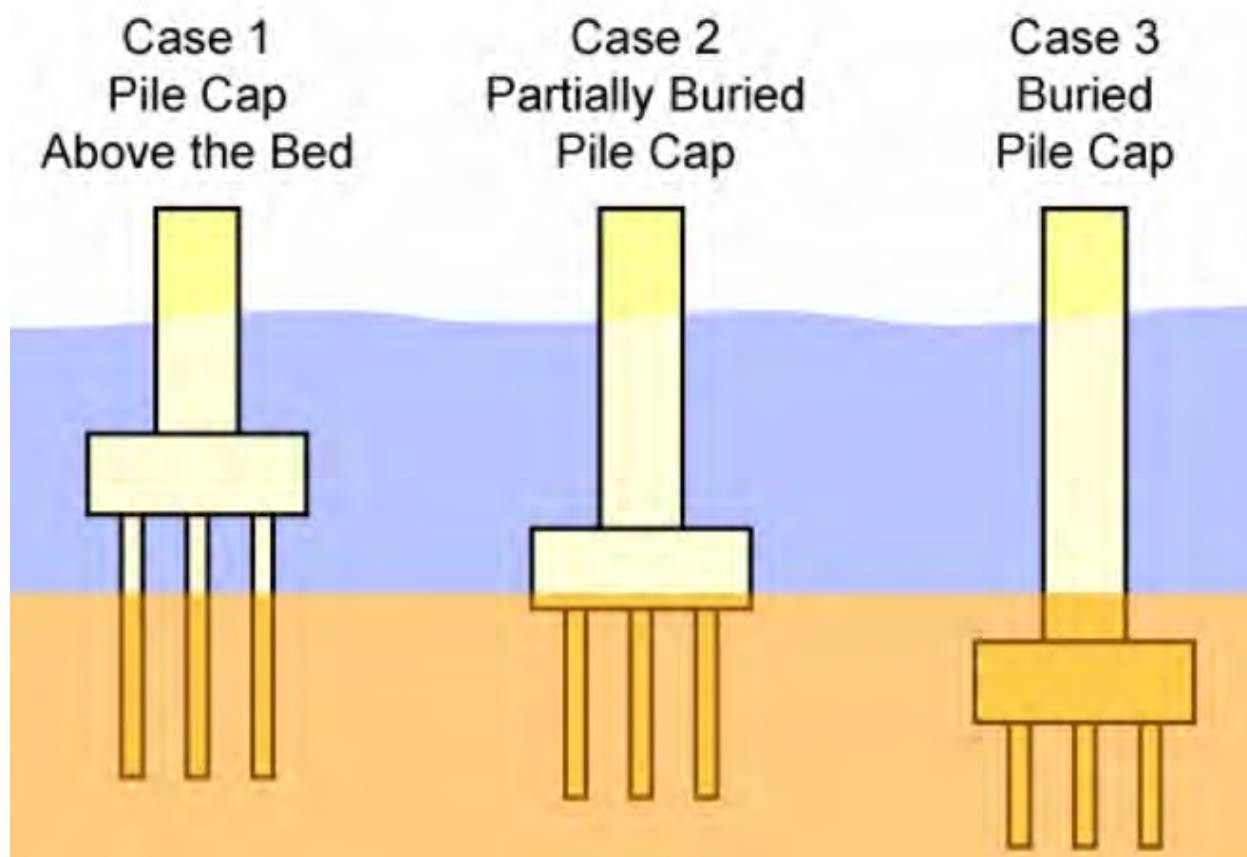


Figure 12.14. Three cases for Sheppard pier scour equations (FDOT 2005)

#### 12.3.4.3 Example: Johns Pass (Florida)

Large Bascule piers are a contributing factor to local scour for a bridge at Johns Pass, Florida (Figure 12.15). Johns Pass is still evolving in response to engineering that occurred decades ago. Most of Florida's inlets have been artificially created and stabilized by engineering works. Their tidal prisms have been significantly affected by engineering of the bays and by other inlets connected to those bays.

Johns Pass illustrates three important lessons regarding scour and coastal bridges. First, because of its relative size, the presence of a Bascule pier has a larger than normal effect on the resulting scour prediction. This usually is handled with application of HEC-18's wide or complex pier scour approaches (see also FDOT 2005). Second, the multiple inlets into the bay illustrate an important concern about attempts to numerically model such bridges and locations (Figure 12.16).

Each inlet could require a separate boundary condition to ensure overall hydrodynamic circulation. Additionally, the direction of the surge event could complicate the hydrodynamics, and thus adequacy of the modeling results. Third, the multiple inlets are evolving geomorphologically in response to previous engineering and thus the tidal flows through the pass may be gradually changing (see Section 6.6).



Figure 12.15. Johns Pass, Florida (2002)

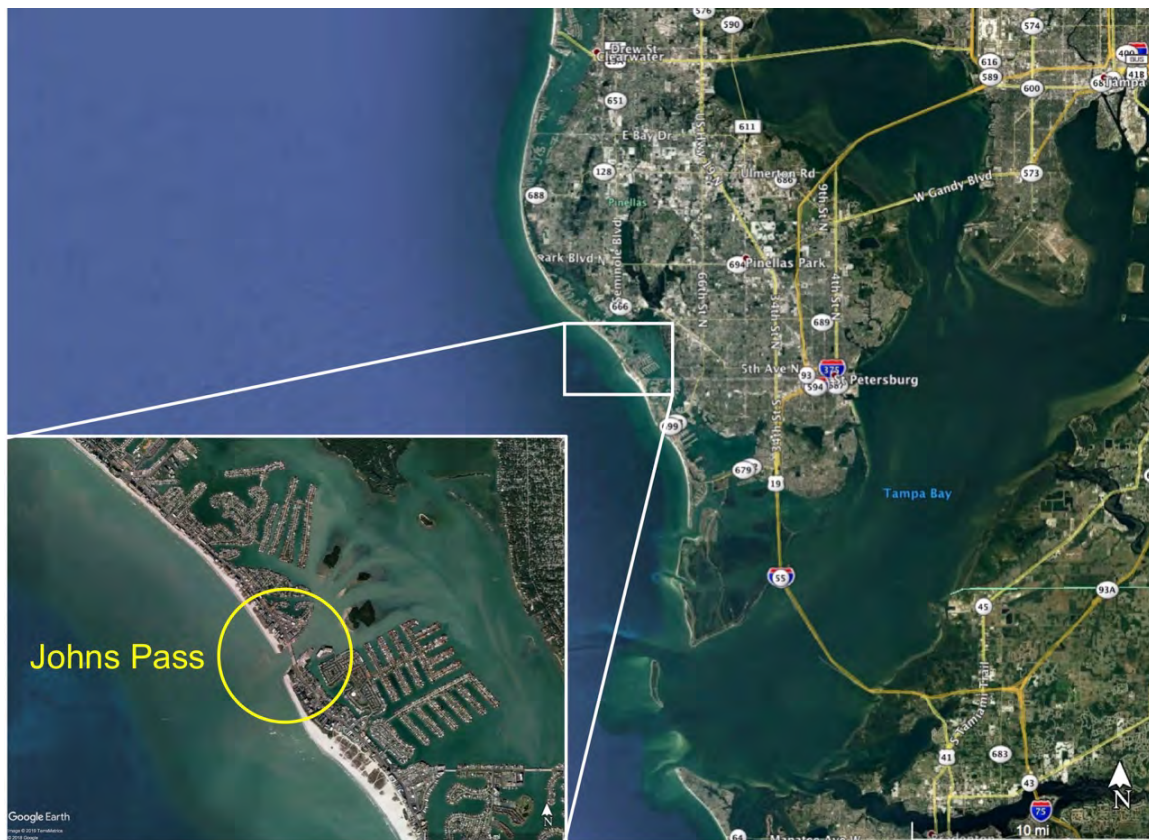


Figure 12.16. Location overview for Johns Pass, Florida

### 12.3.5 Local Scour at Bridge Abutments

Scour at bridge abutments is another form of local scour. HEC-18 provides methods for estimating abutment scour due to currents. Application of these methods, originally developed for the riverine environment, should account for the many complexities mentioned previously regarding coastal processes. For example, estimation of abutment scour at a coastal bridge should account for the flood and ebb tidal velocities, storm velocities associated with the rising and falling limb of the storm hydrograph, and/or potential combinations of ebbing or receding flows and fluvial inputs.

Waves also lead to scour at abutments, or vertical walls more generally, and erosion of approach embankments during coastal flood events. Wave reflection from abutments, or wave breaking at abutments, increases the bed shear stress at the base of the wall leading to toe scour. The Coastal Engineering Manual (USACE 2002) provides methods for estimating toe scour due to regular, irregular, nonbreaking, and breaking waves. Figure 12.17 graphically demonstrates typical toe scour due to nonbreaking regular and irregular waves. Note that pile bents near abutment walls may experience additional local scour due to the development of bars and troughs running somewhat parallel to the abutment wall.

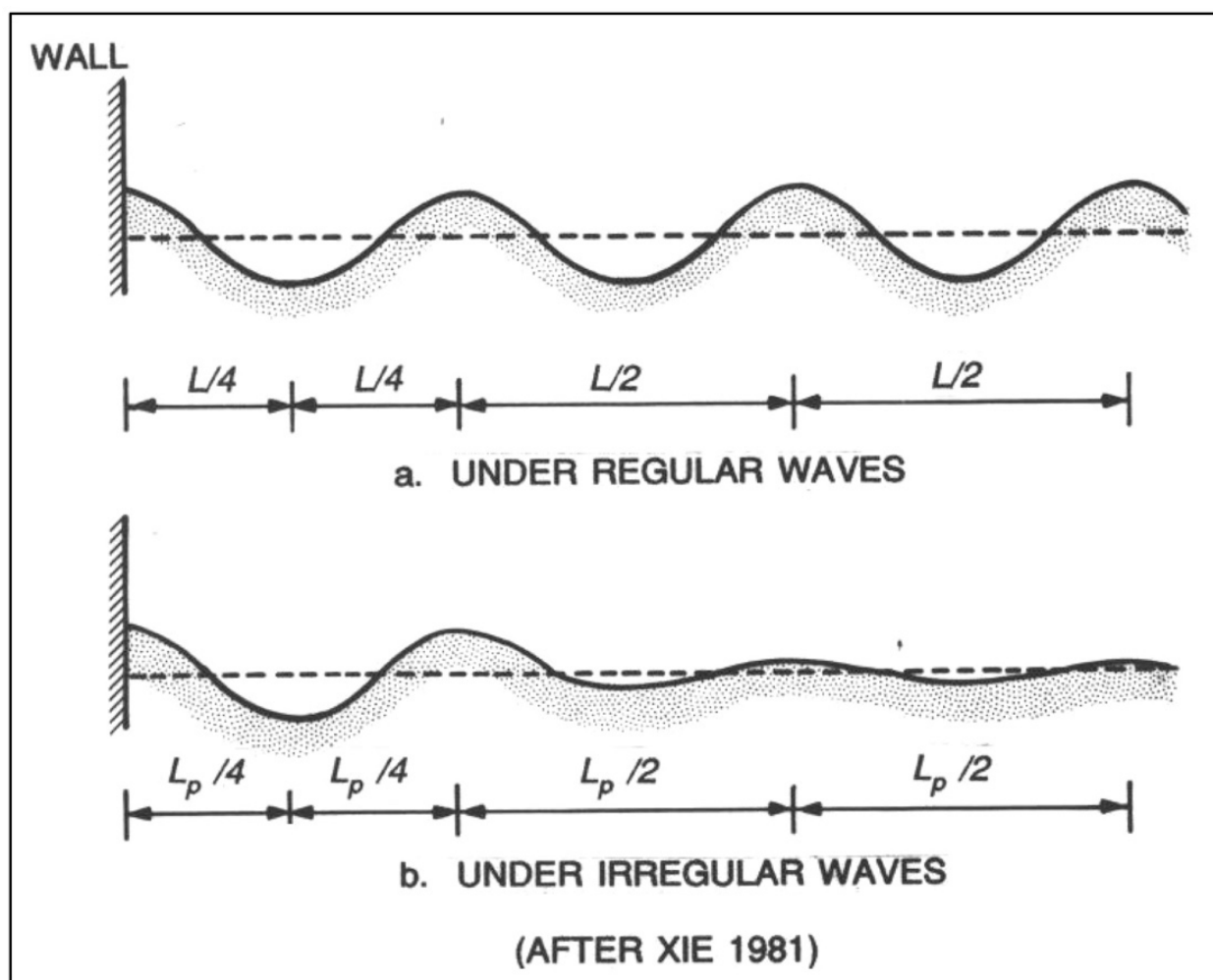


Figure 12.17. Typical scour profiles due to waves at the toe of a vertical wall (from USACE 2002)

Xie (1981, 1985) developed an empirically-based estimate of maximum toe scour by assuming normally incident, nonbreaking, regular waves impinging on an impermeable vertical wall:

$$S_m/H = 0.4/[\sinh(2\pi d/L)]^{1.35} \quad (12.5)$$

where:

- $S_m$  = maximum scour depth at a distance  $L/4$  from the wall;
- $H$  = incident wave height at the wall;
- $d$  = water depth at the wall; and
- $L$  = normally-incident wavelength.

Hughes and Fowler (1991) proposed an equation for toe scour due to normally incident, nonbreaking, irregular waves:

$$S_m/(u_{rms})_m T_p = 0.05/[\sinh(2\pi d/L_p)]^{0.35} \quad (12.6)$$

where:

- $u_{rms}$  = the root-mean-square of the horizontal nearbed wave orbital velocity;
- $T_p$  = peak wave period; and
- $L_p$  = wavelength associated with the peak wave period.

Toe scour due to breaking waves is often greater in magnitude than that attributed to either regular or irregular nonbreaking waves. The CEM (USACE 2002) presents some equations for estimating toe scour due to irregular, breaking waves but use of a simple approximation is more common. That approximation is:

$$S_m \approx H_{max} \quad (12.7)$$

In other words, the maximum expected toe scour depth due to breaking waves is approximately equal to the maximum wave height at the abutment or wall (see Figure 12.18). This wave height is often equivalent to the water depth at the abutment under breaking conditions. If the depth at the abutment is extremely large, then the maximum wave height is instead fetch- or duration-limited instead of depth-limited. In those cases, application of a suitable equation from the CEM is prudent.

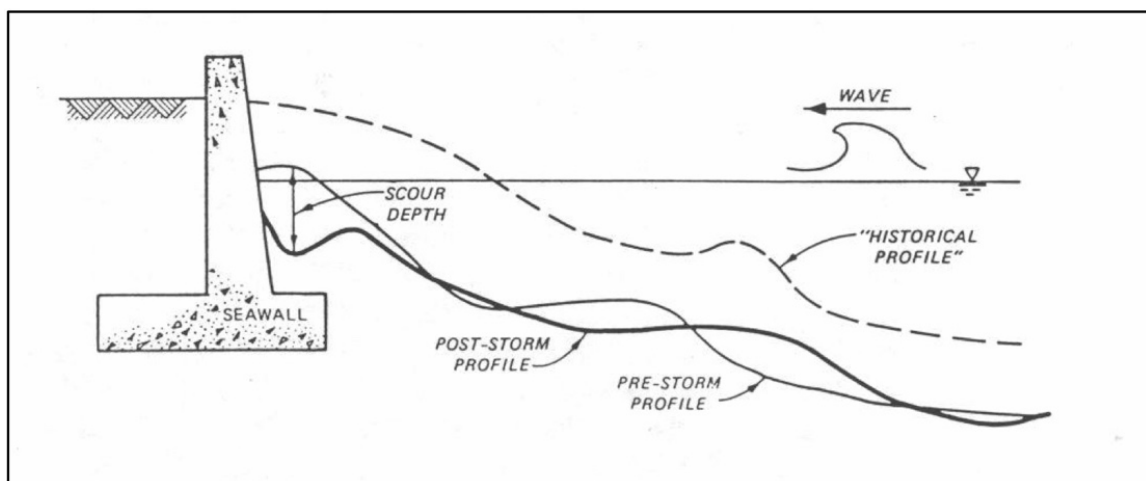


Figure 12.18. Scour due to breaking waves at a vertical wall (USACE 2002)

Use of a spill through or sloping abutment, instead of a vertical wall, reduces the maximum expected toe scour for all types of wave conditions. This is because the amount of wave reflection

from a sloping abutment is less than that from a vertical wall. The use of appropriately sized riprap or armor stone in front of the abutment also reduces wave reflection, ultimately reducing the scour while providing toe protection.

Another form of scour may occur when elevated water levels allow waves to impact approach embankments. Wave action can easily remove embankment soil and undersized riprap during storm events. This erosion can lead to undermining of the approach and flanking of the abutment wall. Figure 12.19 shows an example, where large waves occurring during Hurricane Ivan in 2004 removed small riprap and eroded soil from under approach slabs. The result was undermining and collapse of the approach slab. One way to prevent this damage is to provide an appropriate revetment cross-section including armor stone sized and graded to withstand wave attack (see Section 7.2).



Figure 12.19. Damage to bridge approach behind abutment due to wave action in a hurricane

Some states, like Florida, do not require abutment scour estimates when the design includes minimum abutment protection (FDOT 2012). The minimum abutment protection, including stone size and weight, is a function of either the design velocity (Isbash equation, HEC-23) or the design wave conditions (Hudson's equation, Section 7.2), with the larger of the two governing the design. In the coastal environment, armor stone sized to withstand wave attack is typically adequate to withstand movement by design flow velocities. Also, in fetch-limited situations boat wakes may serve as the design wave event. Section 12.6 provides additional information about scour countermeasures.

### 12.3.6 Wave-Induced Scour

Wave-induced pier scour occurs when the wave orbital velocities interact with bridge foundations and sediments. The literature suggests that the amount of wave-induced scour is typically much less than that estimated using the local pier scour equations mentioned previously (Sumer *et al.* 1992; USACE 2002). Equilibrium scour depths associated with wave action may attain a maximum value of about 1.3 times the pile diameter, though slightly larger multipliers are possible. While these scour depths are often small compared to those associated with currents, the

combination of waves and currents together lead to additional scour. Also, wave-induced scour may be large for complex pile groups as described below. Note that the time periods associated with severe wave attack during storm events are generally short—on the order of hours—and that the equilibrium scour depth due to waves may not occur during the design event.

**Equilibrium scour depths associated with wave action may attain a maximum value of about 1.3 times the pile diameter (though slightly larger multipliers are possible).**

Wave scour processes occur due to different mechanisms. A dimensionless parameter called the Keulegan-Carpenter (KC) number describes the relative magnitude of the flow and structure length scales as:

$$KC = (U_m T)/D \quad (12.8)$$

which describes the ratio of wave orbital velocity (flow) length scale to the size of the pile or pier, where:

$U_m$  = maximum nearbed wave orbital velocity (see Section 5.1)  
 $T$  = wave period; and  
 $D$  = pile diameter.

When  $KC < 1$ , interactions between the wave field and pile or pier dominate the scour process. These conditions typically occur due to very large pile or pier diameters. Wave-induced scour at the base of a bascule pier may fall into this category. When  $6 < KC < 1,000$ , vortex shedding of wave orbital velocities around the pile or pier govern scour formation. In this range, the flow length scale is approximately six times greater than the pile, so the structure is characterized as a slender element. Beyond  $KC > 1,000$  the scour process attains an equilibrium value due to the quasi-steady nature of the flow relative to the size of the pile.

Separate equations exist for the steady streaming (e.g., Sumer and Fredsoe 2001; Khalfin 2007) and vortex shedding (e.g., Sumer *et al.* 1992; Dey *et al.* 2006; Sumer *et al.* 2007) ranges of KC. However, a transition zone between them ( $1 < KC < 6$ ) is mostly ignored in published literature. An evaluation of numerous published scour studies by Webb and Matthews (2014) focused on this transition zone. They proposed a set of equations that covered the continuous range of KC values from 0.1 to infinity. Figure 12.20 shows the empirical data used to derive the equations and the best fit of the suggested equations to those data. The dashed gray line represents the best fit to all scour data considered in the analysis ( $N = 256$ ). The dotted black line is a more conservative upper bound equation that captures nearly 95 percent of all values considered in the analysis. These two equations are as follows:

$$S/D = 1.3 (1 - 0.99 \exp[-0.022 \{KC - 0.1\}]) \quad (\text{best fit}) \quad (12.9)$$

$$S/D = 1.3 (1 - 0.97 \exp[-0.05 \{KC - 0.1\}]) \quad (\text{upper estimate}) \quad (12.10)$$

where:

$S$  = equilibrium scour depth;  
 $D$  = pile diameter; and  
 $KC$  = Keulegan-Carpenter number.

For complex pier geometries, or where the spacing between piles is relatively small, individual scour holes will coalesce or the pile group will behave as one larger pile and a deeper scour hole

will form. The literature for estimating wave-induced scour for complex pier geometries and pile groups is still quite immature, but Webb and Matthews (2014) proposed a temporary solution for pile groups. When the ratio of the gap between piles ( $G$ ) to the individual pile diameter ( $D$ ) is less than five ( $G/D < 5$ ), an effective diameter ( $D_e$ ) is substituted in place of  $D$  in the scour prediction equations above. However, the individual pile diameter ( $D$ ) should still be used to estimate the value of  $KC$  in those equations. This methodology could be applied to Case 1 and Case 3 conditions illustrated by Figure 12.14.

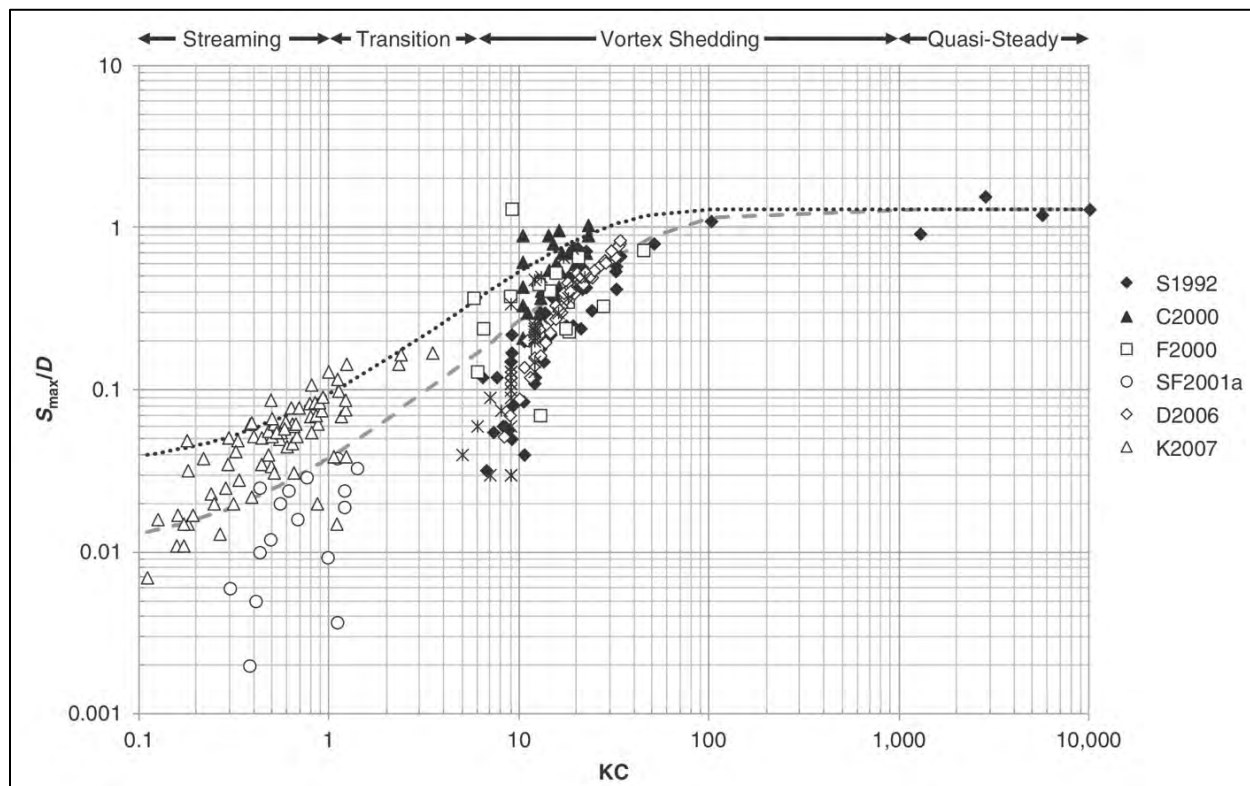


Figure 12.20. Wave-induced local pier scour (Webb and Matthews 2014)

This effective diameter, which is different than the one described for the FDOT scour equations, yields a cross-sectional pile area that is equivalent to the area of the entire pile group. The effective diameter is estimated as demonstrated in Figure 12.21):

$$D_e = \sqrt{4LW / \pi} \quad (12.11)$$

where:

- $D_e$  = effective diameter of the pile group;
- $L$  = length of the pile group; and
- $W$  = width of the pile group.

Breaking waves, as might occur during a storm event, will exacerbate the scour process. The FHWA and SDOTs have documented several situations where significant scour occurred during severe coastal events. For example, during Hurricane Katrina, upland portions of the US-90 Biloxi Bay bridge became subject to surge and waves. As seen in Figure 12.22, a large scour hole formed in the vicinity of a pile bent. While bridge superstructure failure occurred for other reasons (see Section 11.2), the size and extent of the scour hole was significant. This figure also shows the potential for large scour holes to develop around entire pile groups as previously noted.

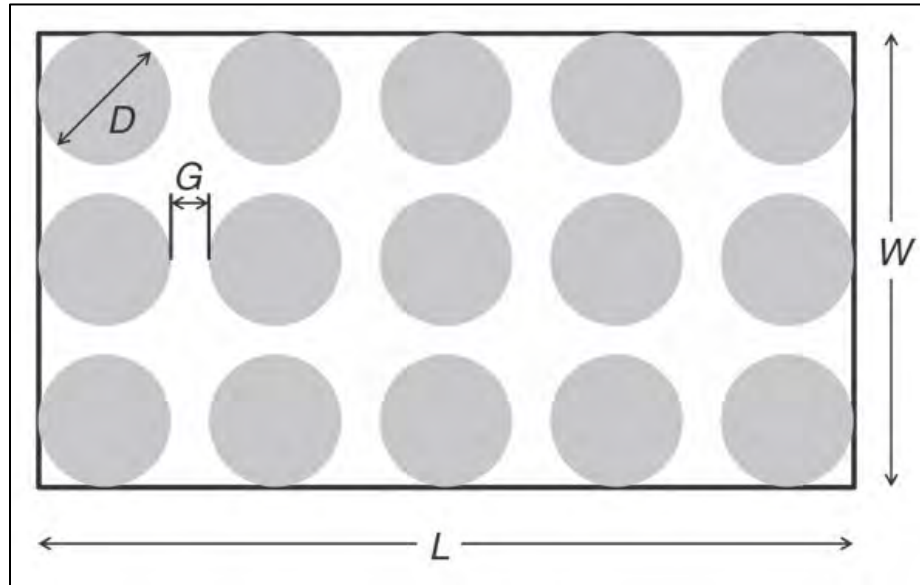


Figure 12.21. Definition sketch for effective diameter of pile groups for wave-induced pier scour (Webb and Matthews 2014)



Figure 12.22. Scour hole formed by Hurricane Katrina (permission to use photograph provided by Joe Krolak)

### 12.3.6.1 Example: Jensen Beach Causeway (Florida)

In 2005, the Jensen Beach, Florida causeway (Figure 12.23) experienced wave scour episodes. The passage of two successive tropical events along similar storm tracks produced waves within the embayment. These waves struck the causeway abutments and bridge piers producing scour to depths of over 30 ft (Figure 12.24). FDOT engineers had concerns about structural integrity of the foundations should a third storm event occur before installation of scour countermeasures.

In trying to determine what had occurred, FDOT expressed concerns that standard HEC-18 approaches did not predict such scour depths even when using advanced two-dimensional hydrodynamic and wave modeling. Only when investigators also considered and modeled, using SED2D, sediment transport resulting from both currents and waves did the simulations agree with post-event measurements (Glasser and Gosselin 2006).

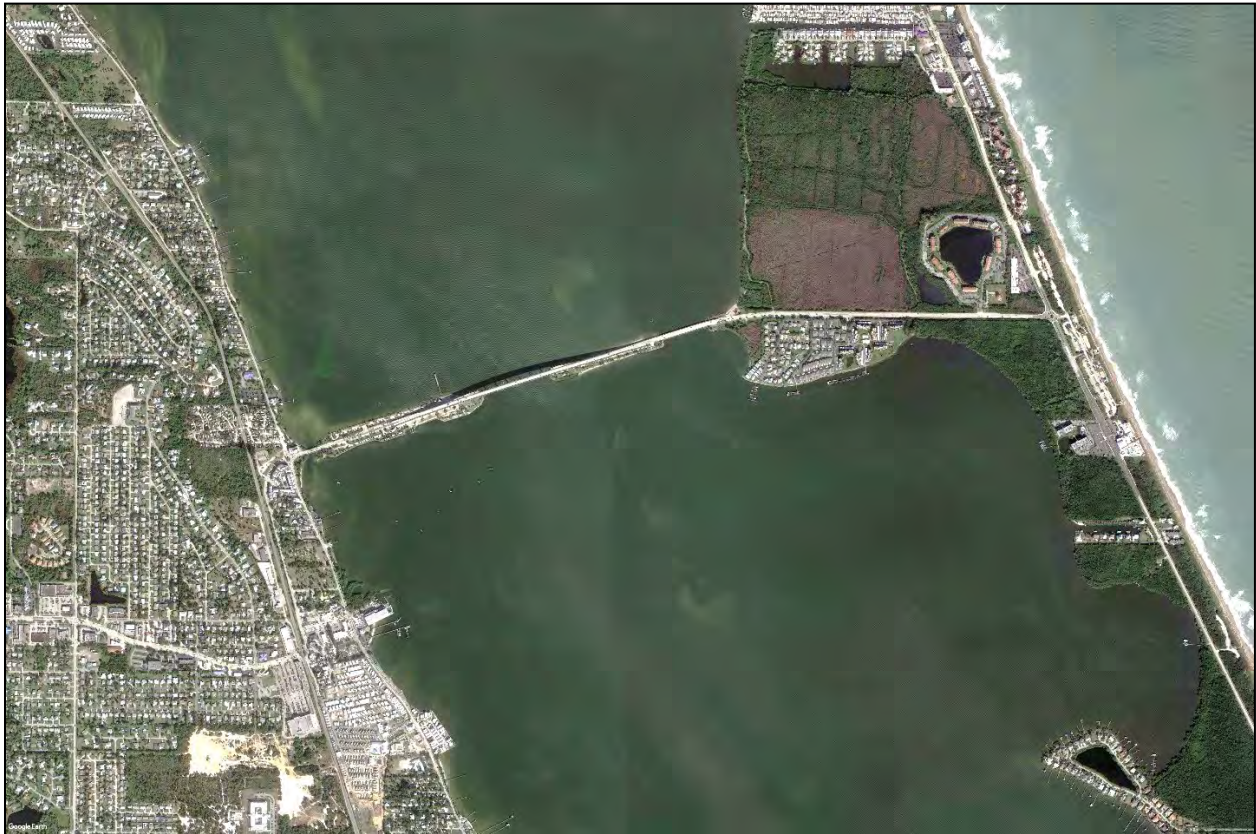


Figure 12.23. Jensen Beach Causeway bridge

### 12.3.7 Tsunami-Induced Scour

Tsunamis are a coastal hazard for many bridges along the US West Coast, Pacific Islands, and Alaska. Tsunami-induced scour around foundations is known to cause building collapse. However, tsunami-induced bridge scour is not a topic that has received much attention. While some information exists, the understanding has not matured to the point of describing all of the scour processes that can occur at a bridge crossing. Most published literature describes local scour. There are no specific methodologies or data for contraction scour in published literature.

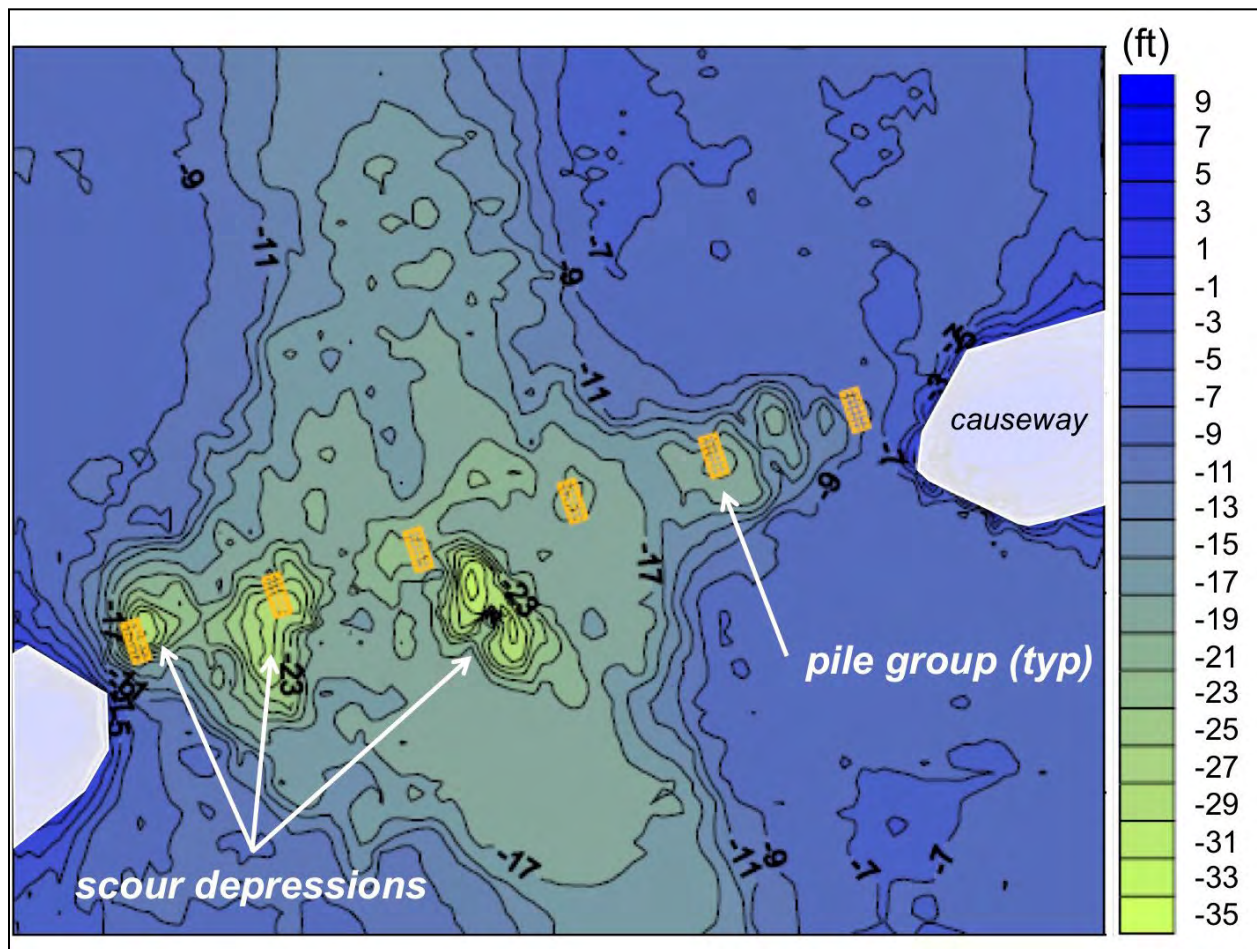


Figure 12.24. Jensen Beach Causeway bridge post-event scour bathymetry (2005)

Our current understanding of scour during tsunamis acknowledges contributions from both velocity/shear and pore pressure relief. Regarding the latter, published literature describes the potential effects of liquefaction on scour enhancement during rapid tsunami drawdown. An evaluation of scour at roadways and bridges reported in Francis (2006) found that a set of predictive equations proposed by Tonkin *et al.* (2003) explained observed scour depths very well for the 2004 Sumatra tsunami. The Tonkin *et al.* (2003) equations include a scour enhancement factor that accounts for the pore water mechanics that lead to liquefaction. However, their complex equations use input data that are not always readily available.

Extensive field observations following the 2004 Sumatra tsunami and the 2011 Tohoku tsunami found that scour depths were generally less than 10 ft (Francis 2006; Chock *et al.* 2013; Bricker *et al.* 2015). The vast number of scour depth observations contained in published reports may point to a practical limit on local scour due to the relatively short duration of tsunami inundation and drawdown.

Some very simple qualitative estimates of tsunami induced local scour are perhaps appropriate for screening bridge foundations for tsunami scour vulnerability. One relationship is cast in terms of a simple ratio of maximum scour depth ( $d_s$ ) to tsunami height ( $h_0$ ). Triatmadja *et al.* (2011) and Kuswandi *et al.* (2017) suggest that ratio ranges from 0.25 to 0.60. In other words, maximum estimated scour depths range from 25 percent to 60 percent of the tsunami height.

Another simple method for estimating scour depth is based on a percentage of the flow depth ( $d$ ). This concept, based on the work of Dames and Moore (1980), is presented in FEMA (2012) as guidance for estimating approximate scour depths resulting from tsunami inundation events. The scour depths are further refined based on soil type and distance from the shoreline (coast) in Table 12.1. For sand, the scour depths range from 35 to 80 percent of the tsunami flow depth depending on distance from the coast.

Table 12.1. Tsunami-induced scour guidance from Dames and Moore (1980) and FEMA (2012).

Soil Type	Scour Depth (% of $d$ ) ( $< 300$ ft from Shoreline)	Scour Depth (% of $d$ ) ( $> 300$ ft from Shoreline)
Loose sand	80	60
Dense sand	50	35
Soft silt	50	25
Stiff silt	25	15
Soft clay	25	15
Stiff clay	10	5

Triatmadja *et al.* (2011), who performed an evaluation of tsunami scour around coastal structures, found good agreement between measured equilibrium local scour depths and estimates using the HEC-18 local pier scour equations. ASCE (2016) outlines an Energy Grade Line (EGL) method for estimating the maximum tsunami inundation depth and velocity. This depth and velocity could be used along with the HEC-18 equations to arrive at a very conservative estimate of local pier scour.

Bricker *et al.* (2015) also found reasonable estimates using the HEC-18 equations. They compared eight separate scour equation predictions to field measurements following the 2011 Tohoku tsunami. The various methods underestimated or overestimated the measured scour depths by approximately a factor of 0.5 to 2, respectively. Of the methods evaluated, the HEC-18 equations for local pier scour and abutment scour were included and generally overestimated measured scour by a factor of 1.5. The tsunami bore propagates with a long period and the flow dynamics may have similarities with the riverine conditions for which the HEC-18 equations were derived, but not sufficiently long enough to produce equilibrium scour.

### 12.3.8 Time-Dependent Scour

Time-dependent scour equations have been suggested as more appropriate in the coastal environment. In addition to the typical physical processes, the short duration of the typical design storm is considered. Also, piers that are impacted by waves are subjected to very short duration pressure gradient fluctuations and shear stress variations which are difficult to quantify.

The University of Florida has conducted research and developed such a set of equations (Gosselin and Sheppard 1998; Miller 2003). The Florida equations use a time-marching solution for the depth of scour adjacent to bridge piers. In other words, the governing equation is discretized and solved at successive time intervals using the results of preceding time steps. Input time-varying estimates of depth-averaged storm surge velocities at the bridge are based on numerical modeling of the hydrodynamics. The Florida equations include calibration coefficients which are primarily based on laboratory investigations. Miller (2003) discusses how the equations can be used to estimate scour at prototype coastal bridges. Gosselin and Sheppard (1998) concluded that more research would be needed before meaningful relationships could be

developed for time-dependent local scour. More recent research on this topic exists but is limited to scour at the base of monopiles used in offshore structures. Those results may not be transferable to bridge foundations. Therefore, this remains an area of needed research.

### 12.3.9 Other Types of Coastal Scour

Scour also occurs at other types of coastal structures, such as a revetment, breakwater, groin, or jetty. Fewer semi-empirical scour equations exist for these rubble mound structures. In place of scour equations, rules of thumb are often applied to evaluate scour potential at the base of rubble mound structures.

At the toe of a sloping rubble mound structure, such as Figure 7.14, the maximum scour is often less than toe scour at an impermeable vertical wall under the same conditions. The CEM (USACE 2002) states that a conservative estimate of scour depth is then:

$$S_m < H_{max} \quad (12.12)$$

where:

$$\begin{aligned} S_m &= \text{maximum scour depth; and} \\ H_{max} &= \text{maximum wave height at the structure toe.} \end{aligned}$$

Decreasing a structure's reflection coefficient leads to similar reductions in scour depth. Flattening the structure slope and/or increasing its porosity reduce wave reflections and, therefore, scour depth. Currents flowing parallel to the structure in the presence of waves generate more scour.

Waves approaching at oblique angles to a structure will also lead to larger scour depths due to two separate effects. First, oblique waves generate currents that flow parallel to the structure. These currents are effective at transporting sediment away from the structure. Second, short-crested waves will increase in height along the structure due to the mach-stem effect (USACE 2002). Larger wave heights have the potential to cause more scour.

## 12.4 Bridge Scour Evaluation Methods

### 12.4.1 Tidally-Influenced Bridge Scour Evaluation

Many of the methods and tools used in the evaluation of riverine scour today are likely transferable to tidally-influenced bridges. Figure 12.25 shows a proposed workflow for evaluating design event scour at tidally-influenced bridge crossings. A practitioner should consider the downstream tidal/coastal boundary condition in evaluations of scour and bridge freeboard for tidally-influenced bridge crossings. The scour analysis should consider the design riverine discharge event, yielding the worst-case scour conditions, with a downstream boundary condition at the MLLW tidal datum. This set of conditions should lead to enhanced velocities and larger estimates of scour. Evaluating bridge freeboard, on the other hand, calls for an elevated downstream boundary condition. A likely choice there is a return period coastal flood elevation. Regulatory flood maps show the 100-yr return period (1 percent annual chance) coastal flood elevations. The corresponding Flood Insurance Study reports may provide coastal flood elevations for higher and lower probability events as well.

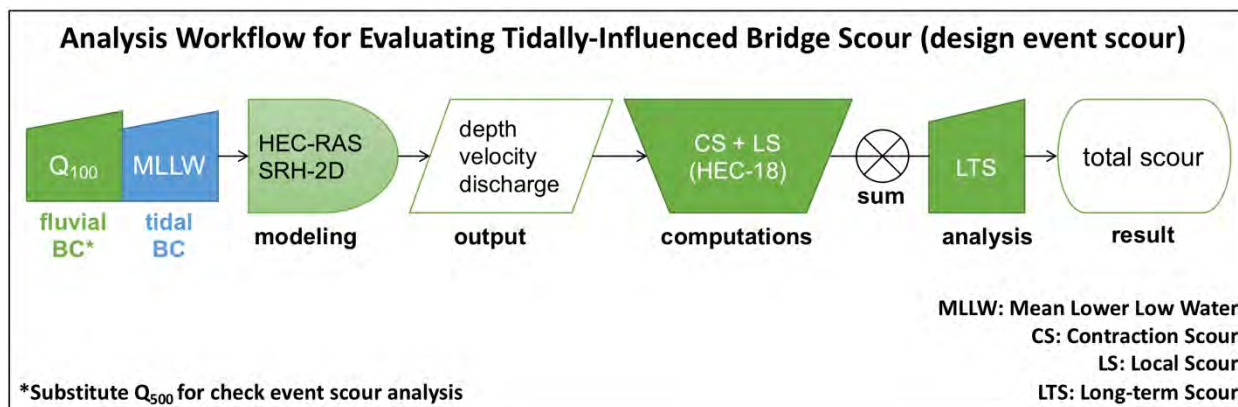


Figure 12.25. Proposed design scour analysis workflow for a tidally-influenced bridge crossing

### 12.4.2 Tidally-Dominated Bridge Scour Evaluation

The evaluation of scour at tidally-dominated bridges may involve consideration of fluvial, tidal, and coastal flood events, as well as their combinations, in order to determine which governs the design. Figure 12.26 illustrates a possible analysis workflow for evaluating design event scour at a tidally-dominated bridge crossing. Note that riverine and tidal event return periods, while specified as a 100-yr event in the graphic, should be selected to produce the worst-case scour for an appropriate design event.

Evaluation of the riverine and coastal flood events may call for different modeling approaches depending on the exposure of the bridge to wave action. A one-dimensional or two-dimensional HEC-RAS model, or a two-dimensional SRH-2D model, may be appropriate for estimating design event parameters for the riverine flood event. These are standard approaches for scour evaluation in the riverine environment that most practitioners use today.

Modeling the design coastal flood condition suggests, at a minimum, a two-dimensional unsteady hydraulic or hydrodynamic model. If the distance between the bridge and the coastal boundary condition is large, the influence of local storm winds on water levels and currents may contribute to flow velocity and depth in a substantial manner. A modeler can incorporate those processes into an appropriate coastal hydrodynamic model. Standard hydraulic models, like those listed above, generally do not have those capabilities. Appropriate hydrodynamic models will provide the flood depths, velocities, discharges, and wave characteristics needed to estimate contraction and local scour. Some coastal models, like the Coastal Modeling System and Delft3D, also simulate sediment transport and changes in bed elevation. However, sediment transport models have much greater uncertainties than hydrodynamic models.

When the effects of wind on waves, currents, and water levels are negligible, a two-dimensional unsteady hydraulic model, like SRH-2D, may prove useful. In this case, the coastal storm surge hydrograph serves as the downstream, time-varying boundary condition for the hydraulic model. The hydraulic model will propagate the coastal flood throughout the model domain in a manner like that of a hydrodynamic model. Obtaining or defining an appropriate coastal storm surge hydrograph is not a trivial matter. Representative hydrographs from past storms are often suitable candidates.

Tidally-dominated bridges may experience increased flow velocities and enhanced scour during the recession of a coastal flood event. As coastal flood waters recede, their velocities combine with fluvial inputs to the coast, thereby resulting in higher velocities (see Figure 12.3). Although the joint probability of fluvial discharge and coastal storm events is low in many cases (Wahl *et al.* 2015), simulating some appropriate amount of fluvial discharge may be prudent in order to

develop the worst-case scour conditions for the design and check event frequencies (e.g., 100-yr and 500-yr return period events). This is particularly true for crossings of tidal inlets (next section), where the inland bay or estuary can have a significant storage effect on ebb-directed velocities.

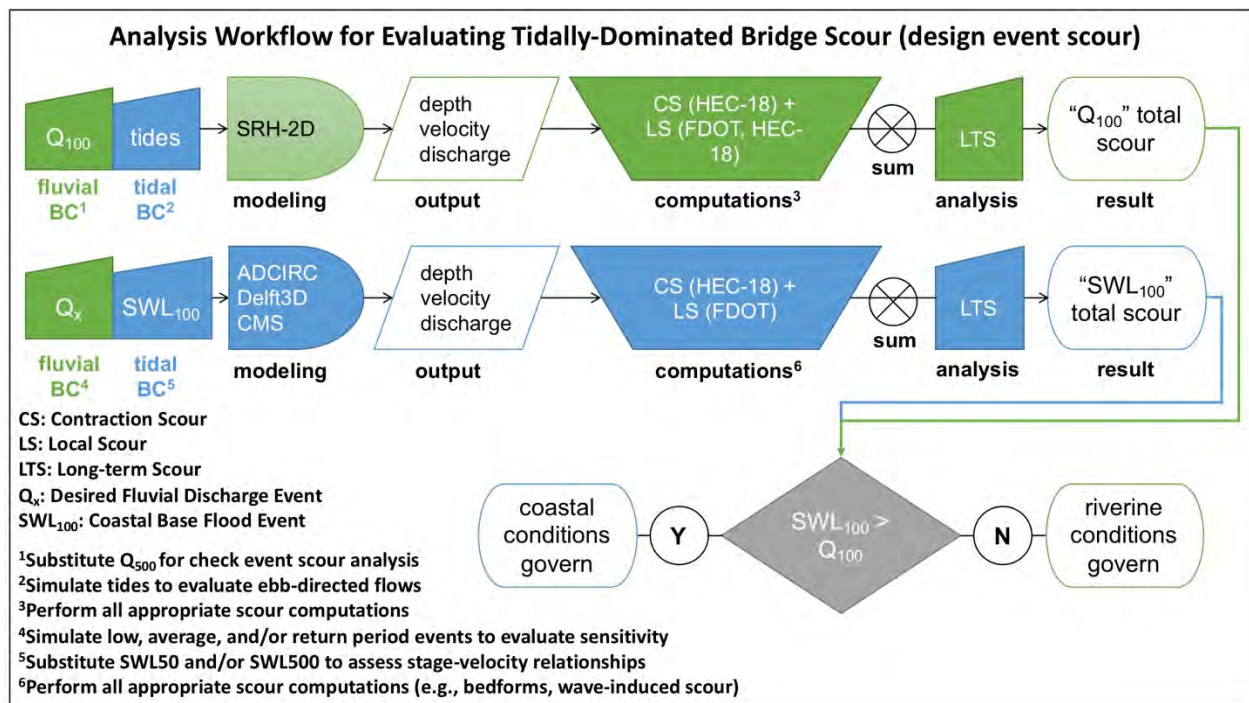


Figure 12.26. Proposed design scour analyses workflow for a tidally-dominated bridge crossing

### 12.4.3 Tidal Bridge Scour Evaluation

Determining the design event parameters for tidal bridges will, in almost all cases, call for the use of two-dimensional hydrodynamic models. The widespread availability and use of these models make it difficult to justify application of simple, analytical approximations of coastal flows. For example, the tidal prism method uses a lot of assumptions: the bay-ocean tidal phase lag, friction, entrance/exit losses, etc. Its results are strictly only applicable to simple tidal inlets and do not work well when applied in other coastal settings.

Figure 12.27 shows a proposed analysis workflow for evaluating design event scour at a tidal bridge crossing. Note that while the graphic indicates use of the 100-yr event return period, it is best practice to also simulate the 50-yr and 500-yr return period coastal events to evaluate the behavior of stage and velocity through the bridge opening.

The evaluation of scour at tidal bridges should consider the relevant design conditions that govern bridge hydraulics (see 23 CFR § 625, § 650.115 and § 650.117). Depending on the region of the US and the coastal setting, design conditions may be related to tides, tsunamis, hurricanes, nor'easters, or strong frontal systems (i.e. Great Lakes region). The selection of an appropriate hydrodynamic model will depend on which of these design conditions governs the depths, discharges, and velocities that lead to bridge scour. The practitioner should also consider relevant combinations of forcing in these models (i.e. tides+surge+waves, tides+surge+waves+discharge, and others).

It is necessary to simulate the design event parameters on both the rising and falling limbs of the coastal flood event, as one will likely dominate over the other. To that end, the simulation should include the complete time history of the event, not just one phase or stage. The practitioner should

consider the time histories of stage, velocity, and discharge during the design event to determine which combinations lead to greatest scour.

Finally, it should be stressed that defining the design event frequency for scour in the coastal environment is not analogous to the riverine environment. Coastal bridge hydraulic design is typically related to an event frequency based on extreme water levels. Riverine bridge hydraulic design is related to an event frequency based on discharge values. In the coastal environment, for example, the 100-yr return period water levels are often the basis of design for vertical clearance and loads. Scour estimates are often based on the velocities and depths corresponding to this design event threshold, though their values are also checked for the 500-yr event. But strictly speaking, the maximum velocity, and therefore the resulting scour depths, determined from such an event do not necessarily have the same return period or exceedance probability.

The maximum scour may occur for a coastal event with a stage that is lower or higher than the 100-yr event. See Figure 12.29 for an example illustration of stage and velocity data for a bridge crossing in Texas. In Figure 12.29 the velocity corresponding to the 100-yr coastal flood event is less than that of the 50-yr event. The practitioner should consider combinations of velocity and flow depth for enough design event return periods, or stages, to discern their potential trends before determining the appropriate conditions for estimating bridge scour.

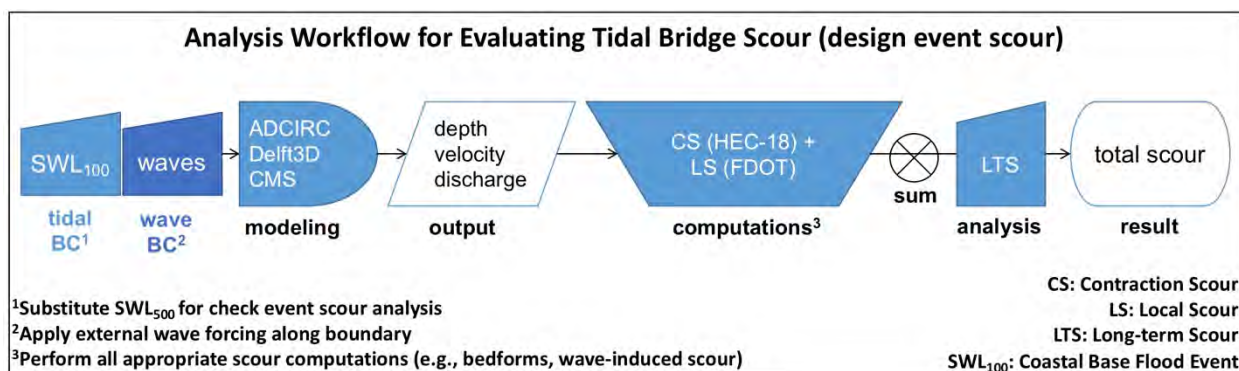


Figure 12.27. Proposed design scour analyses workflow for a tidal bridge crossing

#### 12.4.4 Example of Tidal Bridge Scour Calculations

The following text provides a general example of design event scour calculations for a tidal bridge crossing exposed to hurricane storm surge and waves. Note that some of the values used in the preparation of this example may not reflect actual design conditions or parameter values at this location. The bridge is located in Pensacola Bay, Florida along the northern Gulf of Mexico (see Figure 12.28). There is no appreciable fluvial input to this system and the bridge hydraulics are governed by water levels, waves, and velocities associated with extreme coastal storm events. The following example text summarizes the appraisal of long-term scour; the effects of bedforms on scour depths; horizontal contraction scour; local pier scour; and total resulting scour for the 100-yr design event and the 500-yr check event.



Figure 12.28. Location overview for the Pensacola Bay Bridge scour example

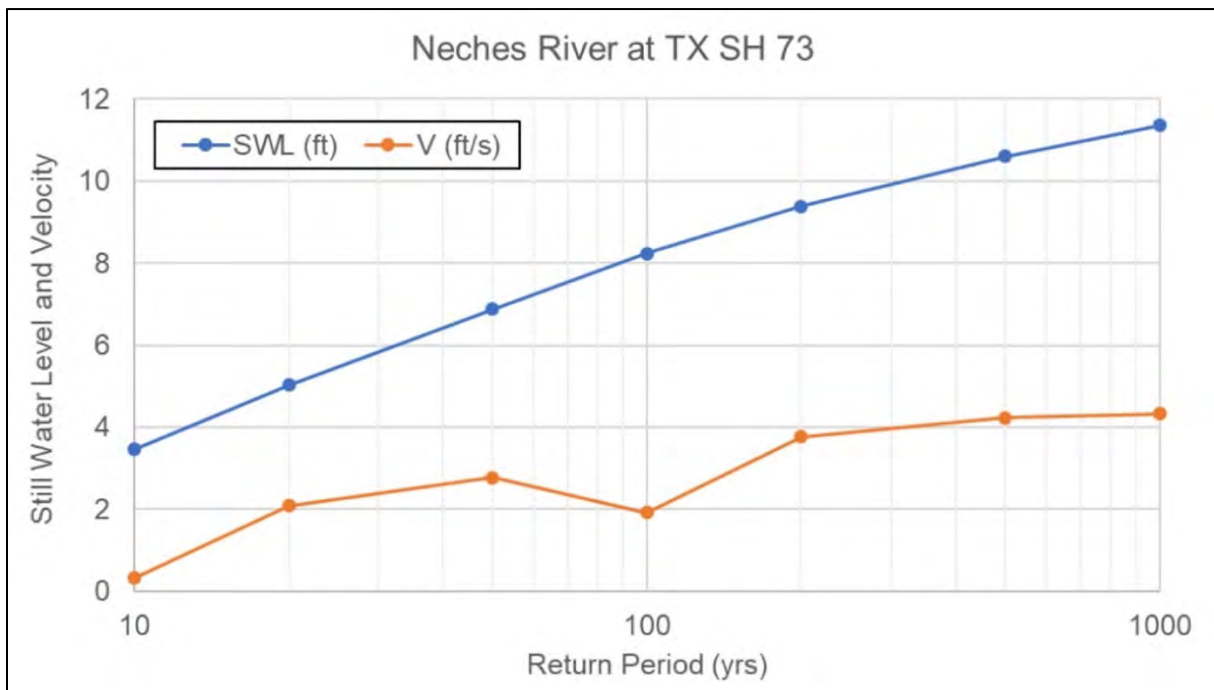


Figure 12.29. Return period still water levels and corresponding event velocity magnitudes on Neches River, TX

**Step 1 – Determine the long-term bed elevation changes:**

Historical bed elevation cross-sections parallel to the bridge alignment were reviewed using data provided as part of bridge inspection reports over a 15-year period. An average rate of erosion along the entire bridge length was calculated as -0.02 ft/yr. Over the specified 75-year service life of the bridge, this average erosion rate leads to an estimated 1.5-ft lowering of the channel bed, which is **rounded to 2.0 ft** for conservatism. This value for long-term scour will be added to the local scour values at the end of this design example. The lateral stability of the channel was similarly evaluated using the historical channel cross sections. The channel is stable and has not migrated during the period covered by those reports.

**Step 2 – Estimate bedform height and length:**

The potential for large wave-generated bedforms is estimated using the equations described in Section 12.3.2. A simulation of the design coastal storm event provides the water depths and wave characteristics (height and period) needed in this step. At a specific pile bent, the water depth is 38 ft, the wave height is 14 ft, and the wave period is 6 s. A sediment analysis determined the sediment angle of repose as 30 degrees. Using these parameters, the estimated bedform length and height are:

$$L_o = \frac{gT^2}{2\pi} = \frac{(32.2 \text{ ft/s}^2)(6 \text{ s})^2}{2\pi} = 184.5 \text{ ft}$$

$$L = L_o \sqrt{\tanh\left(\frac{2\pi d}{L_o}\right)} = (184.5 \text{ ft}) \sqrt{\tanh\left(\frac{2\pi[38 \text{ ft}]}{184.5 \text{ ft}}\right)} = 171.1 \text{ ft}$$

$$\lambda = 1.33 \frac{HL_o}{2L \cosh\left(\frac{2\pi d}{L}\right)} = 1.33 \frac{(14.5 \text{ ft})(184.5 \text{ ft})}{2(171.1 \text{ ft}) \cosh\left(\frac{2\pi[38 \text{ ft}]}{171.1 \text{ ft}}\right)} = 4.7 \text{ ft}$$

$$\eta = 0.32 \lambda \tan(\phi) = 0.32 (4.7 \text{ ft}) \tan(30^\circ) = 0.9 \text{ ft}$$

The calculated ripple height is **rounded to 1.0 ft** and incorporated into the total scour calculation at the end of this example.

**Step 3 – Estimate contraction scour:**

Horizontal contraction scour values are found using the Laursen equations in HEC-18. Conditions at the bridge were evaluated to determine whether scour occurs as live-bed or clear-water scour. For this example, the contraction scour occurs as live-bed scour and the Modified Laursen live bed contraction scour equation in HEC-18 provides the scour estimate. An appropriate “upstream” section was identified on either side of the bridge alignment, chosen such that flow streamlines were as straight and parallel as possible. The Laursen equations were applied for each “upstream” section to determine the maximum contraction scour during the rising and falling limbs of the storm surge hydrograph. The width of, and discharge across, each “upstream” section was extracted from the storm surge model output. The resulting live-bed contraction scour calculations produced a **100-yr design event value of 2.0 ft and a 500-yr check event value of 8.1 ft**.

**Step 4 – Estimate local pier scour:**

Estimates of local scour around the complex bridge piers (Case 1, Figure 12.14) were found using the FDOT (2005) method, pier and pile foundation design sections, sediment characteristics, and storm surge model output. These calculations account for additional local scour induced by the foundation of the twin span alignment, as well as scour associated with the remains of a nearby abandoned bridge foundation. The influence of adjacent and abandoned foundation elements on

local scour should always be evaluated, particularly when the ratio of effective pile diameter to the distance between foundations is small. Taking these issues into account, the estimated local pier scour at a representative bent location is **15.3 ft for the 100-yr design event, and 16.6 ft for the 500-yr check event**. Note that FDOT (2005) contains detailed calculation examples for Case 1, Case 2, and Case 3 complex bridge pier geometries.

#### Step 5 – Estimate wave-induced scour:

Because of the greater depths along this bridge alignment, the contributions of wave-induced scour to local pier scour are expected to be small. Wave-induced scour could potentially be important for approach foundations that experience small velocities, due to friction from shallow flooding depths, during surge events.

The foundation design for this bridge contains an array of 24-inch-square concrete piles below a rectangular cap. The piles are spaced 10 ft apart in the longitudinal direction and 15 ft apart in the transverse direction. Therefore, the gap to diameter ratio is greater than or equal to 5 in both cases; the effective diameter does not apply under these conditions. The equations described in Section 12.3.4 are applied to estimate the wave-induced scour at each foundation pile as follows:

$$U_m = \frac{\pi H}{T} = \frac{\pi(14 \text{ ft})}{6 \text{ s}} = 7.3 \text{ ft/s}$$

$$KC = \frac{U_m T}{D} = \frac{(7.3 \text{ ft/s})(6 \text{ s})}{(2 \text{ ft})\sqrt{2}} = 15.6$$

$$\frac{S}{D} = 1.3 (1 - 0.99 \exp[-0.022\{KC-0.1\}]) = 1.3 (1 - 0.99 \exp[-0.022\{15.6-0.1\}]) = 0.38$$

$$S = 0.38 [(2 \text{ ft})\sqrt{2}] = 1 \text{ ft}$$

The contribution of wave-induced scour to local pier scour is **approximately 1 ft**.

#### Step 6 – Calculate total scour:

The total scour is the sum of values determined in Steps 1-5. Note that the scour values calculated in Steps 2, 4, and 5 are location-dependent and will be unique for each pile bent. The values determined in Steps 1 and 3 are applied to each bent location. Therefore, for the bent location selected in this example, the total estimated scour is as follows:

$$100\text{-yr Total Scour} = 2.0 \text{ ft} + 1.0 \text{ ft} + 2.0 \text{ ft} + 15.3 \text{ ft} + 1.0 \text{ ft} = \mathbf{21.3 \text{ ft}}$$

$$500\text{-yr Total Scour} = 2.0 \text{ ft} + 1.0 \text{ ft} + 8.1 \text{ ft} + 16.6 \text{ ft} + 1.0 \text{ ft} = \mathbf{28.7 \text{ ft}}$$

#### Step 7 – Estimate abutment scour:

The abutments at this bridge are only exposed to wave action during the design flood event. The method of Hughes and Fowler (1991), described in Section 12.3.5, is used to estimate the local toe scour due to nonbreaking irregular waves. Using the same values described earlier for maximum wave orbital velocity, wave period, and water depth the calculations are as follows:

$$S_m / [(u_{rms})_m T_p] = 0.05 / [\sinh(2\pi d / L_p)]^{0.35} = 0.05 / [\sinh(2\pi(38 \text{ ft}) / (171.1 \text{ ft}))]^{0.35} = 0.04$$

$$S_m = 0.04 (7.3 \text{ ft/s})(6 \text{ s}) = 1.8 \text{ ft}$$

The local toe scour under breaking wave conditions could be substantially larger, growing to approximately 80 percent of the flood depth at the abutment wall under the design event conditions.

## **12.5 Scour Appraisal Methodologies**

### **12.5.1 Low-Risk Crossings**

Small, low-risk bridges crossing tidal creeks and minor tributaries in the coastal environment are unlikely candidates for sophisticated coastal hydrodynamic modeling. For very small bridges or bridge openings, their scale may actually prohibit all but the most advanced forms of numerical modeling. However, for these bridges (as per 23 CFR § 650 subpart C), an owner may determine whether they may be unstable as a result of scour based on either the observed or evaluated scour condition (23 CFR § 650.305). For the evaluated condition, this requires analysis of scour, which typically requires hydraulic computations of flow velocity and depth (see 23 CFR § 650.117). One simple way to estimate flow velocity for a given flood event is to consider the phase speed of a shallow-water wave described in Section 5.1 (Equation 5.6). This is a conservative estimate of velocity that increases with the total flow/flood depth. This estimate provides a magnitude but no direction. For very small bridge openings the flow direction may align with the tidal creek or tributary that conveys the flow. If this is not the case, assume an orientation or skew that yields a conservative estimate of bridge scour.

### **12.5.2 Typical Crossings**

The evaluation of scour at most typical bridge crossings will almost always call for the use of an appropriate numerical model. Exceptions may include cases where design event data are available within a database, or where the flood depths, discharges, and velocities can be estimated with some certainty. These exceptions notwithstanding, it is difficult to justify not using numerical models to estimate scour at all but the smallest of bridges in the coastal setting. For tidally-influenced bridges, this may be a 1D or 2D hydraulic model. The HEC-RAS (1D) and SRH-2D (2D) models mentioned previously are appropriate for bridge crossings over clearly definable rivers or streams not directly exposed to open waters and/or substantial wave action. For tidally-dominated bridges adjacent to open water, for tidal bridges crossing open water, and for non-tidal bridges exposed to coastal processes, the use of 2D coastal hydrodynamic and/or wave models is necessary.

Numerical models are typically used in a complete bridge hydraulics study. The flood depths, discharges, velocities, and waves predicted by these models serve as input to the contraction and local scour equations mentioned previously. Because the scour prediction equations were derived for steady, uniform flow conditions, and because the coastal flood events are typically of short duration (on the order of a few hours), ultimate scour may not be reached at some coastal bridges. Due to the uncertainties inherent in defining the storm event, the model predictions, and those of the scour equations themselves, it is difficult to state that the resulting scour estimates are conservative. Experience and sound engineering judgment should be relied upon when evaluating the scour predictions for coastal bridges.

### **12.5.3 Special Cases**

More sophisticated numerical models or reduced scale physical models are useful in resolving uncertainty or complexity in the scour predictions. The practitioner may consider these more comprehensive evaluation methodologies when the existing scour equations yield questionable results, or when the bridge crossing and coastal setting are extremely complex. This level of

analysis is likely only justifiable for some bridges as the level of effort (i.e. time and cost) is considerable.

The use of more sophisticated numerical models may include the direct simulation of sediment transport and/or morphologic updating. These models are typically two- or three-dimensional (3D) models. For very complex coastal settings, the use of a 3D model is preferable. Furthermore, the use of a morphologic model can explicitly simulate the positive feedback that occurs between hydrodynamics and morphology as the bed elevation changes. It may be impractical to resolve the disparity in spatial scales small enough to simulate development of local scour around a pier as well as the hydrodynamic conditions of the entire bridge crossing, simultaneously. In such cases, a larger scale numerical model could be used to first develop an estimate of the contraction scour, with those conditions then used as input to higher resolution numerical models that better refine hydrodynamics and sediment transport around a set of bridge piers or the bridge abutment and approaches.

The development of reduced scale physical models is challenging but may be necessary in some special situations. Here the physical dimensions of the problems are scaled down from prototype (true) to model (reduced) scale using Froude scaling. The horizontal and vertical scaling may be the same or distorted depending on the geometry of the problem and the size of the laboratory facility. In order to be truly compatible between the prototype and model scales, Reynolds scaling would also have to be satisfied for the sediments. However, simultaneously satisfying Froude and Reynolds number scaling in a laboratory is often impossible. Scour experiments conducted at reduced scale often assume that the Reynolds scaling can be relaxed due to the fully turbulent conditions typical of design events. For those conditions, the variation in Reynolds number is said to be insignificant for scour development.

## **12.6 Scour Countermeasures**

Scour prevention, or scour mitigation, can be achieved through the use of countermeasures. A countermeasure is typically a layer or some arrangement of less erodible material on the seabed or wherever scour is expected to occur. The countermeasure is typically placed near the toe, or at the base, of the structure where scour is to be prevented. A revetment prevents erosion of earthen embankments exposed to flow or wave attack. However, the toe of the revetment is also vulnerable to scour so it is designed with scour countermeasures integrated into its cross-section (see Section 7.4). A vertical wall can need a separate countermeasure as part of its design.

In the coastal environment, scour countermeasures often consist of scour blankets, appropriately sized riprap or armor stone, and possibly even precast reinforced concrete armor units. For all of these examples, an appropriate geotextile fabric or layer of adequate bedding stone should be used as an underlayment to prevent piping of the soil through the scour countermeasure. In the case of scour blankets, also called marine mattresses, these fabrics are often integrated into the blanket/mattress framework.

The design of scour countermeasures depends on two primary criteria. First, the stability of the countermeasure itself should be analyzed under design conditions. If the countermeasure is exposed to strong currents and wave action, both stability criteria should be satisfied, resulting in stone sizes for each criterion. Unlike revetments that only consider waves, and thus can apply Hudson's equation (Section 7.2), designers need to consider additional criteria to also capture current. Eckert (1983) suggests that the larger of the two stone sizes be increased by a factor of 1.5 to resist the combination of waves and currents. The stability of countermeasures to resist strong currents can be determined using the Izbash equation in HEC-23. Armor unit stability to wave attack can be evaluated using Hudson's equation (Section 7.2).

The stability of marine mattresses and special concrete armor units may use alternative methods. Equations for sizing scour apron stone and for evaluating scour blanket stability in current fields are outlined in the CEM (USACE 2002).

Second, the appropriate extent or dimensions of the countermeasure needed to protect against scour and/or slip failure should be estimated. The extents of the countermeasures will be different for each type of structure. The following methods provide suggested scour apron widths for cantilevered or anchored retaining walls, gravity retaining walls, sloping structures, and piles.

For cantilevered or anchored retaining walls, providing a scour apron can prevent scour at the toe and/or to provide the stability needed to prevent slip failure. Failure of the apron's edge may occur due to bed scour and/or lowering of the channel bottom over time. Consult FHWA (2019) for additional information on shallow abutment foundation countermeasures for tidally-influenced and tidally-dominated bridge crossings.

Eckert (1983) provides equations for the recommended scour apron width based on geotechnical conditions and hydrodynamic conditions, where the appropriate size will be the larger of the two estimates (see definition sketch Figure 12.30). To protect against slip failure, Eckert (1983) recommends that the scour apron width ( $W$ ) be:

$$W = d_e / \tan(45^\circ - \phi/2) \approx 2.0 d_e \quad (12.13)$$

where:

- $d_e$  = depth of wall penetration below the seabed; and
- $\phi$  = sediment angle of internal friction.

The width of the scour apron to satisfy hydrodynamic conditions should be taken as the greater of the following two expressions:

$$W = 2.0 H_i \quad (12.14)$$

or,

$$W = 0.4 d_s \quad (12.15)$$

where:

- $H_i$  = incident wave height; and
- $d_s$  = depth at the toe of the structure.

In the case of gravity retaining walls, the scour apron need not be as wide as for cantilevered walls due to the lack of slip failure vulnerability. Eckert (1983) recommends a scour apron width approximately equal to the height of the incident nonbreaking wave.

Mitigation of local scour at the base of existing at-risk piles or piers may be accomplished through the use of scour aprons as well. For individual piles exposed to tidal flows, Hoffmans and Verheij (1997) recommend an apron width that is at least four times the pile diameter in each direction parallel to the dominant tidal velocities, and a width of at least 2.5 times the pile diameter in each transverse direction. Therefore, the total apron size would be 8D in the streamwise dimension, and 5D in the spanwise dimension.

An alternative formulation by Carstens (1976) relates the scour apron width to the maximum scour depth ( $S_m$ ):

$$W/S_m = F_s / \tan \varphi \quad (12.16)$$

where:

- $F_s$  = a factor of safety; and  
 $\varphi$  = sediment angle of repose.

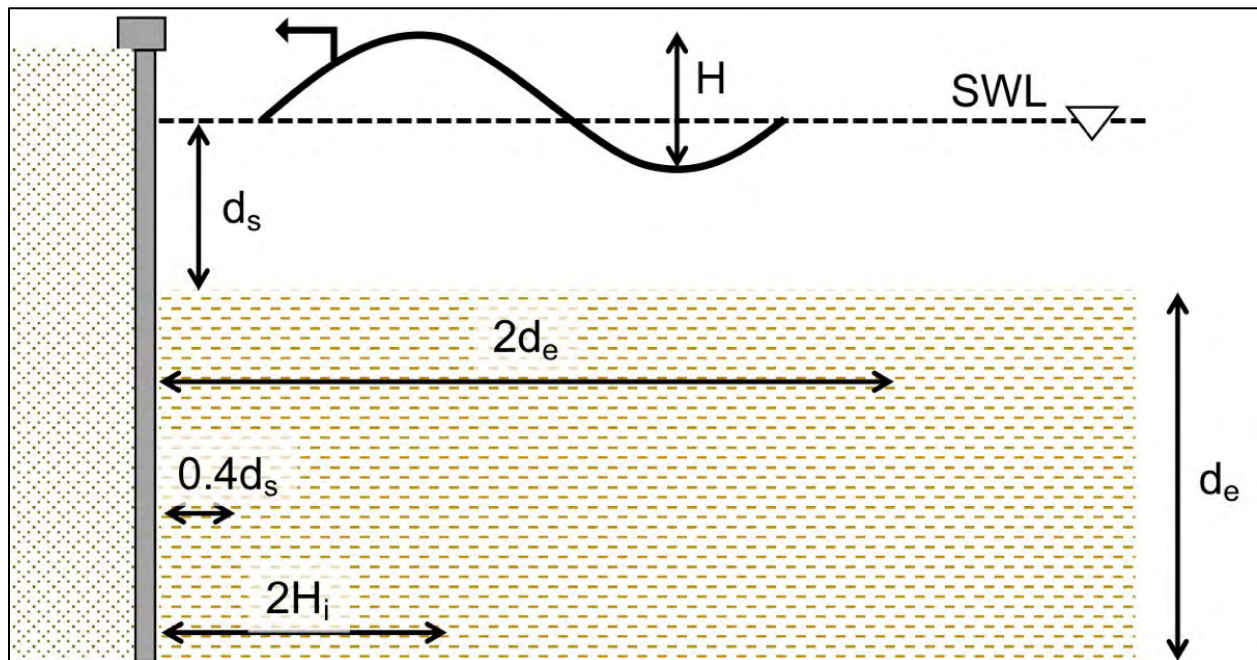


Figure 12.30. Definition sketch for scour protection at the base of vertical walls

The design of coastal scour countermeasures for complex pier geometries and pile groups, however, lacks general processes and applicability. This is partially a result of the unique conditions encountered at coastal bridges. For example, as described in Section 12.3.1, addition of very large dumped rip rap at complex piers in the Indian River Inlet exasperated the scour formation. As related in that earlier discussion, after years of continued scour and stability concerns, the “countermeasure” for this crossing required spanning the entire inlet with a replacement bridge. Likewise, various coastal conditions at Oregon Inlet resulted in situations where scour removed bed material almost entirely at specific bridge pile groups, necessitating emergency remediation (e.g., lane and bridge closures, adding concrete jacks, building pile crutches, forced sand replacement, etc.) (Henderson and Krolak, 2016). After such episodes, the bridge owner engaged a multi-disciplinary team that instituted a comprehensive and aggressive scour monitoring plan of action with a variety of countermeasures (Henderson and Krolak, 2016). The first example demonstrates that simply adding countermeasures does not resolve the issue. The second demonstrates that not acting could have potentially disastrous consequences. However, the lessons learned in both examples were that any scour countermeasure for such complex coastal bridges requires a proactive approach, working through a multi-disciplinary team (including coastal engineers), and focused on solutions that encompass the service life of the structure.

Scour protection at the base of piles may also be provided to withstand wave-induced scour. While specific relationships are lacking, an estimate of the scour apron dimension is approximately twice the expected scour depth (USACE 2002). This general approximation of scour apron size has many additional uses for mitigating wave-induced erosion and is applied in some upland situations as well to protect against erosion initiated by wave overtopping of walls and revetments.

Additional considerations for scour countermeasures at highway bridges are found in HEC-23 (Lagasse *et al.* 2009). However, caution should be exercised when using these countermeasures in the coastal environment. The unsteady, multi-directional flow conditions and wave action make the design of scour countermeasures unique to the coastal environment. The Coastal Engineering Manual should be taken to heart:

*“It should be recognized that scour protection in coastal engineering differs from scour protection encountered in typical transportation projects both in the magnitude of the forces and in their reversing directions. Though scour protection design for highways is a well-developed art with extensive documentation, the direct transferal of highway riprap experience to coastal problems is usually unsatisfactory.” Page III-1-4, USACE (2002)*

## **Part 4 – Coastal Highway Vulnerability Assessment**

*Page Intentionally Left Blank*

## Chapter 13 - Engineering Risk at the Coast

The broad concept of “risk” typically captures both (a) the probability of an extreme event, and, (b) the consequences to human health, the environment and economic activity associated with that event. This chapter discusses the tools appropriate for the quantitative engineering evaluation of probability and risk applied to coastal highways. While the general concepts of return period and probability of occurrence are exactly that same as for all of engineering, the coastal analysis tools differ significantly from riverine flooding tools.

### 13.1 Return Period and Probability of Occurrence

This section discusses the common engineering concept of design storm based on return period, e.g. the “100-year storm” or the “1%-Annual-Chance-Flood.” This section also discusses a common misunderstanding of risk levels implied by the return period terminology.

Extreme natural events, such as river floods or coastal floods, vary in ways that appear to be random and can often be considered to be random for the purposes of engineering analysis and design. Techniques of probability and statistics are used to analyze these random flood events in water resources engineering. Historical records are used to understand the frequency of occurrence of a range of flood event magnitudes.

Probability of exceedance is often referred to in terms of the average “**return period**,”  $T$ , of a given flood magnitude. For example, a flood with a return period of 100 years has a 1 percent (1/100) probability of being equaled or exceeded in any year. Note that the return period is the average number of years between floods equal to or greater than this magnitude. Return period,  $T$ , is related to probability of exceedance,  $P_e$ , by the equation,

$$P_e = 1/T \quad (13.1)$$

It should be emphasized that the return period or recurrence interval  $T$  is a long-term average. It is an average over a very large number of floods over a very long time span. To fully determine this average, one would need to observe and analyze a very long record of floods – perhaps thousands of years of floods. These fundamental concepts of return period are explained in many engineering textbooks (e.g. Roberson *et al.* 1998) and other FHWA manuals including HDS 2 (FHWA 2002).

**The use of the term “1%-annual-exceedance-probability-flood” is often preferred to the equivalent “100-year flood” which confuses the general public, including decision-makers.** For example, to avoid such potential confusion, the FHWA regulation 23 CFR § 650.105(b) defines the base flood as “... the flood or [storm] tide having a 1-percent chance of being exceeded in any given year.” The flood with a return period of 100 years ( $P = 0.01$ ) has a 0.01 or 1% chance of occurring or being exceeded this year or any year. Likewise, a 50-year flood has a 2% chance of occurrence in any year. A layperson may assume a 100-year flood is not going to occur for another hundred years or that there is only a 1% chance it will occur in the next 100 years. The terminology may not adequately communicate the risk (nor address statistical complications, such as a non-homogeneous historical record).

From the perspective of an asset’s service life (or design life), the longer the service life, the greater the risk of such an extreme event level occurring. The probability that a design flood level will be equaled or exceeded at least once during the service life of the project (the probability of occurrence)

$$P = 1 - (1 - 1/T)^n \quad (13.2)$$

where:

- P = probability that the design flood level will be equaled or exceeded in n years  
 n = design or service life, years  
 T = the return period of the design storm, years

This equation is a reduced form of the binomial distribution common in quantitative risk analysis (see Equation 4.81 of Hydraulic Design Series No. 2, 2<sup>nd</sup> ed., FHWA 2002).

For example, if the design storm for a transportation asset is a 50-year storm,  $T = 50$  and the design or service life is 30 years, then the probability of occurrence in the next 30 years is  $P(\text{occurrence in 30 years}) = 1 - (1 - 0.02)^{30} = 0.45 = 45\%$ . There is a 45% chance that the 50-year flood or greater will occur at least once in the next 30 years.

**There is a 39% chance that the 100-year storm will occur in 50 years... by definition!**

Figure 13.1 shows a family of lines corresponding to different risk levels expressed as  $P =$  probability of occurrence, as a function of  $T =$  design return period, and  $n =$  years of service. The same relationship is shown in Table 13.1. For example, as shown in both Figure 13.1 or Table 13.1, the probability of occurrence of a 100-year storm increases from 1% for a service life of 1 year (by definition), to about 10% for a service life of 10 years, 18% for a service life of 20 years, 39% for a service life of 50 years, and about 63% for a service life of 100 years. In other words, there is a 63% chance that the 100-year flood will be equaled or exceeded at least once in the next 100 years.

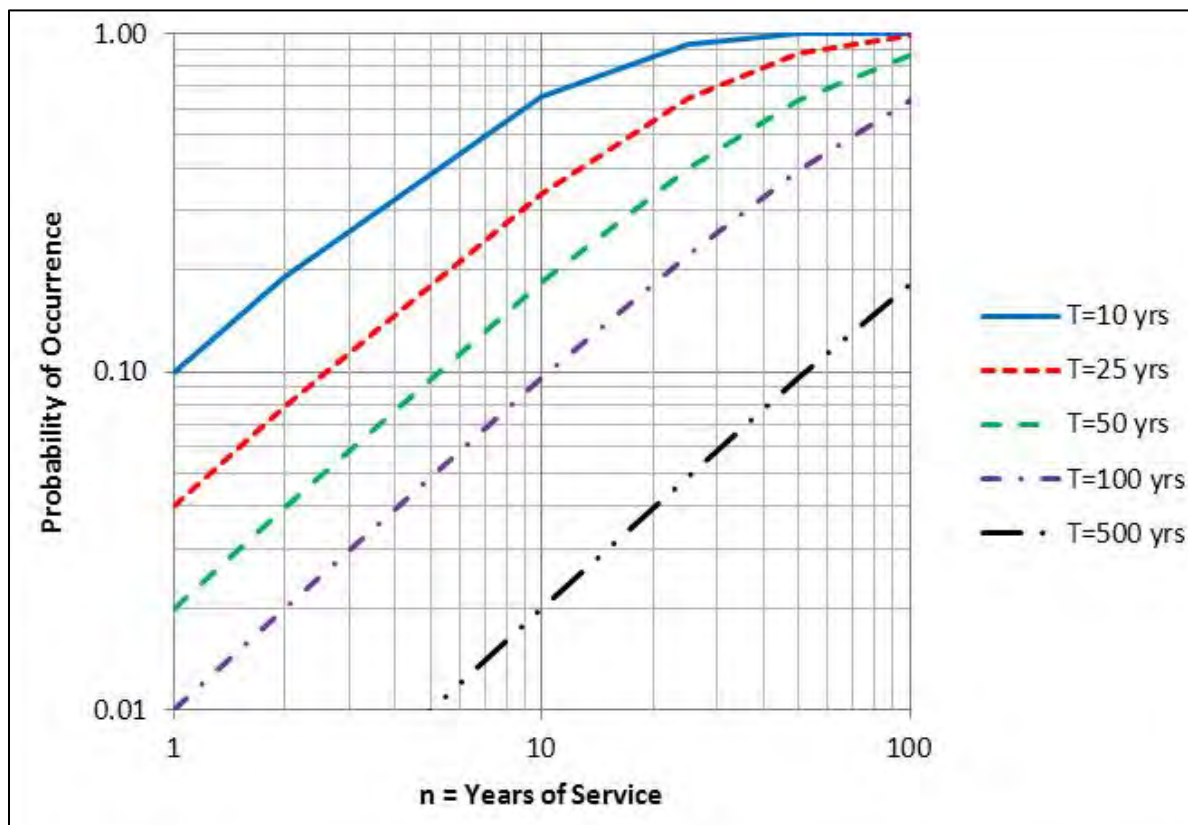


Figure 13.1. Probability of occurrence as a function of return period,  $T$ , and years of service,  $n$

Table 13.1. Probability of extreme event occurrence for various periods of time

Length of Service (Years)	Frequency – Recurrence Interval					
	10-year	25-year	50-year	100-year	500-year	1,000-year
1	0.10	0.04	0.02	0.01	0.002	0.001
10	0.65	0.34	0.18	0.10	0.02	0.01
20	0.88	0.56	0.33	0.18	0.04	0.02
25	0.93	0.64	0.40	0.22	0.05	0.02
30	0.96	0.71	0.45	0.26	0.06	0.03
50	0.99+	0.87	0.64	0.39	0.10	0.05
75	0.99+	0.95	0.78	0.53	0.14	0.07
100	0.99+	0.98	0.87	0.63	0.18	0.10

Another way to use Figure 13.1 or Table 13.1 is to consider what design storm level is needed to attain a given risk level. For example, it might be desired for some facilities to reduce the probability of failure to a smaller level, say a 5% risk of occurrence in the next 25 years. Figure 13.1 or Table 13.1 show that the design storm level would have to be T = 500 years to attain that low level of probability. For extremely important facilities, even less frequent design storms can be adopted. For example, 2,000-year events are used for some spillway designs or some structural designs for earthquake forces and some designs related to nuclear power plants consider design return periods of up to 100,000 years. Design storm return periods used for the evaluation of most types of transportation infrastructure range from 10-year to 500-year depending on the type of infrastructure.

A transportation asset may not experience any damage with a flood level that exceeds its design level. The relationship between flood level and damage depends on numerous other factors including the type of asset (bridge, tunnel, or roadway), the characteristics of the asset (on piles, at grade, on an embankment, etc.), the site-specific topography, and the wave heights at that site. Damage mechanisms common in coastal transportation systems are discussed briefly in Section 15.1 – Typical Coastal Damage Mechanisms.

## 13.2 Coastal Storm Flood Frequencies

This section discusses how the storm surge elevation - return period relationship is typically estimated in coastal areas. Storm flood elevation is often the parameter of primary interest in coastal hazards assessment because it is often responsible for damage, along with waves (which are controlled in part by flood level). The established, general approach for estimating the frequency, or return period, of coastal storm levels was initially developed in the 1970's with the advent of modern computing. It has evolved with better computers and improved methodologies. The numerical modeling involves investments in both computing power and trained personnel skilled in coastal modeling. The approach is fairly complex and varies in different parts of the US because of the regional differences in key coastal processes.

### 13.2.1 Atlantic and Gulf Coast Surge Frequencies

The general approach for estimating the surge-frequency relationship along the Atlantic and Gulf Coasts was originally developed in the 1970's and 1980's by NOAA, USACE, and FEMA. The general approach is to numerically simulate the full complexity of the physical processes

controlling coastal flooding and to derive statistics from the results (the local response) of that analysis (FEMA 2003). Multiple runs of numerical, hydrodynamic storm surge models with some frequency analysis controlling the input modeled storm parameters are used. The surge-frequency relationship is then determined at all locations based on the surge results of the multiple model runs. The numerical model provides the link between the known statistics of the generating forces and the desired statistics of coastal flood levels. The primary reason for the development of such an approach is that the historical coastal storm surge elevation at any location is very dependent on geography and on the path, or track, taken by any individual storm. Thus, if any given historical storm had taken a slightly different track the surge at many locations would have been different.

**Simulating many “synthetic” coastal storms, which have the same statistics as historical storms, results in a reasonable estimate of coastal flood frequency statistics.**

Computer modeling allows for consideration of the impact of similar storms with different tracks and different strength parameters (wind speed, barometric pressure, forward speed, size etc.). Sometimes historical, actual storms are input to the model. “Synthetic” or hypothetical storms which have not actually occurred but could have, based on the frequency analysis of the storm parameters of the historical storms, can also be included so that a realistic coastal flood risk estimate at all locations can be developed. This general approach assumes that future storms will be similar to past storms and thus does not account for possible changes in storm characteristics and frequency. The biggest problem with this approach may be that it traditionally does not include the impacts of future relative sea level rise (RSLR). However, techniques to do just that, and examples of how it has been done, are presented in Chapter 14.

The most common approach to the selection of the input parameters for synthetic hurricanes is the Joint Probability Method (JPM) originally used by NOAA (Ho and Myers, 1975). Historical storm parameters (e.g. wind speed, storm size, landfall location, etc.) are gathered and used to develop a set of statistically representative input storms. The JPM assumes that the probabilities for each parameter are independent and fit some probability distribution. Recently, the JPM has been extended for “Optimal Sampling” to reduce the number of modeled storm events with a goal of not impacting the resulting statistics (Niedoroda *et al.* 2010; Toro *et al.* 2010a; Toro *et al.* 2010b). This JPM-OS technique is needed because the high-performance computational storm surge models have expanded to increase resolution as computing power has increased. An alternative technique to the JPM for developing the surge-frequency relationship at any location is an Empirical Simulation Technique (EST) (Scheffner *et al.* 1996).

Any numerical storm surge model can be used in the general approach for developing coastal surge-frequency estimates (see Section 4.3.2 - Storm Surge Modeling). However, several agencies including FEMA and USACE have begun to use the Advanced CIRCulation Model (ADCIRC) for much of their coastal storm surge modeling for developing surge frequencies (e.g. Algeo and Mahone 2011). The ADCIRC model is used for the storm surge modeling in both the Level 2 and the Level 3 case studies of how to include the effects of sea level rise in vulnerability assessment described in Section 14.8.

Details on risk-based vulnerability assessment for coastal highways along the Atlantic and Gulf Coasts are presented in Sections 14.3 and 14.4.

### 13.2.1.1 Pacific and Great Lakes Coast Surge Frequencies

The methods typically used for the Pacific and Great Lakes Coasts to estimate the surge-frequency relationship differ from those just described for the Atlantic and Gulf Coasts. This is primarily because the damaging storms are so different from the Atlantic/Gulf hurricanes. In Pacific and Great Lakes regions, historical storms are simulated, i.e. hindcast, with numerical surge and wave models to develop a long, say 50-year, database of water levels at all locations. These results are then evaluated directly to estimate the surge-frequency relationship. FEMA (2005) outlines that agency's guidelines for the Pacific Coast. A "total water level" approach is suggested which directly includes wave runup as well as the storm surge. This may also be referred to as the "storm response method" in some literature. Where hindcast storm water levels and waves for a period of at least 30 years can be developed, the extreme values such as the 1%-Annual-Flood are estimated with the Generalized Extreme Value (GEV) Distribution Method.

Similarly, for the Great Lakes, the literature recommends a total water level approach for estimating 1 percent-annual-flood levels based on numerical hindcasts of 50 years of historical storms (Melby *et al.* 2012; FEMA 2014; Nadal-Caraballo *et al.* 2012). The historical approach typical of the Pacific and Great Lakes Coasts avoids the JPM for developing input storms but the numerical modeling effort is still very complex, often with ADCIRC or a similar storm surge model, and needs significant computing resources and experienced coastal modelers.

Details on risk-based vulnerability assessment for coastal highways along the Pacific and Great Lakes Coasts are presented in Sections 14.5 and 14.6, respectively.

## 13.3 Available Estimates of Storm Surge: SSIMs and FIRMs

Two commonly available coastal mapping products are storm surge inundation maps (SSIMs) and flood insurance rate maps (FIRMs). SSIMs are developed by NOAA primarily for input to emergency evacuation decisions. As such, they are created to be conservative so that local decision-makers can use them for evacuation decisions as hurricanes approach. SSIMs show areas which can possibly flood due to different Saffir-Simpson categories of hurricanes. They are essentially maps of modeled (typically with SLOSH) potential inundation areas from the worst possible storms (track and strength) of each Saffir-Simpson storm category. They provide an upper-bound, or worst-case, flood level for each category storm. They are generated by running the storm surge model for numerous possible tracks and strengths in each category storm and recording the highest flood levels from all the storms. Thus, they are not flood maps from any specific storm but the worst-case at each location. Their usefulness for engineering is limited. There is no risk or probability level associated with SSIMs. The "Category 5" SSIMs can provide an overall upper-bound, or worst-case, flood zone for all hurricanes.

A problem with using SSIMs, even for evacuation decisions, is that each storm has its own location and path and may not be the worst-case possible surge generator. For example, the location of Hurricane Irma, a Category 4 storm as it approached the southwest coast of Florida in 2017, meant its track could not physically generate the highest possible Category 4 storm surge in Naples, Florida. That maximum from a Category 4 storm could only have been generated by a storm located west of Naples and moving east. But Irma was south of Naples and moving north. Thus, the forecast surge using the SSIMs was needlessly far too high. This will lead to a major catastrophe if a major hurricane actually approaches Naples from the west in the next few years. People who needlessly evacuated in Irma may not believe that next forecast.

**SSIMs for Category 5 storms estimate the "worst-case" flood at every location from any hurricane with that maximum wind strength.**

Coastal FIRMs are generated by FEMA to be consistent with FIRMs in riverine systems. They are maps of the 100-year coastal flood plain developed with the general approach to surge-frequency estimation described above. The primary purpose of the FIRMs is to establish flood insurance rates in coastal flood plains on a rational, consistent basis. Coastal FIRMs also show the FEMA “Base Flood” depth at specific locations. The base flood includes additional elevation above the still water level (SWL) to account for the wave crest elevations which can exist in that local depth of water. One difference between FIRMs and SSIMs is that the FIRMs are consistent with typical risk-based analysis. The differences between these two commonly available coastal surge map products, the FIRMs and the SSIMs, are explained in FEMA (2011a).

### **13.4 Other Approaches to Quantifying Coastal Risk**

This section discusses other coastal flood risk quantification approaches. One potential alternative for developing the coastal surge-frequency relationship is to use frequency statistics developed directly from measured, historical water level data. Water level data is recorded at a series of tide gages around the United States (see Section 4.1). However, caution should be exercised using these data for vulnerability assessments or designs for extreme events as they often do not reflect the extreme water levels that have occurred. The gages often do not record during extreme events due to physical damage, lost power, or surge elevations beyond their design parameters. Also, because of the complexities of the interaction of storms with coastal geography (bathymetry and topography) surge varies significantly within relatively short distances. Further caution in using water level data directly is that such an approach could be storm-specific, i.e. emphasize planning/designing for the last big storm. Coastal peak flood elevation data can be supplemented with careful high-water mark surveys after storms. However, those data are often subject to interpretation error and have only been collected with significant spatial coverage after major coastal storms in the past several decades. In general, not enough storm surge observations are available to make robust estimates of storm surge-frequency for engineering design.

The Saffir-Simpson Hurricane Scale cannot be used for assessing the vulnerability (or for design) of most coastal transportation infrastructure. This is because wind is not the primary environmental design issue and the Saffir-Simpson scale is a wind speed scale. The winds create the surge and waves, which do the damage, but there is usually only marginal correlation between a hurricane’s wind strength and either surge or waves at any specific location along the coast. For example, the same hurricane will have very different surge and wave effects along the coast to the left of landfall, where peak winds are offshore and reducing surge and waves, than to the right of landfall, where peak winds are onshore and increasing surge and waves. Thus, statements like, “this should be designed to survive a Category 3 hurricane,” as a basis for planning and design decisions are problematic and should be avoided (unless direct wind loads are the damaging phenomenon, e.g. for traffic signs or building roof design).

**The Saffir-Simpson Hurricane scale is not used for coastal engineering design.**

**Life cycle cost analysis approaches for quantifying risk and incorporating it into engineering design are gradually replacing frequency-based analyses in many areas of civil engineering and planning.** The Coastal Engineering Manual (USACE 2002) describes methodologies for risk-based analysis in coastal engineering, and the reader is directed to Thompson *et al.* (1996) and Almodovar *et al.* (2008) for specific case study application of the life cycle approach to coastal infrastructure (not directly related to highways). The life cycle approach addresses a number of possible realizations of project evolution during its design life. It can simulate different cumulative damage scenarios; can incorporate management decisions (i.e.

repair, replace, etc.) and accounts for changing climatic conditions over time. The life cycle approach develops some understanding of the probabilities of key variables and is often a data-driven exercise. Ultimately, probabilities and risk describing the project elements are derived through an analysis of project performance of numerous (i.e. thousands) estimates of the project life cycle. This is most commonly done with Monte Carlo-like simulations or other statistical techniques. Transportation infrastructure/assets typically have long life cycles. Also, the characteristics of the areas surrounding coastal transportation facilities are subject to change either through natural or human impacts. And, within the life cycle of some assets, the statistics and/or characteristics of key variables may change. Economics can be integrated into the life cycle approach and considered simultaneously with technical performance in order to more appropriately describe risk and vulnerability.

*Page Intentionally Left Blank*

## Chapter 14 - Analysis Methods for Assessing Vulnerability to Extreme Coastal Events

The US coastal transportation system is vulnerable to extreme storms today and this vulnerability will increase as sea levels rise (Jacobs, *et al.* 2018b). Assessments of this vulnerability are becoming common in planning and design. Vulnerability assessment, the process of identifying and quantifying the vulnerabilities of a system, is a part of risk management in many different aspects of society (business, national security, infrastructure, etc.). Vulnerability is function of an asset's (or system's) exposure, its sensitivity, and its adaptive capacity (Figure 14.1).

“Exposure” refers to the degree to which the asset is impacted. In this case, this is the amount of, or level of, damaging forces/hazards, e.g. the wave height or loads in a storm.

“Sensitivity” refers to how the asset responds. This can be how, and how much, physical damage is done to the asset (and the cost of that damage). “Sensitivity” mechanisms for coastal roads, i.e. how they are damaged in storms, are discussed briefly in Section 15.1.

“Adaptive capacity” refers to the ability of the asset (e.g. road, bridge, etc.) or the larger system containing the asset, to accommodate and/or recover from the impact. This can include considerations of whether, and for how long, the asset is out of service. Adaptation strategies for coastal highway infrastructure are briefly discussed in Section 15.2.

Figure 14.2 schematically summarizes the FHWA's (non-binding) vulnerability assessment “framework.”

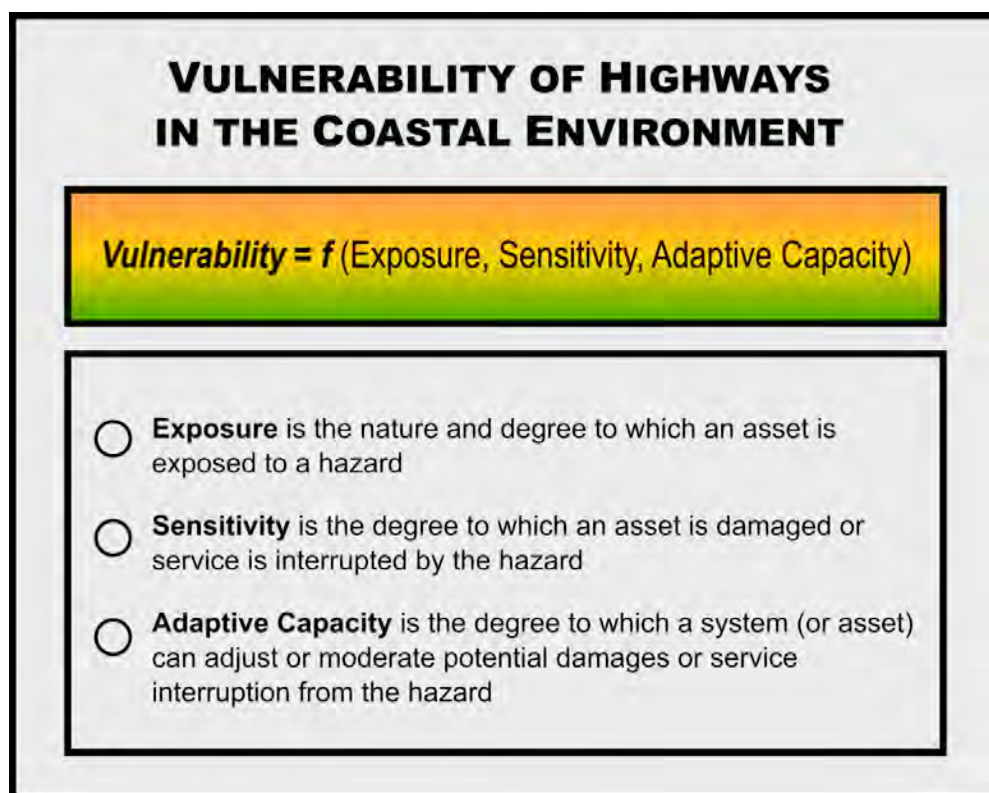


Figure 14.1. Vulnerability of highways in the coastal environment

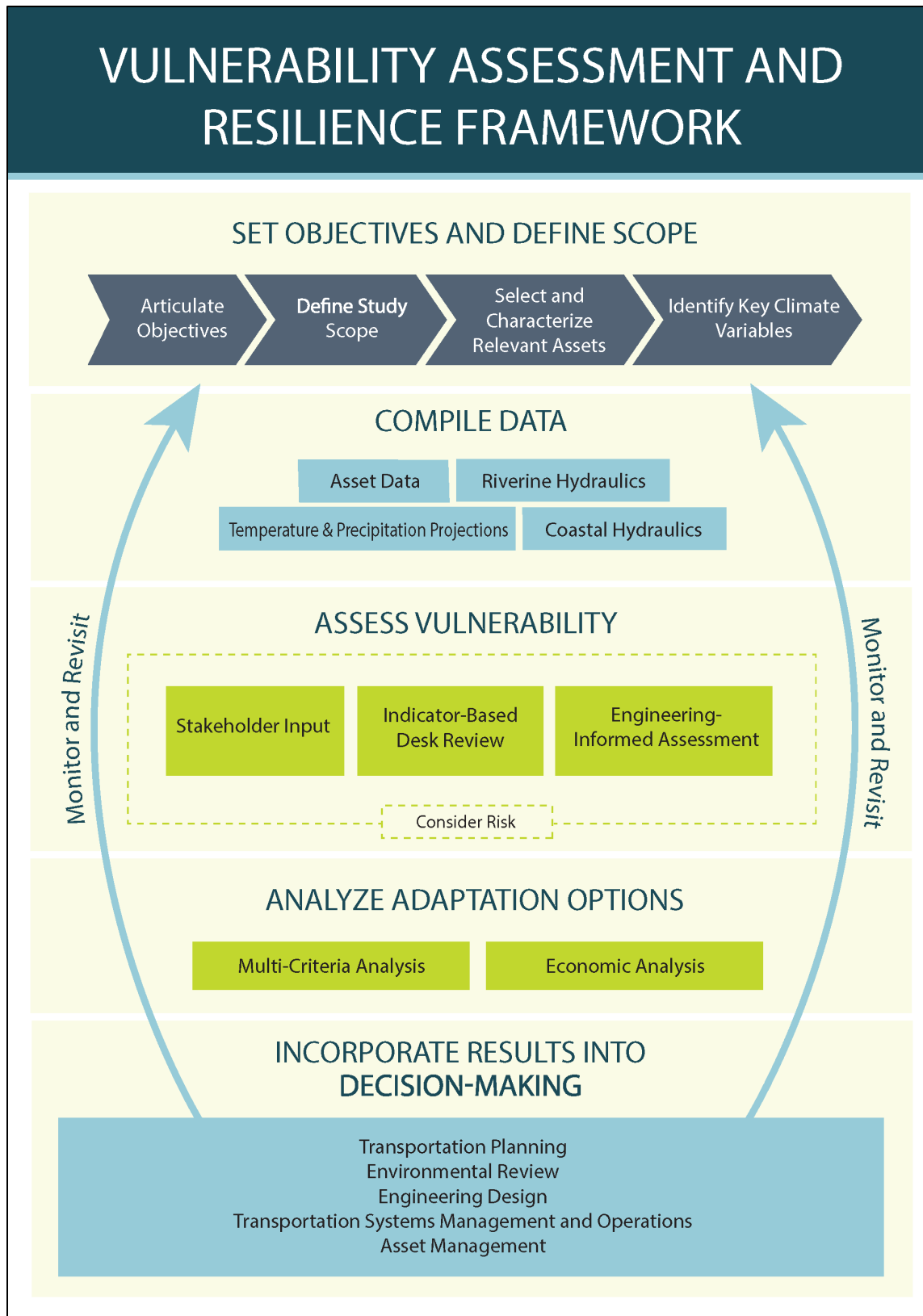


Figure 14.2. FHWA’s Vulnerability Assessment and Resilience “Framework” (FHWA 2017d)

This “framework” outlines five broad components for such studies:

- Set objectives and define scope,
- Compile data,
- Assess vulnerability,
- Analyze adaptation options, and
- Incorporate results into decision making.

The first component, defining objectives and scope, includes articulating the objectives, selecting/characterizing the relevant transportation assets, and identifying variables for study. This includes consideration of the intended outcomes, the target audience, the geographical and temporal limits of the study, and the level of detail needed.

**This chapter presents detailed, technical methods for assessing the “exposure” of coastal transportation infrastructure to extreme events including future sea level rise.** These methods were originally outlined in Douglass *et al.* (2014).

This chapter describes three levels of effort/analysis and provides some specific regional approaches. The availability and location of existing products, data, tools, and methodologies that can be considered at each level of effort for each region, are discussed. Examples of specific information include where to find and how to use flood hazard maps, the selection of an appropriate hydrodynamic model(s) to simulate the coastal processes of interest in that region, and some references to existing methodologies for estimating water levels, waves, currents, and erosion. The coastal tsunami hazard is included in this chapter because of its increasingly more frequent inclusion in engineering planning and design considerations in the Pacific states and territories.

Section 14.8 summarizes three case studies which are examples of excellent applications of the techniques outlined in this chapter. Vulnerability assessments should be done for the planning and design of all high-value US coastal transportation assets using analyses like these case studies (particularly the Level 2 and Level 3 case studies).

## **14.1 Literature on Assessing the Impacts of Future Environmental Conditions**

This section is a brief summary of the literature on assessing the impacts of future environmental conditions on coastal highways. Most investigations have focused on the impacts of sea level rise and some have included the impacts of changing storm characteristics.

Hyman *et al.* (2008) summarized the limited research into the effects of future environmental conditions on highways available at that time. The literature in the field has expanded rapidly in the past decade. ICF (2009) summarized the literature on vulnerability assessments, risk assessment, and adaptation approaches, including some efforts outside of the US.

Many investigators have used a mapping overlay technique with projected future sea levels and roadways for beginning to characterize the extent of road inundation as a surrogate to vulnerability (e.g. Titus 2002). The technique has been dubbed the “bathtub” approach because it considers primarily inundation by sea level rise. Gesch *et al.* (2009) provides a partial list of the investigations which have used the basic technique and NOAA (2012) describes many of the details related to the mechanics of how to apply a basic inundation mapping technique.

Earlier studies used only sea level but later studies combine that with storm surge estimates. The sea level rise and the storm surge after sea level has risen can be estimated by linear addition of

the two components (Gill *et al.* 2009). Douglass *et al.* (2005) used a form of the technique to assess the existing vulnerability of the US coastal highway system to storm surge alone (with no consideration of sea level rise) by overlaying the FEMA 100-year flood plains on road maps to estimate that there are roughly 60,000 road miles occasionally exposed to coastal surge and waves today (see Section 3.2).

Kafalenos *et al.* (2008) used the basic inundation mapping technique in what is commonly referred to as the “Gulf Coast” study. That study was a multi-year, multi-phase study. Phase 1 of the study, “Gulf Coast 1,” quantified the highway miles in areas with ground elevations below levels selected to account for storm surge and sea level rise in the study area from Galveston, Texas to Mobile, Alabama.

Phase 2 of the study, “Gulf Coast 2,” used a more complex method for mapping exposure that is highlighted as a case study in this chapter (see Section 14.8.2). Numerical models with different assumed input future sea levels are used to map future exposure to storm surge and waves. Thus, any nonlinear aspects of the relationship between future sea levels and surge levels are inherently accounted for. Some of those mapping results were directly included in the 3<sup>rd</sup> NCA (Melillo *et al.* 2014).

Long-term Relative Sea Level Rise (RSLR) has already contributed to damage of one major US bridge during a hurricane. Interstate 10 (I-10) crosses Escambia Bay just east of Pensacola, Florida on elevated twin span bridges. The bridge was severely damaged during passage of Hurricane Ivan September 15-16, 2004. Section 11.2.1 explains that the RSLR which occurred in the three to four decades between the design of the bridge and Hurricane Ivan, caused a significant increase in wave-induced loads on the bridge during the storm which caused the worst damage.

**Relative Sea Level Rise (RSLR) has already contributed to damage of a major US bridge.**

Coastal exposure and vulnerability mapping efforts not specifically focused on transportation infrastructure have been done by others using similar approaches. Smith *et al.* (2010) evaluated storm surge and waves across the marshes of southern Louisiana with assumed scenarios of sea level rise. They found that **increases in maximum surge elevations are not linear with the sea level rise assumptions**. In particular, for moderate hurricanes the surge levels could increase significantly more than the sea level rise (see Section 4.3.4). The reason is the interaction of the surge with the bathymetry and coastal topography. Li *et al.* (2013) assessed the impacts of future sea level rise on the naval facilities in the Norfolk area. Atkinson *et al.* (2013) modeled sea-level rise effects on storm surge and nearshore waves on the Texas coast. They conclude that because of the complexities, “there is no one-size-fits-all response to relative sea level rise descriptive of all locations” and that “site-specific computer modeling should be used to evaluate the risk facing coastal communities.” Hagen and Bacopoulos (2012) did probabilistic modeling of extreme event surge for some Florida counties with sea level rise. They found the nonlinear effect of sea level rise on surge, which they called the “dynamic” response of flooding as compared to simply estimating the static response (i.e. the “bathtub” approach), was significant in terms of both coastal flood inundation areas and depths.

Transportation vulnerability to sea level rise is described in studies by Caltrans (2018), Han *et al.* (2017), Lu and Peng (2011), Neumann *et al.* (2015), and Oswald and Treat (2013). Fakhruddin *et al.* (2015) find that transportation systems in American Samoa are the most vulnerable infrastructure sector with regards to impacts of sea level rise. Some recent studies provide, and demonstrate, assessment tools or methodologies for sea level rise vulnerability. These include Bloetscher and Romah (2015), Demirel *et al.* (2015), and Lambert *et al.* (2013). Transportation

adaptation for sea level rise is described in Cooper and Dolan (2012), Filosa *et al.* (2016), and Shilling *et al.* (2016). In addition to sea level rise vulnerability, many numerical modeling studies address coastal bridge and coastal highway vulnerability to combinations of sea level rise and coastal storms. Examples of such numerical studies include Chorzepa *et al.* (2016), Dompe *et al.* (2015), Filosa *et al.* (2016), Kim *et al.* (2015), and Tang *et al.* (2013). A recent study by Anarde *et al.* (2018) provides an example of a numerical modeling study that incorporates expected landscape changes/responses to sea level rise into an assessment of coastal bridge vulnerability to storm surge and sea level rise. Examples of studies that focus on transportation vulnerability to tsunami hazards include Yu *et al.* (2014) and Capozzo *et al.* (2017).

A few papers describing general aspects of coastal highways are also available. Knott *et al.* (2017) demonstrate, in a study of coastal New Hampshire roads, that rising groundwater attributed to sea level rise leads to reductions in pavement service life. The magnitude and timing of pavement degradation is sensitive to the current depth to groundwater, the pavement structure, and the nature of the subgrade (and the sea level rise scenario governs the timing). Other states likely have similar vulnerabilities. Other recent literature describes the impact to roads, or of roads, near receding shorelines (e.g. Kim *et al.* 2011; Zoulas and Orme 2007).

The FHWA has co-sponsored “pilot” planning level studies on vulnerability and risk assessments of infrastructure to the projected impacts and extreme weather events (FHWA 2012b). Most of the coastal studies use some form of an inundation mapping approach for sea level rise, storm surge, or some combination (ART 2012; NJTPA 2011; Oahu Metropolitan Planning Organization 2011; and Washington DOT 2011). Most found a high level of vulnerability to coastal storms today that will increase with increasing sea levels:

- Metropolitan Transportation Commission, **San Francisco Bay**, in a multi-agency collaboration including NOAA, assessed the vulnerability of transportation systems to sea level rise and flooding, as well as impacts to shoreline protection systems. The Adapting to Rising Tides project is one of the case studies of coastal vulnerability assessments highlighted at the end of this chapter (see Section 14.8.1).
- **New Jersey** Transportation Planning Authority assessed the vulnerability of roads, bridges, tunnels, transit, freight rail, maritime assets, and airports to sea level rise and coastal flooding.
- **Oahu** Metropolitan Planning Organization, Hawaii evaluated five high-priority sites with existing vulnerability to extreme weather events including the impacts of sea level rise, storm surge, and strong winds.
- Virginia DOT evaluated the vulnerability and sensitivity of transportation infrastructure in the **Hampton Roads** region.
- **Washington State** DOT assessed the vulnerability of all state-owned and stated-managed assets to 2-ft, 4-ft, and 6-ft sea level rise scenarios.
- Alaska DOT and FHWA Western Federal Lands assessed the vulnerability of **Kivalina Airport** to sea level rise and coastal storm impacts.
- Caltrans District 1 evaluated the impacts of sea level rise on **California SH 101** as well as the potential performance of various adaptation strategies to reduce flooding.
- **Hillsborough** Metropolitan Planning Organization, Florida assessed the vulnerability of surface transportation systems to flooding from sea level rise and storm surge.

- **Maine** DOT evaluated the impacts of sea level rise and storm surge on state-owned roads, bridges, and culverts, as well as the impacts of transportation systems on marsh migration with sea level rise.
- **Maryland** State Highway Administration evaluated the vulnerability of roads and bridges to sea level rise, storm surge, and flooding in two coastal counties.
- Massachusetts DOT evaluated the impacts of sea level rise and extreme event flooding on the **Boston** I-93 Central Artery/Tunnel system. This study is highlighted below at the end of this chapter as an excellent example of a coastal transportation vulnerability assessment (see Section 14.8.3).
- **Oregon** DOT evaluated the vulnerability of roads and bridges in two coastal counties to coastal flooding and storm surge.
- In **South Florida**, three MPOs and a County planning department collaborated to assess the vulnerability of major freeways, arterials, and rail systems to sea level rise and storm surge.

## 14.2 Levels of Effort in Assessments

This section provides a broad overview of the proposed levels of effort for performing a vulnerability assessment of coastal transportation infrastructure to extreme coastal events and sea level rise. Vulnerability assessments may range from broad planning overviews involving systems of assets to highly detailed, project-specific investigations employing state-of-the-art modeling tools. In addition to considering the type of assets that may be affected by extreme events, investigators have varying levels of budget and available expertise that may also define the scope of an investigation. Therefore, this chapter presents techniques for different “levels of effort” for the assessments.

The amount of detail and degree of complexity grow with each subsequent level of effort, as does the quality of the assessment. The degree of uncertainty in the results, however, decreases with each subsequent level of effort. The potential levels of effort for coastal planning are broadly:

- **Level of Effort 1: Use of Existing Data and Resources** - Use of existing inundation (FEMA or USACE) or tsunami data to determine the exposure of infrastructure under selected sea (lake) level change scenarios, and sensitivity to depth-limited wave or wave runup processes.
- **Level of Effort 2: Original Modeling of Storm Surge and Waves** - Modeling of surge and wave fields for specified storm and sea level rise scenarios, or modeling of tsunami inundation under sea level rise scenarios.
- **Level of Effort 3: Modeling in a Probabilistic Risk Framework** - Modeling of surge, sea levels, currents, and waves, or tsunamis, including the impacts of sea level rise, in a probabilistic risk framework.

### 14.2.1 Level of Effort 1: Use of Existing Data and Resources

**The purpose of the “Level 1” approach is to provide some meaningful information about the level and coverage of exposure to damaging storm parameters without having to perform complex modeling or calculations.** This lowest level of effort is simpler to perform and relies on the use of established maps and tools to determine the degree to which a particular asset or area is exposed to the effects of extreme events with future sea level rise. The analysis team for Level 1 should include a trained coastal engineer to insure proper interpretation and

integration of the input coastal flood map products (see Section 3.6 Coastal Engineering as a Specialty Area).

Since the Level 1 approach is relatively simple, a number of sea level rise scenarios can be considered. The goal of a Level 1 study might be to capture the sensitivity of a particular asset or area to the effects of sea level rise instead of predicting an accurate value of flooding depth or wave height, etc. Thus, the Level 1 approach can be used as a screening tool to identify those areas or infrastructure assets that are exposed to the effects of sea level rise. These specific areas can be evaluated in more detail through additional refinements of a Level 1 approach or by including them in assessments with higher levels of effort.

**The USACE Coastal Hazards System is a powerful online resource for vulnerability assessments.**

The degree of uncertainty in results obtained in a Level of Effort 1 assessment will be relatively high. The results will include all of the assumptions and uncertainties inherent in existing inundation or flood hazard maps (or other existing tools used). The most commonly available, existing data are typically the FEMA flood insurance rate maps (FIRMs) and the corresponding Flood Insurance Studies (FIS) or USACE Coastal Hazards System Annual Exceedance Probability data (USACE 2019). In some cases, other agency flood maps and studies may be available.

**An example of a comprehensive Level 1 study is highlighted in Section 14.8.1 Case Study: Adapting to Rising Tides - San Francisco Bay.** This case study developed inundation maps for one county for planning purposes. Two sea level rise scenarios (16 inches and 55 inches) were evaluated. The primary process of interest was flood depths, but some additional evaluation of waves was included.

#### 14.2.2 Level of Effort 2: Modeling of Storm Surge and Waves

The purpose of the “Level 2” approach is to provide detailed information about exposure under extreme events with sea level rise. In such a study, one or more sea level rise scenarios can be explicitly incorporated into model simulations so their effects on the important coastal processes can be determined. Performing a Level 2 analysis uses sophisticated hydrodynamic models that simulate storm surge and waves, or tsunamis. The development and application of these models, as well as interpretation of their results, should generally be performed by a trained coastal engineer with expertise in hydrodynamic modeling.

**Level 2 and Level 3 coastal assessments use sophisticated hydrodynamic models.**

Part of a Level 2 study is thoughtful selection of extreme events of interest for the modeling. These could be events of record for a region (e.g. a specific hurricane), a storm that had a notable impact on a specific piece of infrastructure (e.g. bridge failure), or perhaps even an event that has not yet occurred (e.g. hurricane with a shifted track, tsunami, etc.). A goal of the Level 2 study could be to demonstrate the degree to which sea level rise will modify the exposure of an asset or area relative to a present-day (baseline) scenario. The results of a Level 2 study will generally not be probabilistic in nature. However, it may be possible to assign a return period to a scenario if a historical storm or event (i.e. one that has previously occurred) is selected for analysis or if assumptions about the appropriate storm characteristics are developed. It may be helpful to

consider a range of possible event and sea level scenarios that span from more frequent, lower-intensity events to infrequent, higher-intensity events. Practically, the Level 2 study may be limited to modeling less than approximately two dozen, extreme event and sea level scenarios.

While each Level 2 study will be unique, an underlying methodology will be common to all studies. Every Level 2 study should include:

- selection of extreme event and sea level rise scenarios appropriate for the region,
- development of suitable hydrodynamic modeling tools,
- validation of the hydrodynamic model(s) using hindcast simulations and observations,
- simulation of the extreme event and sea level rise scenarios, and
- mapping of the hazards (e.g. inundation, waves, wave runup) as assessments of exposure under each scenario.

While a Level 1 study uses inundation or flood hazard maps developed by others, a Level 2 study should develop new maps. Such mapping constitutes a significant amount of work and serves purposes beyond the exposure assessment, like communication and public outreach. Therefore, it is crucial that great care is taken in the preparation of these maps and that they are readily understood by laypersons.

The time and effort inherent in a Level 2 study is significantly greater than a Level 1 study. Accordingly, the cost of a Level 2 study is likely to be much higher than a Level 1 study. But with an increase in time, effort, and cost comes a significant reduction in uncertainty and a narrower range of possible answers. The reduction in uncertainty is mostly attributed to use of the hydrodynamic models, which provide specific estimates of the important regional coastal processes of interest, like water levels, wave heights and periods, velocities, etc. Note that the quality and utility of these estimates is not that they are necessarily “larger” values than those obtained in the Level 1 study, but rather that they are more accurate.

An example of a comprehensive Level 2 assessment is highlighted in Section 14.8.2 Case Study: The Gulf Coast 2 Study – Mobile, Alabama below. That study used original, high-resolution modeling to map storm surge and waves in extreme events for a variety of sea level rise scenarios.

#### 14.2.3 Level of Effort 3: Modeling in a Probabilistic Risk Framework

**A “Level 3” study characterizes exposure in terms of probability and risk.** While the general methodology is similar to that of a Level 2 study, probability is known. The Level 3 study uses many more simulations in order to determine the probability of events. Whereas the Level 2 study is based on perhaps tens of unique event scenarios, this type of study may use on the order of one hundred simulations. This probabilistic approach is essentially the same as that currently used by most federal agencies for developing modern flood hazard maps (e.g. FEMA 2003), except here relative sea level rise (RSLR) scenarios are included.

The Level 3 study involves a significant investment. It takes longer to complete and has a higher cost than the Level 1 and Level 2 assessments. However, this highest level of effort also provides the greatest reduction in uncertainty. **Overall project costs, including construction costs, can be reduced by the use of a higher level of analysis for design since the lower analysis levels can overestimate both the magnitude and the duration of coastal flooding** (Bosma 2016). The number of simulations allows for a range of return period events to be considered and the results may be applicable over a much larger area. For instance, a Level 2 study might consider storm events that lead to failure or damage of a specific asset, like a bridge. These

results are valuable but only near that bridge. The event probabilities derived from a Level 3 assessment may be applicable to more than one area when multiple storm tracks or tsunami events are modeled.

A Level 3 study incorporates expertise in coastal engineering, numerical modeling, hazard analysis, probability and risk. Accordingly, such studies should be performed by accomplished engineers with demonstrated expertise in modeling extreme events as well as an understanding of the appropriate regional RSLR scenarios.

An example of a comprehensive Level 3 approach is highlighted in Section 14.8.3 Level 3 Case Study: Central Artery Project, Boston, Massachusetts. That case study used high-resolution storm surge modeling to develop probabilistic inundation maps, and other products, for all coastal storms with sea level rise.

### **14.3 Gulf of Mexico and South Atlantic Coast**

The multi-level approach to evaluating exposure is described on a regional basis, beginning in this section and continuing through Section 14.7. Each region of the US experiences hazards, or combinations of hazards, unique to its particular characteristics.

This section outlines the levels of effort, existing tools and data, appropriate models, and methodologies for determining exposure in the Gulf of Mexico and along the South Atlantic Coast (see Figure 14.3 for one South Atlantic shoreline). Some of the tools outlined here are also useful in the other regions. In this region of the US, tropical storms and hurricanes are the predominant extreme events, and the storm surge and waves they generate are the important coastal processes of interest. This section describes a multi-level approach for evaluating exposure to extreme events with future RSLR in the Gulf of Mexico and along the South Atlantic Coast.

#### **14.3.1 Level of Effort 1: Gulf of Mexico and South Atlantic Coast**

The major steps for developing the information needed to perform a Level of Effort 1 exposure assessment on the Gulf of Mexico and South Atlantic Coasts are summarized in Table 14.1. The steps include the processes of interest:

- Flood depths (Step 6),
- Wave heights (Step 7),
- Wave crest elevations (Step 8), and
- Flow velocities (Step 9).

If only flood depths are needed, steps 7-9 are unnecessary.

A Level 1 approach in this region can be based upon the use of existing FEMA inundation maps, or FIRMS, to determine the exposure of infrastructure to coastal flooding. An alternative may be the USACE Coastal Hazards System (USACE 2019). In this region of the US, the FEMA flood hazard maps delineate the 100-year (1 percent annual chance) flood plain and in some cases the 500-year (0.2 percent annual chance) flood plain. For coastal areas, these flood plains are mostly determined by storm surge from tropical storms and hurricanes. Existing flood hazard maps, however, do not account for future changes in sea level, nor do they explicitly provide information about wave heights or flow velocities.



Figure 14.3. Deerfield Beach, Florida (2018)

FEMA FIRMs describe the 1 percent annual chance still water elevation at various locations throughout the flood plain, as well as the base flood elevations (BFE) at specific locations (see Section 13.3). The BFE accounts for the elevation of wave crests that could exist in the local flooded depth. Use of the FEMA products calls for an understanding of their terminology (BFE, FIRM, etc.) as well as basic coastal engineering terminology (e.g. HEC-25).

Four of the important, extreme event, coastal exposure processes can be evaluated in a Level 1 study:

1. spatial coverage of flooding,
2. depth of flooding,
3. wave characteristics, and
4. flow velocity.

Table 14.1. Exposure assessment steps for level of effort 1: Gulf of Mexico/South Atlantic Coast

Step	Activity
1	Obtain appropriate FEMA flood map elevations for study area
2	Choose desired RSLR scenarios
3	Modify RSLR increments to account for nonlinearity
4	Add the result of Step 3 to the elevations obtained in Step 1
5	Obtain appropriate ground surface elevation maps for study area
6	Subtract ground elevations (Step 5) from values found in Step 4 to obtain flood depth
7	Multiply flood depths (Step 6) by 0.8 to determine maximum wave height
8	Multiply wave heights (Step 7) by 0.75, add to Step 4 for wave crest elevations
9	Use Equations 4.1 and/or 4.2 to estimate flood flow velocity
10	Consider shoreline retreat and erosion based on historical trends in study area
11	Map the damaging coastal processes (results from Steps 6-9)
12	Evaluate exposure of transportation infrastructure

Only the first of these steps is explicitly provided by the FEMA flood hazard maps. The most current FEMA flood hazard maps can be obtained from the FEMA Map Service Center (<https://msc.fema.gov>) for use in GIS software applications. These maps are now part of what FEMA refers to as the National Flood Hazard Layer (NFHL). The maps describe the spatial coverage of the flood plain(s), as well as different flood hazard zones, in a geographic reference system. The flood hazard layer can be combined with other spatially-explicit data organized into GIS layers, like transportation systems, to quickly determine whether a specific area or asset falls within the FEMA flood plain. But this methodology does not immediately reveal whether an asset like a road or bridge will be affected by flooding, flood flows, or waves. It also does not account for increased exposure due to future RSLR impacts.

After the appropriate FEMA flood map has been obtained, RSLR should be considered. In this region, the relevant sea level change scenario is the RSLR that accounts for both land subsidence and global eustatic sea level rise. Appropriate regional RSLR rates, increments, or targeted values at specific planning horizons (e.g. 2020, 2050, 2100, etc.), should be determined for the study area.

#### 14.3.1.1 RSLR Data

Section 4.1 provides discussions and material on sea level rise (including relative sea level rise or RSLR). A practical way to apply this information is with the USACE online sea level change calculator that accounts for local rates of subsidence and eustatic sea level rise by using NOAA tide gages near any selected study area.

#### 14.3.1.2 Increased Flood Levels: Nonlinear SLR-Surge Relationship

The effect of RSLR on storm surge can be nonlinear (see Section 4.3.4). In other words, if the depth of flooding under present-day conditions is  $A$  and the sea level rise increment is  $B$ , the resulting future flood depth may be greater than  $A+B$ . This nonlinearity can be accounted for by multiplying each selected relative sea level change increment considered by a constant ranging from 1 to 5. A value of 1 represents a linear coupling while a value of 5 represents a strongly nonlinear coupling (i.e. the surge increases 5 times the sea level change increment). The degree of nonlinearity is likely both site and scenario specific, as described in Smith *et al.* (2010) who found only isolated cases of surge increasing 5 times the sea level rise increment.

Instead Smith *et al.* (2010) found widespread areas where the surge increased 1 to 2 times the sea level rise increment.

**One foot of future sea level rise can increase storm flood levels more than one foot! There is a nonlinear relationship between sea level and flood level.**

Therefore, an appropriate singular value to apply over an entire study area might be 1.5. Currently very little literature about this nonlinearity exists and all of the published documentation comes from studies in the Gulf of Mexico. This is an area of research that needs more attention. Selection of a larger value could be justified to provide a more conservative estimate. This uncertainty is one of the limitations of a Level 1 approach.

After multiplying the selected sea level change increments by an appropriate nonlinear constant, the resulting values should be added to the still water elevations shown on the FEMA flood map for each sea level scenario considered. Recall that FEMA flood maps provide the elevation of the still water (i.e. waves removed) relative to a fixed vertical datum, like the North American Vertical Datum (NAVD). It is important to note that these values are elevations, not flood depths.

#### 14.3.1.3 Coastal Land Elevation Data

In order to determine flood or total depths within the study area under the selected sea level scenarios, the local ground surface elevations should be known and subtracted from the modified still water elevations. Appropriate sources of information include USGS topographic maps for ground surface elevations (<http://www.usgs.gov/>) and NOAA nautical charts for bathymetric elevations (<http://www.nauticalcharts.noaa.gov/>). Such maps, however, may not always provide the needed resolution to determine elevations near a specific asset. Many coastal areas of the US have been mapped using high-resolution light detection and ranging (LiDAR) systems that provide closely spaced data. A good source for LiDAR and other coastal elevation data is the NOAA Coastal Services Center Digital Coast web data portal (<https://coast.noaa.gov/digitalcoast/>). Other excellent sources of combined topographic and bathymetric elevation data sets, commonly available as GIS layers, include the NOAA National Geophysical Data Center's Coastal Relief Models and the USGS National Map Viewer: (<http://www.ngdc.noaa.gov/mgg/bathymetry/relief.html>) and (<http://viewer.nationalmap.gov/viewer/>). State organizations, like the Texas Natural Resources Information System (TNRIS) at <https://tnris.org>, may also provide more detailed elevation data than national sources.

#### 14.3.1.4 Wave Characteristics

Wave characteristics and flow velocities can be determined as part of the exposure assessment once the spatial coverage and depth of inundation are estimated. In a Level 1 approach, waves can be assumed to be depth-limited and will break when their height is approximately 80 percent of the water depth (see Section 5.2).

Also, the elevations of the wave crests under depth-limited conditions can be approximated by adding 75% of the maximum wave height to the still water elevation flood level. See Section 11.6 for more information about estimating wave crest elevations. This is essentially the same computation that FEMA uses to determine the base flood elevation (BFE) shown on many coastal flood maps.

### 14.3.1.5 Storm Surge Flow Velocity Estimates

The estimation of flood flow velocity magnitude and direction during a storm event is difficult. Conservatism and professional judgment should be applied when estimating and applying these values as part of a hazard analysis. ASCE (2016) provides general guidance on the estimation of flood flow velocity as a function of flood depth. A recommended lower bound on the velocity is equivalent to the flood depth divided by one second:

$$V_{low} = d_s / (1 \text{ second}) \quad (14.1)$$

where:

$$d_s = \text{design flood depth}$$

For example, if the design flood depth is 5 ft, a low estimate of the velocity magnitude is 5 ft/s. A recommended upper bound on the velocity is given as the square root of the product of the gravitational constant and the flood depth:

$$V_{high} = \sqrt{gd_s} \quad (14.2)$$

where:

$$g = \text{gravitational constant having a value of } 32.2 \text{ ft/s}^2 \text{ (} 9.81 \text{ m/s}^2\text{)}$$

This equation is the same as that used to estimate the shallow-water wave celerity as described in Section 5.1 Definitions, Theories and Properties of Waves. Using the same example as before, an upper estimate for the magnitude of flow velocity using a design flood depth of 5 ft is nearly 13 ft/s, more than twice the lower estimate.

### 14.3.1.6 Other Considerations in Level 1 Studies

The spatial coverage and depth of inundation, wave heights, wave crest elevations, and flow velocity for extreme events with selected sea level scenarios can be mapped and used for exposure assessments. This information can be used to determine if an area or asset falls within the modified 100-year flood plain, but it can also be used to determine the sensitivity of transportation infrastructure to waves and flow velocity. Some common types of damage are described in Section 15.1 Typical Coastal Roadway Damage Mechanisms. Additional guidance for mapping hazards in sheltered waters, like coastal embayments, is available in FEMA (2008).

One specific limitation of all these approaches is the inability to account for short- or long-term shoreline change. This may be a particularly important process to consider for highways near receding shorelines. The reader is encouraged to consider future shoreline positions that result from retreat and erosion in their exposure assessment. Additional information about where to obtain and how to use shoreline change data is provided in Chapter 8 - Roads in Areas of Receding Shorelines.

## 14.3.2 Level of Effort 2: Gulf of Mexico and South Atlantic Coast

**A Level 2 study uses some original modeling of storm surge and waves for selected extreme storm events under specific sea level scenarios.** Extreme event scenarios may include storm intensification through increased central pressure deficit and maximum winds. The fundamental steps in a Level 2 analysis for the Gulf of Mexico and South Atlantic Coast are summarized in Table 14.2.

Table 14.2. Exposure assessment steps for level of effort 2: Gulf of Mexico/South Atlantic Coast

Step	Activity
1	Identify damaging coastal processes of interest (e.g. storm surge, waves, etc.)
2	Select and characterize storm and RSLR scenarios of interest
3	Select, develop, and prepare appropriate numerical modeling tools
4	Validate and/or calibrate the models through hindcast simulations and analyses
5	Incorporate RSLR scenarios into numerical model simulations
6	Perform model simulations of selected storm and sea level scenarios
7	Map the damaging coastal processes for each scenario
8	Evaluate exposure and sensitivity of transportation infrastructure for each scenario

In the Gulf of Mexico and along the South Atlantic Coast, storm surge and waves generated by tropical storms and hurricanes are the primary concerns. Episodic, storm-induced shoreline change may also be of concern for highways near receding shorelines, causeway islands, bridge approaches, etc. While the tide range in the Gulf of Mexico is generally small (less than 2 ft), it does grow larger moving north along the South Atlantic Coast and should be considered in exposure assessments. This is especially true for low-lying areas that are particularly sensitive to the effects of sea level rise on tidal inundation (see Hagen and Bacopoulos 2012). Also, the contributions of coastal watersheds through increased stream flows may play an important role in the increase in local water levels, especially in areas distant from the coastline (see Section 4.4). Finally, the combination of the wind-driven storm surge, tidal stage, and river stage are of concern when they occur simultaneously.

#### 14.3.2.1 Storm Selection and Characterization

A range of storm levels can be considered in a Level 2 study. The selection and characterization of storm events for a Level 2 study should not be based solely on the worst-case scenario. Since risk is not a product of this approach it is important to consider the exposure and sensitivity of infrastructure to a wide range of storm and future sea level rise scenarios. The scenarios may include the frequent but low-intensity tropical storms, as well as infrequent but high-intensity hurricanes, that have previously impacted the study area. Other storms having properties that fall somewhere between these limits may also be considered, especially if they produced notable impacts to an area or piece of infrastructure in the past. This is the approach that was applied to the selection of storm events for the Gulf Coast 2 study described in Section 14.8.2.

Some numerical models, like ADCIRC, use only basic storm parameters to develop meteorological forcing for the model. The time and geographic position of the storm, its central pressure, maximum winds, and radius to maximum winds generally constitute the minimum information to model the storm. Some models also allow the user to characterize the asymmetry of a storm by defining winds in each of its four quadrants. Historical storm characteristics and information can be obtained from the NOAA National Hurricane Center (NHC) data archive (<http://www.nhc.noaa.gov/data/>). The NHC Best Track data archive provides general storm characteristics in six-hour increments for the duration of the storm event. Detailed storm characteristics are found in the archived NOAA NHC storm forecast and observation reports.

Synthetic storms, storms based on historical storms but with some possible differences, can be evaluated directly in a Level 2 modeling study. In particular, shifting the track of a storm is a common exercise in model studies because of the sensitivity of coastal storm surge to storm track. Other parameters which can be modified are storm movement speed, wind strength, etc., but care should be taken to alter only the characteristics of interest without affecting those that

should remain constant. For example, shifting the track and landfall location of Hurricane Katrina for the Gulf Coast 2 study (Choate *et al.* 2012) was done while simultaneously preserving the storm's forward speed and decay characteristics appropriately.

Expected future changes in the damaging coastal processes include RSLR and storm intensification. Also, local rates of subsidence can be very different. Care should be taken when developing RSLR scenarios for your study area. Section 4.1 (Sea Levels) provides discussions and materials related to sea level rise.

The selected sea level rise scenarios should be incorporated into the numerical model before the simulation is performed. Doing so provides the deterministic results to capture the nonlinear effects of sea level rise on storm surge and waves. Incorporating relative sea level rise into hydrodynamic models can be achieved in two possible ways: first, the sea level position can be increased relative to its present-day elevation or; second, the ground surface elevations can be reduced relative to their present-day positions. If the model provides an option for the user to prescribe a sea level offset, this will generally be the simpler and preferred method for incorporating sea level change as it does not call for one to modify the computational ground surface grid or mesh.

Associated effects of increasing sea level in a model simulation can be considered. Many hydrodynamic models call for the user to prescribe frictional constants throughout the computational domain. Frictional constants for dry land are typically based on land use and land cover data and represent the "roughness" of coastal landscapes. As new, low-lying areas are inundated by each sea level rise scenario, their frictional resistance should be lowered to be consistent with values of the surrounding water body (Smith *et al.* 2010). It may also be appropriate to consider and incorporate other major changes to the newly-inundated landscape. Examples include the abandonment and/or removal of major infrastructure; the recession and erosion of barrier islands; and the incorporation of new coastal engineering defenses like sea walls, dikes, levees, and beach fill projects.

**Future sea level rise will increase the vulnerability of our coastal highways.**

While the future intensification of storms is still an area of ongoing research, limited guidance is available in Knutson and Tuleya (2004), Knutson *et al.* (2007), Knutson *et al.* (2010), and other documents. For example, Knutson *et al.* (2010) state that tropical storms and hurricanes will grow in intensity by +2 percent to +11 percent by the year 2100. This roughly corresponds to a +3 percent to +21 percent central pressure fall. This information can be used to alter storm characteristics like wind speed and central pressure.

#### 14.3.2.2 Surge and Wave Models

One or more numerical models will be used in a Level 2 study. Few models are capable of simulating storm surge, waves, and shoreline change in a fully-integrated package. The selection of appropriate modeling tools is somewhat dependent upon the regional coastal processes of interest, the type of extreme event being considered, and the spatial coverage of the region to be modeled. The common storm surge models are briefly described in Section 4.3.2. In the Gulf and South Atlantic region of the US, USACE modelers and FEMA modeling contractors typically use the ADCIRC model to simulate storm surge from tropical storms and hurricanes because of its proven ability to model surge characteristics in a variety of complex situations.

A number of numerical models for simulating wave characteristics that may be used in a Level 2 study. See Section 5.4 for a discussion of the merits of some of the available wave models. Any appropriate shallow water wave model can be used for Level 2 studies. The case study in Section

14.8.2 used the ADCIRC model to estimate storm surge and the STWAVE model to estimate wave height fields throughout the flooded areas.

#### 14.3.2.3 Mapping of Results

After validating the selected numerical models, the process models storm and sea level scenarios and saves the outputs for analysis. These model results constitute a major source of information needed to assess exposure and evaluate sensitivity. Pertinent model results, like maximum storm surge elevation (or depth), wave height and direction, or overland flow velocity, can be mapped in GIS software for use with other relevant spatial layers, like transportation systems, demographics, etc. Appropriate examples are found in Choate *et al.* (2012) and USDOT (2013). These results can be presented at discrete times throughout the duration of the model simulation, or simply as the maximum values of each quantity. Examples of each include the time history of wave characteristics at a particular location, and the maximum envelope of water (MEOW), respectively.

A unique mapping of the damaging coastal processes can be done for each storm and sea level scenario considered. The effects of sea level on these processes, and the subsequent exposure to them, can be evaluated through direct comparisons to the historical, or model hindcast, results. Furthermore, the degree to which various scenarios modify the degree of exposure can be determined through direct comparisons between them.

Maps of the damaging coastal processes can be used to assess exposure in different ways. For example, maps of storm surge can be used to determine the spatial coverage and extent of inundation within the study area; maps of wave characteristics can be used to determine if, and to what degree, a particular asset will experience wave forces and overtopping; and maps of velocity can be used to determine hydrodynamic loads, scour, and erosion of embankments. Accordingly, practitioners may consider use of these data and maps to evaluate sensitivity when appropriate (e.g. USACE 2002, ASCE 2016, and this manual).

Caution should be exercised in the development of maps based on hydrodynamic model results, particularly those used to reference elevations. Hydrodynamic model results, like water levels, are commonly referenced to a vertical tidal datum (e.g. mean sea level). However, ground surface elevations and GIS layers containing transportation infrastructure are generally referenced to a vertical survey datum like NAVD. The difference between elevations referenced to either datum may be significant and should be accounted for prior to the mapping exercise. Model results referenced to a vertical tidal datum can be transformed to almost any vertical survey datum using NOAA's free software program VDATUM (<http://vdatum.noaa.gov/>). More information about tidal and survey datums is found in Section 4.2.2 Tidal and Survey Datums.

#### 14.3.3 Level of Effort 3: Gulf of Mexico and South Atlantic Coast

The process of conducting a Level 3 study is almost identical to that of a Level 2 study. This type of assessment includes identification of the damaging processes; selection of storm and sea level scenarios; numerical modeling of the selected scenarios; and assessment of exposure, and perhaps sensitivity, based on model outputs. However, the fundamental difference between the Level 2 and Level 3 approaches is the ability to assign probability and risk to scenario outcomes (see Section 3.1.2 Coastal Storm Flood Frequencies). A Level 3 study will consider hundreds of unique storm and sea level scenarios, each having their own assigned probability of occurrence, as compared to the one or two historical storms used in a Level 2 study. As a result, the level of effort, difficulty, cost, and duration of study are all likely to be higher for a Level 3 study.

The major steps for developing the information needed to perform a Level of Effort 3 exposure assessment for the Gulf of Mexico and Atlantic Coasts are summarized in Table 4.3. The

suggested methodology of a Level 3 study is very similar to the process used by FEMA to develop coastal flood hazard maps, or FIRMs and similar to the procedures used by the USACE in the Coastal Hazards System (USACE 2019) and plan formulation of large coastal projects. Specific guidance and details about how the FEMA studies are conducted are available in FEMA (2003).

Table 14.3. Exposure assessment steps for level of effort 3: Gulf of Mexico/South Atlantic Coast.

Step	Activity
1	Identify damaging coastal processes of interest (e.g. storm surge, waves, etc.)
2	Select and characterize storm and RSLR scenarios of interest
3	Select, develop, and prepare appropriate numerical modeling tools
4	Validate and/or calibrate the models through hindcast simulations and analysis
5	Incorporate RSLR scenarios into numerical model simulations
6	Perform model simulations of selected storm and sea level scenarios
7	Derive probabilities associated with water levels, wave heights, velocity, etc.
8	Map the damaging coastal processes for each return period (probability) of interest
9	Evaluate exposure and sensitivity of transportation infrastructure for each return period
10	Estimate risk as a function of scenario probability and time-interval considered

The most significant differences between a Level 2 and Level 3 study, where storm surge and waves are the primary damaging coastal processes of interest, are related to the characterization of storm and sea level scenarios, as well as their results. Instead of modeling only one or two notable historical storms, dozens to hundreds of synthetic storms may be developed and modeled. The parameters of these synthetic storms are initially based on historical storms that impacted the study area, but are altered to yield hundreds, and possibly even thousands, of unique storm events. The storm's track, landfall location, forward speed, central pressure, maximum winds, and radius to maximum winds (i.e. size) are typically the parameters that are adjusted to generate the unique storm scenarios. Each of the synthetic storms is also assigned a probability of occurrence based on its unique parameters. By doing so, the return period of each storm is known. FEMA has already performed this exercise in the process of updating flood hazard maps in many US coastal states and their counties, including many in this region. These storm characteristics, probabilities, and the associated model results are archived and stored by FEMA.

While previous FEMA coastal flood hazard studies represent excellent resources for the characterization of storm and surge frequencies they do not incorporate or account for the effects of sea level rise. Appropriate sea level scenarios could be incorporated into those synthetic storm scenarios, but the associated probabilities would generally be unknown. Until recently, most published sea level rise projections did not have associated probabilities. The IPCC (2007) published sea level rise projections for 2100 with 95 percent confidence intervals (2.5 percent probability of being equaled or exceeded) but those estimates did not fully account for the effects of ice sheet melting in Greenland or Antarctica. Houston (2013) provides updated sea level rise projections for the period 1990 – 2100 that attempted to appropriately account for these contributions as well as thermal expansion and the melting of glaciers and ice caps. The global mean sea level rise (GMSLR) projections for the period 1990 – 2100, as determined by Houston (2013) at the 5 percent, 50 percent, and 95 percent confidence intervals, are 0.59 ft, 1.6 ft, and 2.7 ft, respectively. Houston (2013) also describes the steps to determine sea mean level rise

projections at other confidence intervals. Note, however, that these are global sea level rise projections and do not account for local subsidence or regional variations in the distribution of the global mean (see Section 4.1 Sea Levels). For a fully probabilistic characterization of relative sea level rise, the probabilities associated with local subsidence rates would also have to be known, or at least assumed to be constant and stationary.

Currently no probabilities are associated with future storm intensification. Furthermore, there are currently no probabilities associated with future increases or decreases in landfalling storm frequency. There is some agreement, though, that the global frequency of all storms will decrease with a corresponding increase in the frequency of major storms (Knutson *et al.* 2010). Therefore, it may not be appropriate to assume that the probabilities of intensified storms will be equivalent to their present-day equivalent. This remains an area of needed research.

The inherent benefits in modeling hundreds of unique storm and sea level rise scenarios, each with their associated probability, also represent serious obstacles. The level of effort, time, and cost to perform such a large number of model simulations may be prohibitive.

After all storm scenarios have been modeled, the probabilities of each process of interest (e.g. water levels, wave heights, velocity, and shoreline change) should be derived from the model results. These probabilities are generally extracted from all model results at every geographic node or grid point in the computational domain. This is representative of the process that delineates a coastal flood plain for a specific return period event, as in the 100-year and 500-year flood plains. Statistical approaches for determining event probabilities are briefly described in Section 13.1 and can also be found in most hydraulic engineering texts.

In contrast to a Level 2 study where outcomes are based on specific scenarios, the outcomes of a Level 3 study are based on the probabilities of all scenarios considered. Therefore, the model results capture the frequent, low-intensity events, as well as the infrequent, high-intensity events, and everything in between. Once the values of relevant processes are determined and associated with specific probabilities (i.e. 100-year water level, 100-year wave height, etc.), risk can be assigned as a function of the project duration, life cycle, or for specific planning horizons.

As in the Level 2 study, maps of storm water levels, waves, velocity, and possibly shoreline change are anticipated to be the primary products of the model simulations. Unlike the Level 2 study where maps of each process are generated for each scenario, the relevant coastal processes will be mapped only at desired return periods. Exposure assessment can then be generalized in terms of probability and risk, as can sensitivity analyses.

## **14.4 Mid-Atlantic and New England Coast**

This section outlines the levels of effort, existing tools and data, appropriate models, and methodologies for determining exposure to extreme events along the Mid-Atlantic and New England Coasts. In this region of the US, tropical storms, hurricanes, and extratropical storms are the predominant extreme events, and the storm surge and waves they generate are the important coastal processes of interest (see Figure 14.4 for some New England shorelines). Other processes of interest in this region include tides, episodic shoreline change, and runoff to coastal waters. A multi-level approach for evaluating exposure to extreme events and sea level along these coasts is described in the subsections that follow.

### **14.4.1 Level of Effort 1: Mid-Atlantic and New England Coast**

The suggested methodology for performing a Level 1 study in this region is essentially the same as that described above in Section 14.3.1. The extreme events in this region are similar with the exception of extratropical storms. Accordingly, the damaging coastal processes of interest for this

region are also basically the same: storm surge and waves generated by strong storms. The major steps for developing the information needed to perform a Level of Effort 1 exposure assessment along the Mid-Atlantic and New England Coast are summarized in Table 14.4.

The coastal flood hazard maps produced by FEMA (<https://msc.fema.gov>) in this region are developed similar to those for the Gulf of Mexico and South Atlantic Coasts and give the same types of information. The flood hazard maps in this region show the 100-year return period still water elevations, relative to a survey datum, for different flood zones. In some locations, the BFE is also provided to show the elevation of probable wave attack. Detailed information about the mapping procedures is available in FEMA (2003). Additional guidance for mapping hazards in sheltered waters, like coastal embayments, is provided in FEMA (2008).

This region of the US corresponds to FEMA Regions 1, 2, 3, and part of 4 on the Atlantic Coast. **With the exception of northern Maine, flood map modernization has either been completed or is ongoing for most coastal counties along this coast.** Many of the coastal counties that were impacted by Hurricane Sandy in 2012 were in the process of updating their coastal flood hazard maps. In limited cases, communities adopted “Advisory Base Flood Elevations” (ABFEs) after Sandy. Unlike the BFEs listed on published FEMA FIRMs, these ABFEs are not based on a standard deterministic or probabilistic protocol. ABFEs have been based on storm-specific surge or high water mark elevations plus some increment, e.g. 1 to 3 ft, of freeboard. In general, the published FEMA FIRMs for this region should be used instead of ABFEs in the Level 1 study, unless there is accepted technical logic to use the ABFEs.

Local rates of relative sea level rise and their future projections should be considered in a Level 1 study. All coastal areas in this region are experiencing relative sea level rise, with the Mid-Atlantic region having rates 2 to 3 times higher than those along the New England coast. As previously described in Section 14.3.1, the USACE (2011) material on sea level change can be used along with their web-based tool ([https://cwbi-app.sec.usace.army.mil/rccslc/slcc\\_calc.html](https://cwbi-app.sec.usace.army.mil/rccslc/slcc_calc.html)) in order to develop appropriate relative sea level rise rates and projections for a specific study area.

One issue that remains unclear for this region of the US is the degree of nonlinearity associated with the effects of sea level rise on storm surge. All published studies documenting this effect were conducted in the Gulf of Mexico. The offshore bathymetry and topography of the Mid-Atlantic and New England coasts are very different than those in the Gulf of Mexico, and they likely play an important role in determining how storm surge is affected by higher sea levels. This is a topic for future research and caution should be exercised when applying the multiplier of 1.5 suggested in Section 14.3.1.

#### 14.4.2 Level of Effort 2: Mid-Atlantic and New England Coast

The process for conducting a Level 2 study in this region is almost identical to the one presented in Section 14.3.2, Level of Effort 2: Gulf of Mexico and South Atlantic Coasts. Exceptions include the selection and characterization of storm scenarios, as well as some of the physical processes that should be included in numerical model simulations. The general methodologies for conducting the study and assessing exposure are essentially the same as before and they are not repeated but the differences are outlined below. The major steps for developing the information needed to perform a Level of Effort 2 exposure assessment along the Mid-Atlantic and New England Coast are summarized in Table 14.5.

Table 14.4. Exposure assessment steps for level of effort 1: Mid-Atlantic/New England Coast

Step	Activity
1	Obtain appropriate FEMA flood map elevations for study area
2	Choose desired RSLR scenarios
3	Modify sea level change increments to account for nonlinearity
4	Add the result of Step 3 to the elevations obtained in Step 1
5	Obtain appropriate ground surface elevation maps for study area
6	Subtract ground elevations (Step 5) from values found in Step 4 to obtain flood depth
7	Multiply flood depths (Step 6) by 0.8 to determine maximum wave height
8	Multiply wave heights (Step 7) by 0.75, add to Step 4 for wave crest elevations
9	Use Equations 4.1 and/or 4.2 to estimate flood flow velocity
10	Consider shoreline retreat and erosion based on historical trends in study area
11	Map the damaging coastal processes (results from Steps 6-9)
12	Evaluate exposure of transportation infrastructure



Figure 14.4. Portland Head Lighthouse, Maine (2016)

Table 14.5. Exposure assessment steps for level of effort 2: Mid-Atlantic/New England Coast.

Step	Activity
1	Identify damaging coastal processes of interest (e.g. storm surge, waves, tides, runoff, etc.)
2	Select and characterize storm and RSLR scenarios of interest
3	Select, develop, and prepare appropriate numerical modeling tools
4	Validate and/or calibrate the models through hindcast simulations and analysis
5	Incorporate RSLR scenarios into numerical model simulations
6	Perform model simulations of selected storm and sea level scenarios
7	Map the damaging coastal processes for each scenario
8	Evaluate exposure and sensitivity of transportation infrastructure for each scenario

Extreme events in the Mid-Atlantic and New England coast include tropical storms, hurricanes, and strong extratropical storms. Sometimes, combinations of these events are also possible as demonstrated by Hurricane Sandy in 2012. The selection of an appropriate extreme event or storm scenario might include historical storms of record, low-intensity storms producing notable impacts, or perhaps a synthetic storm that hasn't even occurred. For example, researchers at Stevens Institute and Rutgers University considered a model scenario that combined some properties of Tropical Storm Irene (2011), which produced significant precipitation, with the size and winds of Hurricane Sandy (2012). A separate scenario simulated the effects of Sandy making landfall at the same time as the astronomical high tide, which altered the spatial coverage and extent of flooding.

Since the extreme events in this region are not limited solely to tropical cyclones, simply knowing the historical storm parameters will generally not provide enough information to recreate the meteorological forcing. Instead, measured or reanalyzed meteorological data should be obtained or created for the selected storm scenarios.

Most coastal circulation and wave models accept meteorological input in terms of wind (or wind stress) and pressure fields. An excellent source of meteorological measurements in coastal areas is provided by the NOAA National Data Buoy Center (<http://www.ndbc.noaa.gov/>). These platforms commonly record and archive wind speed, wind direction, and atmospheric pressure at intervals ranging from 6 minutes to 1 hour. While these platforms are robust, they do occasionally fail during extreme storm events, and sometimes their spacing is too coarse to resolve all characteristics of the meteorological forcing. The NOAA National Climatic Data Center (<http://www.ncdc.noaa.gov/>) provides fully reanalyzed meteorological data at a range of spatial scales appropriate for use in numerical models. If these two options do not provide suitable information, there are companies that sell detailed ocean weather data.

Once the desired storms or storm parameters have been selected, future changes in those storms could be incorporated. A storm's maximum winds, pressures, size, and precipitation are parameters of interest, as well as storm speed, track and landfall location. Appropriate regional and local relative sea level rise rates and projections can be developed as described in Section 4.1 and elsewhere in this manual. Changes in surface roughness for areas inundated by sea level rise can be incorporated into the selected numerical models.

A Level 2 exposure assessment in this region of the US calls for original numerical modeling of the selected storm and sea level scenarios. As described previously, the selected scenarios may need a few to tens of simulations. The numerical models should be selected, developed, and implemented in a manner that ensures the relevant physical coastal processes are being

simulated. For example, the contribution of wave setup to storm surge can become significant in this region of the US due to the offshore bathymetry. Numerical models, or combinations of models, that incorporate this additional forcing for storm surge should be used.

**Both nor'easters and hurricanes cause coastal infrastructure damage along the north Atlantic US coast.**

**The effects of tides and runoff from coastal watersheds on storm surge and waves are especially important in the Mid-Atlantic and New England coasts and can be considered in model simulations.** For example, developing a model scenario that considers the peaks of the local storm surge and stream flow hydrographs occurring simultaneously with the astronomical high tide will produce the maximum likely spatial coverage and depth of flooding. The increased flooding will subsequently allow wave impacts to reach further inland. Therefore, both the astronomical tides and stream flows should be included as boundary conditions in model simulations. Tidal characteristics are available at NOAA tide gage locations (<https://tidesandcurrents.noaa.gov/>). The USGS provides historical stream flow data and statistics (<https://waterdata.usgs.gov/usa/nwis/rt>).

If it is not possible to explicitly model the astronomical tides, one may consider an additional offset of the water level corresponding to the local mean higher high water (MHHW) elevation. Tidal datum information can be obtained from NOAA (<https://tidesandcurrents.noaa.gov/>). This is analogous to the process of changing the water level to account for higher future sea levels. The procedures for validating the numerical models, performing the simulations, interpreting the results, and mapping exposure are similar to those presented earlier.

#### 14.4.3 Level of Effort 3: Mid-Atlantic and New England Coast

A Level 3, risk-based, exposure assessment in this region of the US would be performed in a manner similar to that described in above in Section 14.3.3, Level of Effort 3: Gulf of Mexico and South Atlantic Coast. The primary regional differences have been described in the previous two sections. Those differences include the selection and characterization of storms to include both tropical and extratropical events; incorporating regionally appropriate sea level rise values; prescribing appropriate boundary conditions like astronomical tides and stream flows; and using numerical models that explicitly account for wave effects on storm surge. The major steps for developing the information needed to perform a Level of Effort 3 exposure assessment along the Mid-Atlantic and New England Coast are summarized in Table 14.6.

In addition to modeling the storm surge and waves for each of the probability-based storm and sea level scenarios in a Level 3 study, predictions of storm-induced shoreline change may be important for this region of the US. Shoreline change could be estimated using approximations like the “FEMA 540” rule; simple models like EDUNE and SBEACH; or sophisticated models like XBEACH, DELFT3D, MIKE 21, or Beach-fx (see Section 6.4).

Table 14.6. Exposure assessment steps for level of effort 3: Mid-Atlantic/New England Coast

Step	Activity
1	Identify damaging coastal processes of interest (e.g. storm surge, waves, tides, runoff, etc.)
2	Select and characterize storm and RSLR scenarios of interest
3	Select, develop, and prepare appropriate numerical modeling tools
4	Validate and/or calibrate the models through hindcast simulations and analysis
5	Incorporate RSLR scenarios into numerical model simulations
6	Perform model simulations of selected storm and sea level scenarios
7	Derive probabilities associated with water levels, wave heights, velocity, etc.
8	Map the damaging coastal processes for each return period (probability) of interest
9	Evaluate exposure and sensitivity of transportation infrastructure for each return period
10	Estimate risk as a function of scenario probability and time-interval considered

## 14.5 Great Lakes

This section outlines the levels of effort, existing tools and data, appropriate models, and methodologies for determining exposure to extreme events in the Great Lakes region. In this region of the US, frontal storms and extratropical storms are the predominant extreme events, and the storm surge and waves they generate are the important coastal processes of interest (see Figure 14.5). Other processes of interest in this region include changing lake levels, seiching, meteotsunamis, and bluff erosion. A comprehensive coastal flood study of the Great Lakes region can be found at <http://www.greatlakescoast.org>. A multi-level approach for evaluating exposure to extreme events and lake levels along the Great Lakes coasts is described in the subsections that follow. Each approach is described in terms of the existing technical resources available for the region. Some specific comments regarding how these methodologies may be affected by results of the ongoing flood study are provided.

### 14.5.1 Level of Effort 1: Great Lakes Coast

As in other regions of the US, a Level 1 exposure assessment in the Great Lakes might use existing FEMA flood hazard maps, or FIRMs, to determine the depth and spatial coverage of inundation (<https://msc.fema.gov>). The major steps for developing the information needed to perform a Level of Effort 1 exposure assessment on the Great Lakes Coast are summarized in Table 14.7.

Most of the developed and populated shorelines of the Great Lakes have been mapped by FEMA. These coastal areas are served by FEMA Regions 2, 3, and 5. There are considerable reaches of shoreline along Lakes Superior, Michigan, and Huron that remain unmapped.

Table 14.7. Exposure assessment steps for level of effort 1: Great Lakes Coast

Step	Activity
1	Obtain appropriate FEMA flood map elevations for study area
2	Choose desired lake level change scenarios that account for seasonal variability
3	Subtract (or add) the result of Step 2 from (to) the elevations obtained in Step 1
4	Obtain appropriate ground surface elevation maps for study area
5	Subtract ground elevations (Step 4) from values found in Step 3 to obtain flood depth
6	Multiply flood depths (Step 6) by 0.8 to determine maximum wave height
7	Multiply wave heights (Step 7) by 0.75, add to Step 4 for wave crest elevations
8	Use Equations 14.1 and/or 14.2 to estimate flood flow velocity
9	Consider shoreline retreat and erosion based on historical trends in study area
10	Map the damaging coastal processes (results from Steps 6-9)
11	Evaluate exposure of transportation infrastructure

The methodology and resources for performing a Level 1 exposure assessment in the Great Lakes region are essentially the same as those for the regions already described with one significant exception. In the Great Lakes region, we may experience a decrease in lake levels, not an increase (see Section 4.5, Lake Water Level Fluctuations). However, the projected lake level decreases are similar in magnitude to observed long-term oscillations (see Section 4.5). Lake levels also exhibit seasonal variability that should be considered. Historical and real time lake level data can be obtained from the NOAA Great Lakes Environmental Research Laboratory web site (<http://www.glerl.noaa.gov/>). Return period lake levels can be obtained from the USACE coastal storm database (<https://chswetool.erdcdren.mil/>). The database, named CSTORM-DB, is being populated with return period storm, water level, and wave statistics derived from modeling and statistical analysis as portions of the Great Lakes Flood Study are completed.

Falling lake levels will alter how one evaluates exposure, sensitivity, and vulnerability in the Great Lakes region. The spatial coverage and depth of inundation are likely to decrease with falling lake levels. The wave impacts will generally be of a similar magnitude but will impact areas at lower elevations than present-day. This may expose foundations, embankments, revetments, and other structures to very high forces not accounted for in their design. Furthermore, falling lake levels may lead to undercutting of the shoreline and/or bluffs as highly erodible soil layers are directly impacted by wave action. For these reasons, consideration should be given to the extent of wave runup in the various scenarios.

Great Lakes water levels also exhibit season fluctuations that will be superimposed on the projected future trend. Therefore, as lake levels fall there will be times throughout the year when water levels and wave impacts occur at elevations below and above the annual mean lake level. Accounting for these seasonal fluctuations may make it necessary to consider a range of potential elevations that will be exposed to the damaging physical coastal processes.



Figure 14.5. Chicago waterfront (2018)

When using the existing FEMA flood hazard maps for the Great Lakes in a Level 1 analysis, the stated still water elevations and base flood elevations could be incrementally shifted downward to reflect falling lake levels. More information about the expected lake level fluctuations on the Great Lakes can be found at the “Great Lakes Integrated Sciences + Assessments” web site (<http://glisa.msu.edu/index.php>).

In addition to the potential for falling lake levels, the application of the Level 1 methodology in this region is unique because there is no existing literature on the potential nonlinear relationship between the effect of falling sea or lake levels on storm surge and waves. Therefore, a multiplier

is not used for these locations. Further research is needed to quantify and describe these potential effects.

The estimation of shoreline change, dune erosion, and bluff erosion may not be possible using simple rules or historical trends. If they are of concern, some simple numerical modeling may be performed. Appropriate information can be found on the Great Lakes Coastal Flood Study web site. A specific example includes use of the one-dimensional model CSHORE (Johnson *et al.* 2012) to estimate waves, water levels, and beach profile evolution. The Great Lakes Coastal Flood Study web site also provides links to oblique aerial photography, LiDAR bathymetry and topographic elevations, and geodatabases that will be useful for studies in this region of the US.

#### 14.5.2 Level of Effort 2: Great Lakes Coast

A Level 2 exposure assessment or sensitivity analysis will use many of the same steps, and use many of the same models, described above for the other regions of the US. The major steps for developing the information needed to perform a Level of Effort 2 exposure assessment for the Great Lakes Coast are summarized in Table 14.8. As applied to the Great Lakes region, a Level 2 assessment will still need identification of damaging physical coastal processes; selection and development of relevant storm and lake level scenarios; selection and validation of numerical models; model simulations of the desired scenarios; and mapping of exposure. The primary differences in application of the Level 2 approach presented earlier is related to identification of the physical processes and the storm scenarios that create them.

Extreme meteorological events in this region are characterized by frontal systems, extratropical storms, the remnants of tropical low-pressure systems, and combinations thereof. Similar to other regions of the US, these extreme events produce wind-generated surge and waves that cause inundation and damaging wave forces to reach further inland and at higher elevations. In rare cases, these weather systems can produce seiching of the lakes. In even rarer cases, extreme weather systems have generated meteotsunamis that cause damage to infrastructure at higher elevations. These physical processes, as well as their effects on the shoreline, are modified in the winter seasons by the presence of lake ice. As the extent and duration of ice coverage in the Great Lakes, so too will the physical processes and their impacts be modified.

Table 14.8. Exposure assessment steps for level of effort 2: Great Lakes Coast

Step	Activity
1	Identify damaging coastal processes of interest (e.g. storm surge, waves, bluff erosion, etc.)
2	Select and characterize storm and lake level scenarios of interest
3	Select, develop, and prepare appropriate numerical modeling tools
4	Validate and/or calibrate the models through hindcast simulations and analysis
5	Incorporate lake level scenarios into numerical model simulations
6	Perform model simulations of selected storm and lake level scenarios
7	Map the damaging coastal processes for each scenario
8	Evaluate exposure and sensitivity of transportation infrastructure for each scenario

The selection of appropriate storm scenarios in the Great Lakes region can be treated as in other regions of the US. Extreme events of interest may include either infrequent but intense historical storms that have had significant impacts within the study area, or perhaps a frequent, low-intensity

historical storm that had notable impacts. As in other regions, combinations of historical storm parameters may be considered in order to generate a synthetic storm.

Selection of an appropriate extreme event for a study area may also be a function of the damaging physical processes it produces. For example, if the inundation and high flood velocity attributed to a meteotsunami are of concern, then a storm event capable of (or known to have) producing one should be modeled.

As in other Level 2 assessments, a few storm scenarios representative of the study area, or reflective of the processes of interest, should be considered and later modified to account for the expected impacts of lake levels in the region. Development of the meteorological forcing for the numerical model simulations will take some effort. The meteorological forcing can be reconstructed from measured winds and pressures in the study area, or from reanalyzed environmental data. Note here that in addition to winds and pressures, precipitation, temperatures, and lake ice coverage may also be important. Real-time and historical meteorological and hydraulic measurements can be obtained from the NOAA Great Lakes Environmental Research Laboratory (<http://www.glerl.noaa.gov/data/>). The NOAA National Climatic Data Center (<http://www.ncdc.noaa.gov/>), NOAA National Centers for Environmental Prediction (NCEP) (<http://www.ncep.noaa.gov/>), and NOAA NCEP Climate Forecast System Reanalysis (<http://cfs.ncep.noaa.gov/cfsr/>) serve as excellent sources for reanalyzed meteorological data. The Great Lakes Coastal Flood Study web site should also be consulted.

The relevant lake levels scenarios to consider for the Great Lakes region are those that will significantly impact storm surge, waves, and shoreline change; and those that can be readily incorporated into hydrodynamic models. Here, the selected storm scenarios should be simulated on future lake levels, which are projected to be lower than their present-day elevations. The effects of lake ice coverage and duration may also be simulated by decreasing the spatial ice coverage and/or increasing the number of ice-free days for storms occurring in the winter months. Ice coverage is generally accounted for as an increase in friction or drag coefficients in wind-stress formulations. Note that the model should be capable of accepting spatially variable coefficients for this to be possible.

**Frontal-passage storms can cause significant infrastructure damage on the Great Lakes.**

Future lake levels can be incorporated into the selected models as a reduction in the mean lake level position: a negative offset of the present-day lake level. If such an offset is not possible in the numerical model, then all topographic and bathymetric elevations can be shifted upward (positive) by an equivalent amount. Either way, the net effect is that the lake levels will be lower relative to the land surface. Caution should be exercised when using the latter approach, as direct comparisons of model results to existing data referenced to its original vertical datum will not be possible. In this case, the elevations of either the modeled results or the existing infrastructure data should be altered. Preference should be given to correcting modeled results at the completion of the model study, but prior to exposure mapping, to avoid potential errors.

The modeling of storm and lake levels scenarios, as well as the validation of selected numerical models, should be performed in a manner similar to what was described in previous sections. However, the spatial coverage of the general circulation (storm surge) model should receive special attention in this region. An entire lake should likely be modeled in order to properly simulate wind surge and waves. If the specific study area falls within Lakes Michigan or Huron, both lakes should be modeled to capture the coupling between them. The coupling may not impact

wind-wave generation as much as it will the lake water levels, but if the contributions of wave setup to the total water level are of interest then they should be accounted for in this manner.

Upon completion of the storm and lake levels scenario simulations, exposure of infrastructure to water levels, waves, velocity, and shoreline change should be mapped using a methodology consistent with descriptions provided in previous sections of this manual. As in other Level 2 assessments, exposure maps of each process will be generated for each scenario considered and are expected to be the primary products of the study. The maps can also be used to evaluate sensitivity of specific infrastructure to the relevant physical processes and the effects of lake levels on them.

### 14.5.3 Level of Effort 3: Great Lakes Coast

The suggested methodology for performing a Level 3 assessment in the Great Lakes region differs from that described for the Gulf and Atlantic Coasts. In the Great Lakes region, probabilities are associated with the storm response, e.g. resultant water level, rather than assigned to storm characteristics, e.g. wind speed. This methodology is what FEMA refers to as the “storm response method” or “total water level method.” The storm response method is more fully described in FEMA (2005). Additional guidance for mapping hazards in sheltered waters, like embayments, is available in FEMA (2008). The major steps for developing the information needed to perform a Level of Effort 3 exposure assessment in the Great Lakes region are summarized in Table 14.9.

**The storm response method and original numerical modeling are being applied in the ongoing Great Lakes Coastal Flood Study** to develop new maps that communicate risk related to the wind surge, wave, wave runup, and shoreline erosion hazards. These hazards will be communicated at probabilities defined by the 10-, 50-, 100-, and 500-year return period intervals. These correspond to the 10 percent, 2 percent, 1 percent, and 0.2 percent annual chance of exceedance, respectively.

Table 14.9. Exposure assessment steps for level of effort 3: Great Lakes Coast

Step	Activity
1	Identify damaging coastal processes of interest (e.g. storm surge, waves, tides, bluff erosion)
2	Select and characterize relevant lake levels scenarios (i.e. lower lake levels)
3	Select, develop, and prepare appropriate numerical modeling tools
4	Validate and/or calibrate the models through hindcast simulations and analysis
5	Model and derive hazard probabilities using the storm response method or use existing hazard values at design return periods as model boundary conditions
6	Incorporate lake levels scenarios into numerical model simulations
7	Perform model simulations of selected storm and lake levels scenarios
8	Map the damaging coastal processes for each return period (probability) of interest
9	Evaluate exposure and sensitivity of transportation infrastructure for each return period
10	Estimate risk as a function of scenario probability and time-interval considered

In the storm response method, event probabilities like return period water levels and waves, are generated through a combination of traditional frequency analysis, when measurements are available, and hindcast numerical modeling when they are not. Storm response records are

reconstructed by considering peak values over specific thresholds. The storms that produced the peak values are simulated in hindcast mode to recreate the data needed to perform the frequency analysis.

Some probabilistic data are available for the Great Lakes through the USACE WIS and CSTORM-DB web data portals. These data are archived at a number of “save points” along the coast. The spacing of the save points is generally adequate to resolve detailed wave transformation and shoreline processes. A number of companion documents are also available through the study web site.

If the exposure assessment calls for the development of new or different hazard probabilities, then the modeling and frequency analysis inherent to the storm response method should be performed first. Such modeling would use the application of lake-wide surge and wave models to generate the data necessary to perform a frequency analysis.

The amount of modeling needed to generate probabilistic hazard values can be substantially reduced if existing data are available and used in the study. In that case, the number of model scenarios is a function of the number of scenarios considered and/or the number of locations where the modeling is performed. For a Level 3 exposure assessment, the relevant lake levels scenarios should consider future lake levels that are lower than their present-day elevations. The desired return period water levels can then be incrementally lowered for each scenario and applied as boundary conditions in one- and/or two-dimensional process models. The corresponding return period wave characteristics can be applied in a similar manner, as can any meteorological forcing.

Appropriate numerical models for simulating storm surge, waves, and shoreline change in this region are similar to those listed elsewhere in this manual. In order to generate the probabilistic data necessary to perform a Level 3 assessment, the use of one- and/or two-dimensional models is suggested. Application of two-dimensional models may reduce the total number of simulations as they may resolve the entire study area; however, they typically take much more time to complete. As an alternative, a number of one-dimensional process models can be applied at desired transects, or shore-perpendicular reaches, within the study area. A specific example would be the application of CSHORE with the appropriate return period wave and water level values prescribed as boundary conditions.

A benefit of the storm response method is that probabilities are assigned to the hazards, not the storms that generate them. Therefore, the model results will inherently be probabilistic in nature and eliminating a need to derive probabilities from model results. This constitutes a significant difference from the Level 3 methodology described in previous sections. However, keep in mind that in order for the results of the lake levels scenarios to be fully applied in a risk framework, the probabilities associated with future lake levels would also have to be known. Such information is not currently available and the subsequent limitations should be acknowledged and preferably accounted for as part of the Level 3 assessment.

Upon completion of the scenario simulations, mapping of exposure and sensitivity analyses can be performed in a manner similar to what has been described in previous sections of this manual. Particular attention should be given to the fact that as lake levels fall, areas not previously exposed to direct wave attack and high velocity flows will become vulnerable. As a consequence, sensitivity analyses in the Great Lakes region should include structure stability and foundation integrity.

## **14.6 Pacific Coast & Islands – Storms**

This section specifically outlines the levels of effort, existing tools and data, appropriate models, and methodologies for determining exposure to extreme events along the Pacific Coast, including

Alaska, Hawaii and the other islands in this region of the US, extratropical storms and tsunamis are the predominant extreme events (see Figure 14.6 for types of Pacific Coast shorelines). Although rare, southern California and Hawaii have occasionally experienced tropical storms and hurricanes.

This section focuses on storms and their impacts. The coastal processes of interest in this region are water levels, large waves, wave setup, wave runup, tides, storm- induced shoreline change, bluff erosion, and runoff from coastal watersheds. **Water levels and storm intensity in this region are strongly influenced by changes in the Pacific Decadal Oscillation (PDO) and El Nino-Southern Oscillation (ENSO) processes.** A multi-level approach for evaluating exposure to extreme storm events with sea levels along these coasts is described. An approach for assessing exposure to tsunami hazards is provided in Section 14.7.

#### 14.6.1 Level of Effort 1: Pacific Coast – Storms

Similar to other regions of the US, a Level 1 exposure assessment in this region might use existing FEMA flood hazard maps, or FIRMs, to determine the depth and spatial coverage of inundation (<https://msc.fema.gov>) at the 1 percent or 0.2 percent annual chance of flooding. Most of the developed and populated shorelines of Alaska, California, Hawaii, Oregon, and Washington have been mapped by FEMA. Vast reaches of coastline in Alaska remain unmapped, as well as some isolated areas in other states. These coastal areas are served by FEMA Regions 9 and 10.

The major steps for developing the information needed to perform a Level of Effort 1 exposure assessment for the Pacific Coast are summarized in Table 14.10. The process for developing flood hazard maps in this region of the US is essentially the same as that described in Section 14.5 for the Great Lakes region. The storm response method, or total water level method, is applied since the most extreme storm events are non-tropical and, therefore, difficult to assign probabilities to. Therefore, the 1 percent and 0.2 percent flood hazards delineated on the FEMA maps are derived from measurements or model hindcasts describing the response of coastal water levels to historical storms over a 30-, 40-, or 50-year period. More information about the mapping procedures and zones is available in FEMA (2005).

Table 14.10. Exposure assessment steps for level of effort 1: Pacific Coast

Step	Activity
1	Obtain appropriate FEMA flood map(s) for study area
2	Choose desired RSLR scenarios (i.e. magnitude and direction)
3	Subtract or add the result of Step 2 from the still water elevations obtained in Step 1
4	Obtain appropriate ground surface elevation maps for study area
5	Subtract ground elevations (Step 4) from values found in Step 3 to obtain flood depth
6	Multiply flood depths (Step 5) by 0.8 to determine maximum wave height
7	Multiply wave heights (Step 6) by 0.75, add to Step 3 for wave crest elevations
8	Use Equations 14.1 and/or 14.2 to estimate flood flow velocity
9	Consider shoreline retreat and bluff erosion based on historical trends or modeling
10	Map the damaging coastal processes
11	Evaluate exposure of transportation infrastructure

However, the magnitude and direction of sea levels are highly variable in some areas. Most of California, Hawaii, Oregon, and Washington are experiencing RSLR having rates on the order of 0 to 2 ft per century. Isolated portions of northern California, northern Oregon, and northern

Washington are experiencing relative sea level fall on the order of 0 to -1 ft per century. In Alaska, the relative sea level rates vary greatly from +1 ft/century to -6 ft/century.

The selection of an appropriate sea level change scenario will be a function of the study area location and regional extent. It may not be possible to cover large spatial regions in this type of exposure assessment if the sea level change rates are highly variable over the study area.

The contribution of wind-driven surge to the total water level is much smaller in this region due to the steep coastal bathymetry and narrow continental shelf. However, the contribution of wave setup and wave runup is much more significant than in other regions. The nonlinear coupling between sea level change and wave characteristics is not well understood and only limited examples from the Gulf coast exist that quantify those effects. For example, the study of Smith *et al.* (2010) in Louisiana found the increase in wave heights to be equal to or less than the incremental change in sea level. Since only limited information is available, and the potential nonlinear coupling along the Pacific Coast is currently unknown, a multiplier on sea level change should not be used.

Separate shoreline change modeling may be desired to capture the effects of sea levels on beach profile evolution and bluff erosion. FEMA (2005) offers recommendations in this area.

Most of the data resources presented in previous sections will also be useful for exposure assessments in these regions. Specific examples include the NOAA Coastal Services Center Digital Coast web data portal (<http://coast.noaa.gov/digitalcoast/>), the NOAA National Geophysical Data Center (<http://www.ngdc.noaa.gov/mgg/bathymetry/relief.html>), the USGS National Map Viewer (<http://viewer.nationalmap.gov/viewer/>), and the USACE WIS database (<http://www.usace.army.mil/>).



Figure 14.6. Laguna Beach, California

### 14.6.2 Level of Effort 2: Pacific Coast – Storms

The suggested methodology for a Level 2 study in this region is very similar to the process described previously for the Great Lakes. The major steps for developing the information needed to perform a Level of Effort 2 exposure assessment for the Pacific Coast are summarized in Table 14.11. The major differences here include the need to account for tides, water level fluctuations, and relative sea level rise (or fall) that is location-specific. Most of the same steps outlined in previous Level 2 assessments and most of the data resources and models described earlier will also apply here.

Table 14.11. Exposure assessment steps for level of effort 2: Pacific Coast.

Step	Activity
1	Identify damaging coastal processes of interest (e.g. water levels, wave runup, erosion)
2	Select and characterize storm and RSLR scenarios of interest
3	Select, develop, and prepare appropriate numerical modeling tools
4	Validate and/or calibrate the models through hindcast simulations and analysis
5	Incorporate RSLR scenarios into numerical model simulations
6	Perform model simulations of selected storm and sea level scenarios
7	Map the damaging coastal processes for each scenario
8	Evaluate exposure and sensitivity of transportation infrastructure for each scenario

The selection and characterization of extreme storm events and sea level for this region will be somewhat different from others. As in other regions, a range of possible intensities informs the selection of appropriate storm events. However, for statistical robustness it is also important to consider the timing of the events with the highest astronomical tides of the year (locally referred to as king tides). Because of the large tide range in Alaska, it may also be relevant to consider wave impacts at lower elevations, similar to the Great Lakes region. Contributions of runoff from coastal watersheds can also be considered in the selection of storm events or the development of synthetic storms.

Sea level rise is expected to lead to greater inundation, along with broader expanses of possible wave impacts, during astronomical high tides for even mild extratropical storms. Once the selected extreme storm event scenarios have been selected, sea level can be incorporated by considering future sea level projections at desired time intervals or planning targets. Of the selected storm and sea level rise scenarios, at least one should consider an historical storm on present-day sea levels to serve as a hindcast scenario for model validation.

The selection of appropriate numerical models should be based on the relevant processes of interest. Numerical models that simulate astronomical tides, waves, wave setup, wave runup, and shoreline change along the Pacific Coast should be considered. Although wind surge is not a significant component of the total water level along the Pacific Coast, it will typically be accounted for in most general circulation models used to simulate the astronomical tides. Such models are generally capable of accepting stream flows as non-oscillatory, or discharge, boundary conditions as well. Changes in land surface roughness could be incorporated into the selected numerical models as areas are affected by sea level change.

**Storm wave runup is a significant contributor to infrastructure damage on the Pacific coast.**

In some cases, it may be necessary to supplement the tide, wave, and shoreline modeling with other process-based modeling. For example, additional modeling may be needed to capture wave transformations and runup in sheltered waters. These procedures are outlined in FEMA (2008). The use of equations may also be appropriate and necessary, as in the case of estimating wave overtopping rates. The USACE (2002) and Pullen *et al.* (2007) provide information on these situations.

#### 14.6.3 Level of Effort 3: Pacific Coast – Storms

The major steps for developing the information needed to perform a Level of Effort 3 exposure assessment for the Pacific Coast are summarized in Table 14.12. The regionally appropriate processes, storm events, and scenarios described in earlier sections are accounted for and applied here.

Probabilistic flood hazards should be based on a storm response method that accounts for the frequency of all relevant processes. Much of this analysis is part of the FEMA California Coastal Analysis and Mapping Project: Open Pacific Coast study. As new areas are studied in this region, the probabilistic hazard data will become part of the USACE CSTORM-DB. **Return period wave and wind characteristics are available at many save points along the Pacific, Alaskan, and Hawaiian coasts. See the USACE WIS Pacific database at (<http://www.usace.army.mil/>).**

Table 14.12. Exposure assessment steps for level of effort 3: Pacific Coast.

Step	Activity
1	Identify damaging coastal processes of interest (e.g. water levels, waves, erosion)
2	Select and characterize relevant scenarios (e.g. sea levels, runoff)
3	Select, develop, and prepare appropriate numerical modeling tools
4	Validate and/or calibrate the models through hindcast simulations and analysis
5	Model and derive hazard probabilities using the storm response method or use existing hazard values at desired return periods as model boundary conditions
6	Incorporate RSLR scenarios into numerical model simulations
7	Perform model simulations of selected sea level scenarios
8	Map the damaging coastal processes for each return period (probability) of interest
9	Evaluate exposure and sensitivity of transportation infrastructure for each return period
10	Estimate risk as a function of scenario probability and time-interval considered

The selection and application of numerical models for this region should reflect the characteristics of the processes to be modeled. As previously mentioned, astronomical tides, water level fluctuations related to ENSO and PDO, wave transformation, wave runup, wave overtopping, and runoff from coastal watersheds should be simulated to determine the probabilistic flood, wave, and erosion hazards. Many of the numerical models described earlier could be applied appropriately in this region. One modeling system unique to this region is the USGS Coastal Storm Modeling System, or CoSMoS. The system is capable of simulating water levels, waves, coastal erosion and inundation. In addition to providing real-time forecasts of these processes,

CoSMoS has also been successfully applied to recreate historical storms and synthetic scenarios ([http://walrus.wr.usgs.gov/coastal\\_processes/cosmos/](http://walrus.wr.usgs.gov/coastal_processes/cosmos/)).

Application of the CoSMoS system to desired return period and sea level scenarios could provide the probabilistic hazard values needed to perform a Level 3 risk-based exposure assessment in this region. Such detailed assessments will be greatly facilitated as additional flood hazard studies are completed by FEMA and USACE along the Pacific Coast.

## **14.7 Pacific Coast & Islands – Tsunamis**

This section broadly outlines suggested levels of effort, existing tools and data, appropriate models, and methodologies for determining exposure to tsunami events along the Pacific Coast, including Alaska and Hawaii. Specific literature for the determination of tsunami hazards is relatively new and only exists in limited forms. Probabilistic tsunami hazard assessments are even more limited, but a number of pilot studies are ongoing on the Pacific Coast. At the time of the preparation of this document, a multi-state and federal study is developing bridge design guidelines for the estimation of tsunami loads on highway bridges (Transportation Pooled Fund Program 2019).

This section broadly outlines suggested levels of effort, existing tools and data, appropriate models, and methodologies for determining exposure to tsunami events along the Pacific coast, as well as the coasts of Alaska and Hawaii (see Figure 14.7 for Hawaii shoreline). Specific literature for the determination of tsunami hazards is relatively new and only exists in limited forms. Probabilistic tsunami hazard assessments are even more limited, but a number of pilot studies are ongoing on the Pacific Coast. Engineering guidance for the estimation of tsunami loads is presented in ASCE (2016). The multi-level approach for evaluating exposure to tsunami events and sea level along these coasts is described in general terms in this section.

### **14.7.1 Level of Effort 1: Pacific Coast – Tsunamis**

An appropriate Level 1 study of exposure in this region may be based upon existing tsunami inundation maps. Such maps are available for nearly all coastal areas of Alaska, California, Hawaii, Oregon, and Washington. Most of these inundation maps can be obtained through the National Tsunami Hazard Mitigation Program web site (<https://nws.weather.gov/nthmp/>). The Pacific Northwest Seismic Network web site also contains links to many tsunami inundation maps and associated products (<http://www.pnsn.org>), as does the NOAA Center for Tsunami Research (<http://nctr.pmel.noaa.gov/index.html>). The following sites provide access or links to the maps for each state:

- Alaska: <http://www.dggs.alaska.gov/>
- California: <http://www.quake.ca.gov/gmaps/WH/tsunamimaps.htm>
- Hawaii: <http://www.honolulu.gov/demhazards/tsunamimaps.html>
- Oregon: <http://www.oregongeology.org/tsuclearinghouse/pubs-inumaps.htm>
- Washington: [http://www.dnr.wa.gov/Publications/ger\\_tsunami\\_inundation\\_maps.pdf](http://www.dnr.wa.gov/Publications/ger_tsunami_inundation_maps.pdf)

Unlike FEMA flood hazard maps, tsunami inundation maps do not provide the information needed to estimate flood depth. This is because tsunami inundation maps show only the spatial coverage of inundation that would result from the most probable worst-case tsunami (Bernard *et al.* 1996). The concept of a “still water elevation” does not necessarily apply for the description of tsunami hazards. A tsunami is a long period wave and not a wind-driven storm surge. As a result, the flood moves as a wave having a large amplitude, long period, and high speed. These properties allow

the wave to reach a considerable distance inland, demonstrate considerable wave runup, and translate into very high flood velocities and hydrodynamic loads.

Tsunami inundation maps cannot be directly used to determine the spatial extent and depth of flooding, or expected flood velocity. A new tool for estimating some of these properties, based on existing tsunami inundation maps and land surface elevations, can be very useful for Level 1 assessments of the tsunami hazard (Kriebel *et al.* 2017). The methodology applies an Energy Grade Line concept to describe the maximum expected flood depth, flow velocity, and momentum flux along chosen shore-perpendicular transects. The concept is somewhat similar to standard hydraulic equations for calculating water surface profiles that are available in most hydraulic texts.

**Tsunamis have damaged coastal highways and bridges in Hawaii.**

At this time, there are no widespread materials or processes for the assessment of tsunami hazards. The reader is directed to Gonzalez *et al.* (2003) and FEMA (2012) for additional information on understanding and assessing tsunami hazards in this region. For those sources, Table 14.13 summarizes suggested steps for performing a Level of Effort 1 exposure assessment to tsunamis with sea level.

Table 14.13. Exposure assessment steps for level of effort 1: tsunamis.

Step	Activity
1	Obtain appropriate tsunami inundation maps for study area
2	Choose and incorporate desired sea level change scenarios
3	Apply an energy-based concept to estimate flood depth and velocity along a transect
4	Map the damaging coastal processes
5	Evaluate exposure of transportation infrastructure

The potential nonlinear effect of future sea levels on tsunami propagation and transformation are likely insignificant, but the degree to which wave runup will be affected is currently unknown. Therefore, a multiplier should not be applied to the sea level change scenario.

Incorporating probabilistic tsunami hazards into FEMA's Risk Management, Assessment, and Planning (Risk MAP) program is the subject of pilot studies in Crescent City, California (Tsunami Pilot Study Working Group 2006; and Gonzalez *et al.* 2009) and Seaside, Oregon (CGS 2013). The probabilistic tsunami hazard maps for Seaside, Oregon have been developed and communicate flood risk for the 1 percent and 0.2 percent annual chance events. These levels were chosen to be consistent with existing FEMA National Flood Insurance Program guidance.

#### 14.7.2 Level of Effort 2: Pacific Coast – Tsunamis

A suggested Level 2 study for mapping the exposure of transportation infrastructure to tsunami inundation is based on original numerical modeling of selected tsunamigenic events under appropriate sea level scenarios. Here, a tsunamigenic event could be a seismic event or landslide. The selection of an appropriate tsunami event could include consideration of those that have previously impacted the study area, or tsunamigenic events producing a credible worst-case scenario. Relevant sea level scenarios could include sea level rise or fall depending on the location of the study area and its corresponding sea level trends and projections.

Once the selected tsunami event and sea level scenarios have been developed, their effects can be simulated using an appropriate numerical model. A number of complex numerical models are

being applied to the study, and forecasting, of tsunamis. Most of these modern tsunami models simulate three mostly independent processes: tsunami generation (i.e. earthquake), transoceanic propagation, and inundation of dry land. While the first and last processes are somewhat challenging to simulate, modeling the propagation of the tsunami is comparatively easy. In fact, tsunami waves propagate as surface gravity waves and undergo many of the same transformation processes as other ocean waves. The NOAA Center for Tsunami Research (<http://nctr.pmel.noaa.gov/index.html>) provides an overview of current tsunami forecasting and research efforts.

The NOAA Center for Tsunami Research specifically uses the Method of Splitting Tsunami (MOST) model (Titov and Synolakis, 1997; Titov and Gonzalez, 1997). The MOST model system is a suite of numerical models capable of simulating the three processes of tsunami evolution. The model has been extensively validated against previous tsunami events and is actively being implemented in tsunami forecast systems around the US.



Figure 14.7. Wainiha River, on the north shore of the island of Kauai, Hawaii, is an area with an extremely high tsunami hazard and a history of tsunami-induced bridge damage

There are numerous other tsunami models with capabilities similar to MOST, specifically the ability to model the tsunami propagation and inundation of dry land. Some of the more commonly used tsunami models include the TSUNAMOS model developed by Dr. Patrick Lynett and colleagues (<http://coastal.usc.edu/plynett/TSUNAMOS/index.html>); the GeoClaw model of Berger *et al.* (2011); the Cornell Multi-grid Coupled Tsunami (COMCOT) model of Liu *et al.* (1998); the TUNAMI model(s) documented in UNESCO (1997); the JRC Tsunami Model of Annunziato and Best (2005); and special applications of DELFT3D described in Gelfenbaum *et al.* (2006, 2007) and more recently Sasaki *et al.* (2012).

Summarizing and synthesizing such literature, Table 14.14 provides potential steps for developing the information needed to perform a Level of Effort 2 exposure assessment related to tsunami hazards and sea level.

Table 14.14. Exposure assessment steps for level of effort 2: tsunamis

Step	Activity
1	Identify damaging processes of interest (e.g. flood depth, velocity, runup)
2	Select and characterize tsunamigenic and sea level scenarios of interest
3	Select, develop, and prepare appropriate numerical modeling tools
4	Validate and/or calibrate the models through simulation of historical tsunami events
5	Incorporate sea level scenarios into numerical model simulations
6	Perform model simulations of selected tsunami and sea level scenarios, including the potential ground subsidence from subduction zone rupture events
7	Map the damaging coastal processes for each scenario
8	Evaluate exposure and sensitivity of transportation infrastructure for each scenario

The procedures for mapping exposure to tsunami events and sea level rise will be similar to other coastal hazards in other regions of the United States. One particular exception may be the communication of inundation as flood depths as opposed to still water elevations. The expected results of the model studies will be maps of inundation coverage and depth, flow velocity, and possibly momentum flux. As in other Level 2 studies, these maps are anticipated to be the primary products of the mapping effort. Exposure assessments and sensitivity analyses can be performed using the maps of each hazard for each scenario considered. Methods for evaluating tsunami loads and effects are presented in ASCE (2016).

#### 14.7.3 Level of Effort 3: Pacific Coast - Tsunamis

Probabilistic tsunami hazard analysis is a relatively new concept. Tsunami hazards are often defined by the inundation resulting from a probable worst-case scenario for a particular area. However, there are no probabilities associated with such scenarios or the tsunami response. An accepted framework for the probabilistic description of tsunami hazards has been established and is consistent with seismic hazard analysis (Geist and Parsons, 2006). Application of the probabilistic analysis technique for California is described in Thio *et al.* (2010).

A suitable methodology for performing a probabilistic tsunami hazard analysis is described in Gonzalez *et al.* (2009). While the methodology was applied to a specific location, it could be replicated and used as the basis of a probabilistic Level 3 exposure assessment. The methodology was used to derive the 100- and 500-year tsunami inundation areas and elevations. Application and use of a numerical model (MOST), as well as the derivation of exceedance values, are described in Gonzalez *et al.* (2009). A similar technique is currently being used to develop probabilistic tsunami hazard maps for Crescent City, California (CGS 2013).

The probabilistic values of tsunami inundation should be determined through a joint probability analysis that considers both the probability of the tsunamigenic event (i.e. return period of the source event of each specified magnitude) and the flood exceedance (Gonzalez *et al.* 2009). The development of tsunami flood hazard maps currently defines flood levels for the 100- and 500-year return period events. Consideration could be given to the inundation from other return period events as well. For consistency with ASCE-7 seismic hazard analysis, 2,500-year Tsunami design map is offered by ASCE-7 (<https://asce7tsunami.online/>). The Transportation Pooled Fund research TPF-5(307) (Transportation Pooled Fund Program 2019) produced 1,000-year tsunami

inundation map for the participating States (AK, CA, HI, OR, WA). It also produced areal coverage of tsunami design parameter map for California and part of Oregon, which include maximum depth and maximum velocity in the inundated area (1,000-year return period) that can be directly used in tsunami load formulas developed in the same project. These maps include the effect of potential ground subsidence in the subduction zone events.

As in other exposure assessments for the Pacific Coast, appropriate sea level scenarios should be incorporated into the probabilistic tsunami modeling. The most relevant sea level rise scenario is likely to be the local rate or future projections of relative sea level rise (RSLR). These changes in sea level can be incorporated into the numerical models using water level offsets as described previously. It may be possible to assign probabilities to sea level change scenarios using local rates or projections of subsidence in conjunction with the probability-based estimates of global eustatic sea level rise provided in Houston (2013).

Suggested steps for developing the information needed to perform a Level of Effort 3 exposure assessment for tsunami hazards with sea level are summarized in Table 14.15.

Table 14.15. Exposure assessment steps for level of effort 3: tsunamis

Step	Activity
1	Identify damaging processes of interest (e.g. flood depth, velocity, runup)
2	Select and characterize tsunamigenic and sea level scenarios of interest
3	Select, develop, and prepare appropriate numerical modeling tools
4	Validate and/or calibrate the models through simulation of an historical event
5	Incorporate sea level scenarios into numerical model simulations
6	Perform deep water propagation simulations of selected seismic source and sea level scenarios to obtain probability distribution of offshore wave height
7	Derive the joint probability, for multiple tsunami sources/magnitudes, of offshore wave height
8	Disaggregate the source events based on the offshore wave height associated with the return period of interest and identify reasonable number of governing source events for shoaling analysis
9	Map the damaging tsunami processes for each return period (probability) of interest
10	Evaluate exposure and sensitivity of transportation infrastructure for each return period
11	Estimate risk as a function of scenario probability and time-interval considered

## 14.8 Vulnerability Assessment Case Studies

This section highlights three vulnerability assessment case studies as examples that have used analysis methods similar to those outlined in this chapter above. **Coastal engineers with specialized training and experience in coastal modeling were included on each of the study teams for these case studies – even the Level 1 analysis.** The results document both the vulnerability of these transportation assets to extreme coastal events today and how that vulnerability will increase with future sea level rise:

1. Section 14.8.1 is a Level 1 case study that uses a form of basic inundation mapping (with modifications to approximate increased flooding from wave effects) for different storm and tide conditions with increased sea levels.

2. Section 14.8.2 is a Level 2 case study that uses original, high-resolution storm surge and wave modeling and mapping with increased sea levels and storm strengths.
3. Section 14.8.3 is a Level 3 case study that uses original, high-resolution surge modeling and mapping to develop detailed maps of the probabilistic coastal inundation and flooding levels, including depth-frequency curves at specific locations, with increased sea levels.

#### 14.8.1 Level 1 Case Study: Adapting to Rising Tides - San Francisco Bay

This section describes a case study of mapping the level of flooding exposure of transportation infrastructure to coastal extreme events and sea level in a region where coastal storms during El Niño episodes are the dominant destructive storms. This case study is the technical inundation mapping component of the “Adapting to Rising Tides: Transportation Vulnerability and Risk Assessment” pilot project (ART 2011a). It is an example of a Level 1 study using the terminology outlined in this chapter. The approach was a form of basic inundation mapping to assess the depth of inundation along the Alameda County shoreline of San Francisco Bay (see Figure 14.8). The purpose was to inform a vulnerability rating of transportation assets in the study area under future sea level rise scenarios considering different storm and tide conditions. Intended as support planning, the analyses were not intended to represent or replace detailed engineering analyses.

**Case studies can demonstrate how to quantitatively assess the vulnerability of coastal highways**

##### 14.8.1.1 Background

This case study was one component of the multi-agency ART study to enable transportation planners in the San Francisco Bay regions to improve vulnerability and risk assessment practices and to help craft effective adaption strategies. Lead agencies involved in the study included the San Francisco Bay Conservation and Development Commission, the Metropolitan Transportation Commission, the California Department of Transportation (District 4) and the FHWA. The project stakeholder groups included twenty local, state, and federal agencies and governments. The overall goal of the ART project was to increase the preparedness and resilience of Bay Area communities to sea level rise impacts while protecting ecosystem and community services (ART 2011a).

This portion of the project was a pilot planning project on a sub-regional scale to test the FHWA Risk Assessment Model (a predecessor to Figure 14.2). The sub-region studied was the approximately 20-mile long Alameda County bay shoreline. The study evaluated potential shoreline impacts, vulnerabilities, and risks; it identified adaptation strategies; and it developed adaptation planning tools and resources. This case study focuses on the methodology developed to produce the inundation maps for the pilot study (ART 2011b) and is not a summary of the broader ART study.



Figure 14.8. Shoreline Drive, Alameda, California on San Francisco Bay (2018)

#### 14.8.1.2 Storm Selection and Sea Level Scenarios

The ART study focused on sea level rise because of its potential to cause harm. It could damage residential, commercial, and industrial structures in low-lying areas near the shoreline as well as important habitats and wildlife resources. Two sea level rise scenarios were selected based on a review of the literature. The first scenario was an increase of 16 inches consistent with a high-end estimate for mid-century and the second scenario was an increase of 55 inches consistent with a midrange estimate for the end of the century (ART 2011b).

**Three storm/tide conditions were evaluated for each of the sea level rise scenarios: a high tide (MHHW), a 100-year storm water level (still water level), and the 100-year storm water level increased by some effects of wind waves.** These three storm/tide conditions were selected to represent a reasonable range of potential coastal flood levels. The high tide inundation is representative of the area that would be subject to frequent or permanent tidal inundation. The 100-year flood is representative of the area subject to flooding and wave damage in extreme storms. Thus, there were a total of six scenarios evaluated - the two sea level rise scenarios combined with three storm/tide conditions.

#### 14.8.1.3 Inundation Mapping Approach

The method used to assess the vulnerability to sea level was a modified form of the basic inundation mapping (bathtub) approach. Six inundation maps were developed corresponding to the two sea level rise scenarios with each of the three storm/tide conditions. The maps were developed by estimating the water level of interest and then comparing that elevation to the existing upland topography to determine depth of flooding at all locations across the study area. The elevations of the water levels (MHHW, 100-year storm, and 100-year with some increase for wave effects) used for this inundation mapping were selected based on extensive modeling of the bay.

This pilot study was able to use results of two much more extensive modeling efforts focused on developing similar estimates around San Francisco Bay: a recently completed USGS modeling effort and an ongoing FEMA modeling effort to remap the coastal flood plain around the bay. The FEMA effort used a high-resolution hydrodynamic model, MIKE-21, which is comparable to ADCIRC and also includes a wave model. Estimates of the MHHW and the 100-year storm elevation were taken from the USGS modeling effort at 13 locations along the shore of Alameda County for use in this pilot study inundation mapping effort. These MHHW elevations ranged from +6.11 ft to +6.85 ft (NAVD) with the values consistently increasing farther to the south. This compares with a MHHW elevation at the Presidio of +5.83 ft (NAVD). This variation of high tides throughout San Francisco Bay is well-known and results from the bay's response to tidal waves. The tide is amplified in the bay and the amplification increases moving south from the Golden Gate area. The estimated 100-year storm still water elevations at those 13 Alameda County locations were also obtained from the USGS study results. Those values ranged from +9.2 ft to +10.42 ft (NAVD) and the variation was not consistent spatially along the coast.

**San Francisco Bay's Adapting to Rising Tides (ART) study is an example of a Level 1 vulnerability analysis**

This pilot study also then adjusted the 100-year still water levels upward an increment to account for the elevation of wave crests in depth-limited situations. These resulting elevation estimates were referred to as “wind waves” in the pilot study. This adjustment was essentially a professional coastal engineering judgment by the consultant team based on the available modeling results and consistent with the project purpose of a general screening-level tool. Inundation was then mapped as if the still water level was at that higher elevation and referred to as the “potential wind-wave zone.” This adjustment is not standard coastal engineering practice. As stated in the report, the physics of overland wave propagation into the flooded areas is not modeled (ART 2011b). Similarly, this vulnerability mapping effort also includes a non-standard definition of “overtopping” based on whether the elevation of the shoreline feature along the bay is lower than the vertical elevation of the water surface.

#### 14.8.1.4 Inundation Maps

Inundation maps were generated in the San Francisco Bay pilot study by overlaying the flood water elevations on detailed maps of the existing upland topography. The maps illustrate the potential for coastal flooding in relationship to transportation assets under the six scenarios discussed above (2 sea level rise scenarios with MHHW, 100-year flood levels, and 100-year flood levels including the “potential wind-wave zone”).

Examples of the inundation maps from the pilot study showing the inundation areas estimated for the scenario of 16 inches of sea level rise with the 100-year storm levels adjusted upward to account for the “potential wind-wave zone.” are provided in Figure 14.9 and Figure 14.10. Figure 14.9 shows the entire study area and Figure 14.10 shows the same information in more detail for the northernmost portion of the study area. The maps show the major transportation assets as well as the flooded areas. The extent of flooding is shown by the yellow hatching. Specific transportation assets are identified in Figure 14.10. Also shown on are the estimated flood depths. These mapping results were used to develop metrics of the level of exposure and vulnerability of the transportation assets (ART 2011a, ART 2011b).

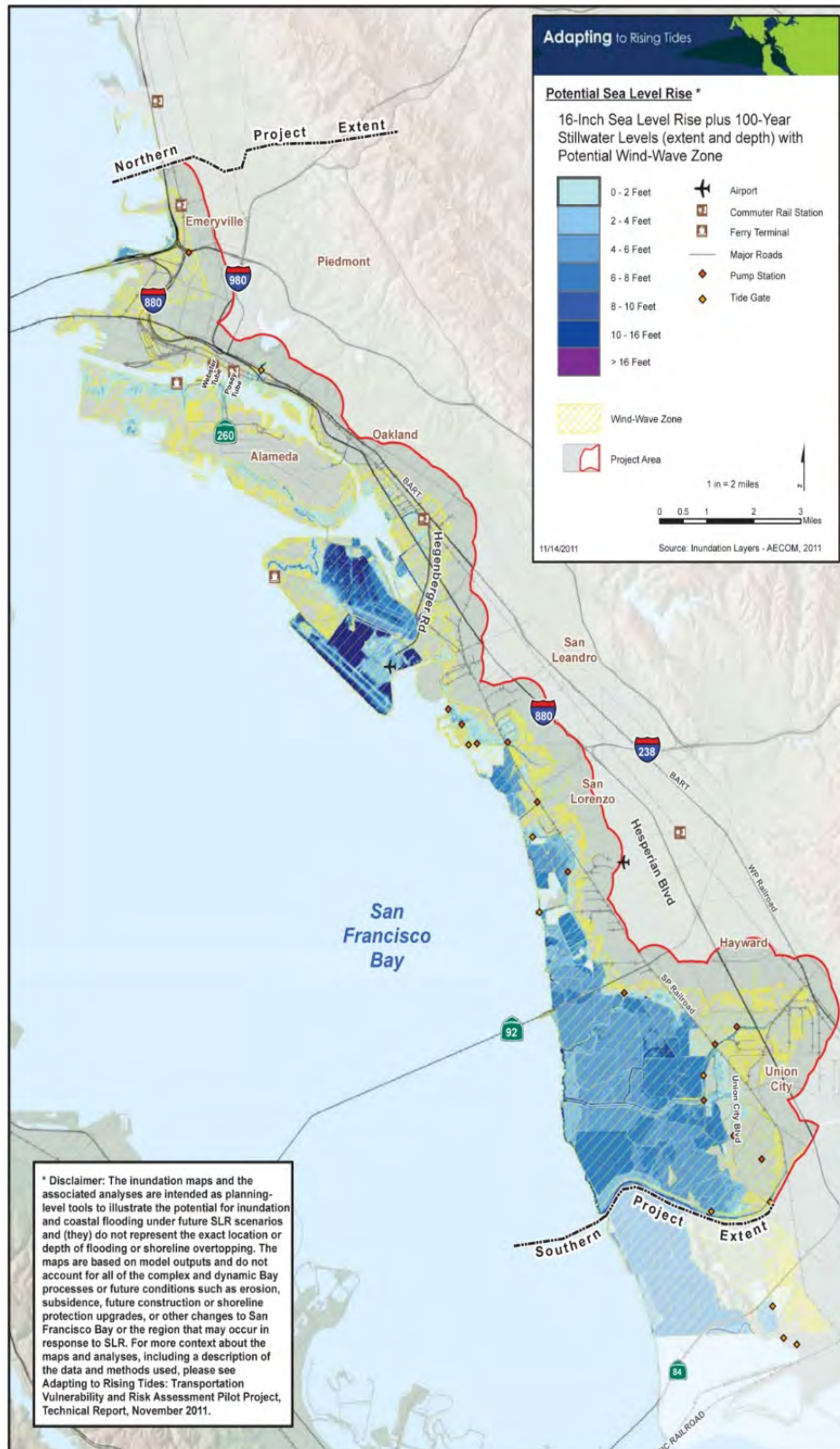


Figure 14.9. Inundation map of Alameda County for 100-year storm flood with 16 inches of sea level rise and additional elevation for wave effects (from ART 2011b)

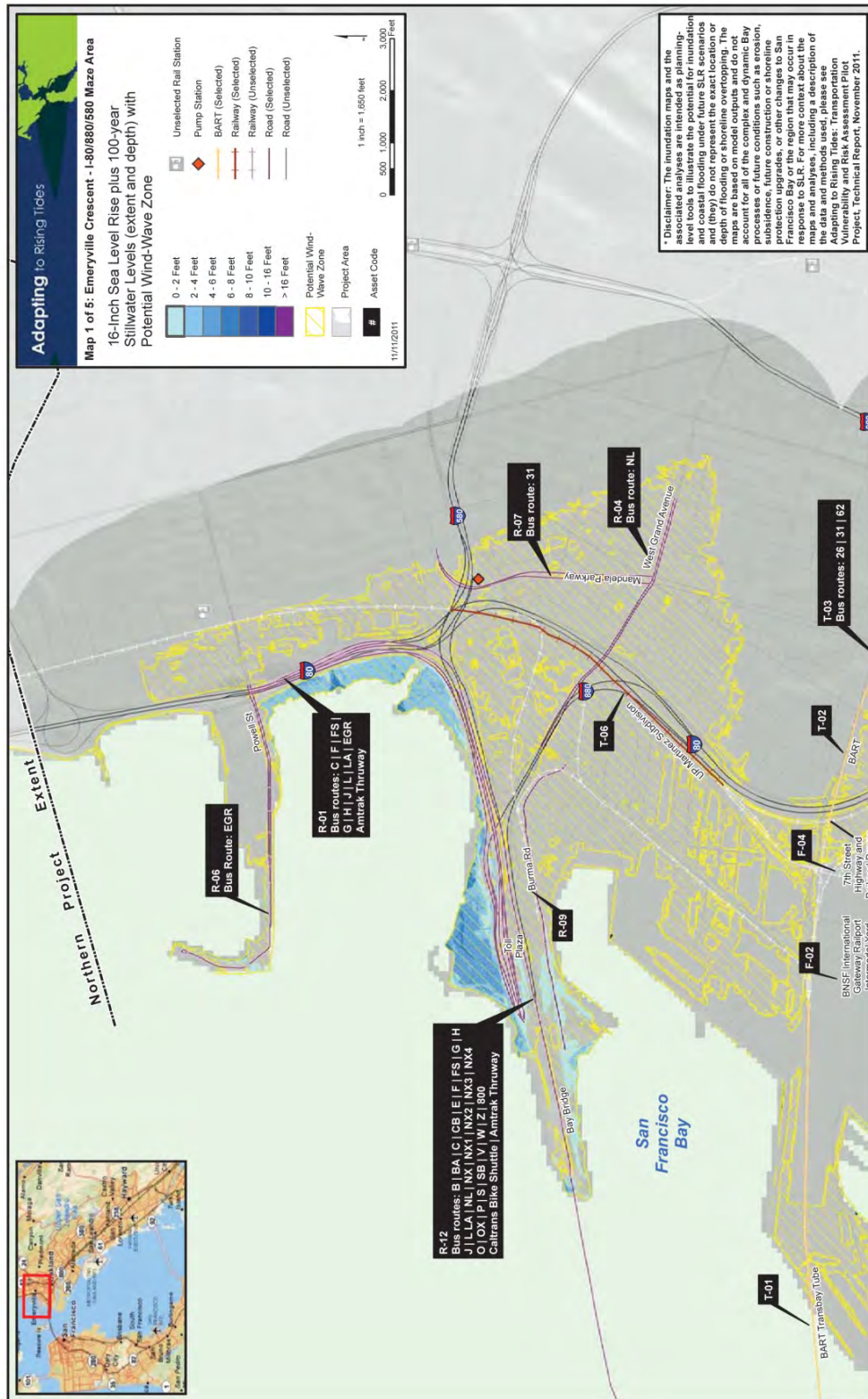


Figure 14.10. Detailed inundation map of the northern portion of Alameda County for the 100-year storm flood with 16 inches of sea level rise and additional elevation for wave effects (from ART 2011b)

### 14.8.2 Level 2 Case Study: The Gulf Coast 2 Study - Mobile, Alabama

This section describes a case study assessing the exposure of transportation infrastructure to coastal extreme events and sea level in a region where hurricanes are the dominant destructive storms. The approach is a scenario-based analysis using high-resolution coastal modeling. Storm surge flood elevation and wave height maps were simulated for different possible future sea level rise (SLR) and storm scenarios. The results are used to assess the vulnerability of road, bridge, tunnel, railway, port, and airport facilities as part of a larger comprehensive study. This case study is an example of a Level 2 type analysis.

#### 14.8.2.1 Background

The USDOT investigated the impacts of sea level on transportation systems in the central Gulf Coast region in a multi-year study (USDOT 2013). This study had two primary phases. Phase 1 (completed in 2008) examined the impacts of sea level on transportation infrastructure at a regional scale. Kafalenos *et al.* (2008) mapped flooding of transportation facilities from Galveston, Texas to Mobile, Alabama by future sea levels. The exposure was determined by identifying areas with ground elevations below the future sea level rise projections/scenarios. Phase 2 was focused on a much smaller study area, Mobile County, Alabama. Phase 2, called the “Gulf Coast 2” or “GC2” study, is a more detailed study that developed and applied more complex methods for assessing sea level exposure and vulnerability.

This case study is a portion of the second major task, GC2: Task 2, using scenario-based modeling of hurricanes with sea level rise. Additional detail on the study methods and results can be found in that task study report (Choate *et al.* 2012). Some of the model results developed in this case study were included as a graphic in the 2014 NCA (Melillo *et al.* 2014).

#### 14.8.2.2 Approach

The GC2: Task 2 study used storm surge and wave models with future sea level rise scenarios. **The results are maps of wave heights and water depths at transportation asset locations.**

Hurricane impacts of surge and waves are the most important coastal process for this study area. Mobile County is susceptible to hurricane storm surge damage because of its location along the northern Gulf coast. The largest city in the study area, the City of Mobile, is in the northwest corner of Mobile Bay, a large, very shallow estuary with a very wide inlet to the Gulf of Mexico, Mobile Pass. Storm surge in the northern portions of the bay can be up to 6 ft higher than in the southern end of the bay. The north end of the bay is also where most of the transportation systems (roads, bridges, ports, and rails) are located. The area is frequently impacted by tropical storms and hurricanes. It has been impacted by at least one named storm in 15 of the last 20 years. Thus, proper estimation of hurricane impacts is vital for quantifying exposure to flooding and wave damage with sea level in Mobile, Alabama.

The storm surge model was validated by comparing simulated results with actual surge measurements for historical storms. The models were then used to simulate surge and waves under a variety of storm and sea level scenarios discussed below. The resulting water levels, velocities, and wave heights were mapped to quantify exposure within a GIS framework. The selection of storm and sea level scenarios and descriptions of the modeling approaches and validation are provided in the following sections.

#### 14.8.2.3 Storm Selection and Sea Level Scenarios

Storms (in this case, hurricanes) and sea level scenarios were selected to bracket a reasonable range of expected conditions. The selected storms included a moderate strength hurricane and an extremely powerful hurricane. Sea level rise scenarios consistent with the projections

presented in Section 4.1 were considered. The storms and sea level scenarios were selected to address two main questions:

1. What are the implications of a moderate hurricane striking the region under a scenario of increased sea levels?
2. What are the implications of a strike by a larger hurricane than the region has experienced in recent history?

Characteristics of two hurricanes which had notable impacts in Mobile County - Hurricane Georges (1998) and Hurricane Katrina (2005) - were used to address these questions. Hurricane Georges was used to evaluate the effects of a moderate storm and Katrina was used to evaluate the effects of a larger, rarer storm. Hurricane Georges made landfall near Biloxi, MS as a Category 2 hurricane. Hurricane Katrina, one of the most destructive hurricanes in US history, made landfall near Buras, Louisiana as a Category 3 hurricane and then again near the Mississippi-Louisiana state line (over 100 miles from Mobile, Alabama). The use of these historical storms, or more correctly, the use of the characteristics of these historical storms (intensity, size, and track) was entered into the numerical models under the assumption that future storms will, in general, have similar characteristics as past storms. Additional scenarios included changes in both the storm track and the storm intensity.

**Mobile's Gulf Coast 2 study is an example of a Level 2 vulnerability assessment.**

The storm and sea level scenarios modeled in this case study are summarized in Table 14.16. The first two scenarios, with no sea level rise, were considered primarily for model validation (discussed later) and comparison purposes. However, their results show that the area is very exposed to extreme events today. All investigators agree that global sea levels will rise in the next century (Section 4.1 Sea Levels). The selected sea level rise scenarios were 0.98 ft (30 cm), 2.5 ft (75 cm), and 6.6 ft (200 cm). These values were selected based on consideration of the published sea level rise projections as well as local vertical land movement estimates (see Choate *et al.* 2012).

**Storm track and intensity were also modified in some scenario simulations** to address the second question. The historical storm track of Hurricane Katrina was shifted eastward such that the strongest onshore, northerly hurricane winds would be blowing up the length of Mobile Bay. This was done without modifying the forward speed of the storm or the rate of decay as the storm moved over the new landfall location.

Intensification of hurricane winds was considered. Some investigators have suggested a chance of a stronger storm than Katrina at any time. Storm intensification was simulated with storm winds and central pressure using information found in Knutson and Tuleya (2004) and Knutson *et al.* (2010). The wind speeds in Hurricane Katrina were increased by 6.5 percent. This value represents an average of the intensification range (+2 percent to +11 percent) suggested in Knutson *et al.* (2010) for hurricane wind intensification by 2100. The central pressure deficit (i.e. difference between ambient and storm central pressure) was decreased by 13 percent, which is consistent with the results of modeling in Knutson and Tuleya (2004), as well as information provided in Knutson *et al.* (2010).

In the final two scenarios listed in Table 14.16, the 150 mph maximum wind speeds of Katrina measured out away from land in the Gulf of Mexico were maintained in the computer simulations until the storm made landfall. More explanation of the selection of the scenarios summarized in Table 14.16 can be found in the GC2: Task 2 study report (Choate *et al.* 2012).

Table 14.16. Scenarios modeled in GC2 (modified from Choate *et al.* 2012)

Scenario Name	Sea Level Rise?	Track Shift?	Intensification?
Georges	No	No	No
Katrina	No	No	No
Georges+30	0.98 ft (30 cm)	No	No
Georges+75	2.5 ft (75 cm)	No	No
Georges+200	6.6 ft (200 cm)	No	No
Katrina+75	2.5 ft (75 cm)	No	No
Katrina-Shift	No	Yes	No
Katrina-Shift+75	2.5 ft (75 cm)	Yes	No
Katrina-Shift-Intensity+75	2.5 ft (75 cm)	Yes	Higher winds and reduced central pressure
Katrina-Shift-MaxWind	No	Yes	Maximum Winds
Katrina-Shift-MaxWind+75	2.5 ft (75 cm)	Yes	Maximum Winds

#### 14.8.2.4 Storm Surge Modeling

Storm surge and the resulting inundation for each scenario were modeled with the Advanced Circulation model ADCIRC. The ADCIRC model is capable of simulating tides, instream flows, hurricane wind fields, and the subsequent water levels and velocities at discrete locations continuously over a specified duration (Luettich *et al.* 1992; Westerink *et al.* 1994). The ADCIRC model is currently used as one of many tools to predict storm surge elevations in the development of flood insurance rate maps for FEMA (see Section 4.3.2 Storm Surge Modeling and see Webb 2017).

Tides were not included in the surge simulations in this case study since the average tide range (about 1.2 ft) is much less than storm surge in the study area. Storm durations were modeled over a 2.5- to 3.0-day period prior to landfall. Storm histories were adapted from the official NOAA National Hurricane Center (NHC) storm database archives that give storm coordinates and characteristics at specified times. The internal wind models of ADCIRC were used to simulate the hurricane wind fields using these basic storm characteristics.

**In the model scenarios considering sea level rise, the water level everywhere in the computational domain was increased by an amount equal to the sea level rise scenario.** This procedure is analogous to lowering the earth surface elevations by an equivalent amount. The ADCIRC model has an option for specifying such adjustments without having to alter the digital elevation model.

The modeling in the GC2 study has been referred to previously in this manual (Section 4.3.2 Storm Surge Modeling). The finite element mesh used in this case study is shown in Figure 4.18. The mesh has 446,459 nodes and 866,496 triangular mesh elements and includes the entire Gulf of Mexico, Caribbean Sea, and much of the western North Atlantic Ocean. To account for upland surge flooding a seamless topographic-bathymetric mesh surface was developed for coastal Alabama as shown in Figure 4.19. Simulated water levels were saved frequently (e.g. each minute) at some discrete locations for comparison with tide gage measurements during the model validation process (see Figure 14.12). Simulated water levels and flow velocities were saved at three-hour increments for every mesh node for the duration of the simulations. Other model output

includes the recording of maximum water levels and velocities at each mesh node over the entire simulation. A map of the maximum envelope of water (MEOW) for each scenario was developed.

Figure 14.11 is an example of estimated surge depths across the study area for the scenario of a moderate hurricane like Hurricane Georges with 2.5 ft (75 cm) of sea level rise. Storm surge depth and inundation maps were generated by combining the ADCIRC model high water results with a GIS-based grid of ground surface elevations.

The implication of Figure 14.11 is that large portions of the study area near the bays and tidal creeks in the study area will be inundated. The modeling approach shows which specific areas and assets will be inundated. These areas include 33 miles of “critical” roads, 114 miles of rails, and 78 percent of port facilities. These values varied by scenario, as expected, with up to 117 miles of critical roads, 154 miles of rails, 100 percent of port facilities, and the downtown airport being inundated in the most extreme event scenarios. More examples of the maximum storm surge results can be found in the GC2: Task 2 study report (Choate *et al.* 2012).

The level of exposure and vulnerability resulting from extreme events today is one of the notable conclusions that can be drawn from this case study. For example, the road and rail inundation mileage results presented for the scenario with 2.5 ft (75 cm) of sea level rise are only slightly higher than those for the same storm with today’s sea level (see Table 25 of Choate *et al.* 2012). Similar results have been found in other vulnerability assessment studies (NJTPA 2011). The damage experienced in extreme events in the past decade, including Hurricane Sandy and Hurricane Katrina, is consistent with and validates this conclusion. The modeling methodology outlined in this case study provides a way to quantitatively address the level of exposure and vulnerability to both extreme events and sea level rise.

#### 14.8.2.5 Validation of Storm Surge Model

The storm surge model was validated as part of this Mobile, Alabama case study investigation before simulating the impacts of sea level on storm surge. The ADCIRC model and mesh were validated by hindcasting Hurricanes Georges and Katrina. Hindcasting is the use of a model to simulate a past time period, i.e. not a forecast. It is a common way to validate that a hydrodynamic model, like ADCIRC, and the project-specific input mesh are working correctly. An example of this model’s hindcast of surge elevation during Hurricane Katrina is shown in Figure 4.20 (Section 4.3.2). The modeled surge matches the actual storm surge well.

Time histories of simulated water levels were compared to NOAA tide gage measurements within and close to the study area. An example comparison of simulated and measured storm surge hydrographs is shown in Figure 14.12 for the Katrina hindcast. Such comparisons show the model’s ability to faithfully recreate the time-dependent nature of storm surge. The simulated peak magnitude, the single most important result, matches the measured value well. The simulated peak occurs earlier than the measured peak and the simulated surge does not model the pre-storm setup well (the day before landfall). Such inconsistencies are not unusual (see Webb 2017 for more discussion of model validations).

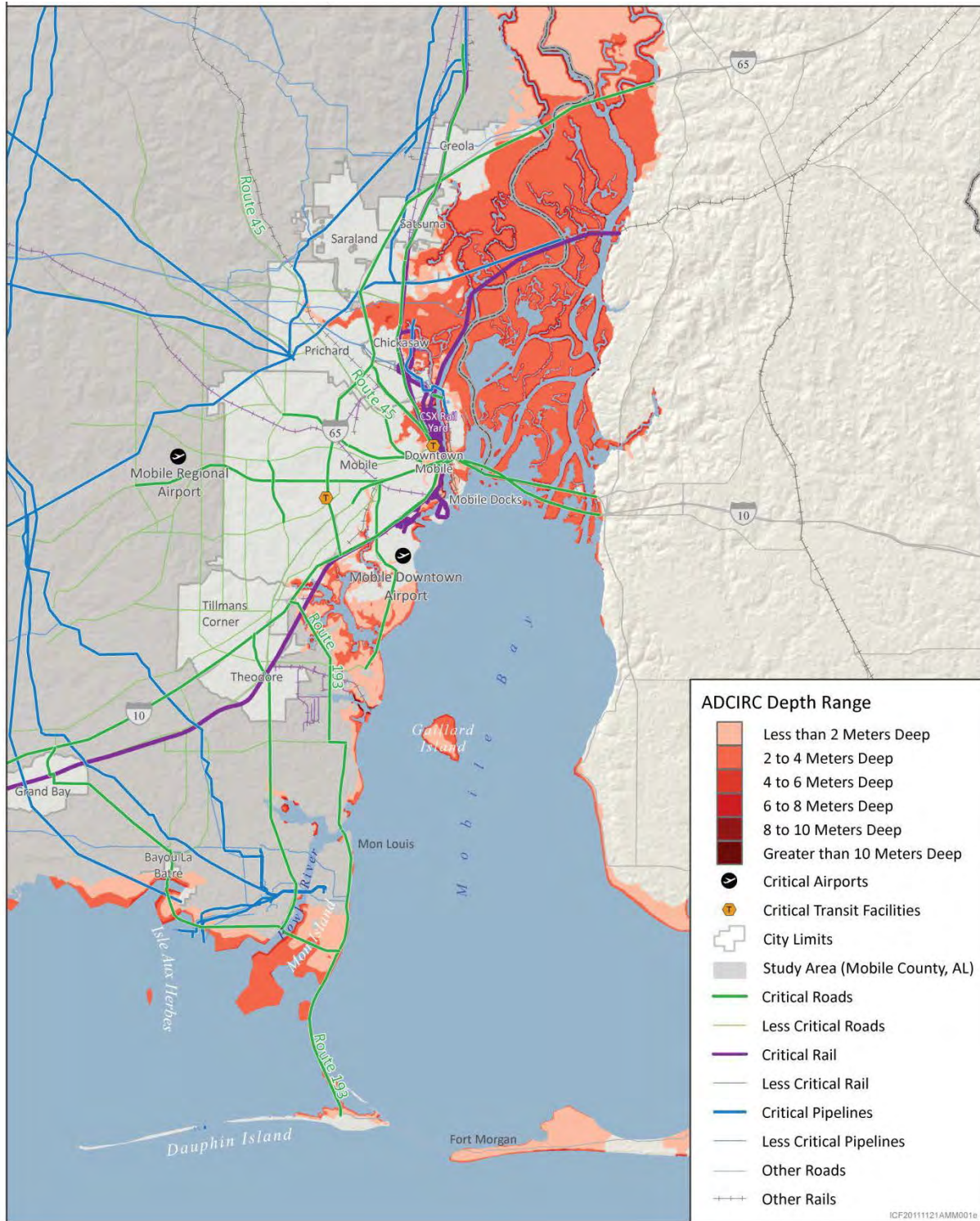


Figure 14.11. Modeled storm surge depths in Mobile County, Alabama for the scenario of Hurricane Georges conditions with 2.5 ft (75 cm) of future sea level rise (from Choate *et al.* 2012)

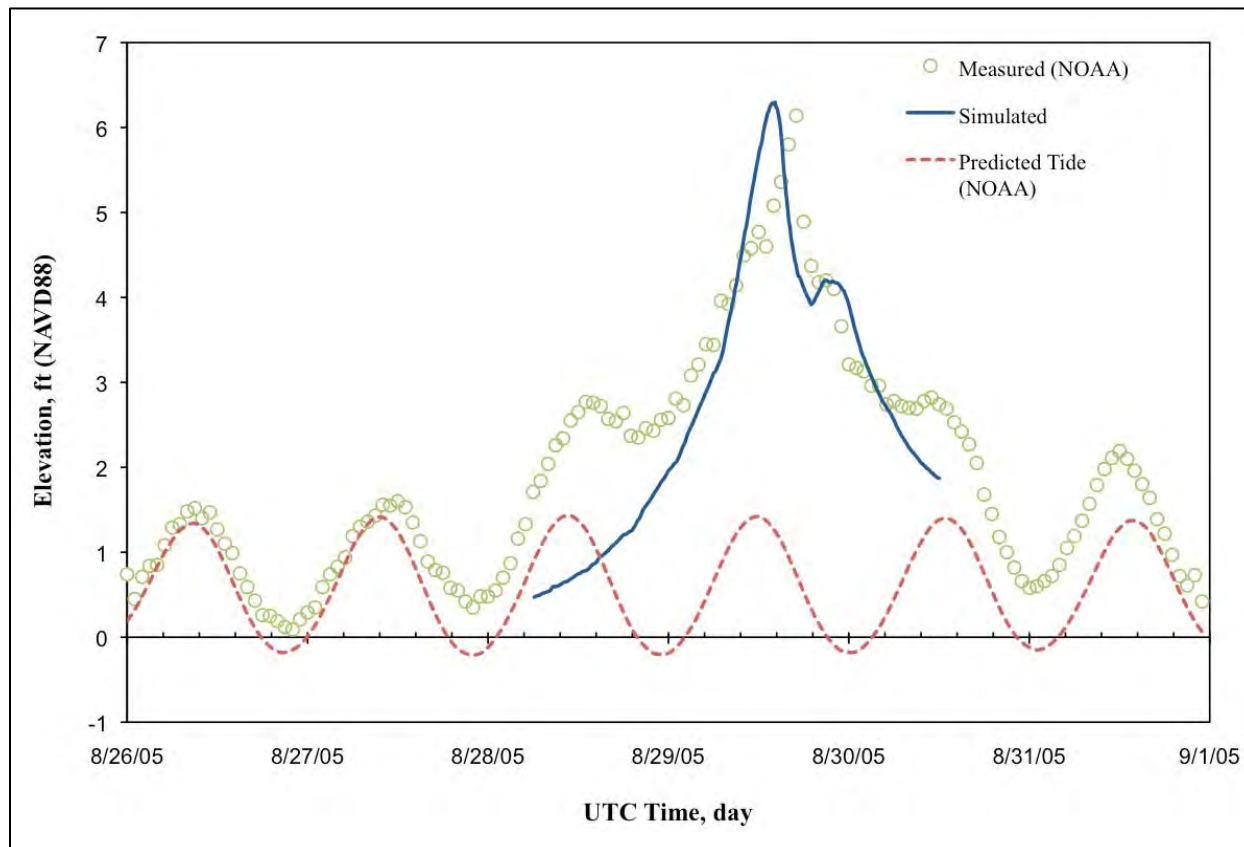


Figure 14.12. Validation of ADCIRC surge estimates by comparison with a tide gage at Dauphin Island, Alabama

A comparison of simulated and measured high water marks (HWMs) was also performed for each storm hindcast to evaluate the potential spatial variability of model errors throughout the study area. An example is provided in Figure 14.13 for the Hurricane Katrina hindcast. The values shown represent the difference in magnitude between simulated and measured maximum still water elevations. Comprehensive documentation of HWMs is available for many recent storms. However, the reporting of HWMs involves subjective determinations that make direct comparisons with simulated water levels difficult.

Additional analysis of the storm surge hydrographs and HWM comparisons was performed to evaluate a range of possible model errors. Calculated model errors are shown in Table 14.17. The root-mean-square (RMS) error provides an error magnitude based on direct comparisons between modeled and measured data over time, in the case of storm surge hydrographs, and in space for the HWM comparisons. An additional error estimate was expressed as the "Percent of Peak," which is the ratio of the RMS error to the measured maximum water level.

Whether the validation is adequate is a matter of professional judgment. The agreement between model and measured surge shown here was acceptable for the purposes and scope of this case study evaluation. The model was then used for the sea level simulations as discussed.

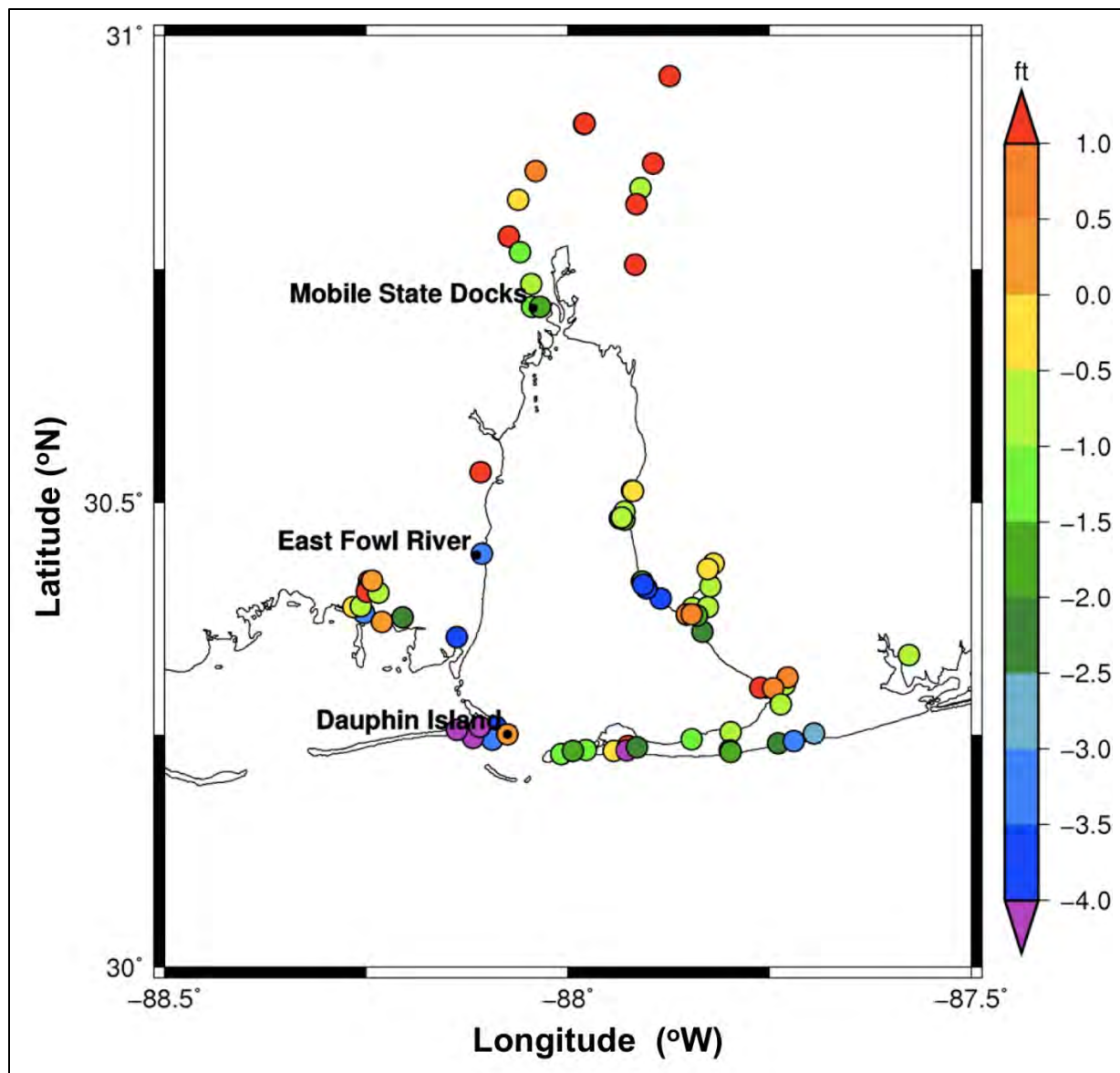


Figure 14.13. Validation of ADCIRC storm surge estimates by comparison with measured high water marks

Table 14.17. Validation analysis of ADCIRC model storm surge estimates

Metric	RMS Error (ft)	Percent of Peak (%)
78 High Water Marks	1.98	13.2
Hydrographs at Pensacola, FL	1.20	19.8
Hydrographs at Dauphin Island, AL	1.00	16.4

#### 14.8.2.6 Wave Modeling

Storm waves were modeled with the Steady-State Spectral Wave model STWAVE. The STWAVE model simulates the generation and transformation of waves over variable bathymetry (Smith *et al.* 2001). The model estimates wave characteristics at every grid point in the model domain assuming that waves have come to a steady state.

The input included the ADCIRC surge simulations, measured winds in Mobile Bay, and measured waves in the Gulf of Mexico. The computational domain for the wave model was developed from a portion of the same digital elevation model used in the ADCIRC simulations but focused on a much smaller area including the bay and offshore into the Gulf. The resulting grid provided wave characteristics at a regular spacing of about 300 ft (100 m). This resolution was sufficient for subsequent exposure and sensitivity analyses in this case study.

Storm waves were simulated for the scenarios outlined in Table 14.16 using the maximum surge depths from the ADCIRC simulation. Input winds for wave generation in the bay were the maximum observed wind speed and direction. Boundary input waves were measured wave characteristics in the Gulf of Mexico during the peak of each historical storm. The results from each wave model scenario included estimates of significant wave height, peak wave period, dominant wave direction, and wave breaking throughout the model domain.

No direct measurements of waves were available within the study area to validate the STWAVE model predictions. Direct measurements of wave characteristics are rarely available close to the coast where comparisons are most useful. However, the model has been extensively validated and those results are available in the published literature.

Figure 14.14 shows an example of the significant wave heights estimated by the STWAVE model. This example is the scenario of a moderate hurricane (Georges) with 2.5 ft (75 cm) of sea level rise. Essentially, these are the waves riding on the surge shown in Figure 4.20. The wave heights are much larger in the Gulf of Mexico but the model estimates the regeneration of waves across Mobile Bay and into the areas inundated by storm surge. More examples of the wave field results corresponding to the scenarios evaluated in Table 14.16 can be found in the GC2: Task 2 study report (Choate *et al.* 2012).

The significant wave heights at one downtown Mobile location will increase from 2 ft (0.6 m) for a moderate hurricane today to over 4.3 ft (1.3 m) for some of the more severe scenarios. This increase is particularly important because most buildings will be severely damaged or destroyed with wave heights around 1 to 3 ft.

Results like Figure 14.11 and Figure 14.14 can be examined to quantify the exposure of specific transportation assets to the primary damaging mechanisms: storm surge and waves. Thus, this type of Level 2 scenario-based analysis provides tools for exposure and vulnerability assessments. In summary, model-based analysis, like this case study from GC2, can provide quantitative estimates of exposure which account for the complex physics of coastal storm surge and wave propagation under different sea level scenarios.

### 14.8.3 Level 3 Case Study: Central Artery Project, Boston, Massachusetts

This section summarizes a case study of probabilistic, high-resolution modeling of storm surge, waves and tides with future sea level rise in the Boston, Massachusetts area. The case study is based on the work of Bosma *et al.* (2015) and more specific details can be found there and in Douglas *et al.* (2016).

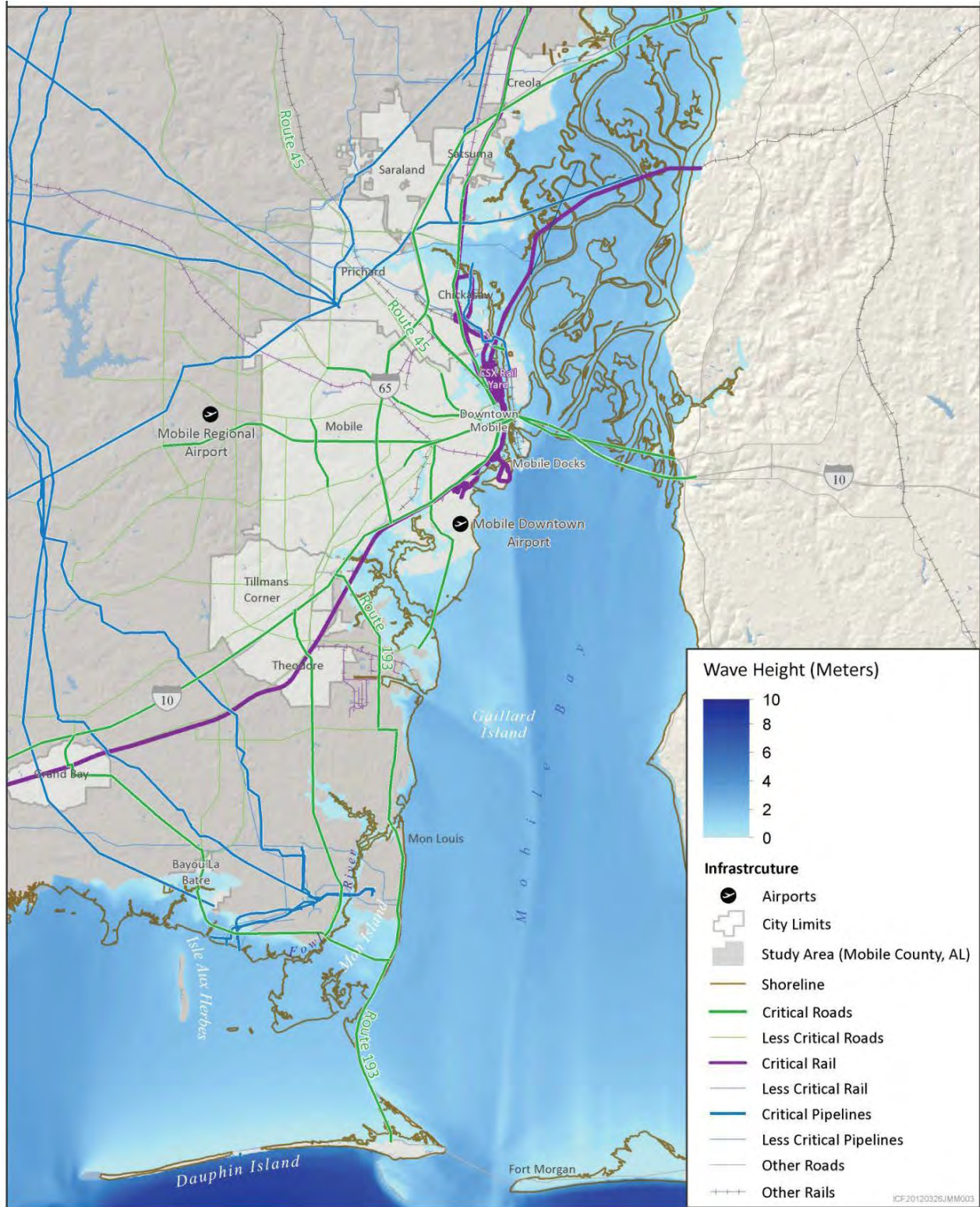


Figure 14.14. Modeled wave heights for the scenario of Hurricane Georges conditions with 2.5 ft (75 cm) of future sea level rise (from Choate *et al.* 2012)

This Boston case study is a comprehensive example of a Level 3 approach to vulnerability assessment because it:

- establishes a methodology for using regional storm characterizations produced through rigorous and defensible applications of science and engineering including sea level rise,
- uses high-resolution tide, surge, and wave models for mapping the extent and coverage of inundation in coastal areas,
- models the dynamic response of flooding to sea level rise as compared to simply estimating the static response (i.e. not the “bathtub” assumption),
- maps, in a probabilistic fashion, the extent of inundation under both tidal and storm conditions including future sea level rise, and
- quantifies the probabilities of flooding (including flood levels, flood pathways, and flood durations) for site-specific transportation assets.

The results demonstrate some of the advantages of the more complex methods of coastal modeling compared to simpler methods. In some parts of the Boston region, the simpler methods underpredict flooding as compared with the more comprehensive analysis methods. In many cases, a “bathtub” approach overpredicts inundation where flooding will not occur and also misidentifies dry area that would actually be inundated. The more complex, probabilistic modeling provides key information such as the flood durations and pathways that simpler methods normally would not include. Such key information can result in cost savings in the planning and design of adaptations (Bosma 2016).

**The Boston Central Artery/Tunnel case study is an example of a Level 3 vulnerability assessment.**

Results from the more complex modeling can also be used to test the effectiveness of various engineering designs and adaptations. For example, green living shoreline alternatives (e.g. restoration of dune, wetlands, and reefs), as well as traditional grey infrastructure (e.g. seawalls), can be simulated individually or in combination.

Level 3 analysis, like that presented in this Boston vulnerability assessment, may be justified for the planning and design of many high-value US transportation assets along the coast which are sensitive to damage in coastal storms (e.g. low bridges, tunnel portals, etc.).

#### 14.8.3.1 Background

This Boston study demonstrates how modeling can estimate the effects of relative sea level rise (RSLR) on the levels of coastal storm flooding and waves at a very high resolution across a broad, highly urbanized area with a focus on transportation assets. The Central Artery/Tunnel system through downtown coastal Boston, Massachusetts is a vital link in the urban regional transportation network and is composed of more than 160 lane-miles (more than half of them in tunnels), 6 interchanges and 200 bridges. As one of the most valuable components of the state’s transportation infrastructure, its maintenance, protection and enhancement are a priority.

The two main objectives of this study were to assess the vulnerability of the Central Artery/Tunnel system to RSLR and extreme storm events, and to investigate and present adaptation options to reduce identified vulnerabilities. This study was jointly funded by MassDOT and the FHWA but a key priority for this project was to develop products that, to the degree possible, are useful to other Boston agencies and stakeholders who are also doing adaptation work.

### 14.8.3.2 Storm Selection and Sea Level Scenarios

Both tropical (i.e. hurricanes) and extra-tropical (i.e. Nor'easters) storm conditions were evaluated in the modeling used in this case study. While hurricanes are intense, fast moving storms that have a significant impact on coastal communities, they are not as common in the northeast US as Nor'easters. Historical water level records and historical meteorological records were used to identify a set of Nor'easters to be simulated in the model. In addition to storm intensity and direction, the timing of a storm relative to the tidal cycle can be an important consideration along the Atlantic Coast. The timing of the peak hurricane surge is very important while the timing of the peak Nor'easter surge has little effect on maximum water levels. This is because hurricanes tend to be fast moving systems, hence the likelihood of peak surge occurring at the same time as peak high tide is relatively low when compared to Nor'easters, which typically last for 24 hours or more. A set of about 400 representative synthetic storms were combined with a set of about 200 Nor'easters. The probability of flooding due to both hurricanes and Nor'easters was estimated by developing composite probability distributions for flooding (see Bosma *et al.* 2015 for details).

Two GMSLR scenarios were evaluated to bracket the potential future sea level rise outcomes for the Boston Harbor area. The selected GMSLR estimates were taken from Parris *et al.* (2012). The actual GMSLR values used in the coastal hydrodynamic modeling were 0, 0.6 and 3.2 ft above present levels:

- 0 ft of GMSLR represents present-day conditions (of 2013 in this study),
- 0.6 ft of GMSLR represents 2030 conditions, and
- 3.2 ft of GMSLR represents both a “high” scenario for 2070 and an “intermediate-high” scenario for 2100.

The GMSLR heights were adjusted for local subsidence of 0 in, 0.74 in, and 2.5 in for 2013, 2030, and 2070/2100 respectively.

Thus, the total RSLR scenarios modelled in the Boston vulnerability assessment were:

- 0 ft for 2013,
- 0.68 ft for 2030, and
- 3.4 ft for 2070/2100.

### 14.8.3.3 Coastal Hydrodynamics Modeling

The hydrodynamic models, ADCIRC to simulate storm surge, circulation, and tide; and SWAN to simulate waves were coupled to include the joint effects of wave setup. Both the ADCIRC circulation model and the SWAN wave model are implemented on an unstructured mesh with 3 levels of nested meshes (see Section 3.1 Grids, Meshes and Nesting of Webb 2017 for an explanation of these terms).

Three resolutions of the mesh are used in the modeling:

- a regional-scale mesh which includes much of the north Atlantic, which is a previously validated model mesh used in numerous FEMA, NOAA, USACE studies,
- a mesh providing an intermediate level of resolution to transition from the regional-scale mesh to the highly resolved mesh needed along the MA coastline, and
- a site-specific fine mesh of sufficiently high resolution to ensure that all important topographic and bathymetric features that influence flow dynamics within the Boston Central Artery/Tunnel system were captured.

The site-specific, fine mesh was developed to delineate the centerlines and banks of waterways within the model domain using a rather painstaking, manual method. In some areas, the resolution of the model is approximately 10 ft. Figure 14.15 shows how highly-resolved the mesh is in a portion of the downtown area.

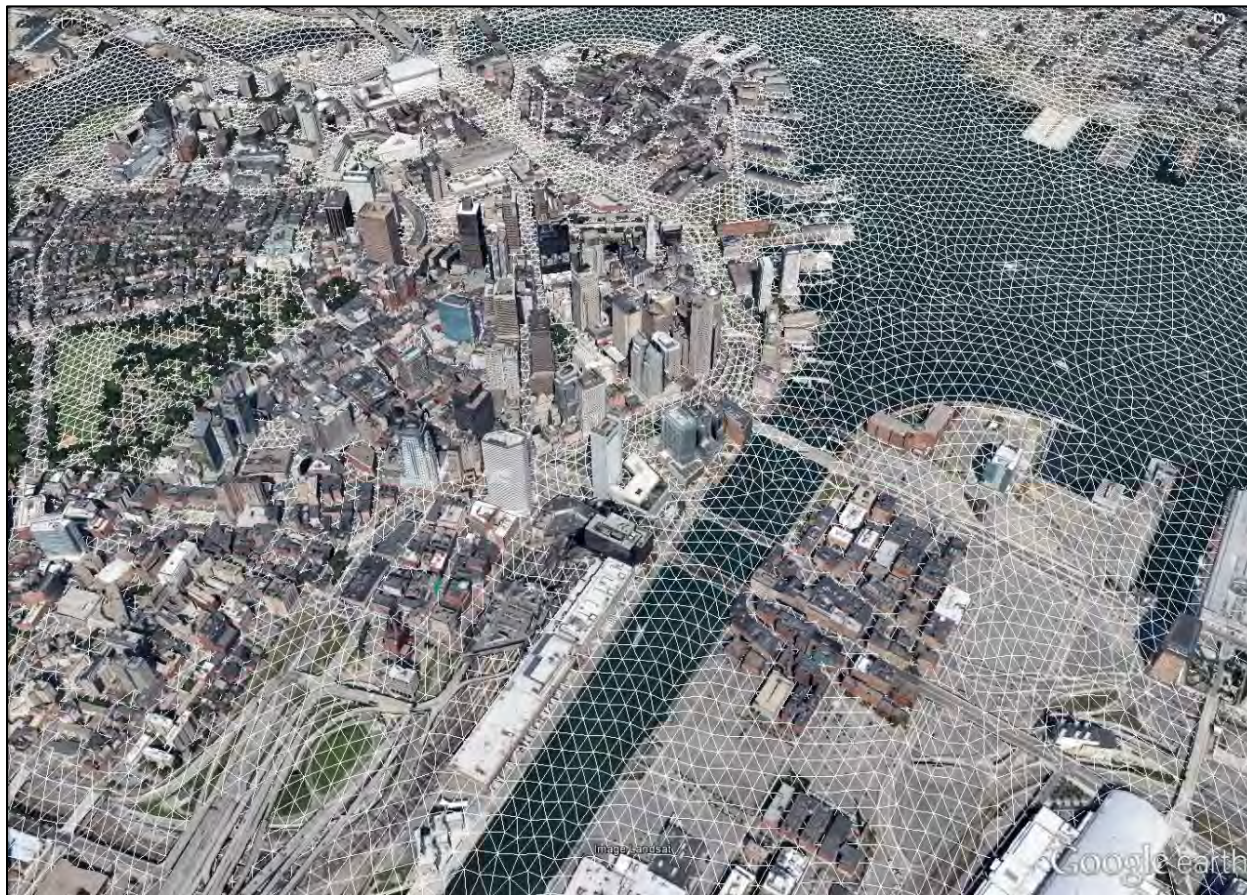


Figure 14.15. Example of the fine, highly-resolved hydrodynamic model mesh used in the Boston Central Artery/Tunnel vulnerability assessment study (from Douglas 2015; permission to use image provided by MassDOT)

#### 14.8.3.4 Calibration and Validation of the Storm Surge Model

The models used in the Boston case study project (ADCIRC, SWAN) are rooted in sound science and utilize standard governing equations of water motion. However, the propagation of water through a unique geographic setting results in site-specific variations that may need adjustment of model parameters, called calibration, to more accurately represent the real-world system. For example, in an urban landscape, an area consisting of numerous buildings will influence flow differently than a marsh, which will influence flow differently than a parking area, which will influence flow differently than an estuary. For these types of cases, it is reasonable to adjust parameters, such as frictional factors, within accepted bounds to better represent the water propagation. The Boston model was calibrated using both normal tidal conditions and a representative storm event for the northeast US. The “Blizzard of 1978” was used for the storm calibration. That storm was a slow-moving Nor’easter on Feb 6-7, 1978. It caused record-setting flood levels from Provincetown, Massachusetts to eastern Maine.

The calibrated model was then validated using another historical storm, the “Perfect Storm of 1991.” This validation used the same model parameters (e.g. bottom friction, diffusivity, etc.) as used to simulate the Blizzard of 1978. The model validation also represents a different type of storm. While the calibration event (Blizzard of 1978) was a purely extra-tropical event, the validation event (Perfect Storm of 1991) was a hybrid of a tropical and extra-tropical event (see Webb 2017 for an explanation of the calibration and validation steps in proper coastal hydrodynamic modeling).

Finally, the calibrated model was used to simulate the full range of storm events (both hurricanes and Nor’easters) and sea level rise conditions using a Monte Carlo statistical approach which accounted for tidal variation.

#### 14.8.3.5 Inundation Mapping

An objective of the study was to assess the vulnerability of the Central Artery/Tunnel system to RSLR and extreme storm events. One way this was achieved was by mapping coastal flooding in a quantified, probabilistic framework.

Figure 14.16 is one example of the inundation maps developed. The color scale shows the probability of flooding in these areas ranges from the 0.1%-risk storm (i.e. the 1,000-year storm) to the 100% risk level (i.e. the bay or the ocean that is always flooded). This example is for 2070/2100 conditions, i.e. with 3.4 ft of RSLR from present-day conditions.

Figure 14.17 shows another, more focused, example of a flood mapping product from the Boston vulnerability assessment study. The probability of flooding in the area of Christopher Columbus Park near Long Wharf is shown on an overlay of an oblique aerial image. This example is for 2030 conditions, i.e. with 0.68 ft of RSLR from present-day conditions.

#### 14.8.3.6 Adaption Engineering Implications

The results of the modeling used in the Boston case study can inform a wide variety of engineering decisions related to adaptations. The flood levels at the specific location of transportation assets are quantified with depth-frequency curves (e.g. 2-year to 1,000-year return period depths). The changes in these curves with sea level rise are also estimated.

Many other highly detailed, site-specific analyses are results of the modeling. One example is demonstrated in Figure 14.18 and Figure 14.19. Specifically, these figures are focused on the 93 Granite Ave. site in Milton, Massachusetts. This location is currently home to the MassDOT Fuel Depot Complex and is also being considered for the potential future residence of the primary MassDOT maintenance facility. As such, this location represents an important site for MassDOT both from a current operational perspective and from an engineering design and future use perspective. The two figures evaluate the site in the present day (2013 for this study) and the near-term future (2030).

Figure 14.18 shows the present day, i.e. 2013, flooding for this area. The dashed black line shows the parcel of interest, while the solid black lines show the existing structures. The map shows the present-day flooding depths corresponding to the 1% flooding probability level (areas of 1% probability or greater). Depths of flooding are generally small for present-day, with depth of water in the parcel of approximately 6 inches and restricted to the southern parking area and the two southern buildings. Accessibility to the site (via Granite Ave.) remains viable for the 1% return period water level in present-day conditions.

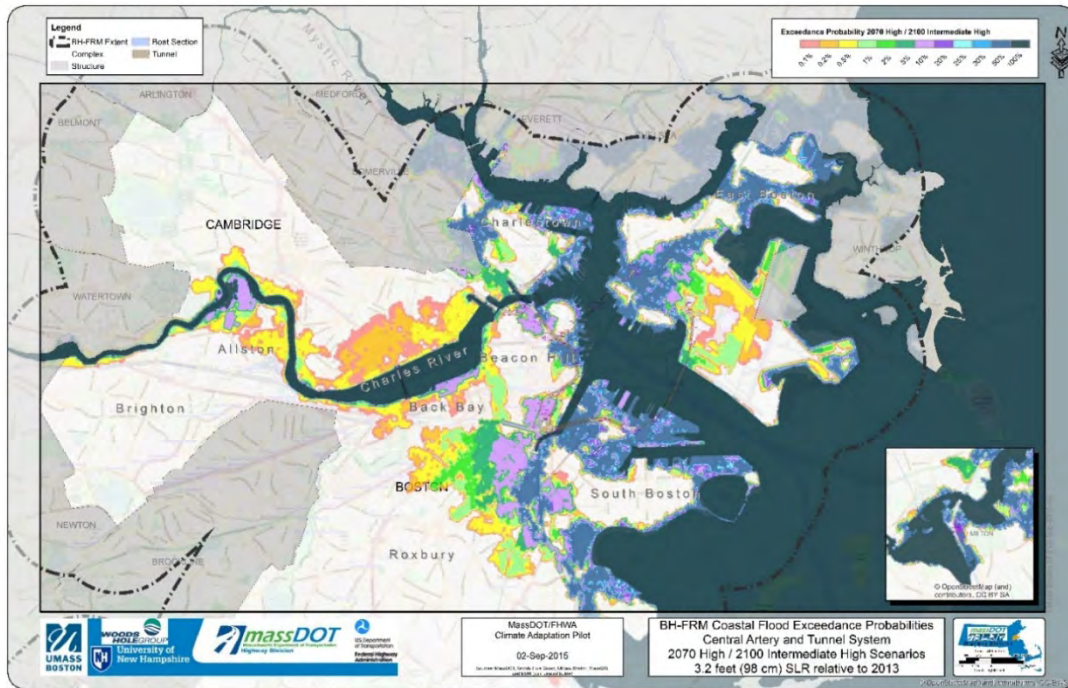


Figure 14.16. Example of the inundation map products from the Boston Central Artery/Tunnel Vulnerability Study. The exceedance probability of coastal flooding in 2070/2100 (from Bosma *et al.* 2015; permission to use image provided by MassDOT)

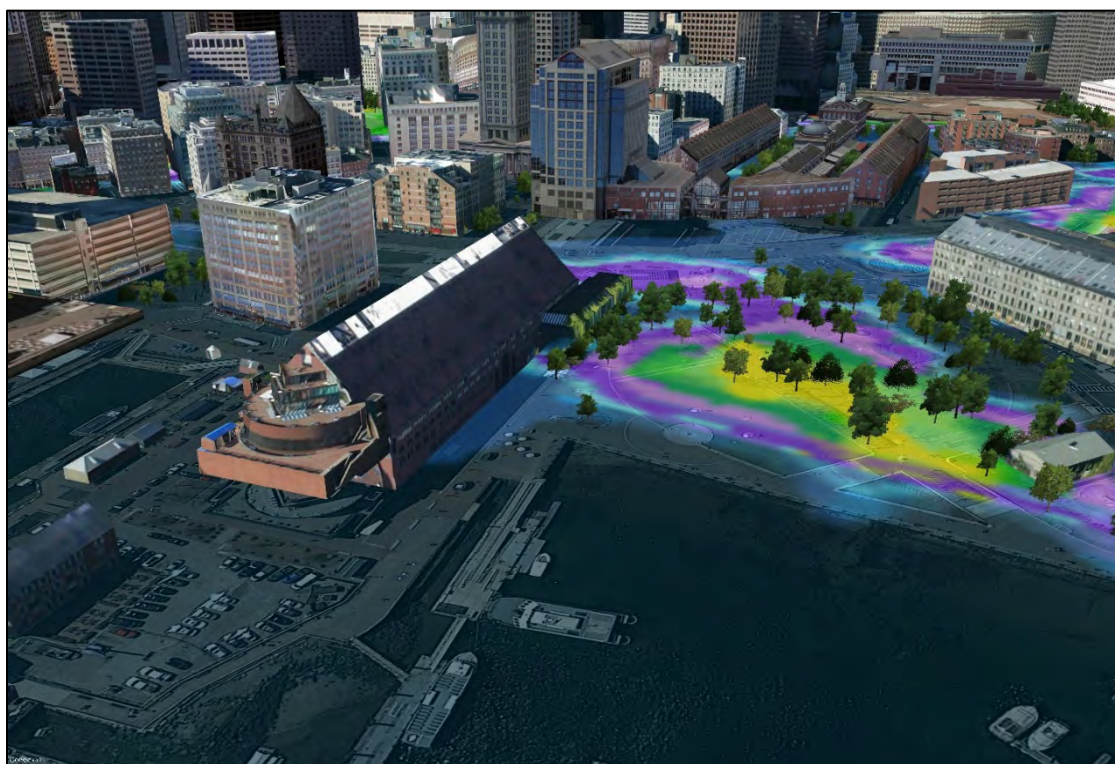


Figure 14.17. Example of coastal flood mapping results from the Boston Central Artery/Tunnel vulnerability study focused on the area around Long Wharf and Christopher Columbus Park (from Bosma 2019; permission to use image provided by MassDOT)

Figure 14.18 also shows the residence time of the flooding and flood pathways to the site. The residence time gives an indication of how long the flooding is expected to last for the 1% probability. This type of information can only be obtained from a coastal hydrodynamic model such as those described here for a Level 2 or Level 3 analysis. For present-day (2013), the residence time of the flooding is 7.33 hours. In other words, the flooding remains at the site for 7.33 hours before it recedes (and peaks at 0.5 ft). The figure also shows the two local flood pathways that influence the area. The flood pathway to the north originates in a small marsh creek that allows water to propagate landward and flood into the local neighborhood and road system. The flood pathway to the south is the low-lying wetland area that connects further to the south to the Neponset River.

Potential adaptations could consider local measures (e.g. raising the elevations of the buildings on the parcel, flood proofing structures, local on-site berms or walls) or more regional approaches (e.g. berms, tide gates, flood walls, etc.) at the source of the flooding for the area that would not only serve to protect the 93 Granite Ave. site, but also other infrastructure (e.g. roads, homes, etc.).

Looking forward to 2030, Figure 14.19 presents the depths for the 1% flooding probability, which have now increased to an average of 1.5 ft for a good portion of the parcel, while also showing inhibited accessibility to the site via Granite Ave. The entire parcel has depths of at least 0.5 ft, and depths reach 2 ft. The residence time is now 10 hours indicating access to the site would be unavailable for that length of time. The pathways of flooding remain the same and I-93 is at a high enough elevation to remain unaffected in this area, as well as to provide a barrier to flooding. This increased risk of flooding at this location gives an indication that, at minimum, careful engineering approaches and planning should be taken if the primary maintenance facility is to be relocated to this site.

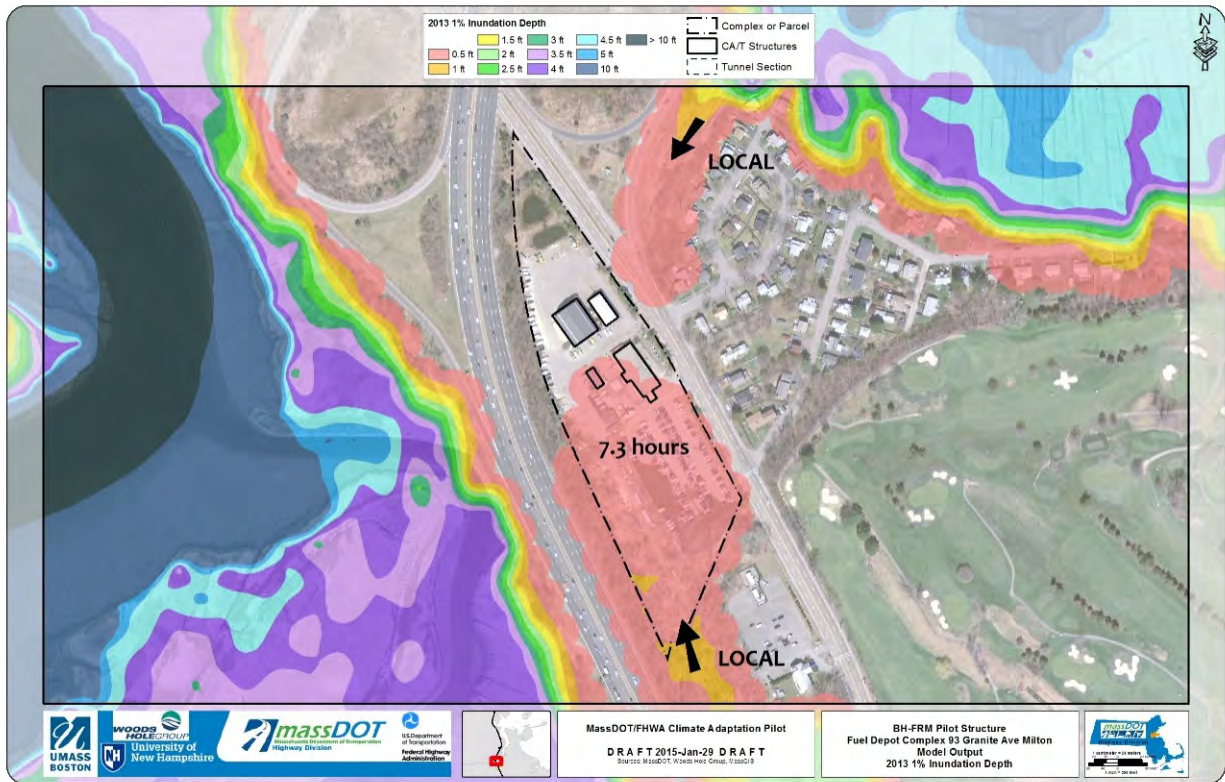


Figure 14.18. Model results showing depth for a 1% flooding probability in 2013 at the 93 Granite Ave. location, as well as residence time and local flood pathways (from Bosma *et al.* 2015; permission to use image provided by MassDOT)

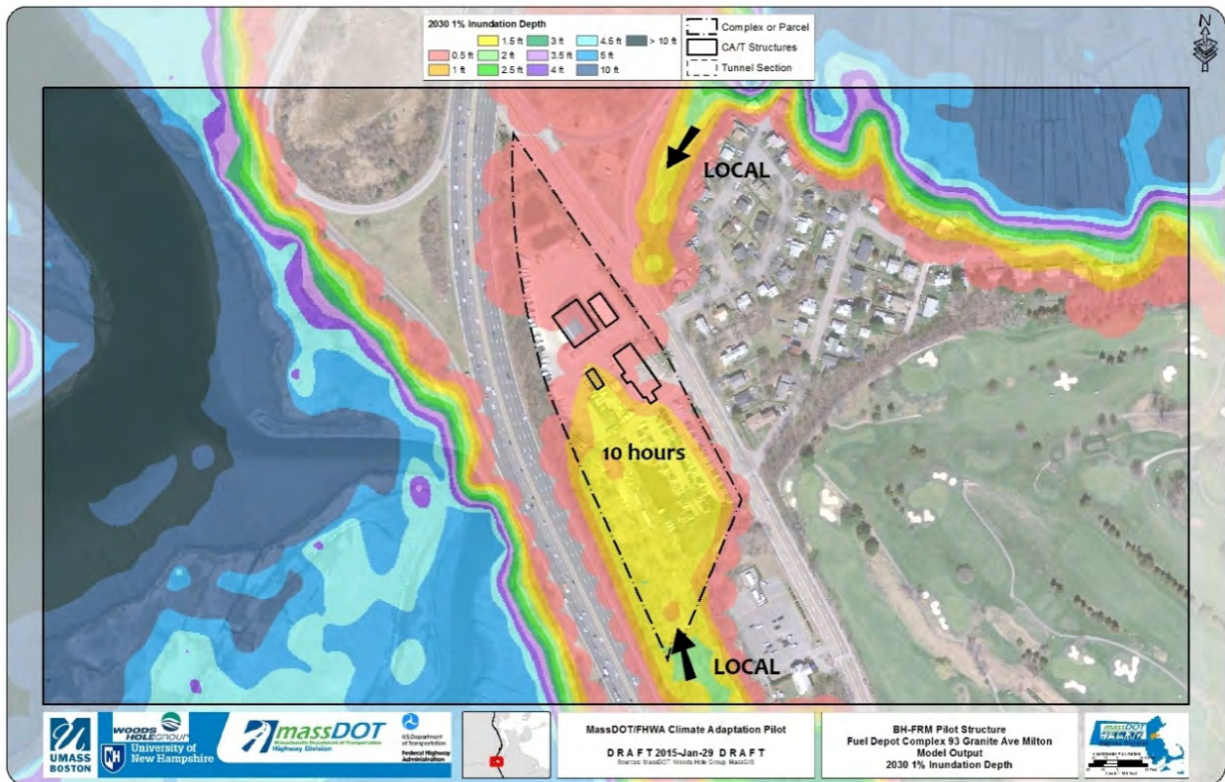


Figure 14.19. Model results showing depth for a 1% flooding probability in 2030 at the 93 Granite Ave. location, as well as residence time and local flood pathways (from Bosma *et al.* 2015; permission to use image provided by MassDOT)

## Chapter 15 - Adaptation Strategies for Coastal Highways

The best coastal highway infrastructure adaptation strategies for coping with extreme events and future sea level rise are most likely forms of coastal engineering and planning already utilized for resilience today. Because society has long lived along the coast, coastal engineering is an ancient field. However, the challenges facing today's engineers and planners are greater than ever. Infrastructure strategies will need to confront the on-going societal migration to coastal areas and sea levels projected to rise to levels society has never experienced.

This chapter briefly summarizes the potential coastal damage mechanisms and adaptation strategies for highways in the coastal environment to extreme events and sea level rise. Many of the technical issues summarized in this chapter are discussed in more detail elsewhere in this document.

### 15.1 Typical Coastal Damage Mechanisms

This section discusses some typical coastal damage mechanisms including damage to roadways, bridges, rails, and tunnels:

- roadway damage by wave attack,
- roadway and railway damage by coastal “weir-flow,”
- roadway damage by bluff erosion and shoreline recession,
- bridge deck damage by waves on surge,
- structure damage by wave runoff,
- loss of function due to more frequent and extensive flooding
- tunnel and road damage by overtopping, and
- damage by tsunamis.

The vulnerability of coastal transportation assets to these damage mechanisms will increase with sea level rise (Jacobs *et al.* 2018b). There is limited information on the details of the “sensitivity” levels for most of these coastal damage mechanisms in the coastal engineering community. More research is needed in this area to improve our ability to assess the vulnerability of our existing coastal transportation system.

#### 15.1.1 Roadway Damage by Wave Attack

Many coastal roads are on constructed embankments or natural bluffs that can be eroded by wave action during extreme events. These embankments are often damaged to the extent that the roadway pavement is undermined and damaged. Embankments used as approaches to coastal bridges are particularly susceptible to this wave attack damage in extreme coastal events as illustrated in Figure 15.1. In this case, the peak storm surge allowed waves to attack an embankment not designed for those wave conditions. Note the undamaged bridge over a coastal water body in the background and the undermined pavement in the foreground.

This susceptibility of the approaches occurs in areas where they are at higher elevations than most of the roadway due to waterway clearance issues. Apparently, the higher elevation subjects

these portions of the embankment to direct action of larger wave heights while nearby lower-elevation embankments are submerged beneath much of the wave action (Douglass *et al.* 2004). The damage can be complete or partial depending on the duration of the storm surge and the design of the embankment. The damage is common on the side of the embankment exposed to large waves during the coastal storm.

**Embankments used as approaches to coastal bridges are particularly susceptible to wave attack damage**

The sensitivity of roadways to wave attack depends on the storm characteristics at the specific location (surge level and duration, wave heights, etc.) as well as the embankment condition/design (grass, exposed sand, slope protection, etc.). The single most important storm parameter is likely wave height at the embankment. For very small waves, embankments designed for rainfall events will survive coastal storms for the duration of a storm surge. In other words, the embankment will be inundated but not damaged if there are only very small waves and very small flow velocities. However, if wave heights are of any significant height, say  $H > 0.5$  ft, most soil embankments will erode. Chapter 7 summarizes proper design of coastal revetments for wave attack. The fundamental tool is Hudson's equation for sizing the revetment armor stone as a function of wave height, slope, etc. Hudson's equation is based on a low level of damage (5 percent of the armor stones moving during design conditions). The USACE Coastal Engineering Manual (USACE 2002) presents methods to evaluate higher percentage levels of revetment damage as well as other methods for designing coastal revetments.



Figure 15.1. Partial embankment damage caused by waves on storm surge during Hurricane Ivan (Pensacola, Florida, 2004)

### 15.1.2 Roadway and Railway Damage by Coastal “Weir-Flow”

Storm surge waters flowing across the road and down an embankment can cause damage as illustrated in Figure 15.2. In this photograph of US 98 (Okaloosa Island, Florida) taken in 2005, the Gulf of Mexico is to the right and storm surge elevation is just slightly greater than the roadway elevation. This is the coastal “weir-flow” damage mechanism described in detail in Chapter 10, Highway Overwashing. **Much of this damage to road pavements is on the landward side of the road and not the seaward side of the road.** Waves on the flowing surge waters can increase the scour potential on the landward side of the road significantly. Two related damage mechanisms occur as storm surge recedes: weir-flow damage on the seaward side of the roadway as surge waters flow back out to sea late in the storm, and scour of the embankment caused by flow parallel to the road as water moves to “breaches” or lower spots in the road as the storm surge recedes.



Figure 15.2. Example of the coastal weir-flow damage mechanism as it occurs (photograph provided by FDOT, circa 2005)

The sensitivity of roadways to damage from the weir-flow damage mechanism depends on both the hydraulics and the embankment conditions (slopes, elevations, cover). However, there is very little information on the rate of damage of roadway embankments to the coastal weir-flow damage mechanism. Both laboratory tests and field observations indicate that embankment shoulders of unvegetated loose sand (common in many coastal areas) erode with even minimal overtopping flow (see Section 10.2.1). Vegetated shoulders and embankments made of compacted sub-soils

will erode slower and thus may experience less than total pavement damage if the storm conditions, particularly surge duration, are mild enough.

Railway embankments can experience the same damage mechanisms as roadway embankments: direct wave attack and the weir-flow mechanism. Figure 15.3 shows damage to a railway embankment which occurred during Hurricane Katrina. The “sediment” here was not unconsolidated sand but unconsolidated gravel (track “ballast”). The incoming or rising-limb storm surge flowed across the tracks from left to right in this photograph. The damage was primarily due to the weir-flow mechanism as the storm surge elevations exceeded the rail elevations.



Figure 15.3. Railway embankment damage caused primarily by the coastal weir-flow damage mechanism during (Mississippi, 2005)

### 15.1.3 Roadway Damage by Bluff Erosion and Shoreline Recession

Roadways along many coasts are threatened and damaged by coastal bluff erosion and shoreline recession. Usually, the damage occurs during an extreme event like a hurricane or northeaster. However, often, shoreline erosion had previously increased the vulnerability of the roadway due to other longer-term processes. Figure 15.4 shows an example of a highway (North Carolina SH 12, the Atlantic Ocean is to the left in the photograph) damaged in the latter stages of Hurricane Ida (2009). The roadway is located along a receding shoreline. That recession had progressively increased the vulnerability of this highway prior to the hurricane.

Understanding the underlying geomorphological framework can be valuable for the highway engineer. This type of damage will continue to occur as sea levels rise. Essentially this barrier island is rolling over itself as a form of migration toward the mainland in response to RSLR. The roadway is now on the beach face. These phenomena are long-term geological processes that impact coastal highways and should be considered in design through engineering or siting. The

rate of bluff and shoreline erosion at different locations is a function of the site-specific geology and coastal processes. Chapter 8 discusses general considerations in this situation. Some states have developed detailed maps of the coastal hazards of bluff erosion which can be used as a basis for evaluating the increased vulnerability to extreme events and sea level rise (see e.g. Revell *et al.* 2011).



Figure 15.4. Pavement damage due to waves and surge in an extreme event (North Carolina SH 12, 2009; permission to use photograph provided by Dave Henderson)

#### 15.1.4 Bridge Deck Damage by Waves on Surge

Bridges over coastal waters can be severely damaged and destroyed by wave-induced loads if storm surge allows the wave to strike the bridge deck (Figure 15.5). Section 11.2 discusses this damage mechanism, loads induced by repeated individual waves striking the bridge superstructure.

Figure 15.5 shows two bridges destroyed by wave loads in Hurricane Katrina. The bridge on the left (US 90) was a wider replacement for the bridge on the right (which was used for fishing only for years prior to Katrina). The newer bridge was designed at about the same elevation as the older bridge despite the older bridge being severely damaged in Hurricane Camille in 1969. This sequence of events implies that:

- a correlation between surge/wave height and vulnerability exists (note the undamaged spans at higher elevations on the left bridge),
- bridges should have a service life at least of 75-years; building a replacement bridge at the same low chord elevation as the damaged bridge resulted in a service life of only 36 years,

- design standards likely will evolve as we learn more about exposure and vulnerability along the coast (Indeed, the Guide Specifications of AASHTO 2008 were developed specifically for this situation shortly after Hurricane Katrina), and
- sea level rise will complicate these correlations.

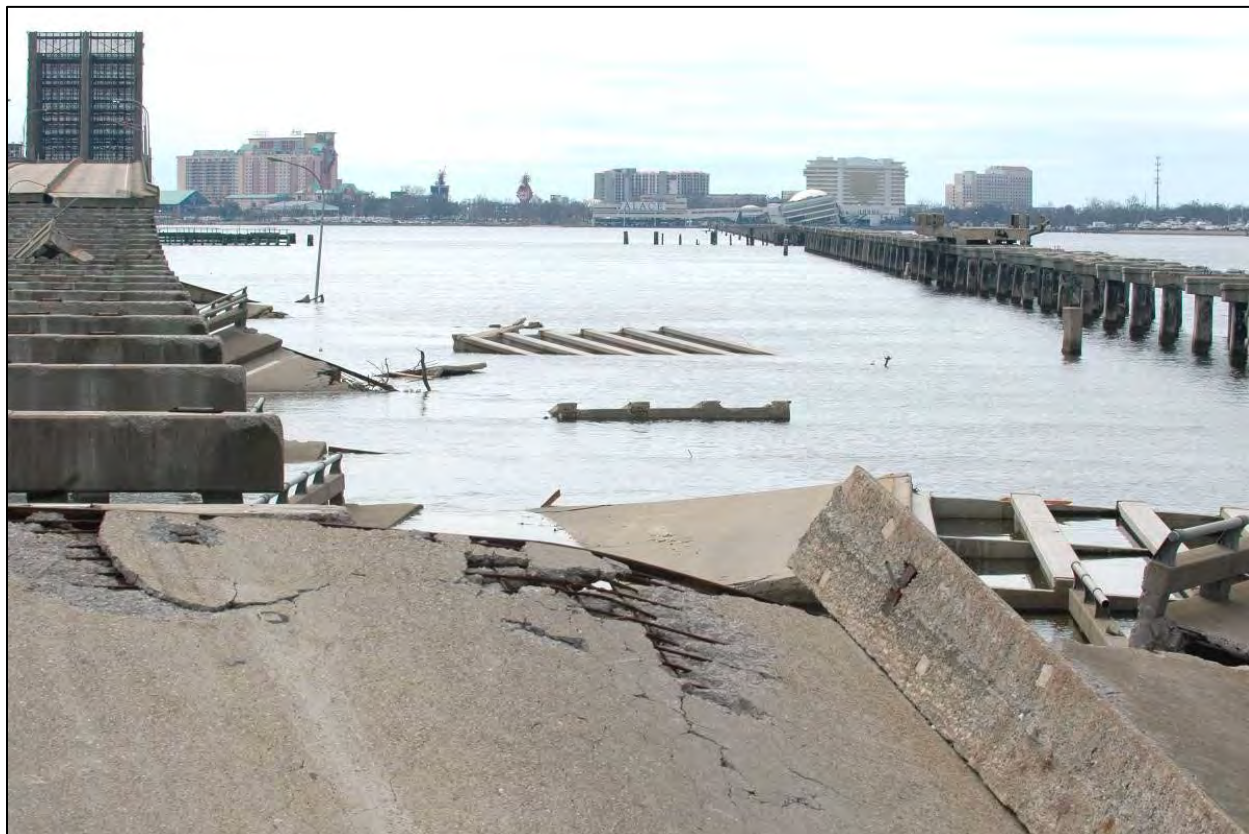


Figure 15.5. Two bridges destroyed by wave loads in Hurricane Katrina (Biloxi Bay, Mississippi)

Sensitivity to this damage mechanism depends primarily on the wave heights which can strike the structure during the peak of the storm and the relative elevation of the storm surge as compared to the bridge elevation (see Chapter 11). Most bridge decks can survive wave-induced loads if just the crests of the largest wave heights are striking the bridge deck. Most damage occurs when the storm surge (still water level) elevation is at or slightly above that of the low chord of the bridge deck. At this condition, the full waves can strike the rigid structures and the loads can be extremely high with each individual wave. Laboratory experiments have found the wave loads to be as much as three times the dead weight of bridge decks when the storm surge (SWL) is very near or just above the bridge deck elevation (Douglass *et al.* 2007).

Evaluating the vulnerability of bridge decks to extreme events and sea level calls for estimating the effect of storm surge, wave heights and sea level rise on the wave loads. Sensitivity of specific bridges to wave-induced loads can be evaluated using available methods for estimating those loads and comparing those loads with the structural resistance (weight and connections) to those loads (e.g. FHWA 2017a). **Sea level rise will increase the vulnerability of many existing coastal bridges** requiring more research into the methods for estimating and reducing wave-induced loads for vulnerability assessment and adaptation planning. Wave loads on bridge decks are extremely sensitive to the storm surge elevation and thus extremely sensitive to sea level rise (see Chapter 14).

### 15.1.5 Structure Damage by Wave Runup

Wave runup is the uprush of a wave's water up a beach (Section 5.5) or structure (Section 7.5). Wave runup causes high velocity flows in individual waves to flow above the storm surge still water elevation where it can cause structural damage and scour. FEMA (2011b) and USACE (2002) provide information for estimating loads on structures (buildings) in the coastal flood plain. These loads include breaking and broken wave-induced loads, hydrostatic and buoyancy loads, and flow-induced hydrodynamic loads. Much of the load information is a function of local depth and/or local, depth-limited, wave height.

The sensitivity of damage caused by wave runup to extreme events and sea level can be evaluated by estimating the effects of storm surge, wave effects of storm surge, wave heights and sea level rise on the loads and the extent of runup. In particular, the damage caused by wave runup will increase as sea levels rise and storm surge increases.

### 15.1.6 Tunnel and Road Damage by Overtopping

Hurricane Sandy flooded some highway and transit tunnels when the storm surge elevation exceeded the elevation of the tunnel entrances, or portals. The basic damage mechanism of overtopping is inundation resulting from flow over the portal walls and down entrances. Tools to estimate the hydraulics of such flows are available in hydraulic engineering textbooks. Several specific damage mechanisms include damage to electrical systems, ventilation systems, and blockage of the tunnel itself. The sensitivity of a specific tunnel to this damage is related to the storm characteristics and the tunnel portal design. The relative elevations of the storm surge and the portal walls are important. A form of a detention pond analysis can be used to evaluate the internal level of flooding in a tunnel for specific storms. Often a small amount of flood water will not damage tunnels as they are designed for some rainwater drippage off vehicles and cleaning. Tunnels may use pumping system to remove these water sources; however, the larger quantities of surge into the portals may overwhelm the capacities of these pumps (if the event hasn't already resulted in a loss of power to those pumps).

**A related issue for some tunnels and many coastal highways is flooding due to wave overtopping.** Wave overtopping is water splashing over a seawall when runup exceeds the elevation of the top of the wall. Wave overtopping onto coastal roads is fairly common during storms in many parts of the US. Two important aspects of overtopping are the time-averaged volumetric rate of overtopping and the intensity or force of a single wave overtopping event (see Section 7.5). Overtopping rate is a function of freeboard (the elevation difference between the storm surge still water level and the wall crest) and wave height. It is particularly sensitive to storm surge level in extreme events and thus, will be extremely sensitive to sea level rise.

### 15.1.7 Damage by Tsunamis

Tsunamis damage transportation assets through extreme hydrodynamic loads, scour, and debris impact loads. The hydrodynamic forces include hydrostatic forces, buoyant forces, drag forces, surge or impact forces (Nistor *et al.* 2010). Bridges and roadways on embankments both suffer damage in tsunamis. The 2011 Japan tsunami destroyed bridges through a variety of damage mechanisms including hydrodynamic loads removing bridge decks (much like the hurricanes in the southeastern US) or damaged substructure. Some lower elevation bridge decks survived while higher elevation decks did not (Chock *et al.* 2013). Many bridge approach embankments were damaged by scour due to water flowing over the embankment (Yashinsky 2011), which appears to be very similar to the weir-flow damage mechanism common in storm surge previously described.

At the time of the preparation of this document, a multi-state and federal study is developing bridge design guidelines for the estimation of tsunami loads on highway bridges (Transportation Pooled Fund Program 2019).

## ***15.2 Adaptation Strategies for Coastal Highway Infrastructure***

This section discusses possible adaptation strategies for coastal transportation infrastructure to extreme events and sea level rise. Adaptation means preparing for the impacts on the nation's transportation infrastructure and systems. Specifically, it refers to planning, designing, constructing, operating, or maintaining transportation infrastructure while incorporating consideration of extreme events and sea level rise. Adaptation strategies may include providing protective countermeasures intended to prevent, delay or reduce the severity of problems related to extreme events and sea level.

Adaptation strategies to respond to coastal infrastructure problems related to extreme events and sea level rise may be categorized as follows:

- Manage and maintain
- Increase redundancy
- Protect
- Accommodate
- Relocate

Combinations of these strategies may also be employed. The next five sub-sections discuss these types of strategies related to highways in the coastal environment.

### **15.2.1 Manage and Maintain**

**One category of adaptation strategies is to maintain existing infrastructure for optimal performance and manage the response to extreme events through advanced preparation.**

Examples include:

- Increase and target maintenance activities (e.g. culvert cleaning, sand sweeping).
- Relocate movable assets prior to forecast storm events (e.g. moving maintenance vehicles and equipment to less vulnerable areas).
- Enhance and practice emergency procedures including vulnerable asset closures.
- Stockpile and strategically place fuel, temporary bridges, and road construction materials for quick deployment.

Coastal SDOT's already use these, and other, forms of specialized management and maintenance to prepare for - and in response to - coastal storms. These procedures have been developed internally and in coordination with other federal, state and local entities to maintain and restore service in response to coastal storms and flooding.

### **15.2.2 Increase Redundancy**

Another general category of adaptation strategy is to **increase the redundancy** of the system. This means ensuring that transportation services provided by infrastructure can be supplied by other means/alternatives. Examples include:

- Identify and enhance, as appropriate, alternative roads, routes, or modes to serve transportation needs during times of compromised service (e.g. enhanced ferry service).
- Consider constructing or enhancing closely spaced roads versus one road.

Coastal transportation organizations often address the redundancy issues such as ferries in planning-level activities in the wake of or in preparation for storm events.

### 15.2.3 Protect

**A common category of adaptation strategies is to protect the existing system.** The goal is to reduce or eliminate damage by providing protective physical barriers to extreme events. This may include “hard” structures such as seawalls and “soft” strategies such as nature-based solutions. Protective strategies keep water away from infrastructure or provide resistance to the damaging forces of water and waves. Examples include:

- New or enlarged seawalls, bulkheads, revetments, etc. (hard structures to provide barriers or resistance to damaging forces),
- Beach nourishment (soft strategy to move water away from infrastructure),
- Dune restoration and vegetation (soft strategies to provide barriers and resistance to damaging forces), or
- Living shorelines along sheltered coasts (combination of hard and soft structures/strategies to increase resistance to damaging forces).

“Hard” engineering structures have been used to protect many coastal transportation assets. These include seawalls, bulkheads, revetments, breakwaters, groins, and jetties. These structures protect many miles of coastal highways today. The functional design purpose of different types of coastal structures is explained in Chapter 7. That material on the structural design of coastal revetments can be easily adapted for future RSLR. USACE (2002) presents more information on the design of seawalls and revetments. The most common successful type of coastal revetment for wave attack is a rubble-mound structure consisting of an engineered slope or pile of rocks (or other armor units). Because the rocks can move, there is an inherent resilience in these structures as compared with completely rigid structures. As sea level rises, these solutions should be considered in more situations to protect assets that are not now threatened. Many highway revetments were built in immediate response to a specific storm but the vulnerability prior to the storm had been increasing for years due to longer term processes of shoreline recession and sea level rise. Also, existing seawall and revetment structures may have to be modified to withstand higher wave conditions as sea level rises. This may include increasing their height and include placement of new layers of rock to strengthen existing seawalls as well as construction of new seawalls (Ewing 2018).

“Soft” engineering includes most of the nature-based solutions discussed in Chapter 8 such as beach nourishment, dune restoration, and marsh creation. **The general goal is to use engineering that more closely mimics the natural systems in the vicinity.** Beach nourishment is the direct placement of large amounts of sand on the beach to widen the beach (see Chapter 8). Beach nourishment is a commonly used adaptation to sea level rise and has been successfully used to stabilize recessional shorelines in many places in the US (NRC 1995, Douglass 2002, Houston 2018). Beach nourishment with sand dune restoration also reduces damage to landward infrastructure. For example, beach communities in New Jersey with nourishment and constructed sand dunes suffered significantly less damage in Hurricane Sandy than other nearby communities (Houston and Dean 2013). Beach nourishment and dune restoration was used extensively along the New Jersey and New York shore in response to

Hurricane Sandy to support the long-term sustainability of the coastal ecosystem and communities as well as to reduce the economic costs and risks associated with future storm events (US Congress 2013).

**Modern coastal engineering solutions often combine some “hard” structures with some “soft” or nature-based approach.**

Modern coastal engineering shoreline stabilization solutions often combine beach nourishment with coastal structures. These solutions are “hybrid” solutions using components of the “soft” and “hard” approach. The primary purpose of the structure is to retain the sand. Some of these “hybrid” solutions emulate natural geomorphology features such as pocket beaches between headlands where the sand nourishment is placed between constructed headland breakwaters (see Chapter 8). During Hurricane Sandy, the presence of a relic stone seawall buried beneath a nourished dune and beach reduced wave forces by a factor of two, effectively protecting the upland infrastructure, including a coastal highway (Smallegan *et al.* 2016).

The term “soft engineering” can also include “green” infrastructure engineering, or “nature-based solutions, such as wetland creation and living shorelines. Living shorelines are combinations of structure, vegetation, and sand (in some cases) to stabilize the shoreline and provide nearshore habitat to allow native species of flora and fauna to flourish. They are particularly attractive alternatives to traditional bulkhead or revetment structures along sheltered bay and river shorelines. More research is needed on the engineering of these green coastal infrastructure approaches.

The FHWA developed “Nature-Based Solutions for Coastal Highway Resilience: An Implementation Guide” (Webb *et al.* 2019). The FHWA designed this implementation guide to help transportation practitioners understand how and where nature-based solutions can be used to improve the resilience of coastal roads and bridges.

#### 15.2.4 Accommodate

Another category of adaptation strategy is to accommodate. The infrastructure is modified or redesigned to better coexist in the future environment. Examples include:

- Increasing bridge deck elevations and strengthen bridge structures,
- Lowering roadway profiles to allow overwash without pavement damage during extreme events, or
- Raising tunnel portal walls to reduce likelihood of flooding.

Careful assessment of the vulnerability of the infrastructure to extreme events and sea level is needed to develop cost-effective accommodation strategies. An understanding of magnitudes, probabilities, and uncertainties of projected stressors such as sea level rise and extreme events is particularly important when considering this strategy for the long-term extension of the design life of infrastructure assets. Accommodation strategies may also be used for short- or medium-term design horizons.

**Increased elevation is the only proven adaptation option for coastal bridges subject to wave attack during extreme events.** Several of the major bridges destroyed by hurricanes in the southeastern US were replaced with new bridges elevated much higher to avoid those wave loads in extreme events. These included:

- I-10 bridge over Escambia Bay near Pensacola, Florida,

- I-10 bridge over Lake Pontchartrain near Slidell, Louisiana,
- US 90 bridge over Bay Saint Louis, Mississippi (see Figure 15.6), and
- US 90 bridge over Biloxi Bay, Mississippi.



Figure 15.6. New, much higher, US 90 bridge across Bay St. Louis, Mississippi built after Hurricane Katrina (June 14, 2007)

Another oft-discussed option is to increase the connection strength to the bridge substructure. This approach, however, will transfer those loads to the substructure and foundation, so care should be taken to evaluate wave-induced load failure mechanisms such as negative bending of the deck, pile bending or shear failure, failure of the pile to bent cap connections, and possible soil failure around the foundation (Douglass *et al.* 2006a, Robertson *et al.* 2011, FHWA 2017a). More research is needed on wave-induced loads for use in design of bridges at low enough elevations to be inundated by storm surge and waves.

Increased elevation is an adaption option for seawalls that protect roadways and tunnel entrances. Increasing the elevation of the roadway is an option for those roads that flood because of wave runup and overtopping and are already protected by seawalls or revetments. Temporary doors or storm surge barriers have been used at some tunnel portals for many years and the further development of these has been suggested as an adaptation for coastal tunnels that can flood in extreme events. More research into effective tunnel options is needed.

### 15.2.5 Relocate

The final category of adaptation strategies is relocation (see Section 8.4). The goal is to lessen or eliminate exposure to coastal stressors by relocating infrastructure away from the coastline. This could be in conjunction with disinvestment, repurposing, abandoning or removing existing exposed infrastructure. Examples include:

- Relocating infrastructure further inland away from the coastline,
- Repurposing or reclassifying paved road to all-terrain vehicle road, or
- Reconditioning a damaged vehicular bridge to serve as a pedestrian bridge or fishing pier.

Relocation or abandonment has long been a common response to shoreline recession and bluff erosion. Recession and erosion are natural processes which become a problem primarily when infrastructure is threatened. For example, storm-related bluff erosion led to a relocation of a portion of the coast-parallel California 1, the Pacific Coast Highway, in April 2013. Chapter 8 discusses other roads that have been relocated in the past several decades. This includes one section of a coast-parallel road in Texas that was abandoned after storm damage in 1989. At that location, relocation of the roadway landward away from the Gulf of Mexico was constrained by the ecological value of the coastal wetlands in a National Wildlife Refuge. Similar issues, the ecological value of natural wetland and barrier island habitat, led to consideration of relocating miles of NC 12 from that barrier island onto a bridge in the bay (FHWA 2010). Portions of coastal road have already been relocated in response to storm damage as shown in Figure 15.7. At some locations, relocation is constrained by private property.

The USACE (2014) presents that agency's guidance concerning adaptation strategies for incorporating sea level change in the planning of coastal works. It addresses a number of concerns that transportation organizations face with coastal infrastructure including discussions about appropriate time horizons and ranges of scenarios for planning.

In alignment with 23 CFR § 515 (Asset Management Plans), for transportation assets vulnerable to extreme events and sea level rise, a SDOT might consider all the adaptation options, including **combinations** thereof: manage and maintain, increase redundancy, protect, accommodate, and relocate, as part of their life-cycle planning and risk identification efforts. For example, some combination of relocation, accommodation (lowering of roadway), and protection (dune construction and a buried revetment on the embankment) have been proposed and constructed for some coast parallel roads that have been damaged by frequent overwashing such as shown in Figure 15.7. This approach is a reasonable adaptation to sea level in these situations. These types of decisions have been made throughout history along the coast in both real-world applications and theoretical analyses. They will likely have to be made more often by coastal engineers in coordination with the transportation engineering community as sea levels rise in the coming decades.

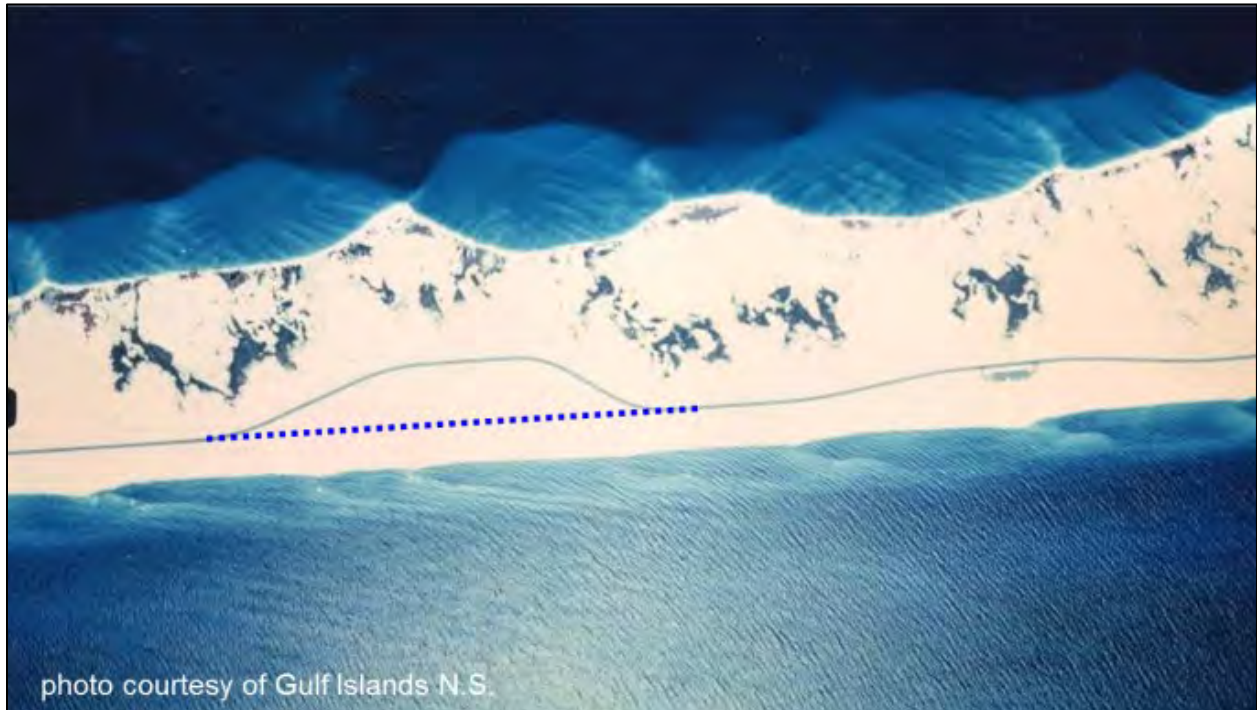


Figure 15.7. Example of coastal highway relocation in Florida (SH 399: the dashed line shows the previous highway location: permission to use image provided by the Gulf Islands National Seashore)

*Page Intentionally Left Blank*

## References

AASHTO (2008) "Guide Specifications for Bridges Vulnerable to Coastal Storms." American Association of State Highway and Transportation Officials, 55 pp.

AASHTO (2014) "AASHTO Drainage Manual." American Association of State Highway and Transportation Officials, 1340 pp.

ACOPNE (2018) Academy of Coastal, Ocean, Port and Navigation Engineers.  
<http://www.acopne.org/> (accessed November 1, 2018)

Akiyama, M., Frangopol, D. M., Arai, M., and Koshimura, S. (2012) "Probabilistic assessment of structural performance of bridges under tsunami hazard." Structures Congress 2012 – Proceedings of the 2012 Structures Congress, p. 1919–1928.

Akiyama, M., and Frangopol, D. M. (2014) "Reliability of Bridges under Seismic and Tsunami Hazards." Vulnerability, Uncertainty, and Risk: Quantification, Mitigation, and Management – Proceedings of the 2nd International Conference on Vulnerability and Risk Analysis and Management, ICVRAM 2014 and the 6th International Symposium on Uncertainty Modeling and Analysis, ISUMA 2014, Hall J.W., Au S.-K., and Beer M., eds., American Society of Civil Engineers (ASCE), p. 1696–1705.

Algeo, L. and Mahoney, T. (2011) "FEMA's Update Process for Coastal Surge and Wave Analysis for Flood Insurance Rate Maps." Proceedings of Solutions to Coastal Disasters Conference, ASCE, p. 569–580.

Almodovar, L., Gravens, M. B. and Curtis, W. R. (2008) "Economics as an Engineering Tool: Life Cycle Risk Analysis of Coastal Projects." COPEDEC VII, Paper 198, Dubai, UAE.

Anarde, K. A., Kameshwar, S., Irza, J. N., Nittrouer, J. A., Lorenzo–Trueba, J., Padgett, J. E., Sebastian, A., and Bedient, P. B. (2018) "Impacts of Hurricane Storm Surge on Infrastructure Vulnerability for an Evolving Coastal Landscape." Natural Hazards Review, Vol. 19, No. 1.

Anderson, E.J., Schwab, D.J., Lombardy, K.A. and LaPlante, R.E. (2012) "Detection and Modeling of a Meteotsunami in Lake Erie During a High Wind Event on May 27, 2012." America Geophysical Union Fall Meeting, on–line abstract.

Andersen, T.L., Moghim, M.N., and Burcharth, H.F. (2014) "Revised Recession of Reshaping Berm Breakwaters." Proceedings of the 34 International Conference on Coastal Engineering, 15 pp.

Angel, J.R. and Krunkel, K.E. (2010) "The response of Great Lakes water levels to future climate scenarios with an emphasis on Lake Michigan–Huron." Journal of Great Lakes Research, Vol. 36, Supplement 2. p. 51–58.

Annunziato, A., and Best, C. (2005) "The Tsunami Event Analyses and Models." Institute for the Protection and Security of the Citizen, Joint Research Centre, European Commission, 42 pp.

Arneson, L.A., Zevenbergen, L.W., Lagasse, P.F., and Clopper, P.E. (2012). "HEC–18: Evaluating Scour at Bridges," 5<sup>th</sup> ed., FHWA–HIF–12–003, 340 pp.

ART (2011a) "Adapting to Rising Tides: Transportation Vulnerability and Risk Assessment Pilot Project: Briefing Book," November, 84 pp.

ART (2011b) "Adapting to Rising Tides: Transportation Vulnerability and Risk Assessment Pilot Project: Technical Report," November, 314 pp.

- ART (2012) "Adapting to Rising Tides Vulnerability and Risk Assessment Report." Chapter 2. Sea Level Rise Mapping and Shoreline Potential Overtopping Analysis, September, 44 pp.
- ASBPA (2018) "A Snapshot of US Coastal Science and Engineering: Training the Next Generation of US Coastal Scientists and Engineers," White Paper by the American Shore & Beach Preservation Science and Technology Committee. October 2018.
- ASCE (2005) ASCE Standard No. 7: Minimum Design Loads for Buildings and Other Structures, ASCE/SEE-7. American Society of Civil Engineers/Structural Engineering Institute, 424 pp.
- ASCE (2016) ASCE Standard No. 7: Minimum Design Loads for Buildings and Other Structures. American Society of Civil Engineers/Structural Engineering Institute, 888 pp.
- ASCE TCLEE (2006) "Performance of Transportation Systems During Hurricane Katrina." Report by the American Society of Civil Engineers Technical Council on Lifeline Earthquake Engineering. Reston, Virginia.
- Ataei, N., Stearns, M., and Padgett, J. E. (2010) "Response Sensitivity for Probabilistic Damage Assessment of Coastal Bridges under Surge and Wave Loading." *Transportation Research Record*, No. 2202, p. 93–101.
- Ataei, N., and Padgett, J. E. (2013a) "Fragility Assessment of Coastal Bridges under Hurricane Events using Enhanced Probabilistic Capacity Models." 2012 ATC and SEI Conference on Advances in Hurricane Engineering: Learning from Our Past, Miami, FL, p. 691–702.
- Ataei, N., and Padgett, J. E. (2013b) "Limit State Capacities for Global Performance Assessment of Bridges Exposed to Hurricane Surge and Wave." *Structural Safety*, 41, p. 73–81.
- Ataei, N., and Padgett, J. E. (2013c) "Probabilistic Modeling of Bridge Deck Unseating during Hurricane Events." *Journal of Bridge Engineering*, Vol. 18, No. 4, p. 275–286.
- Ataei, N., and Padgett, J. E. (2015) "Fragility surrogate models for coastal bridges in hurricane prone zones." *Engineering Structures*, Vol. 103, p. 203–213.
- Atkinson, J., McKee Smith, J., and Bender, C. (2013) "Sea-Level Rise Effects on Storm Surge and Nearshore Waves on the Texas Coast: Influence of Landscape and Storm Characteristics." *Journal of Waterway, Port, Coastal, and Ocean Engineering*, Vol. 139, No. 2, p. 98–117.
- Azadbakht, M. and Yim, S.C. (2014) "Simulation and Estimation of Tsunami Loads on Bridge Superstructures." *Journal of Waterway, Port, Coastal and Ocean Engineering*. American Society of Civil Engineers, Vol. 141, No. 2.
- Baedke, S.J., and Thompson, T.A. (2000) "A 4,700-Year Record of Lake Level and Isostasy for Lake Michigan." *Journal of Great Lakes Research*, Vol. 26, No. 4, p. 416–426.
- Baedke, S.J., Thompson, T.A., Johnston, J.W., and Wilcox, D.A. (2004) "Reconstructing Paleo Lake Levels from Relict Shorelines along the Upper Great Lakes." *Aquatic Ecosystem Health and Management*, Vol. 7, No. 4, p. 1–15.
- Baird, W.F., and Hall, K.R. (1984) "The Design of Breakwaters Using Quarried Stones." *Coastal Engineering Proceedings*, Vol. 19, No. 173, p. 2580–2591.
- Bea, R.G., Xu, T., Stear, J., and Ramos, R. (1999) "Wave Forces on Decks of Offshore Platforms." *Journal of Waterway, Port, Coastal, and Ocean Engineering*. American Society of Civil Engineers. May/June, Vol 125, No. 3, p. 136–144.
- Behrens, J., Terrill, E., Thomas, J.O., and Jensen, R.E. (2018). "CDIP Wave Observations during Hurricanes Irma, Jose, and Maria, And A Nor'easter." *Shore & Beach*, Vol. 86, No. 3, p. 14–20.

- Bendat, J.S., and Piersol, A.G. (2010) *Random Data: Analysis and Measurement Procedures*, 4th Edition, Wiley, 640 pp.
- Bender, M. A., Knutson, T. R., Tuleya, R. E., Sirutis, J. J., Vecchi, G. A., Garner, S. T., and Held, I. M. (2010) "Modeled Impact of Anthropogenic Warming on the Frequency of Intense Atlantic Hurricanes." *Science*, Vol. 327, No. 5964, p. 454–458.
- Berger, M.J., George, D.L., LeVeque, R.J., and Mandli, K.T. (2011) "The GeoClaw Software for Depth–Averaged Flows with Adaptive Refinement." *Advances in Water Resources*, Vol. 34, p. 1195–1206.
- Bernard, E.N. and the Tsunami Hazard Mitigation Federal/State Working Group (1996) "Tsunami Hazard Mitigation Plan." A report to the Senate Appropriations Committee, NOAA report, 28 pp.
- Bloetscher, F. and Romah, T. (2015) "Tools for assessing sea level rise vulnerability." *Journal of Water and Climate Change*, Vol. 6, No. 2, p. 181–190.
- Blumberg, A. F., Georgas, N., Yin, L., Herrington, T. O., and Orton, P. M. (2015) "Street–Scale Modeling of Storm Surge Inundation along the New Jersey Hudson River Waterfront." *Journal of Atmospheric and Oceanic Technology*, Vol. 32, No. 8, p. 1486–1497.
- Bodge, K.R. (1998) "Beach Fill Stabilization with Tuned Structures: Experience in the Southeastern U.S.A. and Caribbean." *Proceedings of Coastlines, Structures and Breakwaters '98*.
- Booij, N., Ris, R.C., and Holthuijsen, L.H. (1999) "A Third–Generation Wave Model for Coastal Regions, Part I: Model Description and Validation." *Journal of Geophysical Research*. Volume 104, No. C4, p. 7649–7666.
- Boon, J.D., Mitchell, M., Loftis, J.D., and Malmquist, D.M. (2018) "Anthropocene Sea Level Change: A History of Recent Trends Observed in the U.S. East, Gulf, and West Coast regions." *Special Report in Applied Marine Science and Ocean Engineering (SRAMSOE) No. 467*. Virginia Institute of Marine Science, College of William and Mary. 77 pp.
- Bosma, K., E. Douglas, P. Kirshen, S. Miller, K. McArthur, C. Watson (2015) "MassDOT–FHWA Pilot Project Report: Climate Change and Extreme Weather Vulnerability and Adaptation Options for the Central Artery/Tunnel System in Boston, Massachusetts," final report.
- Bosma K. (2016) "Climate Change Prioritization: Cost Effectively Building Resilience Using High Resolution Modeling," *ECO*, September 2016, p. 20–25.
- Bosma, K. (2019) personal communication April 16, 2019.
- Bottin, R.R. Jr., McCormick, J.W., and Chasten, M.A. (1993) "Maryland Guidebook for Marina Owners and Operators on Alternatives Available for the Protection of Small Craft Against Vessel–Generated Waves." Prepared for the Maryland Department of Natural Resources. Coastal Engineering Research Center. Vicksburg, Mississippi. 92 pp.
- Bradner, C., Schumacher, T., Cox, D., and Higgins, C. (2011) "Experimental Setup for a Large–Scale Bridge Superstructure Model subjected to Waves." *Journal of Waterway, Port, Coastal and Ocean Engineering*, Vol. 137, No. 1, p. 3–11.
- Bricker, J.D. and Nakayama, A. (2014) "Contribution of Trapped Air, Deck Superlevation, and Nearby Structures to Bridge Deck Failure During a Tsunami." *Journal of Hydraulic Engineering*, Vol. 140, No. 5.
- Bricker, J.D., Francis, M., Nakayama, A. (2015) "Scour Depths near Coastal Structures due to the 2011 Tohoku Tsunami." *Journal of Hydraulic Research* Vol. 50, No. 6, p. 637–641.

- Bruun, P. (1966) Tidal Inlets and Littoral Drift. Volume 2, Stability of Coastal Inlets. University Book Company. Oslo, Norway. 193 pp.
- Buttolph, A. M., Reed, C. W., Kraus, N. C., Ono, N., Larson, M., Camenen, B., ... and Zundel, A. K. (2006) "Two-Dimensional Depth-Averaged Circulation Model CMS-M2D: Version 3.0, Report 2, Sediment Transport and Morphology Change." Technical Report ERDC/CHL-TR-06-9. Engineer Research and Development Center, Vicksburg, Mississippi.
- California (2018) State of California Sea-Level Rise Guidance: 2018 Update, [http://www.opc.ca.gov/webmaster/ftp/pdf/agenda\\_items/20180314/Item3\\_Exhibit-A\\_OPC\\_SLR\\_Guidance-rd3.pdf](http://www.opc.ca.gov/webmaster/ftp/pdf/agenda_items/20180314/Item3_Exhibit-A_OPC_SLR_Guidance-rd3.pdf) (accessed November 8, 2018)
- Caltrans (2018) "Caltrans Climate Change Vulnerability Assessments: Region 4." <http://www.dot.ca.gov/transplanning/ocp/vulnerability-assessment.html>
- Capozzo, M., Rizzi, A., Cimellaro, I. P., Barbosa, A., and Cox, D. (2017) "Earthquake and Tsunami Resiliency Assessment for a Coastal Community in the Pacific Northwest, USA." Structures Congress 2017, Denver, CO, p. 122–133.
- Carstens, T. (1976) "Seabed scour by currents near platforms." Proceedings of the 3<sup>rd</sup> International Conference on Port and Ocean Engineering under Arctic Conditions, p. 991–1006.
- CERA (2018) "Coastal Emergency Risk Assessment." <https://cera.coastalrisk.live/> (accessed September 12, 2018)
- CGS (2013) "Evaluation and Application of Probabilistic Tsunami Hazard Analysis in California." Crescent City Demonstration Projects and the California Probabilistic Tsunami Hazard Analysis Work Group 2013, California Geological Survey Special Report and National Tsunami Hazard Mitigation Program.
- Chen, C., Beardsley, R. C. and Cowles, G. (2006) "An Unstructured Grid, Finite-Volume Coastal Ocean Model (FVCOM) System. Special Issue entitled 'Advance in Computational Oceanography'", Oceanography, Vol. 19, No. 1, p. 78–89.
- Chen, Q., Wang, L., and Xhao, H. (2009). "Hydrodynamic Investigation of Coastal Bridge Collapse During Hurricane Katrina." Journal of Hydraulic Engineering, Vol. 135, No. 3, p. 175–186.
- Chen, Y.H. and Anderson, B.A. (1987) "Development of a Methodology for Estimating Embankment Damage Due to Flood Overtopping." Simons, Li, and Associates report to FHWA. Report No. FHWA/RD-86/126. March 1989. 219 pp.
- Choate, A., Jaglom, W., Miller, R., Rodehorst, B., Schultz, P. and Snow, C. (2012) "Impacts of Climate Change and Variability on Transportation Systems and Infrastructure: The Gulf Coast Study, Phase 2: Climate Variability and Change in Mobile, Alabama: Final Report, Task 2," FHWA-HEP-12-053, 228 pp., [http://www.fhwa.dot.gov/environment/climate\\_change/adaptation/ongoing\\_and\\_current\\_research/gulf\\_coast\\_study/phase2\\_task2/mobile\\_variability/](http://www.fhwa.dot.gov/environment/climate_change/adaptation/ongoing_and_current_research/gulf_coast_study/phase2_task2/mobile_variability/)
- Chock, G., Robertson, I., Kriebel, D., Francis, M., Nistor, I. (2013) "Tohoku, Japan, Earthquake and Tsunami of 2011: Performance of Structures under Tsunami Loads." ASCE, Reston, VA. 366 pp.
- Chorzepa, M. G., Saeidpour, A., Christian, J. K., and Durham, S. A. (2016) "Hurricane Vulnerability of Coastal Bridges using Multiple Environmental Parameters." International Journal of Safety and Security Engineering, Vol. 6, No. 1, p. 10–18.
- Chow, V.T. (1959) Open Channel Hydraulics, McGraw Hill.

- Church, J. A., Gregory, V., Huybrechts, P., Kuhn, M., Lambeck, K., Nhuan, M.T., and Woodworth, P.L. (2001) "11. Changes in Sea Level." Third Assessment Report, Climate Change 2001: The Scientific Basis, Intergovernmental Panel on Climate Change.
- Church, J.A. and White, N.J. (2006) "20th Century Acceleration in Global Sea-Level Rise," *Geophysical Research Letters*, Vol. 33.
- Church, J.A. and White, N.J. (2011) "Sea-Level Rise from the Late 19th to the Early 21st Century," *Surveys in Geophysics*, Vol. 32, p. 585–602.
- Church, J.A., P.U. Clark, A. Cazenave, J.M. Gregory, S. Jevrejeva, A. Levermann, ....and A.S. Unnikrishnan. (2013) "Sea Level Change." In: *Climate Change 2013: The Physical Science Basis. Contribution of Working Group I to the Fifth Assessment Report of the Intergovernmental Panel on Climate Change* [Stocker, T.F., D. Qin, G.-K. Plattner, M. Tignor, S.K. Allen, J. Boschung, A. Nauels, Y. Xia, V. Bex and P.M. Midgley (eds.)]. Cambridge University Press, Cambridge, United Kingdom and New York, NY, USA.
- Citrus County, Florida (2000) "Citrus County Local Mitigation Strategy", Final Report, March 2000.
- Cleary, J.C., Webb, B.M., Douglass, S.L., Buhring, T., and Steward, E. (2018) "Assessment of Engineering Adaptations to Extreme Events and Climate Change for a Simply Supported Interstate Bridge over a Shallow Estuary: Case Study." *Journal of Bridge Engineering*. 23 pp.
- Clopper, P.E. and Chen, Y. (1988) "Minimizing Embankment Damage During Overtopping Flow." Simons, Li, and Associates report to FHWA. Report No. FHWA/RD-188/181. November 1988. 226 pp.
- Clopper, P.E. (1989) "Hydraulic Stability of Articulated Concrete Block Revetment Systems During Overtopping Flow." Simons, Li, and Associates report to FHWA. Report No. FHWA-RD-89-199. November 1989. 131 pp.
- CNES/LECOS/CLS (2018). Centre National d'Etudes Spatiales' AVISO Website. <https://www.aviso.altimetry.fr/en/data/products/ocean-indicators-products/mean-sea-level.html> (website accessed September 1, 2018)
- Coastal Engineering Research Council (2018) "Coastal Engineering Proceedings," <https://journals.tdl.org/icce/index.php/icce>, accessed December 29, 2019)
- Cooper, N., and Dolan, N. (2012). "Adaptation to Coastal Erosion at Lizard Point, Tyne & Wear, UK." *Proceedings of the Institution of Civil Engineers: Maritime Engineering*, Vol. 165, No. 3, p. 139–146.
- Crowell, M., Leatherman, S.P., and Buckley, M.K. (1991) "Historical Shoreline Change: Error Analysis and Mapping Accuracy." *Journal of Coastal Research*, Vol 7, No. 3, p. 839–852.
- Crowell, M., Douglas, B.C., and Leatherman, S.P. (1997) "On Forecasting Future US Shoreline Positions: A Test of Algorithms." *Journal of Coastal Research*. Vol 13, No. 4, p. 1245–1255.
- Cruz-Castro, O., Edge, B.L., and Douglass, S.L. (2006) "Hurricane Forces Measurements on Bridge Decks." *Proceedings of CoastLab 2006*. 9 pp.
- Cuomo, G., Tirindelli, M., and Allsop, W. (2007) "Wave-in-deck Loads on Exposed Jetties." *Coastal Engineering*, Elsevier, Vol. 54, p. 657–679.
- Dabees, M.A. and Kamphuis, J.W. (1998) "ONELINE, A Numerical Model for Shoreline Change." *Proceedings of the 26th International Conference on Coastal Engineering*, American Society of Civil Engineers, p. 2668–2681.

- Dames and Moore (1980) "Design and Construction Standards for Residential Construction in Tsunami-Prone Areas in Hawaii." Prepared by Dames and Moore for the Federal Emergency Management Agency, Washington, D.C.
- Davis, R.A., Jr. (1994) *The Evolving Coast*. Scientific American Library, New York. 231 pp.
- Davis, R. A., Jr. and FitzGerald, D.M. (2009) *Beaches and Coasts*. Wiley-Blackwell, 432 pp.
- Davis, R.A., Jr. (2014) *Beaches of the Gulf Coast*, Texas A&M, 244 pp.
- Dean, R.G. (1965) "Stream Function Representation of Nonlinear Ocean Waves." *Journal of Geophysical Research*. Vol 70, No. 18, p. 4561-4572
- Dean, R.G. (1973) "Evaluation and Development of Water Wave Theories for Engineering Application," Special Report No. 1, Coastal Engineering Research Center, Waterways Experiment Station, USACE.
- Dean, R.G. (1974) "Compatibility of Borrow Material for Beach Fills." Proceedings from the 14th Coastal Engineering Conference. New York. American Society of Civil Engineers.
- Dean, R.G. and Dalrymple, R.A. (1991) *Water Wave Mechanics for Engineers and Scientists*. Singapore. World Scientific Press. 353 pp.
- Dean, R.G. and Dalrymple, R.A. (2002) *Coastal Processes with Engineering Applications*. Cambridge University Press. Cambridge, UK.
- Dean, R.G. (2002) *Beach Nourishment: Theory and Practice*. Advanced Series on Ocean Engineering – Volume 18. World Scientific, New Jersey. 399 pp.
- Dean, R.G. and Walton, T.L. (2018) "Wave Setup," Chapter 2 of *Handbook of Coastal and Ocean Engineering*, Y. Kim (ed.), World Scientific Publishing Co., Singapore, pp. 21-43.
- DeConto, R. M., and D. Pollard (2016) "Contribution of Antarctica to past and future sea-level rise." *Nature*, 531(7596), p. 591-597.
- Demirel, H., Kompil, M., and Nemry, F. (2015). "A framework to analyze the vulnerability of European road networks due to Sea-Level Rise (SLR) and sea storm surges." *Transportation Research Part A: Policy and Practice*, 81, p. 62-76.
- Denson, K.H. (1978) "Wave Forces on Causeway-Type Coastal Bridges." Water Resources Research Institute, Mississippi State University. 42 pp.
- Denson, K.H. (1980) "Wave Forces on Causeway-Type Coastal Bridges: Effects of Angle of Wave Incidence and Cross-Section Shape." Water Resources Research Institute, Mississippi State University. 242 pp.
- Dey, S., Sumer, B.M., Fredsoe, J. (2006) "Control of scour at vertical circular piles under waves and currents." *Journal of Hydraulic Engineering* Vol. 132, No. 3, p. 270-279.
- Dietrich, J. C., Zijlema, M., Westerink, J. J., Holthuijsen, L. H., Dawson, C., Luettich Jr, R. A., and Stone, G. W. (2011). "Modeling Hurricane Waves and Storm Surge Using Integrally-Coupled, Scalable Computations." *Coastal Engineering*, Vol. 58, No. 1, p. 45-65.
- Dompe, P. E., McBee, J. M., and Demir, H. (2015) "Storm surge and wave vulnerability assessment of coastal bridges." *World Environmental and Water Resources Congress 2015: Floods, Droughts, and Ecosystems*, Austin, TX, p. 1256-1263.
- Douglas, B. C., (1992) "Global Sea Level Acceleration." *Journal of Geophysical Research*, Vol. 97, No. C8, p. 12699-12706.

- Douglas, E.M. (2015) "MassDOT–FHWA Pilot Project: Climate Change and Extreme Weather Vulnerability Assessment and Adaptation Options for the Central Artery/Tunnel, Boston, Massachusetts," presentation at the First International Conference on Surface Transportation System Resilience to Climate Change and Extreme Weather Events, Washington, D.C., September 16–18, 2015.
- Douglas, E. M., P. Kirshen, K. Bosma, C. Watson, S. Miller and K. McArthur (2016) "Assessing the Vulnerability of Boston's Central Artery/Tunnel System to Sea Level Rise and Increased Coastal Flooding," *Journal of Extreme Events*, Vol. 3, No. 4, 1650013, <https://doi.org/10.1142/S2345737616500135>
- Douglass, S.L. and Weggel, J.R. (1988) "Laboratory Experiments of the Influence of Wind on Nearshore Wave Breaking," *Proceedings of the 21<sup>st</sup> International Conference on Coastal Engineering*, p. 632–643.
- Douglass, S.L. (2002) *Saving America's Beaches: The Causes of and Solutions to Beach Erosion*, World Scientific Publishing Co., River Edge, New Jersey, 101 pp.
- Douglass, S.L., Bobe, A., and Chen, Q. (2003) "The Amount of Sand Removed from America's Beaches by Engineering Works," *Proceedings of Coastal Sediments '03 Conference (CD-ROM)*. American Society of Civil Engineers.
- Douglass, S.L., Hughes, S.A., Rogers, S. and Chen Q. (2004) "The Impact of Hurricane Ivan on the Coastal Roads of Florida and Alabama: A Preliminary Report," *University of South Alabama Report*, 19 pp.
- Douglass, S.L. (2005) "ASCE–COPRI: Hurricane Katrina Damage Assessment Team: Mississippi/Alabama Coast," presentation to opening session, 2005 Civil Engineering Conference, Los Angeles, CA, October 27, 2005
- Douglass, S.L., Lindstrom, J., Richards, J.M., and Shaw, J. (2005) "An Estimate of the Extent of US Coastal Highways." Presentation to the AFB06 Committee of the Transportation Research Board.
- Douglass, S.L., Chen, Q., Olsen, J.M., Edge, B.L., and Brown, D. (2006a) "Wave Forces on Bridge Decks." report by the Coastal Transportation Engineering Research and Education Center of the University of South Alabama to FHWA. Washington D.C. 74 pp.
- Douglass, S.L., Edge, B. Keith, P., McNeill, L., Reid, C., and Mobley, C. (2006b) "Laboratory Experiment of How Wave Damage Bridges," video at <https://www.youtube.com/watch?v=eMHvtZiOzdE>, (accessed April 22, 2019).
- Douglass, S.L., McNeill, L.P., and Edge, B. (2007) "Wave Loads on US Highway Bridges," *Proceedings of the Coastal Structures '07 International Conference*, Venice, Italy, World Scientific Press, July 2, 2007.
- Douglass, S.L. and Krolak, J. (2008) "Highways in the Coastal Environment," *FHWA Hydraulic Engineering Circular No. 25*, 2nd edition, FHWA–NHI–07–096, 246 pp.
- Douglass, S.L. (2010) "Analyzing the Risk of Coastal Storm Flooding of the I–10 Tunnel in Mobile, Alabama," presentation at the FHWA National Hydraulic Engineering Conference, Park City, Utah.
- Douglass, S.L., Webb, B.M., and Kilgore, R. (2014) "Highways in the Coastal Environment: Assessing Extreme Events," *FHWA Hydraulic Engineering Circular No. 25*, Volume 2, FHWA–NHI–14–006, 147 pp.

- Eckert, J.W. (1983) "Design of toe protection for coastal structures". Proceedings of Coastal Structures 1983, ASCE, Reston, VA, p. 331–341.
- El Ghamry, O.A. (1963) "Wave Forces on a Dock, Hydraulic Engineering Laboratory." Institute of Engineering Research Technical Report HEL–9–1. University of California, Berkeley, California. 206 pp.
- EurOtop (2007) "Wave Overtopping of Sea Defences and Related Structures: Assessment Manual," 201 pp.
- EurOtop (2016) "Manual on Wave Overtopping of Sea Defences and Related Structures. An Overtopping Manual Largely Based on European Research," [www.overtopping-manual.com](http://www.overtopping-manual.com) (accessed September 27, 2018).
- Ewing, L. (2018) "Sea Level Rise: "Major Implications to Coastal Engineering and Coastal Management," in Kim, Y.C. (ed.) Handbook of Coastal and Ocean Engineering, World Scientific, p. 1479–1503.
- Fakhrudin, S. H. M., Babel, M. S., and Kawasaki, A. (2015) "Assessing the vulnerability of infrastructure to climate change on the Islands of Samoa." Natural Hazards and Earth System Sciences, Vol. 15, No. 6, p. 1343–1356.
- FDOT (2005) "Bridge Scour Manual." Office of Design, Drainage Section, Florida Department of Transportation, Tallahassee, FL. May 2005. 129 pp.
- FDOT (2012) "Drainage Handbook: Bridge Hydraulics." Office of Design, Drainage Section, Florida Department of Transportation, Tallahassee, FL. July 2012. 220 pp.
- FEMA (2003) "Guidelines and Specifications for Flood Hazard Mapping Partners."
- FEMA (2005) "Coastal Flood Hazard Analysis and Mapping for the Pacific Coast of the United States," Final Draft Guidelines, 334 pp.
- FEMA (2006) "Final Coastal and Riverine High Water Mark Collection for Hurricane Katrina in Mississippi," FEMA–1604–DR–MS, Task Orders 413 and 420, prepared by URS, March 14, 2006.
- FEMA (2007) CHAMP: Coastal Hazard Analysis Modeling Program: User's Manual, Version 2.0.
- FEMA (2008) "Guidance for Coastal Flood Hazard Analyses and Mapping in Sheltered Waters." Technical Memorandum. February 2008. Washington D.C.
- FEMA (2011a) "Two Coastal Flood Inundation Maps – Which Should I Use?" December, 5 pp. (see [https://www.fema.gov/media-library-data/1508774636839-7ae4bd0c74316ac37ef5ca80a4441fd8/SSIMs\\_vs\\_FIRMs\\_Comparison\\_and\\_Overview.pdf](https://www.fema.gov/media-library-data/1508774636839-7ae4bd0c74316ac37ef5ca80a4441fd8/SSIMs_vs_FIRMs_Comparison_and_Overview.pdf))
- FEMA (2011b) "Coastal Construction Manual: Principles and Practices of Planning, Siting, Designing, Constructing and Maintaining Residential Buildings in Coastal Areas." (Fourth Edition) FEMA P–55, 2 vol.
- FEMA (2012) "Guidelines for Design of Structures for Vertical Evacuation from Tsunamis," 2<sup>nd</sup> Ed. Federal Emergency Management Agency Report P–646, April. 194 pp.
- FEMA (2014) FEMA Great Lakes Coastal Guidelines: Appendix D.3 Update. January 2014 (see <https://www.fema.gov/media-library/assets/documents/130318>).
- FHWA (2002) "HDS–2: Highway Hydrology." Report No. FHWA–NHI–02–001. Washington, D.C.

- FHWA (2005/2007), Office of Bridge Technology, Potential Vulnerability of National Bridge Inventory to Coastal Storms. Unpublished analyses to support Congressional information requests and testimony.
- FHWA (2010) "Record of Decision for NC 12 Replacement of Herbert C. Bonner Bridge," December 2010.
- FHWA (2012a) "Highway Hydraulics State of Practices Report; 50 States and Puerto Rico," January 2012. Washington, D.C.
- FHWA (2012b) Solicitation for Pilot Projects: Climate Change and Extreme Weather Vulnerability Assessments and Adaptation Options Analyses, November 16, 2012.
- FHWA (2014) "Standard Specifications for the Construction of Roads and Bridges on Federal Highway Projects," FP-14, 762 pp.
- FHWA (2017a) "Sea Level Rise and Storm Surge Impacts on a Coastal Bridge: I-10 Bayway, Mobile Bay, Alabama." Report No. FHWA-HEP-17-014. Washington, D.C.
- FHWA (2017b) "Barrier Island Roadway Overwashing from Sea Level Rise and Storm Surge: US 98 on Okaloosa Island, Florida." Report No. FHWA-HEP-17-015. Washington, D.C.
- FHWA (2017c) "Living Shoreline along Coastal Roadways Exposed to Sea Level Rise: Shore Road in Brookhaven, New York." Report No. FHWA-HEP-17-016. Washington, D.C.
- FHWA (2017d) "Vulnerability Assessment and Adaptation Framework, 3<sup>rd</sup> ed." FHWA-HEP-18-020. Washington, D.C.
- FHWA (2019b) "J. Sterling Jones Hydraulics Research Laboratory Overview," FHWA website (accessed April 17, 2019) <https://cms7.fhwa.dot.gov/research/laboratories/hydraulics-research-laboratory/j-sterling-jones-hydraulics-research-laboratory-overview>
- FHWA (2019b) "Hydraulic Considerations for Shallow Abutment Foundations." Report No. FHWA-HIF-19-007. Washington, D.C.
- Filosa, G., Stahl, L., Miller, S., and McArthur, K. (2016) "Keeping climate impacts at bay in Boston." *Public Roads*, Vol. 80, No. 3.
- First Street Foundation (2019) "Defining America's Flood Risk,"
- FitzGerald, D.M., Fenster, M.S., Argow, B.A., and Buynevitch, I.V. (2008), "Coastal Impacts Due to Sea-Level Rise." *Annual Review of Earth and Planetary Sciences*, Vol. 36, p. 601-647.
- Fletcher, C. (2013) *Climate Change: What the Science Tells Us*, John Wiley & Sons, 265 pp.
- Francis, M.J. (2006) "Tsunami Inundation Scour of Roadways, Bridges and Foundations: Observations and Technical Guidance from the Great Sumatra Andaman Tsunami." EERI/FEMA NEHRP Professional Fellowship Report. 53 pp.
- French, J.A. (1970) "Wave Uplift Pressures on Horizontal Platforms." *Proceedings of the Civil Engineering in the Oceans Conference*, American Society of Civil Engineers, p. 187-202.
- Geist, E.L., and Parsons, T. (2006) "Probabilistic Analysis of Tsunami Hazards." *Natural Hazards*, Vol. 37, p. 277-314.
- Gelfenbaum, G., Lesser, G., Jaffe, B., Moore, A., Ruggiero, P. and Morton, R. (2006) "Modeling Tsunami Erosion and Deposition." *EOS, Transactions, American Geophysical Union*, Vol. 87, No. 36.
- Gelfenbaum, G., Vatvani, D., Jaffe, B. and Dekker, F. (2007) "Tsunami Inundation and Sediment Transport in Vicinity of Coastal Mangrove Forest." In: *Proceedings Sixth International*

Symposium on Coastal Engineering and Science of Coastal Sediment Processes, May, p. 1117–1128.

Gesch, D. B., Gutierrez, B. T. and Gill, S. K. (2009) "Coastal Elevations. Coastal Sensitivity to Sea-Level Rise: A Focus on the Mid-Atlantic Region." A report by the U.S. Climate Change Science Program and the Subcommittee on Global Change Research. [J.G. Titus (coordinating lead author), K.E. Anderson, D.R. Cahoon, D.B. Gesch, S.K. Gill, B.T. Gutierrez, E.R. Thieler and S.J. Williams (lead authors)]. U.S. Environmental Protection Agency, Washington DC, p. 25–42.

Gidaris, I., Padgett, J. E., Barbosa, A. R., Chen, S., Cox, D., Webb, B., and Cerato, A. (2017) "Multiple-Hazard Fragility and Restoration Models of Highway Bridges for Regional Risk and Resilience Assessment in the United States: State-of-the-Art Review." *Journal of Structural Engineering*, Vol. 143, No. 3, 04016188.

Gill, S. K., Wright, R., Titus, J. G., Kafalenos, R. S. and Wright, K. (2009) "Population, Land Use and Infrastructure." Coastal Sensitivity to Sea-Level Rise: A Focus on the Mid-Atlantic Region. A report by the U.S. Climate Change Science Program and the Subcommittee on Global Change Research. [J.G. Titus (coordinating lead author), K.E. Anderson, D.R. Cahoon, D.B. Gesch, S.K. Gill, B.T. Gutierrez, E.R. Thieler and S.J. Williams (lead authors)]. U.S. Environmental Protection Agency, Washington DC, p. 105–116.

Glahn, B., Taylor, A., Kurkowski, N. and Shaffer, W. A. (2009) "The Role of the SLOSH Model in National Weather Service Storm Surge Forecasting." *National Weather Digest*, Vol. 33, No. 1, p. 3–14.

Glasser, T., and Gosselin, M. (2006) "Coastal Contraction Scour Study of Jensen Beach Blvd. Bridge." Florida DOT 2006 Design Conference, Session 21.

Goda, Y. (1985). *Random Seas and Design of Maritime Structures*. University of Tokyo Press.

Gonzalez, F.I., Sherrod, B.L., Atwater, B.F., Frankel, A.P., Palmer, S.P., Holmes, M.L., Karlin, R.E., Jaffe, B.E., Titov, V.V., Mofjeld, H.O., and Venturato, A.J. (2003) "Puget Sound Tsunami Sources—2002 Workshop Report." A contribution to the Inundation Mapping Project of the U.S. National Tsunami Hazard Mitigation Program, NOAA/OAR/PMEL, 34 pp.

Gonzalez, F.I., Geist, E.L., Jaffe, B., Kanoglu, U. Nofjeld, H., Synolakis, C.E. (2009) "Probabilistic tsunami hazard assessment at Seaside, Oregon, for near-and far-fields seismic sources." *Journal of Geophysical Research— Oceans*, Vol. 114, No. 11, January 2009.

Good, J. (2018) "From the archives: 'No-name storm' blasted Tampa Bay 25 years ago," *Tampa Bay Times*, March 14, [https://www.tampabay.com/weather/From-the-archives-No-name-storm-blasted-Tampa-Bay-25-years-ago\\_166365944](https://www.tampabay.com/weather/From-the-archives-No-name-storm-blasted-Tampa-Bay-25-years-ago_166365944) (accessed October 10, 2018)

Google (2019) GoogleEarth, <https://www.google.com/earth>

Google (2020) GoogleEarth, <https://www.google.com/earth>

Gosselin, M.S. and Sheppard, D.M. (1998) "A Review of the Time of Local Scour Research." *Stream Stability and Scour at Highway Bridge – Compendium*, E.V. Richardson and P.F. Lagasse, eds., American Society of Civil Engineers. 1040 pp.

Griggs, G. (2011) "Our Ocean Backyard: Tsunami Rocked Alaska's Lituya Bay in 1958." *The Santa Cruz Sentinel*, April 9, 2011. Accessed May 10, 2019. <https://www.santacruzsentinel.com/2011/04/09/gary-griggs-our-ocean-backyard-tsunami-rocked-alaskas-lituya-bay-in-1958/>

- Gronewold, A.D., Clites, A.H., Bruxer, J., Kompoltowicz, K.W., Smith, J.P., Hunter, T.S., and Wong, C. (2015) "Water Levels Surge on Great Lakes," *Eos Earth & Space Science News*, Vol. 96, No. 6.
- Group, The WAMDI (1988) "The WAM Model – A Third Generation Ocean Wave Prediction Model." *Journal of Physical Oceanography*, Vol. 18, No. 12, p. 1775–1810.
- Guo, A., Fang, Q., Bai, X., and Li, H. (2015) "Hydrodynamic Experiment of the Wave Force Acting on the Superstructures of Coastal Bridges," *Journal of Bridge Engineering*, ASCE, Vol. 20, No. 12, DOI: 10.1061/(ASCE)BE.1943-5592.0000758.
- Hagen, S. C. and Bacopoulos, P. (2012) "Coastal Flooding in Florida's Big Bend Region with Application to Sea Level Rise based on Synthetic Storms Analysis." *Terrestrial, Atmospheric & Oceanic Sciences*, Vol. 23, No. 5, p. 481–500, DOI: 10.3319/TAO.2012.04.17.01.
- Hall, J.A., Gill, S., Obeysekera, J., Sweet, W., Knuuti, K., and Marburger, J. (2016) "Regional Sea Level Scenarios for Coastal Risk Management: Managing the Uncertainty of Future Sea Level Change and Extreme Water Levels for Department of Defense Coastal Sites Worldwide." US Department of Defense, Strategic Environmental Research and Development Program.
- Hallermeier, R.J. and Rhodes, P.E. (1988) "Generic Treatment of Dune Erosion for a 100-Year Event." *Proceedings of the 21st International Conference on Coastal Engineering*. American Society of Civil Engineers, p. 1197–1211.
- Hamlington, B.D., Leben, R.R., Nerem, R.S., Han, W. & Kim, K.-Y. (2011) "Reconstructing Sea Level using Cyclostationary Empirical Orthogonal Functions." *Journal of Geophysical Research*, Vol. 116, C12015, 17 pp.
- Hampton, M.A., Griggs, G.B., Edil, T.B., Guy, D.E., Kelley, J.T., Komar, P.D., Mickelson, D.M., and Shipman, H.M. (1999) "Processes That Govern the Formation and Evolution of Coastal Cliffs" in "Formation, Evolution, and Stability of Coastal Cliffs – Status and Trends," USGS Professional Paper 1693.
- Han, Y., Christopher Zegras, P., Rocco, V., Dowd, M., and Murga, M. (2017) "When the Tides Come, Where Will We Go?: Modeling the Impacts of Sea Level Rise on the Greater Boston, Massachusetts, Transport and Land Use System." *Transportation Research Record*, 2653, p. 54–64.
- Hanson, H. and Kraus, N.C. (1989) "GENESIS: Generalized Model for Simulating Shoreline Change." Technical Report CERC-89-19. US Army Engineer Waterways Experiment Station, Vicksburg, Mississippi. 247 pp.
- Hardaway, C.S. Jr. and Gunn, J.R. (2000) "Shoreline Protection: Design Guidelines for Pocket Beaches in Chesapeake Bay, USA." *Carbonate Beaches 2000*, Proceedings from the First International Symposium on Carbonate Sand Beaches. American Society of Civil Engineers, p. 126–139.
- Hasselmann, D.E., Dunckel, M., and Ewing, J. A. (1980) "Directional Wave Spectra Observed During Jonswap 1973." *Journal of Physical Oceanography*. Vol. 10, p. 1264–1280.
- Hayatdavoodi, M., Seiffert, B. and Ertekin, R.C. (2015) "Experiments and Calculations of Cnoidal Wave Loads on a Flat Plate in Shallow-Water," *Journal of Ocean Engineering and Marine Energy* Vol. 1, No. 1, p. 77–99. <https://doi.org/10.1007/s40722-014-0007-x> (accessed April 22, 2019)
- Hayatdavoodi, M., and Ertekin, R.C. (2016) "Review of Wave Loads on Coastal Bridge Decks," *Applied Mechanics Reviews*, ASME, May 2016, Vol. 68 / 030802-1.

- Hayatdavoodi, M., Treichel, K., and Ertekin, R. (2019) "Parametric Study of Nonlinear Wave Loads on Submerged Decks in Shallow Water." *Journal of Fluids and Structures*, Vol. 86, p. 266–289.
- Hayhoe, K., VanDorn, J., Croley, T., Schlegal, N., and Wuebbles, D. (2010) "Regional Climate Change Projections for Chicago and the US Great Lakes." *Journal of Great Lakes Research*, Vol. 36, No. 2, p. 7–21.
- Herbich, J.B. (2000) *Handbook of Coastal Engineering*. McGraw–Hill Handbook. New York, 1152 pp.
- Ho, F.P. and Myers, V.A. (1975) "Joint Probability Method of Tide Frequency Analysis applied to Apalachicola Bay and St. George Sound, Florida", NOAA Tech. Rep. WS 18, 43 pp.
- Hoffmans, G.J.C.M, and Verheij, H.J. (1997) *Scour Manual*. A.A. Balkema, Rotterdam, The Netherlands.
- Holland, G. J., (1980) "An Analytic Model of the Wind and Pressure Profiles in Hurricanes." *Monthly Weather Review*, Vol. 108, No. 8, August, p. 1212–1218. (see [https://doi.org/10.1175/1520-0493\(1980\)108%3C1212:AAMOTW%3E2.0.CO;2](https://doi.org/10.1175/1520-0493(1980)108%3C1212:AAMOTW%3E2.0.CO;2))
- Houston, J. R. and Dean, R. G. (2011) "Sea–Level Acceleration Based on US Tide Gages and Extensions of Previous Global–Gage Analyses." *Journal of Coastal Research*, Vol. 27, No. 3, p. 409–417. (see <https://www.jcronline.org/doi/abs/10.2112/JCOASTRES-D-10-00157.1>)
- Houston, J.R. (2013) "Global Sea Level Projections to 2100 Using Methodology of the Intergovernmental Panel on Climate Change." *Journal of Waterway, Port, Coastal, and Ocean Engineering*, Vol. 139, No. 2, p. 82–87.
- Houston, J.R. and Dean, R.G. (2013) "Beach Nourishment Provides a Legacy for Future Generations," *Shore & Beach*, Vol. 81, No. 3, p. 3–30.
- Houston, J.R. (2018) "The Economic Value of America's Beaches – a 2018 Update," *Shore & Beach*, Vol. 86, No. 2, p. 3–13.
- Houston, J.R. (2019) "The Fate of Beach Nourishment Sand Placed on the Florida East Coast," *Shore and Beach*, Vol. 87, No.2, p. 3–14.
- Hughes, S.A. (1993) *Physical Models and Laboratory Techniques in Coastal Engineering*. Advanced Series in Ocean Engineering – Volume 7. World Scientific, New Jersey. 568 pp.
- Hughes, S.A., and Fowler, J.E. (1991) "Wave–induced scour prediction at vertical walls." *Proceedings of Coastal Sediments 1991*, ASCE, Reston, VA, p. 1186–1900.
- Hyman, R. C., Potter, J. R., Savonis, M. J., Burkett, V. R. and Tump, J. E. (2008) "1.0 Why Study Climate Change Impacts on Transportation?" *Impacts of Climate Change and Variability on Transportation Systems and Infrastructure: Gulf Coast Study, Phase I. A Report by the U.S. Climate Change Science Program and the Subcommittee on Global Change Research*, Savonis, M., V. Burkett and J. Potter (eds.), Department of Transportation, Washington, D.C.
- ICF (2009) "Literature Review: Climate Change Vulnerability Assessment, Risk Assessment and Adaptation Approaches." Report to FHWA Office of Environment and Planning, July 24, 35 pp. ([http://www.fhwa.dot.gov/environment/climate\\_change/adaptation/resources\\_and\\_publications/vulnerability\\_assessment/index.cfm](http://www.fhwa.dot.gov/environment/climate_change/adaptation/resources_and_publications/vulnerability_assessment/index.cfm)) (accessed May 11, 2019)
- Inman, D.L. and Nordstrom, C.F. (1971) "On the Tectonic and Morphologic Classification of Coasts," *Journal of Geology*, Vol. 79, p. 1–21.
- IPCC (2007) "IPCC Fourth Assessment Report," (see <http://www.ipcc.ch>)

- IPCC (2013) "Working Group 1 Contribution to the IPCC Fifth Assessment Report Climate Change 2013: The Physical Science Basis," 2216 pp. (see <http://www.ipcc.ch>)
- Isaacson, M. and Bhat, S. (1996) "Wave Forces on a Horizontal Plate." *International Journal of Offshore and Polar Engineering*. Vol 6, No. 1, p. 19–26.
- Jackson, C.W., Bush, D.M., and Neal, W.J. (2006) "Gabions: A Poor Design for Shore Hardening: The Puerto Rico Experience," *ICS Proceedings, Journal of Coastal Research, Special Issue No. 39*, p. 852–857.
- Jacobs, J.M., Cattaneo, L., Sweet, W. and Mansfield, T. (2018a) "Recent and Future Outlooks for Nuisance Flooding Impacts on Roadways on the US East Coast," *Transportation Research Record* 2018, Vol. 2672, No. 2, p. 1–10.
- Jacobs, J.M., Culp, M., Cattaneo, L., Chinowsky, P., Choate, A., DesRoches, S., Douglass, S. and Miller, R. (2018b) "Transportation." Chapter 12 in *Impacts, Risks, and Adaptation in the United States: Fourth National Climate Assessment, Volume II* [Reidmiller, D.R., C.W. Avery, D.R. Easterling, K.E. Kunkel, K.L.M. Lewis, T.K. Maycock, and B.C. Stewart (eds.)]. US Global Change Research Program, Washington, D.C., USA, p. 479–511. DOI: 10.7930/NCA4.2018.CH
- Jelesnianski, C. P., Chen, J., and Shaffer, W.A. (1992) "SLOSH– Sea, Lake and Overland Surges from Hurricanes." US Department of Commerce, NOAA Tech. Report NWS 48, 71 pp.
- Johnson, B. D., Gravens, M. B., Kobayashi, N. (2012) "Cross–Shore numerical model CSHORE for waves, currents, sediment transport and beach profile evolution." Vicksburg, Miss: US Army Engineer Research and Development Center, Coastal and Hydraulics Laboratory.
- Johnson, B., Heath, R. E., Hsieh, H. H., Kim, K. W. and Butler, H. L. (1991) "Development and Verification of a Three–Dimensional Numerical Hydrodynamic, Salinity and Temperature Model of Chesapeake Bay; Volume I, Main Text and Appendix D." Technical Report HL–91–7, US Army Engineer Waterways Experiment Station, Vicksburg, Mississippi.
- Jones, B.M., Hinkel, K.M., Arp, C.D., and Eisner, W.R. (2008) "Modern erosion rates and loss of coastal features and sites, Beaufort Sea coastline, Alaska." *Arctic*, Vol. 61, No. 4, p. 361–372.
- JPL (2013) Jet Propulsion Laboratory website on Ocean Surface Topography from Space, accessed September 6, 2013. (see <http://sealevel.jpl.nasa.gov/>)
- Kafalenos, R. S., Leonard, K.J., Beagan, D.M., Burkett, V.R., Keim, B.D, Meyers, A., Hunt, D.T., Hyman, R.C., Maynard, M.K., Fritsche, B., Henk, R.H., Seymour, E.J., Olson, L.E., Potter, J.R., and Savonis, M. J. (2008) "What are the Implications of Climate Change and Variability for Gulf Coast Transportation?" In: *Impacts of Climate Change and Variability on Transportation Systems and Infrastructure: Gulf Coast Study, Phase I. A Report by the U.S. Climate Change Science Program and the Subcommittee on Global Change Research* [Savonis, M. J., V.R. Burkett, and J.R. Potter (eds.)]. US Department of Transportation, Washington, D.C., USA.
- Kamphuis, J.W. (2010) *Introduction to Coastal Engineering and Management*, 2<sup>nd</sup> ed., Advanced Series on Ocean Engineering, Vol. 30, World Scientific Press.
- Kaplan, P., Murray, J.J., and Yu, W.C. (1995) "Theoretical Analysis of Wave Impact Forces on Platform Deck Structure." *Proceedings of the 14th International Conference on Offshore Mechanics and Arctic Engineering*. American Society of Mechanical Engineers, Volume 1–A, p. 189–198.
- Kawashima, K. and Buckle, I. (2013) Structural Performance of Bridges in the Tohoku-Oki Earthquake. *Earthquake Spectra*, Vol. 29, No. 1, p. 315–338.

- Keenan, J.M., Hill, T. and Gumber, A. (2018) "Climate gentrification: from theory to empiricism in Miami–Dade County, Florida," *Environmental Research Letters*, Vol. 13, No. 5, <https://doi.org/10.1088/1748-9326/aabb32>.
- Khalfin, I.S. (2007) Modeling and calculation of bed scour around large–diameter vertical cylinder under wave action. *Water Resources* Vol. 34, No. 1, p. 49–59.
- Kilgore, R.T., Herrmann, G., Thomas, W.O., and Thompson D.B. (2016) "HEC–17: Highways in the River Environment." 2nd Edition. Report No. FHWA–HIF–16–018. Washington, D.C.
- Kilgore, R., Thomas, W., Douglass, S., Webb, B., Hayhoe, K., Stoner, A., Jacobs, J., Thompson, D., Herrmann, G., Douglas, E., and Anderson, C. (2019a) "Applying Climate Change Information to Hydrologic and Coastal Design of Transportation Infrastructure – Final Report." NCHRP 15–61, submitted to The National Cooperative Highway Research Program, March 22, 2019, 384 pp. (preliminary, unedited version)
- Kilgore, R., Thomas, W., Douglass, S., Webb, B., Hayhoe, K., Stoner, A., Jacobs, J., Thompson, D., Herrmann, G., Douglas, E., and Anderson, C. (2019b) "Applying Climate Change Information to Hydrologic and Coastal Design of Transportation Infrastructure – Design Practices." NCHRP 15–61, submitted to The National Cooperative Highway Research Program, March 22, 2019, 154 pp. (preliminary, unedited version)
- Kim, K., Pant, P., and Yamashita, E. (2015) "Evacuation planning for plausible worst case inundation scenarios in Honolulu, Hawaii." *Journal of Emergency Management*, Vol. 13, No. 2, p. 93–108.
- Kim, K.–H., Yoo, H.–S., and Kobayashi, N. (2011) "Mitigation of beach erosion after coastal road construction." *Journal of Coastal Research*, Vol. 27, No. 4, p. 645–651.
- Kim, S. C., Chen, J. and Shaffer, W. A. (1996) "An Operational Forecast Model for Extratropical Storm Surges along the US East Coast." In: Preprints, Conf. on Oceanic and Atmospheric Prediction, Atlanta, GA, American Meteorology Society, January, p. 281–286.
- Kim, Y., ed. (2018) *Handbook of Coastal and Ocean Engineering*, World Scientific Press, 1192 pp.
- Kirby, J.T. and Dalrymple, R.A. (1983) "A Parabolic Equation for the Combined Refraction–Diffraction of Stokes Waves by Mildly Varying Topography." *Journal of Fluid Mechanics*. Vol. 136, p. 453–466.
- Klerk, W. J., Winsemius, H. C., van Verseveld, W. J., Bakker, A. M. R., and Diermanse, F. L. M. (2015) "The co–incidence of storm surges and extreme discharges within the Rhine–Meuse Delta." *Environmental Research Letters*, Vol. 10, No. 3, 035005, 9 pp.
- Knott, J. F., Elshaer, M., Daniel, J. S., Jacobs, J. M., and Kirshen, P. (2017) "Assessing the effects of rising groundwater from sea level rise on the service life of pavements in coastal road infrastructure." *Transportation Research Record*, 2639, p. 1–10.
- Knutson, T.R. and Tuleya, R.E. (2004) "Impact of CO<sub>2</sub>–Induced Warming on Simulated Hurricane Intensity and Precipitation: Sensitivity to the Choice of Climate Model and Convective Parameterization." *Journal of Climate*, Vol. 17, No. 18, p. 3477–3495.
- Knutson, T. R., Sirutis, J. J., Garner, S. T., Held, I. M., and Tuleya, R. E. (2007) "Simulation of the Recent Multidecadal Increase of Atlantic Hurricane Activity Using an 18–km–Grid Regional Model." *Bulletin of the American Meteorological Society*, Vol. 88, No.10, p. 1549–1565.
- Knutson T. R., McBride J. L., Chan J., Emanuel, K., Holland, G., Landsea, C., Held, I., Kossin, J. P., Srivastava, A. K. and Sugi, M. (2010) "Tropical Cyclones and Climate Change." *Nature*

- Geoscience, Vol. 3, p. 157–163 (see <http://www.nature.com/ngeo/journal/v3/n3/full/ngeo779.html>)
- Komar, P.D. (1998) *Beach Processes and Sedimentation*. Second Edition. Prentice Hall. Englewood Cliffs, New Jersey. 544 pp.
- Komen, G.J., Cavaleri, L., Donelan, M., Hasselmann, K., Hasselmann, S., and Janssen, P.A.E.M. (1994) *Dynamics and Modelling of Ocean Waves*. Cambridge University Press. 532 pp.
- Kopp, R. E., Horton, R. M., Little, C. M., Mitrovica, J. X., Oppenheimer, M., Rasmussen, D. J., Strauss, B. H. and Tebaldi, C. (2014) “Probabilistic 21st and 22nd century sea-level projections at a global network of tide-gauge sites.” *Earth's Future*, Vol. 2, No. 8, p. 383–406.
- Kopp, R.E., DeConto, R.M., Bader, D.A., Hay, C.C, Horton, R.M, Kulp, S. ...Strauss, B.H. (2017) “Evolving Understanding of Antarctic Ice-Sheet Physics and Ambiguity in Probabilistic Sea-Level Projections,” *AGU Publications, Earth's Future*, Vol. 5, No. 12, p. 1217–1233, <https://doi.org/10.1002/2017EF000663>.
- Kriebel, D.L. and Dean, R. G. (1985) “Numerical simulation of time-dependent beach and dune erosion.” *Coastal Engineering*. Vol. 9, No. 3, p. 221–245. 10.1016/0378-3839(85)90009-2.
- Kriebel, D.L. (1986) “Verification Study of a dune erosion model.” *Shore & Beach*, Vol. 54, No. 3, p. 13–21.
- Kriebel, D.L., Seelig, W., and Judge, C. (2003) “A Unified Description of Ship-Generated Waves.” *Proceedings of the PIANC Passing Vessel Workshop*. Portland, Oregon.
- Kriebel, D.L. and Geiman, J.D. (2014). “A coastal flood stage to define existing and future sea-level hazards.” *Journal of Coastal Research*, Vol. 30, No. 5, p. 1017–1024.
- Kriebel, D.L.; Geiman, J.D., and Henderson, G.R. (2015) “Future Flood Frequency under Sea-Level Rise Scenarios.” *Journal of Coastal Research*, Vol. 31, No. 5, p. 1078–1083.
- Krolak, J., and Henderson, D. (2016) “Implementing a Successful Risk-Based, Data-Driven Scour Program.” *Transportation Research Record: Journal of the Transportation Research Board* 2588, Washington, D.C., p. 163–171. DOI: 10.3141/2588-18
- Kriebel D.L., Lynett P.J., Cox, D., Petroff C.M., Robertson, I.N., and Chock, G. (2017). “Energy Method for Approximating Overland Tsunami Flows.” *Journal of Waterway, Port, Coastal, and Ocean Engineering*, Vol. 143, No. 5, 04017014.
- Kriebel, D.L. and Henderson, G. (2018) “Assessing Current and Future Flood Frequency throughout the US Atlantic Coast.” *Presentation and Proceedings of the 36<sup>th</sup> International Conference on Coastal Engineering*, Baltimore, Maryland, (downloaded April 18, 2019) <http://www.eventscribe.com/uploads/eventScribe/PDFs/2018/6889/675881.pdf>
- Kusisto, L. and Campo-Flores, A. (2018) “Rising Sea Levels Reshape Miami’s Housing Market,” *Wall Street Journal*, April 20, 2018, <https://www.wsj.com/articles/climate-fears-reshape-miamis-housing-market-1524225600> (accessed April 19, 2019).
- Kuswandi, T., Triatmadja, R., Istiarto, M. (2017) “Simulation of scouring around a vertical cylinder due to tsunami.” *Journal of Tsunami Society International*, Vol. 36, No. 2, p. 59–69.
- Lagasse, P.F., Clopper, P.E., Pagán-Ortiz, J.E., Zevenbergen, L.W., Arneson, L.A., Schall, J.D., and Girard, L.G. (2009). “HEC-23: Bridge Scour and Stream Instability Countermeasures: Experience, Selection, and Design Guidelines,” 3<sup>rd</sup> ed., FHWA-NHI-09-111 (Vol. 1), FHWA-NHI-09-112 (Vol. 2).

- Lagasse, P.F., Zevenbergen, L.W., Spitz, W.J., and Arneson, L.A. (2012). "HEC-20: Stream Stability at Highway Structures," 4<sup>th</sup> ed., FHWA-HIF-12-004, 328 pp.
- Lambert, J. H., Wu, Y.J., You, H., Clarens, A., and Smith, B. (2013). "Climate Change Influence on Priority Setting for Transportation Infrastructure Assets." *Journal of Infrastructure Systems*, Vol. 19, No. 1, p. 36-46.
- Larson, M. and Kraus, N.C. (1989) SBEACH: Numerical Model for Simulating Storm-Induced Beach Change. Report 1: Empirical Foundation and Model Development. Technical Report CERC-89-9. US Army Engineer Waterways Experiment Station, Vicksburg, Mississippi. 256 pp.
- Larson, M., Kraus, N. C., and Byrnes, M. (1990) "SBEACH: Numerical Model for Simulating Storm-Induced Beach Change. Report 2. Numerical Formulation and Model Tests." Technical Report CERC-89-9. US Army Engineer Waterways Experiment Station, Vicksburg, Mississippi. 120 pp.
- Laursen, E.M. (1960) "Scour at Bridge Crossings." *Journal Hydraulic Division, ASCE*, 86 (HY2).
- Lehrman, J. B., Higgins, C., Cox, D. (2011) "Performance of Highway Bridge Girder Anchorages Under Simulated Hurricane Wave Induced Loads." *Journal of Bridge Engineering*, Vol. 17, No. 2, p. 259-271.
- Leuliette, E.W., Nerum, R.S., and Mitchum, G.T. (2004). "Calibration of TOPEX/Poseidon and Jason Altimeter Data to Construct a Continuous Record of Mean Sea Level Change," *Marine Geology*, Vol. 27, No. 1, p. 79-94.
- Levin, D.R., Lillycrop, W.J., and Alexander, M.P. (1992) "Sand Wave Shoaling in Navigation Channels." USACE Technical Report HL-90-17. 57 pp.
- Li, H., Lin, L. and Burks-Copes, K.A. (2013) "Modeling of Coastal Inundation, Storm Surge and Relative Sea-Level Rise at Naval Station Norfolk, Norfolk, Virginia, U.S.A." *Journal of Coastal Research*, Vol. 29, No. 1, p. 18-30.
- Li, Y., and Huang, L. (1997) "An Experimental Study on the Wave Uplift Force on the Superstructure of Piers." *Harbor Engineering*, Vol. 6, p. 9-13. (In Chinese)
- Lin, L., Demirbilek, Z., Mase, H., Zheng, J. H. and Yamada, F. (2008) "CMS-Wave: A Nearshore Spectral Wave Processes Model for Coastal Inlets and Navigation Projects." Technical Report ERDC/CHL TR-08-13. US Army Engineer Research and Development Center, Vicksburg, Mississippi.
- Liu, P.L. F., Woo, S.B. and Cho, Y.S. (1998) "Computer Programs for Tsunami Propagation and Inundation," Cornell University, Sponsored by National Science Foundation, p. 104.
- Lofgren, B.M., Hunter, T.S., and Wilbarger, J. (2011) "Effects of using air temperature as a proxy for potential evapotranspiration in climate change scenarios of Great Lakes basin hydrology." *Journal of Great Lakes Research*, Vol. 37, No. 4, p. 744-752.
- Longuet-Higgins, M.S. (1952) "The Statistical Distribution of the Heights of Sea Waves." *Journal of Marine Research*. Vol. 11, p. 245-266.
- Lu, Q.-C., and Peng, Z.-R. (2011) "Vulnerability analysis of transportation network under scenarios of sea level rise." *Transportation Research Record*, 2263, p. 174-181.
- Luetlich, R.A., Jr., Westerink, J.J., and Scheffner, N.W. (1992) "ADCIRC: An Advanced Three-Dimensional Model for Shelves, Coasts, and Estuaries." Report 1: Theory and Methodology of ADCIRC-2DDI and ADCIRC-3DL. USACE. Washington, D.C. 137 pp.

- Mackey, S.D. (2012) "Climate Change Impacts and Adaptation Strategies for Great Lakes Nearshore and Coastal Systems," In: Climate Change in the Great Lakes Region. Eds. T. Dietz and D. Bidwell. 269 pp.
- Maruyama, K., Hosoda, A., Tanaka, Y., Kosa, K., Arikawa, T., Mizutani, N. (2017) "Tsunami Force Acting on Bridge Girders." Journal of Japan Society of Civil Engineers, Vol. 5, No. 1, p. 157–169.
- McAlpine, S.A., and Porter, J.R. (2018) "Estimating Recent Local Impact of Sea-Level Rise on Current Real-Estate Losses: A Housing Market Case Study in Miami-Dade, Florida," Population Research and Policy Review 37, p. 871–895, <https://doi.org/10.1007/s11113-018-9473-5>.
- McConnell, K., Allsop, W., and Cruickshank, I. (2004) Piers, Jetties, and Related Structures Exposed to Waves: Guidelines for Hydraulic Loadings. Thomas Telford Press, London. 148 pp.
- McGuigan, K., Webster, T., and Collins, K. (2015) "A Flood Risk Assessment of the LaHave River Watershed, Canada Using GIS Techniques and an Unstructured Grid Combined River-Coastal Hydrodynamic Model." Journal of Marine Science and Engineering, Vol. 3, No. 3, p. 1093–1116.
- McPherson, R.L. (2008) "Hurricane Induced Wave and Surge Forces on Bridge Decks." Master's thesis, Texas A&M University.
- Melby, J.A., Nadal-Caraballo, N.C., Pagán-Albelo, Y., and Ebersole, B. (2012) "Wave Height and Water Level Variability on Lakes Michigan and St. Clair." USACE Engineer Research and Development Center, Vicksburg, MS, ERDC/CHL TR-12-23.
- Melillo, J., Richmond, T. and Yohe, G. (2014) 3<sup>rd</sup> National Climate Assessment.
- Melville, B.W., and Coleman, S.E. (2000). "Bridge Scour," Water Resources Publications, LLC. Highlands Ranch, Colorado.
- Merrifield, M.A., Merrifield, S.T., and Mitchum, G.T. (2009) "An Anomalous Recent Acceleration of Global Sea-Level Rise." Journal of Climate, Vol. 22, p. 5772–5781.
- Mertz, D. and Hayes, M. (2009). "Assessing the Vulnerability of Delaware's Coastal Bridges to Hurricane Forces." Report to University of Delaware UTC, October 1, 2009. <https://rosap.nrl.bts.gov/view/dot/23058>.
- Miller, I.M., Morgan, H., Mauger, G., Newton, T., Weldon, R., Schmidt, D., Welch, M., and Grossman, E. (2018) "Projected Sea Level Rise for Washington State – A 2018 Assessment." A collaboration of Washington Sea Grant, University of Washington Climate Impacts Group, Oregon State University, University of Washington, and USGS prepared for the Washington Coastal Resilience Project.
- Miller, W. (2003) "Model for the Time Rate of Local Sediment Scour at a Cylindrical Structure." Ph.D. dissertation, University of Florida, 244 pp.
- Miselis, J.L. and Lorenzo-Truebas, J. (2017) "Natural and human-induced variability in barrier-island response to sea level rise." Geophysical Research Letters. Vol. 44, No. 33, p. 11922–11931, DOI: 10.1002/2017GL074811.
- Moftakhari, H.R., AghaKouchak, A., Sanders, B.F., Feldman, D. L., Sweet, W., Matthew, R. A., and Luke, A. (2015) "Increased nuisance flooding along the coasts of the United States due to sea level rise: Past and future." Geophysical Research Letters, Vol. 42, No. 22, p. 9846–9852, DOI: 10.1002/2015GL066072.

- Monserrat, S., Vilibic, I., and Rabinovich, A.B. (2006) "Meteotsunamis: Atmospherically Induced Destructive Ocean Waves in the Tsunami Frequency Band," *Natural Hazards and Earth System Sciences*, Vol. 6, p. 1035–1051.
- Moore, L.J., List, J.H., Williams, S.J., and Stolper, D. (2010) "Complexities in barrier island response to sea level rise: Insights from numerical model experiments, North Carolina Outer Banks." *Journal of Geophysical Research*. Vol. 115, No. F03, p. 1–27, DOI:10.1029/2009JF001299.
- Morris, J.T., Sundareshwar, P.V., Nietch, C.T., Kjerfve, B., and Cahoon, D.R. (2002) "Responses of coastal wetlands to rising sea level." *Ecology*, Vol. 83, No. 10, p. 2869–2877.
- Nadal-Caraballo, N.C., Melby, J.A., and Ebersole, B.A. (2012) "Statistical Analysis and Storm Sampling Approach for Lakes Michigan and St. Clair." USACE Engineer Research and Development Center, Vicksburg, MS, ERDC/CHL TR-12-19.
- NAVFAC (1982) Coastal Protection. NAVFAC Design Memorandum No. 26.2. Washington D.C. 314 pp.
- NCDOT (2018) personal communication September 13, 2018.
- Nerem, R., Beckley, B., Fasullo, J., Hamlington, B., Masters, D., and Mitchum, G.T. (2018) "Climate-change-driven accelerated sea-level rise detected in the altimeter era." *Proceedings of the National Academy of Sciences*, Vol. 115, No. 9, p. 2022–2025, 10.1073/pnas.1717312115.
- Neumann, J. E., Price, J., Chinowsky, P., Wright, L., Ludwig, L., Streeter, R., Jones, R., Smith, J. B., Perkins, W., Jantarasami, L., and Martinich, J. (2015). "Climate Change Risks to US Infrastructure: Impacts on Roads, Bridges, Coastal Development, and Urban Drainage." *Climatic Change*, Vol. 131, No. 1, p. 97–109.
- NGS (2018) National Geodetic Survey. <https://www.ngs.noaa.gov/> (October 1, 2018)
- Niederoda, A. W., Resio, D. T., Toro, G. R., Divoky, D., Das, H. S. and Reed, C. W. (2010) "Analysis of the Coastal Mississippi Storm Surge Hazard." *Ocean Engineering*, Vol. 37, No. 1, p. 82–90.
- Nielsen, P. (1992) *Coastal Bottom Boundary Layers and Sediment Transport*. World Scientific. River Edge, NJ, 340 pp.
- Nistor, I, Palermo, D., Nouri, Y., Murty, T., and Saatcioglu, M. (2010) "Tsunami-Induced Forces on Structures," in Kim, Y.C. (ed.), *Handbook of Coastal and Ocean Engineering*, World Scientific, p. 261–286.
- NJTPA (2011) "Climate Change Vulnerability and Risk Assessment of Transportation Infrastructure." New Jersey Transportation Planning Authority. 165 pp.
- NOAA (2013) "Billion-Dollar Weather/Climate Disasters." web-site accessed 08/06/2013, (see <http://www.ncdc.noaa.gov/billions/events>)
- NOAA (2019) "Tides and Currents;" "Sea Levels Online" website, accessed October 2018 (see <http://tidesandcurrents.noaa.gov/sltrends/index.shtml>)
- NOAA. (2012). *Global Sea level Rise Scenarios for the United States National Climate Assessment*. National Oceanic and Atmospheric Administration, Technical Report OAR CPO-1, 33 pp.

- NRC (1987) Responding to Changes in Sea Level: Engineering Implications. National Research Council, The National Academies Press, Washington, D.C., 160 pp. (see <http://www.nap.edu/catalog/1006.html>)
- NRC (1995) Beach Nourishment and Protection. Committee on Beach Nourishment and Protection. National Research Council. National Academy Press, Washington D.C. 334 pp.
- NTHMP (2018). National Tsunami Hazard Mitigation Program. <https://nws.weather.gov/nthmp/index.html>, (accessed October 1, 2018)
- Oahu Metropolitan Planning Organization (2011) "Transportation Asset Climate Change Risk Assessment." Report prepared by SSFM International, 132 pp.
- Oswald, M., and Treat, C. (2013). "Assessing public transportation vulnerability to sea level rise: A case study application." *Journal of Public Transportation*, Vol. 16, No. 3, p. 59–77.
- Overbeek, J., and Klabbers, I.M. (2001) "Design of Jetty Decks for Extreme Vertical Loads." *Proceedings of the Ports 2001 Conference*. American Society of Civil Engineers. 10 pp.
- Padgett, J. E., Spiller, A., and Arnold, C. (2012). "Statistical analysis of coastal bridge vulnerability based on empirical evidence from Hurricane Katrina." *Structure and Infrastructure Engineering*, Vol. 8, No. 6, p. 595–605.
- Parris, A., Bromirski, P., Burkett, V., Cayan, D., Culver, M., Hall, J., Horton, R., Knuuti, K., Moss, R., Obeysekera, J., Sallenger, A. and Weiss, J. (2012) "Global Sea Level Rise Scenarios for the US National Climate Assessment." NOAA Tech Memo OAR CPO–1, 37 pp.
- Perlin, M. and Dean, R.G. (1983) "A Numerical Model to Simulate Sediment Transport in the Vicinity of Coastal Structures." *Miscellaneous Report MR–83–10*. USACE, Coastal Engineering Research Center Report.
- Pilarczyk, K.W., (1999) "Design of Dikes and Revetments—Dutch Practice." *Handbook of Coastal Engineering*, ed. J.B. Herbich. McGraw–Hill, New York, p. 3.1–3.104.
- Poate, Timothy G., Robert T. McCall, and Gerd Masselink. "A New Parameterisation for Runup on Gravel Beaches." *Coastal Engineering*, Vol. 117 (November 1, 2016), p. 176–190. <https://doi.org/10.1016/j.coastaleng.2016.08.003>.
- Pope, J. and Dean, J. (1986) "Development of Design Criteria for Segmented Breakwaters." *Proceedings from the 20th International Coastal Engineering Conference*. American Society of Civil Engineers, p. 2144–2158
- Pullen, T., Allsop, N.W.H., Bruce, T., Kortenhaus, A., Schüttrumpf, H., and van der Meer, J.W. (2007) *EurOtop – Wave Overtopping of Sea Defences and Related Structures: Assessment Manual*, Die Küste – Heft 73.
- Revell, D.L., Battalio, R., Vandever, J., Spear, B., and Ruggiero, P. (2011) "Planning Level Assessment of the Impacts of Sea Level Rise to the California Coast," *Proceedings of Solutions to Coastal Disasters Conf.*, ASCE, p. 522–538.
- Rienecker, M.M. and Fenton, J.D. (1981) "A Fourier Approximation Method for Steady Water Waves." *Journal of Fluid Mechanics*. Vol. 104, p. 119–137.
- Ris, R. C., Holthuijsen, L. H. and Booij, N. (1999) "A Third–Generation Wave Model for Coastal Regions: 2. Verification." *Journal of Geophysical Research*, Vol. 104, No. C4, p. 7667–7681.
- Roberson, J. A., Cassidy, J. J., and Chaudhry, M. H. (1998). *Hydraulic Engineering*. New York: Wiley, 672 pp.

- Robertson, I., Riggs, H.R., Yim, S., and Young, Y.L. (2007) "Lessons from Hurricane Katrina Storm Surge on Bridges and Buildings." *Journal of Waterway, Port, Coastal, and Ocean Engineering*. Vol. 133, No. 6, p. 463–483.
- Robertson, I., Yim, S., and Tran, T. (2011) "Case Study of Concrete Bridge Subjected to Hurricane Storm Surge and Wave Action," *Proceedings of Solutions to Coastal Disasters Conf.*, ASCE, p. 728–739.
- Roelvink D., Reniers, A., van Dongeren, A., van Thiel de Vries, J., McCall, R., Lescinski, J. (2009) "Modelling Storm Impacts on Beaches, Dunes and Barrier Islands." *Coastal Engineering*. Vol. 56, No. 11–12 (November–December 2009), p. 1133–1152.
- Roelvink, D., Boutmy, A., and Stam, J. (1998). "A Simple Method to Predict Long–Term Morphological Change," *Proceedings of the 26<sup>th</sup> International Conference on Coastal Engineering*.
- Salem, H., Mohssen, S., Nishikiori, Y., Hosoda, A. (2016) "Numerical Collapse Analysis of Tsuyagawa Bridge Damaged by Tohoku Tsunami." *Journal of Performance of Constructed Facilities*, Vol. 30, No. 6.
- Sarpkaya, T. and Isaacson, M. (1981) *Mechanics of Wave Forces on Offshore Structures*, van Nostrand Reinhold, New York, 651 pp.
- Sasaki, J., Ito, K., Suzuki, T., Wiyono, R. U. A., Oda, Y., Takayama, Y., Yokota, K., Furuta, A. and Takagi, H. (2012) "Behavior of the 2011 Tohoku Earthquake Tsunami and Resultant Damage in Tokyo Bay." *Coastal Engineering Journal*, Vol. 54, No. 1, 26 pp.
- Savioli, J., Pedersen, C., Szykarski, S., and Kerper, D. (2003) "Modelling the Threat of Tropical Cyclone Storm Tide to the Burdekin Shire, Queensland Australia [online]." In: Kench, Paul S. (Editor); Hume, Terry M (Editor). *Coasts & Ports 2003 Australasian Conference: Proceedings of the 16th Australasian Coastal and Ocean Engineering Conference, the 9th Australasian Port and Harbour Conference and the Annual New Zealand Coastal Society Conference*. Barton, A.C.T.: Institution of Engineers, Australia, 2003, p. 285–292
- Scheffner, N. W., Borgman, L. E., and Mark, D. J. (1996), "Empirical Simulation Technique Based Storm Surge Frequency Analyses," *Journal of Waterways Ports Coasts and Ocean Engineering*. Vol. 122, No. 2, p. 93–101, DOI:10.1061/(ASCE)0733-950X(1996)122:2(93)
- Seiffert, B., Ertekin, R. C., and Robertson, I. N. (2014). "Experimental Investigation on the Role of Entrapped Air on Solitary Wave Forces on a Coastal Bridge Deck." *ASME 2014 33rd International Conference on Ocean, Offshore and Arctic Engineering, OMAE 2014*, San Francisco, CA.
- Seiffert, B., Ertekin, R.C., and Robertson, I.N. (2016) "Effect of Entrapped Air on Solitary Wave Forces on a Coastal Bridge Deck with Girders," *Journal of Bridge Engineering*. Vol. 21, No. 2, 04015036, 14 pp., DOI: 10.1061/(ASCE)BE.1943-5592.0000799
- Sheng, Y. P. (1990). "Evolution of a Three–Dimensional Curvilinear–Grid Hydrodynamic Model for Estuaries, Lakes and Coastal Waters: CH 3 D." IN: *Estuarine and Coastal Modeling*. American Society of Civil Engineers, New York, p. 40–49.
- Sheng, Y. P., Paramygin, V. A., Alymov, V. and Davis, J. R. (2006) "A Real–Time Forecasting System for Hurricane Induced Storm Surge and Coastal Flooding." In: *Estuarine and Coastal Modeling*, American Society of Civil Engineers, October, p. 585–602.
- Sheppard, D.M. (2001). "A Methodology for Predicting Local Scour Depths near Bridge Piers with Complex Geometries," Unpublished design procedure, University of Florida, Gainesville, FL.

- Sheppard, D.M. and Dompe, P. (2013) NCDOT Bride Superstructure Level III Wave Vulnerability Study, FHWA/NC/2010–06, 86 pp.
- Sheppard, D.M. and Miller, W., Jr. (2003) “Design Storm Surge Hydrographs for the Florida Coast.” Final Report to Florida Department of Transportation. 140 pp.
- Sheppard, D.M., and Marin, J. (2009). “Final Report: Wave Loading on Bridge Decks,” FDOT No. BD545–58, UF No. 00056675, Submitted to Florida Department of Transportation Research Office.
- Sheppard, D.M., Zhao, G., and Ontowirjo, B. (1995). “Local Scour Near Single Piles in Steady Currents.” Proceedings of the 1<sup>st</sup> International Conference on Water Resources Engineering, San Antonio, TX.
- Shijo, R., Aoki, K., Hirose, Y., Suzuki, T., and Koshimura, S. (2015) “Influence of Wave Shapes to Tsunami Wave Force Acting on a Bridge Superstructure.” Proceedings of the International Offshore and Polar Engineering Conference, International Society of Offshore and Polar Engineers, p. 830–837.
- Shilling, F. M., Vandever, J., May, K., Gerhard, I., and Bregoff, R. (2016). “Adaptive Planning for Transportation Corridors Threatened by Sea Level Rise.” Transportation Research Record, 2599, p. 9–16.
- Shoji, G., Hiraki, Y., Fujima, K., and Shigihara, Y. (2011) “Evaluation of Tsunami Fluid Force Acting on a Bridge Deck Subjected to Breaker Bores.” Procedia Engineering, p. 1079–1088.
- Silvester, R., and Hsu, J.R.C. (1993) Coastal Stabilization. Prentice Hall, Englewood Cliffs, New Jersey. 578 pp.
- Smallegan, S.M., Irish, J.L., Van Dongeren, A.R., and Den Bieman, J.P. (2016) “Morphological Response of a Sandy Barrier Island with a Buried Seawall during Hurricane Sandy.” Coastal Engineering, Vol. 110, p. 102–110.
- Smith, H. N., and Carter, R. A. (2011) “Over Twenty–Five Years of Applied Coastal Engineering in Alaska.” Proceedings of Coastal Engineering Practice 2011, American Society of Civil Engineers, p. 64–77.
- Smith, J.M., Anderson, M.E., Taflanidis, A.A., Kennedy, A.B., Westerink, J.J. and Cheung, K.F. (2012) HAKOU v3: SWIMS Hurricane Inundation Fast Forecasting Tool for Hawaii, USACE ERDC/CHL CHETN–I–84.
- Smith, J.M., Sherlock, A.R., and Resio, D.T. (2001) “STWAVE: Steady–State Spectral Wave Model User’s Manual for STWAVE, Version 3.0.” Special Rep. ERDC/CHL SR–01–1, US Army Engineer Waterways Experiment Station, Vicksburg, Miss.
- Smith, J.P, Hunter, T.S., Clites, A.H., Stow, C.A., Slaweki, T., Muhr, G.C., and Gronewold, A.D. (2016) An Expandable Web–Based Platform for Visually Analyzing Basin–Scale Hydro–Climate Time Series Data,” Environmental Modelling & Software, Vol 78, April 2016, p. 97–105, ISSN 1364–8152, <http://dx.doi.org/10.1016/j.envsoft.2015.12.005>
- Smith, M.K., Cialone, M.A., Wamsley, T.V., Mcalpin, T.O. (2010). “Potential Impact of Sea Level Rise on Coastal Surges in Southeast Louisiana.” Ocean Eng, Vol. 37, No. 1, p. 37–47
- Smith, N. (2018) “Climate Change Turns Coastal Property Into a Junk Bond,” Bloomberg, May 3, 2018, <https://www.bloomberg.com/opinion/articles/2018-05-03/flood-risk-makes-coastal-real-estate-look-like-a-junk-bond> (accessed April 19, 2019).

- Smith, S.J., and Smith, J.M. (2001) "Numerical Modeling of Waves at Ponce de Leon Inlet, Florida." *Journal of Waterway, Port, Coastal, and Ocean Engineering.*, American Society of Civil Engineers. Vol. 127, No. 3, p. 176–184.
- Snead, J. (2018) NCDOT Bridge Superstructure Level III Wave Vulnerability Study Report and GIS Database, presentation at National Hydraulic Engineering Conference, Columbus, OH, August 29.
- Sorensen, R.M. (1993) *Basic Wave Mechanics for Coastal and Ocean Engineers*. John Wiley and Sons. 284 pp.
- Sorensen, R.M., (2006) *Basic Coastal Engineering*. Third Edition. Springer Science, New York. 324 pp.
- Southeast Florida (2015) Regional Climate Change Compact Sea Level Rise Work Group (Compact). October 2015. Unified Sea Level Rise Projection for Southeast Florida. A document prepared for the Southeast Florida Regional Climate Change Compact Steering Committee. 35 pp.
- Stockdon, H.F., R.A. Holman, P.A. Howd, and A.H. Sallenger Jr. (2006). "Empirical Parameterization of Setup, Swash, and Runup." *Coastal Engineering*, Vol. 53, No. 7 (2006), p. 573–588. <https://doi.org/10.1016/j.coastaleng.2005.12.005>.
- Sumer, B.M., and Fredsoe, J. (2001). "Wave Scour around a Large Vertical Circular Cylinder." *Journal of Waterway, Port, Coastal, and Ocean Engineering* Vol. 127, No. 3, p. 125–134.
- Sumer, B.M., Fredsoe, J., and Christiansen, N. (1992). "Scour around Vertical Pile in Waves." *Journal of Waterway, Port, Coastal, and Ocean Engineering* Vol. 118, No. 1, p. 15–31.
- Sumer, B.M., Hatipoglu, F., Fredsoe, J. (2007). "Wave Scour around a Pile in Sand, Medium Dense, and Dense Silt." *Journal of Waterway, Port, Coastal, and Ocean Engineering* Vol. 133, No. 1, p. 14–27.
- Sverdrup, H.U. and Munk, W.H. (1947) "Wind, Sea and Swell: Theory of Relations for Forecasting." Hydrographic Office, US Navy. Publication 601. Washington D.C. 50 pp.
- Sweet, W. V. and Park, J. (2014) "From the Extreme to the Mean: Acceleration and Tipping Points of Coastal Inundation from Sea Level Rise." *Earth's Future*, Vol. 2, No. 12, p. 579–600.
- Sweet, W., Park, J., Marra, J., Zervas, C., and Gill, S. (2014). "Sea Level Rise and Nuisance Flood Frequency Changes around the United States." NOAA Technical Report NOS CO–OPS 073.
- Sweet, W.V., Horton, R., Kopp, R.E., LeGrande, A.N., and Romanou, A. (2017a) Sea level rise. In: *Climate Science Special Report: Fourth National Climate Assessment, Volume I* [Wuebbles, D.J., D.W. Fahey, K.A. Hibbard, D.J. Dokken, B.C. Stewart, and T.K. Maycock (eds.)]. U.S. Global Change Research Program, Washington, D.C., USA, p. 333–363, DOI: 10.7930/J0VM49F2.
- Sweet, W., Kopp, R., Weaver, C., Obeysekera, J., Horton, R., Thieler, R., and Zervas C. (2017b). "Global and Regional Sea Level Rise Scenarios for the United States." NOAA Technical Report NOS CO–OPS 083.
- Sweet, W., Kopp, R., Weaver, C., Obeysekera, J., Horton, R., Thieler, R., and Zervas C. (2017c). "Data: Global and Regional Sea Level Rise Scenarios for the United States (CSV)." NOAA Technical Report NOS CO–OPS 083. <https://tidesandcurrents.noaa.gov/publications/techrpt083.csv> (accessed May 10, 2019)

- Sweet, W.V.; Duseket, G.; Obeysekera, J. and Marra, J.J. (2018) "Patterns and Projections of High Tide Flooding Along the U.S. Coastline Using a Common Impact Threshold." Silver Spring, MD, NOAA NOS Center for Operational Oceanographic Products and Services, 44 pp. (NOAA Technical Report NOS CO-OPS 086), DOI: <http://dx.doi.org/10.25607/OBP-128>
- Taflanidis, A.A., Kennedy, A.B., Westerink, J.J., Smith, J.M., Cheung, K.F., Mark, H. and Tanaka, S. (2013). "Rapid Assessment of Wave and Surge Risk during Landfalling Hurricanes: Probabilistic Approach." *Journal of Waterway, Port, Coastal, and Ocean Engineering*, Vol. 139, No. 3, p. 171–182.
- Tang, H. S., Chien, S. I.–J., Temimi, M., Blain, C. A., Ke, Q., Zhao, L., and Kraatz, S. (2013). "Vulnerability of Population and Transportation Infrastructure at the East Bank of Delaware Bay due to Coastal Flooding in Sea–Level Rise Conditions." *Natural Hazards*, Vol. 69, No. 1, p. 141–163.
- Taylor, K.E., Stouffer, R.J., Meehl, G.A. (2012) "An Overview of CMIP5 and the Experiment Design," *Bulletin of the American Meteorological Society*, Vol. 93, No. 4, p. 485–498, DOI:10.1175/BAMS–D–11–00094.1.
- Thio, H.K., Somerville, P., and Polet, J. (2010) "Probabilistic Tsunami Hazard in California," Pacific Earthquake Engineering Research Center College of Engineering University of California, Berkeley Report 2010/108, 331 pp.
- Thompson, E. F., Wutkowski, M. and Scheffner, N. W. (1996) "Risk–Based Analysis of Coastal Projects." *Proceedings of the 25th International Conference on Coastal Engineering* p. 4440–4450.
- Titov, V. V. and Gonzalez, F. I. (1997) "Implementation and Testing of the Method of Splitting Tsunami (MOST) Model." NOAA Technical Memorandum ERL PMEL–112 (see <http://nctr.pmel.noaa.gov/model.html>)
- Titov, V. V. and Synolakis, C. E. (1997) "Extreme Inundation Flows During the Hokkaido–Nansei–Oki Tsunami." *Geophysical Research Letters*, Vol. 24, No. 11, p. 1315–1318. (see <http://nctr.pmel.noaa.gov/model.html>)
- Titus, J. G. (2002) "Does Sea Level Rise Matter to Transportation along The Atlantic Coast?" *The Potential Impacts of Climate Change on Transportation Workshop*, October 1–2, 2002. Washington, D.C, 16 pp.
- Tomiczek, T., Kennedy, A., Zhang, Y., Owensby, M., Hope, M.E., Lin, N., Flory, A. (2017) "Hurricane Damage Classification Methodology and Fragility Functions Derived from Hurricane Sandy's Effects in Coastal New Jersey." *Journal of Waterway, Port, Coastal, and Ocean Engineering*, Vol. 143, No. 5.
- Tonkin, S., Yeh, H., Kato, F., and Sato, S. (2003). "Tsunami scour around a cylinder." *Journal of Fluid Mechanics*, Vol. 496, p. 165–192.
- Toro, G.R., Niedoroda, A.W., Reed, C.W., and Divoky, D. (2010a). "Quadrature–based approach for the efficient evaluation of surge hazard," *Ocean Engineering*, Vol. 37, No. 1, p. 114–124.
- Toro, G.R., Resio, D.T. Divoky, D., Niedoroda, A.W., and Reed, C. (2010b). "Effective joint–probability methods of hurricane surge frequency analysis," *Ocean Engineering*, Vol. 37, No. 1, p. 125–134.

Torres, J. M., Bass, B., Irza, N., Fang, Z., Proft, J., Dawson, C., Kiani, M., and Bedient, P. (2015). "Characterizing the hydraulic interactions of hurricane storm surge and rainfall–runoff for the Houston–Galveston region," *Coastal Engineering*, Vol. 106, p. 7–19.

Transportation Pooled Fund Program (2019) Validation of Tsunami Design Guidelines for Coastal Bridges, Study No. TFP–5–307, <https://www.pooledfund.org/Details/Study/556> (accessed April 22, 2019).

Triatmadja, R., Hijah, S.N., Nurhasanah, A. (2011). Scouring around coastal structures due to tsunami surge. 6<sup>th</sup> Annual International Workshop & Expo on Sumatra Tsunami Disaster and Recovery, TS 3–18, 7 pp.

Tsunami Pilot Study Working Group (2006) Seaside, Oregon Tsunami Pilot Study: Modernization of FEMA flood hazard maps. US Geological Survey Open–File Report 2006–1234 (see <http://pubs.usgs.gov/of/2006/1234/>)

TxDOT (2019) personal communication, April 26, 2019.

UNESCO (1997) IUGG/IOC TIME Project: Numerical Method of Tsunami Simulation with the Leap–Frog Scheme. UNESCO Intergovernmental Oceanographic Commission, Manuals and Guides No. 35. 126 pp. (see [http://ioc-unesco.org/index.php?option=com\\_wrapper&view=wrapper&Itemid=100003](http://ioc-unesco.org/index.php?option=com_wrapper&view=wrapper&Itemid=100003) )

US Congress (2013) H.R. 152 Supplemental Appropriations for Hurricane Sandy, 113th Congress: 1st Session, 109 pp.

US Department of Labor (2017) "Bureau of Labor Statistics, Table B–1. Employees on nonfarm payrolls by industry sector and selected industry detail," <https://www.bls.gov/news.release/empsit.t17.htm>, accessed October 1, 2018)

US Senate (2018) Senate Report 115–138 – Transportation, and Housing and Urban Development, and Related Agencies Appropriations Bill, 2018.

US Travel Association (2017) "Research Report: Travel – The Unsung Hero of Job Creation," <https://www.ustravel.org/research/travel-america-unsung-hero-job-creation>, accessed October 1, 2018)

USACE (1984) Shore Protection Manual. 4th ed., 2 vols. US Army Engineer Waterways Experiment Station, Coastal Engineering Research Center, U.S Government Printing Office, Washington D.C.

USACE (2002) Coastal Engineering Manual. Engineer Manual 1110–2–1100, USACE, Washington, D.C.

USACE (2011) Sea Level Change Considerations for Civil Works Programs, EC 1165–2–212, Washington, D.C., 32 pp. (see: <http://planning.usace.army.mil/toolbox/library/ECs/EC11652212Nov2011.pdf>)

USACE (2014). Procedures to Evaluate Sea Level Change: Impacts, Responses, and Adaptation, USACE ETL 1100–2–1, June 30, 2014, 254 pp. (see [http://www.publications.usace.army.mil/Portals/76/Publications/EngineerTechnicalLetters/ETL\\_1100-2-1.pdf](http://www.publications.usace.army.mil/Portals/76/Publications/EngineerTechnicalLetters/ETL_1100-2-1.pdf))

USACE (2015) "North Atlantic Coast Comprehensive Study: Resilient Adaptation to Increasing Risk." USACE North Atlantic Division. (see <https://www.nad.usace.army.mil/CompStudy> )

USACE (2017). Sea Level Change Curve Calculator, version 2017.55 <http://corpsclimate.us/ccaceslcurves.cfm> (accessed October 1, 2018)

- USACE (2019) Coastal Hazards System. <https://chs.ercd.dren.mil/> (accessed April 17, 2019)
- USACE–Detroit District (2018) Great Lakes Water Level Forecasts <https://www.lre.usace.army.mil/Missions/Great-Lakes-Information/Great-Lakes-Water-Levels/Water-Level-Forecast/> accessed September 24, 2018.
- USDOT (2013) "Impacts of Climate Change and on Transportation Systems and Infrastructure: The Gulf Coast." Web. (accessed February 17, 2013) (see: [http://www.fhwa.dot.gov/environment/climate\\_change/adaptation/ongoing\\_and\\_current\\_research/gulf\\_coast\\_study/index.cfm](http://www.fhwa.dot.gov/environment/climate_change/adaptation/ongoing_and_current_research/gulf_coast_study/index.cfm) )
- USGCRP (2017) Climate Science Special Report: Fourth National Climate Assessment, Volume I [Wuebbles, D.J., D.W. Fahey, K.A. Hibbard, D.J. Dokken, B.C. Stewart, and T.K. Maycock (eds.)]. US Global Change Research Program, Washington, D.C., USA, 470 pp, DOI: 10.7930/J0J964J6.
- USGCRP (2018) Impacts, Risks, and Adaptation in the United States: Fourth National Climate Assessment, Volume II [Reidmiller, D.R., C.W. Avery, D.R. Easterling, K.E. Kunkel, K.L.M. Lewis, T.K. Maycock, and B.C. Stewart (eds.)]. U.S. Global Change Research Program, Washington, D.C., USA, 1515 pp. DOI: 10.7930/NCA4.2018
- USGS (2003) "An Overview of Coastal Land Loss: With Emphasis on the Southeastern United States", USGS Open File Report 03–337
- USGS (2018) "Barrier-Island and Estuarine-Wetland Physical-Change Assessment after Hurricane Sandy." USGS Open-File Report 2017-1157
- van der Meer, J., and Sigurdarson, S. (2017) Design and Construction of Berm Breakwaters. Advanced Series on Ocean Engineering, Volume 40, World Scientific Press.
- Vatvani, D., Zweers, N., van Ormondt, M., Smale, A., de Vries, H., and Makin, V. (2012) "Storm Surge and Wave Simulations in the Gulf of Mexico Using a Consistent Drag Relation for Atmospheric and Storm Surge Models," Natural Hazards and Earth System Science, Vol. 1, p. 2399–2410.
- Vermeer, M. and Rahmstorf, S. (2009) Global sea level linked to global temperature, Proceedings of the National Academy of Sciences, Vol. 106, No. 51, p. 21527–21532, DOI: 1073/pnas.0907765106.
- Wahl, T., Jain, S., Bender, J., Meyers, S. D., and Luther, M. E. (2015). "Increasing risk of compound flooding from storm surge and rainfall for major US cities." Nature Climate Change, Vol. 5, No. 12, p. 1093–1097.
- Walling, K., Miller, J.K., Herrington, T.O., and Eble, A. (2014) "Comparison of Hurricane Sandy impacts in three New Jersey coastal communities." Proceedings of the 34th Conference on Coastal Engineering, Seoul, Korea. 14 pp.
- Wang, H. (1970) "Water Wave Pressure on Horizontal Plate." Journal of the Hydraulics Division. American Society of Engineers. Vol. 96, No. HY10, p. 1997–2017.
- Washington DOT (2011) "Climate Impacts Vulnerability Assessment Report." Report to FHWA, FHWA–HEP–14–004. [https://www.fhwa.dot.gov/environment/sustainability/resilience/case\\_studies/washington\\_state/washington\\_state.pdf](https://www.fhwa.dot.gov/environment/sustainability/resilience/case_studies/washington_state/washington_state.pdf) (accessed May 11, 2019)
- Webb, B.M., and Matthews, M.T. (2014). Wave-induced scour at cylindrical piles: estimating equilibrium scour depth in a transition zone. Journal of the Transportation Research Board Vol. 2436, No. 1, p. 148–155.

- Webb, B.M. (2017) "A Primer on Modeling in the Coastal Environment," FHWA–HIF–18–002, Washington, D.C.: Federal Highway Administration. 71 pp.
- Webb, B., Douglass, S., Dix, B., and Asam, S. (2018) "White Paper: Nature - Based Solutions for Coastal Highway Resilience." FHWA–HEP–18–037. Washington, D.C.: Federal Highway Administration.
- Webb, B., Dix, B., Douglass, S., Asam, S., Cherry, C., and Buhring, B. (2019) "Nature-Based Solutions for Coastal Highway Resilience: An Implementation Guide." FHWA-HEP-19-042. Washington, D.C. Federal Highway Administration.
- Weggel, J.R. (1997) "Breaking–Wave Loads on Vertical Walls Suspended Above Mean Sea Level." Discussion of paper by Chan *et al.* Journal of Waterway, Port, Coastal, and Ocean Engineering. American Society of Civil Engineers. Vol. 123, No. 3, p. 143–146.
- Weggel, J.R. and Sorensen, R.M. (1986) "Ship Wave Prediction for Port and Channel Design." Proceedings from the Ports '86 Conference. American Society of Civil Engineers, p. 794–814.
- Wei, Z., and Dalrymple, R.A. (2016) "Numerical study on mitigating tsunami force on bridges by an SPH model." Journal of Ocean Engineering and Marine Energy, Vol. 2, No. 3, p. 365–380.
- Wei, Z., Dalrymple, R.A., Hecault, A., Bilotta, G., Rustico, E., and Yeh, H. (2015) "SPH modeling of dynamic impact of tsunami bore on bridge piers." Coastal Engineering, Vol. 104, p. 26–42.
- Westerink, J.J., Blain, C.A., Luettich, R.A., Jr., and Scheffner, N.W. (1994) ADCIRC: An Advanced Three–Dimensional Model for Shelves, Coasts, and Estuaries. "Report 2: User's Manual for ADCIRC–22DI." USACE. Washington, D.C. 68 pp.
- Wiegel, R.L. (1964) Oceanographical Engineering. Prentice Hall, Englewood Cliffs, New Jersey. 532 pp.
- Winter, A.O., Motley, M.R., Eberhard, M.O. (2018) "Tsunami-like wave loading of individual bridge components." Journal of Bridge Engineering, Vol. 23, No. 2.
- Xie, S.–L. (1981) "Scouring Patterns in Front of Vertical Breakwaters and their Influences on the Stability of the Foundations of the Breakwaters." Dept. Civil Engineering, Delft University of Technology, Delft, The Netherlands.
- Xie, S.–L. (1985) Scouring patterns in front of vertical breakwaters. Acta Oceanologica Sinica, Vol. 4, No. 1, p. 153–164.
- Yashinsky, M. (2011) "Lessons Learned from the March 11, 2011 M9.0 Great Tohoku Earthquake and Tsunami," 15 pp. (see [http://www.dot.ca.gov/hq/esc/earthquake\\_engineering/PEQIT/Performance%20of%20Bridges.pdf](http://www.dot.ca.gov/hq/esc/earthquake_engineering/PEQIT/Performance%20of%20Bridges.pdf))
- Yu, Q.–S., Wilson, J., and Wang, Y. (2014) "Overview of the Oregon resilience plan for next Cascadia earthquake and tsunami." 10th U.S. National Conference on Earthquake Engineering: Frontiers of Earthquake Engineering, NCEE 2014, Anchorage, AK.
- Zoulas, J. G., and Orme, A. R. (2007) "Multidecadal–scale beach changes in the Zuma littoral cell, California." Physical Geography, Vol. 28, No. 4, p. 277–300.

## Appendix – Workshop Participants

Peer exchange meetings and workshops were held during the development of this 3<sup>rd</sup> edition. The participation by these professionals is gratefully acknowledged.

A one-day peer exchange meeting in March 2018 in Washington, DC provided initial input into the overall revisions for this 3<sup>rd</sup> edition. Participants in that peer exchange included Mary Cialone, Elizabeth Habic, Maria Honeycutt, David Kriebel, Matt Lauffer, Patrick Lynette, Mark Osler, Elizabeth Sciaudone, and William Sweet.

A day and a half meeting at the Turner-Fairbank Hydraulic Research Center in May 2017 focused on coastal highway flooding issues with emphasis on the combined effects of sea level rise and rainfall runoff. Participants in that workshop included Elizabeth Habic, Rick Renna, and Carlton Spirio.

A series of four one-day workshops were held in March and April 2018 focused on emerging issues associated with sea level rise. The workshops were facilitated by FHWA and hosted by SDOTs. These workshops informed the content of Chapter 9 Increased Flooding due to Relative Sea Level Rise. Participants included:

- Hanover, Maryland: Brian Cox, LaTonya Gilliam, Gina Goettler, Robert Graff, Elizabeth Habic, Matt Lauffer, Joy Liang, Peter Mattejat, Andrew McDaniel, Michael Michalski, Karuna Pujara, William Seiger, Eileen Singleton, Steve Sisson, Ryan White, and Russ Yurek,
- Tallahassee, Florida: Jenna Bowman, Jennifer Carver, Kevin Claridge, Samantha Danchuk, Mario Dominguez, Katey Earp, Whitney Gray, Rick Jenkins, Chase Knight, Kenneth Konyha, Abderrahmane Maamar-Tayeb, Steve Nolan, Jayantha Obeysekera, James Poole, Carlos Ribbeck, Ricardo Salazar, Carlton Spirio, and Georgio Tachiev,
- Olympia, Washington: Luke Assink, Craig Boone, William Fletcher, Peggy Fox, Andy Haub, Julie Heilman, John Himmel, Mike Knapp, Casey Kramer, Sharon Love, Mark Mobbs, Gregor Myhr, Simon Page, Carol Lee Roalkvam, Jeff Rudolph, Steve Russel, Alex Steely, James Struthers, Babbak Talebi, Theresa Turpin, and Susan Wimberly
- Boston, Massachusetts: Michael Arpino, Stephen Bartha, David Belange, Peter Collette, Teresa Crean, Jason Dvelis, Hanan Fouad, Mark Griffin, Charlie Hebson, Mike Hogan, Kirsten Howard, Jennifer Jacobs, Julia Knisel, Julie LaBranche, Timothy Mallette, Rick McCullough, Ellen Mecray, Norm Miller, Steven Miller, Timothy Paris, and Daniel Vieira.

*Page Intentionally Left Blank*